Ecotoxicological impact and risk assessment of engineered TiO2 nanomaterials on water, sediments and soil by building a combined RALCA (Risk Assessment – Life Cycle Assessment) model

Véronique Adam

UNIVERSITÉ DE STRASBOURG

ÉCOLE DOCTORALE 413

LHYGES – UMR 7517

THÈSE présentée par :

Véronique ADAM

soutenue le : **25 septembre 2015**

pour obtenir le grade de : **Docteur de l'université de Strasbourg**

Discipline/ Spécialité : Sciences de l'Environnement

Ecotoxicological impact and risk assessment of engineered TiO_2 nanomaterials on water, sediments and soil by building a combined RA-LCA (Risk Assessment – Life Cycle Assessment) model

THÈSE dirigée par :

Mme QUARANTA Gaetana	Maître de conférences, HDR, université de Strasbourg

RAPPORTEURS :

M. BOTTERO Jean-Yves	Directeur de recherche, CNRS
M. FLAHAUT Emmanuel	Directeur de recherche, CNRS

AUTRES MEMBRES DU JURY :

M. ACKERER Philippe	Directeur de recherche, CNRS
Mme LAWNIZCAK Stéphanie	Maître de conférences, université de Strasbourg

ACKNOWLEDGEMENTS

This work took part in the MESONNET (Mesocosm Network for Environmental Nanotechnology Risk Assessment) program of the National Research Agency (ANR). I would like to thank Jean-Yves Bottero, coordinator of this program, for giving me the opportunity to collaborate with chemists and ecotoxicologists from different laboratories (CEREGE at Aix-en-Provence, Ecolab at Toulouse and LIEC at Metz, France). This program enabled the use of ecotoxicity data from LIEC in the modeling.

This research was funded by ADEME (Agence de l'Environnement et de la Maîtrise de l'Energie) and Région Alsace. CEINT (Center for Environmental Impacts of Nanotechnology) also provided financial support. I thank all of them, who made this work possible.

Thank you to all committee members, Jean-Yves Bottero, Emmanuel Flahaut, Philippe Ackerer, Christine Hendren, Hélène Desqueyroux, Aurélie Grégoire and Laurent Liénard, who have accepted to assess my work.

I would like to thank the people that took part in this work, each in their native language.

Tania, Stéphanie, je vous remercie énormément de m'avoir fait confiance pour ce projet, et de m'avoir emmenée jusqu'à son aboutissement. Vous m'avez beaucoup apporté scientifiquement. Votre rigueur scientifique et votre désir d'excellence m'ont poussée à aller toujours plus loin, à être toujours plus exigeante envers moi-même, sur le fond comme sur la forme ! Je vous ai aussi découvert de grandes qualités humaines : Tania, j'ai particulièrement apprécié ta générosité et ta franchise. Tu as su, en m'accompagnant pendant une grande partie de mes études, me transmettre des valeurs importantes qui m'ont permis de me développer, scientifiquement et personnellement. Stéphanie, merci pour ton optimisme et ta bonne humeur, qui m'ont aidée à avancer dans des moments de doute.

Un grand merci à Laurent Liénard, qui nous a ouvert les portes de son entreprise, et grâce à qui nous avons pu faire ce travail. Tu t'es toujours montré disponible et efficace, nos discussions ont permis de soulever des points très intéressants.

Je voudrais également remercier les chercheurs, du LHyGeS bien sûr, mais aussi des différents laboratoires avec qui j'ai pu collaborer grâce à l'ANR MESONNET et au GdRI CEINT. Ils m'ont donné un peu (voire beaucoup) de leur temps pour m'aider au laboratoire et devant mon ordinateur.

Un grand merci à Jérôme Labille, du CEREGE d'Aix-en-Provence, qui m'a accompagnée dans mes expériences d'agrégation. J'ai beaucoup appris à tes côtés, merci pour ta disponibilité. Merci à Jean-Yves Bottero et à Jérôme Rose de m'avoir accueillie dans leur équipe !

Merci à Mathieu Therezien, de l'Université de Duke, et à Philippe Ackerer, du LHyGeS, pour votre aide si précieuse à la programmation. Vous avez toujours été disponibles et patients, je vous en suis réellement reconnaissante. Thank you, Eric Money, for answering my flow of questions and for showing me the route to follow in the Bayesian jungle. Many thanks to Mark Wiesner and Christine Hendren, who made me meet Mathieu, Eric, and other researchers at Duke, always for very interesting talks!

Merci à toute l'équipe d'EcoLab à Toulouse : j'ai énormément appris lors de nos échanges, vous avez été d'une rare efficacité. Un grand merci aussi à Laure Giamberini et à son équipe du LIEC à Metz pour m'avoir fourni les données nécessaires à l'élaboration du modèle. Merci Laure pour ta disponibilité sans faille !

Au LHyGeS, c'est aussi Tiphaine Weber que je voudrais remercier, pour m'avoir aidée à comprendre la théorie derrière les observations de laboratoire. Un grand merci à René Boutin pour les analyses ICP et à Martine Trautmann, du LAS de l'EOST, pour avoir réalisé les analyses de sols et de sédiments. Merci aussi à Sophie Gangloff et Thierry Perrone pour votre gentillesse et vos services rendus au labo, et à Eric Pelt pour m'avoir permis de préciser quelques-uns de mes protocoles.

Merci à Mireille Del Nero et à Catherine Galindo de m'avoir permis d'accéder à leur laboratoire de l'IPHC à Strasbourg.

Un énorme merci à mes compagnons de route, dont certains sont devenus des amis : Adrien, tu as été le premier à m'intégrer dans la *dream team*, ces trois années n'auraient pas été les mêmes si tu n'étais pas venu me chercher ! Jean-Mi et ta « bisounoursattitude », Clio avec ta clairvoyance et Marion avec ton éternel sourire, vous m'avez redonné le moral plus d'une fois, merci, merci, merci ! Julien, merci d'avoir pris du temps pour m'aider à la programmation ! Thiébaud, Harold, à quand nos prochaines discussions philosophiques ? Et puis Pierre, Bastien, Iza, Christian… A tous, merci pour votre soutien, je me suis réellement sentie entourée !

Merci aussi aux Magic' Girls. C'est parce que vous étiez toujours là pour moi, que vous m'avez parfois même nourrie, que j'ai pu me consacrer sereinement à mon travail… Et me détendre quand il le fallait !

Merci Papa, merci Maman, merci Titite Soeurette. Vous avez cru en moi depuis le début, et encore plus à la fin, c'est grâce à vous que j'ai su que je pouvais relever ce défi.

Franck, parfois loin des yeux, mais toujours dans mon cœur. Attentif, réconfortant, encourageant… Tu m'as portée pendant ces trois années. Les mots ne sont pas assez forts pour exprimer toute la gratitude que j'éprouve de te savoir à mes côtés.

RESUME ETENDU

Les nanomatériaux (NMs) font aujourd'hui partie intégrante de nombreux produits de consommation, constituant ainsi une part de plus en plus importante du marché mondial. Les NMs de TiO_2 sont produits à hauteur de 550 à 5500 tonnes par an, se plaçant au deuxième rang européen et mondial en termes de production industrielle de NMs (Piccinno et al. 2012). Ils sont utilisés notamment dans les crèmes solaires pour leurs capacités d'absorbance des rayons ultraviolets, ainsi que dans les procédés de traitement des eaux et les revêtements de façade pour leurs propriétés photo-catalytiques. Ils pourraient donc se retrouver en quantités non négligeables dans les différents compartiments environnementaux (air, sol, eau, sédiments). Les NMs sont définis comme des matériaux contenant au moins 50 % de particules dont au moins une des dimensions est inférieure à 100 nm (European Commission 2012). Du fait de leur petite taille, les nanoparticules (NPs) ont une grande réactivité, ce qui les rend intéressantes pour le développement de nombreuses applications industrielles.

Bien que l'opinion publique s'inquiète de l'exposition potentielle des hommes et de l'environnement à ces NMs, la législation peine à réglementer leur utilisation. Ceci est dû au manque de connaissance que l'on a de leurs propriétés spécifiques, de leur devenir et de leurs effets potentiels dans l'environnement. Le programme européen REACH (Règlement sur l'enregistrement, l'évaluation, l'autorisation et les restrictions des substances chimiques) reconnaît que ces matériaux ont des propriétés spécifiques, et travaille à leur prise en compte dans la législation (European Commission 2008). En France, la loi du Grenelle de l'Environnement (2010-967 du 3 Août 2009, section 42.2009 et 2010-788 du 12 Juillet 2010, section 185.2010) s'applique en termes d'information du public, mais ne régule pas le marché des NMs manufacturés.

La demande sociétale pour une meilleure compréhension du devenir des NMs et de leurs impacts et risques potentiels a été à l'origine du lancement du programme MESONNET (Mesocosm network for Environmental Nanotechnology Risk Assessment) de l'Agence Nationale pour la Recherche, dans lequel s'inscrit cette thèse. MESONNET réunit différents laboratoires de chimie, d'hydrologie et d'écotoxicologie, œuvrant à l'évaluation des risques environnementaux des NMs.

L'objectif principal de cette thèse est donc d'évaluer les impacts et risques environnementaux potentiels des nanomatériaux manufacturés de TiO_2. Pour ce faire, deux méthodologies ont été choisies et combinées en un outil unique, l'ACV-ER : l'Analyse du Cycle de Vie (ACV) et l'Evaluation des Risques (ER). L'ACV est une méthodologie normalisée (ISO 2006a; ISO 2006b) permettant d'évaluer les impacts potentiels d'un produit, d'un service ou d'une substance sur les différents compartiments environnementaux, tout au long de son cycle de vie, c'est-à-dire depuis la production des NMs jusqu'à la fin de vie des nanoproduits dans lesquels ils sont insérés, en passant par leur fabrication et leur utilisation. L'évaluation des risques environnementaux est une méthode d'évaluation environnementale donnant des magnitudes ou des probabilités d'occurrence de dommages causés par les activités humaines ou les catastrophes naturelles (Savolainen et al. 2010). La combinaison de ces deux méthodologies est facilitée par le fait qu'elles requièrent le même type de données : une analyse du devenir des NMs et une analyse de leurs effets. Le devenir des substances comprend leurs émissions, leurs transferts au sein d'un même milieu mais aussi entre différents compartiments environnementaux et leurs transformations (agrégation, dégradation). Ces paramètres sont modélisés afin d'estimer leurs concentrations et leurs temps de résidence dans les différents compartiments environnementaux (air, sol, eau, sédiment). Les effets potentiels des substances sur les organismes sont évalués par des tests de toxicité. C'est la combinaison de ces données de devenir et d'effet qui permet de calculer l'impact ou le risque environnemental de la substance considérée.

Afin de réduire les incertitudes liées au devenir des NMs dans les différents compartiments environnementaux, une échelle « site-spécifique » a été utilisée. Elle permet de prendre en compte les paramètres environnementaux et anthropiques spécifiques au site étudié et d'évaluer les risques et les impacts des NMs de TiO_2 à l'échelle locale. La mise en œuvre de cette échelle « site-spécifique » a été possible grâce à une collaboration avec une entreprise de production de NMs de TiO_2 (CRISTAL, localisée à Vieux-Thann en France). Cette entreprise nous a permis d'échantillonner leurs effluents industriels rejetés vers la rivière et nous a fourni des échantillons de production sur lesquels nous avons pu réaliser des expériences en laboratoire.

L'aire d'étude comprend ainsi l'usine de production de TiO_2 et le site de traitement des déchets qui y est associé, ainsi qu'une surface d'une dizaine de km² autour de cette usine (Figure 1). Plusieurs types d'effluents industriels provenant de l'usine sont dirigés vers la rivière Thur :

- Les effluents T collectent les eaux de pluie et de refroidissement des procédés. S'ils répondent à certains critères de conformité, telle la turbidité, ils sont rejetés dans un canal usinier, qui rejoint la rivière au point 4 (Figure 1).
- Les effluents acides, provenant directement des chaînes de production, sont envoyés vers la station de traitement des déchets de l'Ochsenfeld, qui les neutralise à la chaux avant de les diriger vers la rivière, au point NN.
- Les eaux de ruissellement du terril de l'Ochsenfeld sont rejetées en NNR.

Cette thèse traite donc deux étapes du cycle de vie des NMs, qui sont leur production et leur fin de vie à cette étape de production.

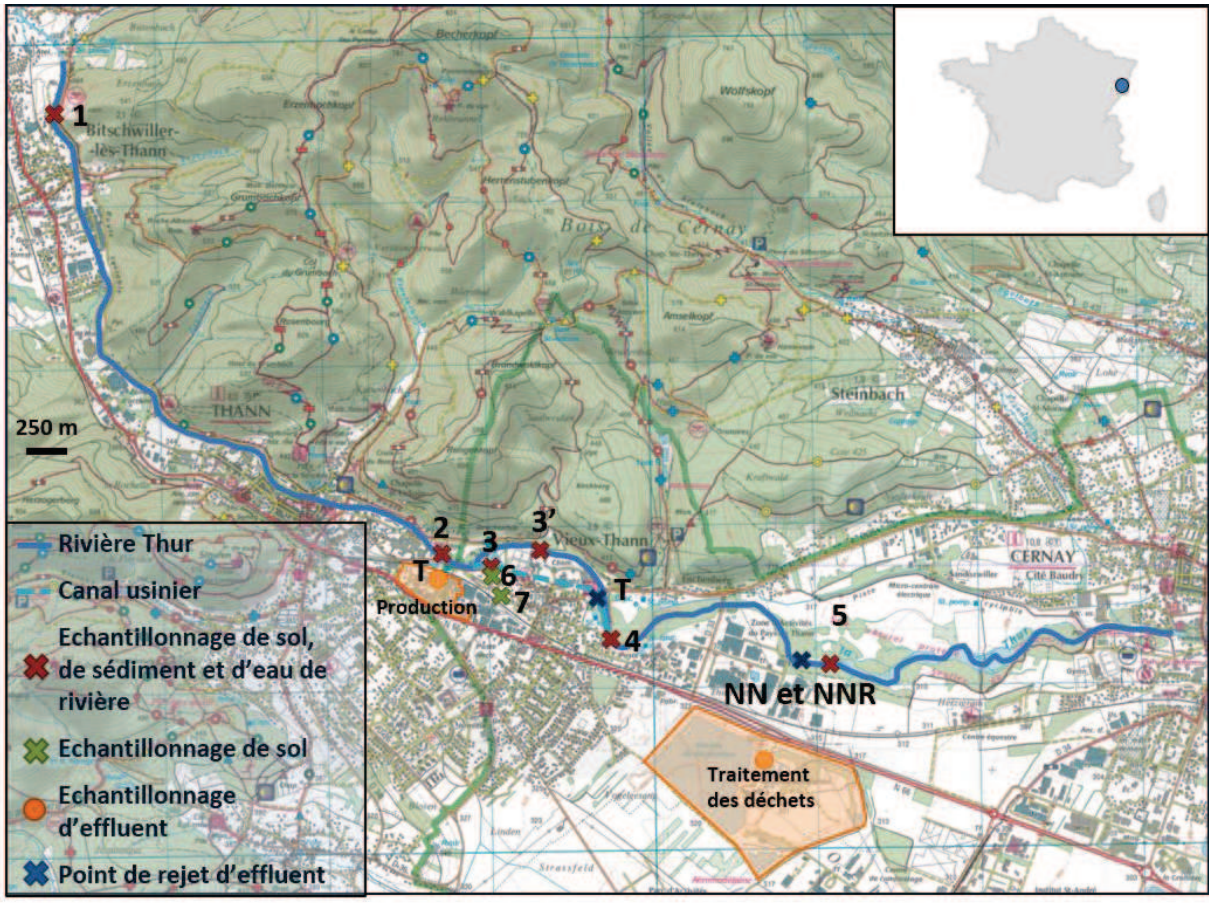

Figure 1 : Localisation de l'aire d'étude et points d'échantillonnages des eaux, sédiments et sols

Les objectifs spécifiques de cette thèse, sont :

- comprendre le comportement des NMs manufacturés de TiO_2 dans le milieu naturel environnant l'usine de production, par la quantification des masses de NMs de TiO_2 disponibles dans l'environnement et par l'étude du comportement d'agrégation de ces NMs dans le milieu naturel (approche analytique) ;
- construire un modèle combinant ACV et ER en utilisant une méthode probabiliste de modélisation, l'approche bayésienne.

Pour y parvenir, une double approche analytique et de modélisation a été menée. Ces deux approches sont étroitement liées, puisque les résultats obtenus sur le terrain et en laboratoire ont permis

d'alimenter le modèle, qui a lui-même permis de déterminer les paramètres devant être obtenus par des mesures et des expériences de laboratoire.

L'approche analytique : présentation et résultats.

Deux volets composent cette approche :

1) Les analyses d'échantillons d'eaux industrielles, d'eau naturelle, de sédiments et de sols ont permis de déterminer les concentrations en TiO_2 auxquelles les organismes sont exposés dans chaque compartiment du milieu, et l'influence potentielle des rejets de l'usine sur la composition chimique des eaux, des sédiments et des sols. L'échantillonnage a été réalisé de façon systématique, sur une dizaine de kilomètres le long de la rivière dans laquelle les effluents industriels sont rejetés, d'amont en aval de l'usine (Figure 1) et à chacune des saisons de l'année 2014 (janvier, mai, août et novembre) ainsi qu'en mars, lorsque seule la chaîne de production des NMs de TiO_2 fonctionnait dans l'usine. Les concentrations en Ti ont été déterminées par ICP-AES, après attaque acide des échantillons d'eau et fusion alcaline des échantillons de sols et de sédiments. L'analyse quantitative des NMs de TiO_2 a été complétée par l'imagerie en microscopie électronique à balayage (MEB) et en transmission (MET) des filtres utilisés lors de la préparation d'échantillons d'effluents industriels (Figure 2).

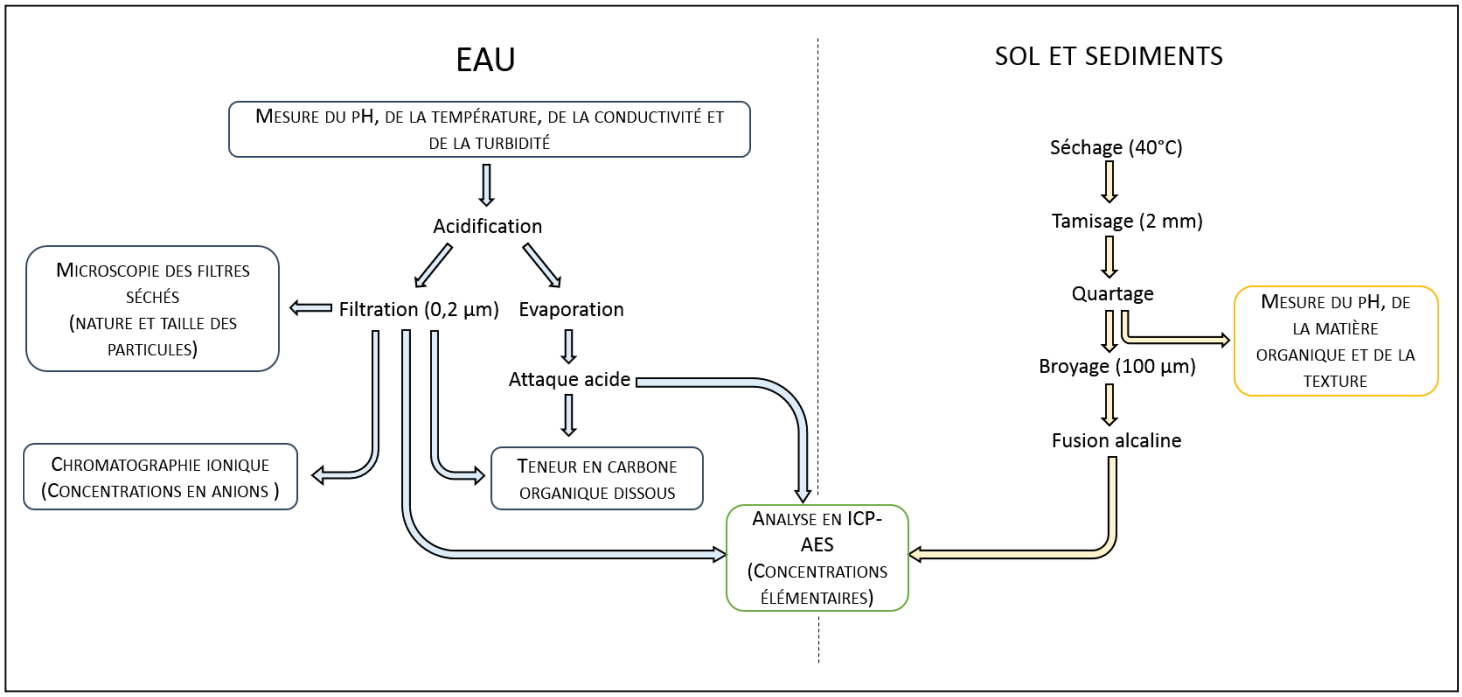

Figure 2 : Techniques utilisées lors de la préparation et de l'analyse des échantillons d'eau, de sédiments et de sols

2) Une caractérisation précise de ces NMs a été réalisée afin de comprendre leur comportement d'agrégation dans l'eau. Les NMs de TiO_2 ont été analysés en diffraction des rayons X pour déterminer leur cristallinité, en microscopie électronique en transmission pour déterminer leur taille et leur forme et par la méthode Brunauer-Emmet-Teller pour obtenir leur surface spécifique. Leur stabilité en suspension a été étudiée en spectrométrie UV-visible et en turbidité sur plusieurs jours. L'évolution de la taille des agrégats de TiO_2 au cours du temps (≥ 30 minutes) a été analysée en diffraction laser et en diffusion dynamique de la lumière (Figure 3), dans l'eau distillée et dans l'eau de rivière filtrée (0.22 µm) pure, après ajout de matière organique dissoute (acides fulviques), et en présence de particules d'argile (illite). Cette argile a été préalablement identifiée comme étant présente en proportion importante dans la matière en suspension transportée par l'eau de rivière.

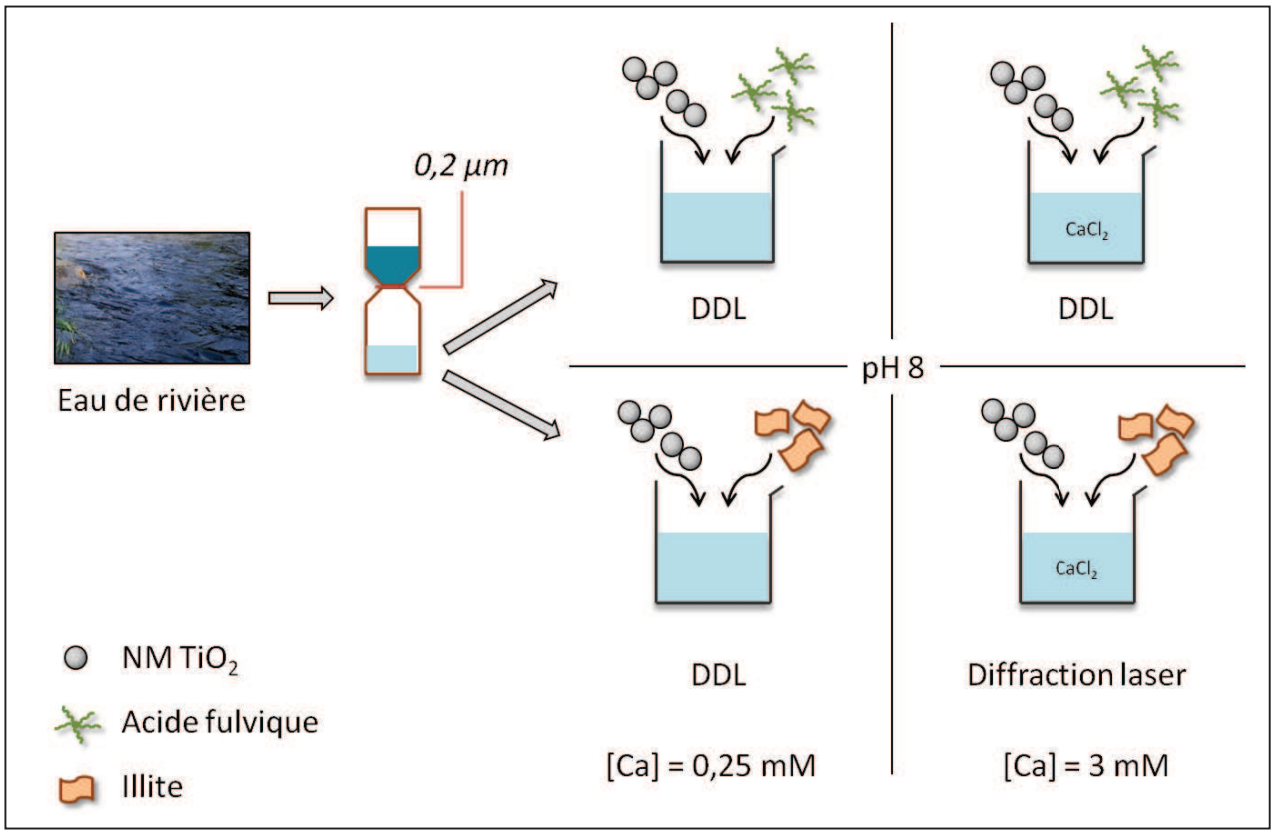

Figure 3 : Conditions expérimentales des expériences d'agrégation des NMs de TiO_2 dans l'eau de rivière. DDL : Diffusion dynamique de la lumière.

Les résultats de microscopie ont révélé la présence des NMs de TiO_2 produits par l'usine dans l'effluent T et dans l'échantillon d'eau prélevé au point 4. Les analyses des échantillons naturels montrent que les mesures réalisées lors de la campagne de mars sont similaires à celles réalisées lors des autres campagnes. Tous les résultats d'analyse des échantillons sont donc représentatifs de l'activité de production des nano-TiO_2. Il a ainsi été montré que les eaux et les sols prélevés sur l'aire d'étude sont significativement impactés par cette activité industrielle, alors que de plus faibles variations de l'amont vers l'aval des concentrations en Ti ont été mesurées dans les sédiments. La faible conductivité mesurée dans l'effluent T ne favorise pas l'agrégation des NMs de TiO_2, ce qui explique le transport préférentiel des NMs vers l'aval plutôt que vers le fond de la rivière, et donc les concentrations en TiO_2 relativement faibles qui ont été mesurées dans les sédiments du point d'échantillonnage 4. A l'opposé, de fortes conductivités ont été mesurées dans les effluents NN et NNR, où les NMs sont certainement

présents sous forme de gros agrégats à la sortie du tuyau et pourraient ainsi sédimenter immédiatement après rejet. Pour mieux comprendre le comportement des NMs de TiO_2 dans la rivière, des échantillons supplémentaires pourraient être collectés plus près des points de rejets industriels.

La concentration relevée dans l'eau de rivière atteint 60 $\mu g.L^{-1}$ au point d'échantillonnage 4. Cette concentration est suffisante pour induire des effets sur les organismes (Ma et al. 2012). L'écosystème aquatique pourrait également être significativement impacté, bien que très localement, par les augmentations de température et de conductivité qui ont été mesurées, induites par les rejets.

Cette étude a montré que l'utilisation d'eau synthétique n'est pas suffisante pour comprendre le comportement des NMs de TiO_2 dans la rivière. Plusieurs paramètres physico-chimiques de ces eaux sont contrôlés (par exemple pH, la concentration en sels et la teneur en matière organique sont ajustés). Mais il est important de réaliser les expériences d'agrégation dans de l'eau naturelle, afin de prendre en compte la grande diversité des molécules organiques et des ions présents dans cette eau.

Dans l'eau de rivière prélevée en amont de l'usine étudiée et de ses rejets, la présence d'acides fulviques en concentration suffisante entraîne une diminution de la taille des agrégats de TiO_2. De plus, lorsque la concentration en TiO_2 est inférieure à 10 $mg.L^{-1}$, les NMs ne s'agrègent pas, ni par homo-agrégation, ni par hétéro-agrégation avec l'argile. Ces résultats suggèrent que dans ces conditions les NMs de TiO_2 sont d'une taille facilement transportable le long de la rivière étudiée (< 600 nm) et peuvent être assimilés par les organismes aquatiques vivant dans la colonne d'eau.

En présence de Ca^{2+} en concentration plus importante, aucun effet de la teneur en carbone organique dissous (COD) n'est observé à des concentrations inférieures à 5 $mg.L^{-1}$. Cependant, il est montré que

les NMs de TiO_2 s'agrègent systématiquement aux particules d'illite, même à de faibles concentrations. Ces résultats permettent de conclure que dans des eaux où les charges cationiques sont importantes, la sédimentation des NMs de TiO_2 et leur transport le long de la rivière sont déterminés par le comportement des particules d'argile. Ce pourrait être le cas, sur le site d'étude, au point d'échantillonnage 5 (en aval des points de rejets NN et NNR), où des concentrations pouvant atteindre 1,73 mM ont été mesurées. A cet endroit, les organismes benthiques seraient ainsi plus facilement exposés au NMs de TiO_2.

La caractérisation précise des NMs, des paramètres environnementaux du milieu dans lequel elles sont rejetées, et la détermination de leur agrégation potentielle dans ce milieu permettent de réduire les incertitudes concernant le devenir des NMs dans l'eau. Toutefois, l'approche « site-spécifique » utilisée ici ne permet pas de les éliminer en totalité. En effet, la stratégie d'échantillonnage et les outils analytiques mis en œuvre n'ont pas permis de déterminer avec certitude la totalité des valeurs des paramètres nécessaires à la modélisation du comportement des NMs de TiO_2 dans les eaux, les sédiments et les sols. En outre, il existe des incertitudes concernant les effets écotoxicologiques de ces NMs. C'est pour cette raison que la modélisation des risques et des impacts des NMs de TiO_2 a été abordée avec une approche probabiliste : le réseau bayésien.

L'approche de modélisation : présentation et résultats.

Les réseaux bayésiens (RBs) se présentent sous forme de graphes acycliques. Cette structure relie des variables par des liens de cause à effet : les états des variables-parents déterminent les états des variables-enfants. Pour chacune des variables, une table de probabilité conditionnelle est déterminée. Elle définit la probabilité que chacun des états d'une variable se produise, en connaissant les distributions de probabilité des variables-parents (Figure 4). Les états des variables, ainsi que les

probabilités qui leur sont associées, peuvent être déterminées d'après la littérature ou par expérimentation en laboratoire, ou encore par calcul.

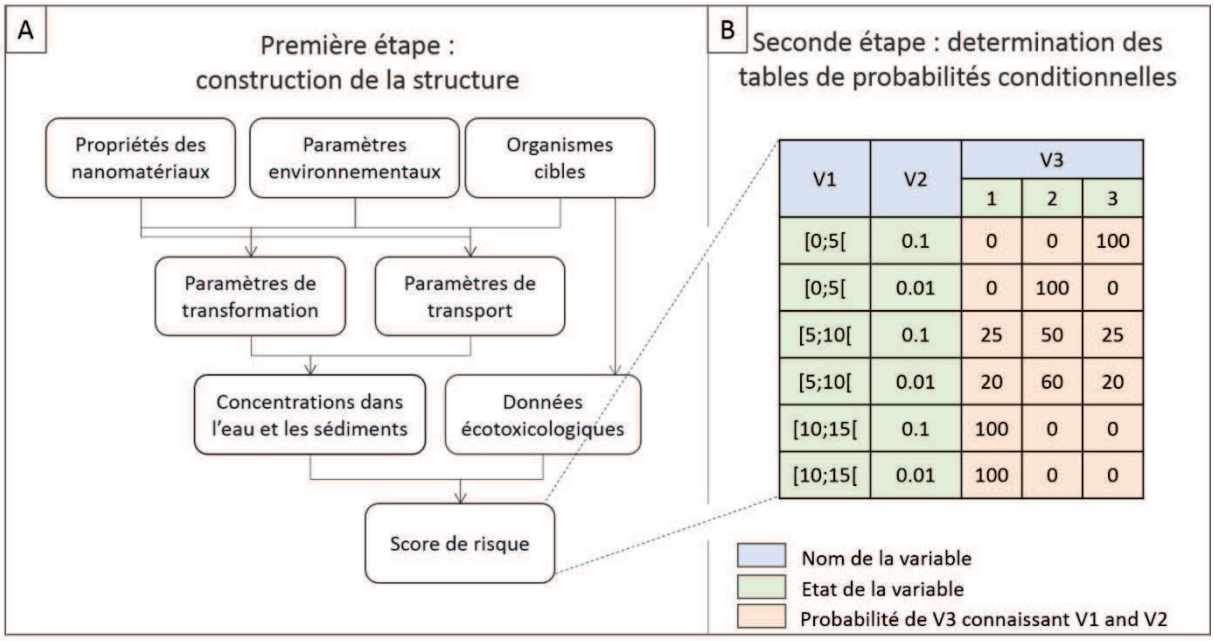

Figure 4 : Construction d'un réseau bayésien

L'utilisation de distributions de probabilités permet de prendre en compte les incertitudes inhérentes au modèle, de les visualiser directement sur le modèle, et donc d'identifier les variables nécessitant des recherches plus approfondies. De plus, les informations relatives à chaque variable peuvent être facilement actualisées à mesure que la recherche avance et que de nouvelles données sont produites. Ce sont ces deux points qui font la force d'un tel modèle, et qui justifient son utilisation pour l'évaluation des risques et des impacts des NMs de TiO_2.

Comme cela a été dit précédemment, le risque d'une substance s'évalue d'une part grâce à des paramètres influant sur son devenir, et d'autre part grâce à des valeurs d'écotoxicité. Un premier RB a été construit, modélisant le devenir des NMs de TiO_2 dans les effluents industriels et dans les eaux

naturelles. Il aboutit à la détermination des concentrations en nombre des NMs et de leurs distributions en taille dans l'eau et les sédiments de la rivière étudiée (Figure 5). Deux effluent (T et NN) et deux sections de rivière (du rejet T au point 4 et du rejet NN au point 5) ont ainsi été considérés (cf. Figure 1).

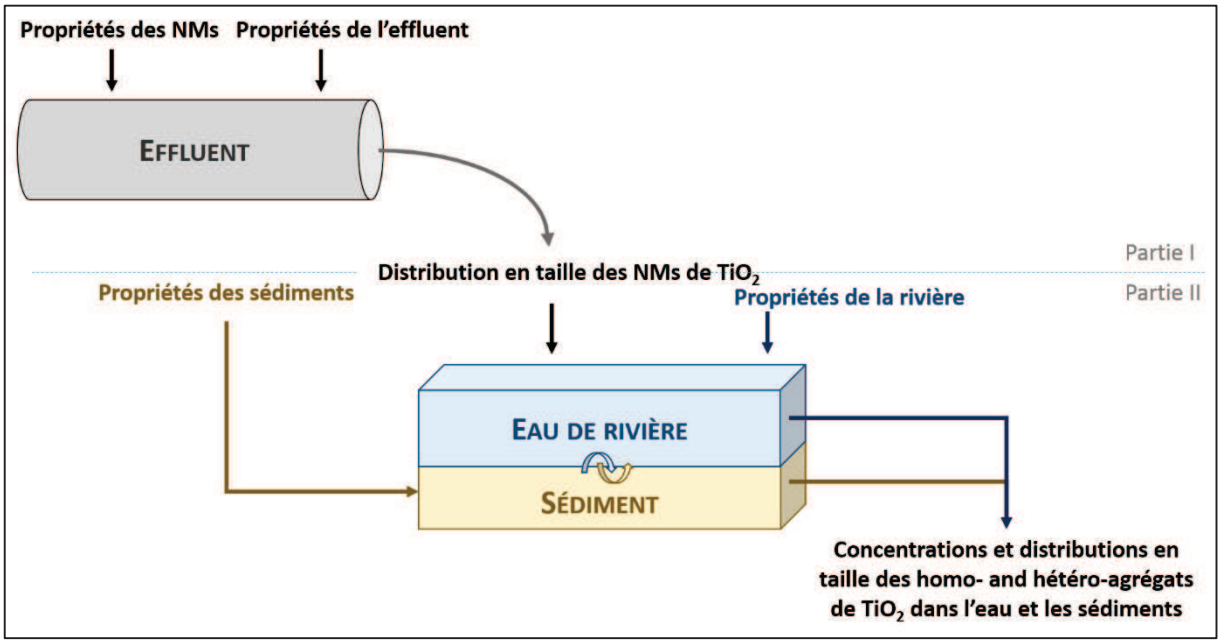

Figure 5 : Conceptualisation du modèle de devenir

La structure de ce réseau a été construite à partir de la littérature disponible et de discussions avec des membres du CEINT (Center for Environmental Impacts of Nanotechnology). Les données concernant les variables sont basées sur des expériences de laboratoire et des analyses d'échantillons collectés sur le site étudié ainsi que sur différents modèles comportementaux des NMs précédemment établis. Les calculs de concentrations et de distributions en taille ont été réalisés à l'aide de code Fortran, en utilisant des équations cinétiques développées par Thill et al. (2001) et Praetorius et al. (2012). Les paramètres anthropiques et environnementaux, ainsi que les concentrations en TiO_2 mesurées dans les effluents à chacune des campagnes ont été intégrés dans les calculs, de façon à réaliser des simulations correspondant à chaque campagne d'échantillonnage et à chaque effluent et

section de rivière étudiés. Les simulations ont été réalisées avec plusieurs valeurs du coefficient d'efficacité d'attachement et de la dimension fractale des agrégats, car ce sont ces paramètres qui présentaient des incertitudes. Cette modélisation a donné lieu à deux types de résultats, obtenus dans les effluents industriels et dans l'eau et les sédiments de la rivière :

- Les concentrations en nombre des NMs de TiO_2 dans chacune des classes de taille étudiées, calculées à partir des codes Fortran ;
- Les probabilités d'occurrence de ces NMs dans chacune des classes de taille considérées, calculées à l'aide de l'application Netica v. 4.16 (Norsys Software Corporation, Figure 6).

Une analyse de sensibilité a ensuite été réalisée, permettant de déterminer l'influence de la variation du coefficient d'efficacité d'attachement et de la dimension fractale des agrégats sur les résultats obtenus.

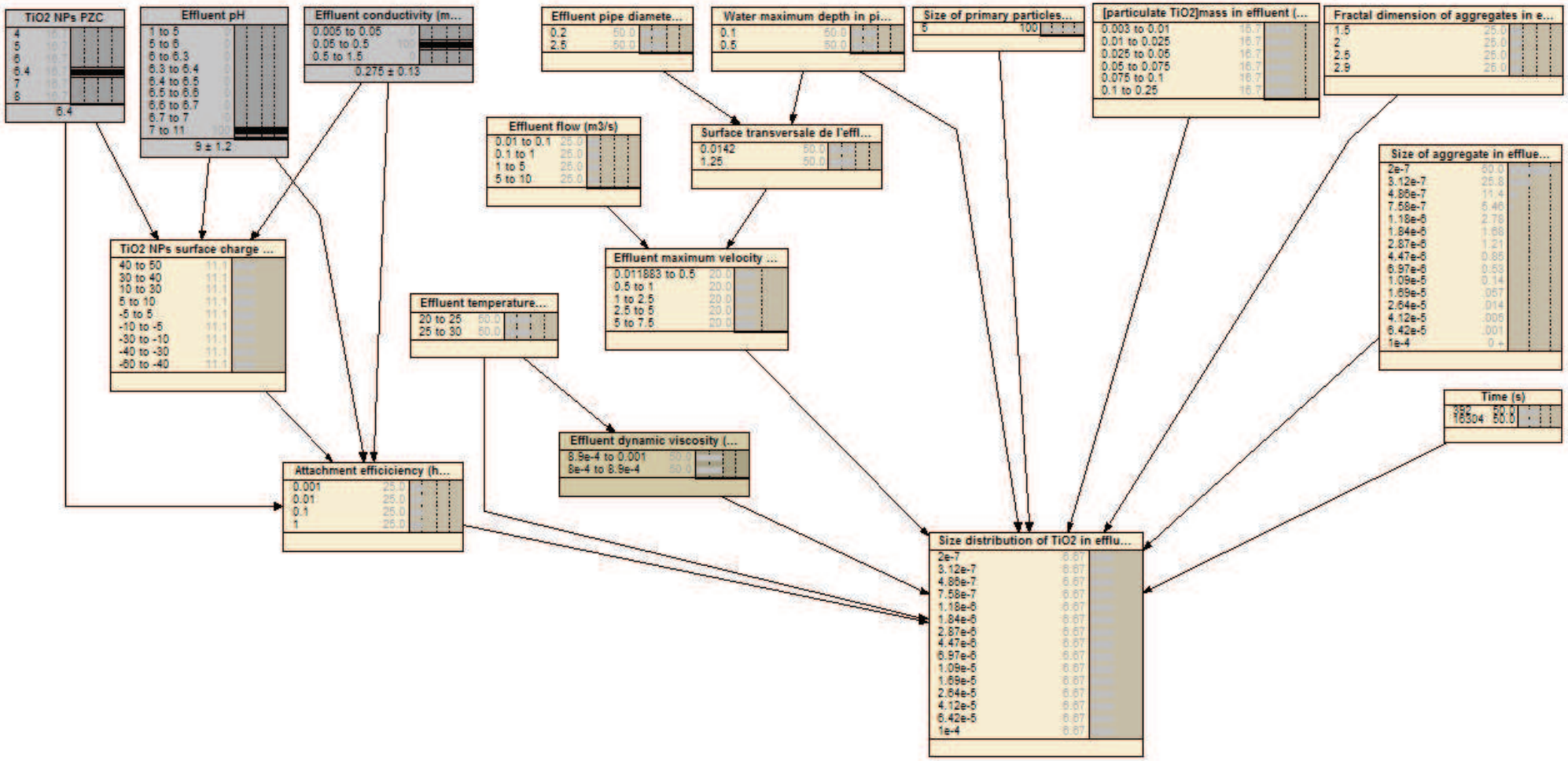

Figure 6 : Réseau bayésien modélisant le devenir des NMs de TiO_2 dans les effluents industriels

Les résultats ainsi obtenus sont cohérents avec les mesures réalisées sur les échantillons naturels, puisqu'ils indiquent de plus faibles concentrations en NMs de TiO_2 dans les sédiments que dans la colonne d'eau. Toutefois, à une dimension fractale de 2,9, la sédimentation des NMs de TiO_2 semble plus rapide que les processus d'homo- et d'hétéro-agrégation. Par ailleurs, l'analyse de sensibilité du modèle a mis en évidence le besoin de caractériser précisément la dimension fractale des agrégats, surtout lorsqu'elle est supposée élevée et lorsque les concentrations en TiO_2 sont importantes. Ce paramètre est encore difficilement déterminé, alors qu'il est déterminant dans la modélisation de la vitesse de sédimentation des agrégats, et donc dans l'estimation des concentrations et des distributions en taille des particules auxquelles les organismes pélagiques et benthiques sont exposés.

Pour calculer le risque associé aux NMs de TiO_2, il est nécessaire de lier les données de devenir avec des données d'effets. Or à l'heure actuelle, aucune donnée écotoxicologique n'est disponible concernant les effets potentiels des NMs de TiO_2 libérés dans la rivière étudiée. Toutefois, des tests ont été réalisés dans le but de déterminer en mésocosmes, simulant un milieu d'eau douce, les effets de NPs d'anatase de forme cubique et en bâtonnets (Figure 7). Ces expériences ont été menées à bien par les partenaires écotoxicologues du projet ANR MESONNET. Ces tests ont été réalisés sur deux espèces vivant en eau douce : *Gammarus roeseli* et *Dreissena polymorpha*, qui ont été exposées à des concentrations de NMs de TiO_2 inférieures à 1 $mg.L^{-1}$ pendant 21 jours. Plusieurs biomarqueurs ont été mesurés, à l'échelle cellulaire (capacité antioxydante totale, peroxydation lipidique, production d'espèces réactives de l'oxygène, viabilité cellulaire et performance de phagocytose) et à l'échelle individuelle (filtration, ventilation, osmolalité, locomotion et mortalité). Un second réseau bayésien a donc été construit, permettant d'inclure ces paramètres écotoxicologiques dans l'évaluation du risque des NMs de TiO_2 (Figure 8).

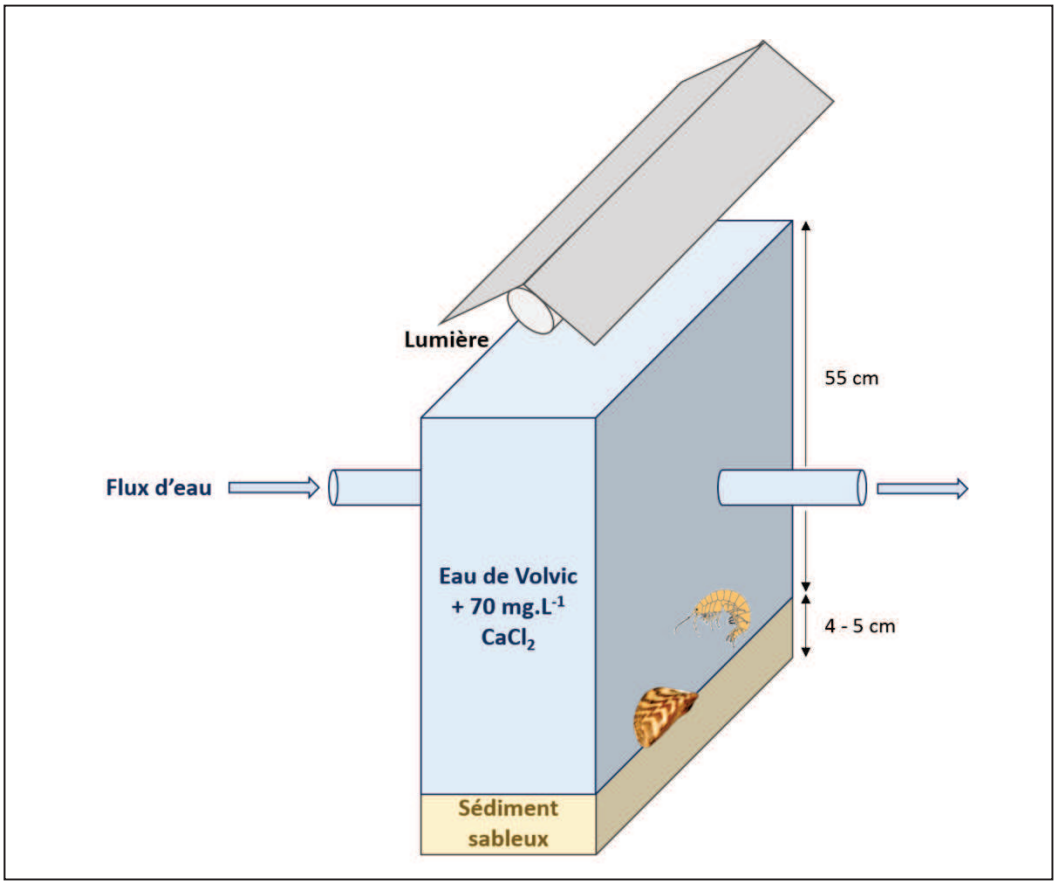

Figure 7 : Montage expérimental des tests d'écotoxicité réalisés en mésocosmes

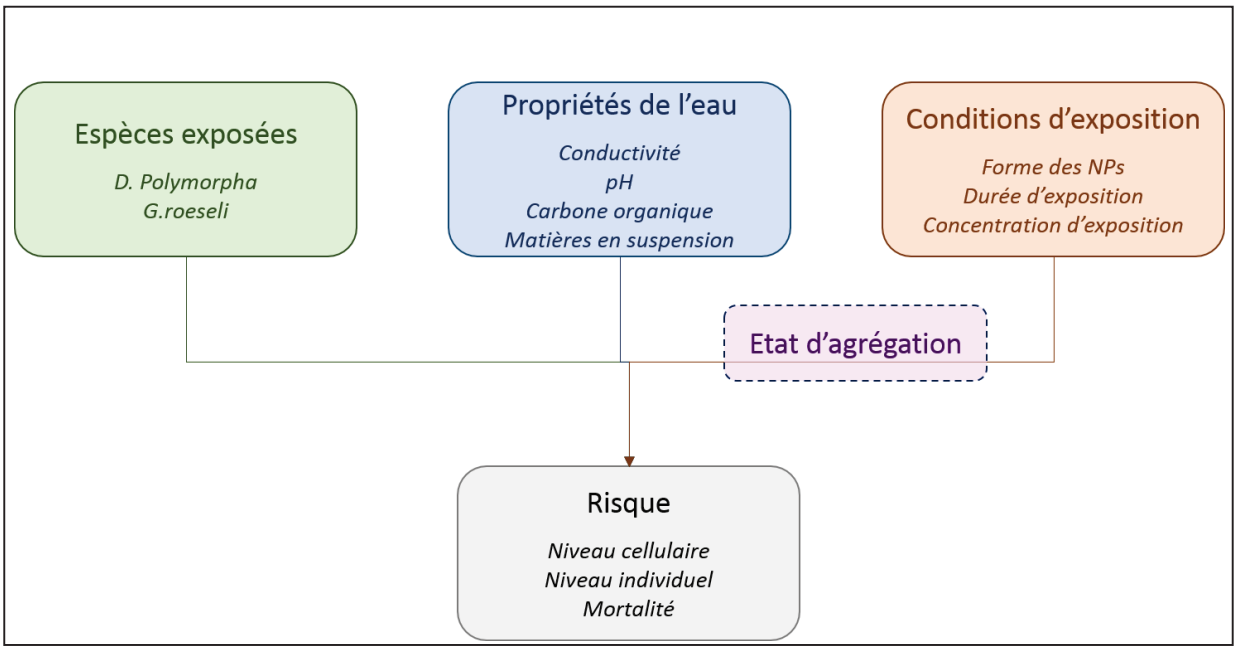

Figure 8 : Structure simplifiée du réseau bayésien modélisant les effets et les risques des NMs d'anatase en mésocosmes

Les résultats ont montré que la forme des NPs d'anatase influence surtout la filtration de *D. polymorpha*. De manière générale, *G. roeseli* est plus sensible aux NPs cubiques, alors que chez *D. polymorpha*, les toxicités les plus élevées sont induites par les NPs en bâtonnets. Les effets les plus importants ont été mesurés sur la locomotion de *G. roeseli* et sur la viabilité cellulaire de *D. polymorpha*.

Il existe donc un risque potentiel des NMs de TiO_2 sur ces organismes. Cependant, une mortalité plus faible a été mesurée chez *D. polymorpha* lorsque ces organismes sont exposés aux NMs que dans le témoin, ceci pour les deux types de NMs testés. Ces NMs pourraient donc avoir un effet protecteur concernant ce biomarqueur. Ceci montre que la mesure des biomarqueurs à l'échelle de l'individu (tels que la mortalité) n'est pas suffisante pour l'évaluation du risque, puisque ceci peut mener à des conclusions différentes des observations faites à l'échelle cellulaire. De plus, même si la toxicité cellulaire peut être visible à l'échelle de l'individu à des temps d'expositions plus longs, il peut être difficile de mettre en œuvre de telles expérimentations. Il est donc nécessaire de déterminer les relations de cause à effet entre les résultats obtenus au niveau cellulaire et ceux obtenus au niveau individuel, afin de conserver les temps d'exposition et le nombre de tests d'écotoxicité nécessaires à l'évaluation du risque aussi bas que possible.

La construction de ce réseau a également souligné le besoin de caractériser de façon précise les NMs étudiés et les milieux-tests, particulièrement leur charge de surface et leur distribution en taille dans le milieu. Les relations entre l'ingestion des NMs par les organismes et leur écotoxicité doivent aussi être déterminées, en se basant sur la quantification des NMs dans les organismes. Ceci est nécessaire pour la détermination des liens entre devenir et effet des NMs, et donc pour la *prédiction* du risque.

Le développement de ce réseau appliqué aux mésocosmes a donc montré l'importance de continuer la recherche dans des conditions environnementales pertinentes, puisque des risques potentiels ont été démontrés à de faibles concentrations en NMs, sur des temps d'exposition de plusieurs semaines. Il est toutefois nécessaire de réaliser ces mêmes tests avec les NMs produits par CRISTAL, puisque l'intégration de ces résultats dans un réseau qui compléterait celui élaboré pour la modélisation du devenir des NMs de TiO_2 sur le site étudié, permettrait d'évaluer les risques environnementaux associés au TiO_2 propres à ce site.

Les deux modèles construits pendant cette thèse ont permis de calculer des constantes d'agrégation, de sédimentation et de transport des NMs de TiO_2 à l'échelle site-spécifique. Ces résultats pourront être intégrés à des méthodes de calcul d'impact en Analyse du Cycle de Vie, répondant au besoin exprimé par la communauté scientifique (Salieri et al. 2015). L'utilisation des réseaux bayésiens s'est montrée pertinente, puisque ce type de modèle permet d'intégrer à la fois des valeurs mesurées de façon précise (par exemple pour les variables de température ou de concentration) et des valeurs pour lesquelles des incertitudes sont encore à prendre en compte (par exemple l'efficacité d'attachement ou la dimension fractale).

Les résultats obtenus par l'approche analytique et par l'approche bayésienne concordent à montrer que la colonne d'eau est le compartiment aquatique le plus impacté. Dans ce compartiment, il existe un risque environnemental potentiel, puisque des concentrations allant jusqu'à environ 60 $\mu g.L^{-1}$ ont été mesurées dans l'eau, alors qu'il a été montré dans la littérature que les NMs de TiO_2 sont toxiques envers les organismes à partir d'une concentration d'environ 30 $\mu g.L^{-1}$. Toutefois, pour confirmer ou infirmer cette hypothèse, il est nécessaire :

- D'une part, de déterminer de façon précise la part nanoparticulaire de TiO_2 présente dans les compartiments environnementaux, par l'utilisation d'outils analytiques complémentaires (tels

que l'ICP-MS et la FFF – *field flow fractionation*) et par le perfectionnement du modèle, pour éviter de surestimer cette concentration ;

- Et d'autre part, de réaliser des expériences de toxicité sur les NMs de TiO_2 produites par l'usine étudiée et dans des conditions les plus proches possible de la réalité, c'est-à-dire dans l'eau de rivière, à des concentrations inférieures ou égales à 60 $\mu g.L^{-1}$ et à des temps d'exposition longs, pour évaluer précisément le risque propre au site étudié.

Différentes perspectives de recherche se dégagent également concernant le modèle ACV-ER. Il pourrait en effet être :

- Affiné, grâce la complexification des études du comportement de ces NMs : d'une part en simulant de mieux en mieux la réalité lors des études de devenir dans l'eau (ajout d'autres types de matière particulaire, d'un compartiment de sédiment, d'un flux d'eau), et d'autre part en insérant des données écotoxicologiques à long terme associées au TiO_2 produit par CRISTAL, à partir de tests réalisés à faibles concentrations (≤ 1 mg/L).
- Complété, par la prise en compte des rejets à la cheminée de l'usine et par la construction d'un modèle détaillant les processus en jeu dans les compartiments atmosphérique et terrestre. Ce modèle, associé à celui construit ici, permettrait de modéliser de façon plus complète les processus environnementaux en jeu. Par ailleurs, la construction de modèles similaires pour les autres étapes du cycle de vie (manufacture, utilisation et fin de vie des nanoproduits) permettrait également de compléter l'évaluation des risques et des impacts.
- Adapté, à d'autres sites de production (en adaptant les valeurs des paramètres) ou à d'autres types de NMs manufacturés (en adaptant les variables nécessaires à la modélisation).
- Simplifié, en confrontant les résultats de l'analyse de sensibilité avec les besoins et les utilisations potentielles des différents acteurs concernés (industriels, collectivités, législateurs). Ceci permettrait d'en faire un outil d'aide à la décision.

Références

European Commission (2012) Communication from the commission to the european parliament, the council and the european economic and social committee - Second Regulatory Review on Nanomaterials.

European Commission (2008) Follox-up to the 6th Meeting of the REACH Competent Authorities for the implementation of Regulation (EC) 1907/2006 (REACH).

ISO (2006a) ISO 14040:2006 Environmental management - Life cycle assessment - Principles and framework.

ISO (2006b) ISO 14044:2006 Environmental management - Life cycle assessment - Requirements and guidelines.

Ma H, Brennan A, Diamond SA (2012) Photocatalytic reactive oxygen species production and phototoxicity of titanium dioxide nanoparticles are dependent on the solar ultraviolet radiation spectrum. Environ Toxicol Chem 31:2099–2107. doi: 10.1002/etc.1916

Piccinno F, Gottschalk F, Seeger S, Nowack B (2012) Industrial production quantities and uses of ten engineered nanomaterials in Europe and the world. J Nanoparticle Res 14:1–11. doi: 10.1007/s11051-012-1109-9

Praetorius A, Scheringer M, Hungerbühler K (2012) Development of Environmental Fate Models for Engineered Nanoparticles—A Case Study of TiO 2 Nanoparticles in the Rhine River. Environ Sci Technol 46:6705–6713. doi: 10.1021/es204530n

Salieri B, Righi S, Pasteris A, Olsen SI (2015) Freshwater ecotoxicity characterisation factor for metal oxide nanoparticles: A case study on titanium dioxide nanoparticle. Sci Total Environ 505:494–502. doi: 10.1016/j.scitotenv.2014.09.107

Savolainen K, Alenius H, Norppa H, et al (2010) Risk assessment of engineered nanomaterials and nanotechnologies—A review. Toxicology 269:92–104. doi: 10.1016/j.tox.2010.01.013

Thill A, Moustier S, Aziz J, et al (2001) Flocs Restructuring during Aggregation: Experimental Evidence and Numerical Simulation. J Colloid Interface Sci 243:171–182.

Table of contents

List of figures

Figures from article: Aggregation behavior of TiO_2 nanoparticles in natural river water

Other figures:

List of tables

Other figures:

GLOSSARY

Agglomerate: ensemble of weakly linked particles, aggregates, or of a mix of both, whose resulting external surface is similar to the sum of the surface areas of each of the components (ISO/TS 27687:2008).

Aggregate: ensemble of particles composed of weakly linked or fused particles, whose resulting external surface may be significantly lower than the sum of the surfaces areas of each of the components (ISO/TS 27687:2008).

Nanoscale: Size range extending from about 1 to 100 nm (ISO/TS 27687:2008).

Nano-object: Material having at least 1, 2 or the three dimensions at the nano-scale (ISO/TS 27687:2008).

Nanoparticle: Nano-object whose three external dimensions are at the nanoscale (ISO/TS 27687:2008).

Nanosheet: Nano-object having one external dimension at the nanoscale and the two others significantly larger (ISO/TS 27687:2008).

Nanofiber: Nano-object having at least two of its external dimensions at the nanoscale and whose third dimension is significantly larger (ISO/TS 27687:2008).

Nanomaterial: Material having one dimension at the nanoscale or having an internal structure or an external structure at the nanoscale (ISO/TS 80004-1:2010).

Manufactured nanomaterial: Nanomaterial intentionally produced with specific properties or composition for commercial purposes (ISO/TS 80004-1:2010).

Nanoproduct: Final product containing manufactured nanomaterials.

NOAA: Nano-objects and their aggregates and agglomerates of more than 100 nm (ISO/TR 13014).

INTRODUCTION

Context and motivation

Nanomaterials (NMs) are emerging as a technical revolution for the past few years. Today, they are ubiquitous in our daily life and represent an important market, as up to 11.5 million tons are produced each year at the global scale (Matrix Insight Ltd 2014). They are used in various products, from automotive industry (e.g. catalyzers, sensors) to textile industry (e.g. "smart" textiles, antibacterial clothes), through building materials (e.g. thermo-isolation, façade coatings, flame retardants) or food industry (e.g. whitening agents, fruit juice clarifiers) (The Royal Society & The Royal Academy of Engineering 2004). Among these, TiO_2 NMs are the second most produced NMs at the European and global scales, with an annual production of 550 to 5500 tons (Piccinno *et al*. 2012). They are used in sunscreens because of their UV-absorbent properties and in façade coatings and water treatment processes because of their photocatalytic properties (Hendren 2010). They present some benefits, especially in medicine (e.g. targeted drug delivery, improved diagnosis and imagery methods, antibacterial material) and in the remediation of contaminated soils and groundwater (The Royal Society & The Royal Academy of Engineering 2004).

However, like any new technology, it supplies the most diverse feelings about the new risks they could induce. In France, as an implementation of the commitments adopted at the end of the Grenelle of Environment, a public debate on nanotechnologies was organized by the National Commission for Public Debate (CNDP), from October 15, 2009 to February 24, 2010. These discussions focused on the socio-economic prospects of the development of nanotechnology, but also on their health, environmental and ethical issues. But they did not bring concrete answers to questions about the societal risk and in the end, the debate turned short and did not provide more answers in the field of regulation. The European REACH program has no specific provisions for NMs, even if it recognizes that these materials have specific properties (European Commission 2008). In France, the Grenelle of Environment law (2010-967 of August 3, 2009, section 42.2009 and 2010-788 of July 12, 2010, section 185, 2010) applies in terms of reporting and public information, but it does not regulate the market of manufactured NMs. This lack of regulation can be explained by the lack of knowledge about the behavior and the effects of NMs in the environment.

This highlights the need to develop research in NMs characterization, toxicology and ecotoxicology. It allows to question the impacts and risks associated with nanoproducts (*i.e.* the final products

containing manufactured nanomaterials) throughout their life cycle. Indeed, NMs are defined as materials containing at least 50% of nanoparticles (NPs) of which at least one dimension sizes less than 100 nm (European Commission 2012). NPs present a high surface/volume ratio, which gives them a high reactivity and allows them to be transferred in significant concentrations to various environmental compartments at each step of their life cycle, that is from the extraction of raw materials to the waste treatment, via the production of NMs, the manufacture of nanoproducts in which they are inserted and their use. The general objective of this thesis is to understand the transfer of titanium manufactured NPs in the environment and their effects in water, soils and sediments, in order to assess quantitatively the associated impacts and risks.

Rationale and originality of this work

With the help of Cristal, a nanoparticulate TiO_2 producer, the study was conducted at a site-specific scale. The specific objectives of this research were (1) the characterization of the industrial TiO_2 NMs and the experimental assessment of their behavior in water, sediments and soils and (2) the impact and risk modeling of the industrial TiO_2 NMs in the aquatic compartment (water and sediment).

Both these approaches were conducted simultaneously: the modeling requirements determined the type of experimentation to be performed in the laboratory and the measurements to make in the field; in turn, the data produced in the laboratory were used to feed the model, in the objective of modeling as precisely as possible the NMs, the environmental compartments and their interactions.

The modeling approach was based on two impacts and risks assessment tools: Life Cycle Assessment (LCA) and Risk Assessment (RA), respectively. Both these methodologies require the same kind of data: (1) data relative to the fate of the studied substance in the different environmental compartments (transfers and transformations), which are transformed into exposure values and (2) ecotoxicological data, enabling the evaluation of the potential effect of a substance on the organisms. Combining both these methodologies allows taking the best of each of them and answering the need for models homogenization (Flemström *et al*. 2004).

Because of the uncertainties regarding the NPs behavior in the environment, a Bayesian probabilistic approach was used. The strength of this kind of model lies in the use of probability distributions. In this way, the inherent uncertainties of NMs data are integrated and directly visualized, so that the model can be easily actualized as new data are produced (Money *et al*. 2012).

The originality of this work relies both on the collaboration with an industrial producer and on the building of a Bayesian network applied to a local scale, fed by data collected in the laboratory and in the field.

Construction of the dissertation

The first chapter of this thesis presents the general background of this work. Two literature reviews are included. The first one describes the NMs properties which are important to know for the understanding of their behavior and potential effects, the analytical tools available for characterizing these properties, and the way in which these parameters are implemented in the LCA and RA models. The second review goes more deeply into the LCA and RA methodologies applied for the ecotoxicity of TiO_2 NMs. The nano-TiO_2 production site, the characteristics of the surrounding environment (Thur River, sediments, soils) influencing their behavior and the potential affected species living in the study area are also detailed in this chapter.

The second chapter of this dissertation aims at understanding the behavior of TiO_2 NMs in the environment in which they are released. The first part presents the estimated concentrations of TiO_2 NMs in water, sediments and soils. Then the aggregation behavior of these TiO_2 NMs is assessed in the river water.

The TiO_2 NMs impacts and risks modeling is addressed in the third chapter. The probabilistic approach and the Bayesian network building are detailed, before the risk scores of TiO_2 NMs are presented. This last chapter is subdivided into three main sections: in the first one, the general Bayesian theory is described, in the second one the nano-TiO_2 behavior is modeled in the Thur River by using the Bayesian approach and in the third one, the risk linked to nano-TiO_2 is modeled within mesocosms by a Bayesian network. It should be noted that because of a lack of ecotoxicological data of NMs in the river, their effects on aquatic species and therefore their risks to aquatic species have been modeled by including data obtained in mesocosms.

CHAPTER I – GENERAL FRAMEWORK OF THE STUDY

The objective of this chapter is to set the background required for the environmental risk and impact assessment of TiO_2 ENMs. The first requirements are to determine the NMs properties needed for the modeling of their behavior, as well as to acquire some knowledge about the analytical tools available for the NPs characterization and about the modeling tools enabling the evaluation of their impacts and risks. This is the aim of the first section of this chapter. The second section discusses more deeply LCA, RA and their combination, in order to choose the best methodology. Finally, the last section gives the required knowledge about the production of the TiO_2 NMs and the environment in which they are released and which needs to be modeled.

I.A. CHARACTERIZATION OF ENGINEERED TiO_2 NANOMATERIALS IN A LIFE CYCLE AND RISK ASSESSMENT PERSPECTIVE

This chapter consists in an article, which was published in Environmental Science and Pollution Research (2015) 22(15): 11175-11192.

Characterization of Engineered TiO_2 Nanomaterials in a Life Cycle and Risk Assessments Perspective

Véronique Adam[a,b], Stéphanie Loyaux-Lawniczak[a], Gaetana Quaranta[a]

[a]: *Laboratoire d'Hydrologie et de Géochimie de Strasbourg / EOST / UDS*
1, rue Blessig
67084 Strasbourg Cedex
France

[b]: *French Environment and Energy Management Agency*
20, avenue du Grésillé
BP 90406
49004 Angers Cedex 01
France

corresponding author
Tel: +33 (0)3 68 85 03 79
Fax: +33 (0)3 68 85 04 02

Email addresses: quaranta@unistra.fr (G. Quaranta), veronique.adam@etu.unistra.fr (V. Adam), s.lawniczak@unistra.fr (S. Loyaux-Lawniczak).

Abstract

For the last ten years, engineered nanomaterials (ENMs) have raised interest to industrials due to their properties. They are present in a large variety of products, from cosmetics to building materials through food additives and their value on the market was estimated to reach $3 trillion in 2014 (Technology Strategy Board 2009). TiO_2 NMs represent the second most important part of ENMs production worldwide (550 – 5500 t/yr).

However, a gap of knowledge remains regarding the fate and the effects of these and consequently impact and risk assessments are challenging. This is due to difficulties in characterizing NMs but also in selecting the NMs properties which could contribute most to ecotoxicity and human toxicity. Characterizing NMs should thus rely on various analytical techniques in order to evaluate several properties and to crosscheck the results.

The aims of this review are to understand the fate and effects of TiO_2 NMs in water and soil and to determine which of their properties need to be characterized, to assess the analytical techniques available for their characterization, and to discuss the integration of specific properties in the Life Cycle Assessment and Risk Assessment calculations.

This study underlines the need to take into account nano-specific properties in the modeling of their fate and effects. Among them, crystallinity, size, aggregation state, surface area and particle number are most significant. This highlights the need for adapting ecotoxicological studies to NP-specific properties, *via* new methods of measurement and new metrics for ecotoxicity thresholds.

Keywords

Nanomaterials, Characterization, Risk Assessment, Life Cycle Assessment, Fate modeling, Effect modeling

Introduction

Engineered nanomaterials (ENMs) are defined as 'intentionally manufactured materials, containing particles, in an unbound state or as an aggregate or as an agglomerate and where, for 50 % or more of the particles in the number size distribution, one or more external dimensions is in the size range 1 nm to 100 nm' (European Commission 2013). These materials raised interest to industrials due to their small size and high reactivity, and are now present in a large variety of products, from cosmetics to building materials through food additives. The market value of these products was estimated to reach $3 trillion in 2014 (Technology Strategy Board 2009). TiO_2 NMs are used in different products such as sunscreens for their UV-absorption properties, and in façade coatings as photocatalysts. They represent the second most important part of ENMs production worldwide (550 – 5500 t/yr (Piccinno *et al*. 2012)) and in Europe (55 – 3000 t/yr (Piccinno *et al*. 2012)) and the most important part in the USA (7800 - 38000 t/yr (Hendren *et al*. 2011)). They consequently represent a priority in impact and risk assessments, and are the theme of this review.

Indeed, scientists point out remaining knowledge gaps concerning the fate of NMs in the various environmental compartments, their effects on living organisms, and consequently their potential impacts and risks on the environment and human health. Furthermore, NMs cannot be considered as one single group of substances having homogeneous impacts on the environment, as they differ in many ways, e.g. composition or shape, so potential risks and impacts of each NM need to be assessed individually.

Impacts and risks of substances are assessed based on standardized methodologies, namely life cycle assessment (LCA) and risk assessment (RA). Both LCA and RA rely on the modeling of the substance fate in the environmental compartments and on the understanding of its effects on the biota. Thus, the properties of NMs and their influences on their behavior (fate and effects) need to be determined in order to predict their potential risks and impacts.

However, NMs small size, high reactivity and most often very low environmental concentrations raise challenges to their characterization. Moreover, there is still discussion about the properties that should be seen as most important for the modeling of their fate and the understanding of their ecotoxicity, and no standardized analytical methodology has yet been published. Characterizing NMs should thus rely on various analytical techniques in order to evaluate several properties and to crosscheck the results.

The first part of this review will aim at understanding the mechanisms underlying of TiO_2 NMs with water, sediment and soil compartments and identifying the properties that are necessary to know in order to model and predict their behavior. The analytical techniques available to determine these properties will be discussed in the second part. Finally, a critical review of available fate and effects models will be performed in the third part of this work.

1. Understanding the mechanisms underlying the interactions of TiO_2 NMs with environmental compartments

TiO_2 NMs can interact with both biotic and abiotic components of the environment. These interactions rely mostly on their agglomeration (or aggregation) state. This will determine the size in which they are present in the environment, and consequently their potential for transport and sedimentation, and for uptake by organisms. A distinction is made between homoaggregation (clusters made of TiO_2 NMs only) and heteroaggregation (clusters made of TiO_2 NMs and other particles).

1.1. NP-NP interactions

TiO_2 NM-NM interactions rely on three main properties: surface charge, size and concentration (Quaranta and Adam 2015).

By definition, at least one dimension of pristine nanoparticles (NPs) is of less than 100 nm: their very little size makes them highly reactive. For NPs having the same shape and surface charge, the smallest size gives the highest specific surface area (surface over volume ratio). High specific surface area means high concentration of reactive sites at the surface of the particle, so high potential for reactivity (Bell 2007). The high reactivity of NMs makes them unstable under most conditions: they tend to be attracted to each other, forming agglomerates ("collection of weakly-bound particles or aggregates or mixtures of the two where the resulting external surface area is similar to the sum of the surface areas of the individual components" (International Organization for Standardization 2008)) or aggregates ("particle comprising strongly-bonded or fused particles where the resulting external surface area may be significantly smaller than the sum of calculated surface areas of the individual components" (International Organization for Standardization 2008)). Decreasing size has been found to enhance aggregation of spherical anatase NPs (Pettibone *et al*. 2008; Aillon *et al*. 2009; Chowdhury *et al*. 2012; Chowdhury *et al*. 2013; Zhou *et al*. 2013).

The aggregation rate of particles primarily depends on their collision rate. Obviously, the collision rate is dependent on the NPs concentration, as chances to collide are higher with increasing number concentration. Collisions between particles can be due to Brownian motion, shear flow or differential sedimentation. Due to their small primary size, NPs are subject to Brownian motion. But as the aggregate diameter increases, it becomes subject to shear flow collisions (relevant at sizes 1 – 10 µm) and differential sedimentation (relevant at sizes 1-10 µm and 10 µm or more, respectively), increasing their collision rates (O'Brien 2003).

Forces involved in the aggregation of NPs can be attractive (van der Waals forces) or repulsive (electrostatic repulsion, steric hindrance) (O'Brien 2003). The van der Waals forces directly arise from the charge of two particles; the electrostatic repulsion is caused by the interaction of the particles electrostatic double layers (EDL), that are the layers of ions (or charges) surrounding the particles; the steric hindrance can be caused by the hydrophilic chains of polymers adsorbed at the surface of the particles, conferring them a high stability. The aggregation of NPs is thus also determined by their surface charge.

The aggregation (or agglomeration) state is often determined by the fractal dimension (D_f) of the aggregate (or agglomerate). This parameter is defined as the distribution of the volume occupied by an aggregate compared to its mass. Thus, a D_f of 1 is assigned to a line, a D_f of 2 is assigned to a flat surface, and a D_f of 3 is assigned to a sphere (Hotze *et al*. 2010). The D_f of an aggregate is also related to its compactness: a high D_f is assigned to a compact aggregate, in which strong bounds are present.

The D_f is an important parameter to know for the prediction of the NMs transport, as NMs with higher D_f will be more influenced by gravitational forces and settle faster down the water column.

1.2. NMs interactions with water and soil – abiotic mechanisms

It has been stated earlier that the NMs surface charge is primordial for understanding their behavior. But this charge does not rely solely on the kind of NPs, it also depends on the pH of the medium. The point of zero charge (PZC) is defined as the pH at which the particle surface is globally neutral. It helps predicting the behavior of the NMs in the environment, as in low ionic strength and low organic matter content, TiO_2 NPs surface charges (or zeta-potential) are positive at low pH and negative at high pH (Dunphy Guzman *et al*. 2006; Adam 2015). In this way, we can predict with relatively good reliability that they will be more stable at these extreme pH values, being highly charged, and that they will readily aggregate at pH values around the pH_{PZC}, as their global charges are low to null.

The surface charge of the particles also depends on the ionic strength of the suspension (water or soil solution). At high pH values, TiO_2 NPs are negatively charged, but dissolved cations can help neutralize these charges, diminishing the absolute charge of the NPs surfaces and enhancing homoaggregation. Divalent cations such as Ca^{2+} are especially effective in forming large aggregates (French *et al*. 2009).

In soil, sediment or water, NPs will encounter natural components and form heteroaggregates. For example, positively charged NMs will readily adsorb onto negatively charged montmorillonite (Zhou *et al*. 2012). Once they adsorb onto clays, NMs transport and uptake will be greatly influenced by the clay behavior.

Natural organic matter (NOM) has also been shown to play a significant role in the aggregation of NMs, though in a more complex way. Organic components are most often negatively charged. So at acidic pH, when NPs are positively charged, they can sorb onto the NMs surface, increasing their steric stability and diminishing their aggregation (Johnston *et al*. 2009). At lower concentrations, NOM can also enhance aggregation by diminishing the global charge of the NPs (Gibson *et al*. 2007). The interactions of NOM with TiO_2 NMs are thus highly dependent on pH and concentrations of both components. Furthermore, the presence of divalent cations (Ca^{2+} or Mg^{2+}) in concentrations exceeding the critical coagulation concentration (CCC) may form bridges between NPs and NOM, enhancing the formation of aggregates (Chen and Elimelech 2007; Chowdhury *et al*. 2012). This occurs at pH values above the pH_{PZC} of the NMs.

1.3. NMs interactions with water and soil – mechanisms of toxicity

Depending on their surface charge, NMs can attach to organisms, e.g. algae, and may obstruct cellular exchange with the medium, inhibiting cell growth and activity (Chen *et al*. 2012b).

Uptake of NPs partly depend on their size (or the size of the aggregate they are part of), smaller NPs and/or aggregates being more readily internalized and transported in the organism (Larue *et al*. 2012; Cho *et al*. 2013). NMs shape will also influence their uptake. For example, fibers (particles with a diameter-to-length ratio higher than 1:3) (WHO/EURO Technical Committee for Monitoring and Evaluating Airborne MMMF 1985) have extended dimensions, and lead to inflammatory responses of the immune system (Hamilton *et al*. 2009). Thin fibers have small aerodynamic diameters, and can be deposited beyond the ciliated airways in the respiratory tract, but they cannot be entirely processed

by immune processes such as phagocytosis (Donaldson *et al*. 2010; Donaldson *et al*. 2013). Natural sunlight, especially UV irradiation, can induce deagglomeration of NMs. Although when stronger forces are entailed NPs remain aggregated, this UV-induced deagglomeration can increase the penetration of NMs through skin (Bennett *et al*. 2012).

The most studied organisms in freshwater are the algae *Pseudokirchneriella subcapitata* (e.g. Lee and An 2013; Mielke *et al*. 2013), the crustacean *Daphnia magna* (e.g. Kim *et al*. 2014; Mansfield *et al*. 2015) and the zebrafish *Danio rerio* (e.g. George *et al*. 2014; Fang *et al*. 2015). Fewer authors have focused on benthic organisms such as *Hyalella azteca* (e.g. Gurkirpal S. 2012; Wallis *et al*. 2014) and *Gammarus fossarum* (e.g. Bundschuh *et al*. 2011; Kalčíková *et al*. 2014). The terrestrial compartment has received less attention, most studies focusing on mammalians (e.g. Chen *et al*. 2014; Meena *et al*. 2015), plants (e.g. Song *et al*. 2013; Larue *et al*. 2014) and bacteria communities (e.g. Nogueira *et al*. 2012; Simonin *et al*. 2015). In most of these organisms, the major mechanism of toxicity is the generation of reactive oxygen species (ROS), enhanced under UV irradiation (Ma *et al*. 2012; Tong *et al*. 2013; Nesic *et al*. 2014). ROS (e.g. hydroxyl radicals (OH●) or superoxide anion ($\bullet O_2^-$)) are generated by the excitement of electrons, inducing the separation of charges and strong reactions with oxygen or water (Ma *et al*. 2012; Li *et al*. 2014). These free radicals can induce cell membrane leakage, oxidation of lipids, proteins and DNA, and cell death (Braydich-Stolle *et al*. 2009; Li *et al*. 2011).

ROS generation depends on several of the NMs properties, including crystallinity: it has been shown that anatase induces more toxicity than rutile to various organisms, because of its higher potential for reactive oxygen species (ROS) generation (Jiang *et al*. 2008; Auffan *et al*. 2009; Lin *et al*. 2014b). In the same way, decreasing particle size may induce more structural defects and more reactive groups on the surface, leading to prooxidant effects, and increased ROS generation (Manke *et al*. 2013; Lin *et al*. 2014b). Increased toxicity of TiO_2 NPs with decreasing size was shown to bacteria and murine macrophages (Jang *et al*. 2007; Xiong *et al*. 2013). However, the toxicity dependence on NMs size cannot be shown in all experiments (Wang *et al*. 2007; Auffan *et al*. 2009; Kobayashi *et al*. 2009; Puzyn *et al*. 2011). Moreover, according to Kobayashi *et al*. (2009), nano-TiO_2 size effects on pulmonary toxicity in rats occur only within 1 week. Beyond this exposure duration, pulmonary effects do not differ according to the size of the NPs. Furthermore, it has been argued that, rather than size, particle surface area could be a better dose metric, because of its more direct relation with surface reactivity (Oberdürster 2000).

The z-potential of NPs influences their oxidative potential and the production of ROS, inducing increased cytotoxicity and inflammatory effects with increasing charge (Stoeger *et al*. 2006; Cho *et al*. 2012; Ma *et al*. 2012; Manke *et al*. 2013; Donaldson *et al*. 2013).

Also, higher number concentration may induce higher chances of contact with organisms, and higher potential toxicity. However, NMs aggregation increases with number concentration, and if the NPs aggregates are large enough, their entrance in organisms, e.g. via dermal penetration, may be less probable.

NOM has been shown to reduce the toxicity of TiO_2 NMs to most organisms (Grillo *et al*. 2015). The mechanisms involved are not fully explained, but authors suggest that (1) NOM could reduce NMs toxicity by changing their surface charge, thus modifying their interactions with the surrounding medium; (2) NOM may react with the ROS and act as an antioxidant; (3) absorption of NOM on the NMs surface might passivate the NMs surface.

Interactions of NPs with each other and with the environmental compartments are complex, and mostly driven by surface reaction and aggregation/agglomeration processes. Crystallinity, size, surface area, surface charge, and concentration of TiO_2 NMs are primordial for predicting their behavior, fate and toxicity in the environment. In the next section, the analytical techniques available for the determination of these properties will be discussed.

2. Determining the prevalent properties of engineered TiO_2 NMs for understanding their behavior in water, sediment and soil

Nanomaterials properties are intermingled: size directly determines surface area, which, associated with crystallinity and surface charge, will determine aggregation/agglomeration processes. The aggregation/agglomeration state will in turn define the "apparent" size and surface area of NMs. All these properties need to be determined in order to evaluate in the most accurate way their potential impacts and risks on the environment. More than 35 analytical methods have been identified to characterize NPs (Salamon 2013), but many of them do not cover wide size ranges (Figure 1) and none is currently able to provide results on all these different properties within one single analysis. Thus, most scientists agree that there is a need for a combination of methods to characterize NPs in the most accurate way (Buffle and van Leeuwen 1992; Buffle and van Leeuwen 1993; Tiede *et al*. 2008; Ju-Nam and Lead 2008). This also allows to cross-check results and to assess potential artifacts. It is also recommended to use *in situ* analytical techniques that allow the analysis of natural samples with minimal, and even no perturbation, in order to remain as close as possible to the natural environment and to understand their behavior in the most accurate way. ENMs are often present in low environmental concentrations, so methods with low detection limits are preferred. This section reviews the analytical techniques available for the identification and characterization of NPs, focusing on TiO_2 NPs in synthetic and environmental samples.

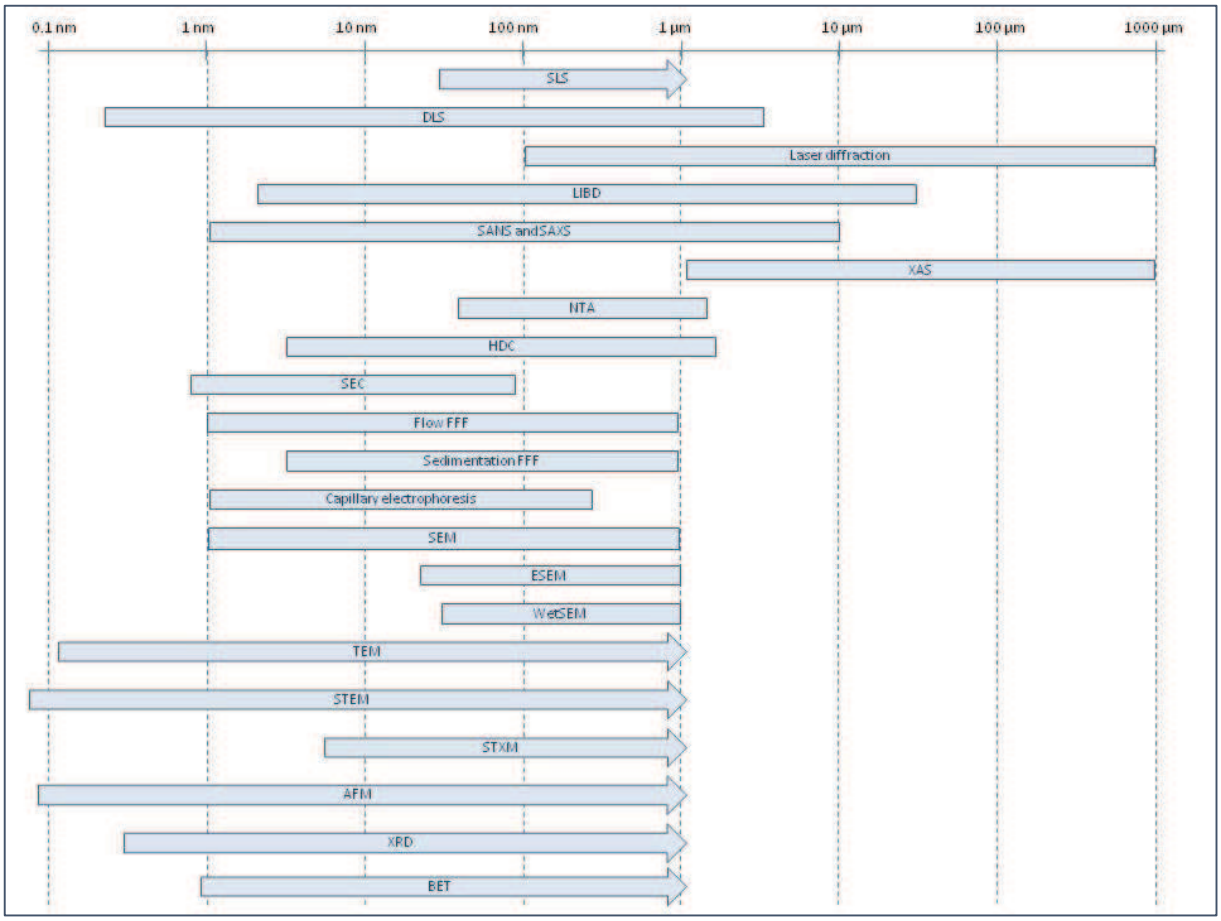

Fig. 1 Analytical methods and their size ranges

2.1. Crystal structure and phase composition

X-Ray diffraction (XRD) is easily implemented, but requires powder samples. It is a non-destructive, relatively quick and inexpensive technique (Burleson *et al*. 2004; Tiede *et al*. 2008) that was used by numerous authors (Burleson *et al*. 2004; Dunphy Guzman *et al*. 2006; Boncagni *et al*. 2009; Chen *et al*. 2011).

For the analysis of aqueous samples, available techniques include nuclear magnetic resonance (NMR) and Raman (Pottier *et al*. 2003; Bassi *et al*. 2005) spectroscopies, cryogenic transmission electron microscopy (cryo-TEM) (Wagner *et al*. 2004), as well as X-ray absorption spectroscopy (XAS) (Chen *et al*. 1997). NMR spectroscopy is a non-destructive technique, and can provide with the 3D structure of NPs (Stone 2009). Cryo-TEM allows the imaging of a frozen sample at liquid nitrogen temperature (Wang *et al*. 2004; French *et al*. 2009; Horst *et al*. 2010; Gmoshinski *et al*. 2013). TEM can be coupled to electron diffraction in order to obtain structure information. In this case, electron energy loss spectroscopy (EELS) has a better spatial resolution (about a fraction of an eV) than energy dispersive x-ray spectroscopy (EDS, >100 eV) (Burleson *et al*. 2004).

XAS is most useful for semi-crystalline and amorphous NPs, and is one of the only methods that can be used for characterizing NPs in soils (Tourinho *et al*. 2012). XAS techniques include extended X-ray absorption fine structure (EXAFS), surface extended X-ray absorption fine structure (SEXAFS) and X-ray absorption near edge structure (XANES). EXAFS and XANES both give information about the structure, the interatomic distances, the coordination number, and the degree of disorder in the NP (Burleson *et al*. 2004). EXAFS can give quantitative measurement of both the type and the percentage of the phases

present in a sample. XANES is more sensitive, but less quantitative than EXAFS. X-ray photoelectron spectroscopy (XPS) can give precise analyzes of crystal structure, though it can perform surface analyzes only.

2.2. Size, size distribution and surface area

2.2.1. Microscopy techniques

Microscopic techniques are quite easily implemented. However, samples are very small, so problems of representativeness can arise. TEM is usually considered as one of the most powerful techniques for the characterization of NPs (Utsunomiya and Ewing 2003; Simonet and Valcárcel 2009; Horst *et al*. 2010; Petosa *et al*. 2012; Zhou *et al*. 2012), partly because it has a better spatial resolution than scanning electron microscopy (SEM) (Hassellöv *et al*. 2008; Boncagni *et al*. 2009; Thio *et al*. 2011; Petosa *et al*. 2012) and can be combined to various additional analytical measurements, e.g. with energy dispersive X-ray spectroscopy (Lin *et al*. 2014a).

Some SEM and TEM techniques have emerged that allow imaging of wet samples, such as environmental SEM (ESEM) (Horst *et al*. 2010), WetSEM, and cryo- and environmental TEM (ETEM). These techniques allow the visualization of the NPs aggregation state *in situ*, though their resolutions can be lowered by the water in the sample or by the membrane of the capsule used in WetSEM. Thus, Doucet *et al*. (2005) recommend using both conventional and Wet or environmental SEM to obtain complementary information.
Scanning transmission electron microscopy (STEM) allows the imaging of biological samples without staining (Tiede *et al*. 2008), at a spatial resolution of less than 0.1 nm. Its optical apparatus is simple, and thick objects can be analyzed (Eberhart 1997). It can also perform analysis of NPs at low concentrations (ppm), which is useful when characterizing environmental samples where NMs concentrations are often very low (Tiede *et al*. 2008). Dark field STEM allows the visualization of biological objects without coating, and is most appropriate for locating NPs, whose characterization can then be completed by high resolution-TEM (Utsunomiya and Ewing 2003). Wet scanning electron microscopy (WetSTEM) can be used for the imaging in liquids (Bogner *et al*. 2005). This technique thus presents many advantages, and should be regarded as a method of choice for the characterization of TiO_2 NPs.

NPs and aggregates can be imaged in three dimensions using scanning transmission X-ray microscopy (STXM) and scanning probe microscopy (SPM). STXM allows the imaging of aqueous samples and can be coupled to computer tomography to obtain 3D images (Ashcroft *et al*. 2008; Tiede *et al*. 2008; Ming *et al*. 2011). However, its resolution of about 30 nm may not be sufficient for the imaging of small NPs.

Atomic force microscopy (AFM) and scanning tunneling microscopy (STM) are the two SPM techniques most commonly used for the analysis of NPs. These techniques have a spatial resolution of up to about 0.1 nm (Table 1) (Burleson *et al*. 2004). AFM can produce 3D surface profiles (Tiede *et al*. 2008; Simonet and Valcárcel 2009). It may be used for the imaging of dry, moist or liquid samples (Hassellöv *et al*. 2008; Kumar *et al*. 2008; Tiede *et al*. 2008; Domingos *et al*. 2009; Thio *et al*. 2011), conductive and non-conductive, so no coating is required (Simonet and Valcárcel 2009). Moreover, it can also be used to visualize interactions of NMs with biomolecules, which is not the case with current electron microscopy techniques (Lin *et al*. 2014b). However, it can induce severe overestimations of the NPs lateral dimension (Kaegi *et al*. 2008; Tiede *et al*. 2008) and may cause damage to the sample through contact with the AFM tip (Burleson *et al*. 2004). STM was used by Song *et al*. (Song *et al*. 2005) to image synthetic TiO_2 NPs, and can also be used on aqueous samples (Ju-Nam and Lead 2008).

Based on microscopy and automatic imaging, nanoparticle tracking analysis (NTA) allows direct visualization of NPs ranging from 30 to 1000 nm in suspension (Petosa *et al*. 2012; Luo *et al*. 2013; Fabricius *et al*. 2014). It presents a high resolution even for polydisperse samples and can be used on dilute samples, as it tracks single particles (Chen and Elimelech 2007; Cho *et al*. 2013). It also induces minimum perturbation of the samples, and can thus be used on environmental samples (Fedotov *et al*. 2011). However, the concentration range is limited (10^7 – 10^9 particles/mL) and the measurement requires more time than with dynamic light scattering (DLS) (Filipe *et al*. 2010).

Table 1: Resolutions of microscopy techniques (adapted from Burleson *et al*. [70])

Microscopy technique	Resolution
AFM	~ 0,1 nm
ESEM	~ 3-4 nm
ETEM	> 0,1 nm
HRTEM	~ 0,1 nm
NSOM	~ 30 nm
SEM	1 nm - 1 µm
STEM	< 0,1 nm
STM	~ 0,1 nm
STXM	~ 30 nm
TEM	> 0,1 nm

2.2.2. Light scattering techniques

Light scattering methods require larger samples than microscopic techniques, and thus give more representative results. However, these methods are not applicable to complex environmental samples due to their broad particle size distributions (US EPA 2011; Fabricius *et al*. 2014), unless samples are fractionated before analysis (Filella *et al*. 1997). Indeed, larger particles tend to mask smaller ones, and a too wide polydispersity may induce errors in the sizing of NPs.

Dynamic light scattering (DLS, also called photon correlation spectroscopy - PCS) allows the determination of a particle hydrodynamic radius, which is the radius of the particle equivalent sphere. It is a fast, *in situ*, non-destructive, real-time sizing and cost-effective technique (Ledin *et al*. 1994; Filella *et al*. 1997; Tiede *et al*. 2008), which needs little to no sample preparation, so it is one of the most commonly used techniques (Stone 2009; Ottofuelling *et al*. 2011; Petosa *et al*. 2012; Zhou *et al*. 2012; Liu *et al*. 2013; Rottman *et al*. 2013). However, this technique is most suited for monodisperse suspensions, because large particles produce higher signals than small ones, inducing biases in the analysis of heterogeneous suspensions (Lin *et al*. 2014b). Moreover, the particles size usually appears to be greater when obtained by DLS than when resulting from microscopy or BET techniques (Stone 2009), so Filella *et al*. (1997) highly recommend checking DLS results with another method, such as TEM. Other disadvantages of DLS are that samples must be in suspension (Burleson *et al*. 2004) and at a particle concentration exceeding 1 mg/L (Kammer *et al*. 2012).

Static light scattering (SLS) or multi angle light scattering (MALS) is used to determine the radius of gyration of particles. As with DLS, the major limitation of this technique is its sensitivity to large

particles, as the signal varies as the sixth power of the particle diameter. Results may thus be biased for heterogeneous suspensions (Egerton and Tooley 2014).

2.2.3. Chromatography techniques

Chromatography and related techniques allow the separation of particles according to their sizes, and can be used to prefractionate samples. In this way, the concentration of NMs present at different sizes and aggregation states can be determined.

Size exclusion chromatography (SEC) and hydrodynamic chromatography (HDC) perform the separation of particles according to their hydrodynamic volume, depending on their size and shape (Song *et al*. 2004; Helfrich *et al*. 2006; Hassellöv *et al*. 2008; Tiede *et al*. 2008). SEC presents good separation efficiency, good resolution (less than 1 nm) and requires small sample volumes. However, there are possible interactions of the solute with the solvent and the column (Tiede *et al*. 2008). In addition, SEC is relatively slow (Powers *et al*. 2006), requires good calibration, and presents a limited separation size range (Figure 1). In HDC, the separation occurs in a column packed with non-porous beads, which reduces the solid phase interactions when compared to SEC. The size separation range is larger, of about 5 to 1200 nm, but the peak resolution is low (Tiede *et al*. 2008). HDC has been coupled with ICP-MS and UV-visible spectrometry for the characterization of different ENPs in environmental and sunscreen samples, including TiO_2 NPs (Philippe and Schaumann 2014). These authors emphasize the need for further investigation on the accuracy of the size determination of HDC, as weak agglomerates could be broken down at the entry of the column.

Field-flow fractionation (FFF) performs the mild fractionation of particles ranging from 1 nm to sub-µm size(Tiede *et al*. 2008; Samontha *et al*. 2011) based on their position in the cross section of a thin (100 to 500-µm thickness) open channel when affected by an applied field (Hassellöv *et al*. 1999; Tiede *et al*. 2008). Advantages of FFF include non-destruction of the sample and minimal exposure to surfaces (Dubascoux *et al*. 2010). However, there may be interactions with the apparatus, increasing the possibility of aggregation in the channel and subsequent biases in the determination of particle size distributions (Bendixen *et al*. 2014). In addition, dilute environmental samples need preconcentration for NP characterization (Dubascoux *et al*. 2010). Furthermore, NPs in natural samples may not be spherical, or may not have a homogeneous shape, so their position in the channel section, and so their FFF separation, may rely on other properties than size only (Kammer *et al*. 2005; Kammer *et al*. 2011). However, it is one of the most sensitive separation methods based on detection limits, especially when coupled with ICP-MS for quantitative elemental analysis (Simonet and Valcárcel 2009). Among the various FFF sub-techniques, sedimentation (SedFFF) and flow FFF (FlFFF) are the most commonly used for the characterization of NPs. FlFFF is easier to implement, has a wider operating range (nm-µm), a lower minimum size limit, and induces very few interactions with the analytical system. But SedFFF has higher size selectivity, although it is not applicable to particles smaller than about 50 nm (Dubascoux *et al*. 2010; Samontha *et al*. 2011). Due to its wider size range covering, FlFFF may be best suited for the analysis of environmental samples.

2.2.4. Other techniques

Confocal correlation spectroscopy (CCS) performs the-real time sizing of small volume (pL-nL) and very dilute samples (Kuyper *et al*. 2006a; Kuyper *et al*. 2006b). SAXS and SANS can be used to determine the size of solid materials and NPs in suspensions (Ridley *et al*. 2006). Both methods can be used to determine the size distribution of monodisperse or polydisperse samples (Tiede *et al*. 2008).

Raman spectroscopy can be used in aqueous samples, for *in situ* experiments (Popović *et al*. 2011). However, Pottier *et al*. (2003) found that the sizes of TiO_2 NPs obtained with Raman spectroscopy were systematically smaller than those obtained with XRD and TEM, due to particle size effect. Li Bassi *et al*. (2005) showed that this technique needed significant improvements before it can give reliable results for TiO_2 NPs.

Advantages of NMR spectroscopy include little sample preparation, and non destruction of the sample. However, large samples are required to compensate for the low detection sensitivity of the method (Sapsford *et al*. 2011).

Conventional XRD can be used on dry samples only (Teleki *et al*. 2007; French *et al*. 2009; Godinez and Darnault 2011), though it is also possible to perform analysis in a controlled atmosphere (Burleson *et al*. 2004).

The BET method is an inexpensive, direct and quick technique, relatively easy to perform, which requires very little sample preparation for the measurement of particles size and surface area (Burleson *et al*. 2004). However, the estimation of particles size is based on the assumption of monodisperse spherical particles, and can thus be inaccurate for some samples (Powers *et al*. 2006).

Among all the sizing techniques, if we consider the size range, detection limit and sample perturbation, LIBD seems to be the most appropriate technique. However, TEM, BET, DLS and FlFFF are the most commonly used techniques. Among these four methods, BET induces the highest sample perturbation (cf. Table 2): moist samples need to be desiccated, which may affect the aggregation state of the particles. DLS induces less sample perturbation than FlFFF, and has equivalent size range (~1-1000 nm), but FlFFF can be coupled to other techniques to allow further characterization of the sample. Also, it is important to keep in mind that microscopic techniques require a large number of particles to be analyzed. According to Egerton and Tooley (2014), 400-500 crystals need to be analyzed in order to have a small standard deviation (5 %) in the sizing of the particles. An auto-scanning technique can avoid spending too much time on the samples.

Table 2: Measurement characteristics of sizing methods from Hassellöv *et al*. (2008)

Sizing technique	Approximate size range (nm)	Limit of detection	Level of sample perturbation
BET	1 to > 1000	dry powder	high
DLS (PCS)	3 to > 1000	ppm	minimum
FlFFF	1 to 1000	UV detection: ppm; ICP-MS detection: ppb	low
SedFFF	50 to 1000		
HDC	5 to 1200	detection dependant	low
LIBD	5 to > 1000	ppt	minimum
NTA	30 to 1000	10^7 particles/mL	minimum
SEC	0,5 to 10	detection dependant	medium
SLS (MALS)	50 to > 1000		minimum
XRD	0,5 to > 1000	dry powder	high

2.3. Surface charge

Surface charge measurements mainly consist in zeta potential measurements (Stone 2009). The zeta potential of a particle is the electric potential at the plane of shear of the particle, and is assimilated to its surface charge (Pyell 2010). This potential is derived from electrophoretic mobility (EPM). This technique induces minimum perturbation of the sample, and performs rapid and simple measurements (Thio *et al*. 2011; Chen *et al*. 2011; Zhou *et al*. 2012; Rottman *et al*. 2013).

Phase analysis light scattering (PALS) systems were used by Lecoanet *et al*. (2004), Kim *et al*. (2009), Boncagni *et al*. (2009), Keller *et al*. (2010), Chowdhury *et al*. (2012;2013) to determine the TiO_2 NPs zeta potential *via* EPM. Capillary electrophoresis is another subtechnique for EPM measurements. The separation is sensitive and fast, but there may be interactions of the sample with the mobile phase, and the data obtained are difficult to interpret (Tiede *et al*. 2008). Laser Doppler electrophoresis has the same limitation as DLS that makes it most suitable for narrow size distributions (Murdock *et al*. 2008; Thio *et al*. 2011; Liu *et al*. 2013; Fabricius *et al*. 2014).

2.4. Concentration

2.4.1. Mass concentration

UV-visible (UV-vis) spectroscopy is an *in situ* characterization technique, with a relatively low sensitivity (Tiede *et al*. 2008). However, the measurement is affected by other parameters than particle concentration, such as size, shape, composition and refractive index of the particles. Consequently, UV-vis spectroscopy cannot be used for a quantitative characterization of polydisperse particles, but gives a good approximation of particle mass concentration for heterogeneous natural particles (Dunphy Guzman *et al*. 2006; Domingos *et al*. 2009; Boncagni *et al*. 2009; Battin *et al*. 2009; Kammer *et al*. 2010).

When using nephelometric turbidity, measures have to be calibrated against known concentrations of the particles that are measured (Ben-Moshe *et al*. 2010; Gondikas *et al*. 2014). Artifacts can arise from the fact that turbidity depends not only on the concentration, but also on the size of the particles.

Inductively coupled plasma – atomic emission spectroscopy (ICP-AES) and mass spectrometry (ICP-MS) allow the simultaneous detection of multiple analytes (Schmidt and Vogelsberger 2006; Zhang *et al*. 2008; Kaegi *et al*. 2008; Samontha *et al*. 2011; Thio *et al*. 2011; Petosa *et al*. 2012; Rottman *et al*. 2013; Lopez-Serrano *et al*. 2014). ICP-MS has a lower detection limit (1-10 pg/mL) than ICP-AES (1-100 ng/mL). Advantages of ICP-AES and ICP-MS include relatively quick and inexpensive measurements, with good detection limits. However, they are destructive techniques, for which sample preparation and matrix effects can cause major artifacts (Burleson *et al*. 2004).

Graphite furnace atomic absorption (GFAA) spectroscopy induces minimal sample perturbation (Bundschuh *et al*. 2001; Walther *et al*. 2006; Olabarrieta *et al*. 2012).

X-ray fluorescence (XRF) is a fast, highly sensitive, and non-destructive (when no dissolution is applied) technique that can be used for elemental concentration determinations of solid, powdered or liquid samples (Solovitch *et al*. 2010).
ICP-MS appears as one of the most powerful techniques for mass concentration analysis of TiO_2 NPs. However, it requires dissolution of solid samples and acidification, and high interferences can arise from Ca if this element is present in high concentrations in the sample (Lopez-Serrano *et al*. 2014). XRF is another powerful method that can be used also on solid samples.

2.4.2. Particle number concentration

The number concentration of NPs can be determined based on several techniques, including SEM, TEM, STM, STXM, LIBD and particle-induced X-ray emission (PIXE).

Coupling electron microscopy with energy dispersive x-ray spectroscopy (EDS) also called energy dispersive x-ray analysis (EDX) gives a clear determination of the composition of elements heavier than oxygen (Kaegi *et al*. 2008). The quantitative analysis presents an uncertainty of about 20%. EDX can be coupled with SEM, TEM or AFM (Walther *et al*. 2006; Tiede *et al*. 2008).

LIBD provides the total number of particles down to 10 nm and less without any special sample preparation (Kertész *et al*. 2005). It is a highly sensitive technique (ppt) (Hassellöv *et al*. 2008; Tiede *et al*. 2008), up to six orders of magnitude more sensitive than conventional light scattering methods (Wagner *et al*. 2004; Kertész *et al*. 2005; Lekki *et al*. 2007; Kaegi *et al*. 2008). This method is very fast and non-invasive (Kaegi *et al*. 2008).

Particle-induced X-ray emission (PIXE) maps the elemental composition of dry or aqueous samples (Reed *et al*. 2012; Lozano *et al*. 2012). Advantages include multi-element acquisition, high sensitivity (ppm), fast measurements and minimal sample preparation. The sensitivity of PIXE is higher than that of EDX spectroscopy (Suter 1993).

To determine particle number concentrations, microscopy techniques require large samples in order to obtain representative results, and counting may appear constraining and time-consuming. LIBD allows processing larger samples more quickly and with a better sensitivity.

2.5. Recommendations

Most studies recommend using different analytical methods simultaneously in order to characterize NPs in the best way, assessing various properties and crosschecking the results obtained with the different techniques (Buffle and van Leeuwen 1992; Chen *et al*. 1997; Burleson *et al*. 2004; Jiang *et al*. 2008; Kaegi *et al*. 2008; Tiede *et al*. 2008; Kammer *et al*. 2010; Samontha *et al*. 2011; Kammer *et al*. 2012).

Among microscopy techniques, AFM and TEM present the highest resolutions and can be used on aqueous samples with virtually no alteration of the aggregation state, so they are methods of choice to image the NPs and to determine their shape. However, numerous pictures are necessary in order to obtain results representative of the whole sample, and this can be quite tedious and time-consuming. DLS is easily implemented and commonly used for the size determination of NPs, but problems can arise if the particle size distribution of the sample is too broad. Even if the use of FFF can require long developments that need to be carried out for each type of sample, it covers a wider range of sizes, and can be coupled to various quantification techniques, such as HDC or ICP-MS. HDC-ICPMS provides a faster separation, but at a lower resolution than FFF-ICPMS (US EPA 2011). SP-ICP-MS coupling is particularly powerful in the characterization of the NPs, as it gives two of the most important parameters, which are size distribution and particle number concentration (Arvidsson *et al*. 2014; Lopez-Serrano *et al*. 2014). NPs charge and structure are determined by more common techniques, respectively electrophoresis and X-ray diffraction.

When aiming at modeling the NPs fate and effects in the environment, both in *situ* analyzes and laboratory experiments are necessary, and complement each other: laboratory experiments allow controlled conditions in simple systems, helping at understanding the mechanisms determining the NPs behavior; *in situ* analyzes helps in predicting environmental concentrations and exposure levels to organisms. *In situ* analyzes are more technically demanding, as NMs are often present at low environmental conditions and broad size distributions. ICP-MS allows low concentration analysis, and can be coupled to FlFFF or HDC to determine their size distributions. Furthermore, NMs are highly reactive, so avoiding altering their environmental state, especially their aggregation/agglomeration state, is tricky. WetSTEM provides high resolution, *in situ* analysis, and broad size range, so that it is highly recommended. Its only disadvantage is that it can induce a lack of representativeness, which is yet an important parameter to take into account in any modeling.

3. Modeling the fate and the effects of TiO_2 NMs in RA and LCA

Research on NMs behavior in the environment is driven by the need for the determination of their potential environmental impacts and risks. Life Cycle Assessment (LCA) and Risk Assessment (RA) are two methodologies that rely both on fate and effect modeling, and will be discussed in the next sections.

3.1. Methodologies of RA and LCA

Risk assessment (RA) is an environmental assessment tool that aims at providing magnitudes and probabilities of adverse effects of human activities and natural catastrophes (Savolainen *et al*. 2010). It includes four steps (ISO 2006a; ISO 2006b):

(1) Hazard identification: identification of substance properties and hazards they may cause to organisms.
(2) Hazard characterization: determination of toxicity mechanisms and values.
(3) Exposure assessment: determination of sources, pathways and routes of exposure, as well as the concentrations to which the organisms are exposed.
(4) Risk assessment: calculation of the risk by the combination of the exposure hazard factors.

Usually, the risk ratio is defined as the ratio of the predicted environmental concentration (PEC) over the predicted no effect concentration (PNEC). However, PECs and PNECs are usually expressed as mass/volume ratios, while using particle number concentrations could lead to more accurate results for the risk assessment of NPs. Moreover, these concentrations cannot be predicted with a satisfying accuracy, because the research in the fields of NPs fate and effect is still recent.

Life cycle assessment (LCA) can be used to assess the impacts of products, processes or services all over their life cycles, from raw material extraction to waste disposal or recycling, through manufacture and use. The aim of LCA is to compare a variety of impacts arising from different scenarios, in order to help stakeholders making decisions about the development of their products. The methodology of LCA has been standardized (Rosenbaum *et al*. 2007; Rosenbaum *et al*. 2008) and includes four steps:

(1) Goal and scope definition: the system boundaries and a functional unit are defined. The functional unit is the unit of product to which all impacts are related.
(2) Life cycle inventory (LCI): input and output data flowing to and from the system are collected and reported to the functional unit.
(3) Life cycle impact assessment (LCIA): LCI results need to be classified into different impact categories (e.g. human toxicity or aquatic ecotoxicity), and the impacts are calculated. The impacts can then be normalized, grouped and weighted, but these steps are optional.
(4) Results interpretation: Results are analyzed in order to give conclusions and recommendations.

In LCIA, impacts are presented as category indicators (CI), which are the results of the product of the total mass of emissions (M) with a characterization factor (CF) (Equation 1).

$$CI = CF \times \sum M_i \quad (1)$$

CFs are substance-specific and can be calculated using various methodologies. USEtox is the most recent one, based on a consensus among experts that had built previous calculation methods. In USEtox, CFs for freshwater aquatic ecotoxicity are calculated according to Equation 2 (Huijbregts *et al*. 2010):

$$CF_i = FF_i \times XF_i \times EF_i \quad (2)$$

Where FF_i is the fate factor of the substance i, equivalent to the residence time of the substance in an environmental compartment; XF_i is the exposure factor of substance i, that is its bioavailable fraction; EF_i is the effect factor of substance i, which is based on ecotoxicity data. The potential ecotoxic impacts are expressed in comparative toxic units (CTUs), which are $PAF.m^3.d.kg^{-1}$ (PAF: Potentially affected fraction of organisms). The USEtox calculations of the different factors are detailed below.

The USEtox fate modeling of a substance in water accounts for adsorption, sedimentation, volatilization, degradation, and advective transport. In soil, degradation, volatilization, leaching to deeper layers of soil, and runoff to surface water are included. Steady state is assumed for the

calculation of the variation of a substance mass in an environmental compartment (Equation 3; (Gottschalk *et al*. 2010):

$$\frac{\overline{dM}}{dt} = \bar{S} + \bar{k} \times \bar{M} \; ; \; \bar{M} = \overline{k^{-1}} \times \bar{S} \qquad (3)$$

With $\bar{S}$ (kg.d^{-1}) the vector of the emission rate S_i in each compartment i, $\bar{M}$ (kg) the vector of chemical masses with elements M_i, and $\bar{k}$ (d^{-1}) the bulk rate coefficient matrix. FF is calculated by dividing the mass increase of the substance in one compartment (kg) by an emission flow (kg.d^{-1}). So, per definition, $\overline{FF} = \overline{k^{-1}}$. The properties necessary for the modeling of metals in USEtox are different from the ones usually considered as important in predicting the fate of metal and metal oxide NPs (Table 3). This demonstrates the need for the development of new fate factors specific to NPs.

Table 3: Comparison of parameters necessary for the modeling of metals fate in USEtox (Gottschalk *et al*. 2013) and that of metal and metal oxide NPs

Metals		**Metal and metal oxide NPs**	
Process	**Parameter**	**Process**	**Parameter**
Dissolution	Dissolution rate constant (k_{diss})	Dissolution	Dissolution rate constant (k_{diss})
Adsorption	• Solid-liquid partitioning coefficients (K_p)	Homoaggregation	• Homoaggregation rate constant ($k_{homoagg}$) • Collision rate constant ($\alpha_{homoagg}$) • Attachment efficiency coefficient ($\beta_{homoagg}$)
Absorption	• Octanol-water partitioning coefficient (K_{ow}) • Organic carbon partitioning coefficient (K_{oc})	Heteroaggregation	• Heteroaggregation rate constant ($k_{heteroagg}$) • Collision rate constant ($\alpha_{heteroagg}$) • Attachment efficiency coefficient ($\beta_{heteroagg}$)

The exposure factor of a substance in freshwater is considered to be the total dissolved fraction of a substance. It is calculated according to Equation 3 (Gottschalk *et al*. 2013):

$$XF_{w,w} = \frac{1}{1+(k_p \times SUSP + k_{DOC} \times DOC + BCF_{fish} \times BIOmass) \times 10^{-6}} \qquad (3)$$

With k_p the partition coefficient between water and suspended solids (L.kg^{-1}), SUSP the suspended matter concentration in freshwater (kg.L^{-1}), k_{DOC} the partition coefficient between DOC and water, DOC the dissolved organic carbon concentration in water (kg.L^{-1}), BCF_{fish} the bioconcentration factor in fish (L.kg^{-1}), and BIOmass the concentration of biota in water (kg.L^{-1}). The size of particulate metal is assumed to be above the bioavailability level, but we have seen earlier that nanometric particles can

enter organisms and cells. So again, a new exposure model needs to be developed, that would take into account the size distribution of the particles.

The USEtox effect factor ($m^3.kg^{-1}$) is calculated according to Equation 4 (Huijbregts *et al*. 2010):

$$EF = \frac{0.5}{HC50_{EC50}} \qquad (4)$$

HC50 is the hazardous concentration at which 50% of the species are exposed above their EC50 (effect concentration affecting 50% of a population). 0.5 stands for a 50% PAF (potentially affected fraction), which is a fraction of 50% of a population that is affected. Here, the concentration is expressed as a mass/volume ratio, but, as seen in section 1, it could be useful to express it as a particle number/volume ratio, or as a surface areas ratio.

We can see that LCIA and RA rely on the same type of data (fate parameters and ecotoxicological data), and in this way they have the same limitations regarding their application to NMs. However, some authors have started overcoming these limitations, as described in the next section.

3.2. Modeling the fate and exposure of TiO_2 NPs in LCA and RA

Gottschalk *et al*. (2010; 2013) and Mueller and Nowack (2008) developed fate and exposure models for TiO_2 NPs in a RA perspective, but at global and regional scales, respectively. These studies did not take into account processes specific to NPs, though Gottschalk *et al*. (2013) used probability distributions to account for the uncertainties of their model. Quik *et al*. (2011) took a step forward and incorporated sedimentation and dissolution of NPs in existing models.

Based on Thill (1999), Praetorius *et al*. (2012) developed a fate model that is able to predict the fate of TiO_2 ENPs in the Rhine River, based on the colloidal theory and thus accounting for all nano-specific fate processes. The river was divided in three compartments (moving water, stagnant water and sediment) in the cross section, and in 520 boxes in the longitudinal dimension. The authors distinguished processes that affect free TiO_2 NPs only (sedimentation and heteroaggregation), TiO_2 NPs bound to suspended particulate matter (SPM) (sedimentation with SPM, sediment resuspension, burial in the deep sediment and horizontal bed load transport) and both free TiO_2 NPs and SPM-bound TiO_2 NPs (river flow and exchange between moving and stagnant water). First order rate constants were derived for each process, assuming steady state of the system. One of the most significant transformation process undergone by NPs is aggregation. This process is commonly described by colloidal science and the Derjaguin-Landau-Verwey-Overbeak (DLVO) theory. Particles undergo three types of motion, depending mostly on their size: Brownian motion (diffusion), shear rate motion, and gravitational settling. These motions lead to collisions, and the actual sticking together of NPs after collision can be predicted by the DLVO theory.

This theory assumes that aggregation of particles is dependent on the sum of two electrical forces: the van der Waals (attractive) and the electrical double layer (repulsive) forces (Hotze *et al*. 2010). However, the DLVO theory cannot be applied in case of high particle concentrations, presence of multivalent counterions, or high particle surface charge (Chen *et al*. 2012a). Moreover, Chen *et al*. (2012a) and Kim *et al*. (2009) showed that other forces play a significant role in NPs aggregation, whose can be included in the extended DLVO (XDLVO) theory. These forces include steric repulsion, which can be caused by adsorbed polymers, polyelectrolyte coatings or natural organic matter. It can lead to the reversibility of aggregation, and was used by Chen *et al*. (2012a) to explain the effects of humic acids on the transport and retention of TiO_2 NPs in porous media. Lewis acid-base hydrophobic

interactions lead to additional repulsive forces, and were used by Kim *et al*. (2009) to explain the interactions of NOM with TiO_2 NPs. Bridging and osmotic forces are also included in the XDLVO theory, as well as magnetic forces (Hotze *et al*. 2010), but these additional forces were not included in the model built by Praetorius *et al*. (2012). Besides, the authors considered the homoaggregation negligible in the Rhine River, as the concentration of TiO_2 NPs expected to be released is low (in the $ng.L^{-1}$ range) so that the NPs are assumed not to collide frequently. The density and concentration of SPM were varied in different runs of the model, their size was assumed log-normally distributed between 1.5 and 80 µm. The NPs were assumed to reach the river in an aggregated state. Their initial size distribution was also assumed to be log-normal, with a mode at 300 nm; five size classes were determined. The incoming flow was expressed as a particle flow for each size class, based on mass flow information and specific density of the NPs. All results are then expressed on the basis of particle *numbers* (Praetorius *et al*. 2012).

Salieri (2013) is the only author that worked on the whole LCIA methodology to adapt it to TiO_2 NPs fate in the aquatic environment. The author carried out the LCIA of TiO_2 NPs in freshwater, taking into account the sediment compartment. Several processes were included in the fate model: advection, aggregation and sedimentation in freshwater, resuspension from sediment to freshwater, bed load transport, and burial to deep sediment. The general equations for constant rates calculations are as follows (Eq. 5-8):

$$k_{w,w,i,} = -(k_{w,adv,i} + k_{sed,i} + k_{diss} + k_{w,het-aggr}) \;\; for\; i = 1, \dots, n_{size}^{ENP} \quad (5)$$

$$k_{sed,sed,i} = -(k_{burial,i} + k_{resusp} + k_{sed,transfer}) \quad (6)$$

$$k_{w,sed,i} = k_{sed,i} \quad (7)$$

$$k_{sed,w,i} = k_{resusp,i} \quad (8)$$

Where $k_{w,w,i}$ and $k_{sed,sed,i}$ are the rate coefficients for the total removal from the water column (advection, hetero-aggregation, dissolution, and sedimentation) and from the sediment (burial, resuspension and bed load transfer), respectively. $k_{w,sed,i}$ and $k_{sed,w,i}$ are the inter-media exchange coefficients between water and sediment, and are equivalent to the sedimentation rate constant from freshwater to sediment, and the resuspension rate constant from sediment to freshwater, respectively. The model equations are based on the USEtox model for advection, burial and resuspension rates, on Quik *et al*. (2011) for dissolution, and on Praetorius *et al*. (2012) for aggregation and bed load sediment transfer. A fate matrix has been developed for different size classes of TiO_2 NPs. The final fate factor has been calculated as the weighted average of the different $FF_{w,w,i}$. But, unlike Praetorius *et al*. (2012), Salieri (2013) did not account for the size distribution of SPM. Photocatalysis and hydrolysis have not been included in the calculations either. The TiO_2 NPs effect factor was calculated based on mass concentrations, thereby not accounting for NPs specific properties.

The MendNano (Multimedia environmental distribution of engineered nanomaterials) model was built by Liu and Cohen (2014). The authors highlighted that the particle size distributions of NMs govern their transport through the different environmental compartments (air, soil, water, sediment, waterborne biota and vegetation), and use first-order kinetic equations to model their multimedia transport and transformations. The dynamic mass balance of each compartment is calculated for each particle size fraction and is given by the general equation:

$$\frac{d}{dt}\left[V_i C_{i,k}\right] = \left(Q_i^{in} \cdot C_{i,k}^{in} - Q_i^{out} \cdot C_{i,k}\right) + \sum_{j=1}^{M} \sum_{l=1}^{P} I_{i,j,k}^{l} + \sum_{n=1}^{U} R_{i,k}^{n} + S_{i,k} \;\; k = 1, \dots, N\,; i = 1, \dots, T (1)$$

The first term on the right side of the equation accounts for advective mass transport, with N the number of particle size fractions, V_i (m^3) the volume of compartment i, $C_{i,k}$ ($g.m^{-3}$) the compartmental ENM concentration associated with particles in size fraction k, Q_i^{in} and Q_i^{out} ($m^3.s^{-1}$) the advective flow rates in and out of compartment i, respectively, and $C_{i,k}^{in}$ ($g.^{m-3}$) the inflow ENM concentration. The intermedia transport rates (second term of the right side of the equation) between compartments i and j, via transport transport process l, is $I^l_{i,j,k}$ ($g.s^{-1}$), P being the number of processes and M the number of compartments. The transformation rate, $R^n_{i,k}$ can be calculated as $r^n_{i,k}.V_i$, with $r^n_{i,k}$ being the volume specific ENM transformation rate ($g.m^{-3}$), or as $\xi_i.K^r_{i,k}.C_{i,k}.V_i$, with $K^r_{i,k}$ the transformation rate constant (s^{-1}) and ξ_i set as +1 or -1 for a production or a consumption transformation. $S_{i,k+}$ is the ENM source release rate ($g.s^{-1}$). The needed input data include ENM properties, meteorological information, geographical parameters, transport parameters and release scenario. The model is able to give temporal profiles, mass distributions and information about intermedia transport (http://mendnano.polysep.ucla.ed). The authors performed two 1-year simulations for TiO_2 NPs in the Los Angeles region and in Switzerland , that resulted in the first case in 73 % of input TiO_2 ending in soil, 0.335 % in water, 26.33 % in sediment, and 0.028 % in the atmosphere compartment. The MendNano model is applicable for regions of minimum 1 km² area (Liu and Cohen 2014). It has been built to give regional average mass tranfers, so that it is recommended to use it for distributed sources, as opposed to singular point sources, for which the fate modeling would result in overestimations for the average compartmental concentrations and underestimations for local concentrations (Liu and Cohen 2014).

Meesters *et al*. (2014) built a multimedia fate model, named SimpleBox4nano (SB4N), based on the European Union System for Evaluation of Substances (EUSES) model, which is widely used in LCIA. This model includes the air, soil, water and sediment compartments. The authors made three major adaptations of this model: (1) transformation processes were not considered as removal processes, (2) dissolution was implemented as a removal process and (3) the thermodynamic equilibrium was not assumed to calculate colloidal concentrations; rather, dissolution, aggregation and attachment rates give the rate at which the NPs reach equilibrium. The third assumption implies that NPs can occur in different forms in each compartment: (1) freely dispersed, (2) heteroaggregated with natural colloidal particles (<450 nm) or (3) attached to larger natural particles (>450 nm). This model is a multimedia mass balance model in which the masses (m) of NPs in the compartments are obtained by solving the steady-state equations. The solutions are expressed as follows:

$$m = -A^{-1} \cdot e \qquad (1)$$

Where A is the system matrix of rate constants (s^{-1}) and e is the vector of emission rates of ENP into the environment ($kg.s^{-1}$). When applying this model to TiO_2 NPs, the authors assumed that the dissolution of these particles was negligible, so that the removal processes were all related to transport processes. Colloidal theory was applied to obtain the mass-balance equations. However, the authors emphasize that experimental results are preferred over modeling with DLVO theory, as it has been established that it cannot be accurately applied to NPs without adding some morphology correction factors. As Praetorius *et al*. (2012), the authors only consider heteroaggregation, disregarding homoaggregation. This was based on previous studies that showed that homoaggregation was negligible in natural conditions, due to the low concentrations of ENPs in the natural aquatic compartment when compared to natural suspended particulate matter (Quik *et al*. 2012;2014). However, SB4N is able to consider homoaggregates as input into the system, if an emission rate and the properties of the aggregates are given.

Modeling the fate and effect of NPs in RA and LCA is based on previously existing methodologies, which were adapted step-by-step to the colloidal theory. One of the most important changes to make in this

direction is to consider no longer the mass of the substance, but the particle number and the aggregation state. In the same way, making the difference between particulate and dissolved metal fractions is not sufficient when working on nanometric particles: their whole size distribution needs to be taken into account. Moreover, there is still a lack of knowledge regarding NPs behavior. This can be accounted for by using probabilistic approaches such as Bayesian networks (BNs) (Adam *et al*. 2015). This type of model has not yet been used on TiO_2 NMs, but was implemented to assess the potential risk of silver NPs (Money *et al*. 2012; Money *et al*. 2014). BNs link the different variables involved in the evaluation of their impacts/risks, based on probability distributions. This allows taking into account the variables uncertainties and visualizing them easily, and makes BNs very useful for prioritizing research needs.

Conclusion

The understanding of NMs behavior in the environment requires taking into account NP-specific properties, such as crystallinity, size, surface charge, aggregation/agglomeration state, surface area and particle number concentration. The determination of these properties needs adapted analytical techniques. Among them, AFM, TEM, X-ray spectroscopy, FlFFF and ICP-MS appear most useful, because they are *in situ* and high resolution techniques. However, none of them can determine all NPs necessary properties within one single run, and some techniques are still emerging. Consequently, it is recommended to combine various analytical tools, as this can also allow cross-checking the results.

Indeed, accurate characterization of NMs properties is necessary for the modeling of predicted environmental concentrations, for the evaluation of toxicity thresholds and for the calculation of LCA characterization factors. However, literature is mostly based on mass concentration instead of particle number concentration or surface area, which makes it difficult to adapt existing LCA and RA models to NPs and to integrate ecotoxicological data in these models. All this adds up to give high uncertainties regarding the potential impacts and risks of TiO_2 NMs. Yet, there is an urgent need for the assessment of their impacts/risks, as NMs are present in a huge quantity of products. So, the best strategy to adopt is using probabilistic approaches such as BNs, which allow both accounting for and visualizing uncertainties, thus facilitating decision making.

Acknowledgements

This work was supported by the French Environment and Energy Management Agency (ADEME), the Région Alsace, and the National Research Agency (ANR) project MESONNET.

Compliance with ethical standards

The compliance with ethical standards is not applicable. (No potential conflicts of interest, research not involving human participants or animals).

References

Adam V (2015) Evaluation des impacts et des risques des nanoparticules manufacturées de TiO_2 sur l'eau par un modèle combiné d'Analyse du Cycle de Vie (ACV) et d'évaluation des risques. 16 pp.

Adam V, Quaranta G, Loyaux-Lawniczak S (2015) Life Cycle Assessment and Ecological Risk Assessment of Nanomaterials - Review of single and combined approaches. Environ Sci Poll Res. submitted

Aillon KL, Xie Y, El-Gendy N, *et al* (2009) Effects of nanomaterial physicochemical properties on in vivo toxicity. Adv Drug Deliv Rev 61:457–466. doi: 10.1016/j.addr.2009.03.010

Arvidsson R, Molander S, Sandén BA (2014) Assessing the Environmental Risks of Silver from Clothes in an Urban Area. Hum Ecol Risk Assess Int J 20:1008–1022. doi: 10.1080/10807039.2012.691412

Ashcroft JM, Gu W, Zhang T, *et al* (2008) TiO_2 nanoparticles as a soft X-ray molecular probe. Chem Commun 2471–2473. doi: 10.1039/b801392f

Auffan M, Rose J, Bottero J-Y, *et al* (2009) Towards a definition of inorganic nanoparticles from an environmental, health and safety perspective. Nat Nanotechnol 4:634–641. doi: 10.1038/nnano.2009.242

Battin TJ, Kammer F v. d., Weilhartner A, *et al* (2009) Nanostructured TiO_2: Transport Behavior and Effects on Aquatic Microbial Communities under Environmental Conditions. Environ Sci Technol 43:8098–8104. doi: 10.1021/es9017046

Bell TE (2007) Understanding risk assessment of nanotechnology. Natl. Nanotechnol. Initiat.

Bendixen N, Losert S, Adlhart C, *et al* (2014) Membrane–particle interactions in an asymmetric flow field flow fractionation channel studied with titanium dioxide nanoparticles. J Chromatogr A 1334:92–100. doi: 10.1016/j.chroma.2014.01.066

Ben-Moshe T, Dror I, Berkowitz B (2010) Transport of metal oxide nanoparticles in saturated porous media. Chemosphere 81:387–393. doi: 10.1016/j.chemosphere.2010.07.007

Bennett SW, Zhou D, Mielke R, Keller AA (2012) Photoinduced Disaggregation of TiO_2 Nanoparticles Enables Transdermal Penetration. PLoS ONE 7:e48719. doi: 10.1371/journal.pone.0048719

Bogner A, Thollet G, Basset D, *et al* (2005) Wet STEM: A new development in environmental SEM for imaging nano-objects included in a liquid phase. Ultramicroscopy 104:290–301. doi: 10.1016/j.ultramic.2005.05.005

Boncagni NT, Otaegui JM, Warner E, *et al* (2009) Exchange of TiO_2 Nanoparticles between Streams and Streambeds. Environ Sci Technol 43:7699–7705. doi: 10.1021/es900424n

Braydich-Stolle LK, Schaeublin NM, Murdock RC, *et al* (2009) Crystal structure mediates mode of cell death in TiO_2 nanotoxicity. J Nanoparticle Res 11:1361–1374. doi: 10.1007/s11051-008-9523-8

Buffle J, van Leeuwen HP (1992) Environmental Particles. Lewis Publishers

Buffle J, van Leeuwen HP (1993) Environmental particles. Lewis Publishers

Bundschuh M, Zubrod JP, Englert D, *et al* (2011) Effects of nano-TiO_2 in combination with ambient UV-irradiation on a leaf shredding amphipod. Chemosphere 85:1563–1567. doi: 10.1016/j.chemosphere.2011.07.060

Bundschuh T, Knopp R, Kim JI (2001) Laser-induced breakdown detection (LIBD) of aquatic colloids with different laser systems. Colloids Surf Physicochem Eng Asp 177:47–55.

Burleson D, Driessen M, Penn RL (2004) On the Characterization of Environmental Nanoparticles. J Environ Sci Health Part A 39:2707–2753. doi: 10.1081/ESE-200027029

Chen G, Liu X, Su C (2011) Transport and Retention of TiO_2 Rutile Nanoparticles in Saturated Porous Media under Low-Ionic-Strength Conditions: Measurements and Mechanisms. Langmuir 27:5393–5402. doi: 10.1021/la200251v

Chen G, Liu X, Su C (2012a) Distinct Effects of Humic Acid on Transport and Retention of TiO_2 Rutile Nanoparticles in Saturated Sand Columns. Environ Sci Technol 46:7142–7150. doi: 10.1021/es204010g

Chen KL, Elimelech M (2007) Influence of humic acid on the aggregation kinetics of fullerene (C60) nanoparticles in monovalent and divalent electrolyte solutions. J Colloid Interface Sci 309:126–134. doi: 10.1016/j.jcis.2007.01.074

Chen LX, Rajh T, Wang Z, Thurnauer MC (1997) XAFS studies of surface structures of TiO_2 nanoparticles and photocatalytic reduction of metal ions. J Phys Chem B 101:10688–10697.

Chen L, Zhou L, Liu Y, *et al* (2012b) Toxicological effects of nanometer titanium dioxide (nano-TiO_2) on Chlamydomonas reinhardtii. Ecotoxicol Environ Saf 84:155–162. doi: 10.1016/j.ecoenv.2012.07.019

Chen Z, Wang Y, Ba T, *et al* (2014) Genotoxic evaluation of titanium dioxide nanoparticles in vivo and in vitro. Toxicol Lett 226:314–319. doi: 10.1016/j.toxlet.2014.02.020

Cho EJ, Holback H, Liu KC, *et al* (2013) Nanoparticle Characterization: State of the Art, Challenges, and Emerging Technologies. Mol Pharm 10:2093–2110. doi: 10.1021/mp300697h

Chowdhury I, Cwiertny DM, Walker SL (2012) Combined Factors Influencing the Aggregation and Deposition of nano-TiO_2 in the Presence of Humic Acid and Bacteria. Environ Sci Technol 46:6968–6976. doi: 10.1021/es2034747

Chowdhury I, Walker SL, Mylon SE (2013) Aggregate morphology of nano-TiO_2: role of primary particle size, solution chemistry, and organic matter. Environ Sci Process Impacts 15:275. doi: 10.1039/c2em30680h

Cho W-S, Duffin R, Thielbeer F, *et al* (2012) Zeta Potential and Solubility to Toxic Ions as Mechanisms of Lung Inflammation Caused by Metal/Metal Oxide Nanoparticles. Toxicol Sci 126:469–477. doi: 10.1093/toxsci/kfs006

Domingos RF, Baalousha MA, Ju-Nam Y, *et al* (2009) Characterizing Manufactured Nanoparticles in the Environment: Multimethod Determination of Particle Sizes. Environ Sci Technol 43:7277–7284. doi: 10.1021/es900249m

Donaldson K, Murphy FA, Duffin R, Poland CA (2010) Asbestos, carbon nanotubes and the pleural mesothelium: a review of the hypothesis regarding the role of long fibre retention in the parietal pleura, inflammation and mesothelioma. Part Fibre Toxicol 7:5.

Donaldson K, Schinwald A, Murphy F, *et al* (2013) The Biologically Effective Dose in Inhalation Nanotoxicology. Acc Chem Res 46:723–732. doi: 10.1021/ar300092y

Doucet FJ, Lead JR, Maguire L, *et al* (2005) Visualisation of natural aquatic colloids and particles - a comparison of conventional high vacuum and environmental scanning electron microscopy. J Environ Monit 7:115. doi: 10.1039/b413832e

Dubascoux S, Le Hécho I, Hassellöv M, *et al* (2010) Field-flow fractionation and inductively coupled plasma mass spectrometer coupling: History, development and applications. J Anal At Spectrom 25:613–623. doi: 10.1039/b927500b

Dunphy Guzman KA, Finnegan MP, Banfield JF (2006) Influence of Surface Potential on Aggregation and Transport of Titania Nanoparticles. Environ Sci Technol 40:7688–7693. doi: 10.1021/es060847g

Eberhart J-P (1997) Analyse structurale et chimique des matériaux. Dunod

Egerton TA, Tooley IR (2014) Physical characterization of titanium dioxide nanoparticles. Int J Cosmet Sci 36:195–206. doi: 10.1111/ics.12113

European Commission (2013) Commission delegated regulation (EU) No 1363/2014 of 12 December 2013 amending Regulation (EU) No 1169/2011 of the European Parliament and of Council on the provision of food information to consumers as regards the definition of “engineered nanomaterials.” 1363/2013:3.

Fabricius A-L, Duester L, Meermann B, Ternes TA (2014) ICP-MS-based characterization of inorganic nanoparticles—sample preparation and off-line fractionation strategies. Anal Bioanal Chem 406:467–479. doi: 10.1007/s00216-013-7480-2

Fang Q, Shi X, Zhang L, *et al* (2015) Effect of titanium dioxide nanoparticles on the bioavailability, metabolism, and toxicity of pentachlorophenol in zebrafish larvae. J Hazard Mater 283:897–904. doi: 10.1016/j.jhazmat.2014.10.039

Fedotov PS, Vanifatova NG, Shkinev VM, Spivakov BY (2011) Fractionation and characterization of nano- and microparticles in liquid media. Anal Bioanal Chem 400:1787–1804. doi: 10.1007/s00216-011-4704-1

Filella M, Zhang J, Newman ME, Buffle J (1997) Analytical applications of photon correlation spectroscopy for size distribution measurements of natural colloidal suspensions: capabilities and limitations. Colloids Surf Physicochem Eng Asp 120:27–46.

Filipe V, Hawe A, Jiskoot W (2010) Critical Evaluation of Nanoparticle Tracking Analysis (NTA) by NanoSight for the Measurement of Nanoparticles and Protein Aggregates. Pharm Res 27:796–810. doi: 10.1007/s11095-010-0073-2

French RA, Jacobson AR, Kim B, *et al* (2009) Influence of Ionic Strength, pH, and Cation Valence on Aggregation Kinetics of Titanium Dioxide Nanoparticles. Environ Sci Technol 43:1354–1359. doi: 10.1021/es802628n

George S, Gardner H, Seng EK, *et al* (2014) Differential Effect of Solar Light in Increasing the Toxicity of Silver and Titanium Dioxide Nanoparticles to a Fish Cell Line and Zebrafish Embryos. Environ Sci Technol 48:6374–6382. doi: 10.1021/es405768n

Gibson CT, Turner IJ, Roberts CJ, Lead JR (2007) Quantifying the Dimensions of Nanoscale Organic Surface Layers in Natural Waters. Environ Sci Technol 41:1339–1344. doi: 10.1021/es061726j

Gmoshinski IV, Khotimchenko SA, Popov VO, *et al* (2013) Nanomaterials and nanotechnologies: methods of analysis and control. Russ Chem Rev 82:48–76. doi: 10.1070/RC2013v082n01ABEH004329

Godinez IG, Darnault CJG (2011) Aggregation and transport of nano-TiO_2 in saturated porous media: Effects of pH, surfactants and flow velocity. Water Res 45:839–851. doi: 10.1016/j.watres.2010.09.013

Gondikas AP, Kammer F von der, Reed RB, *et al* (2014) Release of TiO_2 Nanoparticles from Sunscreens into Surface Waters: A One-Year Survey at the Old Danube Recreational Lake. Environ Sci Technol 48:5415–5422. doi: 10.1021/es405596y

Gottschalk F, Kost E, Nowack B (2013) Engineered nanomaterials in water and soils: A risk quantification based on probabilistic exposure and effect modeling. Environ Toxicol Chem 32:1278–1287. doi: 10.1002/etc.2177

Gottschalk F, Scholz RW, Nowack B (2010) Probabilistic material flow modeling for assessing the environmental exposure to compounds: Methodology and an application to engineered nano-TiO_2 particles. Environ Model Softw 25:320–332. doi: 10.1016/j.envsoft.2009.08.011

Grillo R, Rosa AH, Fraceto LF (2015) Engineered nanoparticles and organic matter: A review of the state-of-the-art. Chemosphere 119:608–619. doi: 10.1016/j.chemosphere.2014.07.049

Gurkirpal S. M (2012) The Chronic Toxicity of Titanium Dioxide Nanoparticles to the Freshwater Amphipod Hyalella azteca. Wilfried Laurier University

Hamilton RF, Wu N, Porter D, *et al* (2009) Particle length-dependent titanium dioxide nanomaterials toxicity and bioactivity. Part Fibre Toxicol 6:35. doi: 10.1186/1743-8977-6-35

Hassellöv M, Lyvén B, Haraldsson C, Sirinawin W (1999) Determination of Continuous Size and Trace Element Distribution of Colloidal Material in Natural Water by On-Line Coupling of Flow Field-Flow Fractionation with ICPMS. Anal Chem 71:3497–3502. doi: 10.1021/ac981455y

Hassellöv M, Readman JW, Ranville JF, Tiede K (2008) Nanoparticle analysis and characterization methodologies in environmental risk assessment of engineered nanoparticles. Ecotoxicology 17:344–361. doi: 10.1007/s10646-008-0225-x

Helfrich A, Brüchert W, Bettmer J (2006) Size characterisation of Au nanoparticles by ICP-MS coupling techniques. J Anal At Spectrom 21:431–434. doi: 10.1039/b511705d

Hendren CO, Mesnard X, Dröge J, Wiesner MR (2011) Estimating Production Data for Five Engineered Nanomaterials As a Basis for Exposure Assessment. Environ Sci Technol 45:2562–2569. doi: 10.1021/es103300g

Horst AM, Neal AC, Mielke RE, *et al* (2010) Dispersion of TiO2 Nanoparticle Agglomerates by Pseudomonas aeruginosa. Appl Environ Microbiol 76:7292–7298. doi: 10.1128/AEM.00324-10

Hotze EM, Bottero J-Y, Wiesner MR (2010) Theoretical Framework for Nanoparticle Reactivity as a Function of Aggregation State. Langmuir 26:11170–11175. doi: 10.1021/la9046963

Huijbregts M, Hauschild M, Jolliet O, *et al* (2010) USEtoxTM - User manual.

International Organization for Standardization (2008) Nanotechnologies - Terminology and definitions for nano-objects - Nanoparticle, nanofibre and nanoplate. ISOTS 276872008 7.

ISO (2006a) ISO 14040:2006 Environmental management - Life cycle assessment - Principles and framework. ISOTC 207SC 5 23.

ISO (2006b) ISO 14044:2006 Environmental management - Life cycle assessment - Requirements and guidelines. ISOTC 207SC 5 46.

Jang H, Kim S, Kim S (2007) Effect of particle size and phase composition of titanium dioxide nanoparticles on the photocatalytic properties. J Nanoparticle Res 3:141–147.

Jiang J, Oberdörster G, Elder A, *et al* (2008) Does nanoparticle activity depend upon size and crystal phase? Nanotoxicology 2:33–42. doi: 10.1080/17435390701882478

Johnston HJ, Hutchison GR, Christensen FM, *et al* (2009) Identification of the mechanisms that drive the toxicity of TiO2 particulates: the contribution of physicochemical characteristics. Part Fibre Toxicol 6:33. doi: 10.1186/1743-8977-6-33

Ju-Nam Y, Lead JR (2008) Manufactured nanoparticles: An overview of their chemistry, interactions and potential environmental implications. Sci Total Environ 400:396–414. doi: 10.1016/j.scitotenv.2008.06.042

Kaegi R, Wagner T, Hetzer B, *et al* (2008) Size, number and chemical composition of nanosized particles in drinking water determined by analytical microscopy and LIBD. Water Res 42:2778–2786. doi: 10.1016/j.watres.2008.02.009

Kalčíková G, Englert D, Rosenfeldt RR, *et al* (2014) Combined effect of UV-irradiation and TiO2-nanoparticles on the predator–prey interaction of gammarids and mayfly nymphs. Environ Pollut 186:136–140. doi: 10.1016/j.envpol.2013.11.028

Keller AA, Wang H, Zhou D, *et al* (2010) Stability and Aggregation of Metal Oxide Nanoparticles in Natural Aqueous Matrices. Environ Sci Technol 44:1962–1967. doi: 10.1021/es902987d

Kertész Z, Szikszai Z, Gontier E, *et al* (2005) Nuclear microprobe study of TiO2-penetration in the epidermis of human skin xenografts. Nucl Instrum Methods Phys Res Sect B Beam Interact Mater At 231:280–285. doi: 10.1016/j.nimb.2005.01.071

Kim J, Shan W, Davies SHR, *et al* (2009) Interactions of Aqueous NOM with Nanoscale TiO_2: Implications for Ceramic Membrane Filtration-Ozonation Hybrid Process. Environ Sci Technol 43:5488–5494. doi: 10.1021/es900342q

Kim K-T, Klaine SJ, Kim SD (2014) Acute and Chronic Response of Daphnia magna Exposed to TiO_2 Nanoparticles in Agitation System. Bull Environ Contam Toxicol 93:456–460. doi: 10.1007/s00128-014-1295-5

Kobayashi N, Naya M, Endoh S, *et al* (2009) Comparative pulmonary toxicity study of nano-TiO_2 particles of different sizes and agglomerations in rats: Different short- and long-term post-instillation results. Toxicology 264:110–118. doi: 10.1016/j.tox.2009.08.002

Kumar SA, Lo P-H, Chen S-M (2008) Electrochemical synthesis and characterization of TiO_2 nanoparticles and their use as a platform for flavin adenine dinucleotide immobilization and efficient electrocatalysis. Nanotechnology. doi: 10.1088/0957-4484/19/25/255501

Kuyper CL, Budzinski KL, Lorenz RM, Chiu DT (2006a) Real-Time Sizing of Nanoparticles in Microfluidic Channels Using Confocal Correlation Spectroscopy. J Am Chem Soc 128:730–731. doi: 10.1021/ja0569252

Kuyper CL, Fujimoto BS, Zhao Y, *et al* (2006b) Accurate Sizing of Nanoparticles Using Confocal Correlation Spectroscopy. J Phys Chem B 110:24433–24441. doi: 10.1021/jp064865w

Larue C, Castillo-Michel H, Sobanska S, *et al* (2014) Fate of pristine TiO_2 nanoparticles and aged paint-containing TiO2 nanoparticles in lettuce crop after foliar exposure. J Hazard Mater 273:17–26. doi: 10.1016/j.jhazmat.2014.03.014

Larue C, Laurette J, Herlin-Boime N, *et al* (2012) Accumulation, translocation and impact of TiO_2 nanoparticles in wheat (Triticum aestivum spp.): Influence of diameter and crystal phase. Sci Total Environ 431:197–208. doi: 10.1016/j.scitotenv.2012.04.073

Lecoanet HF, Bottero J-Y, Wiesner MR (2004) Laboratory Assessment of the Mobility of Nanomaterials in Porous Media. Environ Sci Technol 38:5164–5169. doi: 10.1021/es0352303

Ledin A, Karlsson S, Düker A, Allard B (1994) Measurements in situ of concentration and size distribution of colloidal matter in deep groundwaters by photon correlation spectroscopy. Water Res 28:1539–1545. doi: 10.1016/0043-1354(94)90220-8

Lee W-M, An Y-J (2013) Effects of zinc oxide and titanium dioxide nanoparticles on green algae under visible, UVA, and UVB irradiations: No evidence of enhanced algal toxicity under UV pre-irradiation. Chemosphere 91:536–544. doi: 10.1016/j.chemosphere.2012.12.033

Lekki J, Stachura Z, Dąbroś W, *et al* (2007) On the follicular pathway of percutaneous uptake of nanoparticles: Ion microscopy and autoradiography studies. Nucl Instrum Methods Phys Res Sect B Beam Interact Mater At 260:174–177. doi: 10.1016/j.nimb.2007.02.021

Li Bassi A, Cattaneo D, Russo V, *et al* (2005) Raman spectroscopy characterization of titania nanoparticles produced by flame pyrolysis: The influence of size and stoichiometry. J Appl Phys. doi: 10.1063/1.2061894

Li M, Czymmek KJ, Huang CP (2011) Responses of Ceriodaphnia dubia to TiO_2 and Al_2O_3 nanoparticles: A dynamic nano-toxicity assessment of energy budget distribution. J Hazard Mater 187:502–508. doi: 10.1016/j.jhazmat.2011.01.061

Lin P-C, Lin S, Wang PC, Sridhar R (2014a) Techniques for physicochemical characterization of nanomaterials. Biotechnol Adv 32:711–726. doi: 10.1016/j.biotechadv.2013.11.006

Lin X, Li J, Ma S, *et al* (2014b) Toxicity of TiO2 Nanoparticles to Escherichia coli: Effects of Particle Size, Crystal Phase and Water Chemistry. PLoS ONE 9:e110247. doi: 10.1371/journal.pone.0110247

Li S, Wallis LK, Ma H, Diamond SA (2014) Phototoxicity of TiO2 nanoparticles to a freshwater benthic amphipod: Are benthic systems at risk? Sci Total Environ 466-467:800–808. doi: 10.1016/j.scitotenv.2013.07.059

Liu HH, Cohen Y (2014) Multimedia Environmental Distribution of Engineered Nanomaterials. Environ Sci Technol 48:3281–3292. doi: 10.1021/es405132z

Liu X, Chen G, Keller AA, Su C (2013) Effects of dominant material properties on the stability and transport of TiO2 nanoparticles and carbon nanotubes in aquatic environments: from synthesis to fate. Environ Sci Process Impacts 15:169. doi: 10.1039/c2em30625e

Lopez-Serrano A, Munos Olivas R, Sanz Landaluze J, Carmen C (2014) Nanoparticles: a global vision. Characterization, separation, and quantification methods. Potential environmental and health impact. Anal Methods 6:38–56. doi: 10.1039/C3AY40517F

Lozano O, Mejia J, Tabarrant T, *et al* (2012) Quantification of nanoparticles in aqueous food matrices using Particle-Induced X-ray Emission. Anal Bioanal Chem 403:2835–2841. doi: 10.1007/s00216-012-5895-9

Luo P, Morrison I, Dudkiewicz A, *et al* (2013) Visualization and characterization of engineered nanoparticles in complex environmental and food matrices using atmospheric scanning electron microscopy. J Microsc 250:32–41. doi: 10.1111/jmi.12014

Ma H, Brennan A, Diamond SA (2012) Photocatalytic reactive oxygen species production and phototoxicity of titanium dioxide nanoparticles are dependent on the solar ultraviolet radiation spectrum. Environ Toxicol Chem 31:2099–2107. doi: 10.1002/etc.1916

Manke A, Wang L, Rojanasakul Y (2013) Mechanisms of Nanoparticle-Induced Oxidative Stress and Toxicity. BioMed Res Int 2013:1–15. doi: 10.1155/2013/942916

Mansfield CM, Alloy MM, Hamilton J, *et al* (2015) Photo-induced toxicity of titanium dioxide nanoparticles to Daphnia magna under natural sunlight. Chemosphere 120:206–210. doi: 10.1016/j.chemosphere.2014.06.075

Meena R, Kumar S, Paulraj R (2015) Titanium oxide (TiO_2) nanoparticles in induction of apoptosis and inflammatory response in brain. J Nanoparticle Res. doi: 10.1007/s11051-015-2868-x

Meesters JAJ, Koelmans AA, Quik JTK, *et al* (2014) Multimedia modeling of engineered nanoparticles with simpleBox4nano: Model definition and evaluation. Environ Sci Technol 48:5726–5736. doi: 10.1021/es500548h

Mielke RE, Priester JH, Werlin RA, *et al* (2013) Differential Growth of and Nanoscale TiO_2 Accumulation in Tetrahymena thermophila by Direct Feeding versus Trophic Transfer from Pseudomonas aeruginosa. Appl Environ Microbiol 79:5616–5624. doi: 10.1128/AEM.01680-13

Ming H, Ma Z, Huang H, *et al* (2011) Nanoporous TiO_2 spheres with narrow pore size distribution and improved visible light photocatalytic abilities. Chem Commun 47:8025–8027. doi: 10.1039/C1CC12557E

Money ES, Barton LE, Dawson J, *et al* (2014) Validation and sensitivity of the FINE Bayesian network for forecasting aquatic exposure to nano-silver. Sci Total Environ 473–474:685–691. doi: 10.1016/j.scitotenv.2013.12.100

Money ES, Reckhow KH, Wiesner MR (2012) The use of Bayesian networks for nanoparticle risk forecasting: Model formulation and baseline evaluation. Sci Total Environ 426:436–445. doi: 10.1016/j.scitotenv.2012.03.064

Mueller NC, Nowack B (2008) Exposure Modeling of Engineered Nanoparticles in the Environment. Environ Sci Technol 42:4447–4453. doi: 10.1021/es7029637

Murdock RC, Braydich-Stolle L, Schrand AM, *et al* (2008) Characterization of Nanomaterial Dispersion in Solution Prior to In Vitro Exposure Using Dynamic Light Scattering Technique. Toxicol Sci 101:239–253. doi: 10.1093/toxsci/kfm240

Nesic J, Rtimi S, Laub D, *et al* (2014) New evidence for TiO_2 uniform surfaces leading to complete bacterial reduction in the dark: Critical issues. Colloids Surf B Biointerfaces 123:593–599. doi: 10.1016/j.colsurfb.2014.09.060

Nogueira V, Lopes I, Rocha-Santos T, *et al* (2012) Impact of organic and inorganic nanomaterials in the soil microbial community structure. Sci Total Environ 424:344–350. doi: 10.1016/j.scitotenv.2012.02.041

Oberdürster G (2000) Toxicology of ultrafine particles: in vivo studies. Philos Trans R Soc Math Phys Eng Sci 358:2719–2740. doi: 10.1098/rsta.2000.0680

O'Brien CS (2003) A mathematical model for colloidal aggregation.

Olabarrieta J, Zorita S, Peña I, *et al* (2012) Aging of photocatalytic coatings under a water flow: Long run performance and TiO_2 nanoparticles release. Appl Catal B Environ 123-124:182–192. doi: 10.1016/j.apcatb.2012.04.027

Ottofuelling S, Von Der Kammer F, Hofmann T (2011) Commercial Titanium Dioxide Nanoparticles in Both Natural and Synthetic Water: Comprehensive Multidimensional Testing and Prediction of Aggregation Behavior. Environ Sci Technol 45:10045–10052. doi: 10.1021/es2023225

Petosa AR, Brennan SJ, Rajput F, Tufenkji N (2012) Transport of two metal oxide nanoparticles in saturated granular porous media: Role of water chemistry and particle coating. Water Res 46:1273–1285. doi: 10.1016/j.watres.2011.12.033

Pettibone JM, Cwiertny DM, Scherer M, Grassian VH (2008) Adsorption of Organic Acids on TiO_2 Nanoparticles: Effects of pH, Nanoparticle Size, and Nanoparticle Aggregation. Langmuir 24:6659–6667. doi: 10.1021/la7039916

Philippe A, Schaumann GE (2014) Evaluation of Hydrodynamic Chromatography Coupled with UV-Visible, Fluorescence and Inductively Coupled Plasma Mass Spectrometry Detectors for Sizing and Quantifying Colloids in Environmental Media. PLoS ONE 9:e90559. doi: 10.1371/journal.pone.0090559

Piccinno F, Gottschalk F, Seeger S, Nowack B (2012) Industrial production quantities and uses of ten engineered nanomaterials in Europe and the world. J Nanoparticle Res 14:1–11. doi: 10.1007/s11051-012-1109-9

Popović Z v., Dohčević-Mitrović Z, Šćepanović M, *et al* (2011) Raman scattering on nanomaterials and nanostructures. Ann Phys 523:62–74. doi: 10.1002/andp.201000094

Pottier A, Cassaignon S, Chanéac C, *et al* (2003) Size tailoring of TiO_2 anatase nanoparticles in aqueous medium and synthesis of nanocomposites. Characterization by Raman spectroscopy. J Mater Chem 13:877–882. doi: 10.1039/b211271j

Powers KW, Brown SC, Krishna VB, *et al* (2006) Research Strategies for Safety Evaluation of Nanomaterials. Part VI. Characterization of Nanoscale Particles for Toxicological Evaluation. Toxicol Sci 90:296–303. doi: 10.1093/toxsci/kfj099

Praetorius A, Scheringer M, Hungerbühler K (2012) Development of Environmental Fate Models for Engineered Nanoparticles—A Case Study of TiO_2 Nanoparticles in the Rhine River. Environ Sci Technol 46:6705–6713. doi: 10.1021/es204530n

Puzyn T, Rasulev B, Gajewicz A, *et al* (2011) Using nano-QSAR to predict the cytotoxicity of metal oxide nanoparticles. Nat Nanotechnol 6:175–178. doi: 10.1038/nnano.2011.10

Pyell U (2010) Characterization of nanoparticles by capillary electromigration separation techniques. Electrophoresis 31:814–831. doi: 10.1002/elps.200900555

Quaranta G, Adam V (2015) Nano TiO_2 Life Cycle Assessment Perspective. Encycl. Nanotechnol. Springer, p 15

Quik JTK, Stuart MC, Wouterse M, *et al* (2012) Natural colloids are the dominant factor in the sedimentation of nanoparticles. Environ Toxicol Chem 31:1019–1022. doi: 10.1002/etc.1783

Quik JTK, Velzeboer I, Wouterse M, *et al* (2014) Heteroaggregation and sedimentation rates for nanomaterials in natural waters. Water Res 48:269–279. doi: 10.1016/j.watres.2013.09.036

Quik JTK, Vonk JA, Hansen SF, *et al* (2011) How to assess exposure of aquatic organisms to manufactured nanoparticles? Environ Int 37:1068–1077. doi: 10.1016/j.envint.2011.01.015

Reed RB, Higgins CP, Westerhoff P, *et al* (2012) Overcoming challenges in analysis of polydisperse metal-containing nanoparticles by single particle inductively coupled plasma mass spectrometry. J Anal Spectrom 27:1093–1100. doi: 10.1039/c2ja30061c

Ridley MK, Hackley VA, Machesky ML (2006) Characterization and Surface-Reactivity of Nanocrystalline Anatase in Aqueous Solutions. Langmuir 22:10972–10982. doi: 10.1021/la061774h

Rosenbaum RK, Bachmann TM, Gold LS, *et al* (2008) USEtox—the UNEP-SETAC toxicity model: recommended characterisation factors for human toxicity and freshwater ecotoxicity in life cycle impact assessment. Int J Life Cycle Assess 13:532–546. doi: 10.1007/s11367-008-0038-4

Rosenbaum RK, Margni M, Jolliet O (2007) A flexible matrix algebra framework for the multimedia multipathway modeling of emission to impacts. Environ Int 33:624–634. doi: 10.1016/j.envint.2007.01.004

Rottman J, Sierra-Alvarez R, Shadman F (2013) Real-time monitoring of nanoparticle retention in porous media. Environ Chem Lett 11:71–76. doi: 10.1007/s10311-012-0381-3

Salamon AW (2013) The Current World of Nanomaterial Characterization: Discussion of Analytical Instruments for Nanomaterial Characterization. Environ Eng Sci 30:101–108. doi: 10.1089/ees.2012.0330

Salieri B (2013) The challenges and the limitations in Life Cycle Impact Assessment for metal oxide nanoparticles, a case study on nano-TiO_2. PhD. Dissertation, Bologna, Italy

Samontha A, Shiowatana J, Siripinyanond A (2011) Particle size characterization of titanium dioxide in sunscreen products using sedimentation field-flow fractionation–inductively coupled plasma–mass spectrometry. Anal Bioanal Chem 399:973–978. doi: 10.1007/s00216-010-4298-z

Sapsford KE, Tyner KM, Dair BJ, *et al* (2011) Analyzing Nanomaterial Bioconjugates: A Review of Current and Emerging Purification and Characterization Techniques. Anal Chem 83:4453–4488.

Savolainen K, Alenius H, Norppa H, *et al* (2010) Risk assessment of engineered nanomaterials and nanotechnologies—A review. Toxicology 269:92–104. doi: 10.1016/j.tox.2010.01.013

Schmidt J, Vogelsberger W (2006) Dissolution Kinetics of Titanium Dioxide Nanoparticles: The Observation of an Unusual Kinetic Size Effect. J Phys Chem B 110:3955–3963. doi: 10.1021/jp055361l

Simonet BM, Valcárcel M (2009) Monitoring nanoparticles in the environment. Anal Bioanal Chem 393:17–21. doi: 10.1007/s00216-008-2484-z

Simonin M, Guyonnet JP, Martins JMF, *et al* (2015) Influence of soil properties on the toxicity of TiO_2 nanoparticles on carbon mineralization and bacterial abundance. J Hazard Mater 283:529–535. doi: 10.1016/j.jhazmat.2014.10.004

Solovitch N, Labille J, Rose J, *et al* (2010) Concurrent Aggregation and Deposition of TiO_2 Nanoparticles in a Sandy Porous Media. Environ Sci Technol 44:4897–4902. doi: 10.1021/es1000819

Song U, Jun H, Waldman B, *et al* (2013) Functional analyses of nanoparticle toxicity: A comparative study of the effects of TiO_2 and Ag on tomatoes (Lycopersicon esculentum). Ecotoxicol Environ Saf 93:60–67. doi: 10.1016/j.ecoenv.2013.03.033

Song Y, Heien ML, Jimenez V, *et al* (2004) Voltammetric Detection of Metal Nanoparticles Separated by Liquid Chromatography. Anal Chem 76:4911–4919. doi: 10.1021/ac049223o

Song Z, Hrbek J, Osgood R (2005) Formation of TiO2 Nanoparticles by Reactive-Layer-Assisted Deposition and Characterization by XPS and STM. Nano Lett 5:1327–1332. doi: 10.1021/nl0505703

Stoeger T, Reinhard C, Takenaka S, *et al* (2006) Instillation of Six Different Ultrafine Carbon Particles Indicates a Surface Area Threshold Dose for Acute Lung Inflammation in Mice. Environ Health Perspect 114:328–333. doi: 10.1289/ehp.8266

Stone V (2009) Engineered Nanoparticles: Review of Health and Environmental Safety - Project Final Report. 426.

Suter GW (1993) Ecological Risk Assessment, Lewis Publishers. Boca Raton, FL

Technology Strategy Board (2009) Nanoscale Technologies Strategy. 47 pp.

Teleki A, Wengeler R, Wengeler L, *et al* (2007) Distinguishing between aggregates and agglomerates of flame-made TiO2 by high-pressure dispersion. Powder Technol 179:131–139. doi: 10.1016/j.powtec.2007.05.016

Thill A (1999) Agrégation des particules : structure, dynamique et simulation. Application au cas d'un écoulement stratifié : l'estuaire du Rhône. Ph.D. Dissertation, Université d'Aix-Marseille 3, France

Thio BJR, Zhou D, Keller AA (2011) Influence of natural organic matter on the aggregation and deposition of titanium dioxide nanoparticles. J Hazard Mater 189:556–563. doi: 10.1016/j.jhazmat.2011.02.072

Tiede K, Boxall A, Tear S, *et al* (2008) Detection and characterization of engineered nanoparticles in food and the environment. Food Addit Contam Part A 25:795–821. doi: 10.1080/02652030802007553

Tong T, Shereef A, Wu J, *et al* (2013) Effects of Material Morphology on the Phototoxicity of Nano-TiO2 to Bacteria. Environ Sci Technol 47:12486–12495. doi: 10.1021/es403079h

Tourinho PS, van Gestel CAM, Lofts S, *et al* (2012) Metal-based nanoparticles in soil: Fate, behavior, and effects on soil invertebrates. Environ Toxicol Chem 31:1679–1692. doi: 10.1002/etc.1880

US EPA (2011) Screening Methods for Metal-Containing Nanoparticles in Water. 41 pp.

Utsunomiya S, Ewing RC (2003) Application of High-Angle Annular Dark Field Scanning Transmission Electron Microscopy, Scanning Transmission Electron Microscopy-Energy Dispersive X-ray Spectrometry, and Energy-Filtered Transmission Electron Microscopy to the Characterization of Nanoparticles in the Environment. Environ Sci Technol 37:786–791. doi: 10.1021/es026053t

Von Der Kammer F, Baborowski M, Friese K (2005) Field-flow fractionation coupled to multi-angle laser light scattering detectors: Applicability and analytical benefits for the analysis of environmental colloids. Anal Chim Acta 552:166–174. doi: 10.1016/j.aca.2005.07.049

Von der Kammer F, Ferguson PL, Holden PA, *et al* (2012) Analysis of engineered nanomaterials in complex matrices (environment and biota): General considerations and conceptual case studies. Environ Toxicol Chem 31:32–49. doi: 10.1002/etc.723

Von der Kammer F, Legros S, Larsen EH, *et al* (2011) Separation and characterization of nanoparticles in complex food and environmental samples by field-flow fractionation. Trends Anal Chem 30:425–436. doi: 10.1016/j.trac.2010.11.012

Von der Kammer F, Ottofuelling S, Hofmann T (2010) Assessment of the physico-chemical behavior of titanium dioxide nanoparticles in aquatic environments using multi-dimensional parameter testing. Environ Pollut 158:3472–3481. doi: 10.1016/j.envpol.2010.05.007

Wagner T, Bundschuh T, Schick R, Köster R (2004) Detection of aquatic colloids in drinking water during its distribution via a water pipeline network. Water Sci Technol 50:27–37.

Wallis LK, Diamond SA, Ma H, *et al* (2014) Chronic TiO_2 nanoparticle exposure to a benthic organism, Hyalella azteca: impact of solar UV radiation and material surface coatings on toxicity. Sci Total Environ 499:356–362. doi: 10.1016/j.scitotenv.2014.08.068

Walther C, Büchner S, Filella M, Chanudet V (2006) Probing particle size distributions in natural surface waters from 15 nm to 2 µm by a combination of LIBD and single-particle counting. J Colloid Interface Sci 301:532–537. doi: 10.1016/j.jcis.2006.05.039

Wang C, Böttcher C, Bahnemann DW, Dohrmann JK (2004) In situ electron microscopy investigation of Fe (III)-doped TiO_2 nanoparticles in an aqueous environment. J Nanoparticle Res 6:119–122.

Wang J, Zhou G, Chen C, *et al* (2007) Acute toxicity and biodistribution of different sized titanium dioxide particles in mice after oral administration. Toxicol Lett 168:176–185. doi: 10.1016/j.toxlet.2006.12.001

WHO/EURO Technical Committee for Monitoring and Evaluating Airborne MMMF (1985) Reference methods for measuring airborne man-made mineral fibres (MMMF). Copenhagen

Xiong S, George S, Yu H, *et al* (2013) Size influences the cytotoxicity of poly (lactic-co-glycolic acid) (PLGA) and titanium dioxide (TiO_2) nanoparticles. Arch Toxicol 87:1075–1086. doi: 10.1007/s00204-012-0938-8

Zhang Y, Chen Y, Westerhoff P, *et al* (2008) Stability of commercial metal oxide nanoparticles in water. Water Res 42:2204–2212. doi: 10.1016/j.watres.2007.11.036

Zhou D, Abdel-Fattah AI, Keller AA (2012) Clay Particles Destabilize Engineered Nanoparticles in Aqueous Environments. Environ Sci Technol 46:7520–7526. doi: 10.1021/es3004427

Zhou D, Ji Z, Jiang X, *et al* (2013) Influence of Material Properties on TiO_2 Nanoparticle Agglomeration. PLoS ONE 8:e81239. doi: 10.1371/journal.pone.0081239

I.B. LIFE CYCLE ASSESSMENT AND RISK ASSESSMENT FOR THE ECOTOXICITY ASSESSMENT OF NANOMATERIALS – REVIEW OF SINGLE AND COMBINED APPROACHES

Submitted to Environmental Science and Pollution Research, under review.

The previous section reviews the general methodologies for LCA and RA of NMs. The following review of literature details the way in which these methodologies have been used for the NMs ecotoxicity assessment, whether combined or not, and discusses the benefits arising from their combination.

Life Cycle Assessment and Risk Assessment for the ecotoxicity assessment of nanomaterials

– Review of single and combined approaches –

Véronique Adam[ab], Gaetana Quaranta[a*], Stéphanie Loyaux-Lawniczak[a]

[a]: *Laboratoire d'Hydrologie et de Géochimie de Strasbourg / EOST / UDS*
1, rue Blessig
67084 Strasbourg Cedex
France

[b]: *French Environment and Energy Management Agency*
20, avenue du Grésillé
BP 90406
49004 Angers Cedex 01
France

corresponding author
Tel: +33 (0)3 68 85 03 79
Fax: +33 (0)3 68 85 04 02

Email addresses: quaranta@unistra.fr (G. Quaranta), veronique.adam@etu.unistra.fr (V. Adam), s.lawniczak@unistra.fr (S. Loyaux-Lawniczak).

Abstract

New technologies based on nanomaterials have been developed over the last decades, but high uncertainties remain regarding the fate and effects of these new materials in the environment. Life Cycle Assessment (LCA) and Risk Assessment (RA) are two tools that can be used to assess the potential harm of a substance onto different environmental compartments, based on the modeling of their fate and effects. Today there is consensus among authors that large benefits arise from the combination of these two approaches. This work aims at discussing the single and combined approaches of life cycle and risk assessments. It is shown that combining LCA and RA allows time- and site-specific assessments over several impact categories and over the whole life cycles of nanomaterials. However, more research on the ENMs fate, behavior and effects in the environment is needed to provide more reliable results. Consequently, probabilistic approaches such as Bayesian network (linking probability distributions of different variables) are recommended for the combination of LCA and RA of ENMs.

Keywords

Life Cycle Assessment, Risk Assessment, Life Cycle - Risk Assessment, Ecotoxicity, Nanomaterials

Introduction

The emergence of nanotechnologies gave impetus to the development of novel and innovative research both at academic and industrial levels. To date, the development of engineered nanomaterials (ENMs) has largely centered upon material discovery and manufacture, leading to rapid advances in their technological exploitation in different areas, such as textile, coatings, composites and medicine. This issue is addressed by the EU REACH Regulation n. 1907/2006 which gives industries the responsibility of the Chemical Safety Assessment (CSA) for any industrial substances. The CSA includes hazard assessment, exposure assessment and risk characterization. These different steps depend on the ecological risk assessment approach.

The safety of ENMs along their whole life cycle towards the human health and the environment should be ensured by industrials using the REACH guidance. The ENM life cycle assessment (LCA) requires taking into account the fate and the effects of nanoparticles (NPs) and their bulk material, by determining their physicochemical properties, their interactions with different matrices and their behavior towards different organisms in response to various modes of exposure.

However, even if more and more studies were performed on NPs in the last decade, high uncertainties remain regarding their fate, behavior and toxicological effects in the environment, and regarding the methodological approaches to model these parameters for the assessment of their environmental impacts and their risks. Consequently, a framework able to deal with these uncertainties is needed for the environmental assessment of ENMs. LCA, described as an environmental impact assessment tool for products, processes or services over their whole life cycles (ISO 2006), and risk assessment (RA), defined as the process of assessing magnitudes and probabilities of human activities or natural catastrophes adverse effects, are two methodologies used to assess the impacts and risks of substances in the environment. Today, there is consensus among scientists on combining these two tools in order to overcome their respective limitations. This will be the focus of this paper.

This work presents single and combined approaches of LCA and RA applies to ENMs ecotoxicity and highlights the benefits arising from a combined tool.

1. Life Cycle Assessment of nanomaterials

1.1 Conceptual framework of Life Cycle Assessment

Life Cycle Assessment (LCA) is an environmental impact assessment tool for products, processes or services over their whole life cycles (ISO 2006). It is conducted in four stages following the requirements of the ISO 14040 (Figure 1):

(1) determination of the goal, scope and system boundaries
(2) inventory analysis of inputs and outputs
(3) assessment of environmental impacts
(4) interpretation of results with proposals for improvement

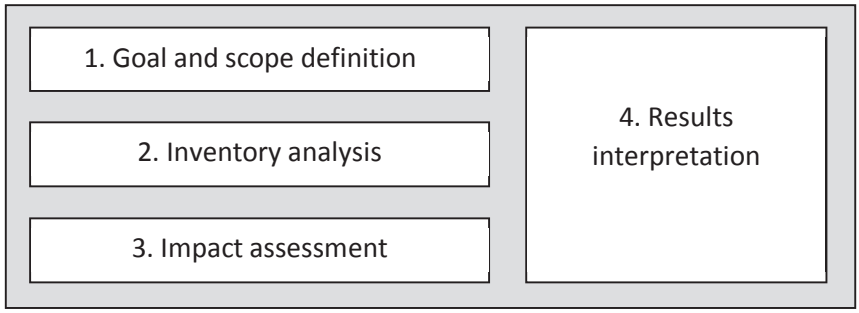

Figure 1: Life Cycle Assessment framework (ISO 14040 2006)

In the determination of the goal, scope and system boundaries, the authors are also requested to define a functional unit, which is the unit to which all inventory data and impact assessment results will be referred to (e.g. 1 kg of product).

The life cycle inventory analysis consists in collecting data concerning energy and material inputs and outputs from the system under study.

In the impact assessment stage (LCIA), inventory data are assigned to different impact categories (such as global warming potential, eutrophication, or ecotoxicity) and the calculation of category indicators (CIs) is achieved using characterization factors (CFs).

The category indicator is the numerical expression of the life cycle inventory results conversion (Eq.1) (Ghazi *et al*. 2011; Huijbregts *et al*. 2000):

$$CI_i = \sum_{e=1}^{e=m} \sum_{x=1}^{x=n} CF_{i,x,e} \times M_{x,e} \qquad (1)$$

Where CI_i is the impact score for category *i*, $M_{x,e}$ the substance mass (LCI results); and $CF_{i,x,e}$ the characterization factor of impact category *i* for substance *x* due to an emission to compartment *e* (dimensionless).

Many LCIA calculation methods/models are available, each providing different CFs for different impact categories. Among the most frequently used are CML, Impact 2002+, and ReCiPe. All of them rely on fate and effect data (transport, transformation, and ecotoxicity values), and calculate characterization factors (CF) as the combination of a fate factor (FF) with an effect factor (EF) specific to a given substance *i* (Equation 2):

$$CF_i = FF_i \times EF_i \quad (2)$$

However, when working on ecotoxicity, and especially in the aim of combining LCA with RA, it is important to explicitly take into account the exposure of organisms to the substance under study. This has been done in the USEtox model with the introduction of an exposure factor. USEtox is defined as an environmental model for the characterization of human and freshwater toxicological impacts, and has been developed by a team of experts that had built previous methods. In this consensus method, the ecotoxicological characterization factor of a chemical is expressed as the product of an exposure factor (XF), with a fate factor (FF) and an effect factor (EF). So according to Rosenbaum *et al*. (2008):

$$CI_i = M_i \times XF_i \times FF_i \times EF_i \quad (3)$$

Here, the exposure factor is defined as the bioavailable fraction of the substance. However, as it is discussed in the following section, it was shown that NPs specific properties (such as size, surface area or functionality) need to be taken into account in the calculation of the exposure, fate, and effect factors (Adam *et al*. 2015, Gavankar *et al*. 2012).

1.2. Assessing the ecotoxicity of NMs with LCA

When studying ENMs, ecological toxicity (terrestrial or aquatic) is rarely included in the impact assessments: to our knowledge, only 14 ENMs LCAs have been conducted on these impact categories. This is mostly due to a lack of data regarding ENMs production processes on one hand, and fate and effects on ecosystems on the other hand, which hampers robust modeling and ecotoxicity assessment (Eckelman *et al*. 2012; Roes *et al*. 2007; Gavankar *et al*. 2012; Upadhyayula *et al*. 2012).

Although a few studies conducted LCAs over the whole life cycle of the studied ENM (Babaizadeh and Hassan 2013; Fufa *et al*. 2013), most of the reviewed LCAs are performed on the production step of the life cycle (e.g. Griffiths *et al*. 2013; Eckelman *et al*. 2012). There is an urgent need for more impact assessments of use and end-of-life stages, as these stages are also potential sources of ENMs releases in the environment (Dahlben *et al*. 2013).

Moreover, the functional units are frequently defined on the basis of ENM mass (Khanna *et al*. 2008), while it was shown that other metrics, such as surface area or number concentration, could be more representative of the toxic effects of NPs at the production stage (Auffan *et al*. 2009; Adam *et al*. 2015; Hischier and Walser, 2012). However, when comparing ENMs impacts with those of traditional materials, the use of functional unit based on the service provided by the nanoproduct or on its performance may be useful (Hischier and Walser 2012). In most studies, it is the amount of produced nanoproduct that is used as a functional unit (Bauer *et al*. 2008; Babaizadeh *et al*. 2013, Fufa *et al*. 2013, Meyer *et al*. 2011, Walser *et al*. 2011; Lloyd and Lave 2003; Lloyd *et al*. 2005).

Finally, most of the time, authors do not use CFs specific to ENMs properties, as they are not currently available in the LCI databases and LCIA calculation methods (Gavankar *et al*. 2012; Hischier *et al*. 2012). To our knowledge, Salieri (2013) is the only one that took into account the size distribution of TiO_2 ENMs in her calculations of a CF for nano-TiO_2 in the USEtox method. Eckelman *et al*. (2012) calculated a CF for CNTs in USEtox, though no distinction was made between the different kinds of CNTs. These CFs differ by several orders of magnitude depending on the data used.

Therefore, even if the USEtox model can be used as a basis for the ecotoxicity assessment of ENMs, it needs to be refined in order to fully account for NM-specific properties (Eckelman *et al*. 2012). This cannot be without concomitant fulfilling of LCI databases with relevant parameters such as size, aggregation state, surface area, etc. (Hischier and Walser 2012). However, the use of the CFs cited above is recommended, as they are the only ones available accounting for some of the specific characteristics of NMs, even if they are calculated at a continental scale.

Besides, ecotoxicity assessment would benefit from the use of a site-specific scale, which is a scale reduced to the study area, implying detailed knowledge of the ecosystem surrounding the site under study and taking into account environmental parameters specific to the study area (Potting and Hauschild 2006, Rodriguez *et al*. 2014). The use of such a scale would reduce uncertainties about the

values of the environmental parameters feeding the fate and ecotoxicity models (Adam *et al*. 2015). This is not the case in any of the studies reviewed here, as all the methods used include CFs averaged at a global or continental scale. This is the main point where LCA would benefit from a combination with RA, as discussed in the following sections.

2. Risk Assessment of nanomaterials

2.1. Conceptual frameworks for Risk Assessment of ENMs

Risk assessment (RA) is defined by Suter (1993) as the process of assessing magnitudes and probabilities to the adverse effects of human activities or natural catastrophes. It is conducted in four steps (Savolainen *et al*. 2010):

(1) Hazard identification: Substance properties that may cause hazards to organisms are identified.
(2) Hazard characterization: Dose-response relationships and mechanisms of toxicity of the substance are defined.
(3) Exposure assessment: Exposure, that is concentration organisms are in contact with, is determined. The sources, pathways and routes of exposure should also be assessed.
(4) Risk assessment: The risk is calculated as the product of an exposure factor with a hazard factor.

Most usually, the ecological risk assessment of a substance is calculated by dividing the PEC (Predicted Environmental Concentration) of a specific chemical in a given compartment (e.g. air, water or soil) by its PNEC (Predicted No Effect Concentration). PNEC is the highest concentration of the substance safe for the environment. It therefore defines the toxicity of the substance in the environment. PEC is the foreseeable concentration of the substance in the environment. It therefore defines the exposure of the natural environment to the substance.

However, uncertainties remain on the behaviour of ENMs in the different environmental compartments and on their effects on organisms. Consequently, probabilistic approaches such as Bayesian networks (that are networks linking probability distributions of different variables) may provide help in accurately assessing the ecological risks of ENMs. Both these approaches and their use in currently available literature are discussed in the following section.

2.2. Assessing the ecotoxicity of ENMs with RA

Most ENMs RA studies concern freshwater, as the ecotoxicological data is the most abundant for this compartment (Table 1). Ag and TiO_2 NMs are most frequently assessed, followed by carbon-based NMs, such as CNTs and fullerenes (Table 2).

Table 1: Number of reviewed studies quantitatively assessing the environmental risks of NMs in different natural environmental compartments

Studied compartment	Risk quotient	Bayesian networks	Total number of studies
Freshwater	7	2	9
Freshwater sediment	1	2	3
Soil	3	0	3
Air	1	0	1

Table 2: Number of reviewed studies quantitatively assessing the environmental risks of NMs

Studied ENM	Risk quotient	Bayesian networks	Total number of studies
Ag	5	1	6
CNT	2	0	2
Fullerene	1	0	1
TiO_2	5	0	5
ZnO	3	0	3

Quantitative risks are most usually calculated as a risk ratio or risk quotient (RQ), dividing the PEC of a specific chemical by its PNEC.

Usually, for conventional chemicals PEC is determined by monitoring data. They should normally be used in preference to calculation. For ENMs, due to lack of data, the authors used data from literature (Stone 2009, Aschberger *et al*. 2011), their own calculations (Johnson *et al*. 2011), estimations (Mueller and Nowack 2008), or probability distributions (Blaser *et al*. 2008, Gottschalk *et al*. 2013) to define a PEC.

The PNEC is usually estimated from laboratory ecotoxicological tests results applied to the studied substance. The PNECs can be derived from ecotoxicological data such as NOECs, using an extrapolation factor of 1/1000 to account for the low data accuracy (Mueller and Nowack 2008; Stone *et al*. 2009, Johnson *et al*. 2011, Gottschalk *et al*. 2009, Williams *et al*. 2009).

When PNECs were not available, the highest observed no-effect concentrations (HONECs) (Blaser *et al*. 2008) or the INEC (indicative no effect concentration) may also be used to take into account the uncertainties in the nanomaterials toxicity assessment (Aschberger *et al*. 2011).

Gottschalk *et al*. (2013) assessed ENMs effects using a generic probability species sensitivity distribution (PSSD). Available toxic values for a species were used to produce a probability density function for each environmental compartment, and single species distributions were combined into the generic PSSD.

Another methodology that uses probability distributions is based on Bayesian networks (BNs). A BN consists of a set of variables (or "nodes") linked by a set of arrows (Figure 2). It takes the form of a directed acyclic graph, meaning that there is no cycle in the network (Kashuba 2010). Nodes represent variables, and arrows represent the probabilistic relations between the variables (Kashuba 2010). Each variable has a finite set of mutually exclusive states, and to each variable B with parents $A_1,...,A_n$ there is an attached conditional probability table (CPT): $P(B|A_1,...,A_n)$ (Jensen and Nielsen 2007).

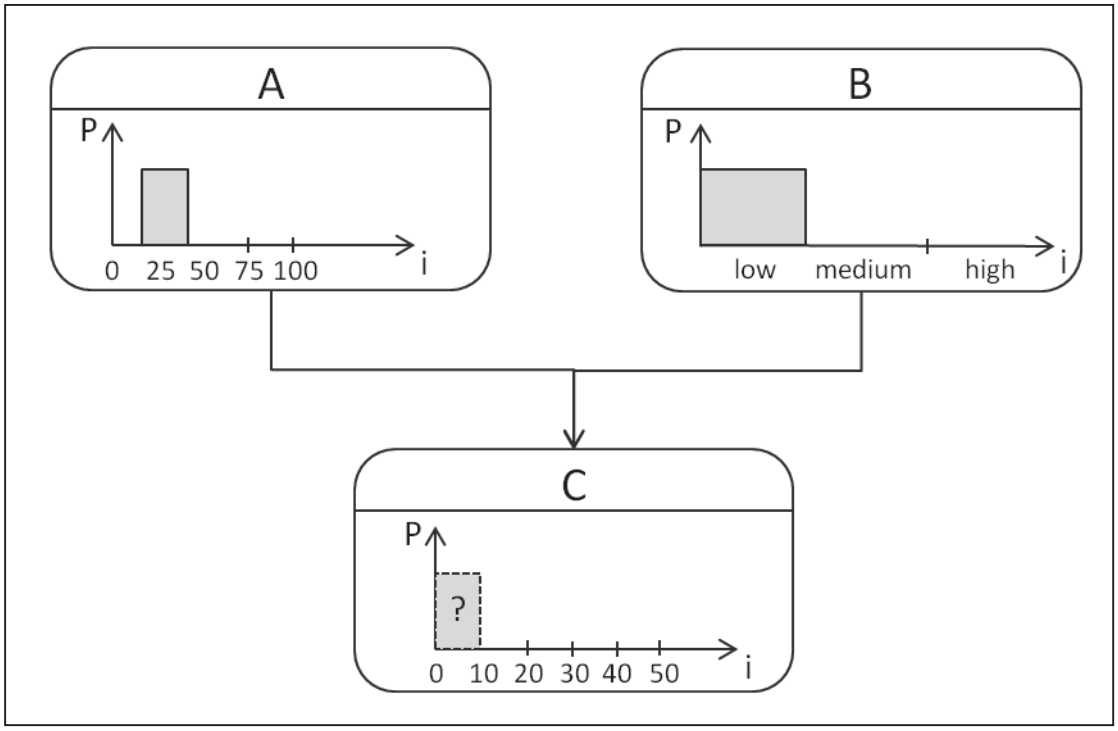

Figure 2: Example of a Bayesian network. Parent variables are A and B, the child variable is C. Probability (P) is assigned for each state (i) of the variables

BNs present various advantages that make them particularly useful to use in nanomaterials RA. Firstly, the results' uncertainties are directly visible in the network, as values are expressed as probability distributions: the higher the uncertainty, the wider the probability distribution (Uusitalo 2007). Another advantage of BNs is that they can be used even when very low data is available (Kontkanen *et al*. 1997; Uusitalo 2007). When little data is available, authors can use expert elicitation to attribute probabilities to parameters values (Kashuba 2010; Morgan 2005; Pollino *et al*. 2007). Finally, BNs can be updated with the calculation of new probability distributions as new data become available (Kashuba 2010). BNs advantages also include the ability to combine categorical and continuous variables, and empirical data with expert judgment (Marcot *et al*. 2001). All these characteristics are particularly appropriate considering the high lack of data regarding ENMs. However, extended use of expert elicitation and high data uncertainty can lead to uninformative models.

To our knowledge, BNs have been used to assess environmental risks of Ag ENMs only (Money *et al*. 2012, 2014). Expert elicitation was used to build the model and to determine the CPTs. Direct expert elicitation of the CPTs was achieved following four steps (Figure 2): (1) experts were presented with a completed diagram of the network, and an empty CPT for each child node; (2) a probability for each cell in the CPT was elicited by asking the following type of questions: "Given that A has a value between 0 and 25 and B is "Low", out of 100 independent experiments, how many times would you expect C to be between 0 and 10?"; (3) the question was repeated using every possible state combination of the parent variables. When the CPT was complete, it was input into the Netica v.4.09 software (a Bayesian network development software); and (4) the experts were asked to rate their confidence in each CPT on a scale from 1 to 10.

3. Combining LCA and RA for the assessment of ENMs ecotoxicity

3.1. Differences and similarities in LCA and RA structures

Even though LCA and RA are two tools used for environmental evaluation, one of the major differences between these two methodologies relies in their final goals. RA aims at assessing the environmental risk of a chemical, whereas LCA aims at assessing the impacts of a whole product (Grieger *et al*. 2012; Olsen *et al*. 2001). Consequently, LCA results are aggregates across substances, and include more industrial processes than RA, which is specific to one substance (Solocof and Geibig 2006; Udo de Haes *et al*. 2006). Furthermore, the final goal of LCA is to *compare* different scenarios, or processes, whereas RA aims at assessing the risk *magnitude* of a substance (Cowell *et al*. 2002), so LCA provides relative results, whereas RA results in an absolute value (Grieger *et al*. 2012; Linkov and Seager 2011; Olsen *et al*. 2001; Socolof and Geibig 2006; Udo de Haes *et al*. 2006). The relative character of LCA is due to the use of a functional unit, to which resources and chemical flows are related (Udo de Haes *et al*. 2006), and which allows the comparison between different scenarios.

Another important difference between these two tools is that RA is fundamentally time- and site-specific, which is not the case of LCA due to the use of a functional unit (Assies 1998; Barnthouse *et al*. 1997; Eason *et al*. 2011; Olsen *et al*. 2001; Socolof and Geibig 2006; Udo de Haes *et al*. 2006; Wegener Sleeswijk *et al*. 2003). This induces higher uncertainties than in RA, where actual flows are used (Bare *et al*. 2006; Udo de Haes *et al*. 2006). Moreover, risk scores are calculated at a given time, while impacts are averaged over several years in LCA.

LCA covers a large number of impact categories, thus including a larger number of environmental impact parameters than RA, which is based primarily on ecotoxicological data (Grieger *et al*. 2012). Furthermore, most-realistic data are used in LCA, whereas worst-case data are often used in RA (Udo de Haes *et al*. 2006). However, the same type of ecotoxicological data is used in both cases.

As stated earlier, both methodologies are conducted in four steps. The classification step of LCIA can be considered similar to the hazard identification step of RA (Table 3). In the same way, life cycle inventory and fate modeling can be likened to exposure assessment in RA; exposure and effect modeling is then considered as the third step of LCA, similar to hazard assessment in RA; and the damage modeling and interpretation of results in LCA is analogous to risk characterization (Udo de Haes *et al*. 2006).

Table 3: Differences and similarities in LCA and RA structures

LCA	RA	LCA + RA
1. Definition of goal and scope of the study	1. Hazard identification	1. Hazard identification and classification
2. Life cycle inventory	2. Dose-response assessment	2. Exposure (fate) assessment
3. Life cycle impact assessment	3. Exposure assessment	3. Hazard (effect) assessment
4. Results interpretation	4. Risk characterization	4. Risk/impact characterization

Moreover, the calculations of exposures and effects in LCA and RA are based on the same chemical and ecotoxicological data and processes (Pennington *et al*. 2006; Udo de Haes *et al*. 2006). This could constitute the basis of the combination of these tools. The aggregation of data is possible in both methods over initial release compartments (Grieger *et al*. 2012; Udo de Haes *et al*. 2006).

3.2. Performing LCRA for the assessment of ENMs ecotoxicity

Various ways of combining RA and LCA have been suggested. For this purpose, Benetto *et al*. (2007) suggested either: (1) combining LCA and RA results into new impact results, (2) substituting LCA results by the ones from (1), and (3) defining new impact categories in addition to LCA categories, in order to include RA results. The second combination had already been identified by Flemström *et al*. (2004), with the use of ecotoxicological models in LCA.

Grieger *et al*. (2012) distinguished two other approaches for combining LCA and RA. (1) The "life cycle-based RA" approach consists in conducting a traditional RA in a life cycle perspective, i.e. at each life cycle stage. This approach has also been proposed by Kuczenski *et al*. (2011), and has been used by Wardak *et al*. (2008). Flemström *et al*. (2004) suggested conducting a RA on every emission identified in the life cycle inventory. (2) The "RA-complemented LCA" approach consists of a conventional LCA complemented by a RA at specific life-cycle steps. In this case, LCA may be used as a screening tool, for identification of critical lifecycle steps requiring RA. According to Grieger *et al*. (2012), this is the only approach which truly combines LCA and RA. It has been used by Linkov and Seager (2011), Shatkin (2008a, 2008b), Som *et al*. (2010), Sweet and Strohm (2006), and has been implemented in the CEA framework (Anastas and Davis 2010; Davis 2007; US EPA 2010a, 2010b, 2009) and Nano LCRA (Shatkin 2009, 2008a, 2008b), as well as in the Nano Risk Framework (Environmental Defense and DuPont 2007a, 2007b, 2007c). Applications of both approaches are detailed in the following sections.

3.2.1. "Lyfe-cycle-based RA" approach

Wardak *et al*. (2008) implemented a life cycle-based approach for qualitative RA using expert elicitation and literature review, in order to identify which ENMs pose greater risks and where these risks occur in the nanoproduct life cycle. Expert elicitation was used to gather information on nanoproducts, to build use and disposal scenarios, and to identify nanoparticles properties (triggers) that induce greater exposure- or hazard-related risks. Once the expert elicitation results were collected, scenarios and triggers were given a score of 1 to 5, (low to high, respectively), considering their severity and probability. This resulted in a score for exposure and another for hazard for both these categories. The higher hazard-related and exposure-related scores of a nanoproduct, the higher its potential risk. Hazard and exposure scores of 3 or more lead to high-risk scenarios and triggers, which were proposed as hot spots where research should be prioritized.

A case study was conducted on an air freshener spray containing silver NPs. Risk hot spots were identified as the intersections of high-risk triggers with high risk scenarios, which lead to high risks (Table 4).

Table 4: Evaluation of environmental risks of an air freshener spray containing silver nanoparticles (Wardak *et al*. 2008)

	Use – inhalation	**Use – skin adsorption**	**Use – air release**	**Disposal – water entrainment**
Dispersibility and bioavailability	Medium	Medium	High	High
Catalytic property	High	Medium	High	Medium
Antibacterial properties	High	High	Medium	High
Susceptible population	High	High	Low	Low
Coating stability	Medium	Medium	High	Medium

3.2.2.“RA-complemented LCA” approach

3.2.2.1 Nano Life Cycle Risk Assessment

Nano Life Cycle Risk Assessment (LCRA) is an adaptive framework in which new information can be implemented as it becomes available on exposure and risk potentials of ENMs. According to Shatkin (2008b), a screening approach was required as not enough information was yet available on nanotechnology to conduct quantitative assessments.

Nano LCRA consists in the ten following steps : (1) Description of the product life cycle, (2) Identification of the materials and assessment of potential hazards at each lifecycle stage, (3) Qualitative exposure assessment for materials at each lifecycle stage, (4) Identification of lifecycle stages at which exposure may occur, (5) Evaluation of the potential ecotoxicity at key lifecycle stages, (6) Analysis of risk potential for selected lifecycle stages, (7) Identification of key uncertainties and data gaps, (8) Development of mitigation/risk management strategies, (9) Gathering additional information, Iteration of the process, revisiting assumptions, and adjustment of evaluation and management steps. This framework has been used by Shatkin *et al*. (2010) to assess occupational risks of quantum dots in paint. Results show low risks to the environment. According to these authors, major advantages of the framework are that it is affordable, easily implemented, and requires little data. It can be used to prioritize future research needs (Shatkin 2008a; 2009; Shatkin *et al*. 2010).

The Nano Risk Framework is an example of the Nano LCRA framework (Eason *et al*. 2011). It has been developed by the Environmental Defense and DuPont (2007a, 2007b, 2007c), and consists in the following steps (ED and DuPont, 2007a): (1) description of the material and its application, (2) lifecycle description, (3) evaluation of risks, (4) assessment of risk management, (5) decision, documentation and action and (6) reviewing and adaptation. This framework was applied to TiO_2 in a light stabilizer (ED and DuPont 2007b), and to CNTs in polymer nanocomposites (ED and DuPont 2007c). Results from the risk assessment of nano TiO_2 in the DuPont™ light stabilizer show low risks to aquatic organisms (ED and DuPont, 2007b). Risks arising from the integration of MWCNTs into polymer nanocomposites by melt processing are low for the aquatic compartment and the soil, as well as those due to incineration ash (ED and DuPont 2007c). Shatkin (2008b) points out that the Nano Risk Framework requires a lot of data that only an organization such as DuPont might be able to implement.

3.2.2.2 Comprehensive Environmental Assessment

The Comprehensive Environmental Assessment (CEA) framework can be used for a quantitative RA providing sufficient data are available. It is conducted in the following steps: (1) qualitative description of the product life cycle, (2) identification of transport and transformation within and across environmental compartments, and (3) exposure and effects assessment of a contaminant in these compartments, across all life cycle stages of a product (Davis 2007; Shatkin 2008b). Exposure characterization includes routes of exposure, aggregate exposure across routes, cumulative exposure to multiple contaminants associated with the NM, and various spatiotemporal dimensions (Shatkin 2008b). The consideration of exposure before conducting effect evaluations avoids unnecessary research (Shatkin 2008b).

The CEA was used by the US EPA which assessed the nano-TiO_2 risks in sunscreen and water treatment (US EPA 2009), and the risks of silver nanomaterials in a disinfectant spray (US EPA 2010b). No general conclusions concerning the overall risks of the NMs could be drawn from these two case studies, due to lack of data.

Ogilvie-Hendren (2010) focused on specific building blocks of the CEA framework, which are assessments of fate and exposure to silver NMs released by a wastewater treatment plant (WWTP). The fate of nano-TiO_2 and four types of nano-Ag surface chemistries were compared in the WWTP. The exposure model considers releases of NMs to various environmental compartments at different life cycle stages. Magnitudes of NM sources were estimated based on publications and patents related to these NMs. Fractions of NMs reaching the WWTP were then estimated from literature review and by direct measurements in wastewater. Population factors and wastewater treatment facility parameters such as detention times or solids concentrations were also estimated, as well as partitioning coefficients, which were estimated from previous scientific work and results from batch partitioning tests. The NM concentrations in wastewater effluent and sludge were then estimated based on Monte Carlo simulations. Finally, a sensitivity analysis was conducted. Results show a high variability of Ag concentrations in wastewater effluent and sludge around the mean values. However, it was concluded that 95% of effluent concentrations would fall below 0.12 $\mu g.L^{-1}$, and that 95% of sludge concentrations would fall below 0.35 $\mu g.L^{-1}$. These concentrations were considered relevant to be used in ecotoxicological tests.

3.2.2.3 An integrated framework combining LCA, RA and multi-criteria decision analysis

Multi-criteria decision analysis (MCDA) has been applied by Canis *et al*. (2010) and Linkov and Seager (2011) to build an integrated framework, with the aim of prioritizing future research needs concerning RA of NMs over their life cycle. This framework consists in four steps:

(1) Definition of the problem and decision context: Problem, boundaries of analysis, relevant effect end-points and a functional unit are identified, and cognitive maps and influence diagrams are constructed.
(2) Identification of stakeholders, decision-makers, assessment criteria, and weight estimates.
(3) Definition and assessment of management alternatives.
(4) Application of MCDA under uncertainty: Data are normalized into uniform or dimensionless units for comparison of results. A weighted average is computed to each criterion, and the different alternatives are ranked according to their weighted scores.

3.3. Benefits arising from the combination of LCA and RA

A limited number of frameworks are available for combined LCA and RA, and to date only three NM types were assessed in the available literature, namely nano-Ag, nano-TiO_2, and CNTs. Furthermore, to our knowledge, no quantitative RA in a life cycle perspective has been conducted on ENMs, due to lack of data.

Combining RA and LCA would allow overcoming their respective limitations. Indeed, environmental risk assessment (ERA) generally considers ecotoxicity only, so that negative impacts on other categories (such as climate change) that could arise from the mitigation of ecotoxicity are not acknowledged. The wide range of impact categories in LCA allows stakeholders to have a more comprehensive view of the system under study (Christensen and Olsen 2004). In the same way, the consideration of all emissions over the whole life cycle of the substance, as it is the case in LCA, would make RA a more powerful decision support (Dusinska *et al*. 2012; Eason *et al*. 2011; Linkov and Seager 2011), and would also allow improving the life cycle processes (Sweet and Strohm 2006). On another hand, the time- and site-specific design of ERA would benefit to LCA, reducing results uncertainties.

Conclusion

Most of the reviewed studies point out the high lack of data regarding ENMs exposure and effects, the need for the implementation of prediction models for their fate and behavior within the environment and consequently the need for further research concerning their environmental risks. Lopez-Serrano *et al*. (2014) specify that further environmental risks of NPs will have to be tested under regulatory schemes such as REACH, to set regulations fixing the limits at which NMs can be found in the environment. However, Pronk *et al*. (2009) have already identified ten kinds of issues that need further attention before all the REACH concepts can be properly applied to nanomaterials. Among these issues, it has been demonstrated that more information is required on physicochemical properties (e.g. on size and size distribution, shape, specific surface area, agglomeration/aggregation state and dissolution characteristics). Another fundamental point is ecotoxicity testing, as the extended use of *in vitro* (screening) methods that is currently occurring under REACH is not a viable option for NMs. Indeed, various knowledge gaps remain, and the issue of the best metric to use in dose-response analysis still needs to be resolved.

Even if it is recognized that the application of ENMs may pose a risk to human health and the environment and even if there is a general consensus that the potential health and environmental risks of ENMs should be evaluated over their entire life cycles (Lazarevic and Finndveden 2013), available LCA and RA results include high uncertainties, and no quantitative combined RA and LCA has yet been published.

Nevertheless, combining LCA and RA into one tool would allow time- and site-specific assessments over a wide range of impact categories and over whole life cycles. Scientists should be able to use such a framework that should also allow a clear visualization of uncertainties. Bayesian networks provide such a basis. They could be used at each step of the NM life cycle, and be readily updated as new information becomes available. Consequently, they are recommended as the best framework for the combination of LCA and RA of engineered nanomaterials.

Acknowledgements

This work was supported by the French National research Agency (MESONNET project), the French Environment and Energy Management Agency (ADEME) and the Alsace Region.

References

Adam V, Loyaux-Lawniczak S, Quaranta G (2015) Characterization of Engineered TiO2 Nanomaterials in a Life Cycle and Risk Assessments Perspective. Envir. Sci Poll Res. DOI 10.1007/s11356-015-4661-x

Anastas P, Davis M (2010) BOSC nanomaterial case studies workshop review letter report. US Environmental Protection Agency Office of Research and Development, Board of Scientific Counselors (BOSC). http://www.epa.gov/osp/bosc/pdf/nano1008rpt.pdf. Accessed 20 March 2013

Aschberger K, Micheletti C, Sokull-Klüttgen B, Christensen FM (2011) Analysis of currently available data for characterizing the risk of engineered nanomaterials to the environment and human health – lessons learned from four case studies. Environ Int 37:1143-1156

Assies JA (1998) A risk-based approach to life-cycle impact assessment. J Hazard Mater 61:23-29

Auffan M, Rose J, Bottero JY, Lowry GV, Jolivet JP, Wiesner MR (2009) Towards a definition of inorganic nanoparticles from an environmental, health and safety perspective. Nat Nanotechnol. DOI:10.1038.NNANO.2009.242

Babaizadeh H, Hassan M (2013) Life cycle assessment of nano-sized titanium dioxide coating on residential windows. Construction Build Mater 40:314-321

Bare JC (2006) Risk Assessment and Life-Cycle Assessment (LCIA) for Human Health Cancerous and Noncancerous Emissions: Integrated and Complementary with Consistency within the USEPA. Hum Ecol Risk Assess 12:493-509

Barnthouse L, Fava J, Humphreys K, *et al*. (eds) (1997) Life-Cycle Impact Assessment: The State-of-the-Art. SETAC, Pensacola, FL, USA

Bauer C, Buchgeister J, Hischier R, Poganietz WR, Shebek L, Warsen J (2008) Towards a framework for life cycle thinking in the assessment of nanotechnology. J Clean Prod 16:910-926

Benetto E, Tiruta-Barna L, Perrodin Y (2007) Combining lifecycle and risk assessments of mineral waste reuse scenarios for decision making support. Environ Impact Assess Rev 27:266-285

Blaser SA, Scheringer M, MacLeod M, Hungerbühler K (2008) Estimation of cumulative aquatic exposure and risk due to silver: Contribution of nano-functionalized plastics and textiles. Sci Total Environ 390:396-409

Canis L, Seager T, Linkov I (2010) Selecting Nanomanufacturing Technology Using Integrated Risk, Life Cycle Assessment And Decision-Analytical Framework. Environ Sci Technol 44(22):8704-8711

Christensen FM, Olsen SI (2004) The potential role of life cycle assessment in regulation of chemicals in the European Union. Int J LCA 9(5):327-332

Cowell SJ, Fairman R, Lofstedt RE (2002) Use of Risk Assessment and Life Cycle Assessment in Decision Making: A Common Policy Research Agenda. Risk Anal 22(5):879-894

Dahlben LJ, Eckelman MJ, Hakimian A, Somu S, Isaacs JA (2013) Environmental Life Cycle Assessment of a Carbon Nanotube-Enabled Semiconductor Device. Environ Sci Technol 47:8471-8478

Davis JM (2007) How to Assess the Risks of Nanotechnology: Learning From Past Experience. J Nanosci Nanotechnol 7:402-409

Dusinska M, Fjellsbo LM, Olsen S, *et al*. (2012) Final Report with Recommendations for Impact Assessment of Engineered Nanomaterials. Institute of Work and Health, Lausanne, Switzerland. www.nanoimpactnet.eu/uploads/Deliverables/D3.10.pdf. Accessed 20 February 2015

Eason T, Meyer DE, Curran MA, Upadhyayula VKK (2011) Guidance to Facilitate Decisions for Sustainable Nanotechnology. EPA/600/R-11/107. http://nepis.epa.gov/Adobe/PDF/P100CH93.pdf. Accessed 20 February 2015

Eckelman MJ, Mauter MS, Isaacs JA, Elimelech M (2012) New Perspectives on Nanomaterial Aquatic Ecotoxicity: Production Impacts Exceed Direct Exposure Impacts for Carbon Nanotubes. Environ Sci Technol 46:2902-2910

Environmental Defense, DuPont (2007a) Nano Risk Framework. http://qsinano.com/wp-content/uploads/2014/05/nano_risk_framework_dupont.pdf. Accessed 20 February 2015

Environmental Defense, DuPont (2007b) Nanomaterial Risk Assessment Worksheet DuPont™ Light Stabilizer. http://epa.gov/oppt/nano/dupont1.pdf. Accessed 20 February 2015

Environmental Defense, DuPont (2007c) Nanomaterial Risk Assessment Worksheet – Incorporation of Single and Multi Walled Carbon Nano Tubes (CNTs) into Polymer Nanocomposites by Melt Processing. www2.dupont.com/Media_Center/en_US/assets/downloads/pdf/NRAW_CNT.pdf. Accessed 20 February 2015

EU (2006) Regulation (EC) No 1907/2006 of the European Parliament and of the Council of 18 December 2006 concerning the Registration, Evaluation, Authorisation and Restriction of Chemicals (REACH), establishing a European Chemicals Agency, amending Directive 1999/45/EC and repealing Council Regulation (EEC) No 793/93 and Commission Regulation (EC) No 1488/94 as well as Council Directive 76/769/EEC and Commission Directives 91/155/EEC, 93/67/EEC, 93/105/EC and 2000/21/EC. Official Journal of the European Union L 396, 30.12.2006, p.1–849; as corrected by OJ L 136, 29.5.2007, p.3–280.

Flemström K, Carlson R, Erixon M (2004) Relationships Between Life Cycle Assessment and Risk Assessment – Potentials and Obstacles. Naturvardsverket Report 5379. www.naturvardsverket.se/Nerladdningssida/?fileType=pdf&downloadUrl=/Documents/publikationer/620-5379-5.pdf. Accessed 20 February 2015

Fufa SM, Jelle BP, Bohne RA, Grossrieder C (2013) LCA of nano-coated wooden claddings utilizing accelerated ageing test results. Proceedings from the 7th Nordic Conference on Construction Economics and Organisation, Trondheim, 12-14 June 2013. Pp. 102-110. http://www.detgarbra.no/publish/tidsskrift/omtidsskrift/35. Accessed 20 February 2015

Gavankar S, Suh S, Keller AF (2012) Life cycle assessment at a nanoscale: review and recommendations. Int J Life Cycle Assess 17:295-303

Ghazi M, Quaranta G, Duplay J, Hadj Amor R, Khodja M, Ait Amar H, Kessaissia Z (2011) The Life-Cycle Impact Assessment of oil drilling mud system in Algerian arid area. Resour Conservat Recycl 55:1222-1231

Gottschalk F, Kost E, Nowack B (2013) Engineered nanomaterials in water and soils: A risk quantification based on probabilistic exposure and effect modeling. Environ Toxicol Chem 32(6):1278-1287

Gottschalk F, Sonderer T, Scholz RW, Nowack B (2009) Modeled environmental concentrations of engineered nanomaterials (TiO_2, ZnO, Ag, Fullerenes) for different regions. Environ Sci Technol 43:9216-9222

Grieger KD, Laurent A, Miseljic M, Christensen F, Baun A, Olsen SI (2012) Analysis of current research addressing complementary use of life-cycle assessment and risk assessment for engineered nanomaterials: Have lessons been learned from previous experience with chemicals? J Nanopart Res 14:958-970

Griffiths OG, O'Byrne JP, Torrente-Murciano L, Jones MD, Mattia D, McManus MC (2013) Identifying the largest environmental life cycle impacts during carbon nanotube synthesis via chemical vapour deposition. J Clean Prod 42:180-189

Hischier R, Walser T (2012) Life cycle assessment of engineered nanomaterials: State of the art and strategies to overcome existing gaps. Sci Total Environ 425:271-282

Huijbregts MAJ, Thissen U, Guinée JB, Jager T, Kalf D, van de Meent D, Ragas AMJ, Wegener Sleeswijk A, Reijnders (2000) Priority assessment of toxic substances in life cycle assessment. Part I: Calculation of toxicity potentials for 181 substances with the nested multi-media fate, exposure and effects model USES-LCA. Chemosphere 41:541-573

ISO 14040 (2006) Environmental management – Life cycle assessment – Principles and framework. http://www.iso.org/iso/catalogue_detail.htm?csnumber=37456. Accessed 5 August 2013

Jensen FV, Nielsen TD (2007) Causal and Bayesian Networks. In: Bayesian Networks and Decision Graphs, Springer Science + Business Media, LLC, Pp. 23-50.

Johnson AC, Bowes MJ, Crossley A *et al*. (2011) An assessment of the fate, behavior, and environmental risk associated with sunscreen TiO_2 nanoparticles in UK field scenarios. Sci Total Environ 409:253-2510

Kashuba RO (2010) Bayesian Methods to Characterize Uncertainty in Predictive Modeling of the Effect of Urbanization on Aquatic Ecosystems. Dissertation, Department of Environment – Duke University

Khanna V, Bakshi BR, Lee LJ (2008) Carbon Nanofiber Production – Life Cycle Energy Consumption and Environmental Impact. J Ind Ecol 12(3):394-410

Kontkanen P, Myllymäki P, Silander T, Tirri H (1997) Comparing predictive inference methods for discrete domains. In: Proceedings of the sixth International Workshop on Artifical Intelligent Techniques, Ft. Lauderdale, USA, pp. 311-318

Kuczenski B, Geyer R, Boughton B (2011) Tracking Toxicants: Towards a Life Cycle Aware Risk Assessment. Environ Sci and Technol 45:45-50

Lazarevic D, Finndeveden G (2013) Life cycle aspects of nanomaterials. Environmental strategies Research, KTH - Royal Institute of Technology, Stockholm, Sweden

Linkov I, Seager TP (2011) Coupling Multi-Criteria Decision Analysis, Life Cycle Assessment, and Risk Assessment for Emerging Threats. Environ Sci Technol 45:5068-5074

Lloyd SM, Lave SB, Matthews HS (2005) Life Cycle Benefits of Using Nanotechnology To Stabilize Platinum-Group Metal Particles in Automotive Catalysts. Environ Sci Technol 39:1384-1392

Lloyd SM, Lave LB (2003) Life Cycle Economic and Environmental Implications of Using Nanocomposites in Automobiles. Environ Sci Technol 37:3458-3466

López-Serrano A, Muñoz Olivas R, Sanz Landaluze J, Cámara C (2014) Nanoparticles: a global vision. Characterization, separation, and quantification methods. Potential environmental and health impact. Anal Methods 6:38-56

Marcot BG, Holthausen RS, Raphael MG, Rowland MM, Wisdom MJ (2001) Using Bayesian belief networks to evaluate fish and wildlife population viability under land management alternatives from an environmental impact statement. For Ecol Manage 153:29-42

Meyer DE, Curran MA, Gonzalez MA (2011) An examination of silver nanoparticles in socks using screening-level life cycle assessment. J Nanopart Res 13:147-156

Money ES, Barton LE, Dawson J, Reckhow KH, Wiesner MR (2014) Validation and sensitivity of the FINE Bayesian network for forecasting aquatic exposure to nano-silver. Sci Total Environ 473-474:685-691

Money ES, Reckhow KH, Wiesner MR (2012) The use of Bayesian networks for nanoparticle risk forecast: Model formulation and baseline evaluation. Sci Tot Environ 426:436-445

Morgan K (2005) Development of a Preliminary Framework for Informing the Risk Analysis and Risk Management of Nanoparticles. Risk Anal 25(6). DOI:10.1111/j.1539-6924.2005.00681.x.

Mueller NC, Nowack B (2008) Exposure modeling of engineered nanoparticles in the environment. Environ Sci Technol 42(12):4447-4453

Ogilvie-Hendren CC (2010) Framing and Assessing Environmental Risks of Nanomaterials. Dissertation, Department of Civil and Environmental Engineering, Duke University

Olsen SI, Christensen FM, Hauschild M, Pederson F, Larsen HF, Torslov J (2001) Life cycle impact assessment and risk assessment of chemicals – A methodological comparison. Environ Impact Assess Rev 21:385-404

Pennington DW, Margni M, Payet J, Jolliet O (2006) Risk and Regulatory Hazard-Based Toxicological Effect Indicators in Life-Cycle Assessment (LCA). Hum Ecol Risk Assess 12:450-475

Pollino CA, Woodberry O, Nicholson A, Korb K, Hart BT (2007) Parameterisation and evaluation of a Bayesian network for use in an ecological risk assessment. Environ Model Softw 22:1140-1152

Potting J, Hauschild MZ (2006) Spatial Differentiation in Life Cycle Impact Assessment – A decade of method development to increase the environmental realism of LCIA. Int J LCA 11 (Special Issue 1):11-13

Pronk MEJ, Wijnhoven SWP, Bleeker EAJ, Heugens EHW, Peijnenburg WJGM, Luttik R, Hakkert BC (2009) Nanomaterials under REACH - Nanosilver as a case study. Report. RIVM, NL. 143. 2009. 145 pp. http://www.rivm.nl/bibliotheek/rapporten/601780003.pdf. Accessed 18 June 2013

Rodriguez C, Ciroth A, Srocka M (2014) The importance of regionalized LCIA in agricultural LCA – new software implementation and case study. Proceedings from the 9th International Conference LCA of Food, San Francisco, USA, 8-10 October 2014.

Roes AL, Marsili E, Nieuwlaar E, Patel MK (2007) Environmental and Cost Assessment of a Polypropylene Nanocomposite. J Polymer Environ 15:212-226

Rosenbaum RK, Bachmann TM, Swirsky Gold L, Huijbregts MAJ, Jolliet O, Juraske R, Koehler A, Larsen HF, MacLeod M, Margni M, McKone TE, Payet J, Schuhmacher M, van de Meent D, Hauschild MZ (2008) USEtox-the UNEP-SETAC toxicity model: recommended characterization factors for human toxicity and freshwater ecotoxicity in life cycle impact assessment. Int J LCA. DOI 10.1007/s11367-008-0038-4

Salieri B (2013) The challenges and the limitations in Life Cycle Impact Assessment for metal oxide nanoparticles, a case study on nano-TiO_2. Dissertation, University of Bologna, Italy

Savolainen K, Alenius H, Norppa H, Pylkkänen L, Tuomi T, Kasper G (2010) Risk assessment of engineered nanomaterials and nanotechnologies – A review. Toxicol 269:92-104

Shatkin JA, Larsen W, Nick R, Hospital J, Coe-Sullivan S (2010) Investigating the Life Cycle Risks of a Nanomaterial in Paint Using Nano LCRA. Proceedings from the New England Nanomanufacturing Summit, UMASS Lowell. http://eprints.internano.org/510/ Accessed 20 February 2015

Shatkin JA (2009) Risk Analysis for Nanotechnology: State of the Science and Implications. USDA, Washington, DC. http://www.usda.gov/oce/risk_assessment/risk_forums/Shatkin100709.pdf. Accessed 20 February 2015

Shatkin JA (2008a) Informing Environmental Decision Making by Combining Life Cycle Assessment and Risk Analysis. J Ind Ecol 12(3):278-281

Shatkin JA (2008b) Nanotechnology – Health and Environmental Risks. CRC Press, Boca Raton, FL

Socolof ML, Geibig JR (2006) Evaluating Human and Ecological Impacts of a Product Life Cycle: The Complementary roles of Life-Cycle Assessment and Risk Assessment. Hum Ecol Risk Assess 12:510-527

Som C, Berges M, Chaudhry Q, Dusinska M, Fernandes TF, Olsen SI, Nowack B (2010) The importance of life cycle concepts for the development of safe nanoproducts. Toxicol 269:160-169

Stone V (2009) Engineered Nanoparticles: Review of Health and Environmental Safety. Project Final Report. 426 pp. http://nmi.jrc.ec.europa.eu/project/ENRHES.htm. Accessed 7 January 2013

Suter GW (1993) Ecological Risk Assessment. Lewis Publishers, Boca Raton, FL, USA

Sweet L, Strohm B (2006) Nanotechnology – Life-Cycle Risk Management. Hum Ecol Risk Assess 12:528-551

Udo de Haes HA, Wegener Sleeswijk A, Heijungs R (2006) Similarities, Differences and Synergisms Between HERA and LCA – An Analysis at Three Levels. Hum Ecol Risk Assess 12:431-449

Upadhyayula VKK, Meyer DE, Curran MA, Gonzalez MA (2012) Life cycle assessment as a tool to enhance the environmental performance of carbon nanotube products: a review. J Clean Prod 26:37-47

US EPA (2010a) State of the Science Literature Review: Nano Titanium Dioxide Environmental Matters. STREAMS Final Report EPA/600/R-10/089. http://www.epa.gov/nanoscience/files/NanoPaper2.pdf. Accessed 20 February 2015

US EPA (2010b) External Review Draft – Nanomaterial Case Study: Nanoscale Silver in Disinfectant Spray. EPA/600/R-10/081. http://cfpub.epa.gov/ncea. Accessed 20 February 2015

US EPA (2009) External Review Draft - Nanomaterial Case Studies: Nanoscale Titanium Dioxide in Water Treatment and in Topical Sunscreen. EPA/600/R-09/057. ofmpub.epa.gov/eims/eimscomm.getfile?p_download_id=490825. Accessed 20 February 2015

Uusitalo L (2007) Advantages and challenges of Bayesian networks in environmental modeling. Ecol Model 203:312-318

Walser T, Demou E, Lang DJ, Hellweg S (2011) Prospective Environmental Life Cycle Assessment of Nanosilver T-Shirts. Environ Sci and Technol 45:4570-4578

Wardack A, Gorman ME, Swami N, Deshpande S (2008) Identification of Risks in the Life Cycle of Nanotechnology-Based Products. J Ind Ecol 12(3):435-448

Wegener Sleeswijk A, Heijungs R, *et al*. (2003) Risk assessment and life-cycle assessment: Fundamentally different yet reconciliable. Green Manage Int 41:77-87

Williams RJ, Keller VDJ, Johnson AC, *et al*. (2009) A national risk assessment for intersex in fish arising from steroid estrogens. Environ Toxicol Chem 28:220-230.

I.C. PRESENTATION OF THE STUDY AREA

Introduction

The state-of-the-art presented above highlights the need for site-specific lifecycle and risk assessments of TiO_2 ENMs. For this purpose, environmental parameters need to be determined based on the specific physical, chemical and biological properties of the site under study. In this work, the study area consists in the factory, its waste treatment site and a near 10 km² area including the river section in which the industrial effluents are released. The first step of such an assessment is to acquire some knowledge about the studied production site, the surrounding environmental compartments and the natural processes taking place in the study area, as they all play a role in the transfer and transformation (aggregation) of TiO_2 NPs in the environment. It is also important to identify the potential targets at risk. This section meets this goal by describing firstly the potential source of engineered TiO_2 NPs that is their production site, then the natural phenomena influencing their behavior in the environmental compartments and finally the potentially affected species present in the study area.

1. Industrial site and processes

1.1. Industrialization of the study area

The nano-TiO_2 NPs producer (CRISTAL) is located in Northern France, in the Thur watershed (Figure 1). This valley has a long history of industrialization, beginning in the late XVIIIth century. On the whole watershed, 382 industrialized sites have been inventoried in the BASIAS database (basias.brgm.fr/donnees.asp), whether abandoned or not. 101 of these sites are upstream of Thann and Vieux-Thann. 4 sites are classified as SEVESO II high level, including CRISTAL FRANCE SAS at Thann, PPC Potasse et Produits Chimiques at Vieux-Thann, as well as DUPONT DE NEMOURS and BIMA 83 at Cernay. This heavy industrialization context induces various pollutions of soils and groundwater, mostly caused by hydrocarbon, arsenic and halogenated solvants upstream of Thann (BASOL database, Table 1). The Thur river water was heavily polluted by mercury in the late XXth century, and such punctual pollutions still occur today. Other potential contamination can be caused mostly by hydrocarbon, metals (e.g. As, Cr, Cu, Zn), sulfates and halogenated compounds (Ministère de l'Ecologie, du Développement Durable et de l'Energie 2014). The studied factory is the only industry releasing titanium in the Thur River.

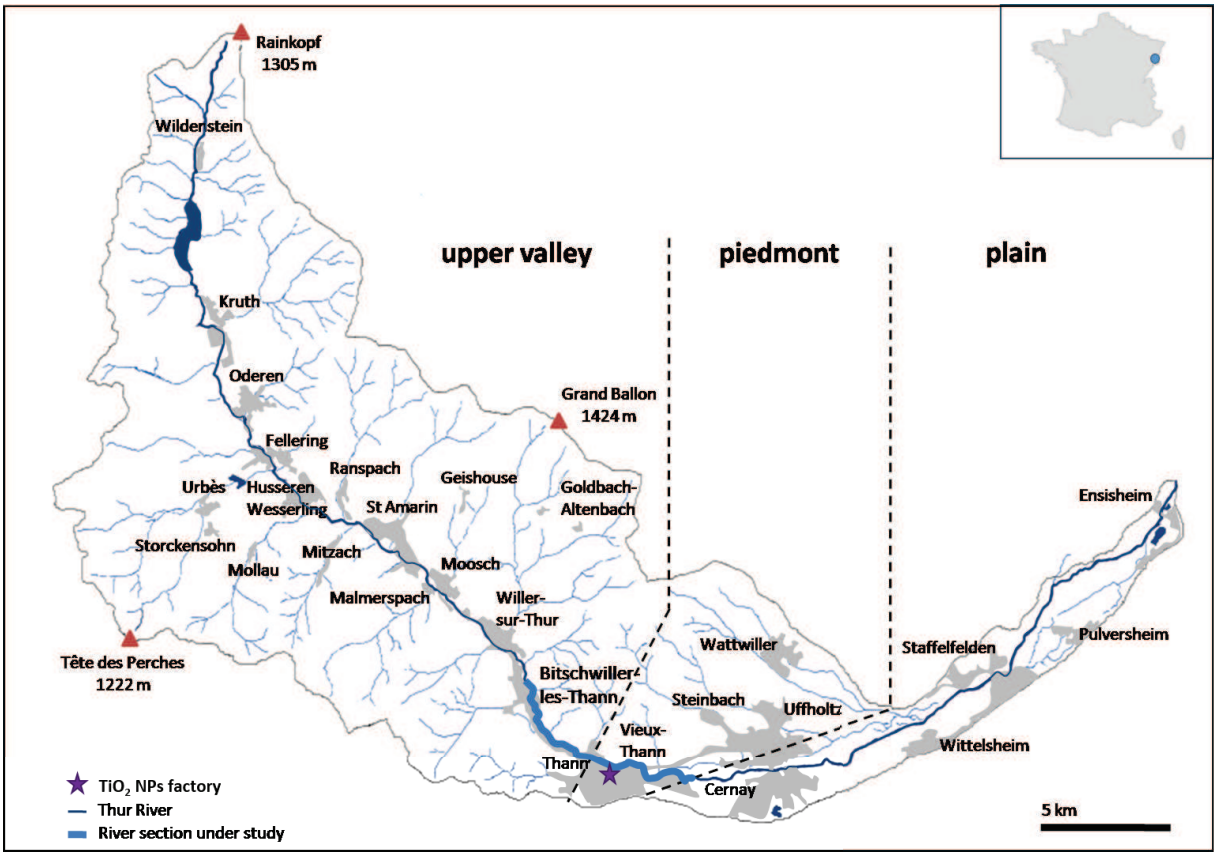

Figure 1: Location of the TiO_2 producing plant and the river section under study. Grey zones are urbanized.

Table 1: Industrialized sites (BASIAS database – *basias.brgm.fr/donnees.asp*) and inventoried pollutions (BASOL database - *basol.developpement-durable.gouv.fr*) in the Thur watershed communes. Potential Ti pollution can appear at Thann and Vieux-Thann.

Commune	**Number of industrialized sites (BASIAS)**	**Number of inventoried (potentially) polluted sites (BASOL)**	**Polluted compartments**	**Nature of pollutants**
Wildenstein	1	0	-	-
Kruth	4	0	-	-
Oderen	5	0	-	-
Urbès	1	0	-	-
Fellering	6	0	-	-
Husseren-Wesserling	4	1	n.a.	n.a.
Ranspach	1	0	-	-
Mitzach	2	0	-	-
St-Amarin	18	2	groundwater and soil	hydrocarbon, As, halogenated solvents
Moosch	11	0	-	-
Malmerspach	10	0	-	-
Goldbach-Altenbach	1	0	-	-
Willer-sur-Thur	15	1	groundwater and soil	hydrocarbons
Bitschwiller-les-Thann	22	0	-	-
Thann	65	2	groundwater and soil	hydrocarbon, As, Cr, Cu, Ni, Pb
Vieux-Thann	31	3	groundwater and soil	As, Cr, Hg, hydrocarbon, cyanides, Ba, halogenated solvents
Cernay	76	4	groundwater and soil	halogenated solvents, pesticides, metals (Cr, Ni, Zn)
Steinbach	6	0	-	-
Uffholtz	7	0	-	-
Wattwiller	7	0	-	-
Wittelsheim	29	0	-	-
Staffelfelden	15	0	-	-
Pulversheim	8	0	-	-
Ensisheim	37	0	-	-

1.2. TiO_2 production process

In the environment, Ti can be found as ilmenite ($FeTiO_3$), sphene ($CaSiTiO_5$), perovskite ($CaTiO_3$), or titanium dioxide (TiO_2). TiO_2 occurs as three crystalline phases: anatase, rutile and brookite, anatase and rutile being the predominant forms.

The factory produces anatase TiO_2 NPs for use in paints and cements, as well as pigmentary TiO_2 (µm size range). The TiO_2 NPs fabrication process is divided in two sectors: the first one, called “black sector”, starts with the extraction of titanium from ilmenite ($FeTiO_3$) and slag ores by sulfuric acid, from which a titanyl sulfate solution is produced. This enters the so-called “white sector”, which includes the hydrolysis of the solution leading to the crystallization of titanium dioxide. The TiO_2 is then washed, neutralized, filtrated, atomized or calcined, and finally sieved or grinded, to obtain the final nanoparticulate and pigmentary TiO_2 (Figure 2).

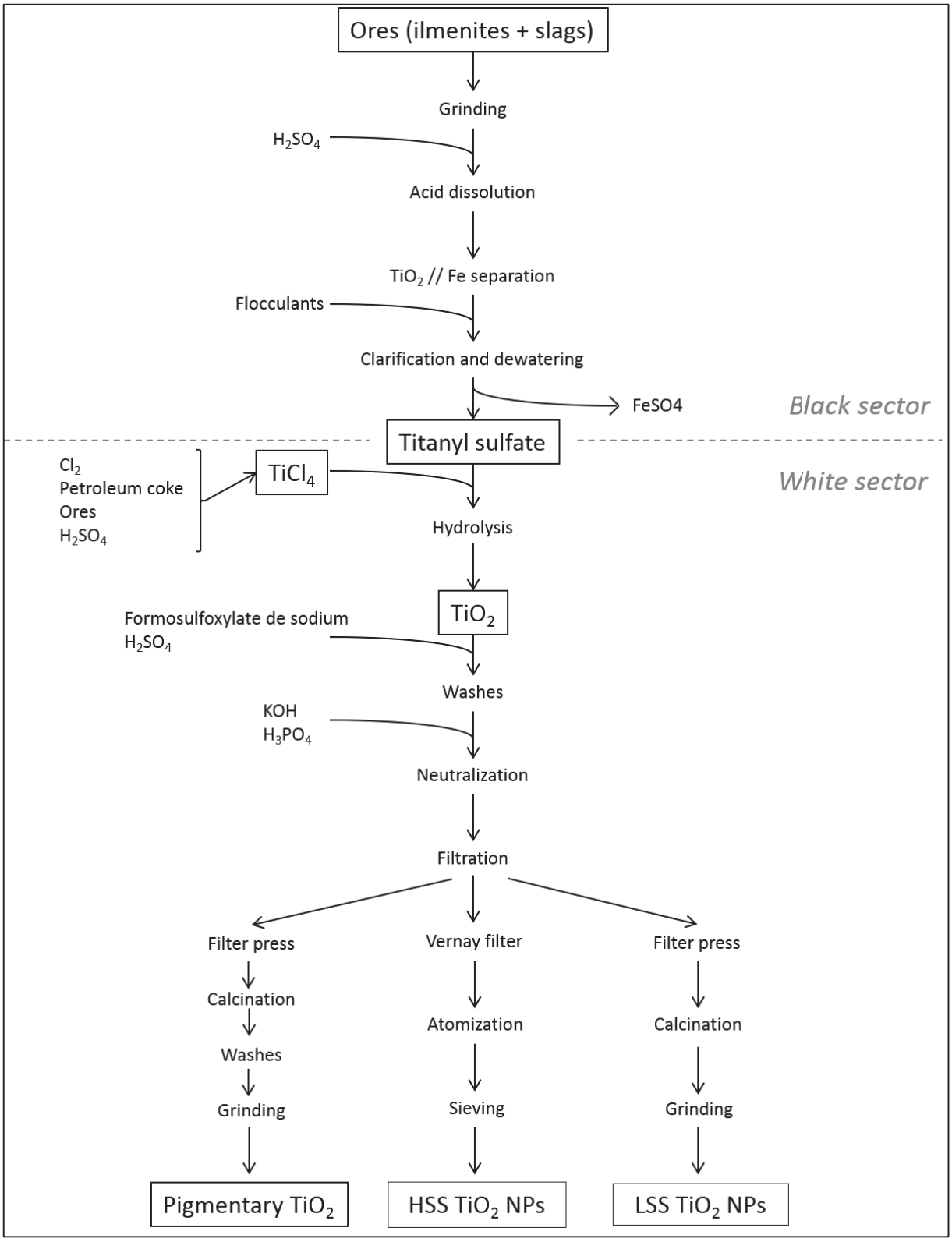

Figure 2: Nanoparticulate and pigmentary TiO_2 fabrication process (adapted from a factory communication)

Three types of industrial effluents are released into the Thur River (Figures 3 and 4):

(1) “blue effluents” are composed of cooling and runoff waters. Flow, temperature, pH and conductivity are monitored continuously. Fe and suspended particulate matter (SPM) concentrations are determined daily; DOC, Cl^-, SO_4^{2-} and Na^+ concentrations are controlled monthly; N, Al, Mg, Mn, Zn, Cu, Cr, As, Hg concentrations are determined quarterly, and Cd, Sn, Pb, Ni and V concentrations are determined once a year. Below conformity thresholds, “blue” effluents are released at point T (mean outflow in 2014: 6778 $m^3.d^{-1}$) in the industrial channel. In case of non-conformity, they are directed into a retention and sedimentation basin before being directed to the Ochsenfeld wastewaster treatment plant (WWTP);

(2) “red effluents” come from the industrial process itself and are treated at the Ochsenfeld WWTP. The treatment consists in neutralizing the effluents with lime. These effluents are released into the river at point NN (mean outflow: 2500 $m^3.d^{-1}$);

(3) other effluents come from the leaching of the Ochsenfeld slag heap. They are released into the river at point NNR (mean outflow: 672 $m^3.d^{-1}$). This slag heap is the result of decades of accumulation of different solid wastes, coming mostly from the potash and TiO_2 industries in the Thur valley. Today, it is covered with red gypsum, coming from the TiO_2 production process and used as a rainproofing.

Effluents NN and NNR are released at the same location in the river.

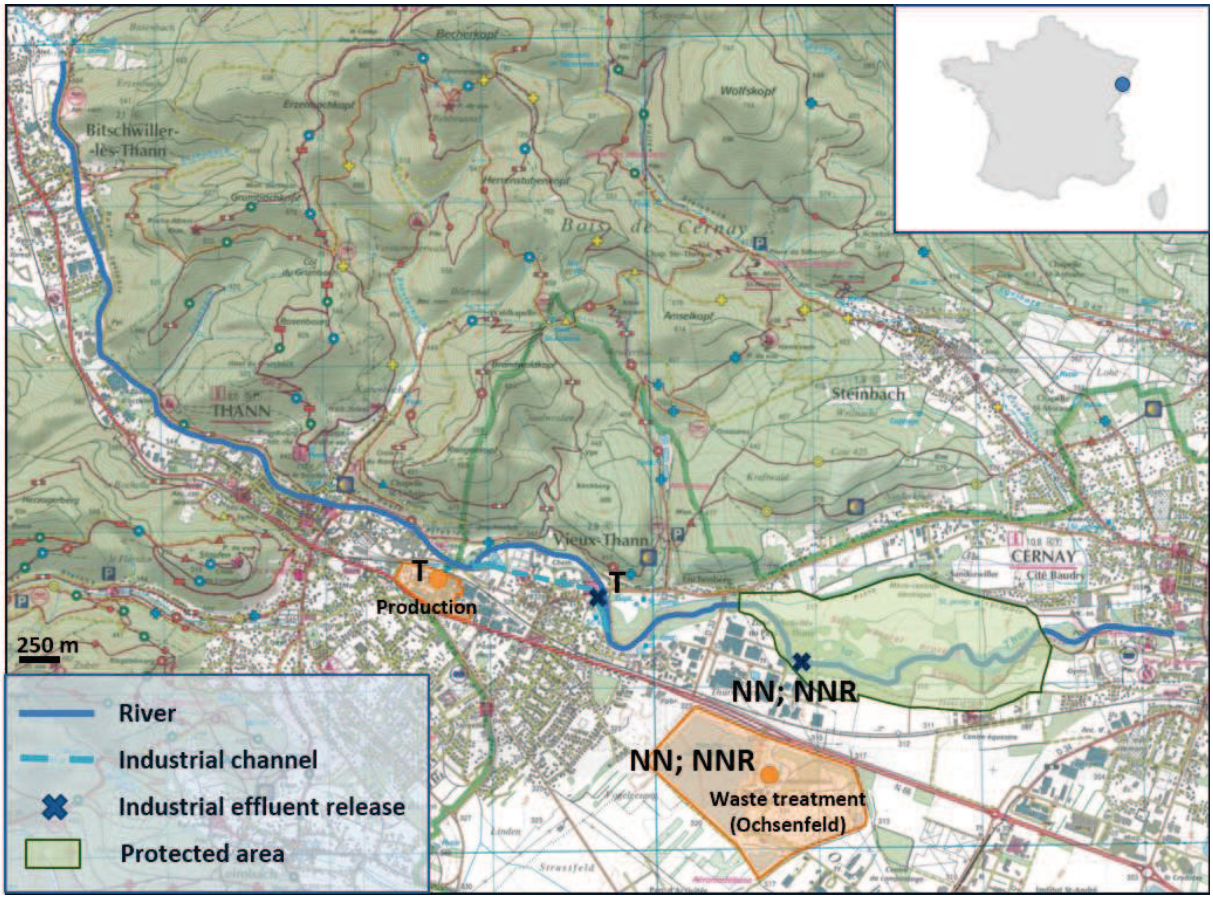

Figure 3: Location of the study site and effluent release points

Figure 4: (A) Junction of the factory channel (left) with the Thur River; (B) Effluents NN and NNR release point

2. Natural processes influencing the fate of TiO_2 NPs in the watershed

2.1. Transport by wind

It was shown that nano-TiO_2 can occur in significant concentrations at TiO_2 NPs manufacturing workplaces (Lee *et al*. 2011) and can thus be transported by the air route, where they may be subject to further agglomeration (Minoura and Takekawa 2005) or break-up (Rothenbacher *et al*. 2008). At Vieux-Thann, the wind mostly blows in two directions (Figure 5): 60% of the recordings were blowing in the downstream direction, towards the East-South-East during 2011 to 2013, the remaining 40% blow in the opposite direction, going up the valley (ASPA 2013). This means that if NPs occur in the air, they are mostly transported downstream of the factory.

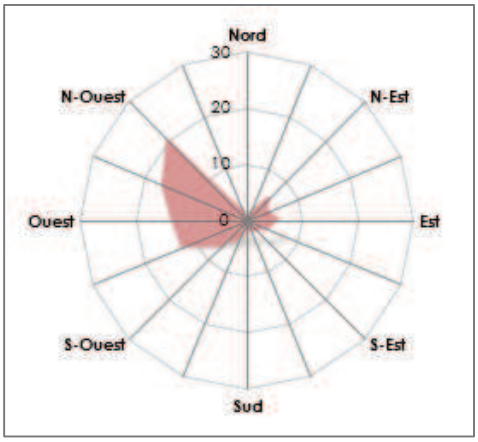

Figure 5: Compass card recorded at Vieux-Thann during the years 2011 to 2013 (wind speed > 0.5 $m.s^{-1}$, ASPA 2013)

2.2. Transport by water

One of the main sources of TiO_2 NPs in the environment are industrial effluents released in the river. As explained earlier, effluent T collects runoff water from the industrial site. Consequently, precipitations play a very important role in the quantities of TiO_2 released by this effluent. The Thur watershed is subject to a maximum rainfall from November to March. At Thann, the mean annual precipitations are 1000 mm (Figure 6).

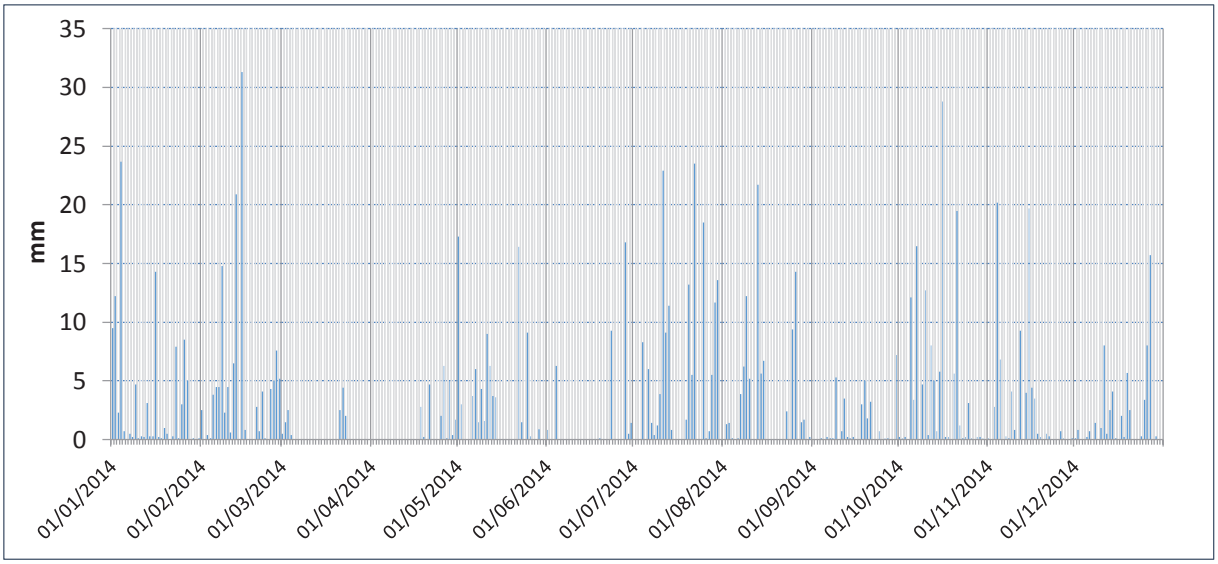

Figure 6: Precipitation fall in Thann during 2014

Precipitations also play a role in determining the magnitude of the river flow, which itself determines the velocity of the potential pollutants transport along the river. Waters are high at the same period as the maximum rainfall and low from June to October (Table 2), which is characteristic of a snow and rain regime (Marbach *et al*. 2013). The first 32 km of the river, from its source to Thann (330 m above sea level), are characterized by a very dynamic regime, as the river flows onto the abrupt slopes of the upper valley. In the lower reach of the valley (also called Piedmont), the valley broadens and the slope diminishes to 4‰. These are the characteristics of our study area, which extends mostly from Thann to Cernay (Figure 3). Downstream of Cernay and down to the confluence with the Ill River at Ensisheim, the river crosses the plain of Alsace. There, the flow is made of a network of phreatic streams that group into “ried”, that are wetlands, composed of floodable plains and gallery forests; the mean slope is 1.7 ‰ (Hissler 2003). The river is canalized at numerous places, especially in Thann, Vieux-Thann and Cernay, to protect industries and human habitat from floods. A wild river section is protected between Vieux-Thann and Cernay, which crosses a protected natural area (Figure 3).

Table 2: Flows ($m^3.s^{-1}$) of the Thur river in 2014 at Bitschwiller-les-Thann, Thann and Vieux-Thann (calculated flows from data from hydro.eaufrance.fr)

	Bitschwiller-les-Thann	Thann	Vieux-Thann
January	6,71	7,24	7,35
February	8,02	8,71	8,85
March	3,87	4,11	4,16
April	1,34	1,41	1,43
May	1,67	1,79	1,82
June	1,19	1,23	1,24
July	1,96	2,28	2,36
August	2,31	2,51	2,55
September	1,99	2,03	2,04
October	2,50	2,69	2,73
November	3,82	4,04	4,08
December	3,68	3,82	3,85

2.3. Transport in sediments

Upon aggregation, TiO_2 NPs may settle down the river column and deposit on sediments. They can aggregate with suspended particulate matter (SPM), coming from rock alteration. Consequently, the geological nature of the area will determine the affinity of the NPs for the SPM and so, will influence their residence time both in water and in the sediment.

Four main lithological units can be distinguished in the Thur watershed (Figure 7). The upper valley mostly comprises sedimentary rocks (schists and graywackes) and granitic rocks, on both sides of the Thur River. The lower reach of the valley is composed of trachy-andesitic rocks, sandstone and conglomerates.

The Thann Series, which is the lithology of Bitschwiller-les-Thann, Thann, and part of that of Vieux-Thann, mainly consists of volcanic (trachites and andesites), and volcano-sedimentary rocks (conglomerates and sandstone) originating from the erosion and reorganization of the former.

During the Quaternary, the valley was subject to successive glaciations that modeled the landscape to its actual shape. Alluvial material were deposited at the Thur outlet, and constitutes the lithology of all the sampling points. The riverbed is composed of recent alluvial material, very coarse and heterogeneous (sandy-rocky, many blocks sizing more than 30 cm, especially in Vieux-Thann). Alluvions are mostly composed of microgranite and granite grauwacke, with some elements of the Thann Series volcanic rocks occurring downstream of Thann (Ménillet *et al*. 1989).

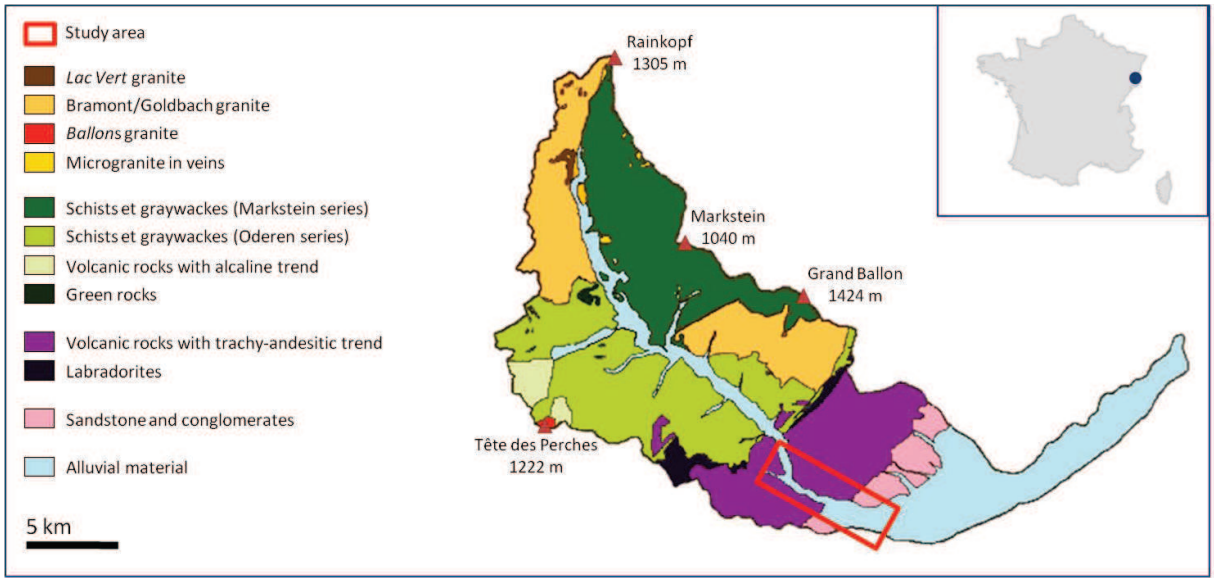

Figure 7: Geology of the Thur watershed (adapted from Hissler, 2003)

2.4. Transport in soils

These geologic formations define the type of soils which are developed in the watershed (Figure 8). The nature of these soils will determine the potential leaching down of TiO_2 NPs, and their bioavailability to biological species. Alluvial soils (constituting all sampled soils) are present near the watercourse and in the alluvial plain. Their pH is acidic; most of them present a high content of coarse material (> 2 cm) and a sandy to loamy texture (Hissler 2003). Alluvial brown soils are developed on alluvial material; this is the type of soil most frequently encountered on the study area. Recent alluvial material produces 40 cm deep sandy (and rocky) soils that are present in the high valley and the piedmont. In the plain, coarse alluvial material produces shallow sandy-loam soils (Appendix I) that are 30 cm deep; and fine alluvial material produces loamy-sand soils that are 50 cm deep (Hissler 2003).

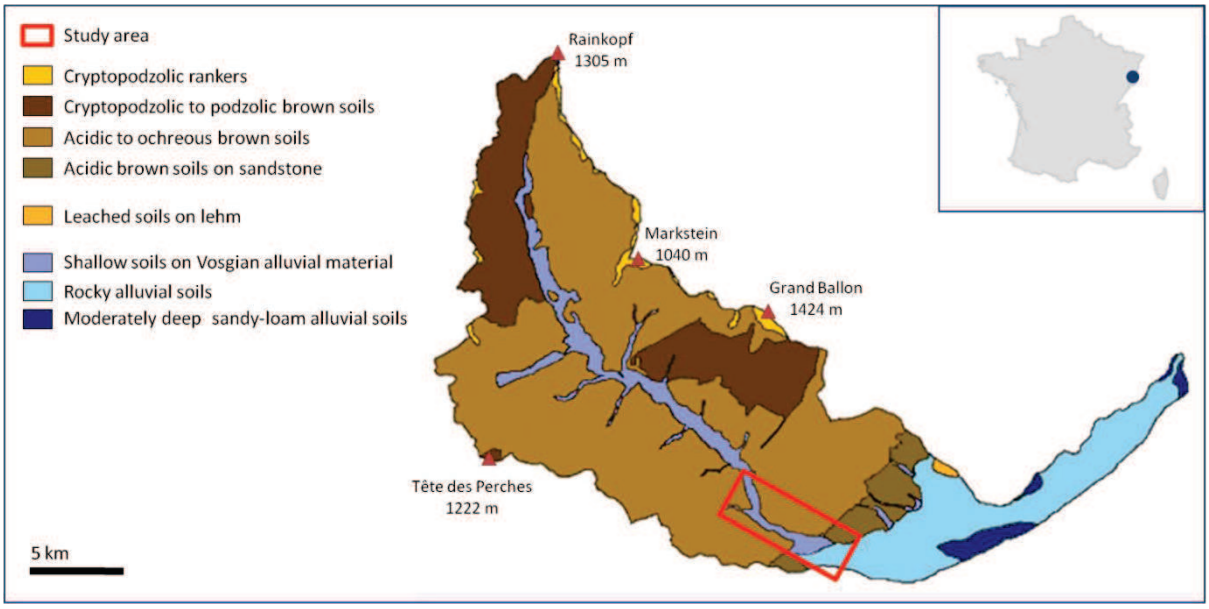

Figure 8: Soil types in the Thur watershed (adapted from Hissler, 2003)

3. Potentially affected species

In the study area, soil is mostly occupied by a low mountain fir forest, as well as vineyards and orchards. Above this cultivated area, coppices of sessile oak and chestnut are in contact with the beech and spruce forest (Marbach *et al*. 2003).

Along the river, the riparian vegetation is mostly composed of pedunculate oak, ash, manna ash, alder and hornbeams (Marbach *et al*. 2003). This is the vegetation encountered at all sampling points, except where soil only was collected, which were under grassy areas.

The Thur river water potentially hosts 16 threatened animal species (Table 3), meaning that the environment in which industrial effluents are released is very sensitive to potential contamination. This highlights the need for an impact and risk assessment in this area. The whole list of threatened animal species present in the study area is presented in the appendix II.

Table 3: Threatened aquatic animal species inventoried in Alsace, in the Thur watershed or in the study area (the most precise location available was reported in the table)

	Latin name	French name	English name	Observed in	Alsace red list status (ODONAT 2014)
Aquatic mollusks	*Theodixus fluviatilis*	Nérite des rivières	River nerite	Alsace[a]	Endangered[d]
	Bithynia leachii	Bithynie nordique	Leach's bithynia	Alsace[a]	Vulnerable[d]
	Belgrandia gfrast	Belgrandie gfrast		Alsace[a]	Vulnerable[d]
	Bythiospeum rhenanum	Bythiospée des rieds		Alsace[a]	Endangered[d]
	Valvata cristata	Valvée plane	Crested valve shell	Alsace[a]	Vulnerable[d]
	Valvata macrostoma	Valvée nordique	Large-mouthed valve snail	Alsace[a]	Vulnerable[d]
	Aplexa hypnorum	Physe élancée	Moss bladder snail	Alsace[a]	Vulnerable[d]
	Anisus spirorbis	Planorbe de Linné		Alsace[a]	Endangered[d]
	Gyraulus crista	Planorbine à crêtes	Nautilus Ram's horn snail	Alsace[a]	Vulnerable[d]
	Gyraulus rossmaessleri	Planorbine des mares		Alsace[a]	Endangered[d]
	Planorbis carinatus	Planorbe carénée	Keeled ramshorn	Alsace[a]	Vulnerable[d]
Crayfishes	*Austropotamobius pallipes*	Ecrevisse à pieds blancs	White-clawed crayfish	Thann and/or upstream[b]	Critically endangered[e]
Fishes	*Thymallus thymallus*	Ombre commun	Grayling	Thur watershed[b]	Vulnerable[e]
	Salmo salar	Saumon Atlantique	Atlantic salmon	Thur watershed[b]	Critically endangered[e]
	Esox lucius	Brochet	Northern pike	Thann and/or upstream[b]	Vulnerable[e]
Amphibians	*Alytes obstetricans*	Alyte accoucheur	Common midwife toad	Thann[c]	Endangered[f]

[a]: Bichain and Orio (2013); [b]: Gerber (2012); [c]: (Inventaire National du Patrimoine Naturel 2013); [d]: (Office des données naturalistes d'Alsace (2014a); [e]: Office des données naturalistes d'Alsace (2014b); [f]: Office des données naturalistes d'Alsace (2014c).

KEYPOINTS

- According to literature analyzes, specific properties of NMs that need to be taken into account for the modeling of their fate and effects include cristallinity, shape, size, surface charge, surface area and aggregation state and
- Bayesian networks appear as the best methodology to use for the RA of NMs.
- The studied factory is the only one to release Ti in the watershed
- Three kinds of effluents are released in the river: runoff and process cooling waters (effluent T), neutralization waters (effluent NN) and slag heap leaching waters (effluent NNR)
- Transport by wind is in the same direction as transport by water
- Soils and sediments present sandy textures; very low quantities of sediments are available on the riverbed

KEY QUESTIONS FOR FURTHER WORK

- Do TiO_2 NPs occur outside the factory and waste treatment sites?
- If so, in what quantities?
- What are the potential interactions of these NPs with the environment?

References

ASPA (2013) Concentrations de mercure dans l'air ambiant en entrée de la vallée de la Thur - Suivi 2011-2012.

Bichain J-M, Orio S (2013) Annotated checklist of the continental molluscs from Alsace (France). MalaCo 9:498–534.

European Commission (2008) Follox-up to the 6th Meeting of the REACH Competent Authorities for the implementation of Regulation (EC) 1907/2006 (REACH).

European Commission (2012) Communication from the commission to the european parliament, the council and the european economic and social committee - Second Regulatory Review on Nanomaterials.

Flemström K, Carlson R, Erixon M (2004) Relationships Between Life Cycle Assessment and Risk Assessment - Potentials and Obstacles. Naturvardsverket

Gerber M (2012) Plan départemental pour la protection du milieu aquatique et la gestion des ressources piscicoles du Haut-Rhin (PDPG) 2012-2016. Partie 1 : Thur et Doller.

Hendren CO (2010) Framing and Assessing Environmetnal Risks of Nanomaterials. Ph.D. Dissertation, Duke University, USA, 125 pp

Hissler C (2003) Dynamique et bilan des flux de mercure dissous et particulaire dans un hydrosystème anthropisé. Cas du bassin versant de la Thur (Sud du Massif Vosgien). Université Louis Pasteur

Inventaire National du Patrimoine Naturel (2013) Liste des espèce recensées dans Commune : Thann.

Lee JH, Kwon M, Ji JH, *et al* (2011) Exposure assessment of workplaces manufacturing nanosized TiO2 and silver. Inhal Toxicol 23:226–236. doi: 10.3109/08958378.2011.562567

Marbach S, Guillot C, Spetz L (2013) Elaboration du Schéma de Cohérence Territoriale (SCOT) Thur Doller - Etat Initial de l'Environnement. Fellering

Matrix Insight Ltd (2014) A Study to support the Impact Assessment of relevant regulatory options for nanomaterials in the framework of REACH.

Ménillet F, Coulon M, Fourquin C, *et al* (1989) Geological map of France - Thann sheet (412).

Ministère de l'Ecologie, du Développement Durable et de l'Energie (2014) Registre français des émissions polluantes.

Minoura H., Takekawa H (2005) Observation of number concentrations of atmospheric aerosols and analysis of nanoparticle behavior at an urban background Japan. Atm Envir 39:5806-5816

Money ES, Reckhow KH, Wiesner MR (2012) The use of Bayesian networks for nanoparticle risk forecasting: Model formulation and baseline evaluation. Sci Total Environ 426:436–445. doi: 10.1016/j.scitotenv.2012.03.064

Office des données naturalistes d'Alsace (ODONAT) (2014a) Liste rouge des Mollusques menacés en Alsace.

Office des données naturalistes d'Alsace (ODONAT) (2014b) Liste rouge des Poissons menacés en Alsace.

Office des données naturalistes d'Alsace (ODONAT) (2014c) Liste rouge des Amphibiens menacés en Alsace.

Piccinno F, Gottschalk F, Seeger S, Nowack B (2012) Industrial production quantities and uses of ten engineered nanomaterials in Europe and the world. J Nanoparticle Res 14:1–11. doi: 10.1007/s11051-012-1109-9

Rothenbacher S, Messerer A, Kasper G (2008) Fragmentation and bond strength of airborne diesel soot agglomerates. Part Fibre Toxicol 5:9.

The Royal Society & The Royal Academy of Engineering (2004) Nanoscience and nanotechnologies: opportunities and uncertainties.

CHAPTER II – ANALYTICAL ASPECTS AND BEHAVIOR OF TiO_2 NPS AND ASSOCIATED POLLUTANTS

The first part of this chapter aims at determining the concentrations of nano-TiO_2 at which organisms living in different environmental compartments (water, sediments and soils) may be exposed. In the second part of the chapter, the aggregation behavior of TiO_2 NMs in analyzed in the river water, in order to better understand their fate in the aqueous medium.

II.A. BEHAVIOR OF POTENTIAL POLLUTANTS COMING FROM TiO_2 NPS PRODUCTION IN WATER, SEDIMENT AND SOIL

Introduction

Although some studies experimentally assessed the release of TiO_2 NPs in water from nanoproducts such as sunscreen (Labille *et al*. 2010; Holbrook *et al*. 2013; Gondikas *et al*. 2014) and building materials (Hsu and Chein 2006; Kaegi *et al*. 2008), no data is currently available on the direct release of engineered TiO_2 NPs from the production sites. This chapter aims at quantifying the release of TiO_2 ENPs in the river water and at assessing the potential impacts of the TiO_2 NPs production on the surrounding environment (water, sediments and soils).

For this purpose, a methodological approach has been implemented that combines a sampling plan and analytical tools to determine the potential interactions between titanium and other elements and to understand spatial and temporal variations of water, sediments and soils compositions.

1. Sampling strategy

1.1. Sampling points

Industrial effluents as well as surface water, sediments and soils were sampled in the study area (Figure 9). Samples were collected upstream of the production site in order to obtain elemental background concentrations, as well as near and downstream the factory in order to assess the potential impact of the TiO_2 production on water, sediments and soils.

Sampling campaigns took place in January, May, August and November 2014, in order to account for seasonal variations of physico-chemistry and elemental concentrations. Additional water samples were collected in March 2014, when nano-TiO_2 industrial processes were the only ones running.

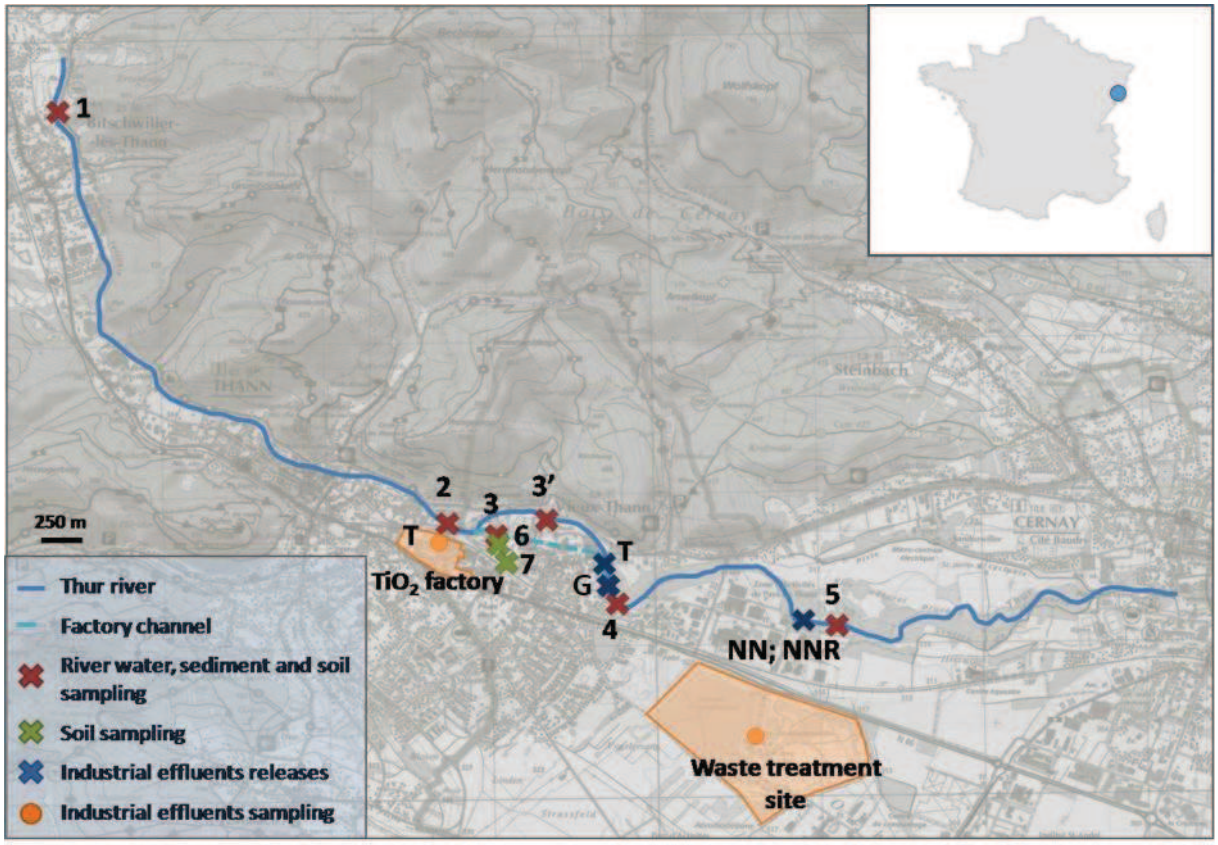

Figure 9: Study area and sampling points

1.2. Sampling techniques

All water samples were collected in 1L perfluoroalkoxy alkane (PFA) vials, at the outlet of the effluents and at the surface of the river.

Sediment samples (200 g - 1 kg dry weight) were taken at the same location as the river water samples, with the help of a polypropylene vial and transported in polyethylene bags. However, because the riverbed is mostly composed of coarse sand and pebbles, sediment samples must be taken at the limit between the bed and the banks of the river.

Soil samples (0-20 cm deep, about 1 kg dry weight) were taken with an auger, 1 to 2 meters away from the river banks. Two additional samplings were performed downwind of the plant chimney (points 6 and 7), in grassy areas.

2. Analytical methods

2.1. Determination of nanoparticles and suspended particulate matter size and shape

Nano-TiO_2 powders were observed by TEM (JEOL JEM 2100). Stabilized suspensions were prepared by dispersing 300 mg $TiO_2.L^{-1}$ in HCl (pH 2), placing these suspensions in an ultrasonic bath (Branson 5510) for 30 minutes, and let to settle down for 8 days. The supernatant (about 10 $mg.L^{-1}$ TiO_2) was then diluted 10 times in ethanol before observation.

In order to characterize the SPM occurring in industrial and river waters, filters used for the water samples preparation were observed in TEM and SEM (Vega 2, Tescan, equipped with an EDAX Pegasus X-ray analyzer), respectively. Drops of ethanol were deposited on the filter, which was then scrubbed with a diamond tip, and rubbed with the TEM Cu grid.

2.2. Measurement of physico-chemical parameters

Temperature, turbidity (2100P ISO Turbidimeter, Hach), pH and conductivity (HQd Field Case, Hach) were measured at each sampling point, on each sampling campaign, in industrial and natural waters.

Soil and sediment samples granulometry was determined by laser diffraction (LS 13320, Coulter Beckmann). pH was measured with a WTW INOLAB PH7110 pH meter, equipped with a Sentix 41 electrode in water suspensions (20 g soil/50 mL DIW). Organic matter content was measured by calcination of dried samples at 375°C during 16 hours.

2.3. Determination of elemental concentrations

2.3.1. Water samples preparation and analysis

At each sampling point, including in the effluents, two sets of water samples were taken (Figure 10). One set was filtered with 0.2 µm polycarbonate filters and acidified with HNO_3 (2%). The other set was submitted to an acid digestion protocol: it was firstly acidified with 1 mL of HNO_3 (12 N) and put to evaporate at 120 °C. When the solid residue was formed, it was covered with an acid solution containing 3 mL of ultrapure water for 1 mL of HNO_3 (7.5 N) and 2 mL of HCl (6 N). Each PFA vial was then closed and heated again at 100°C. After 12h, 1 mL of HF (40%) was added and heating was continued at 70°C during 12 h. After subsequent evaporation in the oven, the volume of the digested sample was adjusted with HNO_3 (0.75 N). All water samples (filtered or digested) were analyzed with inductively coupled plasma – atomic emission spectroscopy (ICP-AES, ICAP 6000 Series ICP Spectrometer, ThermoScientific).

In this way, both particulate and “dissolved” (< 200 nm, commonly considered as the size threshold for separation of particulate from dissolved content) concentrations could be determined.

Anions (Cl^-, NO_3^-, SO_4^{2-}) concentrations were measured with ionic chromatography (ICS 3000, Dionex). Dissolved (DOC) and total organic carbon (TOC) concentrations were measured with a TOC-V CPH analyzer (Shimadzu).

2.3.2.Soil and sediment samples preparation and analysis

Soil and sediment samples were dried at 40°C in a stove before sieving at 2 mm and quartered in order to obtain 100 – 150 g of sample, which were crushed to 250 µm with an agate crusher. After homogenization, 30 g were taken and crushed to 100 µm before alkaline fusion: 4 g of sample were dried at 110°C to evaporate all water and calcined at 1000°C to remove organic matter. Then, 750 mg of lithium tetraborate ($Li_2B_4O_7$, Spectromelt A100, Merck) were added to 100 mg of calcined sample and the mixture was heated during 20 minutes at 1000°C under argon flow, in order to form a pearl. The pearl was dissolved by addition of 20 mL of a solution (4 mL of glycerol (85%), 1 mL of bi-distilled HNO_3 (65%,) 15 mL of ultrapure water) and heating at 80°C under agitation. After 30 minutes, the sample volume was adjusted to 25 mL with ultrapure water and filtrated on filter paper. This treatment was applied to soils and sediments samples before analysis by ICP-AES (ThermoScientific ICAP 6000 Series ICP Spectrometer).

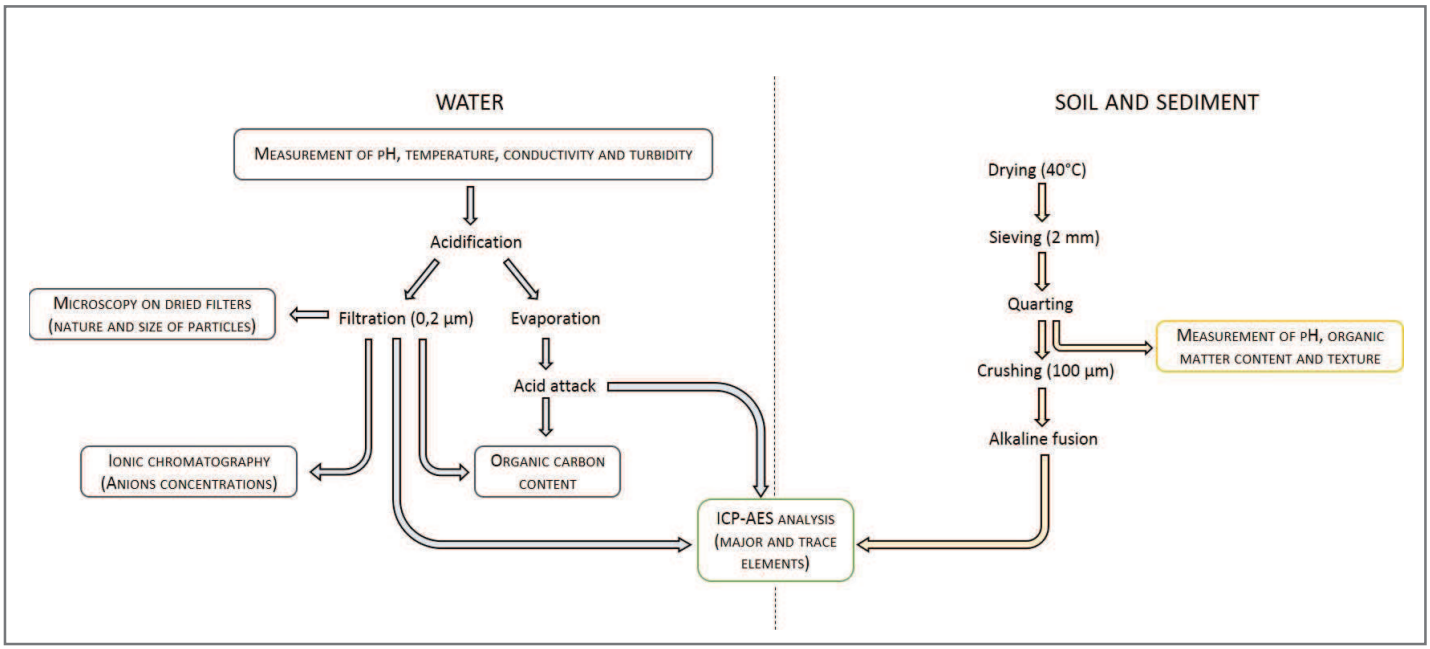

Figure 10: Water, sediment and soil preparation and analyzes

2.4. Representativeness and uncertainties

The sampling strategy was built in order to obtain as high a representativeness as possible. However, some uncertainties arise both from the sampling and the analysis techniques.

Firstly, only surface samples were taken, so that vertical changes of composition were not assessed in the environmental compartments. This choice was made for soils because the objective was to assess only the potential deposition of TiO_2 ENPs from the atmosphere. In river water, the transfer down the water column ends up in the sediment, so the sediment sampling should allow the estimation of TiO_2 NPs travel down the river water column.

Secondly, although soils collected on the river banks were all alluvial soils, the two other ones (samples 6 and 7, Figure 9) were industrial soils, so their composition is inherently different from those of natural soils.

Other uncertainties could arise from the samples preparation. Quartering was performed on sample quantities high enough to be representative of the collected soil (Gy 1992). Acid attack and alkaline fusion tests were performed in order to ensure that all TiO_2 NPs were dissolved. A recovery of 99% was determined for the acid attack of waters. Alkaline fusion was tested on the reference upstream soil (sample 1), doped with 10% TiO_2 NPs (w/w). 100% of these TiO_2 NPs were recovered.

Moreover, although microscopy imagery was used to assess the shape of the particulate content of water samples, this tool cannot be used for quantification. Also, the images were taken in a vacuum chamber, so that the aggregation state of the observed particles give no information on their state in the river.

Finally, detection and quantification levels, as well as analysis uncertainties (Table 4) must be taken into account in the determination of elemental concentrations.

Table 4: Detection levels, quantification levels and uncertainties arising from the samples elemental analysis

Device	**Detection level**	**Quantification level**	**Uncertainties**
TOC analyzer	0.14 ppm	-	5%
Ionic chromatograph	Cl^-: $1.1*10^{-4}$ mM NO_3^-: $3.9*10^{-4}$ mM SO_4^{2-}: $5.9*10^{-4}$ mM	Cl^-: 0.006 mM NO_3^-: 0.008 mM SO_4^{2-}: 0.006 mM	5%
ICP-AES	Cf. Appendix	3*detection level	2% for concentrations > 50 ppb 5% for concentrations < 50 ppb

3. Results obtained by microscopic imagery

3.1. Imagery of NPs powder

Both types of ENPs provided by the factory were observed by TEM. The so-called “high specific surface area” (HSS) sample is composed of spherical 5 nm crystallites (Figure 11A). The second sample (low specific surface area – LSS) is made of larger primary particles (20 – 40 nm) which present an oval shape (Figure 11B). X-ray diffraction (XRD) analysis of these crystallites showed that both were anatase (Appendix III). They present high purity, but their analysis with energy dispersive X-ray (EDS) revealed the presence of Si and Zn in these particles.

3.2. Imagery of suspended particulate matter in industrial and natural waters

Filters used for samples preparation were imaged by TEM, which showed that nanoparticulate TiO_2 was released by effluent T, as numerous homo- and heteroaggregates, most often associated with Fe (Figure 12). The electron diffraction confirmed that they were anatase TiO_2.

Over nine EDS measurements on aggregates observed on the filter used for the sample preparation of effluent NN, Ti was always associated with other elements, especially Fe (Figure 13). Its crystal phase could not be determined. No Ti particle was observed in NNR samples.

Some titanium was also observed as NPs by SEM (Figure 14A) on the filter used for the preparation of sample 4 collected on March, at the exit of the industrial channel, and as a bigger single particle in sample 4 collected on August (Figure 14B).

SEM observations of 8 filters collected in the river allowed the determination of the maximum size threshold in the river water, which was around 100 µm.

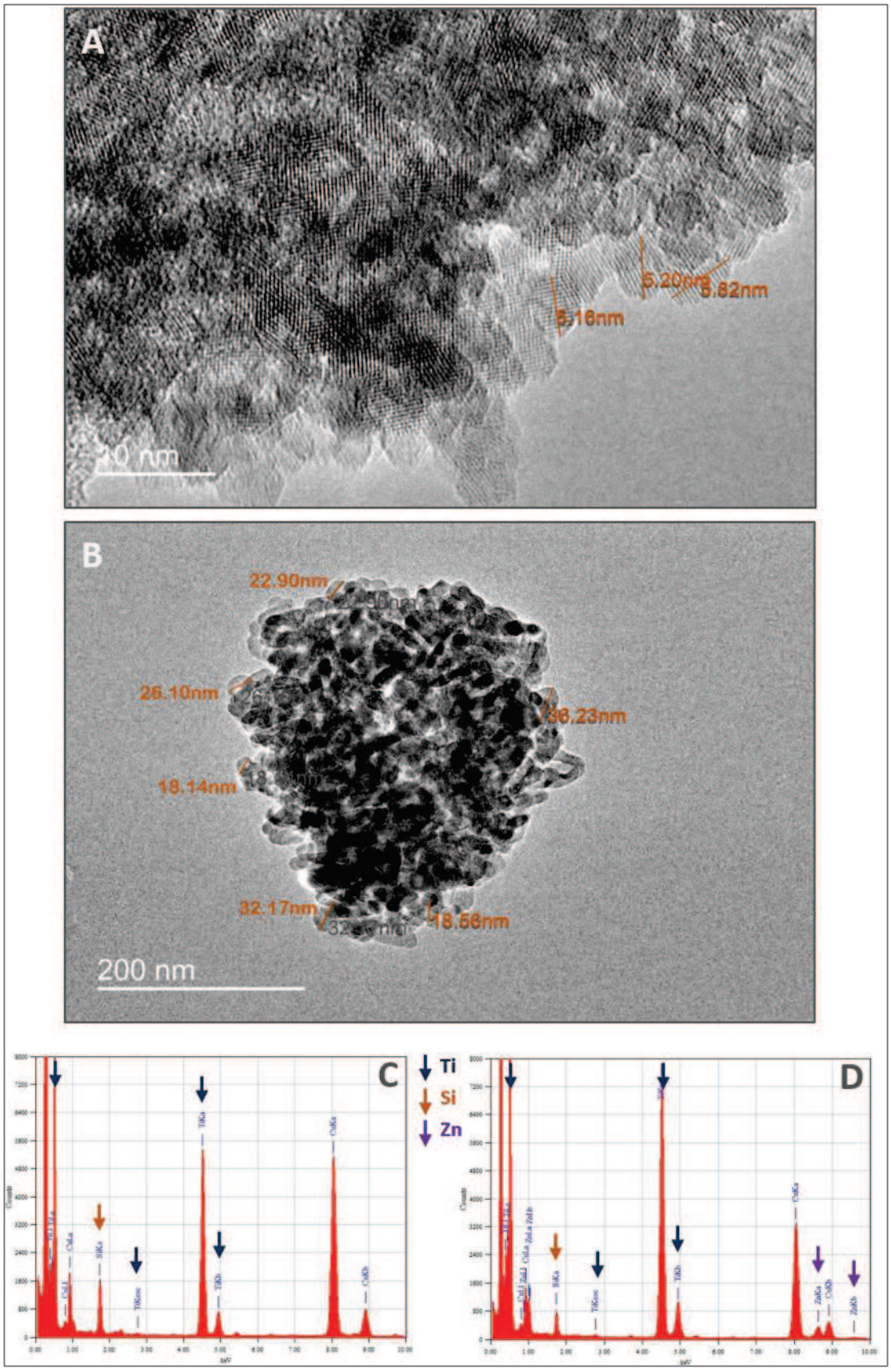

Figure 11: MET images of HSS (A) and LSS (B) samples and corresponding EDS spectra (C and D, respectively)

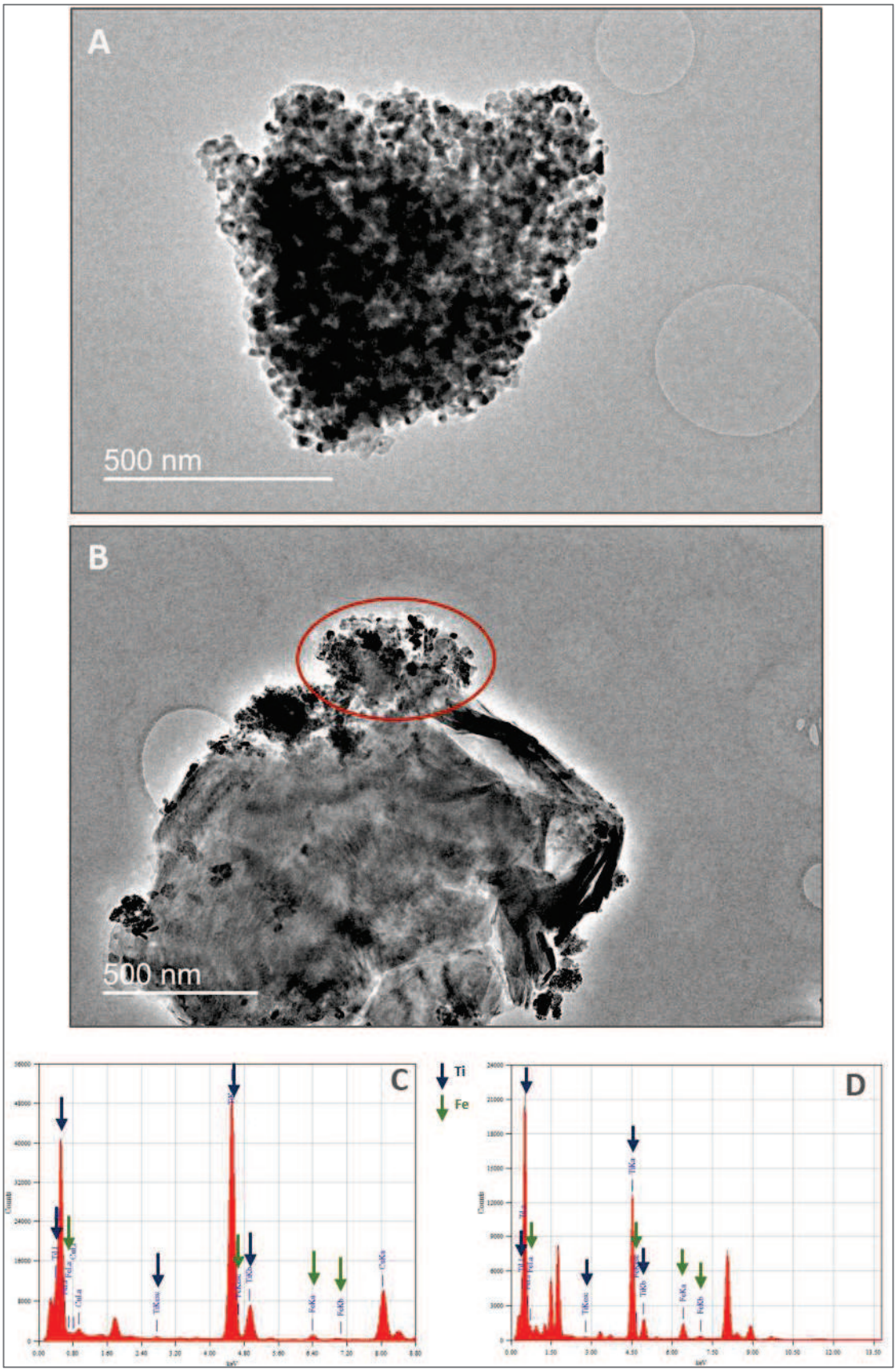

Figure 12: TEM images of TiO_2 retained on the filter used for the sample preparation of effluent T collected on March, present as homoaggregates (A) and heteroaggegates (B). Corresponding EDS spectra are presented in C and D, respectively

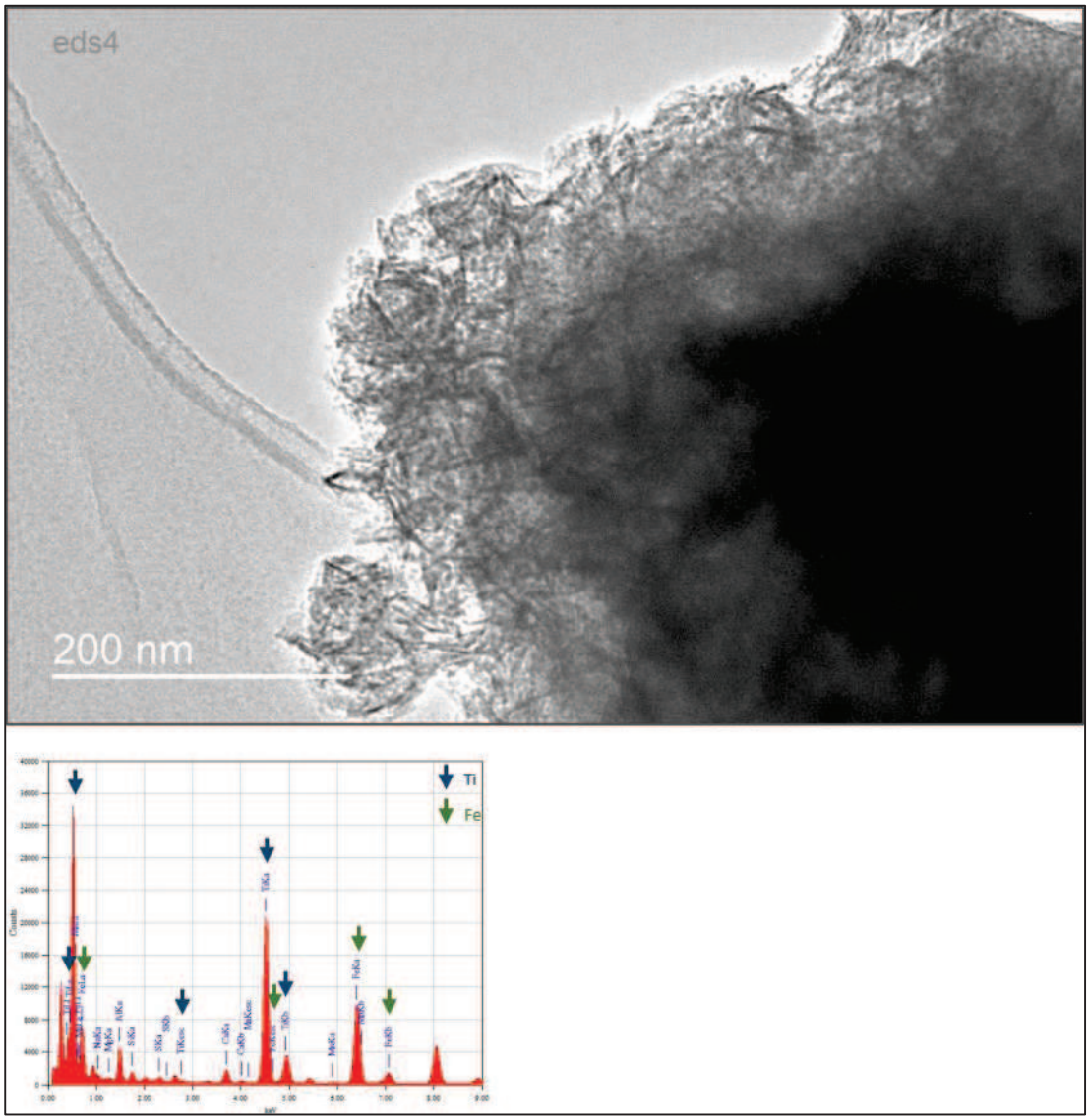

Figure 13: TEM image and EDS spectrum of an aggregate observed on the filter used for the sample preparation of effluent NN collected on November 2014

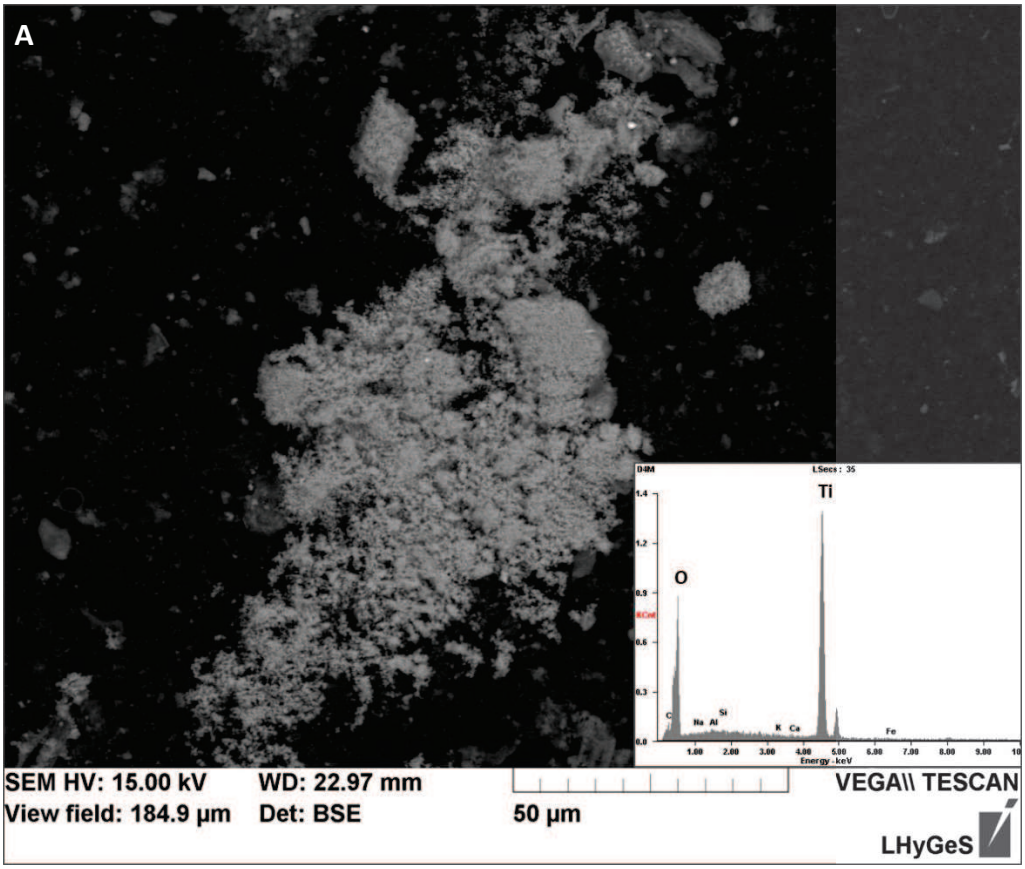

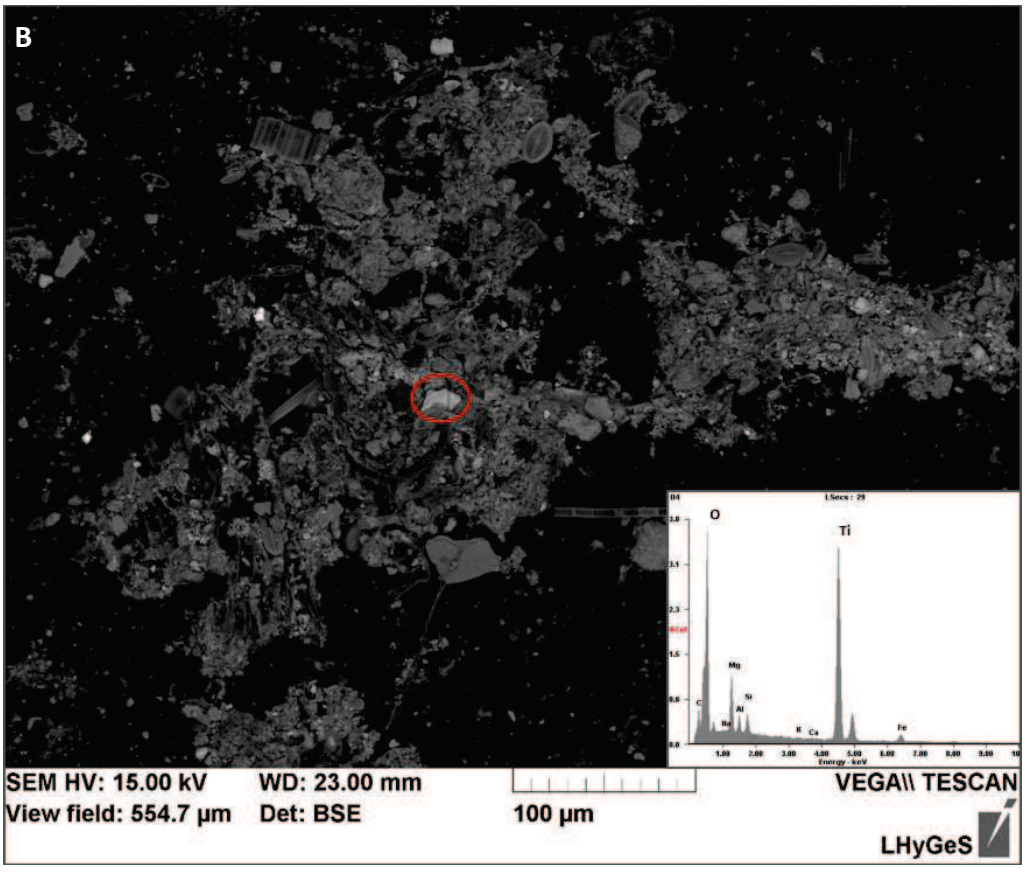

Figure 14: Ti particles observed with SEM as (A) NPs observed on the filter of sample 4 collected on March 2014 (B) a bigger particle (O) observed on the filter used for the preparation of sample 4 collected on August 2014

4. Potential impacts of TiO_2 NMs production wastewater on physico-chemical parameters

The turbidity measured in all samples was below 5 NTU (Nephelometric Turbidity Unit), except in effluent T, where it was up to 40 NTU higher (Figure 15). Yet no effect was observed on downstream water. pH values were around 7.5 to 8 upstream of the factory, around 7.5 in effluents T and NN, and slightly higher in effluent NNR. No significant impact of the effluents was observed on the river water pH.

Upstream of the factory, the river water temperature follows seasonal variations, being higher in summer. Slight increases of temperatures at points 4 and 5 could be due to the release of the effluents, which were warmer (up to 13°C more) than the river water. This could locally affect the aquatic ecosystem, favoring the development of some species to the detriment of others: an important algal development was indeed observed on the river bed at the NN and NNR effluents release point.

Significant increases of conductivity were measured at points 4 and 5 when compared to upstream values. At point 5, these are due to the release of high quantities of ions in the effluents (cf. section 5.1). However, the increase of conductivity at point 4 cannot be explained solely by the conductivity in effluent T, which is lower. A potash industry also releases wastewaters into the industrial channel, downstream of the effluent T release point and upstream of sampling point 4. High ionic concentrations were measured in this effluent (Appendices IVA and IVB), which may explain the increase in the river conductivity at point 4. More than affecting the ecosystem, these conductivities are high enough to induce potential aggregation of TiO_2 NPs, and to have an impact on their transport in water (see section IIB).

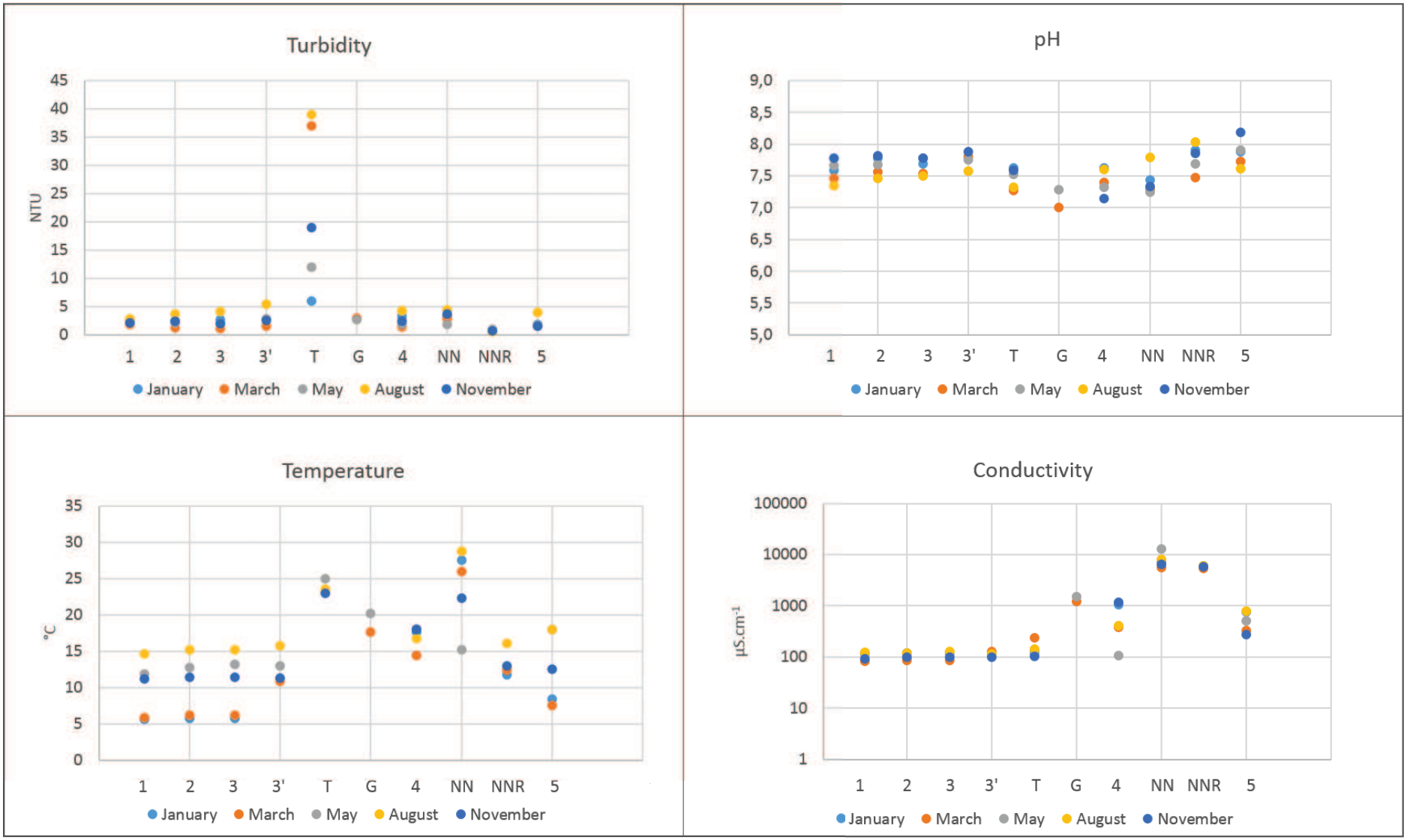

Figure 15: Measurements of turbidity, pH, temperature and conductivity in the industrial and natural waters

5. Behavior of trace elements in water, soil and sediment

As mentioned above, a set of water samples were collected on March 2014, when only the ENPs processes were running at the factory. Results show that all elemental concentrations measured at this time are in the same range as those measured on the other campaigns, at all sampling points (Appendix IV). This means that concentrations measured at all times in these waters are representative of the TiO_2 ENPs process, and valid for the impact evaluation of this production. So, in the following discussion, elemental concentrations were averaged over the 5 sampling campaigns, in order to obtain yearly variations as error bars. These yearly variations upstream of the effluents release points are compared to those measured downstream. Moreover, samples 1 to 3' (see Figure 9 p. 86) were averaged and this mean value was taken as the upstream reference, in order to assess potential spatial variations of elemental concentrations due to the TiO_2 factory.

5.1. Behavior of major and trace elements in the Thur river water

5.1.1.General impacts of the industrial site on elemental concentrations in the river

Dissolved concentrations of Mg, Ca, Na and K were discussed, as this is the form in which they naturally occur in water, and *particulate* concentrations of metals were preferred, in order to potentially associate their behavior to those of TiO_2 ENPs.

At point 4, Mg and Ca dissolved concentrations were in the same range as the upstream values, though a small rise in Ca concentrations was measured (Figure 16, Appendix IVA). However, dissolved Na (50.96 $mg.L^{-1}$) and K (42.50 $mg.L^{-1}$) concentrations were much higher than the upstream mean values (6.03 and 0.91 $mg.L^{-1}$, respectively). This cannot be explained by the release of effluent T, as concentrations were lower in this industrial water (8.92 and 1.32 $mg.L^{-1}$, respectively) than in sample 4. These high concentrations were due to the potash industry wastewater which is released in the channel and contains high concentrations of Ca, Na and K (Appendix IVA).

In sample 5, Mg, Ca, Na and K dissolved concentrations were higher than the upstream values (Figure 16). The mean upstream concentrations were 1.56, 7.72, 6.03 and 0.91 $mg.L^{-1}$ respectively, while the mean concentrations in sample 5 were 3.27, 39.28, 27.96 and 18.79 $mg.L^{-1}$, respectively. This is explained by the neutralization process of "red" effluents, using lime and leading to high concentrations of these elements in NN and NNR, especially in Ca and Na (Figure 16). The raise in these cations concentrations downstream of the industrial site could facilitate the aggregation of TiO_2 ENPs, and lead to a preferential accumulation of TiO_2 in the sediment (French *et al*. 2009; Chowdhury *et al*. 2012; Adam *et al*. submitted to JNR, 2015).

Concentrations of Cl^-, NO_3^- and SO_4^{2-} measured in the river water downstream of both effluents release points were higher than in upstream waters (Table 5, Appendix V). The increase of these concentrations in samples 4 and 5 may be due to the release of the industrial wastewaters. However, conductivity thresholds are respected for release in the river, so no effect on the ecosystem is assumed. Moreover, these anions have no significant effect on the nano-TiO_2 aggregation because they are negatively charged at the river pH value (pH 7 - 8) (Adam *et al*. submitted to JNR, 2015).

Table 5: Anions concentrations (mM) in the collected samples (values averaged over all campaigns)

Sample	Cl^-	NO_3^-	SO_4^{2-}
1	0.25 ±0.07	0.05 ±0.01	0.06 ±0.00
2	0.25 ±0.05	0.05 ±0.01	0.06 ±0.00
3	0.23 ±0.04	0.05 ±0.01	0.06 ±0.00
3'	0.23 ±0.036	0.04 ±0.00	0.07 ±0.01
4	4.398 ±1.56	0.18 ±0.15	0.40 ±0.23
5	2.58 ±0.74	0.28 ±0.25	0.34 ±0.18
T	6.97 ±7.45	0.17 ±0.13	2.66 ±2.85
NN	48.80 ±19.62	2.54 ±2.78	7.13 ±3.35
NNR	32.49 ±2.84	3.30 ±3.19	11.63 ±2.85

Results also show raises in Mn and Cu particulate concentrations downstream of the industrial site, at point 4 (10.54 and 2.83 $\mu g.L^{-1}$ respectively) and at point 5 (10.40 and 2.04 $\mu g.L^{-1}$ respectively) (Figure 16, Appendix IVE). Suppressing the dilution effect occurring from the effluents to the river, by calculating concentrations ratios shows that these concentrations increases can be explained at point 4 by the high concentrations of these elements in effluent T. However, the influence of effluents NN and NNR was not clearly evidenced on downstream Cu and Mn concentrations (Figure 17).

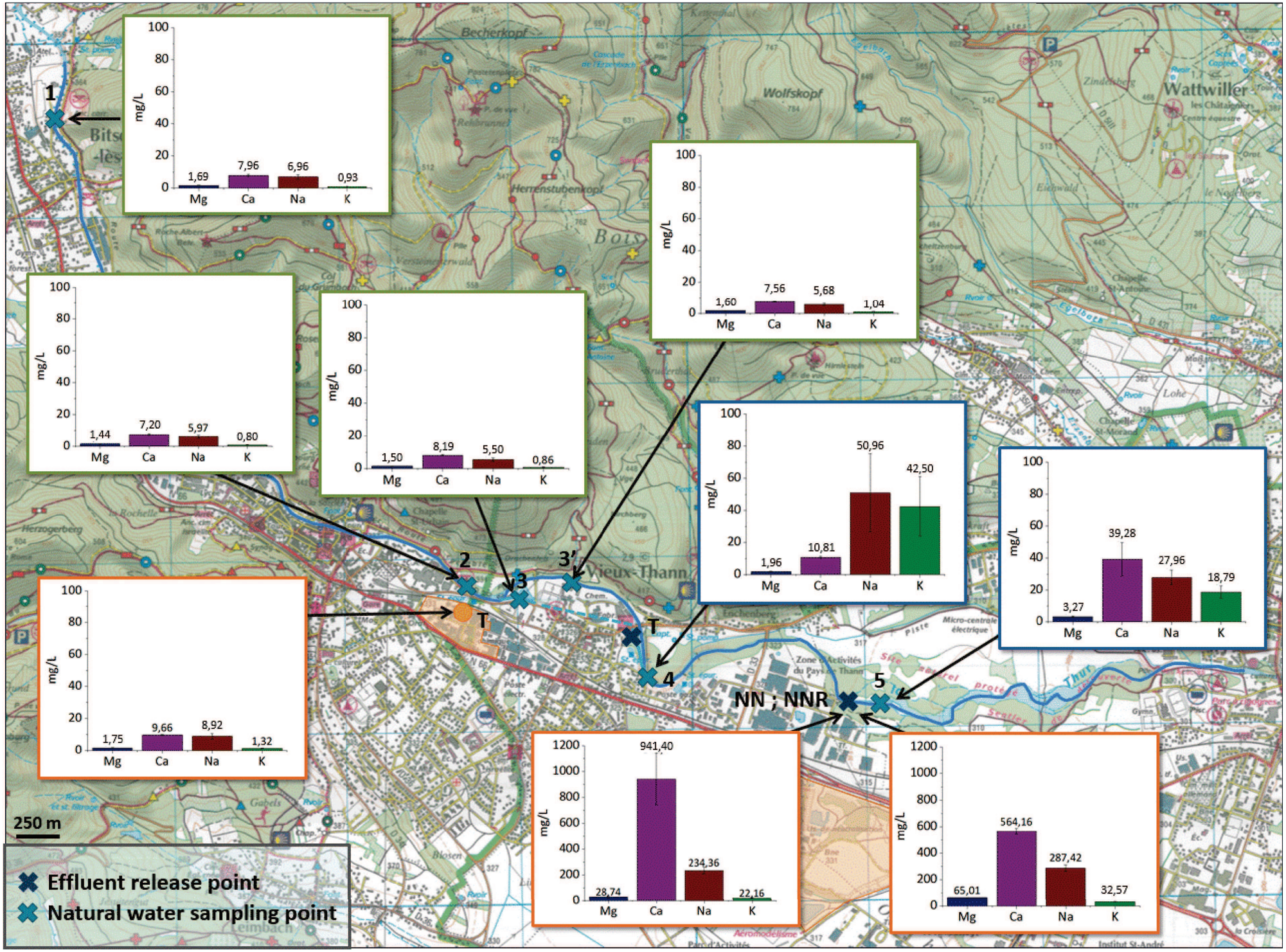

Figure 16: Concentrations of dissolved Mg, Ca, Na and K in industrial and natural waters. Values of each sampling point (Appendix IVA) are averaged over all campaigns, error bars are yearly variations.

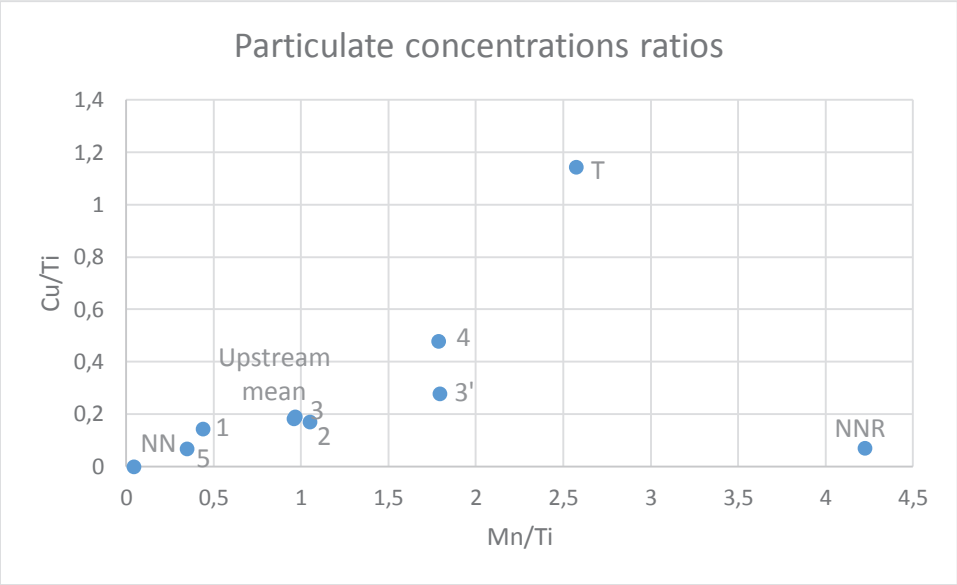

Figure 17: Mn/Ti and Cu/Ti concentration ratios averaged over all campaigns

Concentrations in particulate Al, Fe, Ni and Cr remain relatively stable all along the river water (Figure 18, Appendix IVE). Although Al and Fe are released in high concentrations by effluent T, NN and NNR, they may precipitate rapidly downstream of their release points, explaining the stable concentrations in the river water. Dilution processes should also be kept in mind, as they may as well explain the decrease of elemental concentrations from the effluent waters to the river waters. In order to avoid the dilution effect, Al and Fe concentrations were normalized by Ti concentrations (Figure 19). Results show that Al and Fe content in point 4 are influenced by the effluent T, and that Fe contents in point 5 may be influenced by effluents NN and NNR.

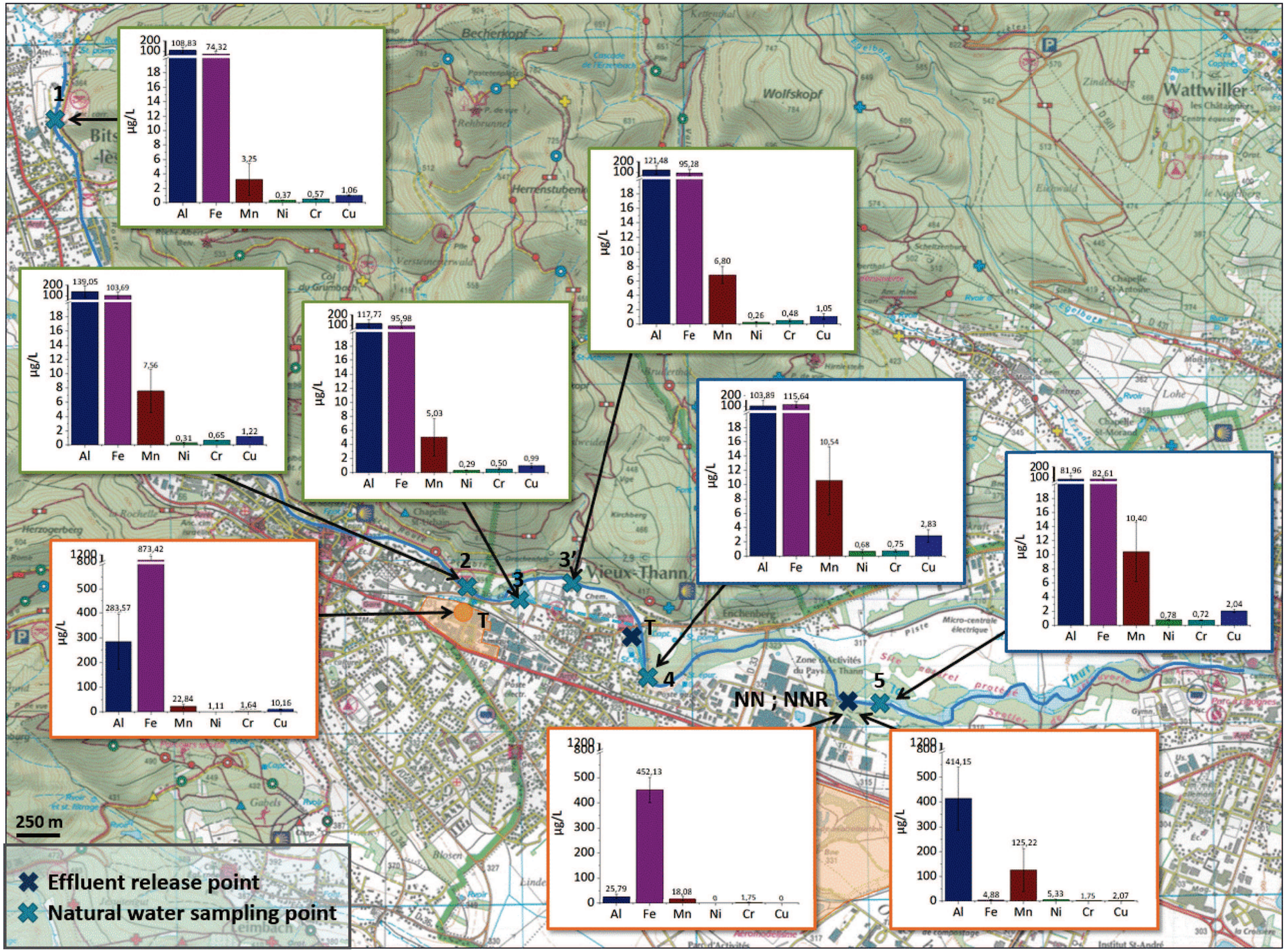

Figure 18: Concentrations of particulate Al, Fe, Mn, Ni, Cr and Cu in industrial and natural waters. Values of each sampling point (Appendix IVE) are averaged over all campaigns, error bars are yearly variations.

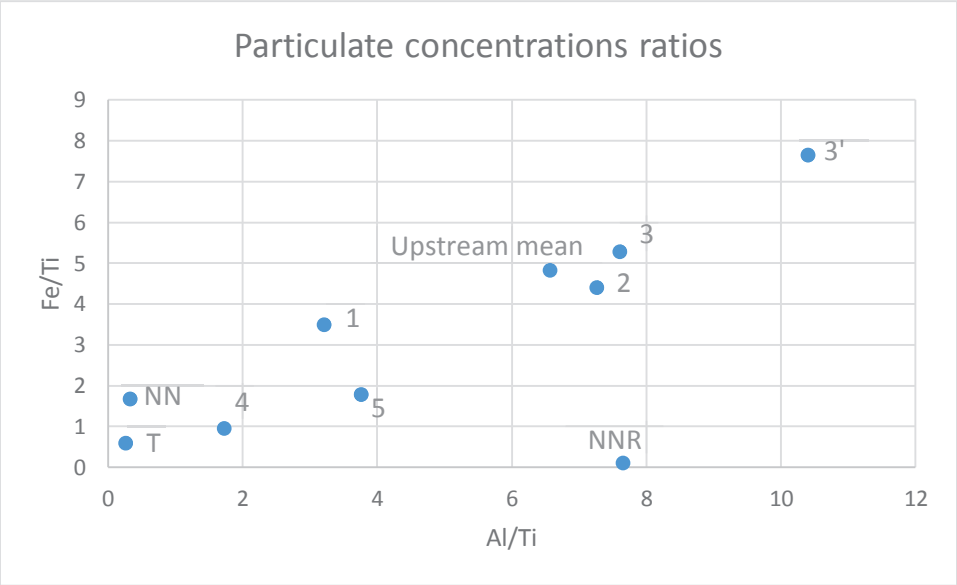

Figure 19: Fe/Ti and Al/Ti concentration ratios averaged over all campaigns

It is thus clear that the industrial effluents released in the river play a significant role in the downstream water composition, both on salt and on metal concentrations. The focus will now be put on the quantification of *nanoparticulate* TiO_2 in the river.

5.1.2.Concentrations variations of TiO_2 and associated elements

Preliminary alkaline fusion tests were performed on the reference soil sample (sample 1), doped with 10% TiO_2 ENPs (w/w) and prepared and analyzed following the same protocol as the other samples. Two replicates were analyzed for each NP type (HSS and LSS), a blank sample (sample 1 alone) was also analyzed for comparison. It was thus shown that Co and V impurities occur in the ENPs samples, as their concentrations increased with ENPs doping (Figure 20). We will focus the following discussion on these elements, together with Zn which was measured by EDS in a LSS TiO_2 sample (Figure 11 p. 91), in the objective of quantifying the nanoparticulate part of TiO_2.

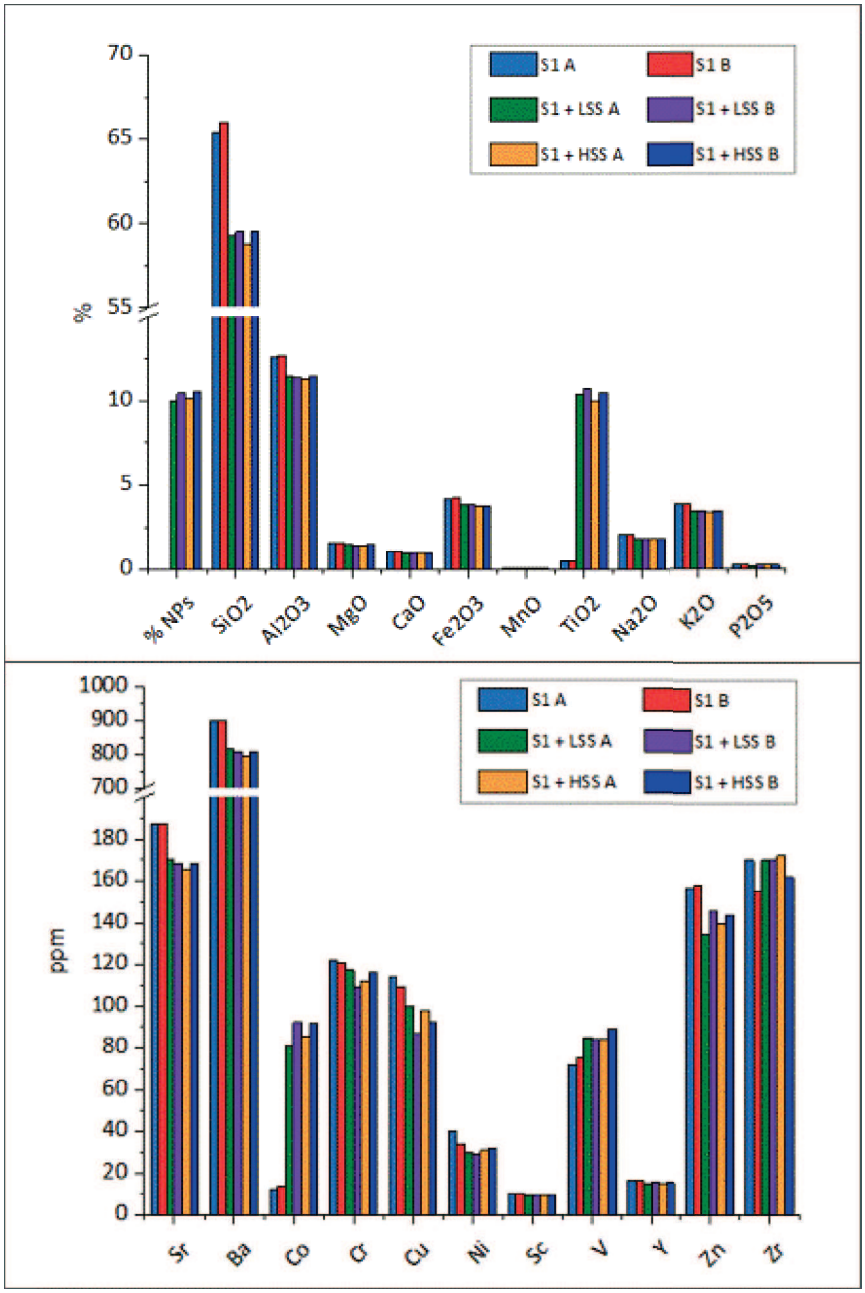

Figure 20: Elemental determination by ICP-AES after alkali fusion of soil sample 1 and soil sample 1 doped with HSS or LSS at 10 % (w/w). Duplicates are named A and B.

All particulate Ti concentrations were transformed into TiO_2 (the most common form of Ti) concentrations, based on molar masses.

Upstream of the effluents release points, the average particulate TiO_2 concentration was 9.84 ppb, with variations of ±3.34 ppb from one campaign to another (Figure 21, Appendix IVH). These variations can be assimilated to seasonal variations, as they occur in uncontaminated natural water. In sample 4, the mean TiO_2 particulate concentration is as high as 49.99 ppb (+ 408.08 % compared to the upstream value, Table 3), with yearly variations of ±9.98 ppb. At point 5, the mean particulate TiO_2 concentration is 14.80 ppb (+ 50.44% compared to the upstream value), with yearly variations of ±5.92 ppb. Higher yearly variations in samples 4 and 5 compared to seasonal variations can be explained, at least partly, by those observed respectively in effluents T (±225.98 ppb), and in NN (±22.37 ppb) and NNR (±18.88 ppb). Both higher TiO_2 concentrations and yearly variations in sample 4 show that the river water is impacted by the release of effluents T. The same observation can be made at point 5, although increases are lower.

Particulate V concentrations remain in the same order all along the river water, though it is released in quite high concentrations in effluents T and NN (Table 6). Dissolution of particulate V could have explained this observation, but it is not the case, as dissolved V was not found in significant concentrations all along the river (Appendix IVG). However, the absence of change in the river concentrations may be due to insufficient concentrations in the effluents. Indeed, when removing the dilution effect by calculating concentration ratios (Figure 22), only a very slight effect of effluent T was shown on sample 4 and no effect on V concentrations was shown in sample 5.

In the opposite, particulate Co and Zn concentrations are subject to high rises. However, the fact that all these elements do not increase in the same range, and especially not in the same range as TiO_2, does not allow us to determine the nanoparticulate part of TiO_2.

Table 6: Changes in water downstream concentrations compared to upstream mean values. For each element, the first column is the concentration difference between the upstream mean value and the downstream value, the second column expresses this difference as a percentage of increase or decrease.

Mean values	TiO_2 (ppb)	TiO_2 (%)	V (ppb)	V (%)	Co (ppb)	Co (%)	Zn (ppb)	Zn (%)
Upstream mean	9,84	0	0,58	0	0,07	0	1,52	0
Sample 4 - upstream	+40,15	+408,08	+0,01	+2,50	+0,08	+109,19	+3,34	+219,21
Sample 5 - upstream	+4,96	+50,44	-0,02	-3,08	+0,12	+164,23	+1,00	+65,71

Nevertheless, it was shown earlier that variations in aquatic concentrations of these elements in natural water seem correlated to those in the effluents (Figure 22). But differences in these concentrations are not only due to the potential presence of TiO_2 NMs in water, as they can also occur in residues of production (extraction from ore) and treatment processes. This may explain why they

do not increase in the same way as TiO_2 and why they cannot be used for the quantitative determination of TiO_2 NMs in water: they may not occur in the effluent only as associated with TiO_2.

Overall, this study shows that TiO_2 NMs occur in the river water, as they were observed by TEM and SEM in effluent T and at point 4. However, they were also observed as associated with Fe, meaning that Ti in the nanometric range occurring in water is not always the final product of the factory. Moreover, the analysis of the NMs impurities in the river water does not allow us to determine the exact concentration of TiO_2 NMs in the river water. Further research must be carried on, using for example isotopic ratios and ICP-MS in order to determine the different origins of TiO_2 in the river water. For modeling purposes, it could be assumed as a "worst case" scenario that all particulate Ti were TiO_2 NPs, as no analytical tool was available for quantifying the nanoparticulate portion of TiO_2.

The potential deposition of NMs down the water column was assessed by performing elemental concentration analysis on the sediment samples. These results are developed in the next section.

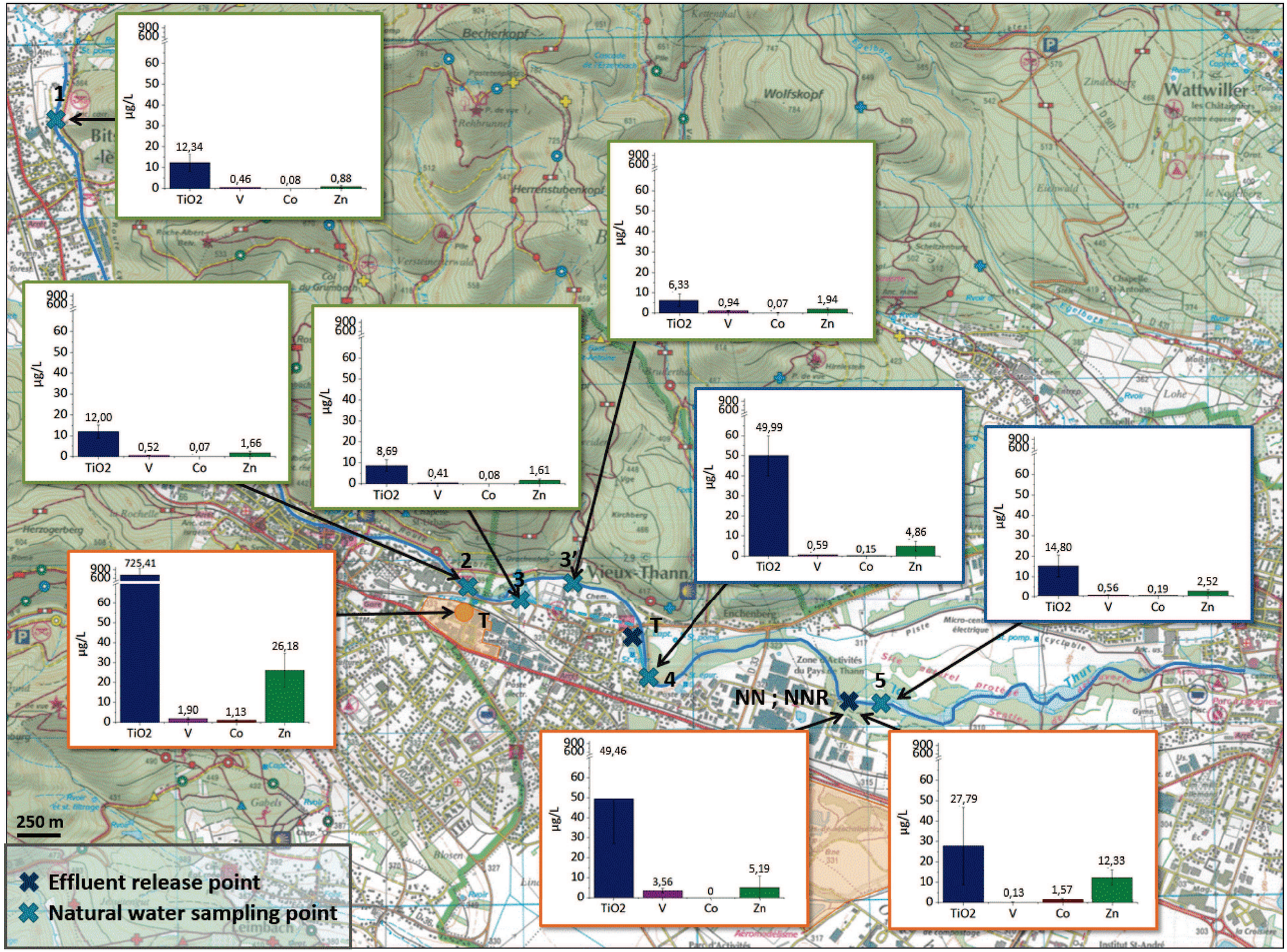

Figure 21: Concentrations of particulate TiO_2, V, Co and Zn in industrial and natural waters. Values at each sampling points (Appendix IVH) are averaged over all campaigns, error bars are yearly variations.

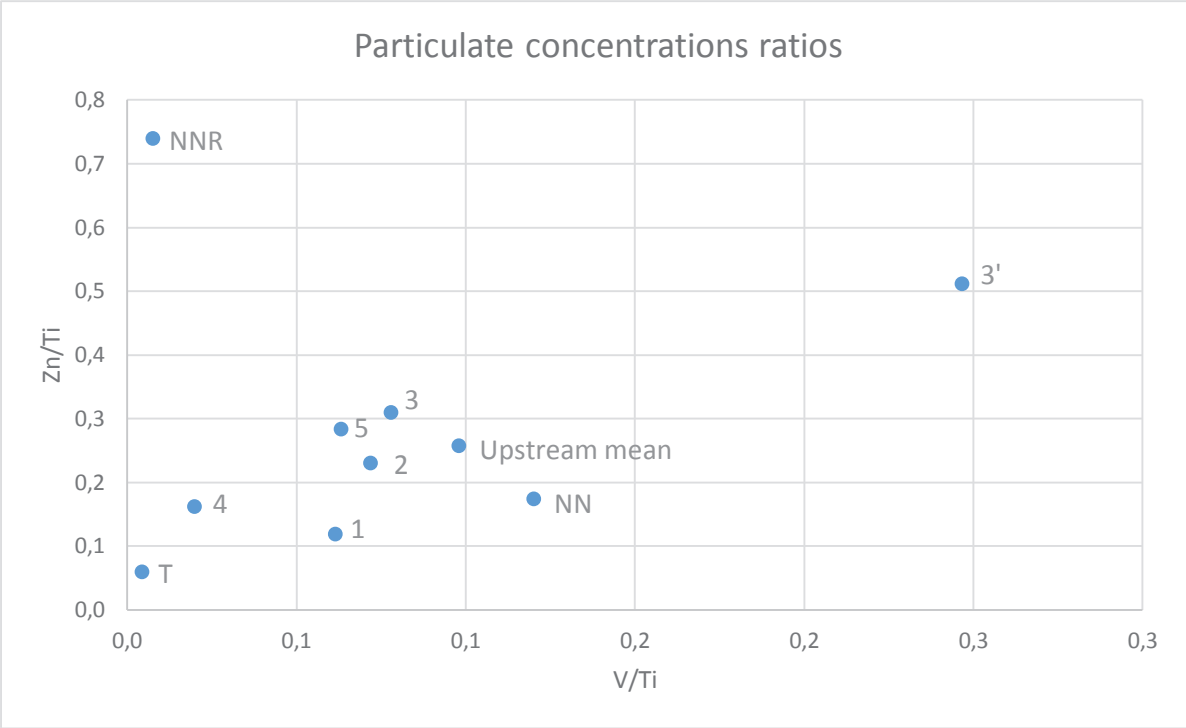

Figure 22: V/Ti and Zn/Ti concentration ratios averaged over all campaigns

5.2. Behavior of TiO_2 and associated elements in the Thur surface sediments

As for water samples, values measured at each sampling point were averaged over all campaigns. "Upstream mean" values were averaged over samples 1, 2, 3 and 3'.

The mean upstream TiO_2 concentration is 5481.52 $mg.kg^{-1}$ dry weight, with seasonal variations of ±94.31 $mg.kg^{-1}$ dry weight. In samples 4 and 5, increases of 2210.45 $mg.kg^{-1}$ (+40.33%) and 624.58 $mg.kg^{-1}$ (+11.39%) compared to this concentration were measured, respectively (Table 7, Figure 23, Appendix VI). This shows that effluent T is the most impactful one on the studied sediments.

The analysis of impurity elements showed low increases in sample 4: +0.15% V, +7.93% Co, +7.73% Zn. They do not vary in the same order as TiO_2.

Table 7: Changes in downstream sediment elemental concentrations compared to upstream mean values. For each element, the first column is the concentration difference between the upstream mean value and the downstream value, the second column expresses this difference as a percentage of increase or decrease.

Mean values	TiO_2 (ppm)	TiO_2 (%)	V (ppm)	V (%)	Co (ppm)	Co (%)	Zn (ppm)	Zn (%)
Upstream mean	5481,52	-	76,58	-	13,46	-	164,67	-
Sample 4 - upstream	+ 2210,45	+ 40,33	+ 0,11	+ 0,15	+ 1,07	+ 7,93	+ 12,73	+ 7,73
Sample 5 - upstream	+ 624,58	+ 11,39	- 8,95	- 11,69	- 3,53	- 26,26	- 34,79	- 21,13

So, it seems that sediments are less impacted than waters by the industrial effluents releases. This could be due to the fact that NMs would more likely stay in the river water than settle down the water column. However, even if this could be true at point 4, Ca concentrations at point 5 are high enough to induce the aggregation of TiO_2 NPs and their potential sedimentation (French *et al*. 2009; Chowdhury *et al*. 2012, Adam *et al*. submitted to JNR, 2015). But this aggregation is not an instantaneous process for TiO_2 concentrations as low as those measured in the river (Adam *et al*. submitted to JNR, 2015). So their transport further downstream is still likely. It is also possible that Ca concentration in the NN and NNR effluents are so high that particles are big enough to settle down immediately upon release. If true, it cannot be assessed in this part of the study as samples were not taken at this release point in the river, due to a lack of sediments. Furthermore, as in waters, the use of isotopic analytical tools could enable distinguishing natural from anthropic TiO_2 and help in making firm conclusions about their presence in the sediment.

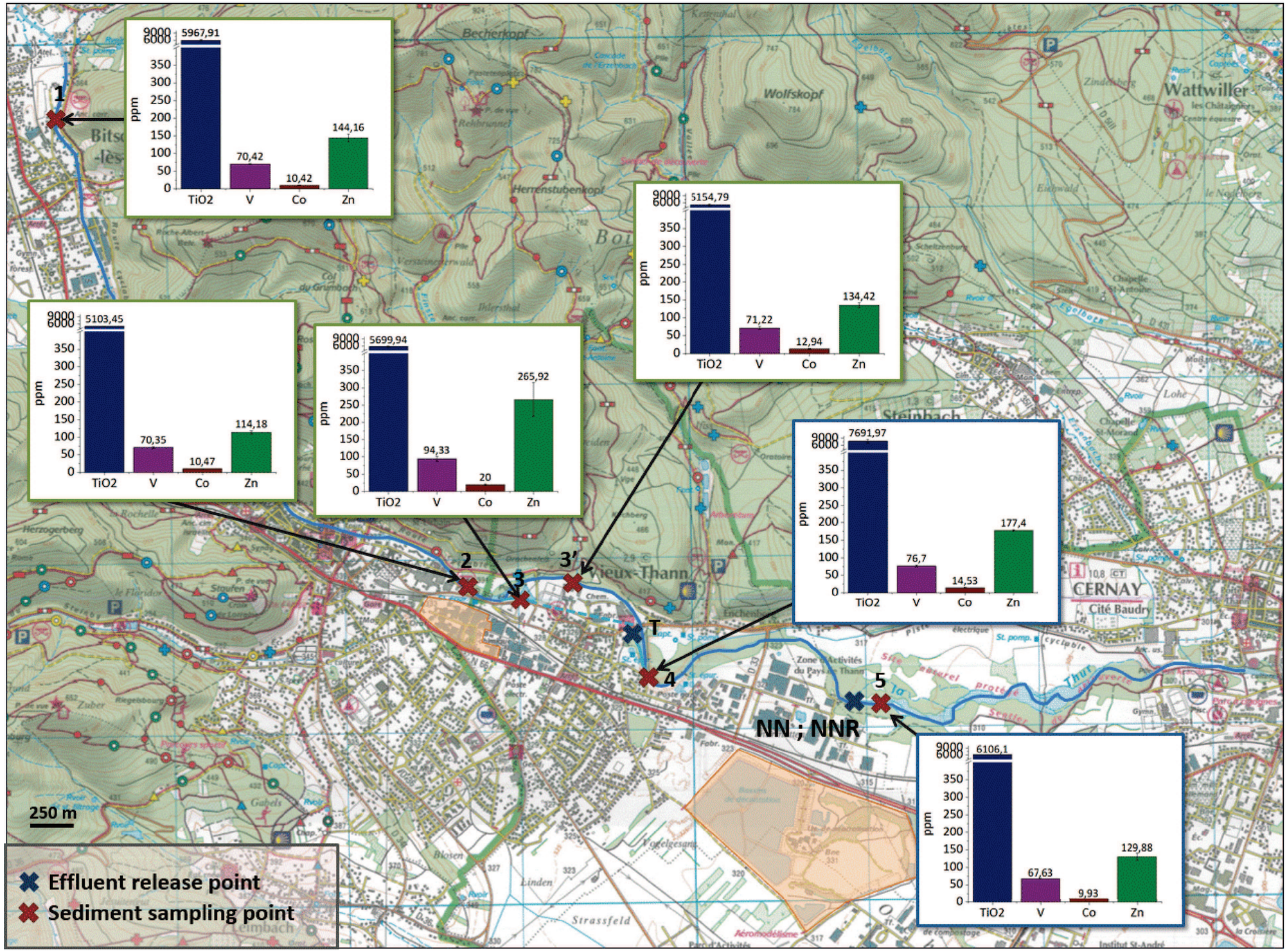

Figure 23: Concentrations of TiO_2, V, Co and Zn in sediments. Values at each sampling point (Appendix V) are averaged over all campaigns, error bars are yearly variations.

5.3. Behavior of TiO_2 and associated elements in soils

The specific objective of this part of the study was to assess the potential atmospheric deposition of TiO_2 onto soil, considering sample 1 as the upstream reference, all others being potentially impacted by atmospheric deposition from the factory.

All soil samples present an increase in Ti concentrations compared with the upstream reference (Table 8, Figure 24, and Appendix VIIA).

Soil 3 is the most impacted soil among the samples, as it presents the highest increases in TiO_2, V and Co and the second most important increase in Zn concentrations compared to the upstream reference (Table 8). Soil 4, 2, 5 and 3' contain lower and lower Ti, V, Co and Zn concentrations, meaning that they are less and less impacted: the industry seems to affect soils compositions less and less as they are located further downstream (3 > 4 > 5). Although soil 2 is the nearest to the factory, it is not located in the main wind direction, which may explain why it does not present the highest elemental concentration of TiO_2 and associated metals. In the same way, soil 3', located on the edge of the forest, is protected by the vegetation, and is the least impacted of the natural soils.

Soil 6 and 7 are industrial soils. Sample 6 presents higher increases than sample 4, but sample 7, which is only a few dozen meters away, presents much lower concentrations. These high concentrations heterogeneities could be explained by their anthropogenic nature. Consequently, no firm conclusions can be drawn on both these soils regarding their content in TiO_2 NMs. The isotopic analysis of vegetation leaves could help in identifying the potential deposition of TiO_2 NPs from the factory.

Table 8: Changes in downstream soil elemental concentrations compared to the upstream reference. For each element, the first column is the concentration difference between the upstream mean value and the downstream value, the second column expresses this difference as a percentage of increase or decrease.

Mean values	TiO_2 (ppm)	TiO_2 (%)	V (ppm)	V (%)	Co (ppm)	Co (%)	Zn (ppm)	Zn (%)
Soil 1	4895,79	0,00	72,84	0,00	12,03	0,00	158,73	0,00
Soil 2 - Soil 1	1839,84	+ 37,58	24,46	+ 33,58	3,45	+ 28,69	48,76	+ 30,72
Soil 3 - Soil 1	3682,22	+ 75,21	45,06	+ 61,85	18,49	+ 153,65	157,57	+ 99,27
Soil 3' - Soil 1	1056,85	+ 21,59	4,27	+ 5,87	1,14	+ 9,47	30,54	+ 19,24
Soil 4 - Soil 1	2325,38	+ 47,50	25,79	+ 35,40	12,35	+ 102,63	149,84	+ 94,40
Soil 5 - Soil 1	1541,02	+ 31,48	2,38	+ 3,26	1,49	+ 12,34	39,71	+ 25,02
Soil 6 - Soil 1	2772,71	+ 56,63	28,69	+ 39,39	8,90	+ 74,01	214,93	+ 135,40
Soil 7 - Soil 1	1970,29	+ 40,24	20,04	+ 27,51	3,62	+ 30,08	85,20	+ 53,68

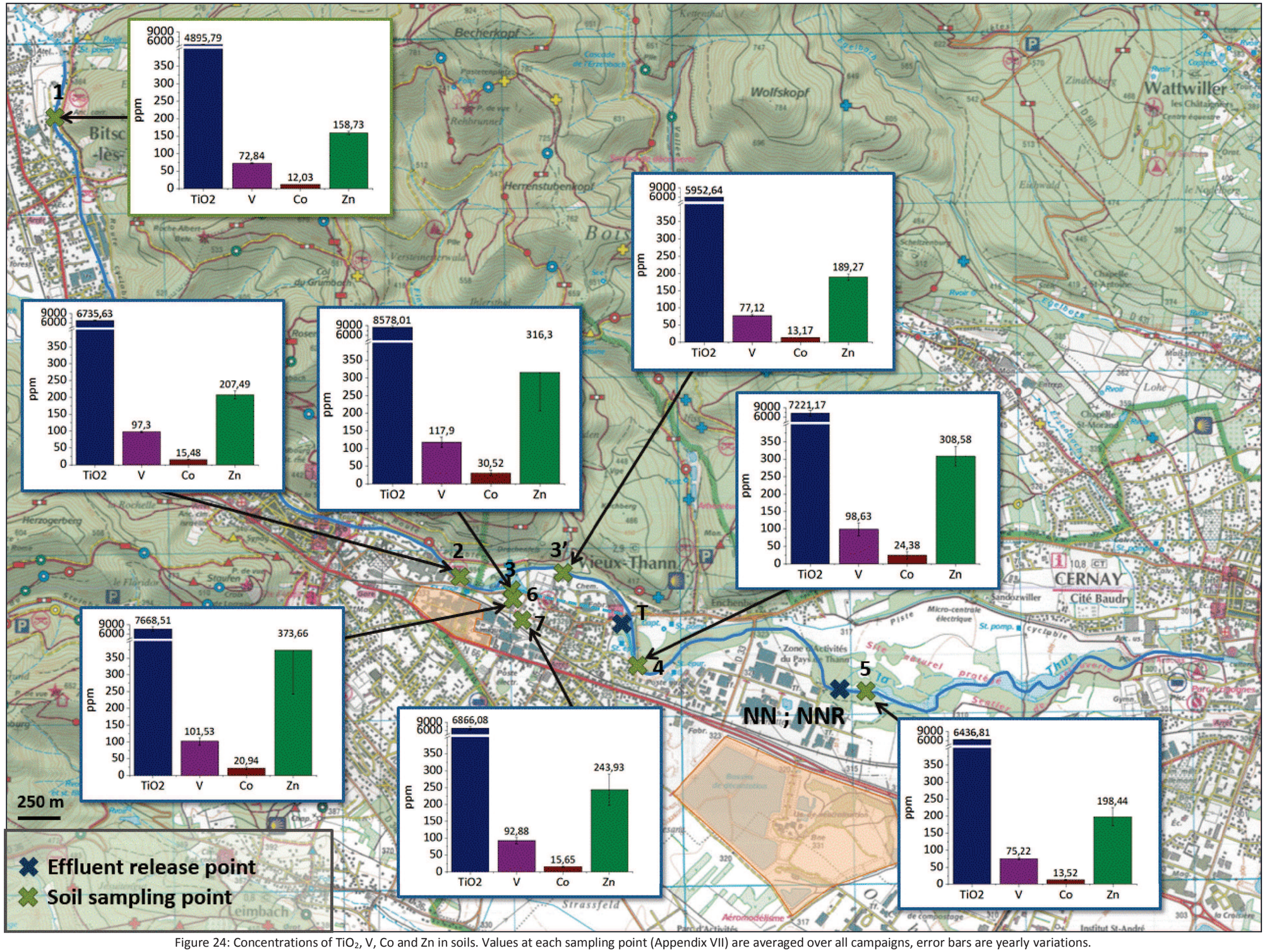

Figure 24: Concentrations of TiO_2, V, Co and Zn in soils. Values at each sampling point (Appendix VII) are averaged over all campaigns, error bars are yearly variations.

Conclusion

This study shows that both water and soils collected on the study area are significantly impacted by the TiO_2 NPs production activity. Lower Ti concentrations increases were measured in sediments than in water. At point 4, this may be due to the transport of NPs further downstream, as the low conductivity measured in effluent T does not favor the TiO_2 NMs aggregation. In the opposite, high conductivity values were measured in effluents NN and NNR, so NPs are likely to occur as big aggregates at the exit of these pipes, and settle down the water column immediately upon release. In order to better assess the behavior of TiO_2 in water, more samples could be taken nearer to the effluents release points. Also, in order to determine the TiO_2 NMs exact concentrations in the environment, an isotopic analytical methodology should be developed. With the coupling of field-flow fractionation in water samples, there is a high potential for determining both the TiO_2 NPs concentrations and aggregates size, which is of first necessity to determine their fate, bioavailability and potential reactivity.

When assuming that all measured particulate TiO_2 is nanoparticulate, its concentrations at point 4 might have an effect on the ecosystem. Indeed, lethal concentration as low as 29.8 $\mu g.L^{-1}$ have been shown in the laboratory, under simulated solar radiations (Ma *et al*. 2012). Even if this result has to be taken with caution, as it was not obtained on the TiO_2 NMs produced by the studied factory, it shows that more ecotoxicity tests are needed in order to make firm conclusions about the potential effect on the TiO_2 NMs release on the ecosystem. Besides NPs, the aqueous ecosystem might be significantly impacted by the rises in temperature and conductivity induced by the effluents release, although very locally.

In order to better understand the dominant processes at stake, the behavior of TiO_2 NPs in river water was studied in the laboratory under various conditions. This is the purpose of the next section.

References

Adam V, Loyaux-Lawniczak S, Labille J, Galindo C, del Nero C, Weber T, Quaranta G (submitted to Journal of Nanoparticle Research) Aggregation behavior of TiO_2 nanoparticles in natural river water

Chowdhury I, Cwiertny DM, Walker SL (2012) Combined Factors Influencing the Aggregation and Deposition of nano-TiO_2 in the Presence of Humic Acid and Bacteria. Environ Sci Technol 46:6968–6976. doi: 10.1021/es2034747

Holbrook DR, Motabar D, Quiñones O, *et al* (2013) Titanium distribution in swimming pool water is dominated by dissolved species. Environ Pollut 181:68–74. doi: 10.1016/j.envpol.2013.05.044

French RA, Jacobson AR, Kim B, *et al* (2009) Influence of Ionic Strength, pH, and Cation Valence on Aggregation Kinetics of Titanium Dioxide Nanoparticles. Environ Sci Technol 43:1354–1359. doi: 10.1021/es802628n

Gondikas AP, Kammer F von der, Reed RB, *et al* (2014) Release of TiO_2 Nanoparticles from Sunscreens into Surface Waters: A One-Year Survey at the Old Danube Recreational Lake. Environ Sci Technol 48:5415–5422. doi: 10.1021/es405596y

Gy PM (1992) Sampling of heterogeneous and dynamic material systems, theories of heterogeneity, sampling and homogeneizing. Elsevier, Amsterdam

Hsu L-Y, Chein H-M (2006) Evaluation of nanoparticle emission for TiO_2 nanopowder coating materials. J Nanoparticle Res 9:157–163. doi: 10.1007/s11051-006-9185-3

Kaegi R, Wagner T, Hetzer B, *et al* (2008) Size, number and chemical composition of nanosized particles in drinking water determined by analytical microscopy and LIBD. Water Res 42:2778–2786. doi: 10.1016/j.watres.2008.02.009

Labille J, Feng J, Botta C, *et al* (2010) Aging of TiO_2 nanocomposites used in sunscreen. Dispersion and fate of the degradation products in aqueous environment. Environ Pollut 158:3482–3489. doi: 10.1016/j.envpol.2010.02.012

Ma H, Brennan A, Diamond SA (2012) Photocatalytic reactive oxygen species production and phototoxicity of titanium dioxide nanoparticles are dependent on the solar ultraviolet radiation spectrum. Environ Toxicol Chem 31:2099–2107. doi: 10.1002/etc.1916

II.B AGGREGATION BEHAVIOR OF TiO_2 NANOPARTICLES IN NATURAL RIVER WATER

This part consists in a paper accepted in the Journal of Nanoparticle Research in September 2015.

The supplementary information is provided in Appendix VIII.

Aggregation behavior of TiO_2 nanoparticles in natural river water

Véronique Adam [a,b], Stéphanie Loyaux-Lawniczak[a], Jérôme Labille[c], Catherine Galindo[d], Mireille del Nero[d], Tiphaine Weber[a], Gaetana Quaranta*[a]

[a] *Laboratoire d'Hydrologie et de Géochimie de Strasbourg / EOST / UDS, 1 rue Blessig, 67084 Strasbourg Cedex, France.*

[b] *French Environment and Energy Management Agency, 20 avenue du Grésillé, BP 90406 49004 Angers Cedex 01, France*

[c] *Aix-Marseille Université, CNRS, IRD, CEREGE, UMR 7330, 13545 Aix-en-Provence, France*

[d] *Institut Plurisdisciplinaire Hubert Curien, 23 rue du Loess, BP 28, 67037 Strasbourg Cedex 2, France*

**corresponding author: quaranta@unistra.fr, 0033 368 85 0379*

Abstract

The purpose of this study was to determine and understand the aggregation behavior of industrial nanoparticulate TiO_2 (NPs) in the river water near a TiO_2 production plant. Aggregation was tested in near-reality conditions, with industrial NPs and filtered river water in which they are potentially released. The evolution of the hydrodynamic diameters of the TiO_2 aggregates in the presence of added Suwannee River Fulvic Acid (SRFA) and illite in the filtered river water was measured at pH 8 for at least 30 minutes with dynamic light scattering and laser diffraction. The experiments performed in filtered river water allowed to determine the attachment efficiency coefficients, while the experiments performed in conditions facilitating aggregation (higher Ca^{2+} content) were used to understand the potential aggregation processes. When no Ca^{2+} was added into the river water, the initially aggregated TiO2 did not develop a secondary aggregation in the presence of SRFA and illite. Upon the addition of 2.75 mM Ca^{2+}, TiO_2 was shown to heteroaggregate with illite at all tested concentrations. Consequently, in the studied river, the fate of TiO_2 NPs does not seem to be related to that of clay suspended particles upstream of the plant. In the opposite, the behaviors of TiO_2 NPs and clays are closely linked in a water with higher salt content, as it is the case downstream of one of the industrial effluents release points.

Introduction

Engineered nanoparticles (ENPs) are present in many consumer products (e.g. in biomedicine, textile and electronics) (Piccinno *et al*. 2012). ENPs research has developed in the last decade, but their diversity and their special behavior due to their small size prevent authors from making general conclusions about their potential risks and impacts on human health and on the environment. Nevertheless, it is known that ENPs aggregation is one of the most important processes to take into account in order to understand and predict their transport in the environment and their potential effects on target organisms: the aggregation state of NPs and their particulate size distributions will determine both their transport in environmental compartments and their bioavailability (Johnston *et al*. 2010; Chowdhury *et al*. 2013; Liu and Cohen 2014).

Nanoparticulate TiO_2 represents the second most important ENP market at the European and global scales. They are used in a wide variety of applications, such as cosmetics, food, cements and paints compositions (Piccinno *et al*. 2012).

In this work, the focus has been put on industrial TiO_2 ENPs, produced by the third most important TiO_2 producer worldwide, and destined to various applications. A site-specific scale (including the factory, the waste treatment site, and the river section in which the effluents are released) was used, in order to assess the aggregation behavior of ENPs in the natural environment in which they occur: the water used in this study was sampled in the river in which the plant industrial effluents are released.

Literature is scarce on the aggregation behavior of TiO_2 ENPs in natural freshwater: to our knowledge, only four studies published such results, and only two of them studied TiO_2 stability in river water (Keller *et al*. 2010; Sillanpää *et al*. 2011; Ottofuelling *et al*. 2011; Praetorius *et al*. 2012). The complexity of natural water composition makes results interpretation difficult, but it is necessary to perform experiments on such waters, in order to have a better knowledge of the behavior of ENPs in the environment in which they are released.

The particles aggregation behavior can be described by the attachment efficiency coefficient. It is defined as the fraction of effective collisions that are leading to actual sticking of the particles to one another. It has been used in numerous modeling studies of ENPs fate (Petosa *et al*. 2010; Praetorius *et al*. 2012; Meesters *et al*. 2014; Therezien *et al*. 2014; Sani-Kast *et al*.), but few authors have experimentally calculated TiO_2 attachment efficiencies. Moreover, only deionized or ultrapure water was used and not natural water. These calculations were used to explain homoaggregation variations with ionic strength (Chowdhury *et al*. 2013; Zhou *et al*. 2013; Zhu *et al*. 2014; Labille *et al*. 2015), to understand TiO_2 ENPs and clay particles interactions (Zhou *et al*. 2012; Labille *et al*. 2015; Wang *et al*.

2015) and to analyze TiO_2 ENPs aggregation in the presence of SiO_2 colloids and humic acids (Praetorius *et al*. 2014; Wang *et al*. 2015).

This paper takes a step forward in current ENPs research, by determining experimentally the aggregation behavior of TiO_2 ENPs in filtered river water in presence of added dissolved organic matter (DOM) and clay, in order to determine the attachment efficiency coefficients of TiO_2 in these natural conditions. Filtered natural water was chosen because natural dissolved contents remained, but particulate matter can be controlled. The approach consisted in (1) experimenting aggregation in the filtered river water to determine attachment efficiency in near-reality conditions, and (2) experimenting aggregation in facilitating conditions (high salt content), in order to understand the aggregation processes.

1. Materials and methods

1.1. Materials

Water was sampled in the river flowing nearby the TiO_2 producing plant, upstream of the point at which the industrial effluents are released (Table 1). The conductivity measured in this river was low compared to those of other rivers in its hydrographic network. These rivers presented in 2013 conductivities of about 0.6 and 0.5 $mS.cm^{-1}$ (AERM 2013). The river water was filtered (0.2 µm polycarbonate filters) on the day of sampling and stored at -20 °C in the dark.

Table 1: Physical parameters and concentrations of elements in the river water upstream of the TiO_2 plant

pH	7.8	**Fe (mM)**	$1.79x10^{-4}$
Conductivity ($mS.cm^{-1}$)	0.15	**K (mM)**	0.038
DOC ($mg.L^{-1}$)	2	**Mg (mM]**	0.091
Cl^- (mM)	0.356	**Mn (mM)**	$1.092x10^{-3}$
NO_3^- (mM)	0.055	**Na (mM)**	0.415
SO_4^{2-} (mM)	0.103	**P (mM)**	$1.25x10^{-3}$
Al (mM)	$1.85x10^{-4}$	**Si (mM)**	0.107
Ca (mM)	0.244	**Ti (mM)**	$< 4.18x10^{-4}$

TiO_2 NPs provided by the producer were used for all experiments. They were delivered as an aggregated powder of several hundreds of nm in size and of 0.5 g.cm-3 bulk density. They were well crystallized spherical anatase, with a crystallite size of about 5 nm (Fig. S1 and S2, Supplementary Information). Due to the aggregated nature of the TiO2 (NPs), the relevant primary constituent size should not be the crystallite size but should rather be the as-is aggregate size as measured in the below stock suspensions.

Stock suspensions were prepared monthly by dispersing 2 g of NPs in 100 mL of filtered river water adjusted to pH 11 with NaOH, then placed in an ultrasonic bath (Ultrasonic cleaner 5510, Branson Electronics) for 30 minutes and centrifuged at 218 g during 20 minutes. The supernatant was taken as the stock suspension. The particle size distributions were measured by dynamic light scattering (DLS, ZetaSizer NanoZS, Malvern Instruments) before each experiment to check that they did not vary with time. The mean hydrodynamic diameter was 465 ±136.5 nm, meaning that the NPs were already aggregated at the beginning of the aggregation experiments. The TiO_2 concentrations in the suspensions were measured by drying and weighing 5 mL of suspension, and found to be 500 $mg.L^{-1}$. TiO_2 stock suspensions were also prepared in deionized water following the same protocol, with particle size distributions (PSDs) narrowing around a hydrodynamic diameter of 350 ±40.9 nm and TiO_2 concentrations of 850 $mg.L^{-1}$ in the suspensions.

Clay suspensions were prepared with illite originating from the Puy-en-Velay, France. 1 g of illite was dispersed in 100 mL of filtered river water, sonicated for 5 min, allowed to settle for 2 hours and centrifuged at 1000 rpm for 10 min. The supernatant constituted the purified illite stock suspension (Fig. S3, Supplementary information) with a concentration of 1 $g.L^{-1}$ measured by drying and weighing 5 mL of suspension. The mean hydrodynamic diameter of illite in these suspensions was 554 ±59.0 nm. TiO_2 and illite stock suspensions were prepared monthly and stored in the dark at 4°C; PSDs were measured before each experiment to verify that they did not change in time.

Suwannee River Fulvic Acid (SRFA, Standard I) was purchased from the International Humic Substance Society and used as a surrogate for dissolved organic carbon (DOC). Stock solutions were prepared weekly by diluting 15 mg of SRFA in 100 mL of river water and stored at 4°C in the dark.

The pH value of the stock suspensions, the test suspensions and the SRFA solution were adjusted to 8 using NaOH or HCl. This value was chosen to be very close to the natural pH of the river water (pH = 7.8). $CaCl_2$ was chosen to facilitate the aggregation because Ca^{2+} is a divalent cation, implying higher efficiency in aggregation of negatively charged particles, and it is the dominant divalent cation in the river water (Table 1). Preliminary experiments were performed in river water in order to determine the lowest $CaCl_2$ concentration leading to the formation of illite homoaggregates with diameters constant for at least 30 minutes (data not shown). The obtained 2.75 mM concentration (leading to a total 3 mM Ca concentration in river water) was used in the experiments where aggregation had to be facilitated.

1.2. Surface charge measurements

Illite (25 mg.L^{-1}) and TiO_2 ENPs (10 mg.L^{-1}) electrophoretic mobilities (EPMs) were measured in filtered river water, with and without an added $CaCl_2$ concentration of 2.75 mM. Measurements were performed using Laser Doppler electrophoresis (ZetaSizer Nano ZS, Malvern Instruments) at pH values between 2 and 11, adjusted with HCl or NaOH. The Smoluchowski approximation was used to convert the EPMs into zeta potentials (Elimelech *et al*. 1995), eq. 1):

$$U = \frac{\varepsilon\zeta}{\mu} \qquad (1)$$

Where U is the electrophoretic mobility, ε is the dielectric constant of the solution, ζ is the zeta potential and μ is the viscosity of the solution.

1.3. Aggregation kinetics measurements

TiO_2 aggregation with fulvic acids

The aggregation of TiO_2 ENPs in presence of SRFA in deionized and river waters was assessed by measuring the aggregates PSDs using DLS. The data fit was performed using the cumulant algorithm. Its validity was controlled and only satisfactory residual is presented here. Homoaggregation of TiO_2 ENPs was tested in preliminary experiments with TiO_2 concentrations from 10 to 100 mg.L^{-1} in triplicates, at pH 8, in the presence of 2.75 mM of added $CaCl_2$ and during 30 minutes. While the kinetics of aggregation through 30 minutes is not measurable at the predicted environmental concentration (PEC < 2 μg.L^{-1}; (Gottschalk *et al*. 2013), our aim is to determine a sticking efficiency at these high but measurable concentrations, which can be extrapolated to lower and more relevant PECs. The homoaggregation was significant from 40 mg TiO_2.L^{-1}. This concentration was retained to evaluate the effect of SRFA on TiO_2 NPs aggregation. The SRFA concentration added in the river water was fixed at 2.5, 5 and 10 mg.L^{-1}. Other tests were performed in deionized water where 3.81 and 8.81 mg.L^{-1} of SRFA were added in order to obtain total DOC concentrations similar, respectively, to those of the river water and of the river water + 5 mg.L^{-1} SRFA (Table 2). Test suspensions were prepared by diluting the proper volumes of SRFA and TiO_2 in the water, adjusting the pH value to 8 and adding 2.75 mM $CaCl_2$ where necessary. The DLS hydrodynamic diameters measurements (ZetaSizer Nano ZS, Malvern Instruments) were started immediately after adjusting the pH value and adding $CaCl_2$. They were stopped after 30 min.

Table 2: Tested SRFA concentrations and corresponding DOC concentrations in river and deionized waters

	$[SRFA]_{added}$ ($mg.L^{-1}$)	$[DOC]_{total}$ ($mg.L^{-1}$)
River water	0	2
	2.5	3.31
	5	4.62
	10	7.25
Deionized water	0	0
	3.81	2
	8.81	4.62

TiO_2 aggregation in presence of illite

The aggregation of TiO_2 ENPs and illite was tested in river water by measuring the aggregates hydrodynamic diameters for at least 30 minutes, using laser diffraction (MasterSizer 3000, Malvern Instruments) when $CaCl_2$ was added in suspension and with DLS when no $CaCl_2$ was added. The measurement technique was chosen as a function of the expected aggregates size: the measurement was performed with laser diffraction when expected diameters were above 5 µm (Adam *et al.* 2015). The illite concentration was set at 25 $mg.L^{-1}$ for all experiments. TiO_2 concentrations were varied from 2.5 to 100 $mg.L^{-1}$ to simulate variations in potential accidental releases of TiO_2 from the industrial effluents.

When using laser diffraction, for each test suspension, two separate suspensions were prepared, one of illite and one of TiO_2 NPs, each 100 mL in volume. The illite suspension was placed in the test beaker and circulated in the Mastersizer with a $CaCl_2$ solution until the median diameter of illite aggregates was stabilized, around 45 µm. The TiO_2 suspension in the presence of $CaCl_2$ was then smoothly added in the test beaker as the measurement continued (1 measurement in 30 seconds). The final illite concentration was then 25 $mg.L^{-1}$, the Ca^{2+} concentration was kept constant, at 3 mM in total. Final concentrations in TiO_2 were 0 (dilution test) to 100 $mg.L^{-1}$ to simulate variations in potential releases of TiO_2 from the industrial effluents.

When using DLS, test suspensions were prepared by diluting suitable volumes of illite and TiO_2 in the river water, and adjusting the pH value to 8. The measurements were started right after pH adjustment.

1.4. Calculation of attachment efficiencies

The attachment efficiency (α) of two particles (or aggregates) is defined as the fraction of collisions leading to the attachment of the particles over the total number of collisions; it is also called the sticking factor (Wilkinson and Lead 2007). Where no collision results in attachment, α equals 0; where

all collisions lead to attachment, α equals 1. This coefficient is also defined as the inverse of the stability ratio (W) between these two entities, depending itself on attraction (van der Waals and Lewis type) and on repulsion (electrical double layer – EDL and steric) forces. The Derjaguin-Landau-Verwey-Overbeek (DLVO) theory is most frequently used to calculate the total interaction energy, as the sum of the van der Waals and the EDL forces (see supporting information for calculations details). However, large discrepancies have been observed between such calculations and experimental results (Wilkinson and Lead 2007). These differences are explained by the occurrence of other forces at stake, such as hydration forces or steric repulsion due to organic matter (Petosa *et al*. 2010). The attachment efficiency coefficient (α) was calculated from experimental data, by measuring the evolution of the hydrodynamic diameters of the aggregates in suspension at the very beginning of the aggregation (Elimelech *et al*. 1995), eq. 2):

$$\alpha = \frac{\left({}^{d_H(t)}/_{dt}\right)_{t\to 0}}{\left({}^{d_H(t)}/_{dt}\right)_{t\to 0,fast}} \qquad (2)$$

where d_H is the hydrodynamic diameter of aggregates and the subscript *fast* indicates favorable aggregation conditions, in which the ionic strength is at least equal to the critical coagulation concentration (CCC) (Zhang *et al*. 2012). At the CCC and above, α is equal to unity (Zhou *et al*. 2012).

The aggregation model SmoluCalc developed by Thill *et al*. (Thill *et al*. 2001) was used to characterize in term of an α value the experimental aggregation kinetics measured here (see model details in SI).

2. Results and discussion

2.1. Zeta potential measurements

Zeta potential measurements showed that both illite and TiO_2 particles presented a negative surface charge in the whole range of tested pH values (Figure 1), although the point of zero charge of these NPs was found at pH 6.4 in deionized water (Figure S4 in supp. info.). This difference may be explained by the presence of dissolved organic matter in river water, which is assumed to form a coating on the NPs, thus reducing their surface charge. The carboxylic functions are partially deprotonated at pH values above 5 (pH 4 < pK < pH 5; Benlot and Blanchouin 2005), which matches with and explains the observed threshold at which the NPs surface charge reaches a stable level up to pH 10.

The presence of $CaCl_2$ in the river water seemed to decrease the TiO_2 surface charge of about 13 mV. This can be explained by the positive charge of Ca^{2+} cations, which partially neutralized the surface charges. However, illite particles present a similar surface charge at all tested pH values and $CaCl_2$ concentrations. This is certainly due to the permanent and negative structural charge of the clay.

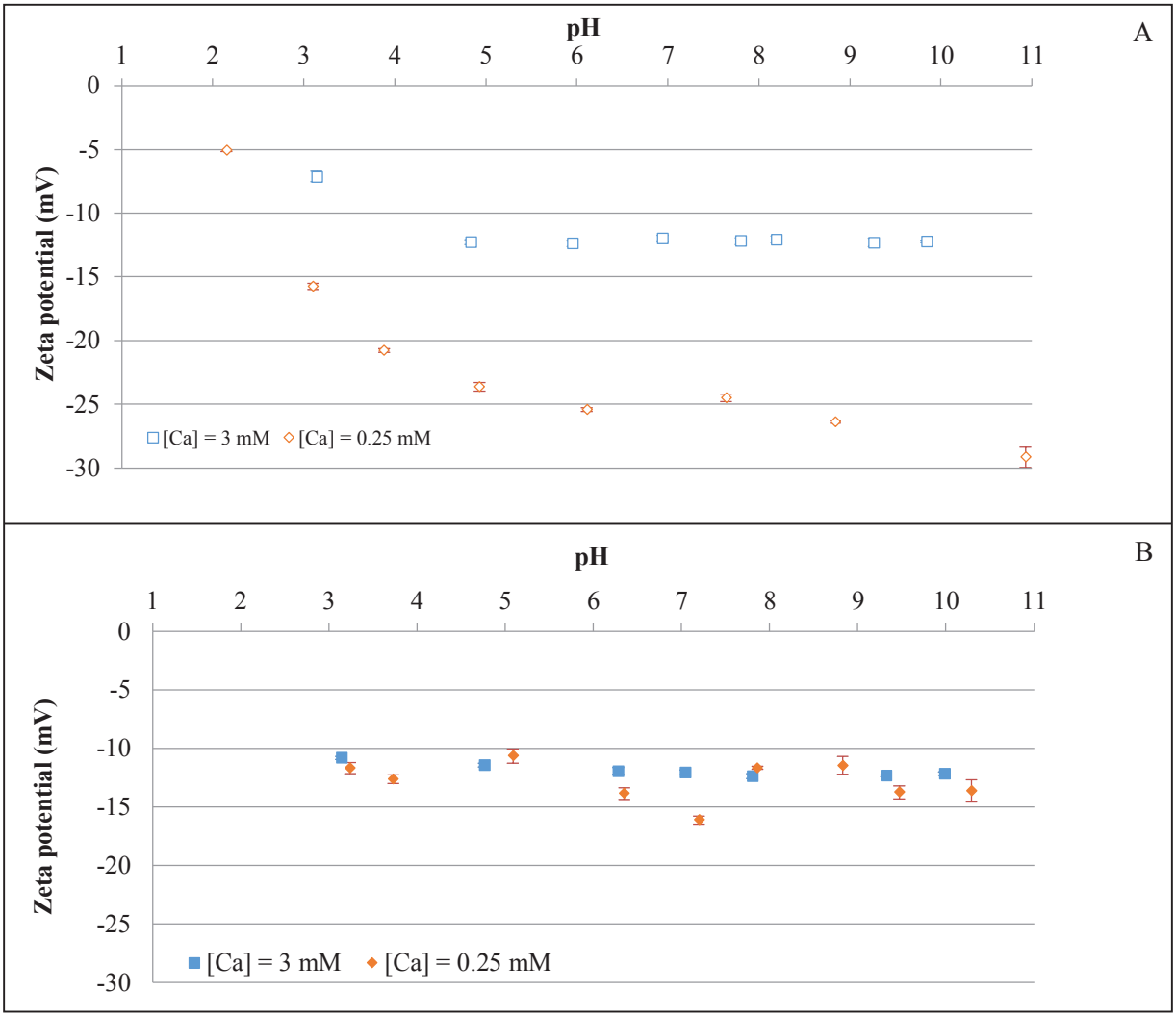

Figure 1: Zeta potential of TiO_2 NPs (A) and illite (B) as a function of pH in river water ([Ca] = 0.25 mM) and in Ca supplemented river water ([Ca] = 3 mM)

2.2. Homoaggregation kinetics

TiO_2 NPs aggregation with fulvic acids

In deionized water free of $CaCl_2$ (Fig. 2A), the addition of SRFA at concentrations up to 4.62 $mg.L^{-1}$ did not produce any effect on the TiO_2 aggregation. Upon the addition of $CaCl_2$, the presence of Ca^{2+} led to charge screening, making van der Waals forces prevailing and allowing the bridging of two negatively charged particles. However at pH 8, SRFA carboxylic functions were deprotonated (pK_1 = 4.42; (Richie and Perdue 2003), so they also carried negative charges. Cations attached to TiO_2 NPs could attract the SRFA molecules, increasing the net surface charge and the steric effect, which led to the observed decreased aggregation with increased SRFA concentration.

In river water free of $CaCl_2$ (Figure 2B), the results showed a decrease in the TiO_2 aggregates sizes with the addition of SRFA, which was the same at all concentrations tested. This was caused both by the repulsion of the negative charges of TiO_2 and SRFA (electrostatic forces) and by the steric effect of dissolved organic matter (Domingos *et al*. 2009). The absence of TiO_2 aggregation led to an attachment efficiency equal to zero.

In the presence of added $CaCl_2$ in river water (Figure 2B), no effect of SRFA was shown. This might be due to the higher cationic charge of the river water than that of deionized water, leading to more efficient neutralization of SRFA carboxylic functions by positive charges (Erhayem and Sohn 2014). Moreover, SRFA was not the only type of DOM in water in these experiments. The diversity of DOM types in the river water implied different surface densities of functional groups and charges, which could be another reason for the much lowered effect of DOC concentration on the TiO_2 aggregation.

Overall, the experiments of TiO_2 NPs aggregation in presence of SRFA showed that the SRFA/cations concentration ratio and the type of DOM played most significant roles in the TiO_2 aggregation. Results were different when working whether with deionized or with river water, which showed that simulating natural water in the laboratory is not sufficient.

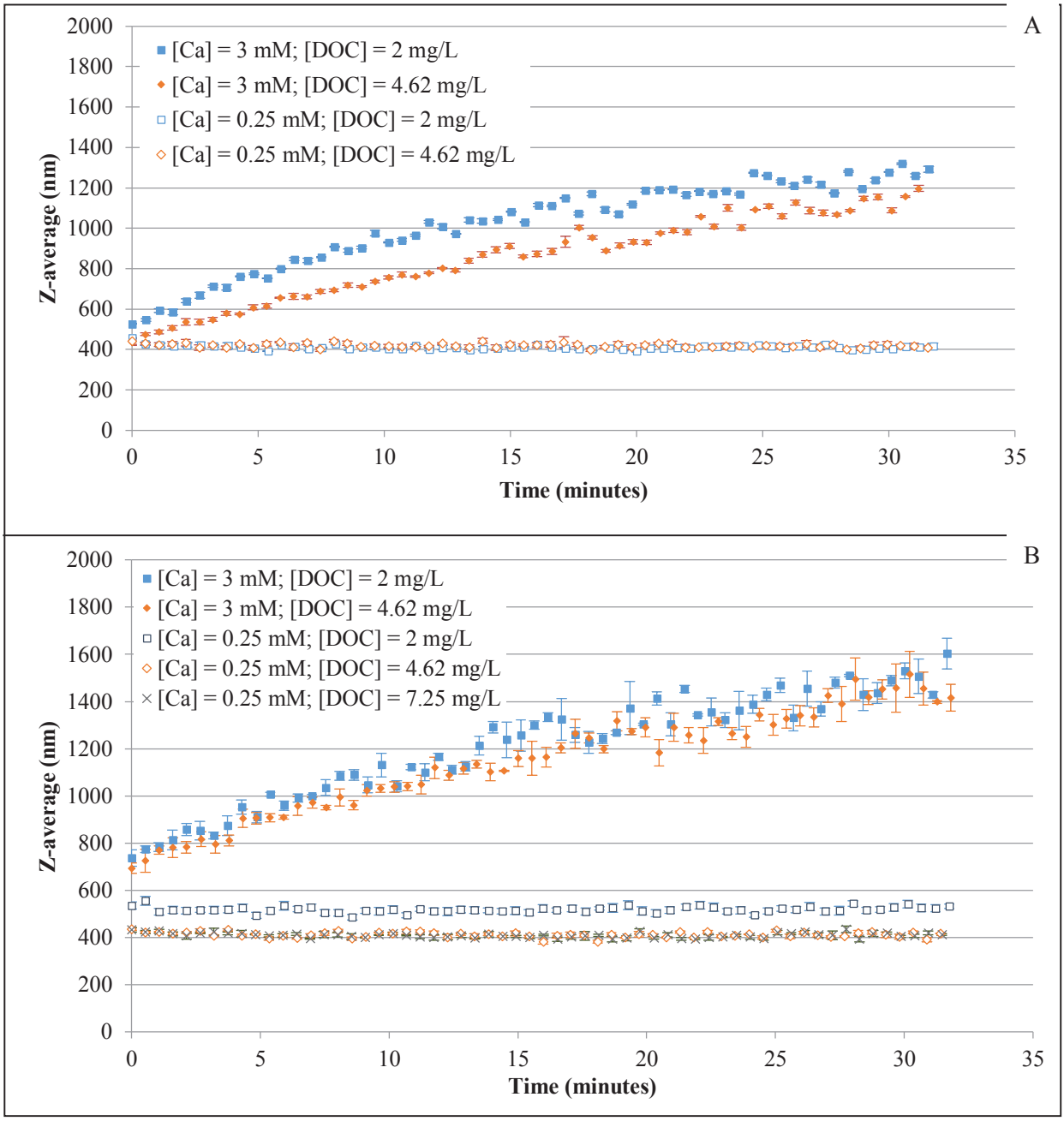

Figure 2: Evolution of TiO_2 NP aggregates diameters in deionized water (A) and river water (B) at pH 8; [TiO_2] = 40 $mg.L^{-1}$

2.3. TiO_2 NPs aggregation in the presence of illite

In river water adjusted to pH 8, illite and TiO_2 aggregates sizes did not change within more than 30 minutes. This was most certainly due to strong negative surface charges of both illite and TiO_2, preventing aggregation through electrostatic repulsion (Figure 3). In these conditions, the attachment efficiency of illite and TiO_2 was null.

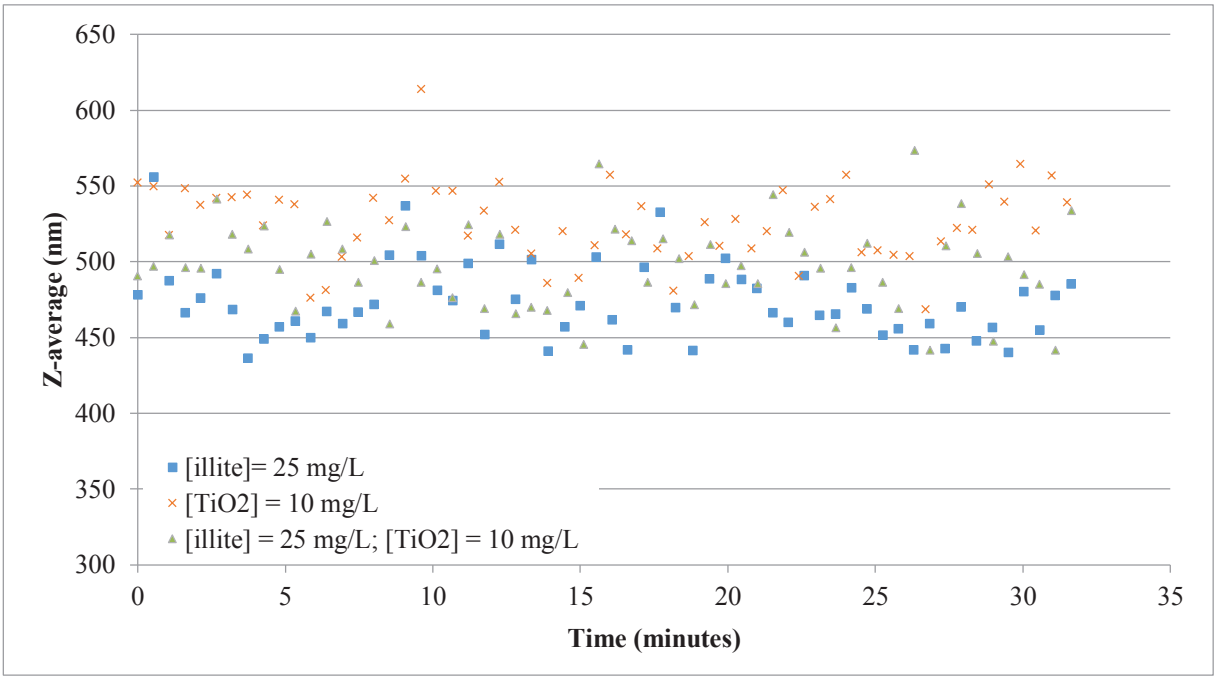

Figure 3: Hydrodynamic diameters of illite and TiO_2 aggregates in river water at pH 8 (DLS measurements)

When $CaCl_2$ was added to the suspension, the aggregation kinetics measured in the presence of the lowest tested TiO_2 concentrations (2.5, 5 and 10 $mg.L^{-1}$) were similar to each other: aggregation was slow (1 $\mu m.min^{-1}$), comparable to that observed after the dilution of the test suspension with 100 mL of electrolyte free of TiO_2 NPs (Figure 4). The aggregates mean size was stabilized around 85 µm after 40 minutes of experiment.

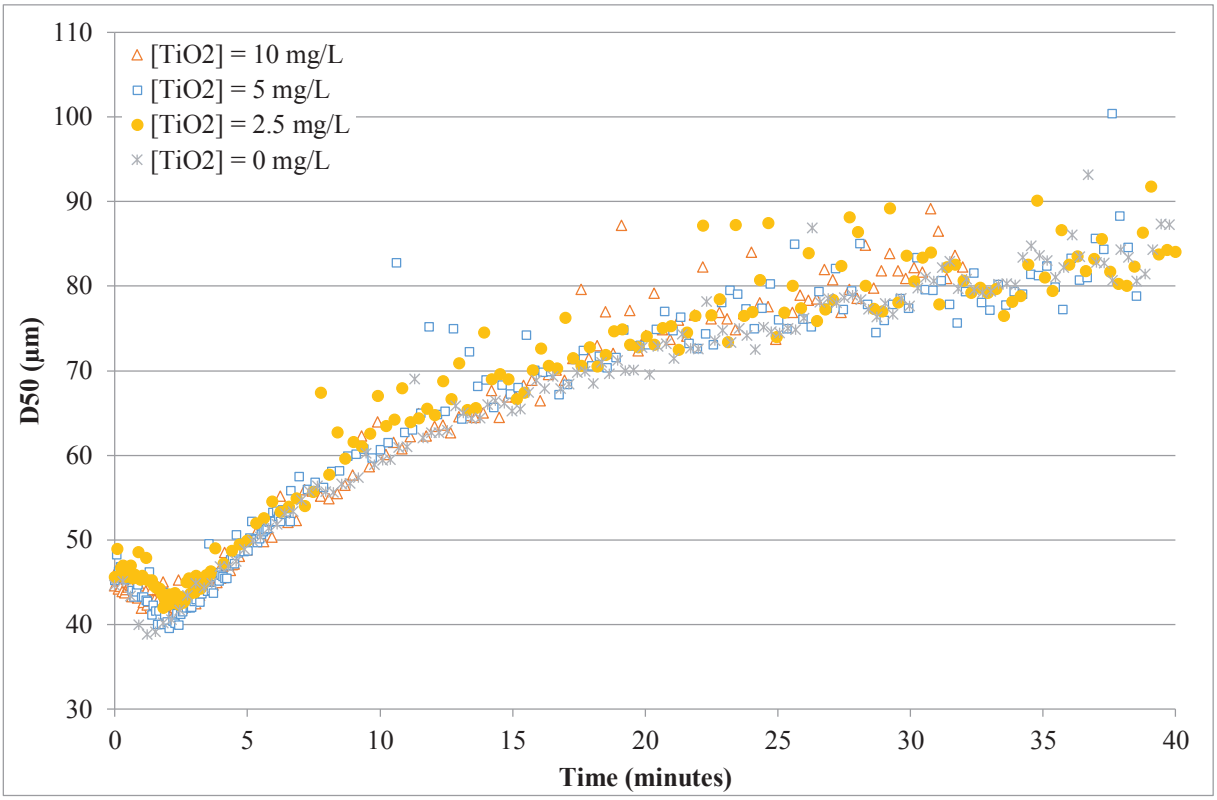

Figure 4: Evolution of illite and TiO_2 NPs aggregates diameters with time in river water ([Ca] = 3 mM; pH 8). Laser diffraction measurements, D50 = median diameter of aggregates

Significant aggregation was observed when higher TiO_2 concentrations were tested (Figure 5). A concentration threshold appeared at 20 $mg.L^{-1}$ of TiO_2. At this concentration and above, the aggregation increased with TiO_2 concentration. So it is clear that TiO_2 played a role in the observed aggregation. However, TiO_2 and illite were both negatively charged in the tested conditions. Cations were the only possible bridge between these negative aggregates: they allowed the formation of "illite-Ca^{2+}-TiO_2-Ca^{2+}-illite" secondary aggregates.

At concentrations of 50 mg $TiO_2.L^{-1}$ and above, the aggregates were very unstable during the 40 minutes measurements. This high instability was due to the fast aggregation kinetics (about 13 and 23 $\mu m.min^{-1}$ at 50 and 100 mg $TiO_2.L^{-1}$, respectively, in the first 5 minutes of measurement), which lead to the formation of big, sparse and fragile aggregates (Bouyer and Coufort 2005; Labille *et al*. 2015).

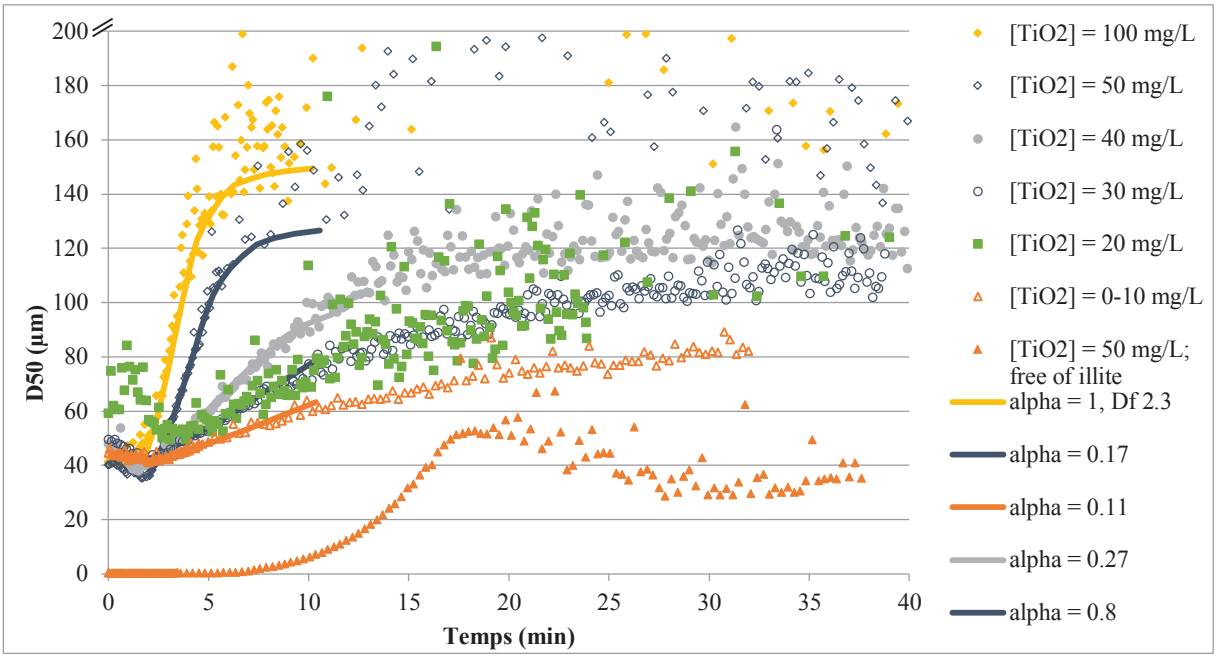

Figure 5: Evolution of illite and TiO_2 aggregates hydrodynamic diameters with time in river water ([illite] = 25 $mg.L^{-1}$); [Ca] = 3 mM; pH 8). Laser diffraction measurements, D50 = median aggregate diameter

The comparison of the aggregation of TiO_2 in the presence of illite with those of TiO_2 and illite alone (Figures 4 and 5) showed different aggregate sizes after 40 minutes of experiment. When TiO_2 nanoparticles were alone at a concentration of 50 $mg.L^{-1}$, aggregates reached a diameter of 30 µm whereas, in the presence of 25 $mg.L^{-1}$ of illite, the aggregate diameter grew up above 150 µm. Aggregates containing only illite presented a median diameter of 85 µm within 40 minutes. This proved that the aggregates formed in the presence of illite were heteroaggregates composed of TiO_2 and illite.

Using the SmoluCalc model to fit these aggregation data (model details given in SI) returned a range of global sticking efficiency values varying with the nanoparticle dose. In absence of NP, the further homoaggregation of the clay following the dilution step at time t0 is characterized by a sticking efficiency of 0.11. No enhanced aggregation was measured upon addition of NPs up to 10 mg/L. At higher nanoparticle dosage, the global sticking efficiency increased from 0.17 to 1 as the NP concentration increased from 30 to 100 mg/L. This evidences an aggregation mechanism of the clay limited by the nanoparticle dose. This is probably not a heteroaggregation mechanism where the attaching nanoparticles bridge neighbor colloids, as proposed elsewhere for lower nanoparticle / colloid ratios (Praetorius *et al*. 2014; Labille *et al*. 2015). Here, the nanoparticle / colloid surface area ratio ranges from approximately 1 to 10 for nanoparticle doses from 10 to 100 mg/L (see detailed ratios calculated in SI). This means that if the nanoparticles attach to the colloids, they potentially saturate the surface, and bridging is thus not favored. Meanwhile, if the amount of attached nanoparticles

cannot increase, this suggests that the increasing amount of non-attaching nanoparticles, remaining free in suspension, plays a key role in the observed aggregation. Depletion flocculation can thus reasonably be proposed as the driving aggregation mechanism here. Indeed, the nanoparticles / clay volume ratio ranges from 4 to 40 %, which might be significant to enhance the colloidal destabilization of the clay already undergoing salt-induced aggregation.

Moreover, at the beginning of all experiments, as illite alone was present in the suspension, results showed a size peak at 45 µm (Figure 6). After dilution with water free of TiO_2, the illite aggregates diameters stabilized around 85 µm. When adding TiO_2 NPs, a peak appeared below 1 µm, in accordance with TiO_2 aggregates size. It is interesting to note that as these are volume distributions, the minor area under this peak is not negligible given the size difference with the clay aggregates initial size. The area under this peak decreased with time, meaning that free TiO_2 aggregates were less and less present in the suspension as they were aggregated to illite particles. So, in the presence of $CaCl_2$, there was heteroaggregation of TiO_2 ENPs to illite in river water, even at concentrations as low as 2.5 $mg.L^{-1}$, which was not visible when considering only the median diameter of the aggregates (Figure 4).

PSDs in figure 6 also showed the destabilization of the aggregates at 50 $mg.L^{-1}$ of TiO_2: these PSDs were wider than those obtained at a TiO_2 concentration of 30 $mg.L^{-1}$ and showed multiple size peaks.

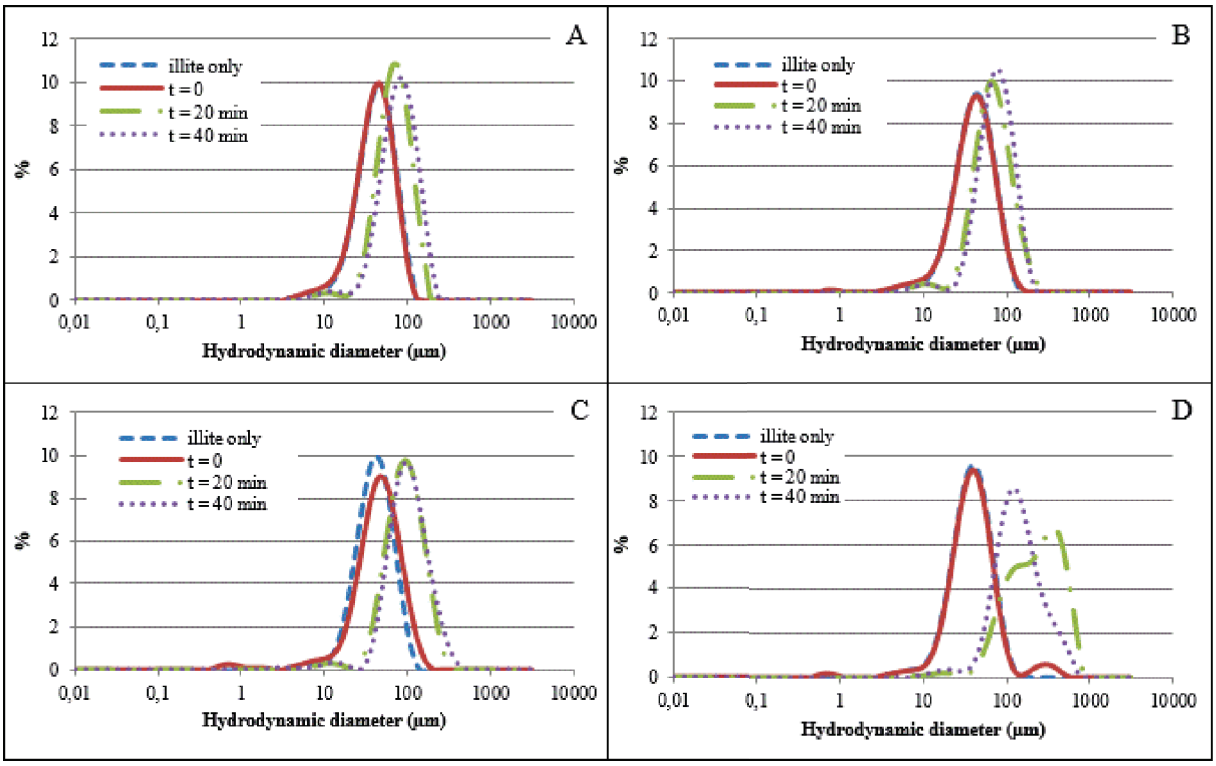

Figure 6: Particle size distributions of TiO_2 and illite aggregates with time in river water at pH 8; $[CaCl_2]_{added}$ = 2.75 mM. A: Water dilution; B: $[TiO_2]$ = 2.5 $mg.L^{-1}$; C: $[TiO_2]$ = 30 $mg.L^{-1}$; D: $[TiO_2]$ = 50 $mg.L^{-1}$

Overall, the results obtained when mixing TiO_2 and illite in the presence of 3 mM of Ca in river water show that heteroaggregation always occurred, even at low TiO_2 concentrations. From 2.5 to 10 $mg.L^{-1}$ of TiO_2, "primary" aggregates (about 85 µm) were formed, constituting one unit. From 20 $mg.L^{-1}$ of TiO_2, these units aggregated to each other, forming so called secondary aggregates, up to 120 µm in size ($[TiO_2]$ = 40 $mg.L^{-1}$). Above 50 $mg.L^{-1}$ of TiO_2, even bigger aggregates were formed, building very unstable structures which should lead over time to their recombination into smaller, denser and more stable aggregates (Labille *et al*. 2015).

3. Environmental implications

Results obtained in this work show that experiments conducted in synthetic solutions such as deionized water with controlled pH, salt concentration and natural organic matter are not sufficient to determine accurately the behavior of TiO_2 NPs in natural water. Indeed, the diversity of dissolved organic macromolecules and the variety of ions present in natural waters are not taken into account although they influence the aggregation of NPs.

Moreover, in the conditions of the studied river (upstream of the plant) the presence of fulvic acids in sufficient concentration leads to a decrease in the TiO_2 aggregates sizes. In addition, at TiO_2 concentrations ≤10mg/L (probable case of an accidental release from the industrial effluents), no NPs aggregation occurs, to themselves or to illite. This means that these NPs are readily transported along the studied river and that they can be assimilated by the organisms living in the water column.

In the presence of Ca^{2+} cations at higher concentration, no effect of DOC content is observed at concentrations below 5 $mg.L^{-1}$. However, TiO_2 NPs are shown to attach to illite particles systematically, even at low concentrations. This leads to the conclusion that in waters where higher cationic charges occur, the transport of TiO_2 down the water column and along the river is driven by those of clay particles. This could be the case in the studied river, about 200 meters downstream of one of the industrial effluents release points, where Ca^{2+} concentrations up to 1.73 mM were measured. There, benthic organisms are more likely to be exposed to TiO_2 NPs.

This work provides new data relevant to TiO_2 behavior in environmental conditions that can help modeling the fate of ENMs in river water. However, several limitations prevent the authors from making general conclusions about their fate in freshwater, as the filtered water is still a much simpler medium than natural water. Further studies need to take into account other components, such as oxy-hydroxides and particulate organic matter in order to further approach real conditions. In the same way, the added simulation of the velocity flow (and shear rate) of the river water would give more accurate collision rates and so more precise results about the potential aggregation of TiO_2 NPs.

Acknowledgements

This work was supported by the French Environment and Energy Management Agency (ADEME), the Région Alsace and the National Research Agency (ANR) project MESONNET.

Supporting information available

Supporting information provides the characterization figures of TiO_2 NPs and illite, as well as the interaction energy (DLVO theory) calculations and results and the methodology used for the SmoluCalc model calculations.

References

Adam V, Loyaux-Lawniczak S, Quaranta G (2015) Characterization of engineered TiO_2 nanomaterials in a life cycle and risk assessments perspective. Environ. Sci. Pollut. Res. 105:731-738.

AERM (Agence de l'Eau Rhin Meuse) (2013) http://rhin-meuse.eaufrance.fr/choixtheme?lang=fr. Consulted on 10 June 2015.

Benlot C, Blanchouin N (2005) www.snv.jussieu.fr/bmedia/aa/aa1.html. Consulted on June 2015.

Bouyer D, Coufort C (2005) Experimental analysis of floc size distributions in a 1-L jar under different hydrodynamics and physicochemical conditions. J Colloid Interface Sci 292:413–428.

Chowdhury I, Walker SL, Mylon SE (2013) Aggregate morphology of nano-TiO_2: role of primary particle size, solution chemistry, and organic matter. Environ Sci Process Impacts 15:275. doi: 10.1039/c2em30680h

Domingos RF, Tufenkji N, Wilkinson KJ (2009) Aggregation of Titanium Dioxide Nanoparticles: Role of a Fulvic Acid. Environ Sci Technol 43:1282–1286. doi: 10.1021/es8023594

Elimelech M, Gregory J, Jia X, Williams RA (1995) Particle Deposition & Aggregation: Measurement, Modelling and Simulation. Elsevier, New York

Erhayem M, Sohn M (2014) Stability studies for titanium dioxide nanoparticles upon adsorption of Suwannee River humic and fulvic acids and natural organic matter. Sci Total Environ 468-469:249–257. doi: 10.1016/j.scitotenv.2013.08.038

Gottschalk F, Sun T, Nowack B (2013) Environmental concentrations of engineered nanomaterials: Review of modeling and analytical studies. Environ Pollut 181:287–300. doi: 10.1016/j.envpol.2013.06.003

Johnston BD, Scown TM, Moger J, *et al* (2010) Bioavailability of nanoscale metal oxides TiO_2, CeO_2, and ZnO to fish. Environ Sci Technol 44:1144–1151.

Keller AA, Wang H, Zhou D, *et al* (2010) Stability and Aggregation of Metal Oxide Nanoparticles in Natural Aqueous Matrices. Environ Sci Technol 44:1962–1967. doi: 10.1021/es902987d

Labille J, Harns C, Bottero J-Y, Brant J (2015) Heteroaggregation of Titanium Dioxide Nanoparticles with Natural Clay Colloids. Environ Sci Technol. doi: 10.1021/acs.est.5b00357

Liu HH, Cohen Y (2014) Multimedia Environmental Distribution of Engineered Nanomaterials. Environ Sci Technol 48:3281–3292. doi: 10.1021/es405132z

Meesters JAJ, Koelmans AA, Quik JTK, *et al* (2014) Multimedia modeling of engineered nanoparticles with simpleBox4nano: Model definition and evaluation. Environ Sci Technol 48:5726–5736. doi: 10.1021/es500548h

Ottofuelling S, Kammer F Von Der, Hofmann T (2011) Commercial Titanium Dioxide Nanoparticles in Both Natural and Synthetic Water: Comprehensive Multidimensional Testing and Prediction of Aggregation Behavior. Environ Sci Technol 45:10045–10052. doi: 10.1021/es2023225

Petosa AR, Jaisi DP, Quevedo IR, *et al* (2010) Aggregation and Deposition of Engineered Nanomaterials in Aquatic Environments: Role of Physicochemical Interactions. Environ Sci Technol 44:6532–6549. doi: 10.1021/es100598h

Piccinno F, Gottschalk F, Seeger S, Nowack B (2012) Industrial production quantities and uses of ten engineered nanomaterials in Europe and the world. J Nanoparticle Res 14:1–11. doi: 10.1007/s11051-012-1109-9

Praetorius A, Labille J, Scheringer M, *et al* (2014) Heteroaggregation of titanium dioxide nanoparticles with model natural colloids under environmentally relevant conditions. Environ Sci Technol. doi: 10.1021/es501655v

Praetorius A, Scheringer M, Hungerbühler K (2012) Development of Environmental Fate Models for Engineered Nanoparticles—A Case Study of TiO_2 Nanoparticles in the Rhine River. Environ Sci Technol 46:6705–6713. doi: 10.1021/es204530n

Richie JD, Perdue EM (2003) Proton-binding study of standard and reference fulvic acids, humic acids, and natural organic matter. Geochim Cosmochim Acta 67:85–96.

Sani-Kast N, Scheringer M, Slomberg D, *et al* Addressing the complexity of water chemistry in environmental fate modeling for engineered nanoparticles. Sci Total Environ. doi: 10.1016/j.scitotenv.2014.12.025

Sillanpää M, Paunu T-M, Sainio P (2011) Aggregation and deposition of engineered TiO_2 nanoparticles in natural fresh and brackish waters. J Phys Conf Ser 304:012018. doi: 10.1088/1742-6596/304/1/012018

Therezien M, Thill A, Wiesner MR (2014) Importance of heterogeneous aggregation for NP fate in natural and engineered systems. Sci Total Environ 485-486:309–318. doi: 10.1016/j.scitotenv.2014.03.020

Thill A, Moustier S, Aziz J, *et al* (2001) Flocs Restructuring during Aggregation: Experimental Evidence and Numerical Simulation. J Colloid Interface Sci 243:171–182.

Wang H, Dong Y, Zhu M, *et al* (2015) Heteroaggregation of engineered nanoparticles and kaolin clays in aqueous environments. Water Res 80:130–138. doi: 10.1016/j.watres.2015.05.023

Wilkinson KJ, Lead JR (2007) Environmental Colloids and Particles: Behaviour, Separation and Characterisation. John Wiley & Sons

Zhang W, Crittenden J, Li K, Chen Y (2012) Attachment Efficiency of Nanoparticle Aggregation in Aqueous Dispersions: Modeling and Experimental Validation. Environ Sci Technol 46:7054–7062. doi: 10.1021/es203623z

Zhou D, Abdel-Fattah AI, Keller AA (2012) Clay Particles Destabilize Engineered Nanoparticles in Aqueous Environments. Environ Sci Technol 46:7520–7526. doi: 10.1021/es3004427

Zhou D, Ji Z, Jiang X, *et al* (2013) Influence of Material Properties on TiO2 Nanoparticle Agglomeration. PLoS ONE 8:e81239. doi: 10.1371/journal.pone.0081239

Zhu M, Wang H, Keller AA, *et al* (2014) The effect of humic acid on the aggregation of titanium dioxide nanoparticles under different pH and ionic strengths. Sci Total Environ 487:375–380. doi: 10.1016/j.scitotenv.2014.04.036

KEYPOINTS

- No firm conclusion can be made concerning the NP part of TiO_2 in the environment without using isotopic and/or sizing analytical tools
- Transport of nanoparticulate TiO_2 is likely from release at point T, because of low attachment efficiencies between particles.
- Immediate aggregation and sedimentation is probable at effluents NN and NNR release point, because of high attachment efficiencies between particles.

NEXT RESEARCH QUESTIONS

- How can we model the NPs fate (size distribution and concentration) in the river water and in sediments, based on the measurements performed in the field and in the laboratory?
- What data are available on their potential effects on target organisms, for integration in a RA model?
- How can we model a risk score taking into account the exposure duration of organisms to NMs?

CHAPTER III: MODELING THE POTENTIAL RISKS OF TiO_2 NMS

This chapter aims at describing the development of Bayesian networks for modeling the potential risks of TiO_2 NMs in the aqueous media, taking into account water and sediment compartments. The network structure of the second model was built in collaboration with EcoLab, Toulouse and LIEC, Metz, France. The ecotoxicological data were provided by LIEC, Metz, France.

Introduction

As it has been underlined in the first chapter, the nano science needs to develop methodologies to assess the impacts and risks due to nanoproducts, nanomaterials, nanoparticles. It has been shown in the second review of chapter I that the impact assessment methodology (LCA) and risk assessment methodology (ERA) have many similarities related to their mathematical expressions and to data required for the calculations (fate, exposure and effect) and that it would be interesting to combine both methodologies.

To date, most of the RA methodologies developed for NMs are qualitative or semi-quantitative, because of the remaining uncertainties regarding their fate and effects in the environment. Such methodologies include CENARIOS (TÜV SÜD Industrie Service 2008), SMAA-TRI (Tervonen *et al*. 2009) and NanoRiskCat (Hansen *et al*. 2011), which result in the classification of NMs into risk categories. These methods assess the NMs risks using data concerning their characteristics (e.g. size, composition, state of integration in the matrix), their fate in the environment (i.e. transport and transformation) and the damage they may cause to the environment (i.e. toxicity potential). Some of this data, if not all, is elicited by expert judgment, meaning that they are qualitative. This ends in qualifications such as “low”, “medium” and “high”, for example in SMAA-TRI, or in color codes (red for the highest risk, green for the lowest), such as in CENARIOS and NanoRiskCat. These models answer the need for rapid integration of NMs in RA, as the results can be produced without the need of acquiring new data on NMs. Moreover, risk categories are easily understood by everyone, so that the communication to public audience is facilitated. However, they may lack some accuracy in the determination of the NMs risks, which explains the choice of a quantitative methodological approach in this research.

Regarding life cycle impact assessment methodologies, USEtox does assess quantitatively the fate, the exposure and the potential effects of a substance by calculating a fate factor, an effect factor and an exposure factor (Rosenbaum *et al*. 2008). Salieri and co-workers (Salieri 2013; Salieri *et al*. 2015) worked on the adaptation of the calculation methodology of these factors to NMs, by adapting the fate and effect modeling to these new substances. However, USEtox is not yet applicable to a site-specific scale (Kennel and Schindler 2015), which is yet the object of this study.

In order to provide a quantitative risk score for TiO_2 NMs accounting for the uncertainties inherent to the NMs fate and effect in the environment, a probabilistic approach may be used, such as Bayesian modeling. Money and coworkers (Money *et al*. 2012; Money *et al*. 2014) developed the FINE model for the RA of Ag NMs. They were the first (and only) ones to use Bayesian networks (BNs) for the RA of NMs, including mostly quantitative parameters, although some of them were still estimated by expert elicitation.

The work described below takes a step forward in current research by (1) developing BNs for TiO_2 NMs RA at a site-specific scale and using fate and effect parameters which were all quantitatively estimated and (2) considering the life cycle of TiO_2 NPs with industrial releases into the Thur river coming from both their production and their waste treatment sites.

After a presentation of Bayesian theory and networks, the second part of this chapter shows the development of a BN to model the behavior of TiO_2 ENPs from the industrial effluents to the river, including water and sediment compartments. No data is yet available concerning the effect of these precise TiO_2 NPs in the aqueous media, so the network focused on the fate factor of TiO_2 NPs.

Meanwhile, in the third chapter, a complete yet simplified network was developed for other anatase TiO_2 ENPs, which were tested in mesocosms, using natural water and water/sediment interface.

1. Bayesian theory and Bayesian networks

The Bayesian theory is based on the fundamental rule of conditional probability. For two events A and B, this rule is given by (Equation 1):

$$P(A|B) = \frac{P(A \cap B)}{P(B)} \quad (1)$$

Which reads as "the probability of A given B is the ratio of the probability of A and B over the probability of B". From this statement, Bayes (1763) wrote the following rule (Equation 2):

$$P(A|B) = \frac{P(B|A) \cdot P(A)}{P(B)} \quad (2)$$

Where

$P(A)$ and $P(B)$ are the probabilities of A and B without regard to each other, $P(A|B)$ the conditional probability of A given that B is the true and $P(B|A)$ is the probability of B given that A is true.

This formulation enables updating the knowledge one has on A, provided one gets new information about B. This is most important when working on such a recent field as NMs environmental behavior, as it allows the user to easily update the results as research goes on.

Bayesian networks (BNs) are acyclic graphs used to represent the knowledge about an uncertain domain. Each node in the graph represents a random variable, while the edges between the nodes represent probabilistic dependencies among the corresponding random variables. Variables, represented by boxes, are linked by causality relationships (Figure 25A) and can take different states,

which can be either continuous or discrete. Continuous variables can be difficult to handle in complex models, so they are most often discretized by defining a set of intervals in which they occur. Causality relationships are represented by arrows linking the parent variables to their children variables, the prior having an effect on the latter.

In this study, the defined variables include NPs properties (e.g. size, surface charge, cristallinity), abiotic environmental parameters (e.g. pH, conductivity, flow rate, elemental concentrations) and biological parameters (e.g. type of species, stage of development). The discretization of continuous variables was based on literature and when applicable, to measurements performed in the field (such as temperature) or in the lab (such as mass concentration). In order to avoid too much complexity arising from too many variables states, the number of intervals was kept as low as possible, using a logarithmic scaling when needed (e.g. for the attachment efficiency coefficient).

Once the structure is built, conditional probability tables (CPTs) must be implemented (Figure 25B). These tables relate the states of the parent nodes to those of a child node, including entries for all possible combinations of the child and parent nodes states. They determine the probability of occurrence of each state of a child variable, given the occurrence of the combined states of its parent variables. This is where probability distributions can be used, allowing the integration of uncertainties inherent to the variable outcome. These probabilities are propagated down the network, to further children variables. Wide probability distributions arise from high uncertainties. Since they can be directly visualized on the BN, priority research needs can be identified as the variables presenting the widest probability distributions.

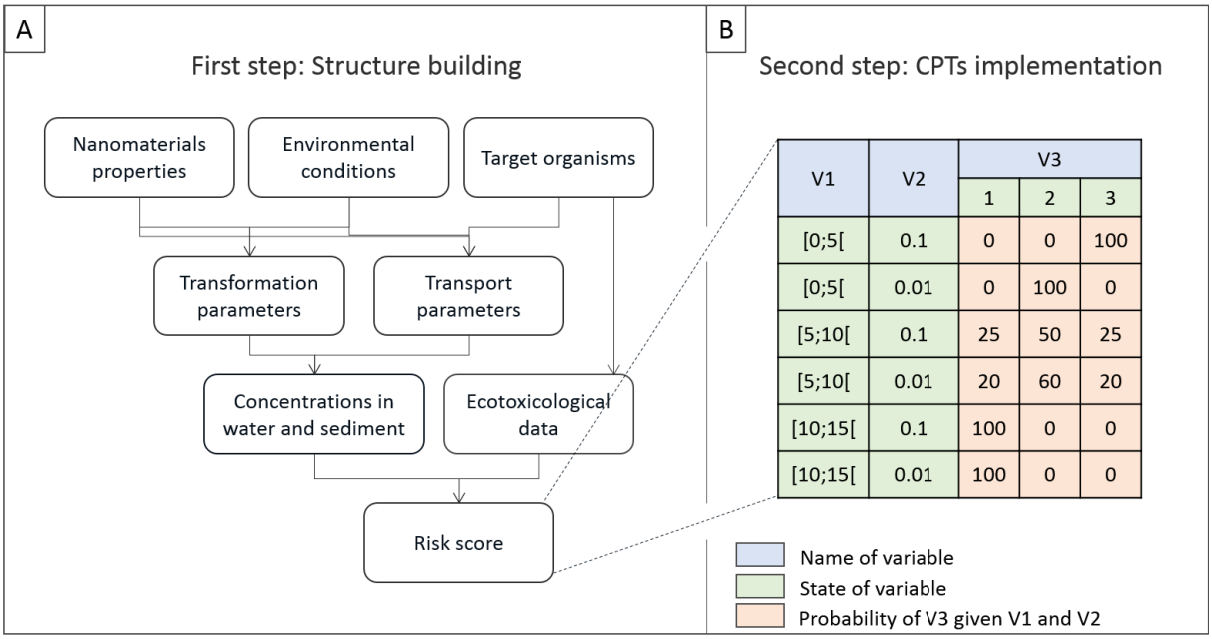

Figure 25: Building a Bayesian network. V1 is continuous (discretized as intervals), V2 is discrete.

The chosen variables, states of variables and the causality relationships between them are described in the next sections. They have been implemented in the Netica application v.4.16 (Norsys Software Corporation).

2. Building a BN for the fate of TiO_2 ENPs in river water

2.1. Building the structure of the models

2.1.1.Structure of the effluent model

A BN was built to assess the fate of the studied TiO_2 NMs in the river in which they are released. The first part of the network models the NMs fate in the industrial effluent, using both the NPs characteristics measured in the lab and the effluent properties measured in the field, to calculate the NMs size distribution in the effluent (Figure 26). Processes at stake were modeled with kinetic equations based on the particle aggregation theory (Wiesner 1992; Thill *et al*. 2001) using 15 variables.

The size distribution determined in the first part of the model is one of the inputs of the second part, which aims at determining concentrations and size distributions of TiO_2 NMs homo- and heteroaggregates in water and sediment. Aggregation and transport processes were modeled using kinetic equations adapted from Praetorius *et al*. (2012), who modeled the fate of TiO_2 NMs in the Rhine River. A total of 23 variables were included in this part of the model.

The purpose here was to give a holistic view of the parameters needed for the determination of TiO_2 NMs concentrations in water and in sediments.

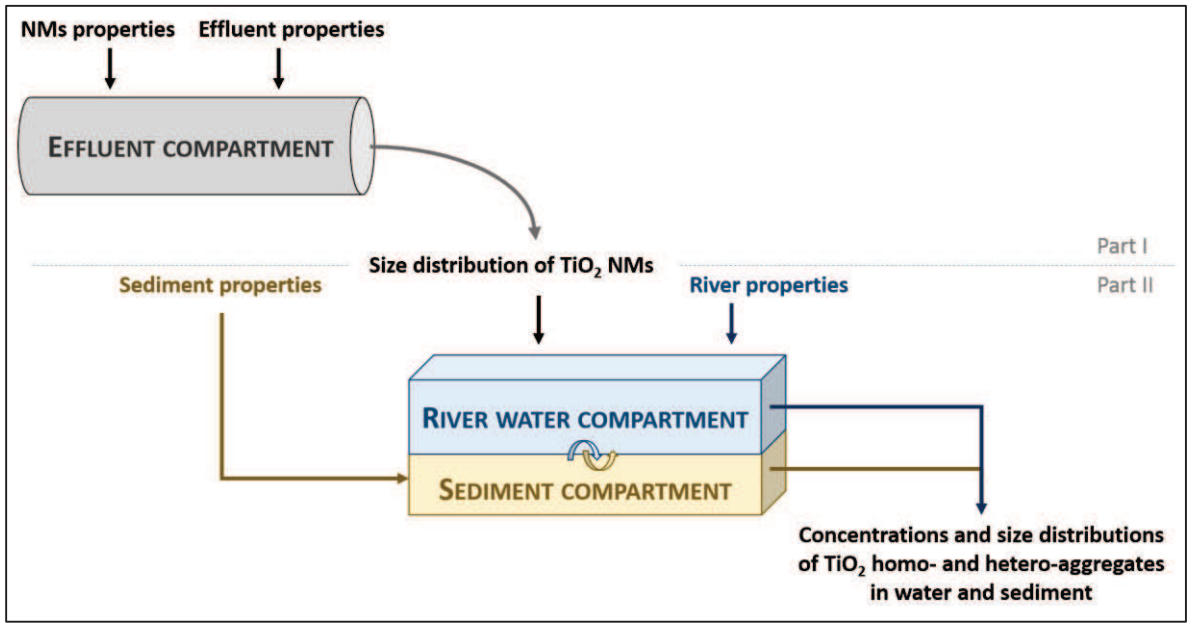

Figure 26: Conceptualization of the fate model

The size distribution of TiO_2 NMs aggregates in the effluent was defined over 15 size classes. The minimum aggregate size was defined as 200 nm, because very low to null Ti concentrations were measured in the industrial effluents water filtrated using this pore size. The maximum aggregate size was set at 100 µm, taking Praetorius *et al*. (2012) as a reference and observing the same limit in SEM imaging (cf. Chapter II, p. 90). This size range was divided on a logarithmic scale, in order to keep a reasonable number of size classes on such a big interval (Thill *et al*. 2001). The initial particle size distribution was similar to that used by Praetorius *et al*. (2012), which is a lognormal distribution with a mode at 300 nm (logarithmic mean = 5.8 nm, logarithmic standard deviation = 0.37 nm).

Two strong assumptions were made in this part of network, modeling aggregation processes in the effluent. Firstly, TiO_2 concentrations were assumed to be high compared to other particulate content, so collision rates with SPM was assumed to be negligible compared to collision rates between TiO_2 particles. There was no way to distinguish quantitatively between SPM free of TiO_2, SPM bound to TiO_2 and free TiO_2 in the effluent, so only homo-aggregation was taken into account. Second, the fragmentation of the aggregates to smaller size classes was not included, as no current model makes consensus between researchers without additional experiments for calibration. Both are strong assumptions.

According to Smoluchovski (1917, Equation 1), the evolution of the aggregates size distribution depends on two constant parameters, the attachment efficiency coefficient (α) and the collision rate (β) of the aggregates:

$$\frac{dN_k}{dt} = \frac{1}{2} \cdot \alpha \cdot \sum_{i+j=k} \beta_{ij,effluent} \cdot N_i \cdot N_j - \alpha \cdot N_k \cdot \sum_{i=1}^{\infty} \beta_{ik,effluent} \qquad (1)$$

Where N_i, N_j and N_k are the number (or number concentrations) of aggregates in size classes i, j and k. The number concentrations of aggregates in each size class can be calculated based on the measured mass concentration and on the particle size probability distribution: the mass is allocated to each size class based on this distribution, then the TiO_2 mass obtained in each size class in divided by the mass of a single particle, in order to obtain the number concentration of aggregates in each size class.

In order to obtain the mass of an aggregate, its density has to be calculated accounting for their fractal dimension (D_f), as it defines the compactness of an aggregate: the more an aggregate is compact, the higher is its D_f. There is thus a direct impact of the D_f on the aggregate density. In this way, the volume of solid TiO_2 in the aggregate was calculated based on Equation 2 (Thill *et al*. 2001):

$$V_{TiO_{2,i}}^{solid} = \frac{4}{3} \cdot \pi \cdot \left(\frac{d_{primary}}{2}\right)^3 \cdot \left(\frac{d_{TiO_{2,i}}}{d_{primary}}\right)^{D_f} \qquad (2)$$

Where $d_{primary}$ is the diameter of a primary particle and $d_{TiO_{2,i}}$ is the diameter of the aggregate of size class i. In this way, one was able to differentiate the mass of TiO_2 from the mass of water in the aggregate and so, to calculate the density of the aggregate ($\rho^*_{TiO_{2,i}}$, Equation 3):

$$\rho^*_{TiO_{2,i}} = \frac{\rho_{TiO_2} \cdot V^{solid}_{TiO_{2,i}} + \rho_{effluent} \cdot \left(V^{total}_{TiO_{2,i}} - V^{solid}_{TiO_{2,i}}\right)}{V^{total}_{TiO_{2,i}}} \quad (3)$$

Where ρ_{TiO_2} is the density of bulk TiO_2, $\rho_{effluent}$ is the density of the effluent, $V^{total}_{TiO_{2,i}}$ is the total volume of the aggregate of size i and $V^{solid}_{TiO_{2,i}}$ is the volume of solid in the aggregate of size i.

The attachment efficiency coefficient α is also called the sticking coefficient: it is the probability that two particles remain attached to each other after collision. It can be determined experimentally (cf. Chapter IIB, p. 121):

In water, collisions between particles can be caused by Brownian motion or diffusion (β^{Br}), differential settling (β^{ds}) or shear (β^{sh}) (Thill *et al*. 2001, Equations 4 to 6). Each of these mechanisms results in a separate collision rate, β being the sum of these collision rates:

$$\beta^{Br}_{ij,effluent} = \frac{2k_B T_{effluent}}{3\mu_{effluent}} \cdot \left(\frac{1}{r_i} + \frac{1}{r_j}\right) \cdot \left(r_i + r_j\right) \quad (4)$$

$$\beta^{ds}_{ij,effluent} = \pi \cdot (r_i + r_j)^2 \cdot \left|U_i - U_j\right| \quad (5)$$

$$\beta^{sh}_{ij,effluent} = \frac{4}{3} \cdot \left(r_i + r_j\right)^3 \cdot G_{effluent} \quad (6)$$

Where k_B is the Boltzmann constant, $T_{effluent}$ is the temperature of water in the effluent, $\mu_{effluent}$ is the dynamic viscosity of the effluent, r_i and r_j are the radii of aggregates of size classes i and j, respectively and $G_{effluent}$ is the shear rate in the effluent. The dynamic viscosity of the effluent is determined based on its temperature (Kestin *et al*. 1978), which can be measured in the field.

The settling velocity U_i of the aggregate is determined by the Stokes' law (Equation 7):

$$U_i = \frac{2}{9} \cdot \frac{\rho^*_{TiO_{2,i}} - \rho_{effluent}}{\mu_{effluent}} \cdot g \cdot r_i^2 \quad (7)$$

Where g is the acceleration of gravity.

One term was added to Eq. 1, in order to account for the loss of aggregates by sedimentation (Equation 8):

$$\frac{dN_k}{dt} = \underbrace{\frac{1}{2} \cdot \alpha \cdot \sum_{i+j=k} \beta_{ij,effluent} \cdot N_i \cdot N_j}_{\text{gain by aggregation}} - \underbrace{\alpha \cdot N_k \cdot \sum_{i=1}^{\infty} \beta_{ik,effluent} \cdot N_i}_{\text{loss by aggregation}} - \underbrace{\frac{U_k}{z_{effluent}} \cdot N_k}_{\text{loss by sedimentation}} \quad (8)$$

Where $z_{effluent}$ is the depth of water in the effluent and U_k is the settling velocity of aggregates of size k.

The interrelationships between the variables are described in the model structure (Figures 27 and 28). In order to calculate the required parameters, a number of NP and effluent characteristics (parent variables) was determined (Tables 9 and 10). Most of them were measured, except from the TiO_2 bulk density which was taken from the literature (Praetorius *et al*. 2012), the effluent density which was assumed to be equal to that of water and D_f and α, which could not be assessed experimentally in the effluents. The sensitivity of the model to these parameters was tested by varying D_f from 1.5 to 2.9 and α from 0.001 to 1 in the calculations. Low α are to be tested in low conductivity waters, high α are to be tested in high conductivity waters (cf. Chapter II, p. 129).

Table 9: Values and types of NPs properties (parent variables) included in the effluent network

Parameter	Value	Unit	Type of variable	Number of states	Reference
Diameter of primary particles	5	nm	discrete	1	Measurement
Point of zero charge	4 - 8	-	discrete	6	Measurement
Surface charge	-60 - +40	mV	continue	9	Measurement
Size of aggregates in the effluent	200 - 100000	nm	discrete	15	Measurement
TiO_2 density	4,23	$g.cm^{-3}$	discrete	1	Praetorius *et al*. 2012
Attachment efficiency coefficient	0 - 1	-	discrete	5	Adjusted, based on measurements
Fractal dimension	1.5 – 2.9	-	discrete	4	Adjusted

Table 10: Values and types of effluent properties (parent variables) included in the effluent network

Parameter	Value	Unit	Type of variable	Number of states	Reference
pH	1 - 11	-	continue	9	Measurement
Conductivity	0,005 - 1,5	$mS.cm^{-1}$	continue	3	Measurement
Temperature	20 - 30	°C	continue	2	Measurement
Pipe diameter	0,2 or 2,5	m	discrete	2	Measurement
Water depth	0,1 or 0,5	m	discrete	2	Measurement
Effluent flow	0,01 - 10	$m^3.s^{-1}$	continue	4	CRISTAL data
Particulate TiO_2 mass concentration	0,003 - 0,25	$mg.L^{-1}$	continue	6	Measurement

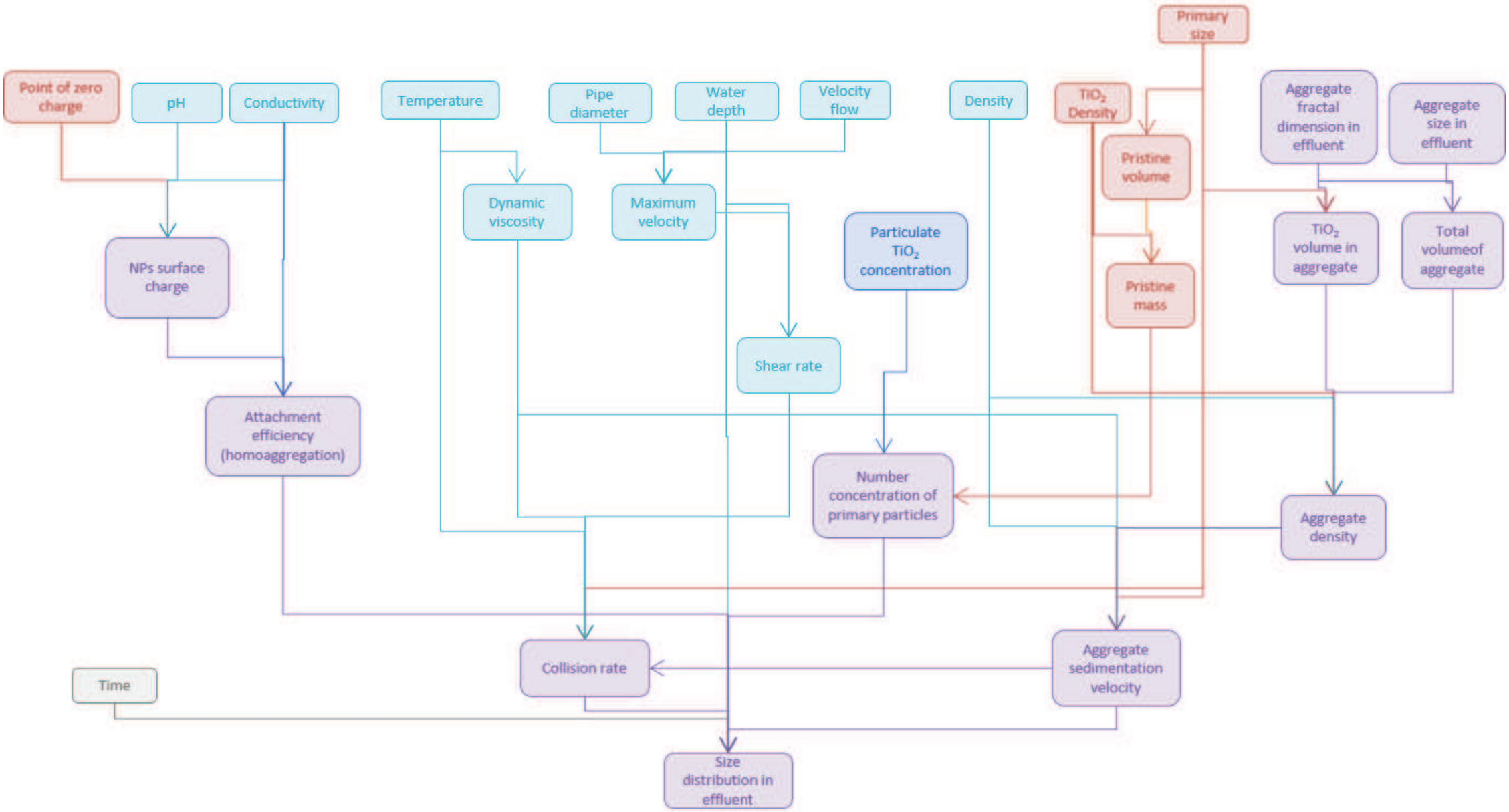

Figure 27: Structure of the BN developed for the TiO_2 NMs fate in the effluent

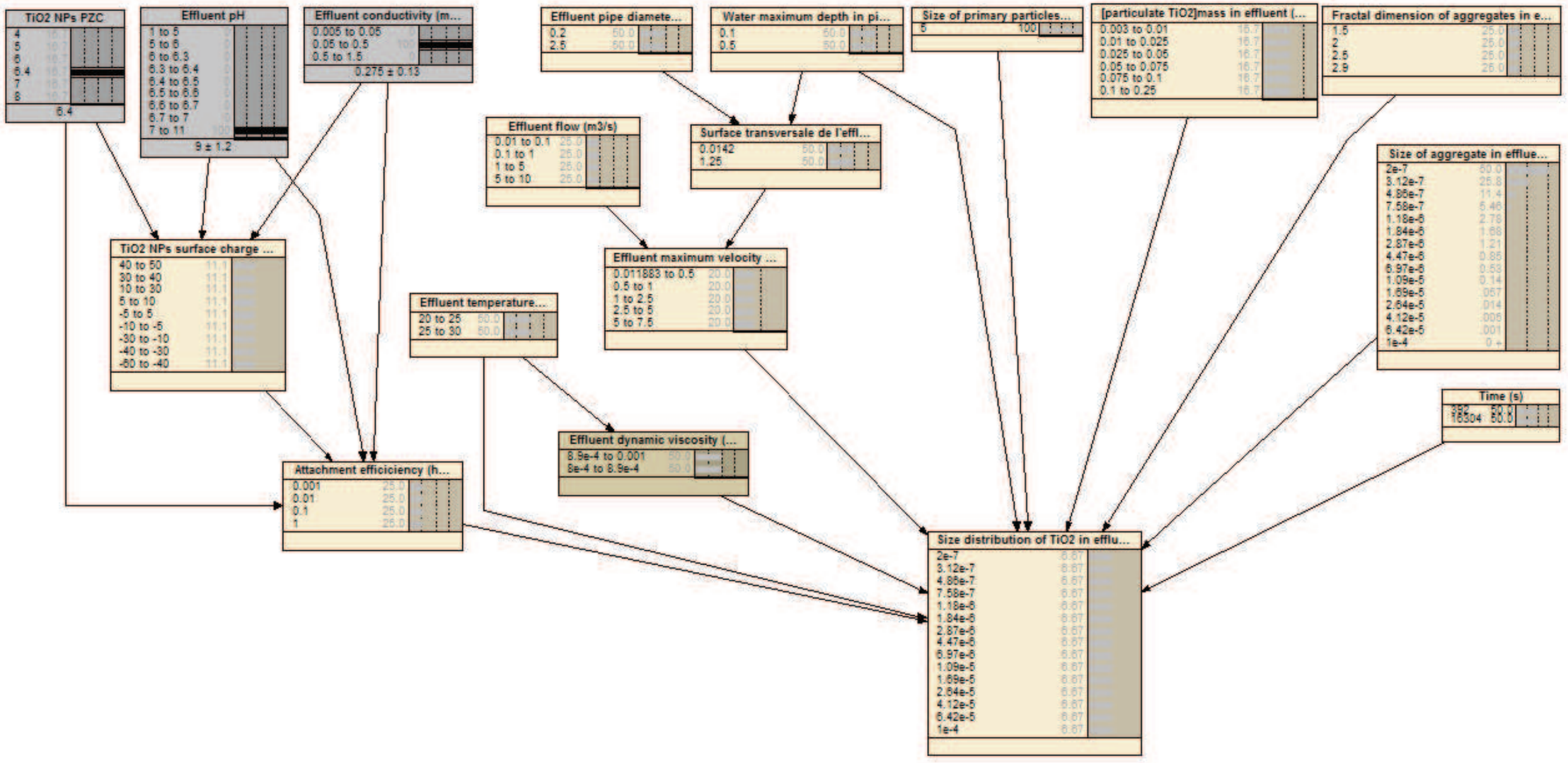

Figure 28: Bayesian network modeling the fate of the TiO_2 NMs in the industrial effluent

2.1.2.Structure of the river model

The size distribution and concentration of TiO_2 NMs aggregates in the effluent are some of the inputs of the river model. Kinetic equations describing the evolution of concentrations of homo- and heteroaggregates in water and sediments were taken from Praetorius *et al*. (2012). Adaptations were made on the calculation of the densities of homo- and heteroaggregates (Equations 2 and 3), taking Thill *et al*. (2001) as a reference. Moreover, due to the shallow river depths, no stagnant water compartment was not included. Due to low TiO_2 concentrations in the river (< 100 µg.L^{-1}), it was assumed that homo-aggregation of TiO_2 NMs was negligible in this compartment.

The concentration and size distribution of TiO_2 homoaggregates in water is expressed by Equation 9: it depends on the TiO_2 incoming flow ($q_{TiO_{2,i}}^{input}$, that is the concentration and size distribution of TiO_2 in the effluent), but also on the transport of TiO_2 by the river flow, their deposition on sediments, and their heteroaggregation onto SPM:

$$\frac{dC_{water}^{TiO_{2,i}}}{dt} = -\left(k_{river,flow} + k_{dep}^{TiO_{2,i}} + \sum_{j=1}^{n_{sizes}^{SPM}} k_{het-agg,ij}\right) \cdot C_{water}^{TiO_{2,i}}(t) + q_{TiO_{2,i}}^{input} \quad (9)$$

loss by transport, deposition and aggregation — *inflow from effluent*

Where $k_{river,flow}$ is the river flow rate constant, $k_{dep}^{TiO_{2,i}}$ is the deposition rate constant of TiO_2 of size class i, $k_{het-agg,ij}$ is the hetero-aggregation constant rate of TiO_2 of size i and SPM and size j.

The river flow rate constant is defined by (Equation 10):

$$k_{river,flow} = v_{river,flow} \cdot \frac{A_{water}}{V_{water}} \quad (10)$$

Where $v_{river,flow}$ is the river flow velocity, A_{water} is the cross-sectional area of the river and V_{water} is the volume of water in the studied river section.

The deposition rate constant of TiO_2 aggregates is calculated by (Equation 11):

$$k_{dep}^{TiO_{2,i}} = \frac{U_{river}^{TiO_{2,i}}}{z_{river}} \quad (11)$$

Where $U_{river}^{TiO_{2,i}}$ is the settling velocity of aggregates of size i in the river, and z_{river} is the depth of river water, measured in the field.

The heteroaggregation rate constant of TiO_2 and SPM is defined as (Equation 12):

$$k_{het-agg,ij} = \alpha_{het-agg} \cdot \beta_{ij,river} \cdot C_{particle}^{SPM_j} \quad (12)$$

Where $\alpha_{het-agg}$ is the hetero-aggregation attachment efficiency coefficient, determined experimentally, $\beta_{ij,river}$ is the collision rate of TiO_2 of size i with SPM of size j, determined in the same way as in the effluent, and $C_{particle}^{SPM_j}$ is the particulate concentration of SPM of size j in the river. Mass concentration of SPM in the river can be determined by weighing the filters used for sample preparation. The size distribution of SPM was defined over 15 size classes, from 1 to 100 µm with a lognormal particle size distribution (Praetorius *et al*. 2012). As for the calculation of TiO_2 number concentrations, the number concentration of SPM in each size class was calculated by allocating the mass concentration to each size class based on the lognormal probability function used by Praetorius *et al*. (2012), with a mode at 5 µm, a logarithmic mean of 8.9 nm and a standard deviation of 0.59 nm. The mass concentration of each size class was then divided by the mass of a single particle in each size class.

The TiO_2 NMs input $q_{TiO_{2,i}}^{input}$ was calculated by multiplying the number concentration of TiO_2 in each size class, which is the output of the first part of the model, by the river flow constant rate, $k_{river,flow}$.

The heteroaggregates of TiO_2 bound to SPM in the river water ($C_{water}^{TiO_{2,i}+SPM_j}$) is expressed as follows (Equation 13):

$$\frac{dC_{water}^{TiO_{2,i}+SPM_j}}{dt} = -\left(k_{river\ flow} + k_{dep}^{TiO_{2,i}+SPM_j}\right) \cdot C_{water}^{TiO_{2,i}+SPM_j}(t) + k_{het-agg,ij} \cdot C_{water}^{TiO_{2,i}}(t) + k_{resusp} \cdot \frac{V_{sed}}{V_{water}} \cdot C_{sed}^{TiO_{2,i}+SPM_j}(t) \quad (13)$$

loss by transport and deposition *gain by aggregation* *gain by resuspension*

Where V_{water} and V_{sed} are the volumes of water and sediment in the considered river section. The resuspension rate constant k_{resusp}, was calculated with Equation 14:

$$k_{resusp} = \frac{v_{resusp}}{z_{sed}} \quad (14)$$

Where z_{sed} is the sediment depth and v_{resusp} is the resuspension velocity of sediment. $k_{dep}^{TiO_{2,i}+SPM_j}$, the deposition rate of heteroaggregates, was calculated based on the density of TiO_2 and SPM and on their volumes in the aggregate (Equations 15 and 16):

$$k_{dep}^{TiO_{2,i}+SPM_j} = \frac{U_{river}^{TiO_{2,i}+SPM_j}}{z_{river}} \quad (15)$$

$$U_{TiO_{2,i}+SPM_j} = \frac{2}{9} \cdot \frac{g \cdot r_{TiO_{2,i}+SPM_j}^2}{\mu_{riverwater}} \cdot \left(\frac{V_{TiO_{2,i}}^{total}}{V_{TiO_{2,i}}^{total}+V_{SPM_j}} \cdot \rho_{TiO_{2,i}}^{*} + \left(1 - \frac{V_{TiO_{2,i}}^{total}}{V_{TiO_{2,i}}^{total}+V_{SPM_j}}\right) \cdot \rho_{SPM}\right) - \rho_{riverwater} \quad (16)$$

Where $U_{river}^{TiO_{2,i}+SPM_j}$ and $r_{TiO_{2,i}+SPM_j}$ are the settling velocity and the radius of the heteroaggregate, is, $V_{TiO_{2,i}}^{total}$ and V_{SPM_j} are the volume of TiO_2 and SPM in the aggregate, and ρ_{SPM} and $\rho_{riverwater}$ are the density of SPM and water, respectively.

The concentrations of homo- and heteroaggregates are expressed by Equations 17 and 18, respectively:

$$\frac{dC_{sed}^{TiO_{2,i}}}{dt} = -\left(k_{resusp} + k_{burial} + k_{sed,transfer}\right) \cdot C_{sed}^{TiO_{2,i}}(t) + k_{dep,water}^{TiO_{2,i}} \cdot \frac{V_{water}}{V_{sed}} \cdot C_{water}^{TiO_{2,i}}(t) \quad (17)$$

loss by resuspension, burial and transport — *gain by deposition*

$$\frac{dC_{sed}^{TiO_{2,i}+SPM_j}}{dt} = -\left(k_{resusp} + k_{burial} + k_{sed,transfer}\right) \cdot C_{sed}^{TiO_{2,i}+SPM_j}(t) + k_{dep}^{TiO_{2,i}+SPM_j} \cdot \frac{V_{water}}{V_{sed}} \cdot C_{water}^{TiO_{2,i}+SPM_j}(t) \quad (18)$$

loss by resuspension, burial and transport in sediment — *loss by deposition*

The burial rate constant k_{burial} and sediment horizontal transfer rate constant $k_{sed,transfer}$ were calculated as follows:

$$k_{burial} = \frac{v_{burial}}{z_{sed}} \quad (19)$$

$$k_{sed,transfer} = \frac{v_{sed,transfer}}{m_{sed}} \quad (20)$$

Where v_{burial} and $v_{sed,transfer}$ are the burial velocity and the horizontal transfer velocity of sediment, respectively. Jones (1997) describes the SPM flow as 14 times the bedload transport. $v_{sed,transfer}$ was thus determined based on this relation, calculating the SPM flow by multiplying the SPM concentration by the water flow. m_{sed} is the mass of sediment, determined from its density. Van De Meent (1993) calculates the bulk sediment density considering that it is composed of 20% mineral and 80% water. The mineral density was determined based on the sediment texture (Appendix I). The components (sand and illite) densities were taken from the webmineral database (www.webmineral.com).

As in the effluent, as many parameters as possible were measured in the field, while others had to be estimated from the literature (Tables 11 and 12). Most uncertainties remain regarding the sediments rate constants, which could not be assessed experimentally. The interrelationships between all these variables are illustrated in Figures 29 and 30.

Table 11: Values and types of water properties (parent variables) included in the river network

Parameter	Value	Unit	Type of variable	Number of states	Reference
Length of river box	50 - 750	m	continue	4	Measurement
Depth of water	0,1 - 5	m	continue	4	Measurement
Flow velocity	0,005 - 50	$m.s^{-1}$	continue	4	hydro.eaufrance.fr
Density of SPM	1,1 - 2,5	$g.cm^{-3}$	continue	3	Praetorius *et al.* 2012
Size of SPM	10^{-6} - 10^{-4}	m	continue	2	Praetorius *et al.* 2012, measurement
Concentration of SPM	0 - 20	$mg.L^{-1}$	continue	5	Measurement
Temperature	0 - 20	°C	continue	4	Measurement
Conductivity	50 - 1500	$\mu S.cm^{-1}$	continue	9	Measurement
pH	7 - 8,5	-	continue	3	Measurement

Table 12: Values and types of sediment properties (parent variables) included in the river network

Parameter	Value	Unit	Type of variable	Number of states	Reference
Porosity	0,2 - 0,6	-	continue	4	Granulometry measurement, Calvet 2003
Density of dry sediment	sand (90-95% vol.): 2,6; illite (5-10% vol.): 2,6-2,9	$g.cm^{-3}$	continue	4	webmineral.com
Density of bulk sediment	20% mineral + 80% eau = 1640 - 2280	$g.cm^{-3}$	continue	4	van de Meent 1993
Depth	0,05	m	discrete	1	Praetorius 2012
Volume of sediment	1 – 750	m^3	continue	5	Calculated from measurement of river section length and 5 cm depth (Praetorius *et al.* 2012)
Horizontal transfer velocity	0,001 - 2	$kg.s^{-1}$	continue	5	Jones 1997
Burial velocity	8,88.10-4	$m.s^{-1}$	discrete	1	van de Meent 1993
Resuspension velocity	2,89.10-10	$m.s^{-1}$	discrete	1	van de Meent 1993

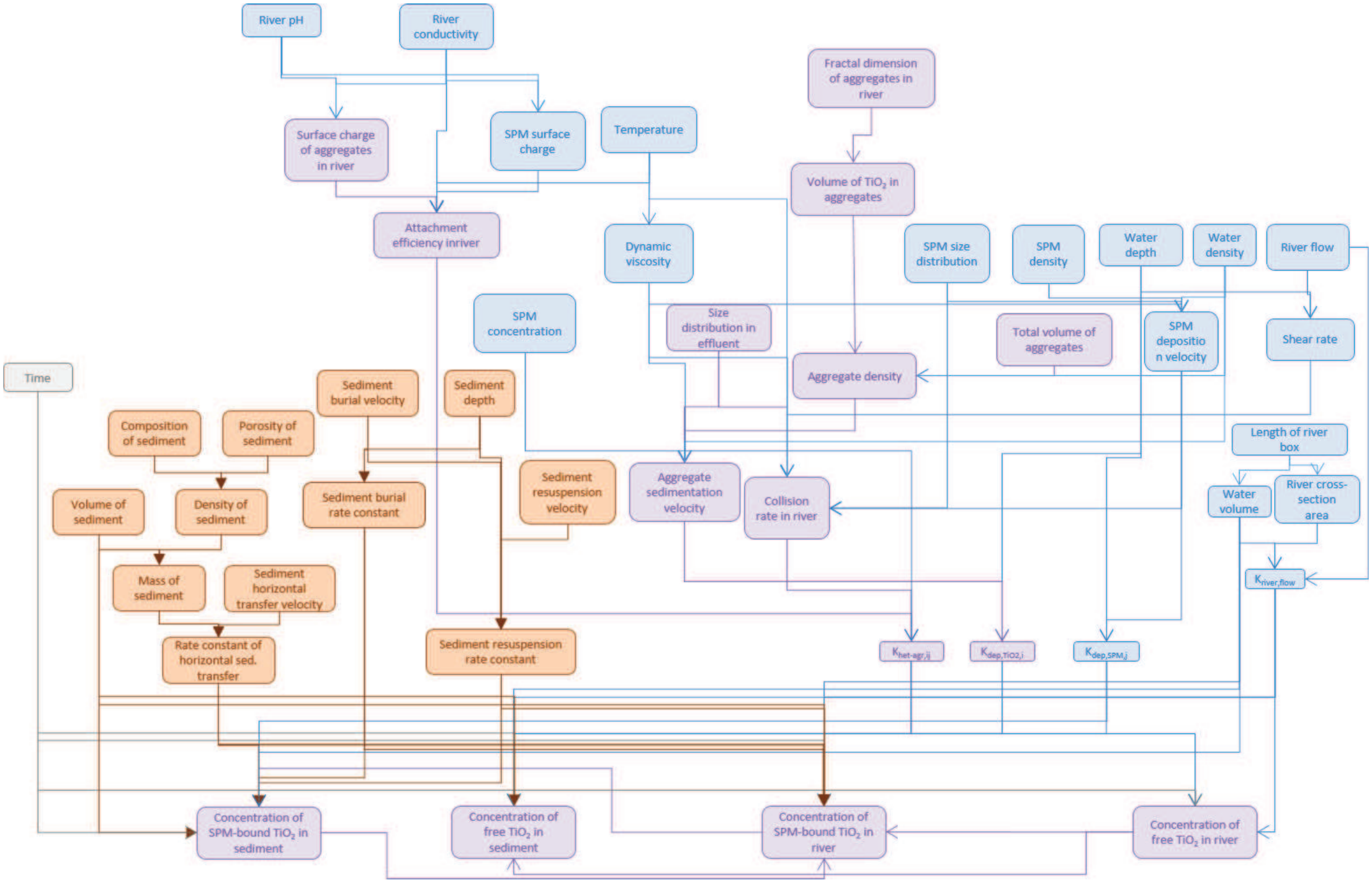

Figure 29: Structure of the BN modeling the fate of TiO_2 NMs in the river

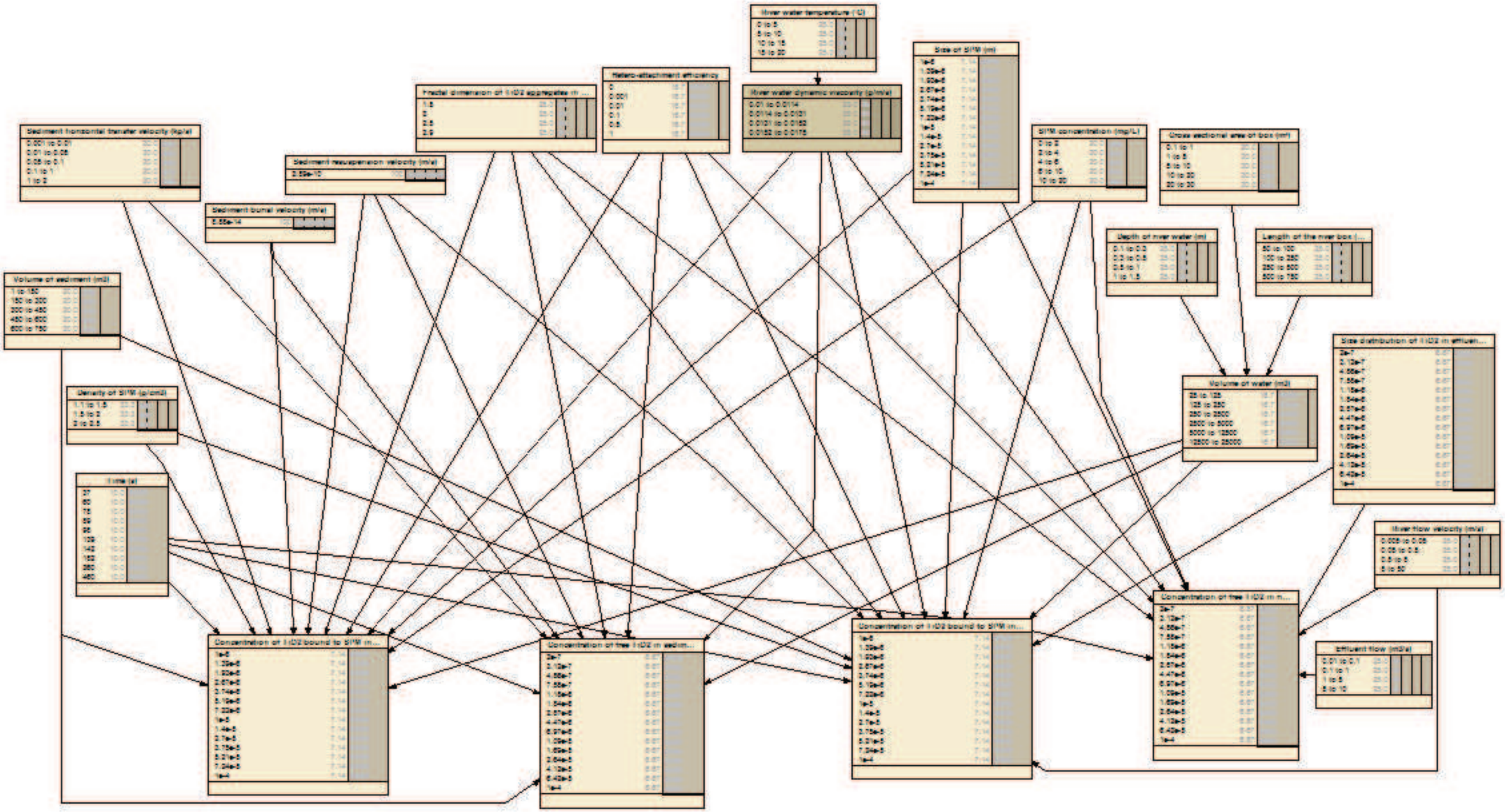

Figure 30: Bayesian network modeling the fate of the TiO_2 NMs in the river

2.2. Implementing the conditional probability tables

In order to reduce even further the uncertainties in the fate of TiO_2 NMs in the river, discrete values were used for each parameter, most of them measured in the field. This enabled the modeling of the fate of TiO_2 in effluent T up to sample point 4, and in effluent NN up to sampling point 5 (Figure 31). Thus, two river sections were considered, one extending from the release of effluent T to the sampling point 4, the other extending from the release of effluent NN to the sampling point 5. Effluent NNR was not considered in the risk modeling, as it comes from the slag heap, which has a long history and cannot be related to the TiO_2 production only. The environmental and anthropic parameters and effluent TiO_2 concentrations measured on each sampling campaigns were integrated in the calculations (Appendix IX), resulting in different outcomes for each sampling campaign and each river section. As no quantification of the nanoparticulate part of TiO_2 could be made (cf. Chapter II, p. 105), TiO_2 NMs concentrations were assimilated to total TiO_2 particulate concentrations in the effluent, as a "worst-case" scenario.

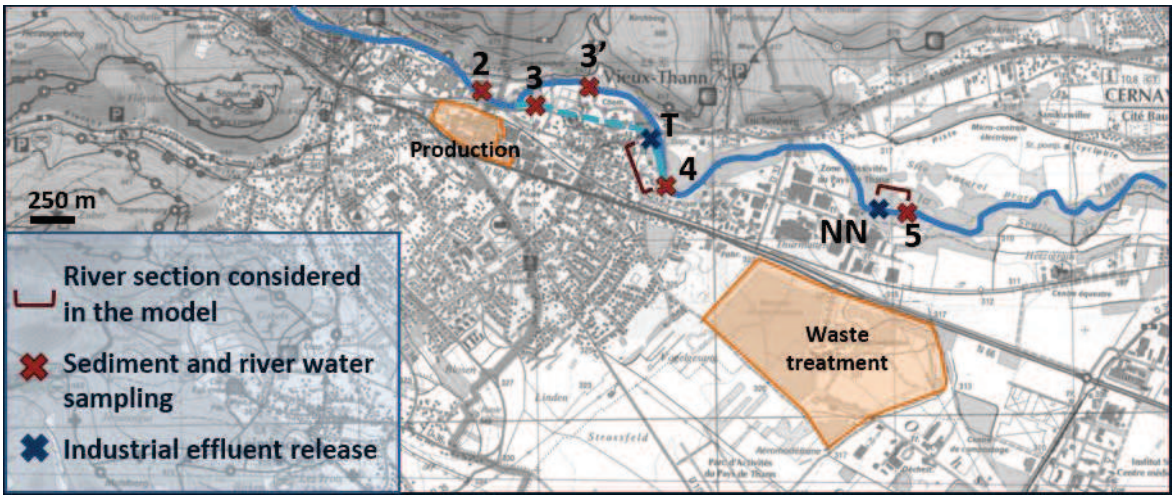

Figure 31: River sections considered in the modeling

Environmental parameters and TiO_2 concentrations were considered homogenous all along the river sections. Concentrations and size distributions were calculated at the time at which NMs were supposed to reach on the one hand the exit of the effluent pipe and on the other hand the corresponding sampling point, based on the effluent/river flow velocity and the length of the effluent pipe/river section.

The model equations were implemented in two Fortran codes (Appendix X), enabling the calculation of aggregation and transport rate constants as well as concentrations and size distributions in each sub-model (effluent and river). In order to obtain as much stability as possible (meaning that the total volume of NMs be kept constant all along the calculation), the analytical solutions of all kinetic equations were used. They were written as:

$\frac{dC(t)}{dt} + a \cdot C(t) = b$ (21)

With $C(t)$ being the number concentration of TiO_2 particles, a and b being constants to be determined for each equation. In this way, the analytical solution is given by Equation 22, γ being an integration constant:

$C(t) = \gamma \cdot e^{-at} + {}^{b}/_{a}$ (22)

And:

$C(0) = \gamma + {}^{b}/_{a} = C(t-1);$ so: $\gamma = C(t-1) - {}^{b}/_{a}$ (23)

Finally, by the analytical solution was obtained replacing γ in Eq. 22 and used in the Fortran codes (Equation 24):

$C(t) = \left[C(t-1) - {}^{b}/_{a}\right] \cdot e^{-at} + {}^{b}/_{a}$ (24)

However, because of the logarithmic initial definition of size classes, the size of an aggregate resulting from the aggregation of two smaller aggregates (of sizes i and j) may not be exactly one of the sizes defined initially. In this case, the aggregate volume was allocated to the two adjacent size classes (Figure 32, Thill *et al*. 2001).

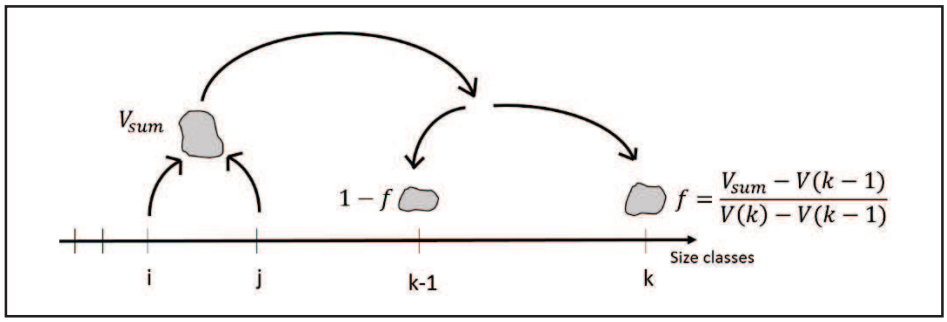

Figure 32: Methodology used for the aggregates volume fractionation (adapted from Thill *et al*. 2001)

2.3. Results interpretation

The integration of NMs- and site-specific parameters in a BN enabled the determination of the fate of TiO_2 NMs in the river in which they are released. Two different kinds of results were produced: firstly, concentrations of aggregates in each size class were calculated in the Fortran codes (Appendix XI). These size distributions were then expressed as probabilities of occurrence in the BN, with the help of the Netica application (Norsys). Both results are complementary.

The initial concentration of TiO_2 NMs in sediments was considered as null, so number concentrations in the sediment must be taken as the numbers of aggregates that settle down the water column in a given time, and not as total NMs concentrations in the sediments. They can be used to calculate partitioning coefficients between water and sediment at the local scale. Furthermore, aggregation and transport rate constants were also calculated at the site-specific scale. All these parameters may be used for calculating fate factors adapted to the local scale, and so answering the need expressed by Salieri (2013) of adapting the USEtox LCIA methodology to the local scale.

In order to calculate these concentrations and size distributions, most parameters were assessed experimentally. It results that concentrations in the sediments were lower than in the water, up to 7 to 8 orders of magnitude, with parameters measured on March, (Appendix XI), which is consistent with the results obtained in the laboratory. However, the attachment efficiency coefficient and the fractal dimension could not be determined precisely in the effluent and in the studied river sections, so the sensitivity of the results to these parameters and to TiO_2 concentration are analyzed in the next sections.

2.3.1.Sensitivity to attachment efficiency coefficients (α)

The attachment efficiency coefficient of TiO_2 NMs was determined experimentally in upstream water, with very low conductivity, and shown to be null (section IIB). However, both industrial effluents and downstream waters show higher conductivities and cations concentrations, so that higher attachment efficiency could occur. In the network, low α were tested in effluent T and in river water, while higher α were tested in effluent NN, where very high cations concentrations (> 500 $mg.L^{-1}$) were measured.

In the effluents, an increase in the attachment efficiency coefficient from 0.1 to 0.5 and 1 results in faster aggregation, and consequently in a slight shift of the particle size distribution towards bigger sizes. However, the distribution mode stays the same, at 312 nm (Figure 33).

In the river, no effect of α was shown on the size distributions of homo- and heteroaggregates in water and sediments (Figure 34). However, when increasing α from 0.001 to 0.01, the concentration of heteroaggregates was 10 times higher, both in water and in sediments (Appendix XI).

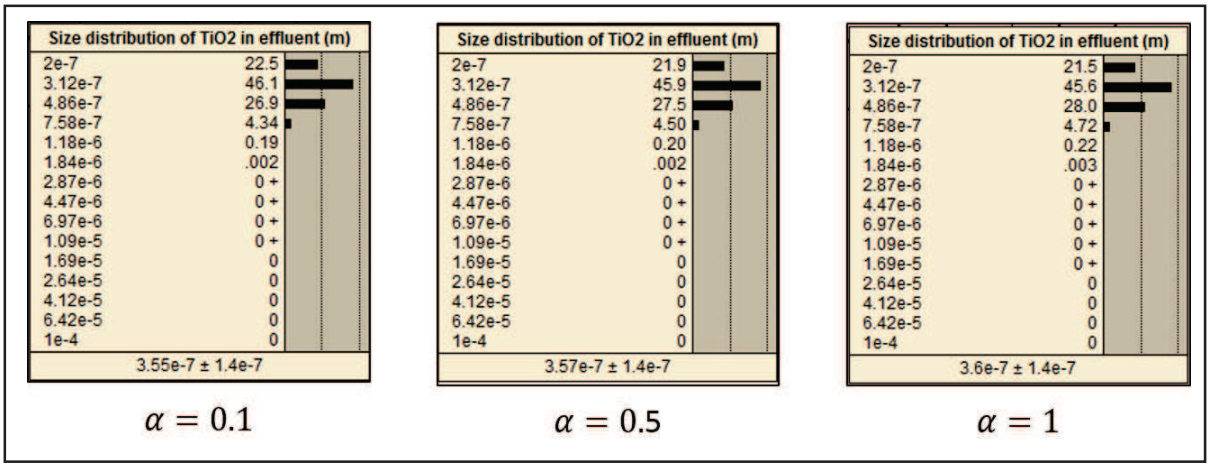

Figure 33: Sensitivity of size distribution results in effluent NN (March campaign, D_f = 2.5, sizes expressed in meters)

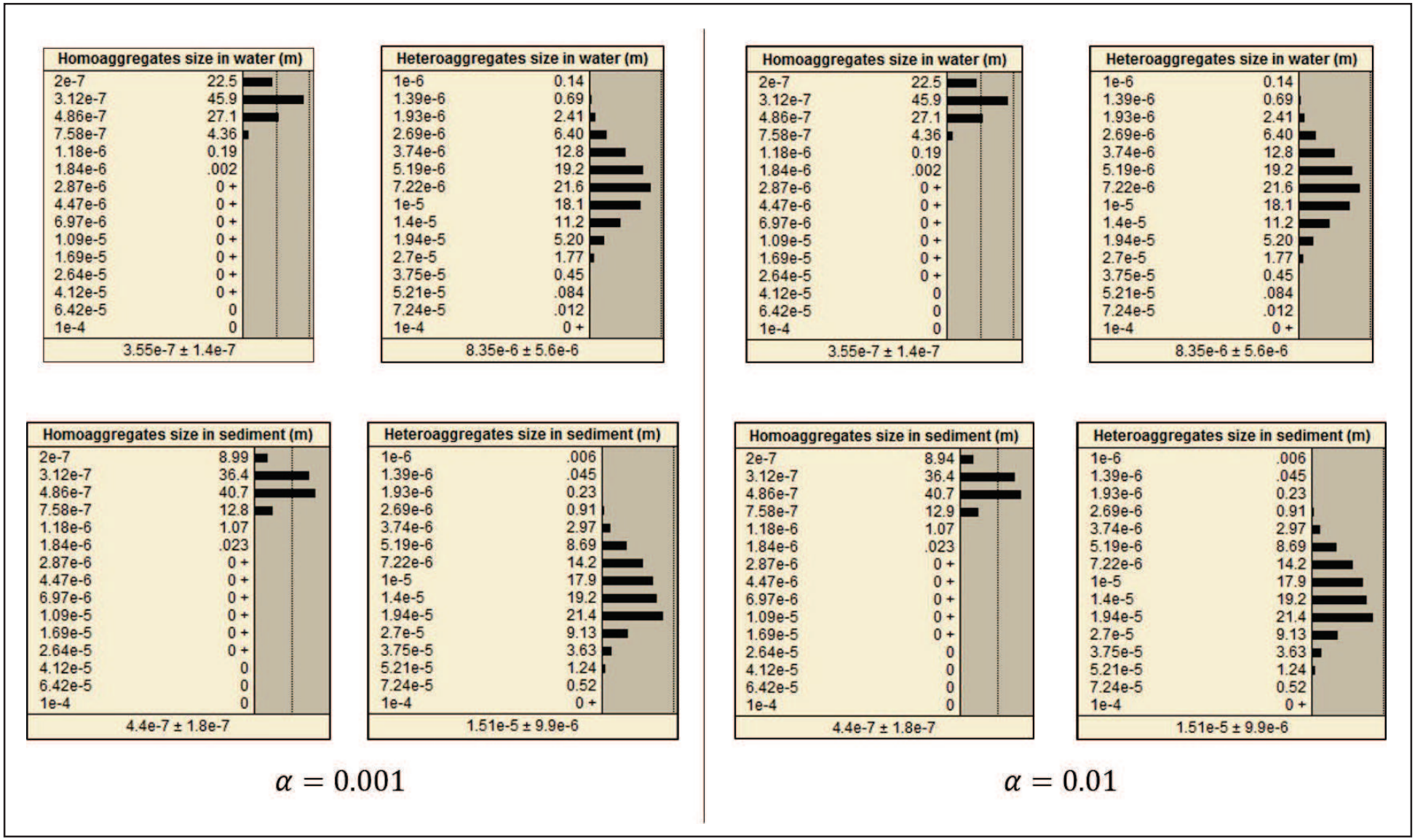

Figure 34: Sensitivity of size distributions to the attachment efficiency coefficient in the river (sampling point 4, January campaign, D_f = 2.5, sizes expressed in meters)

2.3.2.Sensitivity to fractal dimension

In water (river and effluents), the concentration of homo-aggregates in suspension decreases with an increase of the fractal dimension, from 1.5 and 2.9 (Appendix XI). This is due to the aggregates higher density, leading to faster sedimentation out of the water column (Eq. 2, 3 and 12). This effect is most important as D_f increases from 2.5 to 2.9, where a much higher number of aggregates is lost by sedimentation. Consequently, more aggregates are found in the sediments as D_f increases, meaning that fewer aggregates are available for hetero-aggregation in water. This explains why they are present in smaller quantities as heteroaggregates in both water and sediments with increasing D_f. This leads to the conclusion that sedimentation occurs at a faster rate than aggregation, at all tested α and at a D_f equal to 2.9.

No significant effect was shown on the aggregates size distributions in the water column, but TiO_2 homo- and heteroaggregates tend to be bigger in the sediment when the D_f is increased (Figure 35). This is explained by the fact that, in the calculation of the sedimentation rate constant, the aggregate size is raised to the power of D_f (Eq. 2, 3 and 12): the increased D_f enlarges the effect of increasing size on the sedimentation rate.

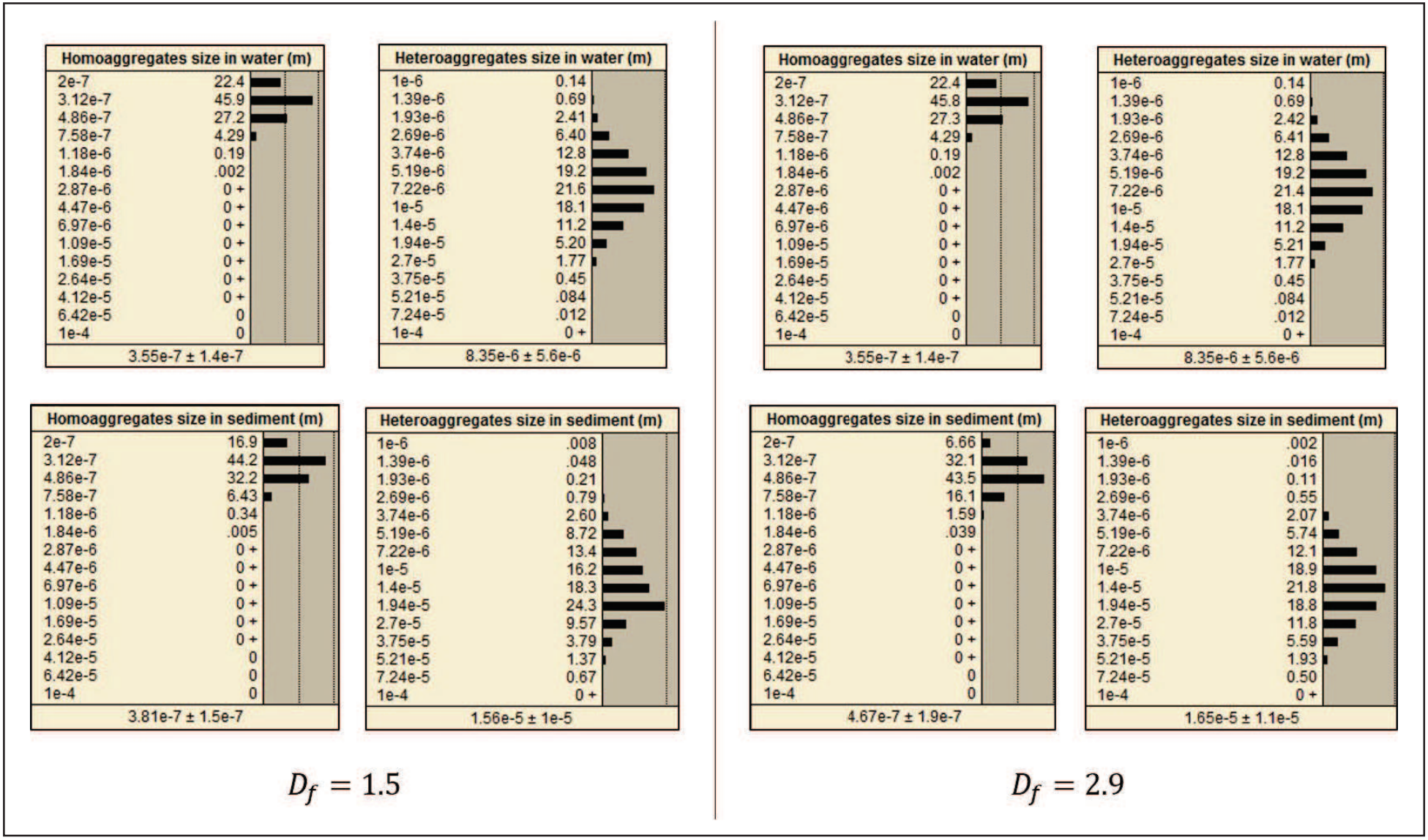

Figure 35: Sensitivity of size distributions to the aggregates fractal dimension in the river (sampling point 4, January campaign, α=0.001, sizes expressed in meters)

2.3.3.Sensitivity to TiO_2 concentration

The effect of a raise in the TiO_2 concentration was analyzed in effluent T, comparing the January (31 $\mu g.L^{-1}$), March (922 $\mu g.L^{-1}$) and August campaigns (1250 $\mu g.L^{-1}$), all other parameters being constant. In the effluent, at D_f equal to 1.5, 2 and 2.5, the increased concentration leads, by definition, to higher numbers of aggregates in suspension (Appendix XI). However, at D_f = 2.9, the term of loss by deposition in Eq. 10 becomes very important, as both Df and concentration are raised, in such a way that deposition counterbalances the concentration raise and leads to fewer aggregates in suspension. The trace of this phenomenon is still observable in the river: at high initial concentrations, fewer aggregates are available for hetero-aggregation and sedimentation, so that all concentrations are decreased at D_f = 2.9.

No significant change was observed in the size distributions of aggregates in the effluent and in the river water as the TiO_2 concentration increases, although aggregates tend to be slightly bigger with increased concentrations (Figures 36 and 37). This is expected from the higher collision rates induced by higher concentrations, which lead to faster aggregation.

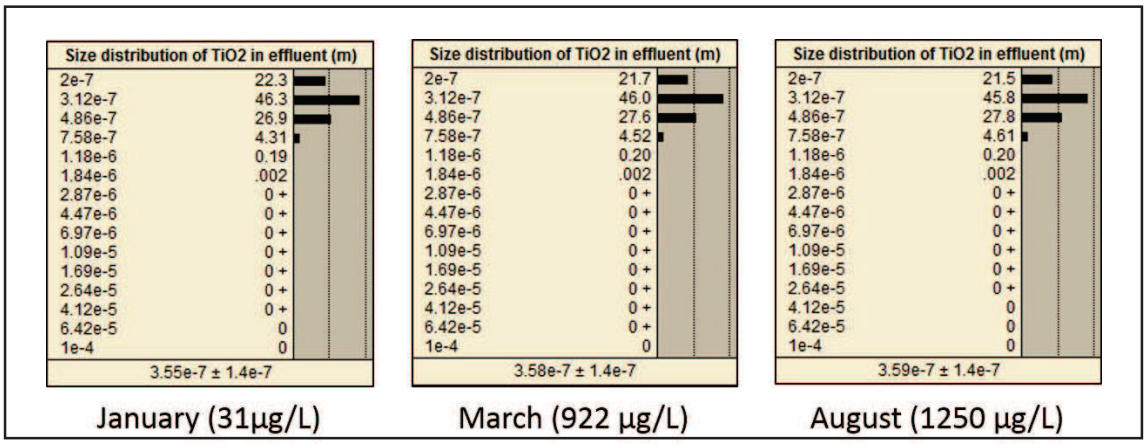

Figure 36: Sensitivity of size distributions to TiO_2 number concentration (effluent T, D_f = 2.5, α=0.001, sizes expressed in meters)

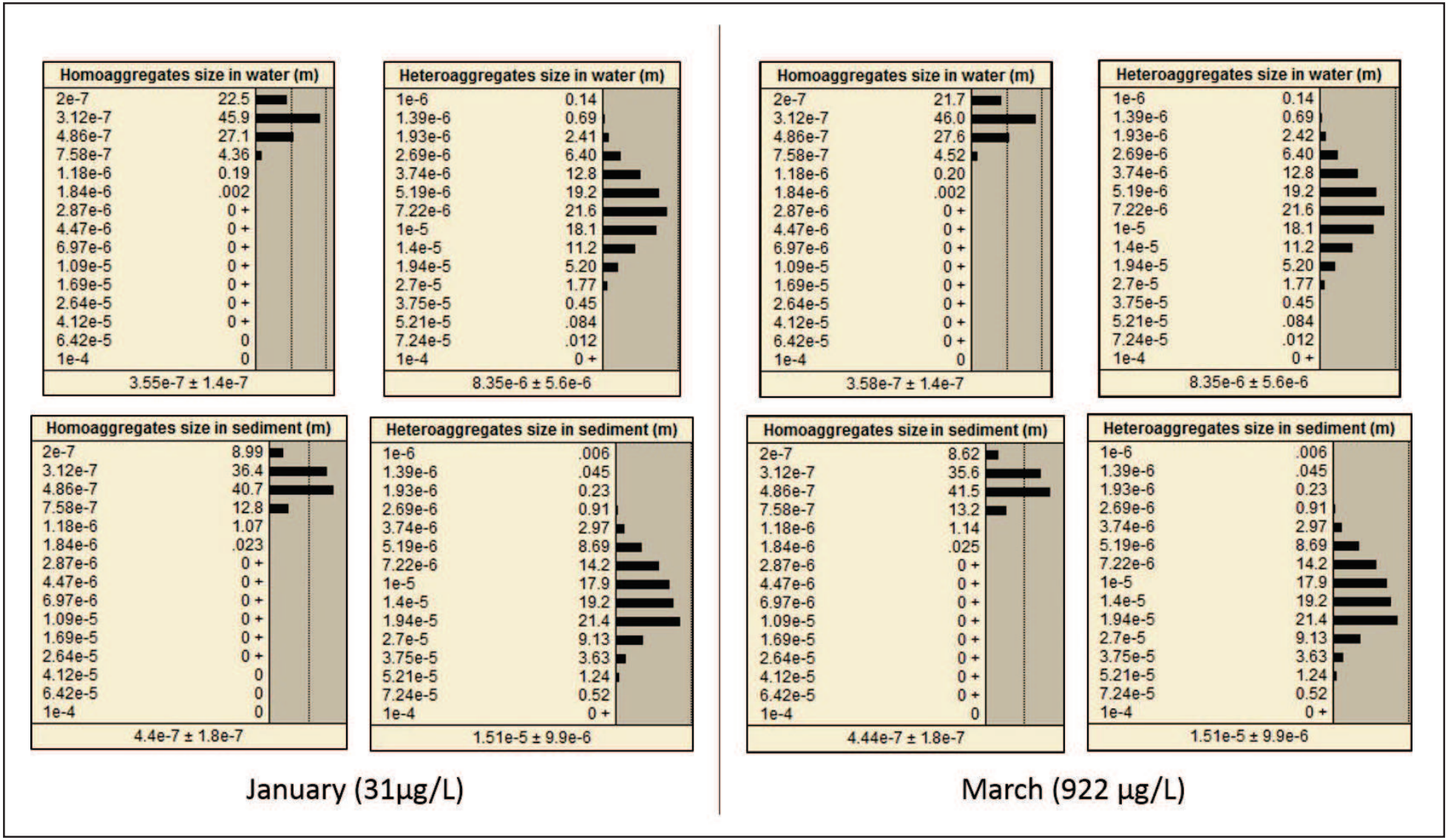

Figure 37: Sensitivity of size distributions to TiO_2 number concentration (sampling point 4, D_f = 2.5, α=0.001, sizes expressed in meters)

Overall, the size distributions of TiO_2 NMs seem most sensitive to variations in their fractal dimension, especially from 2.5 to 2.9. This sensitivity is even higher at high concentrations. Furthermore, the results analysis shows that sedimentation is a faster process than homo- and hetero-aggregation at a D_f equal to 2.9. However, an experimental assessment of α in the effluent and in the river would allow a more accurate determination of the fate of the NMs in these waters.

This model has to be combined to ecotoxicological data in order to obtain a risk score. However, no data is currently available on the ecotoxicity of TiO_2 NMs produced by CRISTAL. Thus, we built a BN adapted to the ecotoxicity tests performed in the mesocosms studied in the Mesonnet ANR.

3. Building a BN for the risk assessment of TiO_2 NMs

A battery of biomarkers was measured on *Dreissena polymorpha* and *Gammarus roeseli* exposed to cubic and rod-shaped anatase in mesocosms (Figure 38). These data were chosen for implementation in the BN, because they were obtained in near-reality conditions, which were natural freshwater (Volvic), environmentally relevant concentrations (max. 1 $mg.L^{-1}$) and long exposure times (up to 28 days).

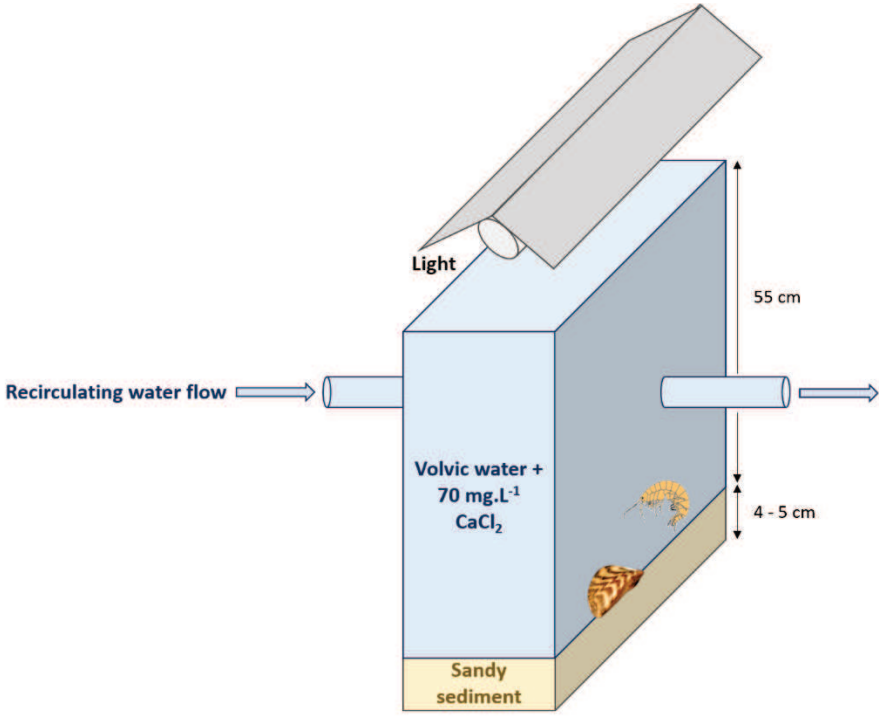

Figure 38: Mesocosms experimental design

3.1. Generating the ecotoxicity data

3.1.1.Simulation of a natural aqueous medium

G. roeseli is a freshwater amphipod (crustacean) and *D. polymorpha* is a freshwater bivalve (mollusk). Both live in temperate rivers, are ubiquitous and were collected in Eastern France, which make them relevant to the study area.

The mesocosms in which they were introduced were preliminary filled with an artificial sediment composed of 89% SiO_2, 10% kaolinite and 1% $CaCO_3$, and with Volvic water (56 L, Table 13). The water was supplemented with 70 $mg.L^{-1}$ $CaCl_2$ (0.63 mM) in order to obtain an optimal mineralization for *D. polymorpha* (Table 14). A natural inoculum of water-saturated sediment, composed of algae, bacteria, hyphomycete and alder leaves was added three weeks before the introduction of the tested organisms, so that the presence of primary producers was ensured (Figure 39).

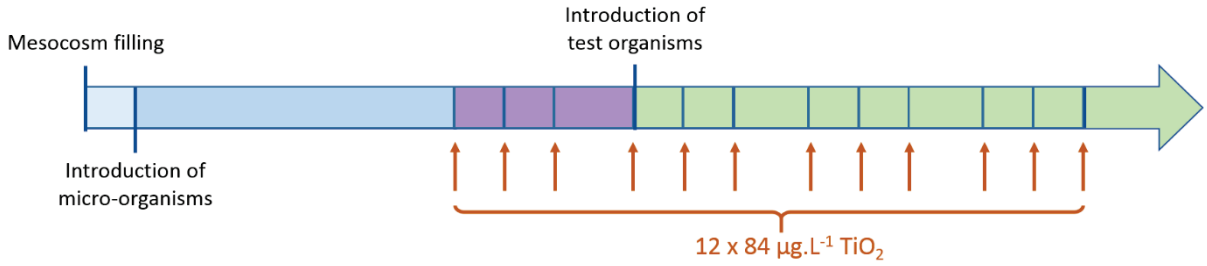

Figure 39: Time schedule for mesocosms experiments

Table 13: Composition of Volvic water (concentrations are expressed in $mg.L^{-1}$)

Ca^{2+}	Mg^{2+}	K^{+}	Na^{+}	Cl^{-}	HCO_3^{-}	NO_3^{-}	SO_4^{2-}	SiO_2
11.5	8.0	6.2	11.6	13.5	71.0	6.3	8.1	31.7

Table 14: Physicochemical parameters of mesocosms water (Auffan *et al.* 2014)

Temperature	pH	Conductivity	Redox potential	Dissolved O_2	Total organic carbon
19 ±2°C	7.9 ±0.1	250 – 330 $\mu S.cm^{-1}$	+270 ±20 mV	8.0 ±0.2 $mg.L^{-1}$	1.80 ±0.08 $mg.L^{-1}$

3.1.2.Exposure conditions

Two types of anatase NMs were tested, both provided as dispersed in stock suspensions. One was composed of cubic NPs, the other one was made of rod-shaped NPs (Table 15, Figure 40). 84 $\mu g.L^{-1}$ of NPs were injected at the surface of the water mesocosms 12 times over 25 days, in order to obtain 1 $mg.L^{-1}$ at the end of the experiment (Figure 39). This enabled the simulation of a continuous release of NPs in the aqueous media.

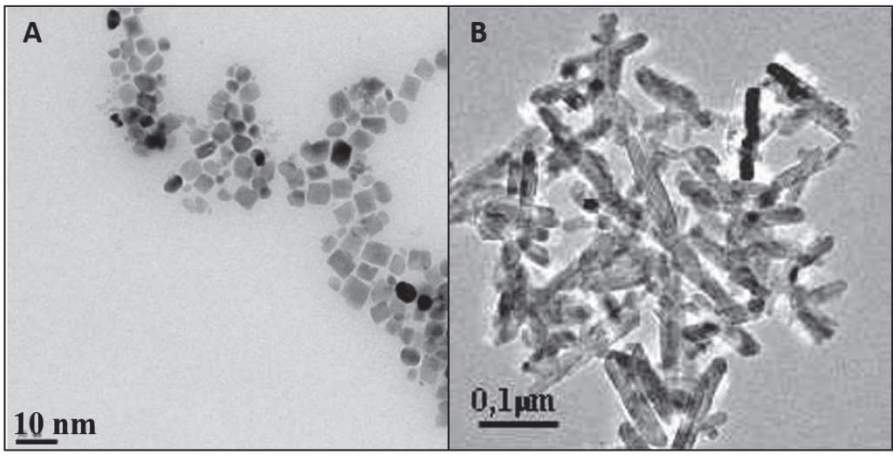

Figure 40: TEM images of (A) cubic and (B) rod-shaped anatase NMs tested in mesocosms (Garaud *et al*. 2013)

Table 15: Characterization of anatase TiO_2 NMs in stock suspensions (Garaud *et al*. 2013)

Shape	TEM primary size	DLS hydrodynamic diameter	Specific surface area	Zeta potential
cubic	25-30 nm	149 nm	100 $m^2.g^{-1}$	+46 mV
rod-shaped	20 x 200 nm	93 nm	140 $m^2.g^{-1}$	+57 mV

3.1.3.Measurements of effect parameters

25 biomarkers were measured on *D. polymorpha* and 14 on *G. roeseli*, so a choice had to be made in order to avoid too much complexity of the BN (Table 16), in accordance with ecotoxicologists and with a discriminating statistic analysis they performed.

Oxidative stress is an important toxicity mechanism of TiO_2 (Manke *et al*. 2013) so total antioxidant capacity (TAC) and lipid peroxidation were included in the network. They were tested on both organisms. The TAC shows the capacity of the organisms to resist to oxidative stress. It was measured on the cytosolic fraction of the digestive gland as the bleaching upon reduction by antioxidants and expressed in µmol Trolox equivalent/g protein/min (Trolox being a calibration standard). A decrease in the value of this biomarker shows a toxicity towards the tested organism. The oxidative stress can result in lipid peroxidation, inducing cellular damage. It was measured as the lipid hydroperoxide (LOOH) concentration in the whole homogenate of the digestive gland. An increase of this concentration reveals a higher toxicity.

Three of the most sensible immunological parameters tested on *D. polymorpha* were the reactive oxygen species (ROS) production, the cell viability and the phagocytosis performance, so they also appear in the network. They were all measured in the heamocytes. ROS production was assessed by

fluorescence and expressed as arbitrary units (AU). The number of damaged cells was the most sensitive biomarker for cell viability. It was assessed by flow-cytometry and expressed in %. Phagocytosis activity was assimilated to the percentage of phagocytic cells that had engulfed at least one latex bead (2 µm size). A decrease in phagocytic activity shows a decreased cellular defense capacity, and so a higher toxicity.

Finally, all biomarkers measured at an individual level appear in the model, as they are representative of a global toxicity, induced by the various toxicity mechanisms occurring at smaller scales (cellular level). They were filtration and mortality for *D. polymorpha*, and ventilation, osmolality, locomotion and mortality for *G. fossarum*. The filtration capacity of *D. polymorpha* is expressed in mL/individual/h, so a decrease in the value shows an increased toxicity. Ventilation is an indicator of blood oxygenation: lower ventilation shows a toxicity towards the organism. It was measured as the number of swimmeret fluttering per minute. Osmolality is the concentration of molecules actually in solution. For example, 1 mole of NaCl (electrolyte) gives 2 osmoles of solute (1 osmol of Na^+ and 1 osmol of Cl^-). Thus, it is an indication of the organism electrolyte-water balance: a decrease in osmolality shows a toxicity towards *G. roeseli*. Finally, locomotion was measured as the percentage of mobile individuals, and mortality as the percentage of dead individuals.

Table 16: Biomarkers included in the BN, measurement times and tested species (d = day)

Biomarker	**Measurement time**	**Tested species**
Total antioxidant capacity (TAC)	d7, d14, d21	*G. roeseli*; *D. polymorpha*
Lipid peroxidation	d7, d14, d21	*G. roeseli*; *D. polymorpha*
ROS production	d7, d14, d21	*D. polymorpha*
Cell viability	d7, d14, d21	*D. polymorpha*
Phagocytosis performance	d7, d14, d21	*D. polymorpha*
Filtration	d21	*D. polymorpha*
Ventilation	d7, d14, d21	*G. roeseli*
Osmolality	d7, d14	*G. roeseli*
Locomotion	d7, d14, d21	*G. roeseli*
Mortality	d7, d14, d21	*G. roeseli*
	d28	*D. polymorpha*

The structure and probability tables of the BN were adapted to these available data, as described in the next section.

3.2. Integrating the data in a BN

3.2.1.Modeling the natural medium

A single BN was developed for both species, in order to read all the results on the same document (Figures 41 and 42). For this purpose, a box called “species” was created in the network, so that the user can choose the organism to be analyzed.

The water properties determining the aggregation state of the particles also appear on the BN, because the particle size distribution must be assessed to determine their potential sedimentation and uptake by the organisms. However, the fate model developed above could not be used to predict it, because it was built based on theories which are valid for spherical primary particles, which present a relatively uniform surface reactivity. This is not the case of cubic and rod-shaped NPs, whose faces present different reactivity. Furthermore, no SPM characterization was performed in the mesocosms, neither regarding its concentration nor its size distribution, so hetero-aggregation could not be assessed. Measurements of TiO_2 in water and in sediments, which are planned to be performed shortly, will help in assessing the NMs fate in the mesocosms system.

3.2.2.Modeling the exposure conditions

As for species, a box called “NP type” allows to choose the tested NPs for which the risk is assessed. In the experiments design, the NPs concentration is function of the exposure time (Table 17), so a link was made between these variables.

Table 17: Relationship between exposure duration and NP concentration in the test medium

Exposure duration	NPs concentration
7 days	588
14 days	840
21 days	1008

3.2.3.Modeling the risks

The risk of TiO_2 NMs was expressed in the same way for all biomarkers, as a comparison to the control (% increase or % decrease compared to the value measured in the control organisms). Mean values were directly entered in the probability tables (Appendix XIIA and XIIB).

Biomarkers were placed on one of three levels: the top one includes all cellular endpoints, on the second one are individual biomarkers except mortality, which is placed at the bottom of the network. Ideally, causality links should be made between these three levels, as cellular toxicity induces effects at the individual level and *in fine*, mortality. It would indeed be very interesting to reduce the number of biomarkers to be tested by predicting the effects of TiO_2 NMs at the individual level from the effects

observed at the cellular level. However, these relationships could not be quantitatively assessed in the current state of knowledge, so the links were not represented in the network.

The risk probability distributions narrow down as the species, the shape and the concentration of NPs are selected. However, biomarkers were not always measured for both species. In the case of the absence of data, the risk probability distribution stays uniform, meaning that no knowledge exists on this variable.

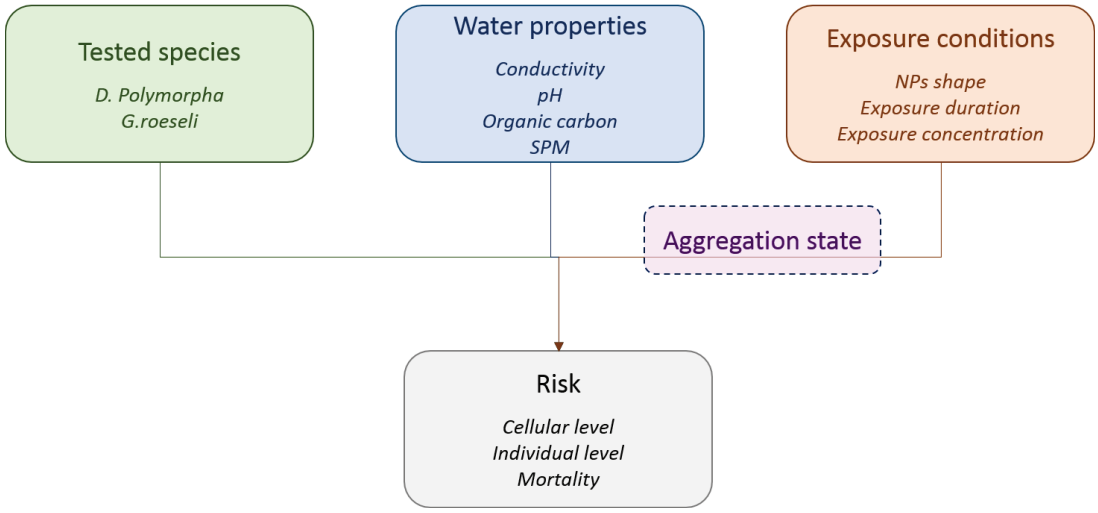

Figure 41: Simplified structure of the BN developed for TiO_2 NPs RA in mesocosms

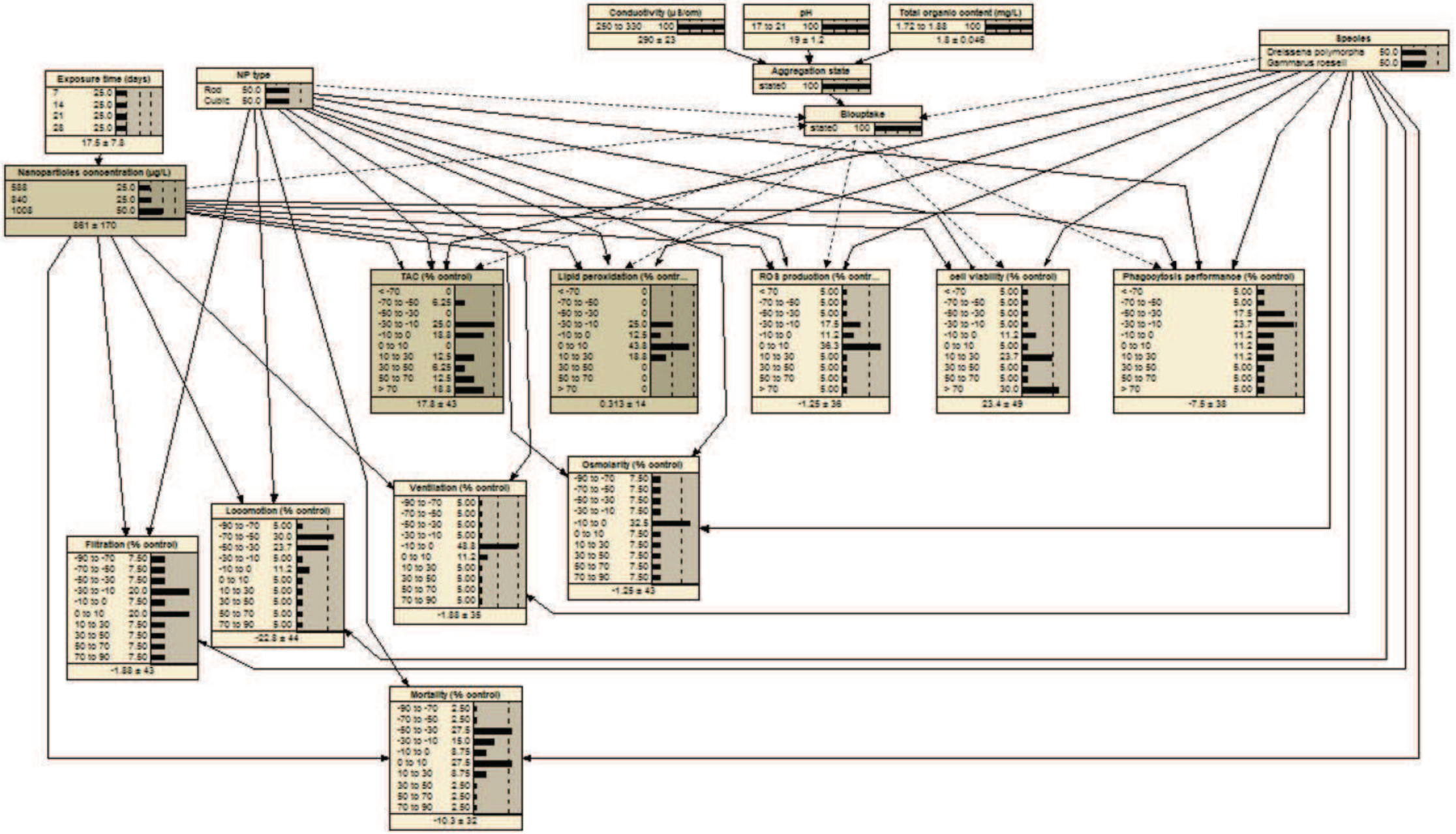

Figure 42: Structure of the BN developed for the risk assessment of cubic and rod-shaped TiO_2 NMs on *D. polymorpha* and *G. roeseli.* Dot lines represent the links that need to be made with the biouptake. This variable has to be linked to all effect variables.

3.3. Results and discussion

3.3.1.Risks towards Gammarus roeseli

Gammarids exposed to rod-shaped and cubic anatase NMs presented a lower TAC than the control after 7 days of exposure, but a higher TAC than the control at longer exposure durations (Figures 43 and 44). Lipid peroxidation did not seem sensitive to NMs concentration in these organisms. So both NMs did not show a high oxidative toxicity to *G. roeseli*. In the same way, very low effects were measured on their ventilation. The most impacted biomarker was locomotion, decreasing with longer exposure durations and higher TiO_2 concentrations, with more than 50% difference to the control. This represents the highest potential risk of TiO_2 NMs observed on *G. roeseli*.

Cubic anatase NMs induced higher toxicity than rod-shaped NMs, both on TAC and on locomotion, showing higher potential risks of the latter on *G. roeseli*.

High mortalities were observed in both control and exposed organisms, so the risks specific to TiO_2 NMs on this endpoint are difficult to assess. No firm conclusion could be drawn, although differences with the control remained within about 10%.

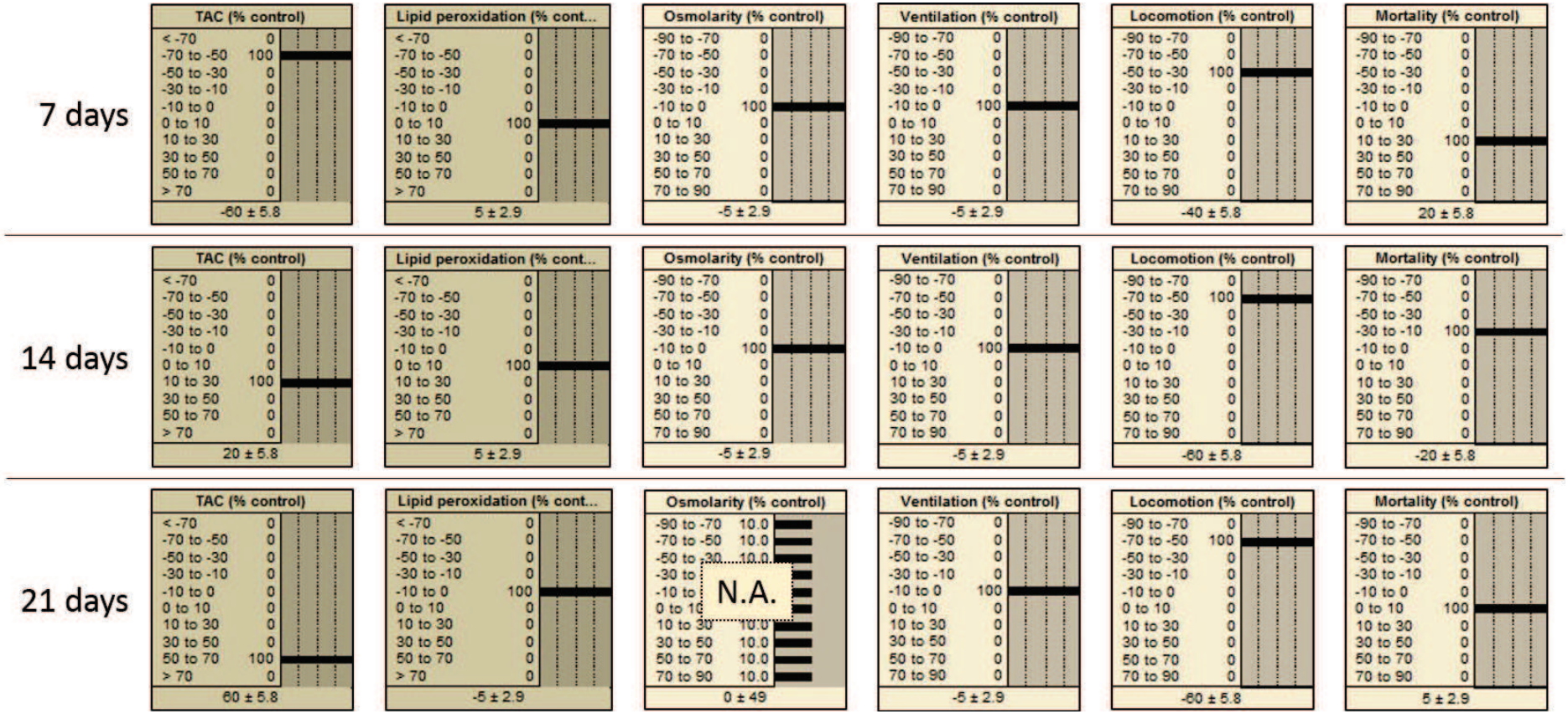

Figure 43: Risk assessment of cubic anatase NMs on *Gammarus roeseli.* Exposure durations are indicated on the left of the figure.

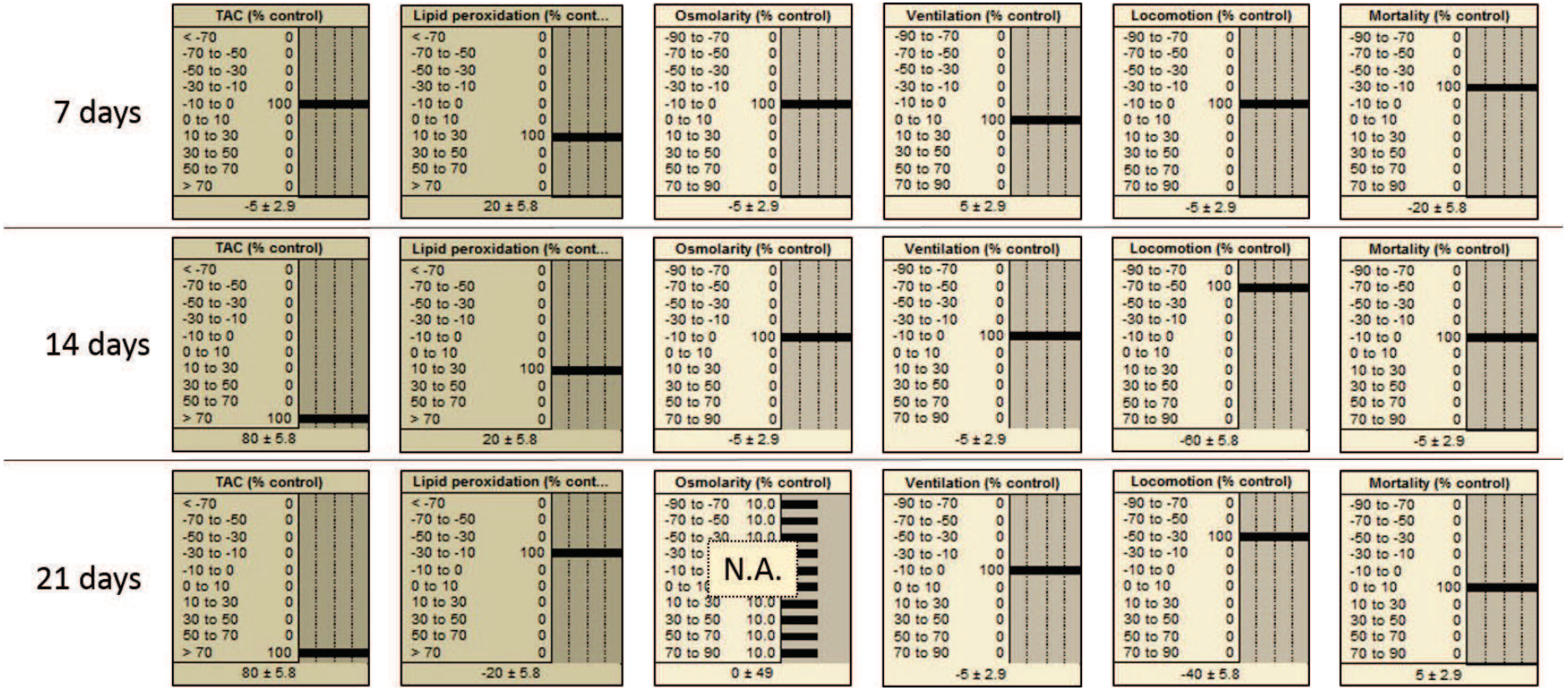

Figure 44: Risk assessment of rod-shaped anatase NMs on *Gammarus roeseli.* Exposure durations are indicated on the left of the figure.

3.3.2.Risks towards Dreissena polymorpha

Mussels exposed to rod-shaped NMs showed contradictory results concerning the risks arising from oxidative stress (Figures 45 and 46). The difference of TAC with the control was negative after 7 days of exposure, positive after 14 days, and negative again after 21 days. The ROS production gave results that lead to the same conclusion, which was that the organisms seemed to adapt to the NMs exposure at days 7 and 14, but not anymore at day 21. Meanwhile, the difference in lipid peroxidation with the control was positive and increased from 7 to 14 days, while it decreased to negative values after 21 days of exposure, which could show an adaptation of these organisms after 21 days. Consequently, the effect of oxidative stress induced by rod-shaped anatase NMs to *D. polymorpha* remains unclear.

Regarding cubic anatase, low effects on lipid peroxidation were measured in mussels. The TAC behaved in the same way as for rod-shaped NMs, although the difference with the control was very low at the end of the experiment. The difference of ROS production with the control was negative and decreased from 7 to 14 days of exposure, but was positive after 21 days of exposure.

The percentage of damaged cells was the most sensitive of the biomarkers tested on *D. polymorpha*: difference with the control were positive, up to 245% for rod-shaped NMs after 21 days of exposure. This showed a high toxicity towards *D. polymorpha*.

Both NMs induced similar trends of phagocytosis performance: after 14 days of exposure, an adaptation seemed to appear with positive differences with the control. However, after 21 days of exposure, these differences were negative, more than 10% and 30% for cubic and rod-shaped NMs, respectively, showing a potential risk towards the organisms.

Filtration was measured after 28 days of exposure, which showed a higher risk induced by rod-shaped than by cubic NMs. Mortality was the same for both NMs, and lower than in the control (Figure 47).

D. polymorpha reacted in the same way when exposed to cubic and to rod-shaped TiO_2 NMs, apart from ROS production and filtration, which showed higher effects of rod-shaped NMs.

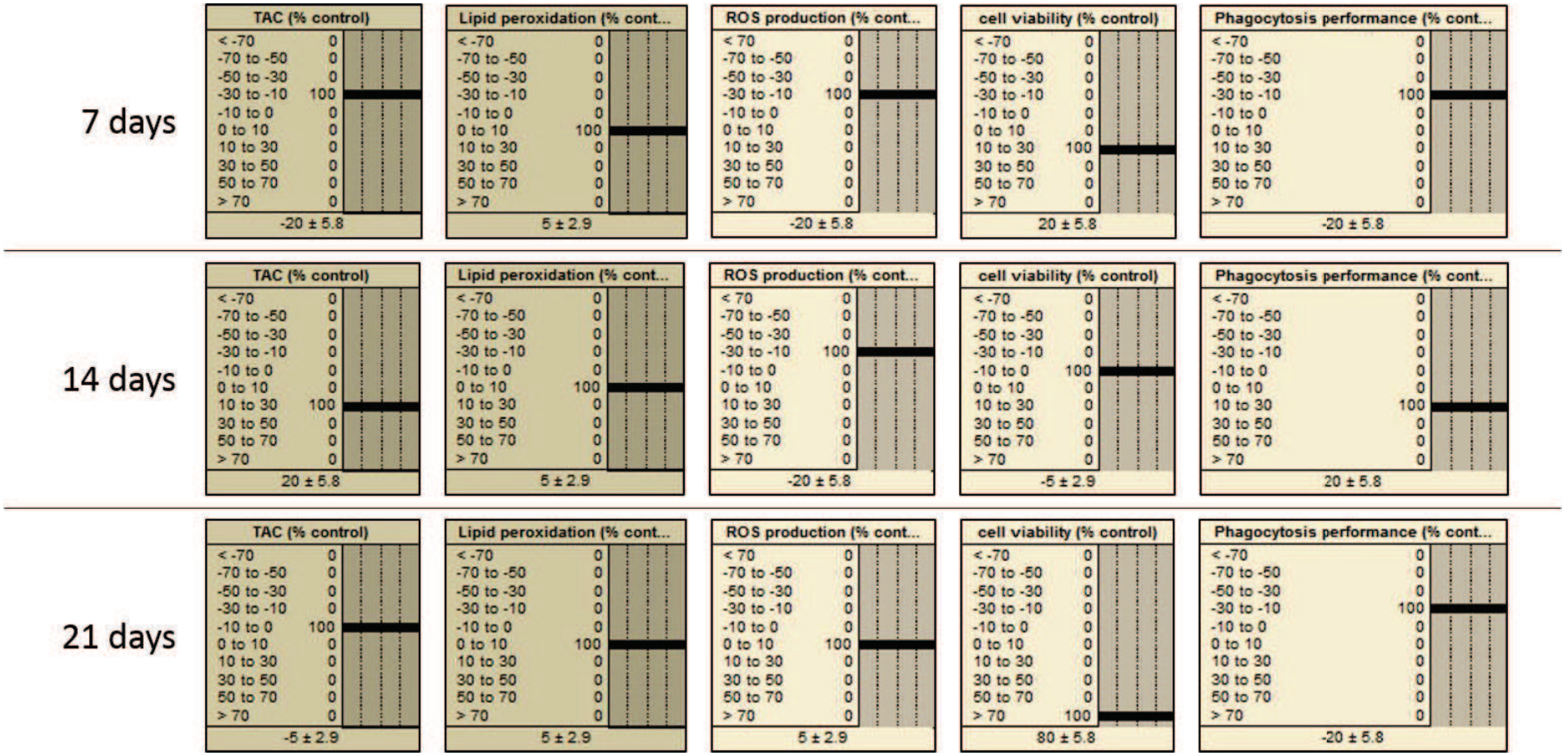

Figure 45: Risk assessment of cubic anatase NMs on *Dreissena polymorpha* at the cellular level. Exposure durations are indicated on the left of the figure.

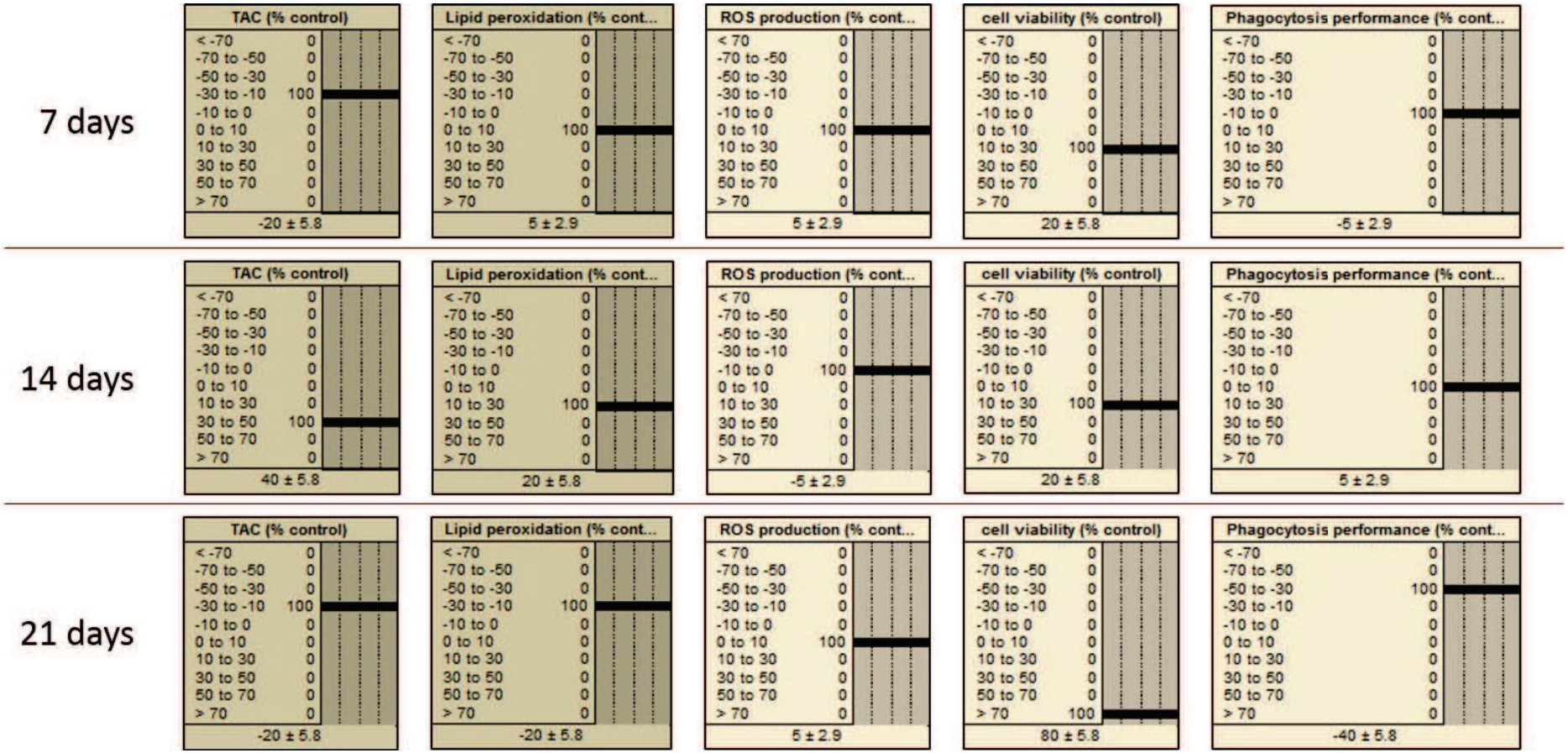

Figure 46: Risk assessment of rod-shaped anatase NMs on *Dreissena polymorpha* at the cellular level. Exposure durations are indicated on the left of the figure.

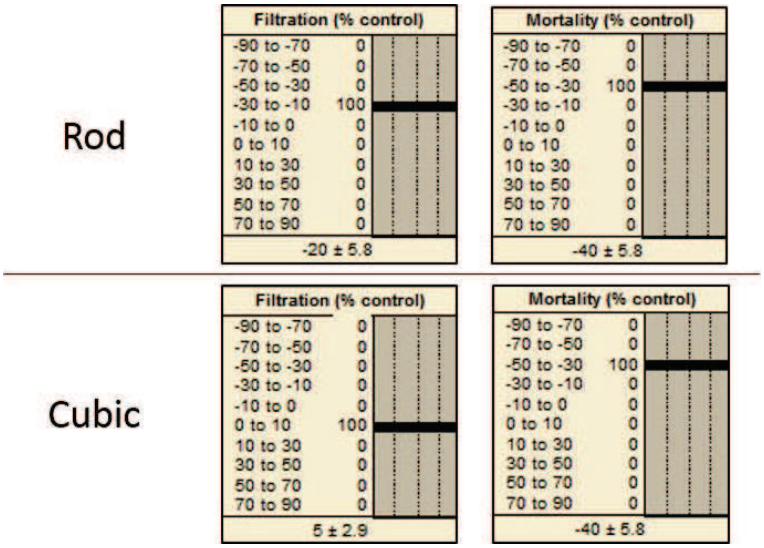

Figure 47: Risk assessment of rod-shaped and cubic anatase NMs on *Dreissena polymorpha* at the individual level. Filtration was measured after 21 days of exposure; Mortality was measured after 28 days of exposure. NP types are indicated on the left of the figure.

3.3.3.Discussion

The integration of ecotoxicological data in a BN enabled the direct visualization of the potential risks induced by two types of NPs towards two types of species on the same document.

The design of the experiment and especially the cumulative character of the exposure concentration do not allow to make the distinction between time- and concentration-dependent effects. Nevertheless, this same character simulates well the accumulation of NMs in the sediment upon continuous release in water, so that the exposure conditions are very similar to those encountered in the study area.

These experiments also answered the need for ecotoxicological data obtained at environmentally relevant concentrations and over long exposure durations. Results showed that the shape of anatase NMs influences most the filtration of *D. polymorpha*, at concentrations less than 1 $mg.L^{-1}$. Cubic anatase were the most toxic on *G. roeseli*, while the highest toxicity was induced by rod-shaped NMs on *D. polymorpha*.

The highest negative effects were measured on the locomotion of *G. roeseli* and on the cell viability of *D. polymorpha*, showing a potential risk induced by TiO_2 NMs on these organisms. However, a lower mortality was measured on *D. polymorpha* exposed to NMs than in the control, meaning that both NMs may have a protective effect on these organisms regarding this biomarker. This shows that measuring biomarkers at the individual level is not sufficient for risk assessment, as they may leed to

different conclusions than observations at the cellular level. The result of the cellular toxicity might be visible at the individual level over longer exposure durations, but it might be difficult to implement such experiments. Consequently, causality relationships need to be made between the toxicity results obtained at the cellular level and at the individual level, in order to keep as low as possible the required time and number of ecotoxicity experiments for RA.

Moreover, building this network highlighted the need for a thorough characterization of NMs and test media (Table 18), especially their charge and/or size distribution in the exact test medium. The relationship between biouptake and ecotoxicity must also be quantified, based on the NMs dosage in the organisms. These are the only ways a link can be made between the fate and the effects of NMs, and so to *predict* a risk.

Table 18: Minimum required data to be measured in ecotoxicity experiments for further integration in a RA BN. Properties colored in green were measured in the mesocosms, properties colored in orange were missing.

Nanomaterials	**Test medium**
Shape	Conductivity / ionic strength
Size of primary particles	pH
Crystal phase	Organic carbon content
Concentration	Depth of water column
Surface charge / Point of zero charge in the test medium	SPM concentration
	SPM size distribution

KEYPOINTS

- Under the tested conditions, TiO_2 NMs are more abundant in the water column than in the sediment.
- The fate model showed a high sensitivity towards the NMs aggregates fractal dimension, especially at the highest values.
- Ecotoxicological effects are observed at low concentrations (≤ 1 $mg.L^{-1}$) over long exposure durations (up to 28 days).

PRIORITY RESEARCH NEEDS

- To better assess the fractal dimension of NMs aggregates. Precision is most needed at highest values.
- To perform more studies on chronic ecotoxicity of TiO_2 NMs, at environmentally relevant concentrations and using the NMs released in the river.
- To better characterize the tested NMs and the test media in order to predict their behavior in ecotoxicity testing media.

References

Auffan M, Tella M, Santaella C, *et al* (2014) An adaptable mesocosm platform for performing integrated assessments of nanomaterial risk in complex environmental systems. Sci Rep. doi: 10.1038/srep05608

Garaud M, Bennasroune A, Chanéac C, *et al* (2013) Multibiomarker assessment of TiO2 nanoparticles effects on Dreissena polymorpha and Gammarus roeseli: influence of shape and crystal structure.

Garaud M, Trapp J, Brulé N, *et al* Multibiomarker assessment of CeO2 nanoparticle (nCeO2) sublethal effects on the freshwater invertebrates Dreissena polymorpha and Gammarus roeseli.

Hansen SF, Baun A, Alstrup-Jensen K (2011) NanoRiskCat–a conceptual decision support tool for nanomaterials. Danish Ministry of the Environment

Jones JAA (1997) Global hydrology - Processes, Resources and Environmental management. Longman, Essex, U.K.

Kennel C, Schindler P (2015) Caractérisation de l'impacts des nanoparticules de titane appliquée aux environs d'un site de production.

Kestin J, Sokolov M, Wakeham WA (1978) Viscosity of Liquid Water in the Range -8°C to 150°C. J Phys Chem Ref Data 7:941–948.

Manke A, Wang L, Rojanasakul Y (2013) Mechanisms of Nanoparticle-Induced Oxidative Stress and Toxicity. BioMed Res Int 2013:1–15. doi: 10.1155/2013/942916

Money ES, Barton LE, Dawson J, *et al* (2014) Validation and sensitivity of the FINE Bayesian network for forecasting aquatic exposure to nano-silver. Sci Total Environ 473–474:685–691. doi: 10.1016/j.scitotenv.2013.12.100

Money ES, Reckhow KH, Wiesner MR (2012) The use of Bayesian networks for nanoparticle risk forecasting: Model formulation and baseline evaluation. Sci Total Environ 426:436–445. doi: 10.1016/j.scitotenv.2012.03.064

Praetorius A, Scheringer M, Hungerbühler K (2012) Development of Environmental Fate Models for Engineered Nanoparticles—A Case Study of TiO_2 Nanoparticles in the Rhine River. Environ Sci Technol 46:6705–6713. doi: 10.1021/es204530n

Rosenbaum RK, Bachmann TM, Gold LS, *et al* (2008) USEtox—the UNEP-SETAC toxicity model: recommended characterisation factors for human toxicity and freshwater ecotoxicity in life cycle impact assessment. Int J Life Cycle Assess 13:532–546. doi: 10.1007/s11367-008-0038-4

Salieri B (2013) The challenges and the limitations in Life Cycle Impact Assessment for metal oxide nanoparticles, a case study on nano-TiO2. Bologna

Salieri B, Righi S, Pasteris A, Olsen SI (2015) Freshwater ecotoxicity characterisation factor for metal oxide nanoparticles: A case study on titanium dioxide nanoparticle. Sci Total Environ 505:494–502. doi: 10.1016/j.scitotenv.2014.09.107

Smoluchovski M von (1917) Attempt for a mathematical theory of kinetic coagulation of colloid solutions. Z Phys Chem 92:129–168.

Tervonen T, Linkov I, Figueira JR, *et al* (2009) Risk-based classification system of nanomaterials. J Nanoparticle Res 11:757–766. doi: 10.1007/s11051-008-9546-1

Thill A, Moustier S, Aziz J, *et al* (2001) Flocs Restructuring during Aggregation: Experimental Evidence and Numerical Simulation. J Colloid Interface Sci 243:171–182.

TÜV SÜD Industrie Service (2008) Certification Standard CENARIOS.

Van De Meent D (1993) SIMPLEBOX: a generic multimedia fate evaluation model. National Institute of Public Health and Environmental Protection, Bilthoven, The Netherlands

Wiesner MR (1992) Kinetics of aggregate formation upon rapid mix. Water Res 26:379–387.

CONCLUSION

The objective of this work was to assess the environmental risks and impacts of TiO_2 NMs at a site-specific scale. The focus was put on their fate and effects in the aqueous medium, where the industrial effluents of a nanoparticulate TiO_2 producer are released.

This study showed that low concentrations of TiO_2 are released in the river water (< 60 $\mu g.L^{-1}$). Nevertheless, ecotoxic effects were demonstrated below this level (at about 30 $\mu g.L^{-1}$), which shows the need for quantifying the exact concentration of nanoparticulate TiO_2 in the environment, with the help of isotopic and/or sizing analytical tools. Sediments seem to be less impacted than water by the effluents release, as concentrations differences between downstream and upstream samples are lower than in water.

The use of a Bayesian approach in the fate modeling of TiO_2 NMs helped in obtaining a more precise assessment of their behavior in the river, especially on their size distribution and on their partitioning between water and sediments. Results showed that TiO_2 NMs are present in lower quantities in the sediment than in water, giving the same conclusion as the analytical approach, but allowing to quantify this partitioning and its dependency to NM-specific and environmental parameters. All uncertainties could not be removed in the modeling, which demonstrates the usefulness of using Bayesian networks. A sensitivity analysis showed that the aggregates fractal dimension needs to be studied in priority in further works. This fate modeling also answered the need for site-specific LCA, by producing data (especially aggregation and transport constant rates) that may be integrated in LCIA methodologies such as USEtox.

TiO_2 NMs risks were assessed in a second BN, dedicated to mesocosms. The assessment of TiO_2 NMs ecotoxicity in environmentally relevant conditions and long exposure durations demonstrated that environmental risks can arise from low concentrations in water (< 1 $mg.L^{-1}$) and that research must be carried on in this direction. This network was used to complete the first step of risk assessment, which is data compilation. Links were made between the exposure conditions (NMs concentration and type, exposure duration), test species and observed effects, but the causality relationships between the NMs aggregation state, their biouptake and their potential toxicity are yet to be quantified. This may be done based on the dosage of Ti in the organisms, and will help researchers in predicting the potential risks of TiO_2 NMs under various exposure conditions. For this purpose, two additional research paths are suggested, which could be investigated: (1) to better characterize the test medium and the tested NMs, in order to predict their aggregation state (and so their potential sedimentation and biouptake)

based on the fate BN developed in this work, (2) to work on quantifying the relationships between biomarkers assessed at different levels, in order to predict potential effects at the individual level from the effects observed at the cellular level. Furthermore, because different NMs behave differently in the organisms, potential ecotoxic effects must be assessed on the precise TiO_2 NMs produced by CRISTAL, in order to predict accurately their risks in the river in which they are released.

Nano-objects are not only released by water effluents coming from industrial production, they can be released all along their life cycles, as nanoparticles, nanomaterials, nanoproducts, or nanowaste. Including all lifecycle steps in the RA would allow to bridge LCA and RA, and may be done by adapting the present BNs to each of these steps. Integration of data relative to the matrices in which NMs are inserted would be required for assessing the NMs releases from the use of nanoproducts and more information relative to their waste management would be required for the estimations of releases from this last step.

NMs transfer routes from production, use and waste management to the environment include industrial and domestic wastewater, transport by air, and deposition on soils. Understanding the fate of NMs in these compartments and their transfers from one to another would allow to account for all potential target organisms, and so to give a more comprehensive basis for their RA. Different BNs could be developed for each one of these compartments, including compartment-specific parameters and processes. For example, regarding the terrestrial risks of NMs, the main source of NMs in soils is air deposition. A BN specific to air and soil compartments could thus be built, considering (1) the fate of NMs in the air (by adapting the effluent part of the model developed in this work) and determining the state in which they are deposited onto soils and (2) the terrestrial processes determining their fate in soils, based on the output of the first fate model and taking into account soil properties such as porosity, texture, and pH of the soil solution. Both models could then be interrelated through the evaluation of inter-media transfers, such as runoff from soils. This would enable to model the whole ecosystem in which TiO_2 NMs are released.

The environmental impact and risk assessments of NMs concern not only the academic research, but also the society and the economical stakeholders. Collaborations between these worlds make more efficient and useful the results obtained by each field. For this purpose, comparing the sensitivity analysis to the needs and potential uses of the different stakeholders would allow to adapting BNs to make them practical tools, which would help in building NMs-specific regulation and in decision making.

Working on this Ph.D. during 3 years brought me so much, both scientifically and personally, that it gave me the desire to continue on this path. This experience helped me both to enrich and to strengthen myself. I gained in self-confidence, in work endurance and I have higher self-requirements. This work also helped me in learning to structure my ideas, to develop them and to communicate them in an understandable way. I very much enjoyed learning about various domains, such as risk and impact assessments, probabilistic theories, chemistry, ecotoxicology, modeling and programming. This fed my thirst for knowledge, enabled me to relate data coming from very different fields and gave me solid bases to carry on the research on NMs environmental assessment.

APPENDIX

Appendix I: Texture and organic matter content of soils and sediment (analyzes performed on the samples collected in 2014)

JANUARY	% Clay	% Silt	% Sand	% Coarse elements	% Organic matter
	< 2µm	> 2µm and < 50µm	> 50µm and < 2000 µm	> 2 mm	on < 2 mm fraction
Soil 1	/	/	/	/	/
Soil 2	1,55	5,75	92,70	25,57	11,31
Soil 3	3,45	12,25	84,30	9,50	10,94
Soil 3'	/	/	/	/	/
Soil 4	2,23	7,47	90,30	23,69	10,60
Soil 5	2,06	7,47	90,47	19,76	3,45
Soil 6	3,67	13,73	82,60	7,95	14,12
Soil 7	5,64	12,86	81,50	9,64	9,97
Sediment 1	1,58	6,10	92,32	27,17	1,59
Sediment 2	0,97	3,94	95,09	17,63	1,63
Sediment 3	6,28	32,32	61,40	34,71	16,02
Sediment 3'	2,57	10,33	87,10	5,92	4,76
Sediment 4	1,70	5,56	92,74	31,89	1,41
Sediment 5	1,33	4,57	94,10	11,90	1,35

MAY	% Clay	% Silt	% Sand	% Coarse elements	% Organic matter
	< 2µm	> 2µm and < 50µm	> 50µm and < 2000 µm	> 2 mm	on < 2 mm fraction
Soil 1	3,90	14,60	81,50	3,32	7,12
Soil 2	7,01	21,59	71,40	35,12	10,07
Soil 3	9,30	31,60	59,10	21,09	10,89
Soil 3'	2,73	9,87	87,40	24,73	7,81
Soil 4	3,69	10,91	85,40	31,16	10,27
Soil 5	8,20	40,60	51,20	1,01	8,65
Soil 6	1,89	6,12	91,99	48,69	17,60
Soil 7	7,57	18,53	73,90	59,49	10,46
Sediment 1	1,29	4,85	93,86	48,33	2,46
Sediment 2	2,71	7,39	89,90	61,87	1,44
Sediment 3	1,25	3,67	95,08	55,87	4,06
Sediment 3'	1,94	5,93	92,13	80,22	4,92
Sediment 4	2,12	5,90	91,98	34,27	1,51
Sediment 5	1,34	3,31	95,35	38,12	1,69

AUGUST	% Clay	% Silt	% Sand	% Coarse elements	% Organic matter
	< 2µm	> 2µm and < 50µm	> 50µm and < 2000 µm	> 2 mm	on < 2 mm fraction
Soil 1	3,72	8,18	88,10	3,44	8,60
Soil 2	8,44	21,96	69,60	25,01	11,28
Soil 3	4,83	19,27	75,90	26,67	10,37
Soil 3'	3,64	16,26	80,10	25,96	7,77
Soil 4	7,86	28,94	63,20	28,28	11,33
Soil 5	4,85	23,45	71,70	2,95	7,90
Soil 6	7,08	23,22	69,70	103,77	13,26
Soil 7	9,54	25,76	64,70	20,11	10,94
Sediment 1	3,64	7,16	89,20	11,01	2,41
Sediment 2	1,65	8,33	90,02	19,03	2,55
Sediment 3	5,52	15,48	79,00	40,39	4,56
Sediment 3'	14,80	61,50	23,70	48,43	9,36
Sediment 4	3,61	10,89	85,50	3,57	1,88
Sediment 5	1,22	3,43	95,35	21,68	1,89

NOVEMBER	% Clay	% Silt	% Sand	% Coarse elements	% Organic matter
	< 2µm	> 2µm and < 50µm	> 50µm and < 2000 µm	> 2 mm	on < 2 mm fraction
Soil 1	3,27	14,13	82,60	3,16	6,55
Soil 2	6,47	23,53	70,00	49,36	9,02
Soil 3	11,70	43,40	44,90	17,62	11,85
Soil 3'	4,17	14,63	81,20	23,63	10,69
Soil 4	3,90	19,10	77,00	0,74	11,16
Soil 5	4,63	22,37	73,00	1,95	10,46
Soil 6	4,42	10,68	84,90	47,26	16,61
Soil 7	8,15	21,15	70,70	20,78	9,71
Sediment 1	0,56	2,23	97,21	61,91	1,93
Sediment 2	1,44	4,32	94,24	30,95	1,95
Sediment 3	2,71	12,99	84,30	32,08	12,27
Sediment 3'	6,36	29,04	64,60	6,18	7,09
Sediment 4	3,09	6,59	90,32	45,70	1,49
Sediment 5	2,13	4,05	93,82	25,57	2,16

Appendix II: List (not limited) of threatened species observed in the study area

	Latin name	French name	English name	Observed at	Threat	Reference
Mammalians	Lepus europaeus	Lièvre d'Europe	European hare	WST, C	in decline	INPN[a,b], ODONAT[i]
	Myotis myotis	Grand Murin	greater mouse-eared bat	C	in decline	ODONAT[a,i]
Birds	Motacilla alba	Bergeronnette grise	white wagtail	C, T, VT	least concern	ODONAT[b,c,d,j]
	Motacilla flava	Bergeronnette printanière	western yellow wagtail	C	endangered	ODONAT[b,j]
	Emberiza cirlus	Bruant zizi	cirl bunting	VT	vulnerable	ODONAT[c,j]
	Actitis hypoleucos	Chevalier guignette	common sandpiper	C	endangered	ODONAT[b,j]
	Galerida cristata	Cochevis huppé	crested lark	C	vulnerable	ODONAT[b,j]
	Aythya ferina	Fuligule milouin	common pochard	C	vulnerable	ODONAT[b,j]
	Aythya fuligula	Fuligule morillon	tufted duck	C	rare	ODONAT[b,j]
	Larus michahellis	Goéland leucophée	yellow-legged gull	C	vulnerable	ODONAT[b,j]
	Corvus corax	Grand corbeau	common raven	C, T	vulnerable	ODONAT[b,c,j]
	Tachybaptus ruficollis	Grèbe castagneux	little grebe	C	in decline	ODONAT[b,j]
	Hippolais polyglotta	Hypolaïs polyglotte	melodious warbler	C	vulnerable	INPN[b], ODONAT[j]
	Larus melanocephalus	Mouette mélanocéphale	Mediterranean gull	C	vulnerable	ODONAT[b,j]
	Chroicocephalus ridibundus	Mouette rieuse	black-headed gull	C	localized	ODONAT[b,j]
	Anas crecca	Sarcelle d'hiver	Eurasian teal	C	Endangered	ODONAT[b,j]
	Sterna hirundo	Sterne pierregarin	common tern	C	vulnerable	ODONAT[b,j]
	Oenanthe oenanthe	Traquet motteux	northern wheatear	C	vulnerable	ODONAT[b,j]
	Vanellus vanellus	Vanneau huppé	northern lapwing	C	in decline	ODONAT[b,j]
Reptiles	Natrix natrix	Couleuvre à collier	gras snake	T,C	in decline	ODONAT[e,f,k]
	Coronella austriaca	Corneille lisse	smooth snake	T	rare	ODONAT[e,k]
Butterflies	Cupido argiades	Azuré du Trèfle	short-tailed blue	T, C	vulnerable	ODONAT[g,h,l]
	Lasiommata maera	Némusien	large wall brown	T	in decline	ODONAT[g,h,l]
	Plebejus argus	Petit Argus	silver-studded blue	C	in decline	ODONAT[h,l]
	Brenthis daphne	Nacré de la Ronce	marbled fritillary	C	in decline	ODONAT[h,l]
	Brintesia circe	Silène	great banded grayling	C	vulnerable	ODONAT[h,l]

	Latin name	French name	English name	Observed at	Threat	Reference
Batracians	Triturus cristatus	Triton crêté	northern crested newt	C	rare	INPN[c], ODONAT[m]
	Alytes obstetricans	Alyte accoucheur	common midwife toad	T	endanger	INPN[c], ODONAT[m]
Fishes	Gasterosteus aculeatus	Epinoche	three-spined stickleback	VT, WST	vulnerable	INPN[a,d], ODONAT[n]
	Thymallus thymallus	Ombre commun	grayling	upstream and downstream of T	vulnerable	Gerber (2012), ODONAT[n]
	Lampetra planeri	Lamproie de Planer	brook lamprey	upstream and downstream of T	rare	Gerber (2012), ODONAT[n]
	Salmo salar	Saumon Atlantique	Atlantic salmon	upstream and downstream of T	endangered	Gerber (2012), ODONAT[n]
	Esox lucius	Brochet	northern pike	T and/or upstream	in decline	Gerber (2012), ODONAT[n]
Crayfishes	Austropotamobius pallipes	Ecrevisse à pieds blancs	White-clawed crayfish	Thann and/or upstream	Critically endangered	ODONAT[n]

INPN[a]: Inventaire National du Patrimoine Naturel (2013a); INPN[b]: Inventaire National du Patrimoine Naturel (2013b); INPN[c]: Inventaire National du Patrimoine Naturel (2013c); INPN[d]: Inventaire National du Patrimoine Naturel (2013d). ODONAT[a]: Office des données naturalistes d'Alsace - ODONAT (2013a); ODONAT[b]: Office des données naturalistes d'Alsace - ODONAT (2013b); ODONAT[c]: Office des données naturalistes d'Alsace - ODONAT (2012a); ODONAT[d]: Office des données naturalistes d'Alsace - ODONAT (2013c); ODONAT[e]: Office des données naturalistes d'Alsace - ODONAT (2012b); ODONAT[f]: Office des données naturalistes d'Alsace - ODONAT (2012c); ODONAT[g]: Office des données naturalistes d'Alsace - ODONAT (2012d); ODONAT[h]: (Office des données naturalistes d'Alsace (ODONAT) 2013d); ODONAT[i]: Office des données naturalistes d'Alsace - ODONAT (2014a); ODONAT[j]: Office des données naturalistes d'Alsace - ODONAT (2003a) ; ODONAT[k]: Office des données naturalistes d'Alsace - ODONAT (2003b); ODONAT[l]: Office des données naturalistes d'Alsace - ODONAT (2014b); ODONAT[m]: Office des données naturalistes d'Alsace - ODONAT (2014c); ODONAT[n]: Office des données naturalistes d'Alsace - ODONAT (2014d).

References:

Inventaire National du Patrimoine Naturel (2013a) Liste des espèces recensées dans Commune : Willer-sur-Thur.

Inventaire National du Patrimoine Naturel (2013b) Liste des espèces recensées dans Commune : Cernay.

Inventaire National du Patrimoine Naturel (2013c) Liste des espèces recensées dans Commune : Thann.

Inventaire National du Patrimoine Naturel (2013d) Liste des espèces recensées dans Commune : Vieux-Thann.

Office des données naturalistes d’Alsace (ODONAT) (2013a) Liste des mammifères observés à Cernay.

Office des données naturalistes d’Alsace (ODONAT) (2013b) Liste des oiseaux observés à Cernay.

Office des données naturalistes d’Alsace (ODONAT) (2012a) Liste des oiseaux observés à Thann.

Office des données naturalistes d’Alsace (ODONAT) (2013c) Liste des oiseaux observés à Vieux-Thann.

Office des données naturalistes d’Alsace (ODONAT) (2012b) Liste des reptiles observés à Thann.

Office des données naturalistes d’Alsace (ODONAT) (2012c) Liste des reptiles observés à Cernay.

Office des données naturalistes d’Alsace (ODONAT) (2012d) Liste des papillons observés à Thann.

Office des données naturalistes d’Alsace (ODONAT) (2013d) Liste des papillons observés à Cernay.

Office des données naturalistes d’Alsace (ODONAT) (2014a) Liste rouge des mammifères d’Alsace.

Office des données naturalistes d’Alsace (ODONAT) (2003a) Liste rouge des oiseaux d’Alsace.

Office des données naturalistes d’Alsace (ODONAT) (2003b) Liste rouge des reptiles d’Alsace.

Office des données naturalistes d’Alsace (ODONAT) (2014b) Liste rouge des papillons d’Alsace.

Office des données naturalistes d’Alsace (ODONAT) (2014c) Liste rouge des Amphibiens menacés en Alsace.

Office des données naturalistes d’Alsace (ODONAT) (2014d) Liste rouge des Poissons menacés en Alsace.

Appendix III: XRD spectra of LSS (A) and HSS (A) nanoparticulate TiO_2 produced by CRISTAL (analyzes performed by CEREGE, Aix-en-Provence, France).

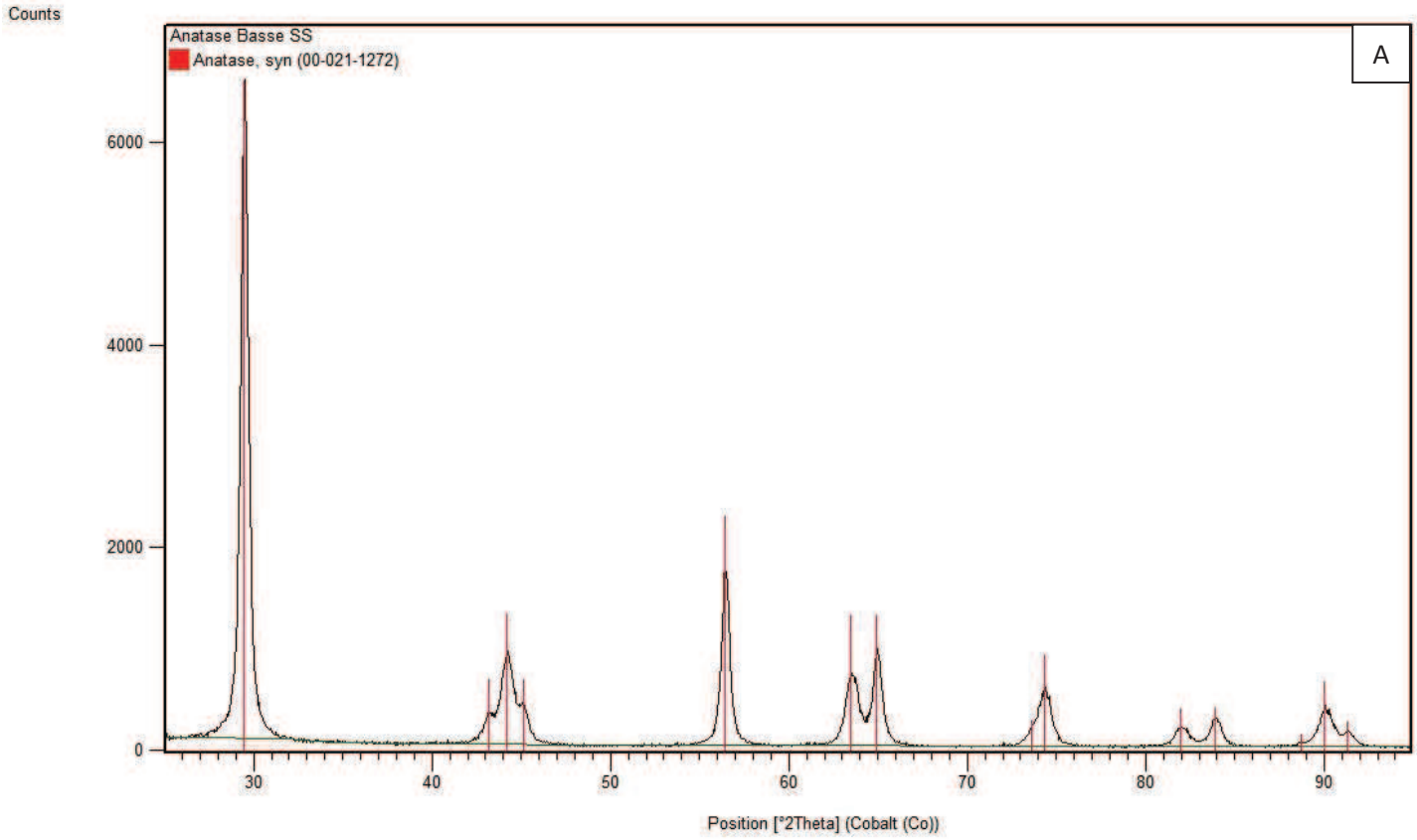

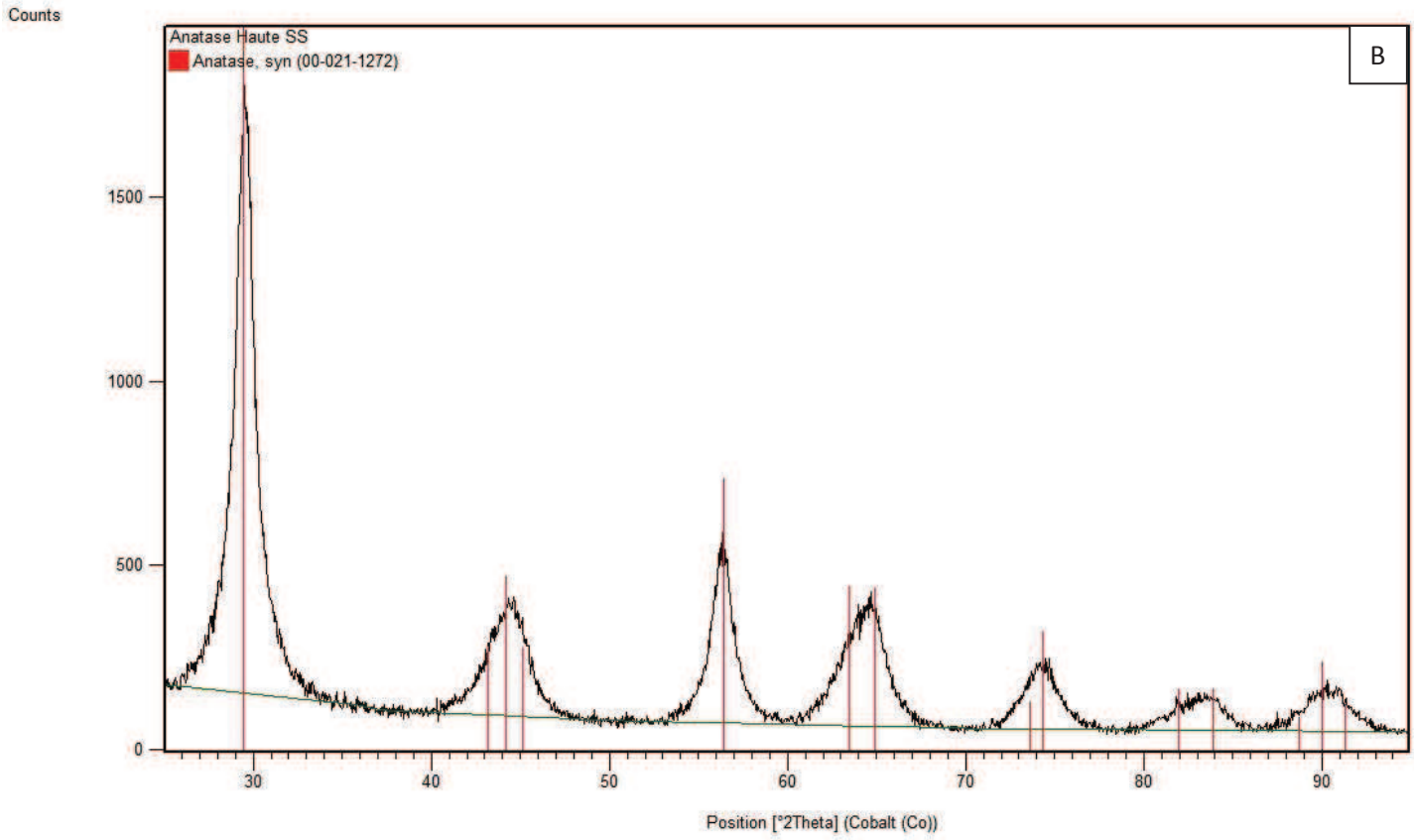

Appendix IVA: Dissolved concentrations (mg.L^{-1}) of Mg, Ca, Na and K in waters (DL = detection limit, strong orange boxes are under DL, light orange boxes are under the quantification level)

January					March					May				
Sample	Mg	Ca	Na	K	Sample	Mg	Ca	Na	K	Sample	Mg	Ca	Na	K
DL	*0,005*	*0,100*	*0,010*	*0,010*	*DL*	*0,040*	*0,010*	*0,020*	*0,030*	*DL*	*0,050*	*2,000*	*0,800*	*0,200*
1	2,249	10,000	11,360	1,400	**1**	1,330	6,900	4,650	0,520	**1**	1,950	9,000	8,700	1,200
2	1,742	8,400	9,020	1,150	**2**	1,360	7,400	4,670	0,520	**2**	2,000	10,000	9,000	1,200
3	1,725	8,300	8,640	1,110	**3**	1,360	7,450	4,540	0,510	**3**	1,980	9,000	8,600	1,300
3'	n.a.	n.a.	n.a.	n.a.	**3'**	1,965	8,897	8,779	1,620	**3'**	1,980	9,000	8,300	1,200
4	2,423	11,800	99,960	48,150	**4**	1,920	10,450	33,690	15,740	**4**	2,550	12,000	110,100	92,700
5	5,371	69,400	31,110	17,080	**5**	3,080	31,650	15,350	3,810	**5**	4,060	29,000	37,200	21,700
T	1,896	8,938	8,700	1,428	**T**	1,480	8,860	6,580	0,870	**T**	2,090	10,000	14,300	1,800
G	n.a.	n.a.	n.a.	n.a.	**G**	2,450	11,700	148,000	115,0	**G**	2,740	13,000	153 ,000	137,000
NN	45,600	899,000	190,000	23,320	**NN**	43,350	755,000	230,000	22,260	**NN**	18,760	1595,000	316,200	16,200
NNR	70,000	583,800	237,000	34,210	**NNR**	64,290	612,000	287,000	33,460	**NNR**	72,980	606,000	357,000	37,400

August					November				
Sample	Mg	Ca	Na	K	Sample	Mg	Ca	Na	K
DL	*0,050*	*2,000*	*0,800*	*0,200*	*DL*	*0,004*	*0,004*	*0,020*	*0,030*
1	1,680	8,000	6,000	0,800	**1**	1,247	5,873	4,110	0,740
2	1,600	8,000	5,700	0,800	**2**	0,474	2,197	1,460	0,310
3	1,560	8,000	5,700	0,800	**3**	0,886	-	0,030	0,580
3'	1,560	8,000	5,600	0,800	**3'**	0,904	4,324	0,030	0,550
4	1,810	9,000	11,000	13,400	**4**	1,084	-	0,030	-
5	3,000	62,000	26,200	16,400	**5**	0,828	4,363	29,950	34,940
T	1,740	10,000	8,500	1,200	**T**	1,557	10,500	6,540	1,300
NN	12,090	772,000	245,600	34,500	**NN**	23,900	686,000	190,000	14,520
NNR	61,780	519,000	322,100	31,700	**NNR**	56,000	500,000	234,000	26,090

Mean					Standard deviation/2				
Sample	Mg	Ca	Na	K	Sample	Mg	Ca	Na	K
1	1,691	7,955	6,964	0,932	**1**	0,196	0,665	1,488	0,198
2	1,435	7,199	5,970	0,796	**2**	0,134	0,556	1,124	0,160
3	1,502	8,188	5,502	0,860	**3**	0,131	0,323	1,038	0,174
3'	1,602	7,555	5,677	1,043	**3'**	0,119	0,275	0,857	0,205
4	1,957	10,813	50,956	42,498	**4**	0,183	0,695	24,402	18,518
5	3,268	39,283	27,962	18,786	**5**	0,553	10,337	4,623	3,831
T	1,753	9,660	8,924	1,320	**T**	0,129	0,318	1,663	0,196
NN	28,740	941,400	234,360	22,160	**NN**	8,508	199,191	26,330	3,814
NNR	65,010	564,160	287,420	32,572	**NNR**	2,567	21,282	25,614	1,192

Appendix IVB: Total concentrations (mg.L^{-1}) of Mg, Ca, Na and K in water (DL = detection limit, strong orange boxes are under DL, light orange boxes are under the quantification level)

January					March					May				
Sample	Mg	Ca	Na	K	Sample	Mg	Ca	Na	K	Sample	Mg	Ca	Na	K
DL	*0,005*	*0,100*	*0,010*	*0,010*	*DL*	*0,001*	*0,003*	*0,007*	*0,010*	*DL*	*0,050*	*2,000*	*0,800*	*0,200*
1	1,643	7,017	8,732	0,976	**1**	1,340	5,653	4,363	0,665	**1**	1,964	7,753	6,624	1,174
2	1,475	7,171	7,684	0,936	**2**	1,338	5,868	4,414	0,680	**2**	2,050	8,876	7,187	1,282
3	1,635	7,452	8,291	1,005	**3**	1,376	6,051	4,437	0,710	**3**	1,989	8,106	6,923	1,299
3'	n.a.	n.a.	n.a.	n.a.	**3'**	0,985	9,253	-	1,124	**3'**	1,921	7,842	6,909	1,263
4	1,817	8,694	> 1200	37,609	**4**	1,778	7,768	0,000	9,474	**4**	2,165	9,469	> 1200	59,082
5	5,130	47,759	29,116	15,046	**5**	-	21,272	-	2,210	**5**	4,014	25,895	30,322	22,766
T	1,758	7,409	5,848	0,999	**T**	1,556	7,506	6,683	1,325	**T**	2,098	9,462	11,384	1,801
G	-	-	-	-	**G**	1,830	7,460	0,000	45,49	**G**	1,848	7,968	> 1200	> 3500
NN	42,489	870,166	218,452	22,992	**NN**	45,959	706,905	305,020	31,419	**NN**	17,727	> 1700	287,185	20,628
NNR	79,072	614,022	321,147	40,543	**NNR**	64,431	500,576	261,687	34,664	**NNR**	69,299	> 1700	> 1200	41,184

August					November				
Sample	Mg	Ca	Na	K	Sample	Mg	Ca	Na	K
DL	*0,050*	*2,000*	*0,800*	*0,200*	*DL*	*0,002*	*0,010*	*0,020*	*0,100*
1	1,823	7,450	5,781	1,271	**1**	1,489	6,391	5,367	0,937
2	2,047	9,342	6,704	1,357	**2**	1,592	7,478	6,312	1,124
3	1,892	7,950	5,799	1,150	**3**	1,564	7,077	5,912	1,071
3'	1,449	6,035	4,448	0,895	**3'**	1,599	7,453	6,184	1,078
4	2,364	10,728	16,748	71,020	**4**	1,020	4,477	76,319	56,801
5	3,328	> 1700	27,151	21,403	**5**	2,026	10,074	12,155	17,739
T	2,243	11,074	11,063	2,189	**T**	1,730	8,914	8,489	1,670
NN	12,579	> 1700	> 1200	42,007	**NN**	26,303	933,882	284,750	18,967
NNR	64,697	> 1700	> 1200	38,574	**NNR**	60,471	656,662	365,736	32,542

Mean					Standard deviation/2				
Sample	Mg	Ca	Na	K	Sample	Mg	Ca	Na	K
1	1,652	6,853	6,174	1,005	**1**	0,125	0,422	0,823	0,117
2	1,700	7,747	6,460	1,076	**2**	0,165	0,696	0,627	0,137
3	1,691	7,327	6,273	1,047	**3**	0,124	0,411	0,717	0,109
3'	1,488	7,646	5,847	1,090	**3'**	0,195	0,662	0,632	0,076
4	1,829	8,227	31,022	46,797	**4**	0,257	1,180	20,056	12,029
5	3,624	26,250	24,686	15,833	**5**	0,649	7,902	4,228	4,100
T	1,877	8,873	8,693	1,597	**T**	0,142	0,759	1,251	0,228
NN	29,011	836,984	273,852	27,203	**NN**	7,389	58,535	19,011	4,781
NNR	67,594	590,420	316,190	37,501	**NNR**	3,569	40,338	26,101	1,881

Appendix IVC: Total concentrations (µg.L^{-1}) of Ti and associated metals (DL = detection limit, strong orange boxes are under DL, light orange boxes are under the quantification level)

January					March					May				
Sample	Ti (ppb)	V (ppb)	Co (ppb)	Zn (ppb)	Sample	Ti (ppb)	V (ppb)	Co (ppb)	Zn (ppb)	Sample	Ti (ppb)	V (ppb)	Co (ppb)	Zn (ppb)
DL	*3,00*	*3,00*	*2,00*	*2,00*	*DL*	*1,00*	*4,00*	*2,00*	*2,00*	*DL*	*3,00*	*3,00*	*1,00*	*1,00*
1	7,38	0,43	0,06	3,93	**1**	4,05	0,37	0,06	1,80	**1**	4,28	0,42	0,07	2,37
2	5,59	0,39	0,05	3,29	**2**	3,73	0,36	0,05	1,67	**2**	4,19	0,49	0,06	2,65
3	5,31	0,39	0,05	3,30	**3**	4,39	0,38	0,05	1,72	**3**	6,49	0,46	0,07	2,59
3'	n.a.	n.a.	n.a.	n.a.	**3'**	2,29	2,12	0,00	3,15	**3'**	3,75	0,46	0,06	2,47
4	37,84	0,57	0,19	11,30	**4**	31,30	0,49	0,16	9,89	**4**	18,31	0,55	0,12	5,12
5	7,61	0,53	0,07	5,27	**5**	2,05	0,00	0,49	2,36	**5**	18,54	0,67	0,20	4,21
T	29,56	1,00	0,46	16,61	**T**	552,65	1,88	1,27	37,49	**T**	361,39	1,85	0,82	20,79
NN	0,00	0,00	0,00	25,12	**NN**	32,98	4,12	0,00	0,00	**NN**	18,08	3,70	0,00	0,82
NNR	0,88	0,00	3,09	28,71	**NNR**	36,68	0,00	2,97	23,79	**NNR**	0,00	0,00	2,33	24,88

August					November				
Sample	Ti (ppb)	V (ppb)	Co (ppb)	Zn (ppb)	Sample	Ti (ppb)	V (ppb)	Co (ppb)	Zn (ppb)
DL	*3,00*	*3,00*	*1,00*	*1,00*	*DL*	*40,00*	*1,00*	*1,00*	*1,00*
1	15,14	0,65	0,11	3,21	**1**	10,13	0,40	0,07	2,22
2	11,22	0,85	0,12	3,97	**2**	11,22	0,48	0,09	2,44
3	9,52	0,79	0,13	3,45	**3**	12,31	0,43	0,08	2,28
3'	9,22	0,70	0,11	2,87	**3'**	12,92	0,46	0,09	2,28
4	44,77	0,96	0,21	16,57	**4**	25,57	0,40	0,07	8,42
5	11,09	0,94	0,12	5,54	**5**	10,07	0,66	0,08	3,23
T	746,87	3,61	1,75	49,93	**T**	494,22	1,96	1,36	66,57
NN	24,77	4,18	0,00	0,67	**NN**	72,39	5,79	0,00	1,21
NNR	0,00	0,00	1,40	21,62	**NNR**	45,72	0,62	1,04	11,64

Mean						Standard deviation/2					
Sample	Ti (ppb)	TiO2 (ppb)	V (ppb)	Co (ppb)	Zn (ppb)	Sample	Ti (ppb)	TiO2 (ppb)	V (ppb)	Co (ppb)	Zn (ppb)
1	8,20	13,68	0,45	0,07	2,71	**1**	2,31	3,85	0,06	0,01	0,43
2	7,19	12,00	0,52	0,07	2,80	**2**	1,87	3,12	0,10	0,01	0,43
3	7,60	12,69	0,49	0,07	2,67	**3**	1,63	2,73	0,09	0,02	0,36
3'	7,04	11,75	0,94	0,07	2,69	**3'**	2,46	4,11	0,40	0,02	0,20
4	31,56	52,66	0,59	0,15	10,26	**4**	5,16	8,60	0,11	0,03	2,10
5	9,87	16,47	0,56	0,19	4,12	**5**	2,99	4,99	0,17	0,09	0,67
T	436,94	729,08	2,06	1,13	38,28	**T**	133,32	222,46	0,47	0,25	10,34
NN	29,64	49,46	3,56	0,00	5,56	**NN**	13,40	22,37	1,07	0,00	5,47
NNR	16,66	27,79	0,12	2,17	22,13	**NNR**	11,32	18,88	0,14	0,46	3,20

Appendix IVD: Dissolved concentrations (µg.L^{-1}) of Ti and associated metals (DL = detection limit, strong orange boxes are under DL, light orange boxes are under the quantification level)

January					March					May				
Sample	Ti (ppb)	V (ppb)	Co (ppb)	Zn (ppb)	Sample	Ti (ppb)	V (ppb)	Co (ppb)	Zn (ppb)	Sample	Ti (ppb)	V (ppb)	Co (ppb)	Zn (ppb)
DL	*3,00*	*0,80*	*1,00*	*0,60*	*DL*	*2,00*	*0,60*	*0,09*	*0,07*	*DL*	*3,00*	*3,00*	*1,00*	*1,00*
1	4,00	0,00	0,00	6,00	**1**	0,00	0,00	0,00	0,00	**1**	0,00	0,00	0,00	0,00
2	0,00	0,00	0,00	4,00	**2**	0,00	0,00	0,00	0,00	**2**	0,00	0,00	0,00	0,00
3	0,00	0,00	0,00	3,00	**3**	0,00	0,00	0,00	0,00	**3**	0,00	0,00	0,00	0,00
3'	**na**	na	**na**	**na**	**3'**	1,00	0,00	0,00	3,00	**3'**	0,00	0,00	0,00	0,00
4	0,00	0,00	0,00	10,00	**4**	0,00	0,00	0,00	0,00	**4**	0,00	0,00	0,00	4,00
5	0,00	0,00	0,00	5,00	**5**	0,00	0,00	0,00	0,00	**5**	0,00	0,00	0,00	0,00
T	11,00	0,80	0	11,50	**T**	0,00	0,00	0,00	0,00	**T**	0,00	0,00	0,00	10,00
NN	0,00	0,00	0,00	0,00	**NN**	0,00	0,00	0,00	0,00	**NN**	0,00	0,00	0,00	0,00
NNR	0,00	0,00	3,00	16,00	**NNR**	0,00	0,00	0,00	0,00	**NNR**	0,00	0,00	0,00	15,00

August					November				
Sample	Ti (ppb)	V (ppb)	Co (ppb)	Zn (ppb)	Sample	Ti (ppb)	V (ppb)	Co (ppb)	Zn (ppb)
DL	*3,00*	*3,00*	*1,00*	*1,00*	*DL*	*3,00*	*5,00*	*2,00*	*2,00*
1	0,00	0,00	0,00	23,00	**1**	0,00	0,00	0,00	2,00
2	0,00	0,00	0,00	0,00	**2**	0,00	0,00	0,00	3,00
3	0,00	0,00	0,00	0,00	**3**	12,00	8,00	0,00	3,00
3'	0,00	0,00	0,00	0,00	**3'**	12,00	0,00	0,00	0,00
4	0,00	0,00	0,00	6,00	**4**	8,00	0,00	0,00	7,00
5	0,00	0,00	0,00	1,00	**5**	5,00	0,00	0,00	2,00
T	0,00	0,00	0,00	14,00	**T**	0,00	0,00	0,00	25,00
NN	0,00	0,00	0,00	1,00	**NN**	0,00	0,00	0,00	8,00
NNR	0,00	0,00	0,00	9,00	**NNR**	0,00	0,00	0,00	9,00

Mean						Standard deviation/2					
Sample	Ti (ppb)	TiO2 (ppb)	V (ppb)	Co (ppb)	Zn (ppb)	Sample	Ti (ppb)	TiO2 (ppb)	V (ppb)	Co (ppb)	Zn (ppb)
1	0,80	1,33	0,00	0,00	6,20	**1**	0,89	1,49	0,00	0,00	4,85
2	0,00	0,00	0,00	0,00	1,40	**2**	0,00	0,00	0,00	0,00	0,97
3	2,40	4,00	1,60	0,00	1,20	**3**	2,68	4,48	1,79	0,00	0,82
3'	3,25	5,42	0,00	0,00	0,75	**3'**	2,93	4,88	0,00	0,00	0,75
4	1,60	2,67	0,00	0,00	5,40	**4**	1,79	2,98	0,00	0,00	1,86
5	1,00	1,67	0,00	0,00	1,60	**5**	1,12	1,87	0,00	0,00	1,04
T	2,20	3,67	0,16	0,00	12,10	**T**	2,46	4,10	0,18	0,00	4,48
NN	0,00	0,00	0,00	0,00	1,80	**NN**	0,00	0,00	0,00	0,00	1,75
NNR	0,00	0,00	0,00	0,60	9,80	**NNR**	0,00	0,00	0,00	0,67	3,19

Appendix IVE: Particulate concentrations (µg.L^{-1}) of Ti and associated metals

January						March						May					
Sample	Ti (ppb)	TiO_2 (ppb)	V (ppb)	Co (ppb)	Zn (ppb)	Sample	Ti (ppb)	TiO_2 (ppb)	V (ppb)	Co (ppb)	Zn (ppb)	Sample	Ti (ppb)	TiO_2 (ppb)	V (ppb)	Co (ppb)	Zn (ppb)
1	3,38	5,64	0,43	0,06	0,00	**1**	4,05	6,76	0,37	0,06	1,80	**1**	4,28	7,15	0,42	0,07	2,37
2	5,59	9,33	0,39	0,05	0,00	**2**	3,73	6,22	0,36	0,05	1,67	**2**	4,19	7,00	0,49	0,06	2,65
3	5,31	8,86	0,39	0,05	0,30	**3**	4,39	7,32	0,38	0,05	1,72	**3**	6,49	10,83	0,46	0,07	2,59
3'	na	na	na	na	na	**3'**	1,29	2,15	2,12	0,00	0,15	**3'**	3,75	6,25	0,46	0,06	2,47
4	37,84	63,14	0,57	0,19	1,30	**4**	31,30	52,22	0,49	0,16	9,89	**4**	18,31	30,55	0,55	0,12	1,12
5	7,61	12,69	0,53	0,07	0,27	**5**	2,05	3,42	0,00	0,49	2,36	**5**	18,54	30,93	0,67	0,20	4,21
T	18,56	30,96	0,20	0,46	5,11	**T**	552,65	922,16	1,88	1,27	37,49	**T**	361,39	603,02	1,85	0,82	10,79
NN	0,00	0,00	0,00	0,00	25,12	**NN**	32,98	55,02	4,12	0,00	0,00	**NN**	18,08	30,17	3,70	0,00	0,82
NNR	0,88	1,47	0,00	0,09	12,71	**NNR**	36,68	61,20	0,00	2,97	23,79	**NNR**	0,00	0,00	0,00	2,33	9,88

August						November					
Sample	Ti (ppb)	TiO_2 (ppb)	V (ppb)	Co (ppb)	Zn (ppb)	Sample	Ti (ppb)	TiO_2 (ppb)	V (ppb)	Co (ppb)	Zn (ppb)
1	15,14	25,26	0,65	0,11	0,00	**1**	10,13	16,91	0,40	0,07	0,22
2	11,22	18,72	0,85	0,12	3,97	**2**	11,22	18,72	0,48	0,09	0,00
3	9,52	15,89	0,79	0,13	3,45	**3**	0,31	0,52	0,00	0,08	0,00
3'	9,22	15,39	0,70	0,11	2,87	**3'**	0,92	1,54	0,46	0,09	2,28
4	44,77	74,70	0,96	0,21	10,57	**4**	17,57	29,32	0,40	0,07	1,42
5	11,09	18,50	0,94	0,12	4,54	**5**	5,07	8,47	0,66	0,08	1,23
T	746,87	1246,24	3,61	1,75	35,93	**T**	494,22	824,67	1,96	1,36	41,57
NN	24,77	41,33	4,18	0,00	0,00	**NN**	72,39	120,80	5,79	0,00	0,00
NNR	0,00	0,00	0,00	1,40	12,62	**NNR**	45,72	76,28	0,62	1,04	2,64

Mean						Standard deviation/2					
Sample	Ti (ppb)	TiO_2 (ppb)	V (ppb)	Co (ppb)	Zn (ppb)	Sample	Ti (ppb)	TiO_2 (ppb)	V (ppb)	Co (ppb)	Zn (ppb)
1	7,40	12,34	0,45	0,07	0,88	**1**	2,56	4,26	0,06	0,01	0,56
2	7,19	12,00	0,52	0,07	1,66	**2**	1,87	3,12	0,10	0,01	0,86
3	5,20	8,68	0,40	0,07	1,61	**3**	1,68	2,79	0,14	0,02	0,74
3'	3,79	6,33	0,94	0,07	1,94	**3'**	1,92	3,20	0,40	0,02	0,61
Upstream mean	5,90	9,84	0,58	0,07	1,52	**Upstream mean**	2,00	3,34	0,17	0,02	0,69
4	29,96	49,99	0,59	0,15	4,86	**4**	5,98	9,98	0,11	0,03	2,45
5	8,87	14,80	0,56	0,19	2,52	**5**	3,17	5,29	0,17	0,09	0,93
T	434,74	725,41	1,90	1,13	26,18	**T**	135,43	225,98	0,60	0,25	8,44
NN	29,64	49,46	3,56	0,00	5,19	**NN**	13,40	22,37	1,07	0,00	5,57
NNR	16,66	27,79	0,12	1,57	12,33	**NNR**	11,32	18,88	0,14	0,56	3,80

Appendix IVF: Dissolved concentrations (µg.L^{-1}) of other metals (DL = detection limit, strong orange boxes are under DL, light orange boxes are under the quantification level)

January							March							May						
Sample	Al	Fe	Mn	Ni	Cr	Cu	Sample	Al	Fe	Mn	Ni	Cr	Cu	Sample	Al	Fe	Mn	Ni	Cr	Cu
DL	*3,00*	*2,00*	*4,00*	*2,00*	*0,90*	*0,80*	*DL*	*1,00*	*1,00*	*10,00*	*2,00*	*0,90*	*2,00*	*DL*	*2,00*	*3,00*	*2,00*	*2,00*	*3,00*	*3,00*
1	58,00	165,00	5,00	0,00	0,00	0,00	**1**	0,00	0,00	0,00	0,00	0,00	0,00	**1**	0,00	7,00	0,00	0,00	0,00	0,00
2	52,00	36,00	0,00	0,00	0,00	0,00	**2**	0,00	0,00	0,00	0,00	0,00	0,00	**2**	0,00	9,00	0,00	0,00	0,00	0,00
3	54,00	25,00	0,00	0,00	0,00	0,00	**3**	0,00	0,00	0,00	0,00	0,00	0,00	**3**	0,00	12,00	0,00	0,00	0,00	0,00
3'	n.a.	n.a.	n.a.	n.a.	n.a.	n.a.	**3'**	8,10	15,00	0,00	0,00	0,00	0,00	**3'**	0,00	9,00	0,00	0,00	0,00	0,00
4	72,00	59,00	24,00	0,00	0,00	0,00	**4**	0,00	8,00	0,00	0,00	0,00	0,00	**4**	0,00	13,00	18,00	0,00	0,00	0,00
5	63,00	13,00	170,00	0,00	0,00	0,00	**5**	7,00	0,00	80,00	0,00	0,00	0,00	**5**	22,00	6,00	193,00	0,00	0,00	0,00
T	73,00	44,00	12,00	0,00	2,50	8,00	**T**	16,00	52,00	0,00	0,00	0,00	0,00	**T**	16,00	38,00	3,00	0,00	0,00	7,00
NN	132,00	4,00	86,00	0,00	6,00	0,00	**NN**	18,00	0,00	70,00	0,00	0,00	0,00	**NN**	38,00	4,00	95,00	0,00	0,00	0,00
NNR	271,00	6,00	8138,00	24,00	7,00	0,00	**NNR**	218,00	0,00	6110,00	0,00	0,00	0,00	**NNR**	307,00	0,00	7061,00	21,00	0,00	0,00

August							November						
Sample	Al	Fe	Mn	Ni	Cr	Cu	Sample	Al	Fe	Mn	Ni	Cr	Cu
DL	*2,00*	*3,00*	*3,00*	*2,00*	*3,00*	*3,00*	*DL*	*2,00*	*4,00*	*4,00*	*2,00*	*4,00*	*4,00*
1	4,00	14,00	14,00	0,00	0,00	0,00	**1**	11,00	27,00	0,00	0,00	0,00	0,00
2	4,00	17,00	0,00	0,00	0,00	0,00	**2**	12,00	9,00	0,00	3,00	0,00	0,00
3	2,00	17,00	5,00	0,00	0,00	0,00	**3**	12,00	27,00	9,00	2,00	9,00	9,00
3'	3,00	16,00	5,00	0,00	0,00	0,00	**3'**	12,00	24,00	6,00	2,00	6,00	5,00
4	7,00	18,00	8,00	0,00	0,00	0,00	**4**	15,00	29,00	9,00	2,00	0,00	4,00
5	13,00	11,00	92,00	0,00	0,00	0,00	**5**	25,00	25,00	7,00	0,00	0,00	0,00
T	37,00	41,00	9,00	0,00	0,00	6,00	**T**	14,00	68,00	44,00	3,00	0,00	0,00
NN	101,00	10,00	30,00	0,00	3,00	0,00	**NN**	19,00	38,00	140,00	2,00	0,00	0,00
NNR	174,00	0,00	6383,00	17,00	0,00	0,00	**NNR**	49,00	6,00	8588,00	18,00	0,00	0,00

Mean							Standard deviation/2						
Sample	Al	Fe	Mn	Ni	Cr	Cu	Sample	Al	Fe	Mn	Ni	Cr	Cu
1	14,60	42,60	3,80	0,00	0,00	0,00	**1**	12,34	34,57	3,05	0,00	0,00	0,00
2	13,60	14,20	0,00	0,60	0,00	0,00	**2**	11,01	6,80	0,00	0,67	0,00	0,00
3	13,60	16,20	2,80	0,40	1,80	1,80	**3**	11,56	5,45	2,04	0,45	2,01	2,01
3'	5,78	16,00	2,75	0,50	1,50	1,25	**3'**	2,66	3,08	1,60	0,50	1,50	1,25
4	18,80	25,40	11,80	0,40	0,00	0,80	**4**	15,19	10,16	4,67	0,45	0,00	0,89
5	26,00	11,00	108,40	0,00	0,00	0,00	**5**	10,94	4,65	37,34	0,00	0,00	0,00
T	31,20	48,60	13,60	0,60	0,50	4,20	**T**	12,60	6,02	8,82	0,67	0,56	1,95
NN	61,60	11,20	84,20	0,40	1,80	0,00	**NN**	25,96	7,70	19,96	0,45	1,34	0,00
NNR	203,80	2,40	7256,00	16,00	1,40	0,00	**NNR**	50,14	1,64	540,00	4,68	1,57	0,00

Appendix IVG: Total concentrations (µg.L^{-1}) of other metals (DL = detection limit, strong orange boxes are under DL, light orange boxes are under the quantification level)

January							March							May						
Sample	Al	Fe	Mn	Ni	Cr	Cu	Sample	Al	Fe	Mn	Ni	Cr	Cu	Sample	Al	Fe	Mn	Ni	Cr	Cu
DL	*1,00*	*3,00*	*3,00*	*3,00*	*4,00*	*7,00*	*DL*	*0,80*	*4,00*	*4,00*	*3,00*	*3,00*	*4,00*	*DL*	*2,00*	*3,00*	*3,00*	*2,00*	*3,00*	*3,00*
1	127,11	106,44	5,41	0,38	0,58	1,25	**1,00**	110,85	76,72	0,00	0,32	0,48	0,74	**1**	91,16	80,34	6,20	0,31	0,56	1,01
2	109,62	85,65	4,53	0,34	0,52	1,20	**2,00**	110,34	73,75	0,00	0,29	0,47	0,80	**2**	100,90	85,69	7,00	0,34	0,64	1,24
3	105,89	87,90	4,48	0,33	0,52	1,30	**3,00**	114,81	77,74	0,00	0,31	0,48	0,82	**3**	85,55	80,30	6,91	0,31	0,57	1,24
3'	n.a.	n.a.	n.a.	n.a.	n.a.	n.a.	**3'**	61,72	53,47	5,55	0,28	0,51	1,68	**3'**	90,09	82,15	6,87	0,30	0,58	1,25
4	90,23	158,46	23,24	1,21	0,62	4,57	**4,00**	112,42	114,47	23,23	0,75	0,62	2,80	**4**	90,18	113,39	23,51	0,75	0,81	2,75
5	10,93	83,84	147,88	0,81	0,71	1,70	**5,00**	103,92	61,12	98,78	0,91	0,58	1,37	**5**	122,35	97,32	200,31	1,06	0,83	2,52
T	125,85	1054,94	15,55	1,36	1,74	12,69	**T**	368,43	564,41	25,34	1,37	1,94	10,05	**T**	166,75	355,56	18,46	0,91	1,55	14,46
NN	125,61	376,83	0,00	0,00	0,00	0,00	**NN**	64,82	478,14	120,57	0,00	0,00	0,00	**NN**	79,31	442,55	102,32	0,00	6,57	0,00
NNR	977,13	5,30	8437,28	27,83	2,34	2,69	**NNR**	837,60	4,96	5897,87	20,82	2,48	2,97	**NNR**	679,50	5,58	6464,81	20,70	2,79	2,09

August							November						
Sample	Al	Fe	Mn	Ni	Cr	Cu	Sample	Al	Fe	Mn	Ni	Cr	Cu
DL	*2,00*	*3,00*	*3,00*	*2,00*	*3,00*	*3,00*	*DL*	*2,00*	*3,00*	*0,10*	*1,00*	*1,00*	*3,00*
1	193,18	160,49	9,80	0,51	0,78	1,32	**1**	94,85	102,07	9,63	0,31	0,46	0,96
2	326,07	227,93	15,98	0,59	1,09	1,67	**2**	116,30	116,43	10,29	0,35	0,53	1,19
3	255,56	210,69	18,08	0,52	0,95	1,60	**3**	95,05	104,29	9,65	0,32	0,49	1,13
3'	237,94	191,40	15,15	0,45	0,84	1,28	**3'**	119,27	118,09	10,63	0,32	0,55	1,18
4	280,75	230,44	25,26	0,69	1,29	4,02	**4**	39,86	88,43	15,69	0,41	0,41	3,41
5	187,53	145,11	111,46	0,71	0,90	2,59	**5**	63,02	80,67	13,47	0,39	0,58	2,00
T	663,89	884,23	57,95	1,92	3,15	22,06	**T**	248,92	1750,95	64,89	1,98	1,55	12,53
NN	117,65	372,88	44,68	0,00	2,18	0,00	**NN**	43,20	646,24	157,84	0,48	2,17	0,00
NNR	476,25	3,84	6208,15	19,01	2,44	1,74	**NNR**	119,28	16,00	8914,81	16,42	1,04	0,83

Mean							Standard deviation/2						
Sample	Al	Fe	Mn	Ni	Cr	Cu	Sample	Al	Fe	Mn	Ni	Cr	Cu
1	123,43	105,21	6,21	0,37	0,57	1,05	**1**	20,76	16,77	2,00	0,04	0,06	0,12
2	152,65	117,89	7,56	0,38	0,65	1,22	**2**	48,55	31,76	3,01	0,06	0,13	0,15
3	131,37	112,18	7,83	0,36	0,60	1,22	**3**	35,15	28,02	3,37	0,04	0,10	0,14
3'	127,25	111,28	9,55	0,34	0,62	1,35	**3'**	38,72	29,80	2,15	0,04	0,07	0,11
4	122,69	141,04	22,19	0,76	0,75	3,51	**4**	46,14	27,99	1,86	0,14	0,17	0,39
5	97,55	93,61	114,38	0,78	0,72	2,04	**5**	33,02	15,78	34,41	0,13	0,07	0,26
T	314,77	922,02	36,44	1,51	1,99	14,36	**T**	108,02	268,68	11,61	0,22	0,33	2,29
NN	86,12	463,33	85,08	0,10	2,18	0,00	**NN**	17,49	55,77	31,35	0,11	1,34	0,00
NNR	617,95	7,14	7184,59	20,95	2,22	2,07	**NNR**	167,67	2,50	693,27	2,12	0,34	0,42

Appendix IVH: Particulate concentrations (µg.L^{-1}) of other metals

January							March							May						
Sample	Al	Fe	Mn	Ni	Cr	Cu	Sample	Al	Fe	Mn	Ni	Cr	Cu	Sample	Al	Fe	Mn	Ni	Cr	Cu
1	69,11	0,00	0,41	0,38	0,58	1,25	1	110,85	76,72	0,00	0,32	0,48	0,74	1	91,16	73,34	6,20	0,31	0,56	1,01
2	57,62	49,65	4,53	0,34	0,52	1,20	2	110,34	73,75	0,00	0,29	0,47	0,80	2	100,90	76,69	7,00	0,34	0,64	1,24
3	51,89	62,90	4,48	0,33	0,52	1,30	3	114,81	77,74	0,00	0,31	0,48	0,82	3	85,55	68,30	6,91	0,31	0,57	1,24
3'	n.a.	n.a.	n.a.	n.a.	n.a.	n.a.	3'	53,62	38,47	5,55	0,28	0,51	1,68	3'	90,09	73,15	6,87	0,30	0,58	1,25
4	18,23	99,46	0,00	1,21	0,62	4,57	4	112,42	106,47	23,23	0,75	0,62	2,80	4	90,18	100,39	5,51	0,75	0,81	2,75
5	0,00	70,84	0,00	0,81	0,71	1,70	5	96,92	61,12	18,78	0,91	0,58	1,37	5	100,35	91,32	7,31	1,06	0,83	2,52
T	52,85	1010,94	3,55	1,36	0,00	4,69	T	352,43	512,41	25,34	1,37	1,94	10,05	T	150,75	317,56	15,46	0,91	1,55	7,46
NN	0,00	372,83	0,00	0,00	0,00	0,00	NN	46,82	478,14	50,57	0,00	0,00	0,00	NN	41,31	438,55	7,32	0,00	6,57	0,00
NNR	706,13	0,00	299,28	3,83	0,00	2,69	NNR	619,60	4,96	0,00	20,82	2,48	2,97	NNR	372,50	5,58	0,00	0,00	2,79	2,09

August							November						
Sample	Al	Fe	Mn	Ni	Cr	Cu	Sample	Al	Fe	Mn	Ni	Cr	Cu
1	189,18	146,49	0,00	0,51	0,78	1,32	1	83,85	75,07	9,63	0,31	0,46	0,96
2	322,07	210,93	15,98	0,59	1,09	1,67	2	104,30	107,43	10,29	0,00	0,53	1,19
3	253,56	193,69	13,08	0,52	0,95	1,60	3	83,05	77,29	0,65	0,00	0,00	0,00
3'	234,94	175,40	10,15	0,45	0,84	1,28	3'	107,27	94,09	4,63	0,00	0,00	0,00
4	273,75	212,44	17,26	0,69	1,29	4,02	4	24,86	59,43	6,69	0,00	0,41	0,00
5	174,53	134,11	19,46	0,71	0,90	2,59	5	38,02	55,67	6,47	0,39	0,58	2,00
T	626,89	843,23	48,95	1,92	3,15	16,06	T	234,92	1682,95	20,89	0,00	1,55	12,53
NN	16,65	362,88	14,68	0,00	0,00	0,00	NN	24,20	608,24	17,84	0,00	2,17	0,00
NNR	302,25	3,84	0,00	2,01	2,44	1,74	NNR	70,28	10,00	326,81	0,00	1,04	0,83

Mean							Standard deviation/2						
Sample	Al	Fe	Mn	Ni	Cr	Cu	Sample	Al	Fe	Mn	Ni	Cr	Cu
1	108,83	74,32	3,25	0,37	0,57	1,05	1	23,68	25,91	2,22	0,04	0,06	0,12
2	139,05	103,69	7,56	0,31	0,65	1,22	2	52,21	31,68	3,01	0,10	0,13	0,15
3	117,77	95,98	5,03	0,29	0,50	0,99	3	39,55	27,49	2,66	0,09	0,17	0,31
3'	121,48	95,28	6,80	0,26	0,48	1,05	3'	39,44	29,07	1,21	0,09	0,18	0,36
4	103,89	115,64	10,54	0,68	0,75	2,83	4	51,66	28,62	4,73	0,22	0,17	0,88
5	81,96	82,61	10,40	0,78	0,72	2,04	5	33,34	15,92	4,22	0,13	0,07	0,26
T	283,57	873,42	22,84	1,11	1,64	10,16	T	110,64	263,92	8,36	0,36	0,56	2,20
NN	25,79	452,13	18,08	0,00	1,75	0,00	NN	9,47	49,68	9,71	0,00	1,43	0,00
NNR	414,15	4,87	125,22	5,33	1,75	2,07	NNR	127,47	1,80	85,87	4,40	0,59	0,42

Appendix V: Anions concentrations in water (mM)

January				March				May				August				November			
Sample	**Cl^-**	**NO_3^-**	**SO_4^{2-}**	**Sample**	**Cl^-**	**NO_3^-**	**SO_4^{2-}**	**Sample**	**Cl^-**	**NO_3^-**	**SO_4^{2-}**	**Sample**	**Cl^-**	**NO_3^-**	**SO_4^{2-}**	**Sample**	**Cl^-**	**NO_3^-**	**SO_4^{2-}**
1	0,49	0,07	0,06	**1**	0,18	0,04	0,05	**1**	0,261	0,046	0,067	**1**	0,168	0,042	0,053	**1**	0,169	0,040	0,047
2	0,42	0,08	0,07	**2**	0,21	0,04	0,05	**2**	0,265	0,047	0,071	**2**	0,170	0,042	0,057	**2**	0,181	0,043	0,053
3	0,35	0,06	0,05	**3**	0,17	0,04	0,06	**3**	0,266	0,046	0,071	**3**	0,169	0,041	0,058	**3**	0,186	0,039	0,054
3'	n.a.	n.a.	n.a.	**3'**	0,294	0,051	0,082	**3'**	0,298	0,042	0,068	**3'**	0,167	0,038	0,058	**3'**	0,173	0,039	0,052
4	5,66	0,70	0,05	**4**	1,85	0,04	0,03	**4**	5,240	0,062	1,020	**4**	0,733	0,049	0,110	**4**	8,505	0,047	0,759
5	4,72	1,17	0,07	**5**	1,81	0,05	0,05	**5**	2,044	0,062	0,636	**5**	3,384	0,053	0,812	**5**	0,961	0,045	0,133
T	0,30	0,06	0,11	**T**	0,26	0,05	0,11	**T**	0,387	0,051	0,120	**T**	0,286	0,061	0,127	**T**	33,640	0,625	12,840
NN	53,00	12,50	0,09	**NN**	32,60	0,06	14,90	**NN**	108,100	0,051	9,400	**NN**	50,060	0,053	11,120	**NN**	0,246	0,049	0,141
NNR	31,00	14,72	1,56	**NNR**	29,20	0,54	15,10	**NNR**	30,100	0,550	14,680	**NNR**	29,570	0,632	14,130	**NNR**	42,560	0,051	12,680

Mean				Standard deviation/2			
Sample	**Cl^-**	**NO_3^-**	**SO_4^{2-}**	**Sample**	**Cl^-**	**NO_3^-**	**SO_4^{2-}**
1	0,253	0,048	0,056	**1**	0,068	0,007	0,004
2	0,248	0,049	0,061	**2**	0,051	0,008	0,004
3	0,229	0,045	0,058	**3**	0,039	0,005	0,004
3'	0,233	0,042	0,065	**3'**	0,036	0,003	0,006
4	4,398	0,180	0,395	**4**	1,563	0,145	0,231
5	2,584	0,276	0,341	**5**	0,739	0,250	0,178
T	6,974	0,171	2,660	**T**	7,453	0,127	2,845
NN	48,801	2,543	7,130	**NN**	19,615	2,783	3,353
NNR	32,486	3,299	11,630	**NNR**	2,836	3,194	2,852

Appendix VIA: Total concentrations (mg.kg^{-1} dry weight) of major elements in sediments

January										
Sample	**Si**	**Al**	**Mg**	**Ca**	**Fe**	**Mn**	**Ti**	**Na**	**K**	**P**
Sed 1	321598,72	71132,54	9666,73	5260,16	31096,69	612,60	2822,93	16128,13	37439,77	981,96
Sed 2	328142,88	68062,84	8563,17	5345,93	29131,29	500,30	2625,15	15556,89	36111,53	947,05
Sed 3	251015,28	64384,48	9286,82	8579,92	30299,34	536,70	4213,42	10697,68	23493,25	1379,11
Sed 3'	316456,88	62452,68	8171,19	6982,58	31873,06	548,32	3224,50	14807,61	31545,71	1056,16
Sed 4	326740,56	67665,89	8312,91	5317,34	35419,17	602,92	4387,23	15226,76	36319,07	888,13
Sed 5	336556,80	69809,39	8725,99	5603,22	27403,70	608,73	2715,05	15816,54	37356,76	859,76

May										
Sample	**Si**	**Al**	**Mg**	**Ca**	**Fe**	**Mn**	**Ti**	**Na**	**K**	**P**
Sed 1	321598,72	64940,20	8201,34	5145,81	34062,28	810,86	2565,00	14763,10	34866,31	885,95
Sed 2	325585,05	67433,65	10455,27	6123,51	39622,47	733,04	2905,93	15105,54	32467,51	910,63
Sed 3	308977,84	77801,22	10197,41	8462,00	46309,31	841,07	3596,09	13464,83	31545,71	1117,26
Sed 3'	316784,09	68388,23	8476,33	5740,44	26544,24	551,29	2762,02	16237,33	36922,76	924,55
Sed 4	318794,08	72614,47	8858,66	5338,78	33194,98	573,10	4884,69	18442,74	42254,65	990,69
Sed 5	331181,24	66051,65	8683,78	5646,10	31439,41	787,24	2691,08	15245,31	35156,86	844,49

August										
Sample	**Si**	**Al**	**Mg**	**Ca**	**Fe**	**Mn**	**Ti**	**Na**	**K**	**P**
Sed 1	286177,05	70214,17	8882,42	4583,20	38055,05	1276,54	3272,98	12265,24	27200,20	6721,03
Sed 2	319918,27	64839,38	7696,90	9912,12	27625,07	415,63	2984,47	18042,88	30368,56	1893,86
Sed 3	329027,74	68326,09	8683,84	5253,80	30779,08	889,07	3494,52	15389,38	33772,84	1713,72
Sed 3'	310831,71	69110,14	8614,55	6686,55	34548,10	796,25	3895,03	14851,68	31985,52	2004,31
Sed 4	306418,14	68087,66	8289,27	5758,23	34511,10	1715,64	6699,34	14977,87	32933,47	1989,86
Sed 5	324030,34	67257,88	8239,88	5151,10	30906,52	646,18	2807,76	15817,81	36854,60	1699,32

November										
Sample	**Si**	**Al**	**Mg**	**Ca**	**Fe**	**Mn**	**Ti**	**Na**	**K**	**P**
Sed 1	284568,12	69722,60	7764,56	4422,25	35460,02	1205,74	3409,46	12808,58	27423,02	3305,87
Sed 2	324116,82	67827,47	7344,89	8199,53	29610,02	434,95	2870,62	18211,95	32398,73	1018,91
Sed 3	329498,46	69978,28	7514,80	4893,95	30356,48	938,20	3850,61	15538,79	37451,06	905,34
Sed 3'	327251,94	69541,06	7484,95	4587,78	29955,29	918,94	3582,84	16146,75	38301,47	892,99
Sed 4	279409,46	68553,99	7949,06	8717,00	30316,13	701,03	5503,75	13609,94	29538,74	1130,59
Sed 5	311430,03	68734,68	7296,33	5212,49	31896,35	818,28	2766,22	15858,90	35277,23	957,31

Mean										
Sample	**Si**	**Al**	**Mg**	**Ca**	**Fe**	**Mn**	**Ti**	**Na**	**K**	**P**
Sed 1	303485,65	69002,38	8628,76	4852,86	34668,51	976,44	3017,59	13991,26	31732,33	2973,70
Sed 2	324440,76	67040,83	8515,06	7395,27	31497,21	520,98	2846,54	16729,32	32836,58	1192,61
Sed 3	304629,83	70122,52	8920,72	6797,42	34436,05	801,26	3788,66	13772,67	31565,71	1278,86
Sed 3'	317831,15	67373,02	8186,76	5999,34	30730,17	703,70	3366,09	15510,84	34688,86	1219,50
Sed 4	307840,56	69230,50	8352,47	6282,84	33360,35	898,17	5368,75	15564,33	35261,48	1249,82
Sed 5	325799,60	67963,40	8236,49	5403,23	30411,49	715,11	2745,03	15684,64	36161,36	1090,22

Standard deviation/2										
Sample	**Si**	**Al**	**Mg**	**Ca**	**Fe**	**Mn**	**Ti**	**Na**	**K**	**P**
Sed 1	10462,74	1385,22	415,46	206,13	1449,73	158,75	196,11	891,62	2606,20	1368,65
Sed 2	1721,75	745,21	695,55	1032,74	2741,24	72,97	77,54	813,17	1195,28	234,83
Sed 3	18500,30	2815,66	562,48	998,09	3959,20	90,39	160,17	1128,54	2953,44	174,35
Sed 3'	3424,52	1657,27	251,60	539,95	1683,38	92,31	243,53	393,83	1713,40	263,98
Sed 4	10358,33	1142,48	188,09	817,71	1112,72	273,86	498,86	1023,18	2710,97	251,63
Sed 5	5433,65	824,37	332,11	128,75	1022,79	51,57	26,13	146,77	555,30	204,56

Appendix VIB: Total concentrations (mg.kg^{-1} dry weight) of trace elements in sediments

January											
Sample	**Sr**	**Ba**	**Co**	**Cr**	**Cu**	**Ni**	**Sc**	**V**	**Y**	**Zn**	**Zr**
Sed 1	195,60	1020,00	11,60	106,00	85,00	31,00	9,50	71,00	14,80	116,00	140,00
Sed 2	193,50	979,00	11,70	102,00	77,00	28,00	9,30	64,00	13,80	110,00	154,00
Sed 3	161,40	756,00	21,65	272,00	151,00	44,00	13,20	94,00	24,85	275,00	313,50
Sed 3'	202,50	2403,00	12,60	147,00	75,00	28,00	8,50	65,00	15,00	120,00	269,00
Sed 4	194,15	1102,50	14,65	135,00	147,00	33,00	9,10	74,00	14,70	174,00	198,50
Sed 5	210,40	1167,00	10,70	86,00	58,00	33,00	9,40	69,00	14,60	113,00	126,00

May											
Sample	**Sr**	**Ba**	**Co**	**Cr**	**Cu**	**Ni**	**Sc**	**V**	**Y**	**Zn**	**Zr**
Sed 1	184,00	982,00	9,00	106,00	230,00	47,00	8,30	71,00	13,40	141,00	161,00
Sed 2	186,48	977,76	10,08	104,83	90,72	49,39	10,79	77,62	15,02	127,01	144,14
Sed 3	224,50	1249,00	26,10	177,00	135,00	57,00	15,40	115,00	25,20	198,00	190,00
Sed 3'	209,84	1643,55	11,04	85,34	70,28	39,16	9,04	63,25	14,06	125,50	155,62
Sed 4	209,10	1105,00	15,40	126,00	144,00	39,00	10,00	75,00	14,70	182,00	149,00
Sed 5	194,50	1136,00	9,50	127,00	75,00	38,50	9,15	68,00	13,95	159,00	145,00

August											
Sample	**Sr**	**Ba**	**Co**	**Cr**	**Cu**	**Ni**	**Sc**	**V**	**Y**	**Zn**	**Zr**
Sed 1	209,46	1113,74	10,07	57,40	50,35	22,15	9,06	66,46	14,40	168,17	160,11
Sed 2	176,05	1175,01	10,06	92,55	60,36	34,20	9,96	69,41	15,69	106,64	224,34
Sed 3	184,46	1002,96	15,12	161,28	50,40	48,38	10,99	81,65	19,35	403,20	290,30
Sed 3'	136,82	1482,84	15,09	92,55	50,30	32,19	12,98	81,49	27,26	148,89	276,65
Sed 4	189,32	1127,34	15,11	146,01	80,57	44,31	9,16	83,08	15,26	182,27	344,89
Sed 5	199,20	1126,63	9,51	83,08	50,05	33,03	9,41	67,57	14,11	127,13	147,65

November											
Sample	**Sr**	**Ba**	**Co**	**Cr**	**Cu**	**Ni**	**Sc**	**V**	**Y**	**Zn**	**Zr**
Sed 1	210,63	1161,47	11,03	72,22	60,18	33,10	9,33	73,22	14,44	151,45	157,47
Sed 2	171,35	1193,42	10,05	89,94	45,22	33,17	9,60	70,35	16,43	113,06	200,52
Sed 3	180,43	951,55	17,14	192,53	100,80	52,42	12,50	86,69	22,38	187,49	301,39
Sed 3'	158,32	1774,54	13,03	105,21	50,10	33,07	11,12	75,15	23,35	143,29	270,54
Sed 4	200,20	1126,48	12,95	110,56	69,72	43,82	9,06	74,70	15,24	171,31	240,04
Sed 5	201,30	1142,89	9,99	80,42	59,94	34,96	9,44	65,93	14,78	120,38	145,88

Mean											
Sample	**Sr**	**Ba**	**Co**	**Cr**	**Cu**	**Ni**	**Sc**	**V**	**Y**	**Zn**	**Zr**
Sed 1	199,92	1069,30	10,43	85,40	106,38	33,31	9,05	70,42	14,26	144,16	154,65
Sed 2	181,85	1081,30	10,47	97,33	68,32	36,19	9,91	70,35	15,24	114,18	180,75
Sed 3	187,70	989,88	20,00	200,70	109,30	50,45	13,02	94,33	22,95	265,92	273,80
Sed 3'	176,87	1825,98	12,94	107,53	61,42	33,10	10,41	71,22	19,92	134,42	242,95
Sed 4	198,19	1115,33	14,53	129,39	110,32	40,03	9,33	76,69	14,97	177,39	233,11
Sed 5	201,35	1143,13	9,93	94,13	60,75	34,87	9,35	67,63	14,36	129,88	141,13

Standard deviation/2											
Sample	**Sr**	**Ba**	**Co**	**Cr**	**Cu**	**Ni**	**Sc**	**V**	**Y**	**Zn**	**Zr**
Sed 1	6,31	41,36	0,57	12,27	41,85	5,14	0,26	1,42	0,30	10,93	4,94
Sed 2	5,01	59,54	0,41	3,60	9,89	4,60	0,32	2,80	0,56	4,47	19,03
Sed 3	13,26	101,44	2,45	24,61	22,25	2,78	0,92	7,34	1,35	49,74	28,33
Sed 3'	17,54	201,37	0,83	13,78	6,55	2,30	1,03	4,31	3,22	6,92	29,16
Sed 4	4,26	6,71	0,55	7,49	20,44	2,63	0,22	2,14	0,16	2,79	41,65
Sed 5	3,33	8,63	0,28	11,02	5,21	1,29	0,07	0,64	0,20	10,13	5,07

Appendix VIIA: Total concentrations (mg.kg^{-1} dry weight) of major elements in soils

January										
Sample	**Si**	**Al**	**Mg**	**Ca**	**Fe**	**Mn**	**Ti**	**Na**	**K**	**P**
Soil 1	n.a.	n.a.	n.a.	n.a.	n.a.	n.a.	n.a.	n.a.	n.a.	n.a.
Soil 2	281398,88	65945,80	10022,52	10806,20	35503,11	936,32	3955,70	13620,63	28308,12	1291,83
Soil 3	283736,08	65522,39	9648,64	7161,25	33803,49	996,73	4507,10	13160,67	27810,03	1492,59
Soil 3'	314587,12	62876,09	7984,25	6339,35	32215,78	1050,94	3572,12	12366,88	29470,33	1003,79
Soil 4	288877,92	64728,50	8973,24	9055,20	31488,37	812,41	3877,79	12337,20	27893,05	1907,19
Soil 5	314587,12	67533,58	9515,97	6839,64	39028,24	798,47	3967,69	14206,70	31462,69	1034,34
Soil 6	285605,84	48744,85	5680,64	6796,76	48043,90	1184,93	4375,25	5541,73	22414,06	1780,63
Soil 7	285605,84	70497,43	9359,18	6460,85	35629,00	1163,24	4597,01	12218,50	27311,94	2526,92

May										
Sample	**Si**	**Al**	**Mg**	**Ca**	**Fe**	**Mn**	**Ti**	**Na**	**K**	**P**
Soil 1	301498,80	66210,43	9226,51	8076,06	29655,86	684,62	2900,85	14392,17	31047,62	1091,07
Soil 2	285891,45	66700,47	9477,20	9157,26	34726,46	902,38	3971,66	15074,90	30413,88	1179,54
Soil 3	233252,56	82458,71	11397,46	16295,07	76307,90	1484,64	5819,68	5860,73	22912,15	2160,32
Soil 3'	305254,68	62212,55	7936,25	7196,77	33402,23	1077,91	3483,72	12795,75	30044,05	1000,77
Soil 4	240264,16	84152,34	11518,06	15651,84	77077,27	1499,36	5993,49	6009,10	23244,21	1911,56
Soil 5	302901,12	57583,49	7718,91	20940,59	30425,24	883,66	3925,74	10905,40	22414,06	2732,04
Soil 6	231616,52	52899,54	6965,11	11649,54	29201,23	765,17	3530,17	9347,49	19882,10	1815,54
Soil 7	290981,40	61870,49	8231,50	6253,59	27802,37	617,63	2942,80	13576,11	29719,38	1012,51

August										
Sample	**Si**	**Al**	**Mg**	**Ca**	**Fe**	**Mn**	**Ti**	**Na**	**K**	**P**
Soil 1	301083,71	67006,86	9543,47	8068,63	30668,64	726,01	3087,17	15329,88	31547,04	2041,77
Soil 2	272790,04	67627,60	10593,94	11625,42	40327,50	1003,16	4199,64	13515,43	27463,90	2497,10
Soil 3	258677,56	78743,73	9361,11	7420,26	45192,18	932,89	4905,65	11291,77	28032,51	2644,26
Soil 3'	303204,02	64369,40	8752,82	7082,56	35776,65	864,39	3582,00	13515,43	30081,49	1703,51
Soil 4	282702,10	66130,83	9147,88	8701,85	31969,86	904,31	3624,79	12882,62	29162,85	3852,48
Soil 5	296994,55	65668,36	9096,80	7211,21	32491,01	785,29	3837,98	14896,56	31845,89	2156,23
Soil 6	277720,13	62463,48	8198,03	12378,82	35568,50	954,58	5208,59	11654,09	26081,99	3460,88
Soil 7	286645,43	69206,57	8640,72	4439,98	37214,05	1243,95	4420,03	12413,91	26950,66	6438,21

November										
Sample	**Si**	**Al**	**Mg**	**Ca**	**Fe**	**Mn**	**Ti**	**Na**	**K**	**P**
Soil 1	306800,97	65562,61	7878,09	8567,77	28019,13	639,07	2814,12	15044,78	32260,55	1011,50
Soil 2	286359,35	63097,90	7628,97	16096,74	38367,13	986,88	4019,65	13960,99	25843,49	1065,95
Soil 3	275152,01	67316,16	8012,57	5908,25	38036,16	769,05	5330,78	12044,02	26210,50	1638,75
Soil 3'	311462,28	64041,52	7553,07	7039,04	34302,88	883,41	3632,14	13494,88	29617,68	986,87
Soil 4	288653,55	65576,58	7854,43	8684,41	32463,10	828,44	3814,52	12635,13	28608,30	1890,87
Soil 5	290849,82	65355,12	8039,46	7262,38	30994,89	793,53	3702,08	14402,77	31149,15	1187,67
Soil 6	212055,79	61264,31	7941,18	21123,16	86315,25	1393,26	5268,94	7059,69	21233,42	1489,85
Soil 7	284282,98	69811,03	7809,55	4489,08	35703,42	1215,35	4499,56	12351,96	27147,24	3341,72

Mean										
Sample	**Si**	**Al**	**Mg**	**Ca**	**Fe**	**Mn**	**Ti**	**Na**	**K**	**P**
Soil 1	303127,83	66259,96	8882,69	8237,49	29447,88	683,23	2934,05	14922,28	31618,40	1381,45
Soil 2	281609,93	65842,94	9430,66	11921,40	37231,05	957,18	4036,66	14042,99	28007,35	1508,60
Soil 3	262704,55	73510,24	9604,94	9196,21	48334,93	1045,83	5140,80	10589,30	26241,30	1983,98
Soil 3'	308627,03	63374,89	8056,60	6914,43	33924,39	969,16	3567,50	13043,23	29803,39	1173,74
Soil 4	275124,43	70147,06	9373,40	10523,32	43249,65	1011,13	4327,65	10966,01	27227,10	2390,53
Soil 5	301333,15	64035,13	8592,79	10563,46	33234,84	815,24	3858,37	13602,86	29217,95	1777,57
Soil 6	251749,57	56343,04	7196,24	12987,07	49782,22	1074,48	4595,74	8400,75	22402,89	2136,73
Soil 7	286878,91	67846,38	8510,24	5410,87	34087,21	1060,04	4114,85	12640,12	27782,31	3329,84

Standard deviation/2										
Sample	**Si**	**Al**	**Mg**	**Ca**	**Fe**	**Mn**	**Ti**	**Na**	**K**	**P**
Soil 1	1593,90	361,70	442,16	143,03	668,47	21,74	69,76	240,36	304,80	286,62
Soil 2	3145,41	977,50	642,38	1483,39	1295,42	23,16	56,00	356,87	951,29	332,71
Soil 3	11108,93	4179,68	695,83	2389,20	9615,92	153,93	281,93	1622,27	1181,58	262,63
Soil 3'	2651,15	502,76	251,33	194,56	750,90	55,41	30,86	280,72	152,94	176,63
Soil 4	11707,74	4677,32	770,16	1711,64	11277,63	163,97	557,88	1656,06	1352,83	487,34
Soil 5	5056,76	2203,64	425,84	3460,33	1979,65	22,97	58,69	910,79	2272,43	403,61
Soil 6	17799,00	3307,43	570,74	2981,54	12790,92	136,59	409,56	1337,07	1330,98	447,38
Soil 7	1450,42	2009,34	329,95	548,10	2126,53	148,41	392,35	314,65	649,90	1142,98

Appendix VIIB: Total concentrations (mg.kg^{-1} dry weight) of trace elements in soils

January											
Sample	**Sr**	**Ba**	**Co**	**Cr**	**Cu**	**Ni**	**Sc**	**V**	**Y**	**Zn**	**Zr**
Soil 1	n.a.	n.a.	n.a.	n.a.	n.a.	n.a.	n.a.	n.a.	n.a.	n.a.	n.a.
Soil 2	179,50	974,00	17,40	120,00	156,00	42,00	11,90	93,00	22,00	186,00	689,00
Soil 3	158,50	844,00	17,90	289,00	125,00	38,00	11,70	88,00	23,70	206,00	520,00
Soil 3'	239,40	6514,00	14,60	133,00	98,00	31,00	9,50	73,00	20,20	167,00	342,00
Soil 4	160,60	917,00	15,60	122,00	108,00	35,00	10,70	80,00	19,10	270,00	487,00
Soil 5	191,70	1342,00	15,50	140,00	158,00	37,00	10,50	84,00	16,70	201,00	222,00
Soil 6	132,90	809,00	20,40	111,00	157,00	49,00	8,40	93,00	25,40	207,00	1307,00
Soil 7	149,80	1260,00	19,60	117,00	103,00	41,00	13,10	109,00	25,40	240,00	766,00

May											
Sample	**Sr**	**Ba**	**Co**	**Cr**	**Cu**	**Ni**	**Sc**	**V**	**Y**	**Zn**	**Zr**
Soil 1	181,00	869,00	12,00	129,00	90,00	42,00	10,10	75,00	16,90	157,00	179,00
Soil 2	186,00	1259,00	14,00	131,00	140,00	49,00	11,80	94,00	21,30	188,00	814,00
Soil 3	301,00	1080,00	53,00	245,00	510,00	190,00	21,10	154,00	45,50	645,00	1607,00
Soil 3'	268,00	7943,00	11,00	168,00	110,00	41,00	9,90	74,00	18,70	213,00	366,00
Soil 4	300,00	1095,00	54,00	175,00	500,00	181,00	21,60	154,00	44,70	393,00	1709,00
Soil 5	168,00	924,00	13,00	103,00	80,00	45,00	10,00	72,00	19,80	273,00	690,00
Soil 6	141,50	739,50	14,50	174,00	85,00	49,50	10,10	79,00	20,30	189,00	564,50
Soil 7	179,00	1158,50	10,00	98,50	70,00	47,50	9,00	66,50	15,10	132,00	168,00

August											
Sample	**Sr**	**Ba**	**Co**	**Cr**	**Cu**	**Ni**	**Sc**	**V**	**Y**	**Zn**	**Zr**
Soil 1	180,43	868,90	13,10	144,14	90,72	42,34	10,38	74,59	16,93	169,34	193,54
Soil 2	170,17	853,85	15,52	131,13	150,15	51,55	12,66	103,10	23,67	233,73	906,91
Soil 3	179,42	1075,54	31,25	364,90	161,28	86,69	18,04	126,00	33,06	238,90	946,51
Soil 3'	229,23	5151,15	14,01	203,20	120,12	76,08	10,11	86,09	19,12	196,20	356,36
Soil 4	162,67	954,09	13,97	112,77	89,82	45,91	10,88	81,84	20,66	294,41	432,13
Soil 5	186,81	1085,91	11,99	122,88	69,93	42,96	10,09	71,93	16,88	163,84	247,75
Soil 6	157,09	1002,97	16,11	103,72	120,84	50,35	10,98	100,70	23,87	343,39	1429,94
Soil 7	144,79	1152,30	17,03	129,26	100,20	51,10	12,32	99,20	21,74	359,22	886,27

November											
Sample	**Sr**	**Ba**	**Co**	**Cr**	**Cu**	**Ni**	**Sc**	**V**	**Y**	**Zn**	**Zr**
Soil 1	182,82	883,12	10,99	133,87	89,91	37,96	9,79	68,93	15,68	149,85	179,82
Soil 2	190,19	834,83	15,02	108,11	300,30	46,05	11,21	99,10	23,32	222,22	1214,21
Soil 3	154,38	865,52	19,92	616,52	159,36	61,75	13,45	103,58	26,19	175,30	1433,24
Soil 3'	207,03	3982,82	13,07	153,77	120,60	44,22	9,95	75,38	18,09	180,90	369,84
Soil 4	162,35	953,17	13,94	127,49	109,56	49,80	11,06	78,68	19,92	276,89	585,65
Soil 5	179,06	971,27	13,58	119,20	80,48	45,28	10,21	72,94	17,10	155,92	261,52
Soil 6	197,37	1217,97	32,73	208,45	6751,94	213,48	14,35	133,43	28,65	755,25	1569,41
Soil 7	147,70	1152,69	15,97	117,76	159,68	48,90	12,38	96,81	21,56	244,51	957,08

Mean											
Sample	**Sr**	**Ba**	**Co**	**Cr**	**Cu**	**Ni**	**Sc**	**V**	**Y**	**Zn**	**Zr**
Soil 1	181,42	873,67	12,03	135,67	90,21	40,77	10,09	72,84	16,51	158,73	184,12
Soil 2	181,47	980,42	15,48	122,56	186,61	47,15	11,89	97,30	22,57	207,49	906,03
Soil 3	198,33	966,27	30,52	378,86	238,91	94,11	16,07	117,90	32,11	316,30	1126,69
Soil 3'	235,91	5897,74	13,17	164,49	112,18	48,07	9,86	77,12	19,03	189,27	358,55
Soil 4	196,41	979,82	24,38	134,32	201,85	77,93	13,56	98,63	26,09	308,57	803,45
Soil 5	181,39	1080,80	13,52	121,27	97,10	42,56	10,20	75,22	17,62	198,44	355,32
Soil 6	157,22	942,36	20,93	149,29	1778,69	90,58	10,96	101,53	24,55	373,66	1217,71
Soil 7	155,32	1180,87	15,65	115,63	108,22	47,13	11,70	92,88	20,95	243,93	694,34

Standard deviation/2											
Sample	**Sr**	**Ba**	**Co**	**Cr**	**Cu**	**Ni**	**Sc**	**V**	**Y**	**Zn**	**Zr**
Soil 1	0,62	4,09	0,53	3,87	0,22	1,22	0,15	1,70	0,36	4,93	4,08
Soil 2	4,36	97,84	0,71	5,48	38,04	2,05	0,30	2,35	0,56	12,07	112,01
Soil 3	34,66	64,53	8,05	83,00	90,75	33,47	2,14	14,34	4,88	110,33	245,83
Soil 3'	12,65	855,73	0,79	14,77	5,32	9,75	0,13	3,03	0,44	9,90	6,20
Soil 4	34,53	39,35	9,88	13,90	99,49	34,50	2,68	18,47	6,21	28,61	303,52
Soil 5	5,17	93,47	0,74	7,59	20,44	1,92	0,11	2,94	0,73	26,73	111,86
Soil 6	14,29	107,46	4,12	25,25	1657,81	40,97	1,25	11,54	1,73	131,78	224,24
Soil 7	7,96	26,41	2,03	6,36	18,71	2,17	0,92	9,18	2,14	46,40	179,82

Appendix VIII: Supplementary information from article: Aggregation behavior of TiO_2 nanoparticles in natural river water

Supplementary Information

Aggregation behavior of TiO_2 ENMs in natural river water

Véronique Adam[a,b], Stéphanie Loyaux-Lawniczak[a], Jérôme Labille[c], Catherine Galindo[d], Mireille del Nero[d], Tiphaine Weber[a], Gaetana Quaranta[a]

[a] *Laboratoire d'Hydrologie et de Géochimie de Strasbourg / EOST / UDS, 1 rue Blessig, 67084 Strasbourg Cedex, France.*

[b] *French Environment and Energy Management Agency, 20 avenue du Grésillé, BP 90406 49004 Angers Cedex 01, France*

[c] *Aix-Marseille Université, CNRS, IRD, CEREGE, UMR 7330, 13545 Aix-en-Provence, France*

[d] *Institut Plurisdisciplinaire Hubert Curien, 23 rue du Loess, BP 28, 67037 Strasbourg Cedex 2, France*

Characterization of TiO_2 NPs

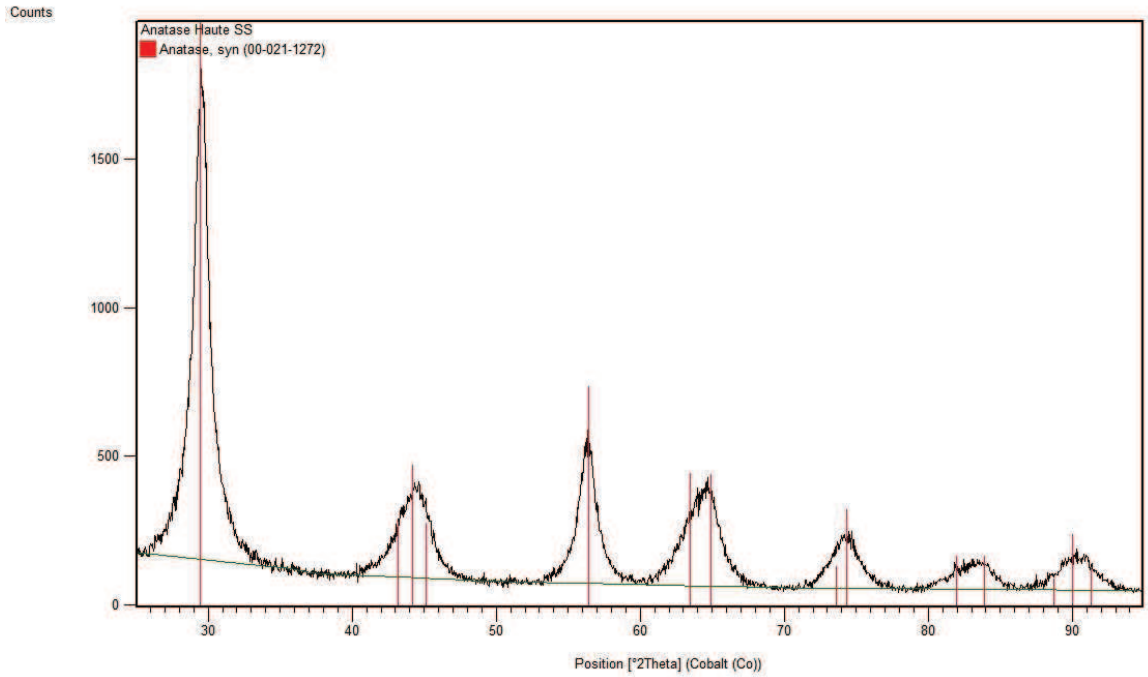

Figure S1: Spectra of TiO_2 NPs obtained in X-Ray diffraction

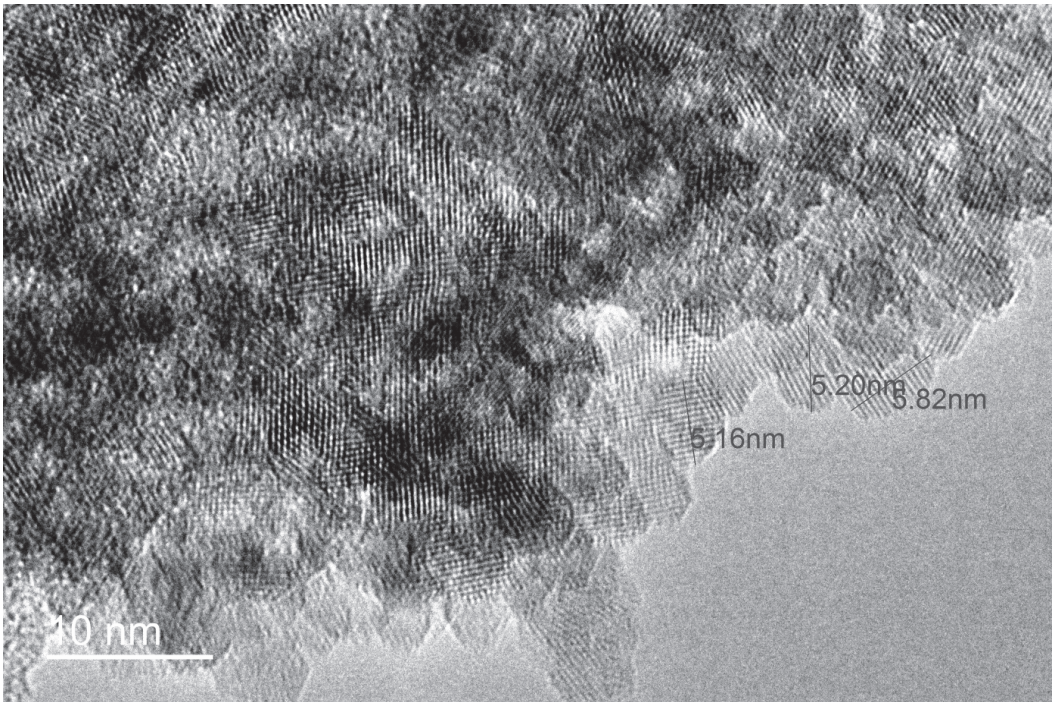

Figure S2: Transmission electronic microscopy micrograph of TiO_2 ENMs in deionized water (Jeol JEM 2100)

Characterization of illite

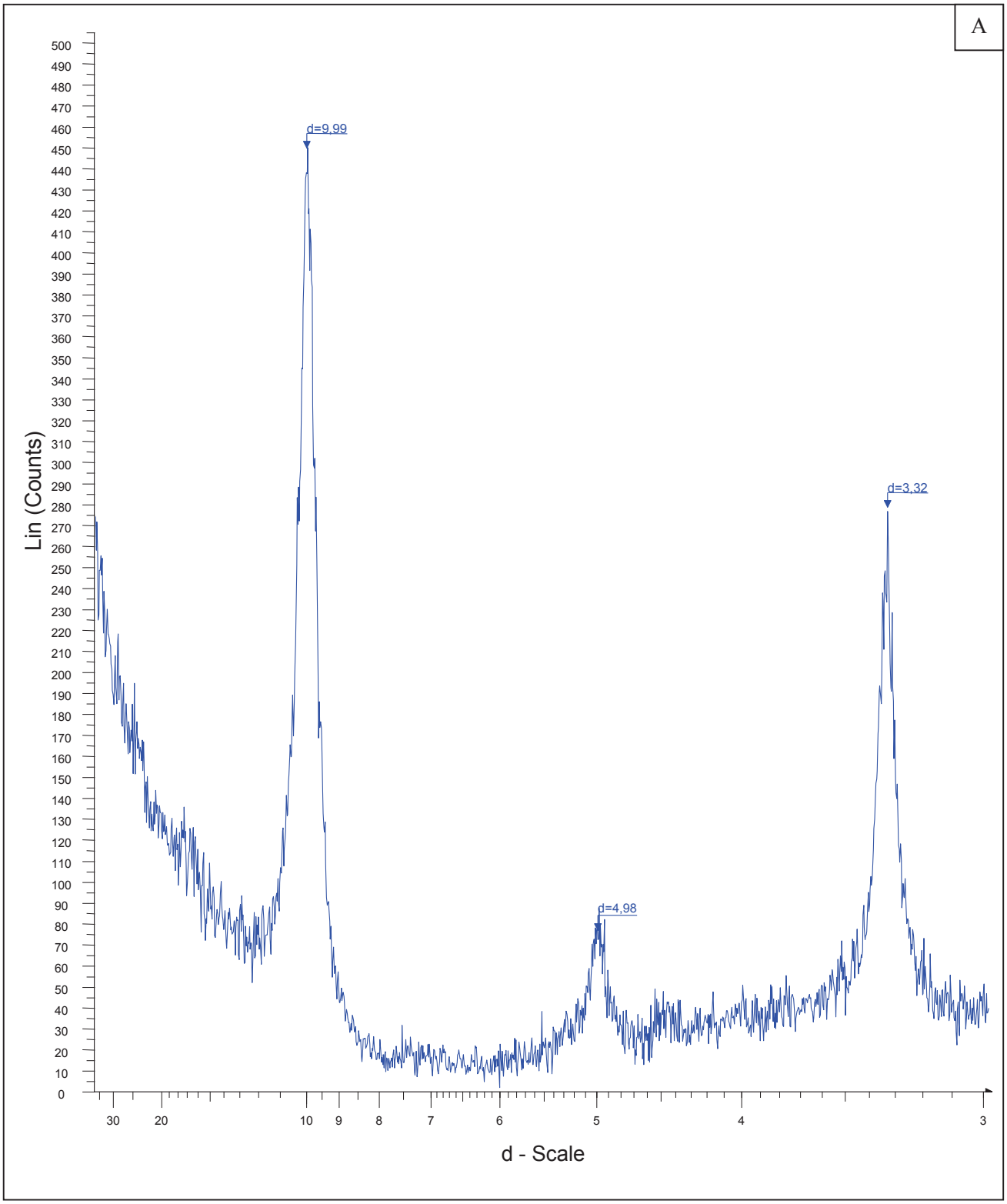

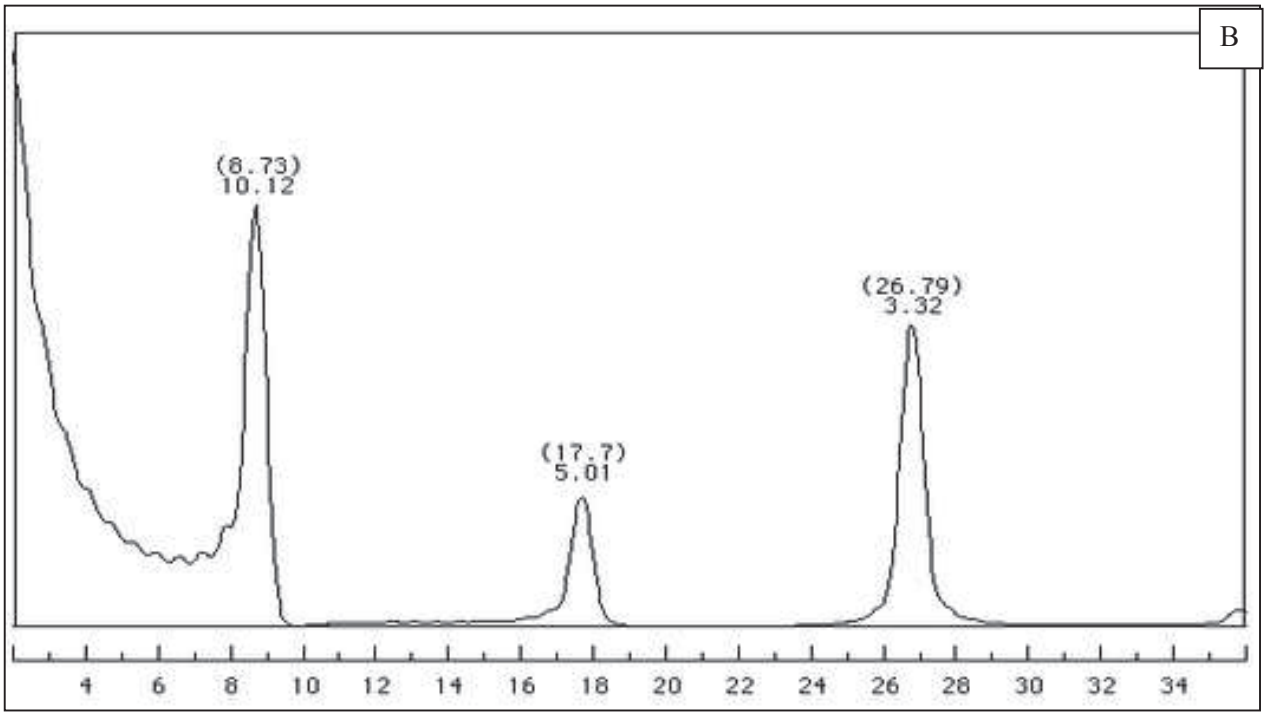

Figure S3A: Spectra of studied illite obtained with X-Ray Diffraction. Figure S3B: Reference illite spectra, 2Θ.[1] The comparison between the two spectra shows that it is pure illite.

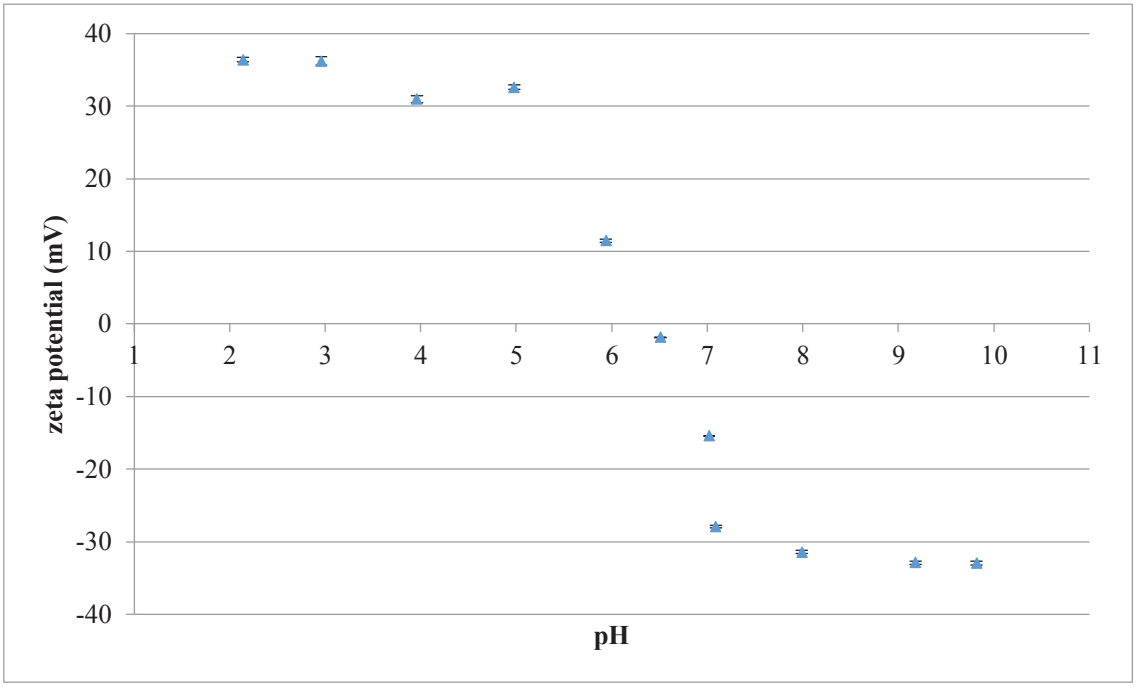

Figure S4: Zeta potential of TiO_2 NPs in deionized water ([NaCl] = 10mM) as a function of pH

Interaction energy calculations according to the DLVO theory

The interaction energy between two particles can be calculated by summing the attractive (van der Waals - vdW) and repulsive (electrical double layer - edl) forces (Equation 1).

$$\Phi_{DLVO} = \Phi_{vdW} + \Phi_{edl} \quad (1)$$

The van der Waals attraction between two spheres is given by Gregory:[2]

$$\Phi_{vdW}(d) = -\frac{A_H}{6d}\frac{R_1 R_2}{R_1+R_2}\left[1 - \frac{b_1 d}{\lambda_d}\ln\left(1+\frac{\lambda_d}{b_1 d}\right)\right] \quad (2)$$

Where A_H [J] is the Hamaker constant, accounting for materials properties, d [m] is the shortest distance between the spheres of radii R_1 and R_2 (m), $b_1 = 5.32$, $b_2 = 14.02$ and $\lambda_d = 100$ nm.

The Hamaker constant between two materials 1 and 2 immersed in a medium 3 can be calculated by:

$$A_{12} = -\sqrt{A_{11}A_{22}} \quad (3)$$

$$A_{132} = A_{12} + A_{33} - A_{13} - A_{23} = \left(\sqrt{A_{11}} - \sqrt{A_{33}}\right)\left(\sqrt{A_{22}} - \sqrt{A_{33}}\right) \quad (4)$$

Where A_{ii} is the Hamaker constant of a material in vacuum, A_{ij} is the Hamaker constant related to the interaction between materials i and j in vacuum.

The electrical double layer repulsion between two spheres is given by:[3]

$$\Phi_{edl}(d) = \frac{\pi\varepsilon_0\varepsilon_r R_1 R_2}{R_1+R_2}\left\{2\zeta_1\zeta_2 \ln\left[\frac{1+e^{-\kappa d}}{1-e^{-\kappa d}}\right] + (\zeta_1^2 + \zeta_2^2) + \ln[1-e^{-2\kappa d}]\right\} \quad (5)$$

Where d is the shortest distance between two spheres of radii R_1 and R_2 [m], ε_0 is the free space permittivity [$F.m^{-1}$], ε_r the liquid permittivity [-], ζ_1 and ζ_2 are the zeta potentials of the particles [V], and κ is the inverse of the Debye length [m^{-1}].

The Debye length, which is the thickness of the double layer, is given by:

$$\kappa^{-1} = \left(\frac{\varepsilon_0\varepsilon_r k_B T}{2e^2 N_{Av} I}\right)^{1/2} \quad (6)$$

With k_B is the Boltzmann constant [$J.K^{-1}$], T is the temperature [K], e is the electron charge [C], N_{Av} is the Avogadro number [-], and I is the ionic strength of the suspension [$mol.m^{-3}$].

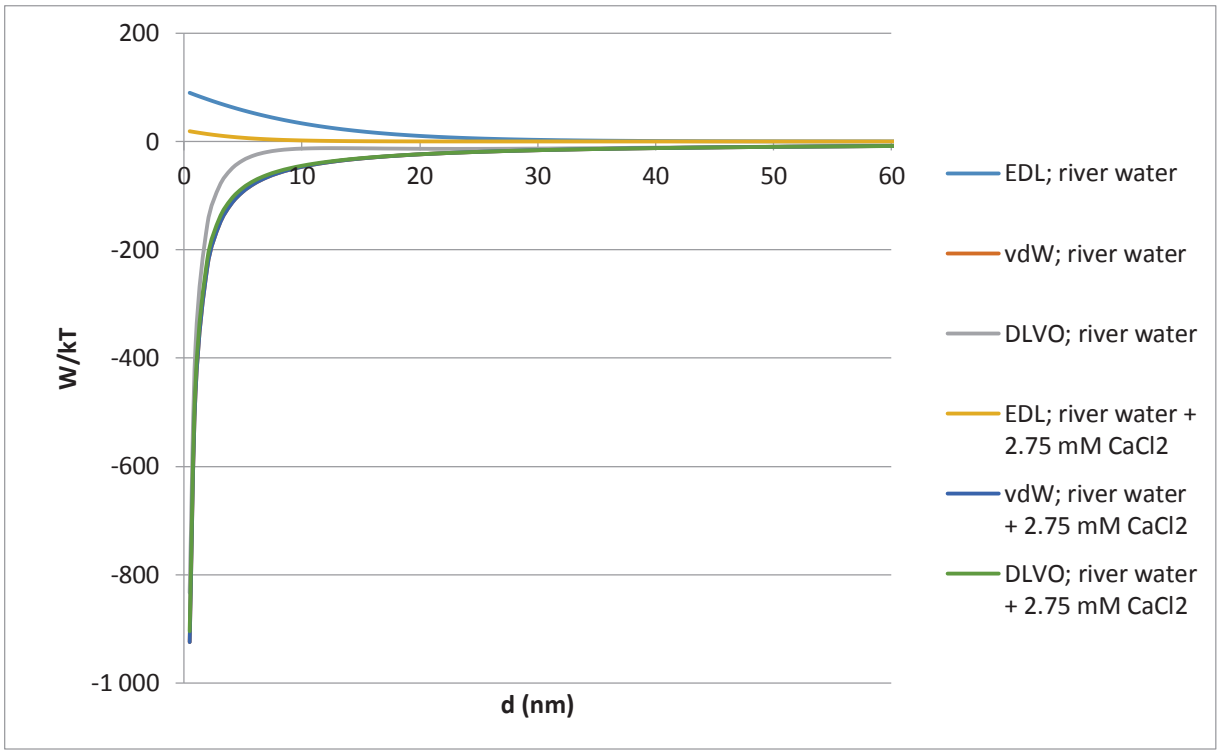

Figure S4: Interaction energies between TiO_2 NPs aggregates in the river water and in the river water with added $CaCl_2$ (pH 8)

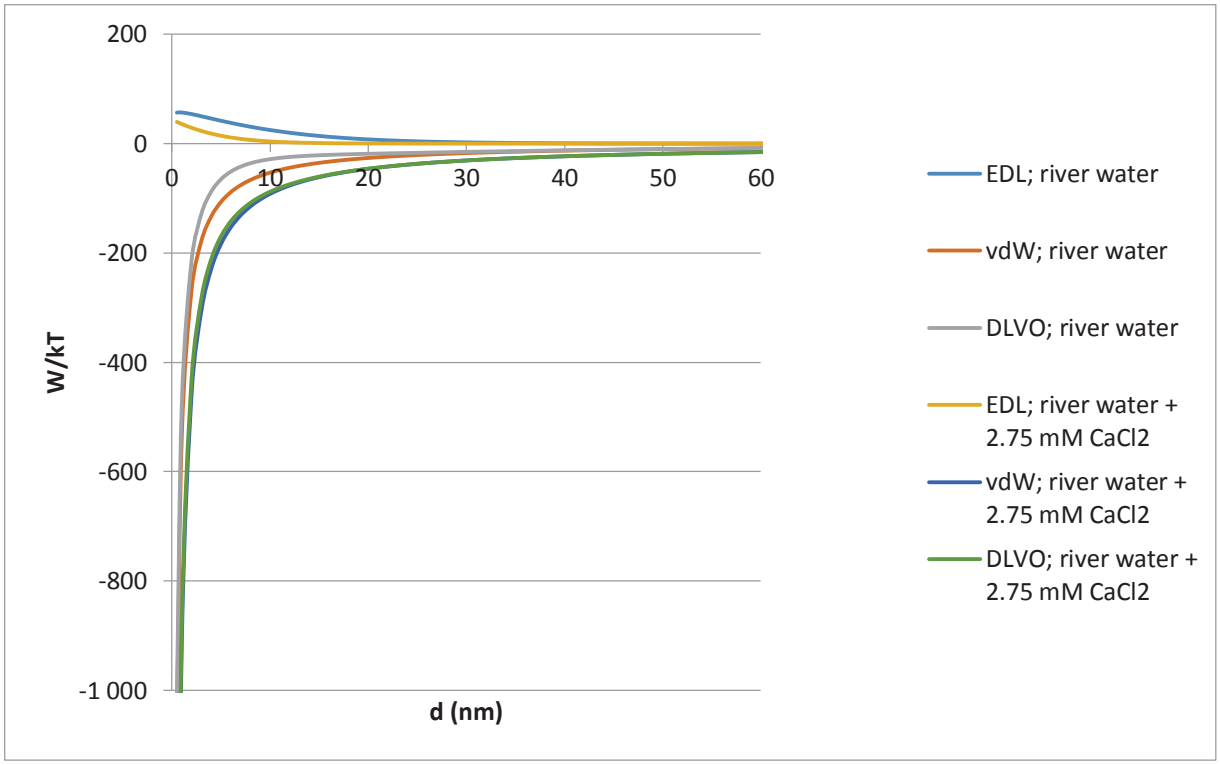

Figure S5: Interaction energies between TiO_2 NPs and illite aggregates in the river water and in the river water with added $CaCl_2$ (pH 8)

SmoluCalc model approach

In this model the Smoluchowski equations are solved numerically using a size gridding procedure to divide the particle population into different size classes and thus controlling the number of differential equations to be solved. On one hand, the sticking efficiency α is an open parameter that is adjusted to fit the measured aggregation kinetics data. On the other hand, the collision frequency β is generated by the model, accounting for the particle properties (size, density, concentration, fractal dimension), the solvent properties (velocity gradient, viscosity, density, temperature) and the type of interparticle collision resulting from the aggregate permeability to the streamlines.[4] In the present work, the aggregate permeability was calculated from Gmachowski model, as derived by Thill et al.[4] Both mechanical agitation and Brownian motion are accounted for in the β simulation, while sedimentation is considered negligible due to the permanent agitation. The mechanical agitation was also responsible for aggregate fractionation effect competing with the aggregation forces. Nevertheless, although it was fitted here by a maximum aggregate size in the model, this effect is not discussed in the present work as our attention is more focused on the very first steps of the aggregation process to determine the driving α while fragmentation remains negligible.

Because the SmoluCalc model only deals with homoaggregation of spherical units, and clay gives the major signal by laser diffraction on the clay / NP mixture, we used the clay characteristics to constrain this unique type of particle input. This latter consists of the clay homoaggregates, 45 µm in average size, preliminary formed in Thur water + $CaCl_2$ (2.75 mM), before NP injection. For a valid estimation of the collision frequency by these clay units, an appropriate estimation of the initial number concentration and density of the clay units in the system was required. It was calculated from the fractal dimension 2.18 measured for the clay units, using the Verapaneni approach. The structural characteristics of the initial clay unit are given in Table S1.

Table S1: Structural characteristics of the initial clay units used in the SmoluCalc modeling

Clay characteristic	**Value**
Mean particle diameter Dv50 of the primary particles	45 µm
Volumic mass of the primary particles	54.7 kg/m^3
Interparticle collision type	Gmachowski
Fractal dimension of the primary particles	2.18
Fractal dimension of the forming aggregates	2.3
Surface of a primary particle	6.39x10^{-9} m^2
Primary particle number	1.94x10^6
Total surface of primary particles	1.23x10^{-2} m^2
Total volume of primary particles	9.25x10^{-8} m^3

Table S2: SmoluCalc results

NP concentration (mg/L)	NP number	total projected area (m^2)	total NP volume (m^3)	number ratio	surface ratio	volume ratio	alpha global
10	6.11E+10	1.20E-02	4.00E-09	3.15E+04	9.73E-01	4.33E-02	0.11
20	1.22E+11	2.40E-02	8.00E-09	6.31E+04	1.95E+00	8.65E-02	
30	1.83E+11	3.60E-02	1.20E-08	9.46E+04	2.92E+00	1.30E-01	0.17
40	2.44E+11	4.80E-02	1.60E-08	1.26E+05	3.89E+00	1.73E-01	0.27
50	3.06E+11	6.00E-02	2.00E-08	1.58E+05	4.87E+00	2.16E-01	0.8
100	6.11E+11	1.20E-01	4.00E-08	3.15E+05	9.73E+00	4.33E-01	1

References

(1) UGA Clay Science website: http://clay.uga.edu/courses/8550/CM11.html. Consulted on 22 June 2015.

(2) Gregory, J. Approximate expressions for retarded van der Waals interaction. *J. Coll. Interface Sci.* **1981**, 83 (1), 138-145.

(3) Hogg, R.; Healy, T.; Fuerstenau, D. Mutual coagulation of colloidal dispersions. *Transactions of the Faraday Society* **1966**, 62, 1638-1651.

(4) Thill, A.; Moustier, S.; Aziz, J.; Wiesner, M.; Bottero, J.Y. Flocs Restructuring during Aggregation: Experimental Evidence and Numerical Simulation. *J. Coll. Interface Sci.* **2001**, 243, 171-182; Doi: 10.1006/jcis.2001.7801.

Appendix IXA: Parameters used for the assessment of the fate of TiO_2 NMs in the effluent

Effluent T	**January**	**March**	**May**	**August**	**November**
TiO_2 mass concentration (g/m^3)	0,031	0,922	0,603	1,25	0,82
pH	7,63	7,27	7,52	7,32	7,59
Conductivity (mS/cm)	0,1189	0,238	0,13	0,1417	0,1036
Attachment efficiency coefficient	0; 0.001				
Temperature (°C)	25	25	25	25	25
Water dynamic viscosity (kg/m/s)	8,90E-04	8,90E-04	8,90E-04	8,90E-04	8,90E-04
Mean water flow (m^3/s)	0,079				
Pipe diameter (m)	2,5				
Water depth (m)	0,5				
Mean water velocity (m/s)	0,06				
Pipe length (m)	980				
Maximum time (s)	16304				
Effluent NN	**January**	**March**	**May**	**August**	**November**
TiO_2 mass concentration (g/m^3)	0	0,055	0,03	0,041	0,121
pH	7,44	7,29	7,24	7,79	7,34
Conductivity (mS/cm)	7,43	5,62	12,95	7,9	6,5
Attachment efficiency coefficient	0.1; 0.5; 1				
Temperature (°C)	27,5	25	20	29	20
Water dynamic viscosity (kg/m/s)	8,00E-04	8,90E-04	1,00E-03	8,00E-04	1,00E-03
Mean water flow (m^3/s)	0,029				
Pipe diameter (m)	0,2				
Water depth (m)	0,1				
Mean water velocity (m/s)	2				
Pipe length (m)	800				
Maximum time (s)	392				

Appendix IXB: Parameters used for the fate assessment of TiO_2 NMs in the river

Point 4	**January**	**March**	**May**	**August**	**November**	**Reference**
pH	7,62	7,4	7,32	7,6	7,15	Measurement
Conductivité (mS/cm)	1,062	0,382	0,108	0,403	1,183	Measurement
Attachment efficiency coefficient	0.001; 0.01; 0.1					Section II
Temperature (°C)	17,6	14,4	18,1	16,8	18	Measurement
Water dynamic viscosity (kg/m/s)	1,00E-03	1,14E-03	1,00E-03	1,14E-03	1,00E-03	Kestin et al. 1978
Water depth (m)	0,3	0,3	0,2	0,4	0,35	Measurement
River width (m)	2,5					Measurement
Mean water flow (m^3/s)	4,67	7,49	1,89	4,73	3,65	hydro.eaufrance.fr database
Mean water velocity (m/s)	6,227	9,987	3,78	4,73	4,17	Calculation
Water volume (m^3)	278,25	278,25	186	371	325	Calculation
Sediment volume (m^3)	46,375					Depth similar to Praetorius et al. 2012
Sediment horizontal transfer velocity (kg/s)	0,405	0,650	0,164	0,411	0,317	van de Meent 1993
River section length (m)	371					Measurement
Maximum time (s)	2310	3705	1402	1755	1547	Calculation
Point 5	**January**	**March**	**May**	**August**	**November**	**Reference**
pH	7,88	7,73	7,9	7,61	8,19	Measurement
Conductivité (mS/cm)	0,751	0,332	0,515	0,778	0,273	Measurement
Attachment efficiency coefficient	0.001; 0.01; 0.1					Section II
Température (°C)	281,55	280,65	291,15	291,15	285,65	Measurement
Water dynamic viscosity (kg/m/s)	1,31E-03	1,31E-03	1,00E-03	1,00E-03	1,14E-03	Kestin et al. 1978
Water depth (m)	0,35	0,3	0,25	0,25	0,15	Measurement
River width (m)	13,5	13,5	13,5	13,5	13,5	Measurement
Mean water flow (m3/s)	4,7	7,54	1,9	4,79	3,68	hydro.eaufrance.fr database
Mean water velocity (m/s)	0,99	1,86	0,56	1,42	1,82	Calculation
Water volume (m3)	174,15	174,15	174,15	174,15	174,15	Calculation
Sediment volume (m3)	0,408	0,654	0,165	0,416	0,319	Depth similar to Praetorius et al. 2012
Sediment horizontal transfer velocity (kg/s)	1,10499E-06	1,77269E-06	4,46698E-07	1,12615E-06	8,65183E-07	van de Meent 1993
River length (m)	258					Measurement
Maximum time (s)	255,42	479,88	144,48	366,36	469,56	Calculation

Appendix XA: Fortran code used for the fate modeling of NMs in effluents

```
      IMPLICIT NONE

      ! Definition of the parameters type:

      INTEGER, PARAMETER ::  Nclass=15
      INTEGER ::  nt,i,j,k,jj,m,d

      REAL(KIND=16) :: dt, tmax,alpha,Temp,mu,df(4),d_primary_TiO2,v_max_effluent, z_effluent,pi,dt_max
      REAL(KIND=16) :: g,mass_concentration(Nclass),dmax,d_min,dstep,frac ,a1,a2,masse,number_concentration(Nclass)
      REAL(KIND=16) :: v_tot,v_tot_old
      REAL(KIND=16) :: sizeclass_log(Nclass) ,sizeclass(Nclass),crit(Nclass)
      REAL(KIND=16) :: N(Nclass),Ngain(Nclass),Nperte(Nclass),N_old(Nclass)
      REAL(KIND=16) :: nombre_NP(Nclass),V_compact(Nclass),V_total(Nclass),ro(Nclass),U(Nclass)
      REAL(KIND=16) :: V_tot_0(Nclass),V_total_sum,V_dum
      REAL(KIND=16) ::
BBr(Nclass,Nclass),BDS(Nclass,Nclass),BSH(Nclass,Nclass),betatotal_1(Nclass,Nclass),V_sed(Nclass),v(Nclass ),fracv(Nclass )


      pi=3.14159

      ! Opening saving files:

      open(41,file='sizedistri_T_mars_alpha0001_Df1.50')
      open(42,file='sizedistri_T_mars_alpha0001_Df2.00')
      open(43,file='sizedistri_T_mars_alpha0001_Df2.50')
      open(44,file='sizedistri_T_mars_alpha0001_Df2.90')

      ! Definition of the duration of timesteps in the command window:
      write(*,*) ' Pas de temps:'
      read(*,*) dt
      ! Maximum time (s):
      tmax=16304
      ! Number of timesteps:
      nt=tmax/dt
      ! Duration of timesteps:
      dt=tmax/nt

      ! Attachment efficiency coefficient:
      alpha = 0.001

      ! Fractal dimension.
      Df = [1.50, 2.00, 2.50, 2.90]

      ! The code is written in order to obtain concentrations distributions at each one of these fractal dimensions:
      do d=1,4
```

```
      ! Temperature (K):
      Temp=296.65
      ! Dynamic viscosity (kg/m/s):
      mu = 8.9d-4
      ! Diameter of primary particles (m):
      d_primary_TiO2 = 5.0d-9
      ! Maximum velocity of effluent (m/s):
      v_max_effluent = 0.06
      ! Water depth in effluent (m):
      z_effluent = 0.5
      ! Water shear rate:
      G = v_max_effluent/z_effluent


      ! Definition of TiO2 sizeclasses (m):
      ! 1. Maximum diameter:
      dmax =100.0d-6
      ! 2. Minimum diameter:
      d_min = 200.0d-9
      ! 3. Length of intervals (logarithmic distribution):
      dstep = (log10(dmax)-log10(d_min))/(Nclass-1)
      ! 4. Definition of sizeclasses:
      do i=1,Nclass
        sizeclass_log (i)= log10(d_min) + (i-1)*dstep
      enddo
      sizeclass = 10.0**sizeclass_log

      ! Initial mass concentration of TiO2 in each size class:
      mass_concentration = [1.99d-1, 4.15d-1, 2.41d-1, 3.85d-2, 1.66d-3, 1.84d-5, 4.92d-8, 3.51d-11, 5.92d-15, 2.26d-19, 4.86d-
24, 5.73d-30, 3.06d-36, 4.07d-43, 1.36d-50]*1d-3



      ! Calculation of sedimentation velocity of TiO2 aggregates, for each size class:
      do i=1,Nclass
        ! number of primary particles in the aggregate:
        nombre_NP(i) = (sizeclass(i)/d_primary_TiO2)**Df(d)

        ! Volume of solid TiO2 in the aggregate:
        V_compact(i) = (4.0*pi/3.0)*nombre_NP(i) *(d_primary_TiO2/2.0)**3
        ! Total volume of the aggregate:
        V_total(i) = 4.0*pi/3.0 *(sizeclass(i)/2.0)**3
        ! Aggregate density:
        ro(i) = (4230.0*V_compact(i) + 1000.0*(V_total(i)-V_compact(i)))/V_total(i)
        ! Aggregate settling velodicity:
        U(i) = sizeclass(i)**2 * 9.81 * (ro(i) - 1000.0) / 36.0 / mu
      enddo
```

```
      ! Mass of the aggregate in each size class:
      masse = V_total (1)* ro(1)
      ! Initial number concentration of aggregates in each size class:
      number_concentration(:) = mass_concentration(:)/masse
      ! Total volume of TiO2, over all size classes:
      V_tot  = sum (V_compact(:))

      ! Calculation of collision rates between aggregates of size classes i and j:
      do i=1,Nclass
        do j=1,Nclass
          ! Collision due to Brownian motion:
          BBr(i,j) =2.0*1.380d-23*temp/3.0/mu*(1.0/(sizeclass(i)/2.0) + 1.0/(sizeclass(j)/2.0))*(sizeclass(i)/2.0 +
sizeclass(j)/2.0)
          ! Collision due to differential settling:
          BDS(i,j) = pi * (sizeclass(i)/2.0 + sizeclass(j)/2.0)**2 * abs(U(i) - U(j))
          ! Collision due to shear rate:
          BSH (i,j) = (sizeclass(i)/2.0 + sizeclass(j)/2.0)**3 * G*4.0/3.0
        enddo
      enddo
      ! Total collision rate:
      betatotal = BBr + BDS + BSH

      ! Setting the initial parameters, N being the particulate concentration of TiO2 in each size class:
      N = number_concentration
      Ngain = 0.0
      Nperte = 0.0

      ! Calculation of initial total volume
      V_tot_0(:) = 4.0*pi/3.0*(sizeclass(:)/2.0)**3*N(:)

      ! Beginning time loop:
      do m = 2,nt
        N_old=N
        NGain=0.0
        NPerte=0.0
        V_tot_old=V_tot

        ! finds the subscript jj, the first one for which the volume is higher than the volume of the sum of the i and j
aggregates:
        do i =1, Nclass
          do j = 1,Nclass
            V_total_sum = V_total(i) + V_total(j)
            do jj=1,Nclass
              if(V_total_sum< V_total(jj)) exit
            enddo
            k = jj
            if(k<Nclass+1) then
              ! Calculation of the fraction used for volume allocation:
```

```
          frac = (V_total(k) - V_total_sum) / (V_total(k) - V_total(k-1))
          ! Allocation of aggregation gains to adjacent size classes using the volume fraction:
          Ngain(k) = Ngain (k) + 0.50*alpha*(1.0-frac)*betatotal_1(i,j)*N_old(i)*N_old(j)
          Ngain(k-1) = Ngain (k-1) + 0.50*alpha*frac*betatotal_1(i,j)*N_old(i)*N_old(j)
          ! Calculation of loss by aggregation to other size classes:
          Nperte(i) = Nperte(i) + alpha*betatotal_1(i,k)*N_old(i)*N_old(k)
        endif
      enddo
    enddo

! Calculation of the analytical solution:
do k = 1,Nclass
  a1=(Ngain(k)-Nperte(k))/(U(k)/z_effluent)
  a2=U_1(k)*dt/z_effluent

  N(k) = (N_old(k)-a1)*exp(-a2) + a1

  ! Calculation of TiO2 volume in size class k:
  V(k) = (4.0*pi/3.0)*(sizeclass(i)/d_primary_TiO2)**Df(d) *(d_primary_TiO2/2.0)**3 * N(k)
enddo

 ! Writting number concentrations in separate files, one for each Df:
 if (d==1) then
 write(41,'(E12.5,<Nclass>(1x,E12.5))') m*dt,(N_1(j),j=1,Nclass)
 endif
 if (d==2) then
 write(42,'(E12.5,<Nclass>(1x,E12.5))') m*dt,(N_1(j),j=1,Nclass)
 endif
 if (d==3) then
 write(43,'(E12.5,<Nclass>(1x,E12.5))') m*dt,(N_1(j),j=1,Nclass)
 endif
 if (d==4) then
 write(44,'(E12.5,<Nclass>(1x,E12.5))') m*dt,(N_1(j),j=1,Nclass)
 endif

! Calculation of total volume of TiO2:
V_tot=sum(V(:))

100  format(' V',i8,2(1x,es12.5))

! Checking that the code returns correct numbers:
do k=1,Nclass
  if(N(k)<1.0d-20) N(k)=0.0
  if(isnan(N(k))) then
    write(*,*) ' nan',m,k
    write(*,*) Ngain(k),Nperte(k)
    write(*,*) N(k)
    stop
```

```
        endif
    enddo

enddo
enddo

! Checking the stability of the code:
write(*,'(E12.5,<Nclass>(1x,E12.5))') (m-1)*dt,(N_1(j),j=1,5)
write(*,*)m,v_tot,v_tot-v_tot_old
end
```

Appendix XB: Fortran code used for the modeling of TiO_2 NMs fate in the river

```
      IMPLICIT NONE

      ! Definition of the parameters type:

      INTEGER, PARAMETER ::  Nclass_TiO2=15
      INTEGER, PARAMETER ::  Nclass_SPM=15
      INTEGER ::  nt,i,j,k,jj,m,d

      REAL(KIND=16) :: dt, tmax,alpha,Temp,mu,Df(4),d_primary_TiO2,v_max_river, z_river,pi
      REAL(KIND=16) :: k_resusp, k_burial, k_transfer, V_water, V_sed, ro_SPM, L_pipe, Area_river, k_river_flow, k_effl_flow
      REAL(KIND=16) :: G,dmin_TiO2, dmax_TiO2, dmin_SPM, dmax_SPM,dstep_TiO2, dstep_SPM, frac
      REAL(KIND=16) :: v_tot,v_tot_old
      REAL(KIND=16) :: sizeclass_log_TiO2(Nclass_TiO2), sizeclass_log_SPM(Nclass_SPM), sizeclass_TiO2(Nclass_TiO2),
sizeclass_SPM(Nclass_SPM), crit(Nclass_SPM)
      REAL(KIND=16) :: N(Nclass_TiO2), q_input_TiO2(Nclass_TiO2)
      REAL(KIND=16) :: V_total_SPM(Nclass_SPM), U_SPM(Nclass_SPM), k_sed_SPM(Nclass_SPM), U_TiO2SPM(Nclass_SPM)
      REAL(KIND=16) :: conc_SPM(Nclass_SPM), conc_SPM_old(Nclass_SPM)
      REAL(KIND=16) :: nombre_NP(Nclass_TiO2),V_compact_TiO2(Nclass_TiO2),V_total_TiO2(Nclass_TiO2),ro_TiO2(Nclass_TiO2)
      REAL(KIND=16) :: U_TiO2(Nclass_TiO2), k_sed_TiO2(Nclass_SPM)
      REAL(KIND=16) :: V_tot_0(Nclass_TiO2),V_total_sum
      REAL(KIND=16) ::
BBr(Nclass_TiO2,Nclass_SPM),BDS(Nclass_TiO2,Nclass_SPM),BSH(Nclass_TiO2,Nclass_SPM),betatotal(Nclass_TiO2,Nclass_SPM),k_hetero(
Nclass_TiO2, Nclass_SPM), v(Nclass_TiO2)
      REAL(KIND=16) :: conc_free_water(Nclass_TiO2), conc_free_water_old(Nclass_TiO2)
      REAL(KIND=16) :: conc_free_sed(Nclass_TiO2), conc_free_sed_old(Nclass_TiO2)
      REAL(KIND=16) :: conc_bound_water(Nclass_SPM), conc_bound_water_old(Nclass_SPM)
      REAL(KIND=16) :: conc_bound_sed(Nclass_SPM), conc_bound_sed_old(Nclass_SPM)
      REAL(KIND=16) :: a_free_water(Nclass_TiO2), b_free_water(Nclass_TiO2), a_free_sed(Nclass_TiO2), b_free_sed(Nclass_TiO2)
      REAL(KIND=16) :: a_bound_water(Nclass_SPM), b_bound_water(Nclass_SPM), a_bound_sed(Nclass_SPM), b_bound_sed(Nclass_SPM)
      REAL(KIND=16) :: k_tot_hetero(Nclass_TiO2), ro_TiO2SPM(Nclass_SPM) ,k_sed_TiO2SPM(Nclass_TiO2), Gain(Nclass_SPM),
V_TiO2(Nclass_SPM)


      pi=3.14159

      ! Opening saving files:

      open(211,file='conc_free_water_janv_alphaT_0001_4_0001_Df150')
      open(212,file='conc_free_water_janv_alphaT_0001_4_0001_Df200')
      open(213,file='conc_free_water_janv_alphaT_0001_4_0001_Df250')
      open(214,file='conc_free_water_janv_alphaT_0001_4_0001_Df290')
      open(221,file='conc_bound_water_janv_alphaT_0001_4_0001_Df150')
      open(222,file='conc_bound_water_janv_alphaT_0001_4_0001_Df200')
      open(223,file='conc_bound_water_janv_alphaT_0001_4_0001_Df250')
      open(224,file='conc_bound_water_janv_alphaT_0001_4_0001_Df290')
```

```
open(231,file='conc_free_sed_janv_alphaT_0001_4_0001_Df150')
open(232,file='conc_free_sed_janv_alphaT_0001_4_0001_Df200')
open(233,file='conc_free_sed_janv_alphaT_0001_4_0001_Df250')
open(234,file='conc_free_sed_janv_alphaT_0001_4_0001_Df290')
open(241,file='conc_bound_sed_janv_alphaT_0001_4_0001_Df150')
open(242,file='conc_bound_sed_janv_alphaT_0001_4_0001_Df200')
open(243,file='conc_bound_sed_janv_alphaT_0001_4_0001_Df250')
open(244,file='conc_bound_sed_janv_alphaT_0001_4_0001_Df290')

! Definition of the duration of timesteps in the command window:
write(*,*) ' Pas de temps:'
read(*,*) dt
! Maximum time (s):
tmax=60
! Number of timesteps:
nt=tmax/dt
! Duration of timesteps:
dt=tmax/nt


! Attachment efficiency coefficient:
alpha = 0.001

! Resuspension rate constant (s-1):
k_resusp = 5.78d-12
! Burial rate constant (s-1):
k_burial = 1.776d-12
! Sediment horizontal transfer rate constant (s-1):
k_transfer = 0.405
! Volume of water (m3):
V_water = 278.25
! Volume of sediment (m3):
V_sed = 46.375
! SPM density (kg/m3):
ro_SPM = 2500
! Temperature (K):
Temp=290.75
! River water dynamic viscosity (kg/m/s):
mu = 1.0d-3
! Fractal dimensions:
Df = [1.5, 2.0, 2.5, 2.9]
! Diameter of primary particles (m):
d_primary_TiO2 = 5.0d-9
! River maximum velocity (m/s):
v_max_river = 6.227
! River water depth (m):
z_river = 0.30
! River water shear rate:
```

```
      G = v_max_river/z_river
      ! Effluent pipe length (m):
      L_pipe = 980
      ! River water cross sectional area (m2)
      Area_river = 0.75
      ! River flow rate constant:
      k_river_flow = v_max_river * Area_river * V_water
      ! Effluent flow rate constant:
      k_effl_flow = 61.544


      ! Definition of SPM sizeclasses (m):
      ! 1. Minimum diameter:
      dmin_SPM = 1.0d-6
      ! 2. Maximum diameter:
      dmax_SPM = 100.0d-6
      ! 3. Length of intervals (logarithmic distribution):
      dstep_SPM = (log10(dmax_SPM)-log10(dmin_SPM))/(Nclass_SPM-1)
      ! 4. Definition of sizeclasses:
      do i=1,Nclass_SPM
        sizeclass_log_SPM (i)= log10(dmin_SPM) + (i-1)*dstep_SPM
      enddo
      sizeclass_SPM = 10.0**sizeclass_log_SPM
      ! Volume of SPM particles in each size class:
      V_total_SPM (:) = (4*pi/3)*(sizeclass_SPM(:)/2.0)**3.0
      ! Settling velocity of SPM partices in each size class:
      U_SPM (:) = (sizeclass_SPM(:)/2.0)*9.81*(ro_SPM-1000)/36.0/mu
      ! SPM deposition constant rate in each size class:
      k_sed_SPM (:) = U_SPM(:)/z_river

      ! Concentration of SPM in each size class:
      conc_SPM = [1.46d9, 2.92d9, 4.25d9, 4.59d9, 3.66d9, 2.15d9, 9.35d8, 3.0d8, 7.08d7, 1.24d7, 1.59d6, 1.52d5, 1.06d4,
5.45d2, 2.07d1]

      ! Definition of TiO2 sizeclasses (m):
      ! 1. Miminum diameter:
      dmin_TiO2 = 200.0d-9
      ! 2. Maximum diameter:
      dmax_TiO2 = 100.0d-6
      ! 3. Length of intervals (logarithmic distribution):
      dstep_TiO2 = (log10(dmax_TiO2)-log10(dmin_TiO2))/(Nclass_TiO2-1)
      ! 4. Definition of sizeclasses:
      do i=1,Nclass_TiO2
        sizeclass_log_TiO2 (i)= log10(dmin_TiO2) + (i-1)*dstep_TiO2
      enddo
      sizeclass_TiO2 = 10.0**sizeclass_log_TiO2
      ! In each size class:
      ! number of primary particles in the aggregate:
```

```
      nombre_NP(:) = (sizeclass_TiO2(:)/d_primary_TiO2)**Df(d)
      ! Volume of solid TiO2 in the aggregate:
      V_compact_TiO2(:) = (4.0*pi/3.0)*nombre_NP(:) * (d_primary_TiO2/2.0)**3
      ! Total volume of the aggregate:
      V_total_TiO2(:) = (4.0*pi/3.0) * (sizeclass_TiO2(:)/2.0)**3
      ! Density of the aggregate:
      ro_TiO2(:) = (4230*V_compact_TiO2(:) + 1000*(V_total_TiO2-V_compact_TiO2))/V_total_TiO2(:)
      ! Settling velocity of the aggregate:
      U_TiO2(:) = (sizeclass_TiO2(:)/2)**2 *9.81 * (ro_TiO2(:)-1000)/36/mu
      ! Aggregate sedimentation constant rate:
      k_sed_TiO2(:) = U_TiO2(:)/z_river
      ! Total volume of TiO2 over all size classes:
      V_tot  = sum (V_compact_TiO2(:))


      ! Definition of initial particle size distribution of homoagggregates, for each fractal dimension, equal to the outputs
of the effluent code:
        do d=1,4
            if (d==1) then
                N = [1.58d12, 3.28d12, 1.91d12, 3.07d11, 1.32d10, 1.46d8, 3.94d5, 2.81d2, 4.77d-2, 1.85d-6, 4.01d-11, 5.44d-17,
2.94d-29, 0, 0]
            elseif (d==2) then
                N = [1.48d12, 3.07d12, 1.79d12, 2.88d11, 1.24d10, 1.37d8, 3.69d5, 2.63d2, 4.46d-2, 1.73d-6, 3.75d-11, 5.10d-17,
2.91d-29, 0, 0]
            elseif (d==3) then
                N = [1.06d12, 2.20d12, 1.28d12, 2.05d11, 8.81d9, 9.75d7, 2.61d5, 1.84d2, 3.07d-2, 1.16d-6, 2.51d-11, 5.05d-17,
1.92d-28, 0, 0]
            elseif (d==4) then
                N = [4.95d11, 1.02d12, 5.95d11, 9.50d10, 4.02d9, 4.30d7, 1.07d5, 6.36d1, 7.26d-3, 1.31d-7, 8.39d-13, 3.35d-18,
1.66d-28, 0, 0]
        endif

      ! TiO2 inflow into the river:
      q_input_TiO2 = N * k_effl_flow * L_pipe


      ! Calculation of collision rates between TiO2 of size class i and SPM of size class j:
      do i=1,Nclass_TiO2
        do j=1,Nclass_SPM
          ! Collision due to Brownian motion:
          BBr(i,j) =2.0*1.380d-23*temp/3.0/mu*(1.0/(sizeclass_TiO2(i)/2.0) + 1.0/(sizeclass_SPM(j)/2.0))*(sizeclass_TiO2(i)/2.0
+ sizeclass_SPM(j)/2.0)
          ! Collision due to differential settling:
          BDS(i,j) = pi * (sizeclass_TiO2(i)/2.0 + sizeclass_SPM(j)/2.0)**2 * abs(U_TiO2(i) - U_SPM(j))
          ! Collitions due to shear rate:
          BSH (i,j) = (sizeclass_TiO2(i)/2.0 + sizeclass_SPM(j)/2.0)**3 * G*4.0/3.0
        enddo
      enddo
```

```
      ! Total collision rate:
      betatotal = BBr + BDS + BSH

      ! Setting the initial concentrations:
      ! Concentration of homoaggregates in water:
      conc_free_water = q_input_TiO2
      ! Concentration of homoaggregates in sediment:
      conc_free_sed = 0.0
      ! Concentration of heteroaggregates in water:
      conc_bound_water = 0.0
      ! Concentration of heteroaggregates in sediment:
      conc_bound_sed = 0.0


     ! Calculation of heteroaggregation constant rate for TiO2 of size class i and SPM of size class j:
     do i=1,Nclass_TiO2
       do j=1,Nclass_SPM
         k_hetero(i,j) = alpha*betatotal(i,j)*conc_SPM(j)
       enddo
       k_tot_hetero = sum (k_hetero,1)
     enddo


      ! Defining constant "a" of the equations analytical solutions:
      do k = 1,Nclass_SPM
        a_free_water (k) = k_river_flow + k_sed_TiO2 (k)+ k_tot_hetero (k)
        a_bound_water(k) = k_river_flow
        a_free_sed(k) = k_resusp + k_burial + k_transfer
        a_bound_sed(k) = k_resusp + k_burial + k_transfer
      enddo


      ! Beginning time loop:
      do m = 2,nt
        conc_free_water_old = conc_free_water
        conc_free_sed_old = conc_free_sed
        conc_bound_water_old = conc_bound_water
        conc_bound_sed_old = conc_bound_sed

        Gain = 0.0
        V_TiO2 = 0.0

      ! finds the subscript jj, the first one for which the volume is higher than the volume of the sum of the i and j
aggregates:
      do i =1, Nclass_TiO2
        do j = 1,Nclass_SPM
          V_total_sum = V_total_TiO2(i) + V_total_SPM(j)
          do jj=1,Nclass_SPM
```

```
          if(V_total_sum< V_total_SPM(jj)) exit
        enddo
        k = jj
        if(k<Nclass_SPM+1) then
          ! Calculation of the fraction used for volume allocation:
          frac = (V_total_SPM(k) - V_total_sum) / (V_total_SPM(k) - V_total_SPM(k-1))
          ! Allocation of aggregation gains to adjacent size classes using the volume fraction:
          Gain(k) = Gain (k) + alpha*(1.0-frac)*betatotal(i,j)*conc_free_water_old(i)*conc_SPM(j)
          Gain(k-1) = Gain (k-1) +alpha*frac*betatotal(i,j)*conc_free_water_old(i)*conc_SPM(j)
          ! Allocation of gained volumes of TiO2 :
          V_TiO2 (k) = V_TiO2 (k) + (1-frac)*V_total_TiO2(i)
          V_TiO2 (k-1) = V_TiO2 (k-1) + frac*V_total_TiO2(i)

        endif
      enddo
    enddo

      ! Calculation of the analytical solutions:
      do k = 1,Nclass_SPM
        ! Density of heteroaggregates:
        ro_TiO2SPM = (ro_TiO2*V_TiO2(k) + ro_SPM*V_total_SPM)/(V_TiO2(k)+V_total_SPM(k))
        ! Settling velocity of heteroaggregates:
        U_TiO2SPM(k) = (sizeclass_SPM(k)/2)**2 *9.81 * (ro_TiO2SPM(k)-1000.0)/36.0/mu
        ! Deposition rate constant of heteroaggregates:
        k_sed_TiO2SPM(k) = U_TiO2SPM(k)/z_river

        ! Calculation of "b" constants in the analytical solutions:
        b_free_water (k) = q_input_TiO2(k)
        b_bound_water(k) = (k_resusp*V_sed/V_water)*conc_bound_sed_old(k) + Gain(k)
        b_free_sed(k) = (k_sed_TiO2(k)*V_water/V_sed)*conc_free_water_old(k)
        b_bound_sed(k) = (k_sed_TiO2SPM(k)*V_water/V_sed)*conc_bound_water_old(k)
        ! Calculations of concentrations:
        conc_free_water (k) = (conc_free_water_old(k) - b_free_water(k)/a_free_water(k))*exp(-a_free_water(k)*dt) +
b_free_water(k)/a_free_water(k)
        conc_bound_water(k) = (conc_bound_water_old(k) - b_bound_water(k)/(a_bound_water(k)+k_sed_TiO2SPM(k)))*exp(-
(a_bound_water(k)+k_sed_TiO2SPM(k))*dt) + b_bound_water(k)/a_bound_water(k)
        conc_free_sed(k) = (conc_free_sed_old(k) - b_free_sed(k)/a_free_sed(k))*exp(-a_free_sed(k)*dt) +
b_free_sed(k)/a_free_sed(k)
        conc_bound_sed(k) = (conc_bound_sed_old(k) - b_bound_sed(k)/a_bound_sed(k))*exp(-a_bound_sed(k)*dt) +
b_bound_sed(k)/a_bound_sed(k)
        ! Calculation of total volume of size class k:
        V(k)= 4.0*pi/3.0*(sizeclass_TiO2 (k)/2.0)**3.0 * (conc_free_water(k) + conc_free_sed(k)) + 4.0*pi/3.0*(sizeclass_SPM
(k)/2.0)**3.0 * (conc_bound_water(k) + conc_bound_sed(k))
        if(conc_free_water(k)<1.0d-30) conc_free_water(k)=0.0
        if(conc_bound_water(k)<1.0d-30) conc_bound_water(k)=0.0
        if(conc_free_sed(k)<1.0d-30) conc_free_sed(k)=0.0
        if(conc_bound_sed(k)<1.0d-30) conc_bound_sed(k)=0.0
      enddo
```

```
        ! Calculation of total volume of aggregates:
        V_tot=sum(V(:))

100   format(' V',i8,2(1x,es12.5))

        ! Checking that the code returns numbers:
        do k=1,Nclass_SPM
          if(isnan(conc_free_water(k))) then
            write(*,*) ' nan_free',m,k
            write(*,*) conc_free_water(k)
            stop
            endif
          if(isnan(conc_bound_water(k))) then
            write(*,*) ' nan_bound',m,k
            write(*,*) conc_bound_water(k)
            stop
          endif
          if(isnan(conc_free_sed(k))) then
            write(*,*) ' nan_free_sed',m,k
            write(*,*) conc_free_sed(k)
            stop
            endif
          if(isnan(conc_bound_sed(k))) then
            write(*,*) ' nan_bound_sed',m,k
            write(*,*) conc_bound_sed(k)
            stop
            endif
        enddo

  ! Writing final concentrations in separate files, one for each Df:
  if ((d==1) .AND. m*dt==tmax) then
       write(211,'(E12.5,<Nclass_TiO2>(1x,E12.5))') m*dt,(conc_free_water(i),i=1,Nclass_TiO2)
       write(221,'(E12.5,<Nclass_SPM>(1x,E12.5))') m*dt,(conc_bound_water(j),j=1,Nclass_SPM)
       write(231,'(E12.5,<Nclass_TiO2>(1x,E12.5))') m*dt,(conc_free_sed(i),i=1,Nclass_TiO2)
       write(241,'(E12.5,<Nclass_SPM>(1x,E12.5))') m*dt,(conc_bound_sed(j),j=1,Nclass_SPM)
  endif

  if ((d==2) .AND. m*dt==tmax) then
       write(212,'(E12.5,<Nclass_TiO2>(1x,E12.5))') m*dt,(conc_free_water(i),i=1,Nclass_TiO2)
       write(222,'(E12.5,<Nclass_SPM>(1x,E12.5))') m*dt,(conc_bound_water(j),j=1,Nclass_SPM)
       write(232,'(E12.5,<Nclass_TiO2>(1x,E12.5))') m*dt,(conc_free_sed(i),i=1,Nclass_TiO2)
       write(242,'(E12.5,<Nclass_SPM>(1x,E12.5))') m*dt,(conc_bound_sed(j),j=1,Nclass_SPM)
  endif

  if ((d==3) .AND. m*dt==tmax) then
```

```
      write(213,'(E12.5,<Nclass_TiO2>(1x,E12.5))') m*dt,(conc_free_water(i),i=1,Nclass_TiO2)
      write(223,'(E12.5,<Nclass_SPM>(1x,E12.5))') m*dt,(conc_bound_water(j),j=1,Nclass_SPM)
      write(233,'(E12.5,<Nclass_TiO2>(1x,E12.5))') m*dt,(conc_free_sed(i),i=1,Nclass_TiO2)
      write(243,'(E12.5,<Nclass_SPM>(1x,E12.5))') m*dt,(conc_bound_sed(j),j=1,Nclass_SPM)
endif

if ((d==4) .AND. m*dt==tmax) then
      write(214,'(E12.5,<Nclass_TiO2>(1x,E12.5))') m*dt,(conc_free_water(i),i=1,Nclass_TiO2)
      write(224,'(E12.5,<Nclass_SPM>(1x,E12.5))') m*dt,(conc_bound_water(j),j=1,Nclass_SPM)
      write(234,'(E12.5,<Nclass_TiO2>(1x,E12.5))') m*dt,(conc_free_sed(i),i=1,Nclass_TiO2)
      write(244,'(E12.5,<Nclass_SPM>(1x,E12.5))') m*dt,(conc_bound_sed(j),j=1,Nclass_SPM)
endif

enddo
enddo


! Checking the code stability:
write(*,*)m,v_tot,v_tot-v_tot_old
end
```

Appendix XIA: Number concentrations of aggregates, obtained at the exit of effluent T

alpha	Df	Month	Sizeclass														
			2,00E-07	3,12E-07	4,86E-07	7,58E-07	1,18E-06	1,84E-06	2,87E-06	4,47E-06	6,97E-06	1,09E-05	1,69E-05	2,64E-05	4,12E-05	6,42E-05	1,00E-04
0	1,5	January	1,58E+12	3,28E+12	1,91E+12	3,06E+11	1,32E+10	1,46E+08	3,91E+05	2,78E+02	4,69E-02	1,79E-06	3,84E-11	4,55E-17	0,00E+00	0,00E+00	0,00E+00
	2		1,48E+12	3,07E+12	1,79E+12	2,87E+11	1,23E+10	1,36E+08	3,67E+05	2,60E+02	4,39E-02	1,68E-06	3,59E-11	4,25E-17	0,00E+00	0,00E+00	0,00E+00
	2,5		1,06E+12	2,20E+12	1,28E+12	2,05E+11	8,79E+09	9,71E+07	2,59E+05	1,82E+02	3,02E-02	1,11E-06	2,20E-11	2,24E-17	0,00E+00	0,00E+00	0,00E+00
	2,9		4,95E+11	1,02E+12	5,95E+11	9,49E+10	4,01E+09	4,29E+07	1,06E+05	6,28E+01	6,87E-03	9,61E-08	1,99E-13	0,00E+00	0,00E+00	0,00E+00	0,00E+00
	1,5	March	4,69E+13	9,78E+13	5,68E+13	9,08E+12	3,91E+11	4,34E+09	1,16E+07	8,27E+03	1,40E+00	5,33E-05	1,15E-09	1,35E-15	0,00E+00	0,00E+00	0,00E+00
	2		4,40E+13	9,17E+13	5,32E+13	8,50E+12	3,67E+11	4,06E+09	1,09E+07	7,75E+03	1,31E+00	4,98E-05	1,07E-09	1,26E-15	0,00E+00	0,00E+00	0,00E+00
	2,5		3,14E+13	6,56E+13	3,81E+13	6,07E+12	2,62E+11	2,89E+09	7,69E+06	5,43E+03	8,97E-01	3,29E-05	6,55E-10	6,65E-16	0,00E+00	0,00E+00	0,00E+00
	2,9		1,47E+13	3,06E+13	1,77E+13	2,81E+12	1,19E+11	1,28E+09	3,16E+06	1,87E+03	2,04E-01	2,85E-06	5,92E-12	3,04E-20	0,00E+00	0,00E+00	0,00E+00
	1,5	May	3,06E+13	6,39E+13	3,72E+13	5,94E+12	2,57E+11	2,83E+09	7,59E+06	5,42E+03	9,12E-01	3,49E-05	7,50E-10	8,84E-16	0,00E+00	0,00E+00	0,00E+00
	2		2,87E+13	5,99E+13	3,49E+13	5,57E+12	2,41E+11	2,65E+09	7,11E+06	5,08E+03	8,54E-01	3,26E-05	7,01E-10	8,25E-16	0,00E+00	0,00E+00	0,00E+00
	2,5		2,05E+13	4,28E+13	2,49E+13	3,98E+12	1,72E+11	1,89E+09	5,03E+06	3,56E+03	5,86E-01	2,16E-05	4,29E-10	4,35E-16	0,00E+00	0,00E+00	0,00E+00
	2,9		9,59E+12	2,00E+13	1,16E+13	1,84E+12	7,84E+10	8,34E+08	2,07E+06	1,22E+03	1,34E-01	1,87E-06	3,87E-12	1,99E-20	0,00E+00	0,00E+00	0,00E+00
	1,5	August	6,36E+13	1,32E+14	7,71E+13	1,23E+13	5,30E+11	5,87E+09	1,57E+07	1,12E+04	1,89E+00	7,24E-05	1,55E-09	1,83E-15	0,00E+00	0,00E+00	0,00E+00
	2		5,96E+13	1,24E+14	7,22E+13	1,16E+13	4,97E+11	5,50E+09	1,47E+07	1,05E+04	1,77E+00	6,77E-05	1,45E-09	1,71E-15	0,00E+00	0,00E+00	0,00E+00
	2,5		4,27E+13	8,88E+13	5,16E+13	8,25E+12	3,55E+11	3,91E+09	1,04E+07	7,36E+03	1,22E+00	4,47E-05	8,87E-10	9,01E-16	0,00E+00	0,00E+00	0,00E+00
	2,9		1,99E+13	4,14E+13	2,40E+13	3,82E+12	1,62E+11	1,73E+09	4,28E+06	2,53E+03	2,77E-01	3,88E-06	8,02E-12	4,13E-20	0,00E+00	0,00E+00	0,00E+00
	1,5	November	4,17E+13	8,70E+13	5,04E+13	8,09E+12	3,49E+11	3,84E+09	1,03E+07	7,35E+03	1,24E+00	4,74E-05	1,02E-09	1,20E-15	0,00E+00	0,00E+00	0,00E+00
	2		3,91E+13	8,15E+13	4,73E+13	7,58E+12	3,27E+11	3,60E+09	9,67E+06	6,89E+03	1,16E+00	4,43E-05	9,52E-10	1,12E-15	0,00E+00	0,00E+00	0,00E+00
	2,5		2,80E+13	5,83E+13	3,38E+13	5,41E+12	2,33E+11	2,56E+09	6,85E+06	4,83E+03	7,99E-01	2,93E-05	5,82E-10	5,91E-16	0,00E+00	0,00E+00	0,00E+00
	2,9		1,31E+13	2,72E+13	1,57E+13	2,50E+12	1,06E+11	1,13E+09	2,81E+06	1,66E+03	1,82E-01	2,54E-06	5,26E-12	2,71E-20	0,00E+00	0,00E+00	0,00E+00
0,001	1,5	January	1,58E+12	3,28E+12	1,91E+12	3,07E+11	1,32E+10	1,46E+08	3,94E+05	2,81E+02	4,77E-02	1,85E-06	4,01E-11	5,44E-17	2,94E-29	0,00E+00	0,00E+00
	2		1,48E+12	3,07E+12	1,79E+12	2,88E+11	1,24E+10	1,37E+08	3,69E+05	2,63E+02	4,46E-02	1,73E-06	3,75E-11	5,10E-17	2,91E-29	0,00E+00	0,00E+00
	2,5		1,06E+12	2,20E+12	1,28E+12	2,05E+11	8,81E+09	9,75E+07	2,61E+05	1,84E+02	3,07E-02	1,16E-06	2,51E-11	5,05E-17	1,92E-28	0,00E+00	0,00E+00
	2,9		4,95E+11	1,02E+12	5,95E+11	9,50E+10	4,02E+09	4,30E+07	1,07E+05	6,36E+01	7,26E-03	1,31E-07	8,39E-13	3,35E-18	1,66E-28	0,00E+00	0,00E+00
	1,5	March	4,53E+13	9,68E+13	5,88E+13	9,78E+12	4,38E+11	5,06E+09	1,44E+07	1,13E+04	2,26E+00	1,21E-04	3,89E-09	3,93E-14	6,55E-25	0,00E+00	0,00E+00
	2		4,26E+13	9,07E+13	5,50E+13	9,12E+12	4,08E+11	4,70E+09	1,33E+07	1,04E+04	2,07E+00	1,10E-04	3,61E-09	3,96E-14	6,94E-25	0,00E+00	0,00E+00
	2,5		3,07E+13	6,51E+13	3,90E+13	6,39E+12	2,82E+11	3,21E+09	8,97E+06	6,92E+03	1,46E+00	1,15E-04	2,30E-08	1,54E-09	1,63E-11	2,25E-21	0,00E+00
	2,9		5,21E+10	1,07E+11	6,00E+10	9,12E+09	3,62E+08	3,48E+06	7,29E+03	3,40E+00	2,76E-04	3,64E-09	3,26E-14	2,91E-17	1,43E-28	1,60E-07	3,19E-15
	1,5	May	3,00E+13	6,34E+13	3,81E+13	6,24E+12	2,77E+11	3,13E+09	8,76E+06	6,64E+03	1,26E+00	6,06E-05	1,69E-09	1,00E-14	1,08E-25	0,00E+00	0,00E+00
	2		2,81E+13	5,95E+13	3,57E+13	5,83E+12	2,58E+11	2,92E+09	8,13E+06	6,15E+03	1,16E+00	5,56E-05	1,58E-09	9,83E-15	1,12E-25	0,00E+00	0,00E+00
	2,5		2,02E+13	4,26E+13	2,53E+13	4,11E+12	1,81E+11	2,02E+09	5,57E+06	4,18E+03	8,10E-01	5,04E-05	4,68E-09	8,64E-12	6,48E-22	0,00E+00	0,00E+00
	2,9		4,31E+10	8,81E+10	4,99E+10	7,58E+09	3,02E+08	2,90E+06	6,12E+03	2,88E+00	2,38E-04	3,32E-09	3,55E-14	8,02E-17	3,28E-28	1,83E-05	3,14E-13
	1,5	August	6,07E+13	1,30E+14	8,07E+13	1,36E+13	6,18E+11	7,24E+09	2,11E+07	1,70E+04	3,61E+00	2,15E-04	7,96E-09	2,69E-19	0,00E+00	0,00E+00	0,00E+00
	2		5,71E+13	1,22E+14	7,54E+13	1,27E+13	5,74E+11	6,70E+09	1,94E+07	1,55E+04	3,28E+00	1,94E-04	7,37E-09	2,53E-19	0,00E+00	0,00E+00	0,00E+00
	2,5		4,13E+13	8,79E+13	5,33E+13	8,83E+12	3,93E+11	4,52E+09	1,28E+07	1,02E+04	2,33E+00	2,32E-04	1,02E-07	1,42E-17	0,00E+00	0,00E+00	0,00E+00
	2,9		5,27E+10	1,08E+11	6,16E+10	9,43E+09	3,75E+08	3,64E+06	7,90E+03	4,25E+00	6,98E-04	2,28E-07	4,60E-05	4,68E-06	2,36E-17	1,31E-03	1,44E-14
	1,5	November	4,05E+13	8,62E+13	5,20E+13	8,64E+12	3,86E+11	4,41E+09	1,25E+07	9,67E+03	1,91E+00	9,89E-05	3,04E-09	2,60E-14	3,84E-25	0,00E+00	0,00E+00
	2		3,80E+13	8,08E+13	4,87E+13	8,06E+12	3,59E+11	4,10E+09	1,16E+07	8,92E+03	1,75E+00	9,02E-05	2,82E-09	2,60E-14	4,04E-25	0,00E+00	0,00E+00
	2,5		2,74E+13	5,79E+13	3,45E+13	5,66E+12	2,50E+11	2,81E+09	7,85E+06	5,99E+03	1,23E+00	9,01E-05	1,41E-08	2,98E-10	6,03E-15	7,36E-25	0,00E+00
	2,9		5,03E+10	1,03E+11	5,80E+10	8,84E+09	3,51E+08	3,36E+06	7,09E+03	3,31E+00	2,71E-04	3,63E-09	3,41E-14	3,90E-17	1,86E-28	8,84E-07	1,71E-14

Appendix XIB: Number concentrations of aggregates, obtained at the exit of effluent NN

alpha	Df	Month	Sizeclass														
			2,00E-07	3,12E-07	4,86E-07	7,58E-07	1,18E-06	1,84E-06	2,87E-06	4,47E-06	6,97E-06	1,09E-05	1,69E-05	2,64E-05	4,12E-05	6,42E-05	1,00E-04
0,1	1,5	January	0	0	0	0	0	0	0	0	0	0	0	0	0	0	0
	2		0	0	0	0	0	0	0	0	0	0	0	0	0	0	0
	2,5		0	0	0	0	0	0	0	0	0	0	0	0	0	0	0
	2,9		0	0	0	0	0	0	0	0	0	0	0	0	0	0	0
	1,5	March	0.28.E+13	5,80E+12	3,41E+12	5,50E+11	2,40E+10	2,73E+08	7,82E+05	6,79E+02	2,20E-01	6,33E-05	0,00E+00	0,00E+00	0,00E+00	0,00E+00	0,00E+00
	2		2,60E+12	5,50E+12	3,20E+12	5,15E+11	2,24E+10	2,55E+08	7,27E+05	6,24E+02	1,95E-01	5,04E-05	0,00E+00	0,00E+00	0,00E+00	0,00E+00	0,00E+00
	2,5		1,90E+12	3,90E+12	2,28E+12	3,67E+11	1,59E+10	1,80E+08	5,04E+05	4,12E+02	1,11E-01	1,89E-05	0,00E+00	0,00E+00	0,00E+00	0,00E+00	0,00E+00
	2,9		8,80E+11	1,80E+12	1,06E+12	1,70E+11	7,35E+09	8,20E+07	2,23E+05	1,71E+02	3,97E-02	5,83E-06	0,00E+00	0,00E+00	0,00E+00	0,00E+00	0,00E+00
	1,5	May	1,50E+12	3,20E+12	1,85E+12	2,97E+11	1,29E+10	1,45E+08	4,02E+05	3,20E+02	7,86E-02	9,99E-06	0,00E+00	0,00E+00	0,00E+00	0,00E+00	0,00E+00
	2		1,40E+12	3,00E+12	1,74E+12	2,78E+11	1,21E+10	1,35E+08	3,75E+05	2,97E+02	7,13E-02	8,50E-06	0,00E+00	0,00E+00	0,00E+00	0,00E+00	0,00E+00
	2,5		1,00E+12	2,10E+12	1,24E+12	1,98E+11	8,61E+09	9,62E+07	2,64E+05	2,03E+02	4,46E-02	4,11E-06	0,00E+00	0,00E+00	0,00E+00	0,00E+00	0,00E+00
	2,9		4,80E+11	1,00E+12	5,79E+11	9,24E+10	3,99E+09	4,43E+07	1,19E+05	8,74E+01	1,73E-02	1,34E-06	0,00E+00	0,00E+00	0,00E+00	0,00E+00	0,00E+00
	1,5	August	2,10E+12	4,30E+12	2,53E+12	4,08E+11	1,78E+10	2,01E+08	5,67E+05	4,70E+02	1,31E-01	2,41E-05	0,00E+00	0,00E+00	0,00E+00	0,00E+00	0,00E+00
	2		2,00E+12	4,06E+12	2,37E+12	3,82E+11	1,66E+10	1,87E+08	5,28E+05	4,34E+02	1,17E-01	1,99E-05	0,00E+00	0,00E+00	0,00E+00	0,00E+00	0,00E+00
	2,5		1,40E+12	2,90E+12	1,70E+12	2,72E+11	1,18E+10	1,33E+08	3,68E+05	2,91E+02	7,02E-02	8,64E-06	0,00E+00	0,00E+00	0,00E+00	0,00E+00	0,00E+00
	2,9		6,50E+11	1,36E+12	7,91E+11	1,27E+11	5,47E+09	6,07E+07	1,64E+05	1,23E+02	2,63E-02	2,91E-06	0,00E+00	0,00E+00	0,00E+00	0,00E+00	0,00E+00
	1,5	November	6,10E+12	1,28E+13	7,53E+12	1,23E+12	5,42E+10	6,32E+08	1,96E+06	2,13E+03	1,31E+00	2,78E-03	4,94E-02	0,00E+00	0,00E+00	0,00E+00	0,00E+00
	2		5,70E+12	1,20E+13	7,05E+12	1,15E+12	5,06E+10	5,89E+08	1,81E+06	1,92E+03	1,10E+00	1,86E-03	1,40E-02	0,00E+00	0,00E+00	0,00E+00	0,00E+00
	2,5		4,10E+12	8,57E+12	5,03E+12	8,14E+11	3,57E+10	4,09E+08	1,21E+06	1,16E+03	5,03E-01	3,60E-04	1,18E-04	0,00E+00	0,00E+00	0,00E+00	0,00E+00
	2,9		1,90E+12	4,01E+12	2,34E+12	3,76E+11	1,63E+10	1,83E+08	5,16E+05	4,39E+02	1,48E-01	8,00E-05	0,00E+00	0,00E+00	0,00E+00	0,00E+00	0,00E+00
0,5	1,5	January	0	0	0	0	0	0	0	0	0	0	0	0	0	0	0
	2		0	0	0	0	0	0	0	0	0	0	0	0	0	0	0
	2,5		0	0	0	0	0	0	0	0	0	0	0	0	0	0	0
	2,9		0	0	0	0	0	0	0	0	0	0	0	0	0	0	0
	1,5	March	2,73E+12	5,76E+12	3,48E+12	5,80E+11	2,66E+10	3,34E+08	1,24E+06	2,13E+03	5,02E+00	1,17E+00	0,00E+00	0,00E+00	0,00E+00	0,00E+00	0,00E+00
	2		2,56E+12	5,40E+12	3,26E+12	5,41E+11	2,47E+10	3,08E+08	1,12E+06	1,83E+03	3,75E+00	5,18E-01	0,00E+00	0,00E+00	0,00E+00	0,00E+00	0,00E+00
	2,5		1,85E+12	3,88E+12	2,32E+12	3,80E+11	1,71E+10	2,06E+08	6,92E+05	9,28E+02	1,08E+00	2,11E-02	0,00E+00	0,00E+00	0,00E+00	0,00E+00	0,00E+00
	2,9		8,71E+11	1,82E+12	1,07E+12	1,73E+11	7,60E+09	8,79E+07	2,66E+05	2,88E+02	2,27E-01	3,81E-03	0,00E+00	0,00E+00	0,00E+00	0,00E+00	0,00E+00
	1,5	May	1,51E+12	3,17E+12	1,87E+12	3,05E+11	1,36E+10	1,61E+08	5,16E+05	6,12E+02	4,93E-01	2,50E-03	0,00E+00	0,00E+00	0,00E+00	0,00E+00	0,00E+00
	2		1,42E+12	2,97E+12	1,75E+12	2,85E+11	1,27E+10	1,50E+08	4,74E+05	5,46E+02	4,05E-01	1,55E-03	0,00E+00	0,00E+00	0,00E+00	0,00E+00	0,00E+00
	2,5		1,02E+12	2,13E+12	1,25E+12	2,02E+11	8,91E+09	1,03E+08	3,13E+05	3,20E+02	1,69E-01	2,23E-04	0,00E+00	0,00E+00	0,00E+00	0,00E+00	0,00E+00
	2,9		4,77E+11	9,95E+11	5,81E+11	9,32E+10	4,06E+09	4,59E+07	1,31E+05	1,16E+02	4,58E-02	4,44E-05	0,00E+00	0,00E+00	0,00E+00	0,00E+00	0,00E+00
	1,5	August	2,05E+12	4,30E+12	2,58E+12	4,26E+11	1,93E+10	2,35E+08	8,09E+05	1,14E+03	1,49E+00	4,04E-02	0,00E+00	0,00E+00	0,00E+00	0,00E+00	0,00E+00
	2		1,92E+12	4,03E+12	2,41E+12	3,98E+11	1,80E+10	2,18E+08	7,38E+05	1,00E+03	1,17E+00	2,16E-02	0,00E+00	0,00E+00	0,00E+00	0,00E+00	0,00E+00
	2,5		1,38E+12	2,89E+12	1,72E+12	2,80E+11	1,25E+10	1,48E+08	4,71E+05	5,47E+02	4,17E-01	1,86E-03	0,00E+00	0,00E+00	0,00E+00	0,00E+00	0,00E+00
	2,9		6,50E+11	1,35E+12	7,95E+11	1,28E+11	5,61E+09	6,41E+07	1,89E+05	1,85E+02	1,07E-01	5,18E-04	0,00E+00	0,00E+00	0,00E+00	0,00E+00	0,00E+00
	1,5	November	0,00E+00	0,00E+00	0,00E+00	0,00E+00	0,00E+00	0,00E+00	0,00E+00	0,00E+00	0,00E+00	0,00E+00	0,00E+00	0,00E+00	0,00E+00	0,00E+00	2,46E+11
	2		0,00E+00	0,00E+00	0,00E+00	0,00E+00	0,00E+00	0,00E+00	0,00E+00	0,00E+00	0,00E+00	0,00E+00	0,00E+00	0,00E+00	0,00E+00	0,00E+00	2,30E+11
	2,5		0,00E+00	0,00E+00	0,00E+00	0,00E+00	0,00E+00	0,00E+00	0,00E+00	0,00E+00	0,00E+00	0,00E+00	0,00E+00	0,00E+00	0,00E+00	0,00E+00	1,51E+11
	2,9		3,51E+09	7,25E+09	4,20E+09	6,64E+08	2,81E+07	3,10E+05	9,40E+02	1,25E+00	2,93E-03	1,52E-02	8,15E-03	6,85E-03	2,38E-06	0,00E+00	8,90E+10

alpha	Df	Sizeclass	2,00E-07	3,12E-07	4,86E-07	7,58E-07	1,18E-06	1,84E-06	2,87E-06	4,47E-06	6,97E-06	1,09E-05	1,69E-05	2,64E-05	4,12E-05	6,42E-05	1,00E-04
1	1,5	January	0	0	0	0	0	0	0	0	0	0	0	0	0	0	0
	2		0	0	0	0	0	0	0	0	0	0	0	0	0	0	0
	2,5		0	0	0	0	0	0	0	0	0	0	0	0	0	0	0
	2,9		0	0	0	0	0	0	0	0	0	0	0	0	0	0	0
	1,5	March	5,69E+03	1,14E+04	6,38E+03	9,31E+02	3,45E+01	3,16E-01	7,62E-04	8,08E-07	0,00E+00	1,78E-08	0,00E+00	0,00E+00	0,00E+00	0,00E+00	1,12E+11
	2		1,24E+08	2,56E+08	1,51E+08	2,39E+07	1,01E+06	1,14E+04	3,79E+01	6,79E-02	3,94E-04	1,55E-02	4,13E-03	8,84E-04	2,96E-07	0,00E+00	1,05E+11
	2,5		1,81E+12	3,85E+12	2,36E+12	3,98E+11	1,86E+10	2,44E+08	1,01E+06	2,30E+03	1,35E+01	1,09E+02	7,26E-06	0,00E+00	0,00E+00	0,00E+00	0,00E+00
	2,9		8,64E+11	1,81E+12	1,08E+12	1,77E+11	7,92E+09	9,58E+07	3,30E+05	5,24E+02	1,59E+00	1,06E+01	0,00E+00	0,00E+00	0,00E+00	0,00E+00	0,00E+00
	1,5	May	1,49E+12	3,15E+12	1,90E+12	3,15E+11	1,45E+10	1,83E+08	6,94E+05	1,27E+03	3,69E+00	1,86E+00	1,47E-05	0,00E+00	0,00E+00	0,00E+00	0,00E+00
	2		1,40E+12	2,95E+12	1,77E+12	2,94E+11	1,35E+10	1,69E+08	6,27E+05	1,09E+03	2,71E+00	7,68E-01	0,00E+00	0,00E+00	0,00E+00	0,00E+00	0,00E+00
	2,5		1,01E+12	2,12E+12	1,26E+12	2,07E+11	9,31E+09	1,13E+08	3,85E+05	5,41E+02	7,25E-01	2,33E-02	0,00E+00	0,00E+00	0,00E+00	0,00E+00	0,00E+00
	2,9		4,75E+11	9,93E+11	5,83E+11	9,41E+10	4,15E+09	4,80E+07	1,47E+05	1,62E+02	1,36E-01	2,65E-03	0,00E+00	0,00E+00	0,00E+00	0,00E+00	0,00E+00
	1,5	August	2,93E+09	6,10E+09	3,63E+09	5,86E+08	2,55E+07	2,95E+05	1,01E+03	1,69E+00	5,99E-03	1,99E-02	1,24E-02	1,35E-02	1,44E-04	0,00E+00	8,31E+10
	2		1,88E+12	4,00E+12	2,46E+12	4,19E+11	1,98E+10	2,62E+08	1,10E+06	2,55E+03	1,51E+01	1,07E+02	1,28E+02	7,60E+01	3,17E+00	5,34E-06	0,00E+00
	2,5		1,36E+12	2,88E+12	1,74E+12	2,91E+11	1,34E+10	1,69E+08	6,32E+05	1,12E+03	2,94E+00	1,14E+00	0,00E+00	0,00E+00	0,00E+00	0,00E+00	0,00E+00
	2,9		6,46E+11	1,35E+12	8,00E+11	1,31E+11	5,81E+09	6,86E+07	2,23E+05	2,99E+02	5,06E-01	2,71E-01	0,00E+00	0,00E+00	0,00E+00	0,00E+00	0,00E+00
	1,5	November	0,00E+00	0,00E+00	0,00E+00	0,00E+00	0,00E+00	0,00E+00	0,00E+00	0,00E+00	0,00E+00	0,00E+00	0,00E+00	0,00E+00	0,00E+00	0,00E+00	2,46E+11
	2		0,00E+00	0,00E+00	0,00E+00	0,00E+00	0,00E+00	0,00E+00	0,00E+00	0,00E+00	0,00E+00	0,00E+00	0,00E+00	0,00E+00	0,00E+00	0,00E+00	2,30E+11
	2,5		0,00E+00	0,00E+00	0,00E+00	0,00E+00	0,00E+00	0,00E+00	0,00E+00	0,00E+00	0,00E+00	0,00E+00	0,00E+00	0,00E+00	0,00E+00	0,00E+00	1,43E+11
	2,9		0,00E+00	0,00E+00	0,00E+00	0,00E+00	0,00E+00	0,00E+00	0,00E+00	0,00E+00	0,00E+00	0,00E+00	0,00E+00	0,00E+00	0,00E+00	0,00E+00	1,16E+08

Appendix XI: Number concentrations of aggregates, obtained at point 4, with alpha (T) = 0

alpha river	Month	State of aggregation	Df	Sizeclass													
				2,00E-07	3,12E-07	4,86E-07	7,58E-07	1,18E-06	1,84E-06	2,87E-06	4,47E-06	6,97E-06	1,09E-05	1,69E-05	2,64E-05	4,12E-05	6,42E-05	1,00E-04
0	January	homoaggregates in water	1,5	7,33E+13	1,52E+14	8,86E+13	1,42E+13	6,13E+11	6,78E+09	1,81E+07	1,29E+04	2,18E+00	8,31E-05	1,78E-09	2,11E-15	0,00E+00	0,00E+00	0,00E+00
			2	6,87E+13	1,42E+14	8,31E+13	1,33E+13	5,71E+11	6,31E+09	1,70E+07	1,21E+04	2,04E+00	7,80E-05	1,67E-09	1,97E-15	0,00E+00	0,00E+00	0,00E+00
			2,5	4,92E+13	1,02E+14	5,94E+13	9,51E+12	4,08E+11	4,51E+09	1,20E+07	8,45E+03	1,40E+00	5,15E-05	1,02E-09	1,04E-15	0,00E+00	0,00E+00	0,00E+00
			2,9	2,30E+13	4,73E+13	2,76E+13	4,40E+12	1,86E+11	1,99E+09	4,92E+06	2,91E+03	3,19E-01	4,46E-06	9,24E-12	0,00E+00	0,00E+00	0,00E+00	0,00E+00
		homoaggregates in sediment	1,5	3,12E+06	8,08E+06	5,87E+06	1,17E+06	6,32E+04	8,73E+02	2,92E+00	2,59E-03	5,46E-07	2,60E-11	6,97E-16	0,00E+00	0,00E+00	0,00E+00	0,00E+00
			2	1,85E+07	5,97E+07	5,42E+07	1,36E+07	9,06E+05	1,56E+04	6,57E+01	7,25E-02	1,91E-05	1,14E-09	3,79E-14	0,00E+00	0,00E+00	0,00E+00	0,00E+00
			2,5	8,36E+07	3,38E+08	3,82E+08	1,19E+08	9,95E+06	2,14E+05	1,11E+03	1,52E+00	4,90E-04	3,51E-08	1,35E-12	0,00E+00	0,00E+00	0,00E+00	0,00E+00
			2,9	1,71E+08	8,18E+08	1,11E+09	4,11E+08	4,04E+07	1,00E+06	5,77E+03	7,94E+00	2,02E-03	6,56E-08	3,16E-13	0,00E+00	0,00E+00	0,00E+00	0,00E+00
				Sizeclass														
				1,00E-06	1,39E-06	1,93E-06	2,69E-06	3,74E-06	5,19E-06	7,22E-06	1,00E-05	1,40E-05	1,94E-05	2,70E-05	3,75E-05	5,21E-05	7,24E-05	1,00E-04
		heteroaggregates in water	1,5	0	0	0	0	0	0	0	0	0	0	0	0	0	0	0
			2	0	0	0	0	0	0	0	0	0	0	0	0	0	0	0
			2,5	0	0	0	0	0	0	0	0	0	0	0	0	0	0	0
			2,9	0	0	0	0	0	0	0	0	0	0	0	0	0	0	0
		heteroaggregates in sediment	1,5	0	0	0	0	0	0	0	0	0	0	0	0	0	0	0
			2	0	0	0	0	0	0	0	0	0	0	0	0	0	0	0
			2,5	0	0	0	0	0	0	0	0	0	0	0	0	0	0	0
			2,9	0	0	0	0	0	0	0	0	0	0	0	0	0	0	0
	March			Sizeclass														
				2,00E-07	3,12E-07	4,86E-07	7,58E-07	1,18E-06	1,84E-06	2,87E-06	4,47E-06	6,97E-06	1,09E-05	1,69E-05	2,64E-05	4,12E-05	6,42E-05	1,00E-04
		homoaggregates in water	1,5	1,36E+15	2,83E+15	1,64E+15	2,63E+14	1,13E+13	1,26E+11	3,36E+08	2,39E+05	4,05E+01	1,54E-03	3,33E-08	3,91E-14	0,00E+00	0,00E+00	0,00E+00
			2	1,27E+15	2,65E+15	1,54E+15	2,46E+14	1,06E+13	1,17E+11	3,15E+08	2,24E+05	3,79E+01	1,44E-06	3,10E-08	3,65E-14	0,00E+00	0,00E+00	0,00E+00
			2,5	9,09E+14	1,90E+15	1,10E+15	1,76E+14	7,58E+12	8,36E+10	2,23E+08	1,57E+05	2,60E+01	9,52E-04	1,90E-08	1,92E-14	0,00E+00	0,00E+00	0,00E+00
			2,9	4,25E+14	8,86E+14	5,12E+14	8,13E+13	3,44E+12	3,70E+10	9,14E+07	5,41E+04	5,90E+00	8,25E-05	1,71E-10	8,80E-19	0,00E+00	0,00E+00	0,00E+00
		homoaggregates in sediment	1,5	3,16E+07	8,22E+07	5,96E+07	1,19E+07	6,39E+05	8,86E+03	2,96E+01	2,63E-02	5,56E-06	2,64E-10	7,12E-15	0,00E+00	0,00E+00	0,00E+00	0,00E+00
			2	1,87E+08	6,08E+08	5,50E+08	1,37E+08	9,22E+06	1,59E+05	6,66E+02	7,38E-01	1,94E-04	1,15E-11	3,86E-13	0,00E+00	0,00E+00	0,00E+00	0,00E+00
			2,5	8,45E+08	3,44E+09	3,88E+09	1,20E+09	1,01E+08	2,17E+06	1,12E+04	1,55E+01	4,97E-03	3,55E-07	1,37E-11	2,72E-17	0,00E+00	0,00E+00	0,00E+00
			2,9	1,73E+09	8,37E+09	1,13E+10	4,15E+09	4,09E+08	1,02E+07	5,87E+04	8,07E+01	2,05E-02	6,64E-07	3,21E-12	0,00E+00	0,00E+00	0,00E+00	0,00E+00
				Sizeclass														
				1,00E-06	1,39E-06	1,93E-06	2,69E-06	3,74E-06	5,19E-06	7,22E-06	1,00E-05	1,40E-05	1,94E-05	2,70E-05	3,75E-05	5,21E-05	7,24E-05	1,00E-04
		heteroaggregates in water	1,5	0	0	0	0	0	0	0	0	0	0	0	0	0	0	0
			2	0	0	0	0	0	0	0	0	0	0	0	0	0	0	0
			2,5	0	0	0	0	0	0	0	0	0	0	0	0	0	0	0
			2,9	0	0	0	0	0	0	0	0	0	0	0	0	0	0	0
		heteroaggregates in sediment	1,5	0	0	0	0	0	0	0	0	0	0	0	0	0	0	0
			2	0	0	0	0	0	0	0	0	0	0	0	0	0	0	0
			2,5	0	0	0	0	0	0	0	0	0	0	0	0	0	0	0
			2,9	0	0	0	0	0	0	0	0	0	0	0	0	0	0	0

alpha river	Month	State of aggregation	Df	Sizeclass													
				2,00E-07	3,12E-07	4,86E-07	7,58E-07	1,18E-06	1,84E-06	2,87E-06	4,47E-06	6,97E-06	1,09E-05	1,69E-05	2,64E-05	4,12E-05	6,42E-05	1,00E-04
0	May	homoaggregates in water	1,5	5,26E+15	1,10E+16	6,40E+15	1,02E+15	4,42E+13	4,87E+11	1,31E+09	9,32E+05	1,57E+02	6,00E-03	1,29E-07	1,52E-13	0,00E+00	0,00E+00	0,00E+00
			2	4,94E+15	1,03E+16	6,00E+15	9,58E+14	4,15E+13	4,56E+11	1,22E+09	8,74E+05	1,47E+02	5,61E-03	1,21E-07	1,42E-13	0,00E+00	0,00E+00	0,00E+00
			2,5	3,53E+15	7,36E+15	4,28E+15	6,85E+14	2,96E+13	3,25E+11	8,65E+08	6,12E+05	1,01E+02	3,72E-03	7,38E-08	7,48E-14	0,00E+00	0,00E+00	0,00E+00
			2,9	1,65E+15	3,44E+15	2,00E+15	3,17E+14	1,35E+13	1,43E+11	3,56E+08	2,10E+05	2,31E+01	3,22E-04	6,66E-10	3,42E-18	0,00E+00	0,00E+00	0,00E+00
		homoaggregates in sediment	1,5	3,63E+08	9,46E+08	6,87E+08	1,37E+08	7,40E+06	1,02E+05	3,41E+02	3,04E-01	6,38E-05	3,05E-09	8,18E-14	0,00E+00	0,00E+00	0,00E+00	0,00E+00
			2	2,15E+09	7,00E+09	6,36E+09	1,58E+09	1,07E+08	1,83E+06	7,65E+03	8,51E+00	2,23E-03	1,33E-07	4,45E-12	0,00E+00	0,00E+00	0,00E+00	0,00E+00
			2,5	9,72E+09	3,95E+10	4,47E+10	1,39E+10	1,17E+09	2,50E+07	1,30E+05	1,78E+02	5,72E-02	4,10E-06	1,59E-10	3,13E-16	0,00E+00	0,00E+00	0,00E+00
			2,9	1,99E+10	9,64E+10	1,30E+11	4,79E+10	4,74E+09	1,17E+08	6,77E+05	9,27E+02	2,37E-01	7,68E-06	3,69E-11	0,00E+00	0,00E+00	0,00E+00	0,00E+00
				Sizeclass														
				1,00E-06	1,39E-06	1,93E-06	2,69E-06	3,74E-06	5,19E-06	7,22E-06	1,00E-05	1,40E-05	1,94E-05	2,70E-05	3,75E-05	5,21E-05	7,24E-05	1,00E-04
		heteroaggregates in water	1,5	0	0	0	0	0	0	0	0	0	0	0	0	0	0	0
			2	0	0	0	0	0	0	0	0	0	0	0	0	0	0	0
			2,5	0	0	0	0	0	0	0	0	0	0	0	0	0	0	0
			2,9	0	0	0	0	0	0	0	0	0	0	0	0	0	0	0
		heteroaggregates in sediment	1,5	0	0	0	0	0	0	0	0	0	0	0	0	0	0	0
			2	0	0	0	0	0	0	0	0	0	0	0	0	0	0	0
			2,5	0	0	0	0	0	0	0	0	0	0	0	0	0	0	0
			2,9	0	0	0	0	0	0	0	0	0	0	0	0	0	0	0
	August			Sizeclass														
				2,00E-07	3,12E-07	4,86E-07	7,58E-07	1,18E-06	1,84E-06	2,87E-06	4,47E-06	6,97E-06	1,09E-05	1,69E-05	2,64E-05	4,12E-05	6,42E-05	1,00E-04
		homoaggregates in water	1,5	2,19E+15	4,54E+15	2,65E+15	4,23E+14	1,82E+13	2,02E+11	5,40E+08	3,85E+05	6,50E+01	2,49E-03	5,33E-08	6,29E-14	0,00E+00	0,00E+00	0,00E+00
			2	2,05E+15	4,26E+15	2,48E+15	3,99E+14	1,71E+13	1,89E+11	5,05E+08	3,61E+05	6,08E+01	2,33E-03	4,98E-08	5,88E-14	0,00E+00	0,00E+00	0,00E+00
			2,5	1,47E+15	3,05E+15	1,77E+15	2,84E+14	1,22E+13	1,34E+11	3,57E+08	2,53E+05	4,19E+01	1,54E-03	3,05E-08	3,10E-14	0,00E+00	0,00E+00	0,00E+00
			2,9	6,84E+14	1,42E+15	8,25E+14	1,31E+14	5,57E+12	5,95E+10	1,47E+08	8,70E+04	9,52E+00	1,33E-04	2,76E-10	1,42E-18	0,00E+00	0,00E+00	0,00E+00
		homoaggregates in sediment	1,5	1,06E+08	2,73E+08	1,99E+08	3,97E+07	2,14E+06	2,95E+04	9,86E+01	8,79E-02	1,85E-05	8,85E-10	2,37E-14	0,00E+00	0,00E+00	0,00E+00	0,00E+00
			2	6,25E+08	2,03E+09	1,84E+09	4,61E+08	3,08E+07	5,31E+05	2,21E+03	2,46E+00	6,47E-04	3,86E-08	1,29E-12	0,00E+00	0,00E+00	0,00E+00	0,00E+00
			2,5	2,83E+09	1,15E+10	1,30E+10	4,04E+09	3,38E+08	7,24E+06	3,75E+04	5,16E+01	1,67E-02	1,19E-06	4,59E-11	9,07E-17	0,00E+00	0,00E+00	0,00E+00
			2,9	5,78E+09	2,79E+10	3,76E+10	1,39E+10	1,37E+09	3,41E+07	1,96E+05	2,69E+02	6,85E-02	2,23E-06	1,07E-11	0,00E+00	0,00E+00	0,00E+00	0,00E+00
				Sizeclass														
				1,00E-06	1,39E-06	1,93E-06	2,69E-06	3,74E-06	5,19E-06	7,22E-06	1,00E-05	1,40E-05	1,94E-05	2,70E-05	3,75E-05	5,21E-05	7,24E-05	1,00E-04
		heteroaggregates in water	1,5	0	0	0	0	0	0	0	0	0	0	0	0	0	0	0
			2	0	0	0	0	0	0	0	0	0	0	0	0	0	0	0
			2,5	0	0	0	0	0	0	0	0	0	0	0	0	0	0	0
			2,9	0	0	0	0	0	0	0	0	0	0	0	0	0	0	0
		heteroaggregates in sediment	1,5	0	0	0	0	0	0	0	0	0	0	0	0	0	0	0
			2	0	0	0	0	0	0	0	0	0	0	0	0	0	0	0
			2,5	0	0	0	0	0	0	0	0	0	0	0	0	0	0	0
			2,9	0	0	0	0	0	0	0	0	0	0	0	0	0	0	0

alpha river	Month	State of aggregation	Df	Sizeclass														
				2,00E-07	3,12E-07	4,86E-07	7,58E-07	1,18E-06	1,84E-06	2,87E-06	4,47E-06	6,97E-06	1,09E-05	1,69E-05	2,64E-05	4,12E-05	6,42E-05	1,00E-04
0	November	homoaggregates in water	1,5	2,12E+15	4,43E+15	2,57E+15	4,12E+14	1,78E+13	1,95E+11	5,24E+08	3,74E+05	6,31E+01	2,41E-03	5,19E-08	6,11E-14	0,00E+00	0,00E+00	0,00E+00
			2	1,99E+15	4,15E+15	2,41E+15	3,86E+14	1,66E+13	1,83E+11	4,92E+08	3,51E+05	5,91E+01	2,26E-03	4,85E-08	5,70E-14	0,00E+00	0,00E+00	0,00E+00
			2,5	1,43E+15	2,97E+15	1,72E+15	2,75E+14	1,19E+13	1,30E+11	3,49E+08	2,46E+05	4,07E+01	1,49E-03	2,96E-08	3,01E-14	0,00E+00	0,00E+00	0,00E+00
			2,9	6,67E+14	1,38E+15	7,99E+14	1,27E+14	5,40E+12	5,75E+10	1,43E+08	8,45E+04	9,27E+00	1,29E-04	2,68E-10	1,38E-18	0,00E+00	0,00E+00	0,00E+00
		homoaggregates in sediment	1,5	1,33E+08	3,46E+08	2,51E+08	5,02E+07	2,70E+06	3,72E+04	1,24E+02	1,11E-01	2,34E-05	1,11E-09	2,99E-14	0,00E+00	0,00E+00	0,00E+00	0,00E+00
			2	7,89E+08	2,56E+09	2,32E+09	5,79E+08	3,89E+07	6,68E+05	2,80E+03	3,11E+00	8,16E-04	4,86E-08	1,63E-12	0,00E+00	0,00E+00	0,00E+00	0,00E+00
			2,5	3,57E+09	1,45E+10	1,63E+10	5,09E+09	4,26E+08	9,12E+06	4,75E+04	6,52E+01	2,10E-02	1,50E-06	5,79E-11	1,14E-16	0,00E+00	0,00E+00	0,00E+00
			2,9	7,31E+09	3,53E+10	4,73E+10	1,75E+10	1,73E+09	4,28E+07	2,47E+05	3,39E+02	8,65E-02	2,81E-06	1,35E-11	0,00E+00	0,00E+00	0,00E+00	0,00E+00
				Sizeclass														
				1,00E-06	1,39E-06	1,93E-06	2,69E-06	3,74E-06	5,19E-06	7,22E-06	1,00E-05	1,40E-05	1,94E-05	2,70E-05	3,75E-05	5,21E-05	7,24E-05	1,00E-04
		heteroaggregates in water	1,5	0	0	0	0	0	0	0	0	0	0	0	0	0	0	0
			2	0	0	0	0	0	0	0	0	0	0	0	0	0	0	0
			2,5	0	0	0	0	0	0	0	0	0	0	0	0	0	0	0
			2,9	0	0	0	0	0	0	0	0	0	0	0	0	0	0	0
		heteroaggregates in sediment	1,5	0	0	0	0	0	0	0	0	0	0	0	0	0	0	0
			2	0	0	0	0	0	0	0	0	0	0	0	0	0	0	0
			2,5	0	0	0	0	0	0	0	0	0	0	0	0	0	0	0
			2,9	0	0	0	0	0	0	0	0	0	0	0	0	0	0	0

alpha river	Month	State of aggregation	Df	Sizeclass													
				2,00E-07	**3,12E-07**	**4,86E-07**	**7,58E-07**	**1,18E-06**	**1,84E-06**	**2,87E-06**	**4,47E-06**	**6,97E-06**	**1,09E-05**	**1,69E-05**	**2,64E-05**	**4,12E-05**	**6,42E-05**	**1,00E-04**
0,001	January	homoaggregates in water	**1,5**	7,33E+13	1,52E+14	8,86E+13	1,42E+13	6,13E+11	6,78E+09	1,81E+07	1,29E+04	2,18E+00	8,31E-05	1,78E-09	2,11E-15	0,00E+00	0,00E+00	0,00E+00
			2	6,87E+13	1,42E+14	8,31E+13	1,33E+13	5,71E+11	6,31E+09	1,70E+07	1,21E+04	2,04E+00	7,80E-05	1,67E-09	1,97E-15	0,00E+00	0,00E+00	0,00E+00
			2,5	4,92E+13	1,02E+14	5,94E+13	9,51E+12	4,08E+11	4,51E+09	1,20E+07	8,45E+03	1,40E+00	5,15E-05	1,02E-09	1,04E-15	0,00E+00	0,00E+00	0,00E+00
			2,9	2,30E+13	4,73E+13	2,76E+13	4,40E+12	1,86E+11	1,99E+09	4,92E+06	2,91E+03	3,19E-01	4,46E-06	9,24E-12	0,00E+00	0,00E+00	0,00E+00	0,00E+00
		homoaggregates in sediment	**1,5**	3,12E+06	8,08E+06	5,87E+06	1,17E+06	6,32E+04	8,73E+02	2,92E+00	2,59E-03	5,46E-07	2,60E-11	6,97E-16	0,00E+00	0,00E+00	0,00E+00	0,00E+00
			2	1,85E+07	5,97E+07	5,42E+07	1,36E+07	9,06E+05	1,56E+04	6,57E+01	7,25E-02	1,91E-05	1,14E-09	3,79E-14	0,00E+00	0,00E+00	0,00E+00	0,00E+00
			2,5	8,36E+07	3,38E+08	3,82E+08	1,19E+08	9,95E+06	2,14E+05	1,11E+03	1,52E+00	4,90E-04	3,51E-08	1,35E-12	0,00E+00	0,00E+00	0,00E+00	0,00E+00
			2,9	1,71E+08	8,18E+08	1,11E+09	4,11E+08	4,04E+07	1,00E+06	5,77E+03	7,94E+00	2,02E-03	6,56E-08	3,16E-13	0,00E+00	0,00E+00	0,00E+00	0,00E+00
				Sizeclass														
				1,00E-06	**1,39E-06**	**1,93E-06**	**2,69E-06**	**3,74E-06**	**5,19E-06**	**7,22E-06**	**1,00E-05**	**1,40E-05**	**1,94E-05**	**2,70E-05**	**3,75E-05**	**5,21E-05**	**7,24E-05**	**1,00E-04**
		heteroaggregates in water	**1,5**	1,04E+05	5,01E+05	1,75E+06	4,63E+06	9,25E+06	1,39E+07	1,56E+07	1,31E+07	8,12E+06	3,76E+06	1,28E+06	3,26E+05	6,07E+04	8,34E+03	9,18E-04
			2	9,75E+04	4,69E+05	1,64E+06	4,33E+06	8,67E+06	1,30E+07	1,46E+07	1,22E+07	7,60E+06	3,52E+06	1,20E+06	3,05E+05	5,68E+04	7,81E+03	8,60E-04
			2,5	6,98E+04	3,36E+05	1,17E+06	3,10E+06	6,21E+06	9,30E+06	1,05E+07	8,77E+06	5,44E+06	2,52E+06	8,59E+05	2,19E+05	4,07E+04	5,59E+03	6,15E-04
			2,9	3,24E+04	1,56E+05	5,44E+05	1,44E+06	2,88E+06	4,32E+06	4,86E+06	4,07E+06	2,53E+06	1,17E+06	3,99E+05	1,02E+05	1,89E+04	2,60E+03	2,85E-04
		heteroaggregates in sediment	**1,5**	8,68E+00	5,43E+01	2,41E+02	8,87E+02	2,92E+03	9,82E+03	1,51E+04	1,82E+04	2,06E+04	2,74E+04	1,08E+04	4,26E+03	1,54E+03	7,51E+02	1,01E-03
			2	8,32E+00	5,27E+01	2,36E+02	8,71E+02	2,84E+03	9,39E+03	1,45E+04	1,74E+04	1,96E+04	2,58E+04	1,02E+04	4,01E+03	1,45E+03	7,04E+02	9,48E-04
			2,5	6,79E+00	4,84E+01	2,44E+02	9,76E+02	3,19E+03	9,33E+03	1,53E+04	1,92E+04	2,06E+04	2,29E+04	9,81E+03	3,90E+03	1,33E+03	5,63E+02	6,79E-04
			2,9	4,71E+00	4,64E+01	3,18E+02	1,60E+03	6,01E+03	1,67E+04	3,52E+04	5,50E+04	6,33E+04	5,45E+04	3,44E+04	1,62E+04	5,59E+03	1,44E+03	3,48E-04
	March			Sizeclass														
				2,00E-07	**3,12E-07**	**4,86E-07**	**7,58E-07**	**1,18E-06**	**1,84E-06**	**2,87E-06**	**4,47E-06**	**6,97E-06**	**1,09E-05**	**1,69E-05**	**2,64E-05**	**4,12E-05**	**6,42E-05**	**1,00E-04**
		homoaggregates in water	**1,5**	1,36E+15	2,83E+15	1,64E+15	2,63E+14	1,13E+13	1,26E+11	3,36E+08	2,39E+05	4,05E+01	1,54E-03	3,33E-08	3,91E-14	0,00E+00	0,00E+00	0,00E+00
			2	1,27E+15	2,65E+15	1,54E+15	2,46E+14	1,06E+13	1,17E+11	3,15E+08	2,24E+05	3,79E+01	1,44E-06	3,10E-08	3,65E-14	0,00E+00	0,00E+00	0,00E+00
			2,5	9,09E+14	1,90E+15	1,10E+15	1,76E+14	7,58E+12	8,36E+10	2,23E+08	1,57E+05	2,60E+01	9,52E-04	1,90E-08	1,92E-14	0,00E+00	0,00E+00	0,00E+00
			2,9	4,25E+14	8,86E+14	5,12E+14	8,13E+13	3,44E+12	3,70E+10	9,14E+07	5,41E+04	5,90E+00	8,25E-05	1,71E-10	8,80E-19	0,00E+00	0,00E+00	0,00E+00
		homoaggregates in sediment	**1,5**	3,16E+07	8,22E+07	5,96E+07	1,19E+07	6,39E+05	8,86E+03	2,96E+01	2,63E-02	5,56E-06	2,64E-10	7,12E-15	0,00E+00	0,00E+00	0,00E+00	0,00E+00
			2	1,87E+08	6,08E+08	5,50E+08	1,37E+08	9,22E+06	1,59E+05	6,66E+02	7,38E-01	1,94E-04	1,15E-11	3,86E-13	0,00E+00	0,00E+00	0,00E+00	0,00E+00
			2,5	8,45E+08	3,44E+09	3,88E+09	1,20E+09	1,01E+08	2,17E+06	1,12E+04	1,55E+01	4,97E-03	3,55E-07	1,37E-11	2,72E-17	0,00E+00	0,00E+00	0,00E+00
			2,9	1,73E+09	8,37E+09	1,13E+10	4,15E+09	4,09E+08	1,02E+07	5,87E+04	8,07E+01	2,05E-02	6,64E-07	3,21E-12	0,00E+00	0,00E+00	0,00E+00	0,00E+00
				Sizeclass														
				1,00E-06	**1,39E-06**	**1,93E-06**	**2,69E-06**	**3,74E-06**	**5,19E-06**	**7,22E-06**	**1,00E-05**	**1,40E-05**	**1,94E-05**	**2,70E-05**	**3,75E-05**	**5,21E-05**	**7,24E-05**	**1,00E-04**
		heteroaggregates in water	**1,5**	1,06E+06	5,09E+06	1,77E+07	4,70E+07	9,39E+07	1,41E+08	1,58E+08	1,33E+08	8,24E+07	3,82E+07	1,30E+07	3,31E+06	6,16E+05	8,46E+04	9,31E-03
			2	9,91E+05	4,77E+06	1,66E+07	4,40E+07	8,80E+07	1,32E+08	1,48E+08	1,24E+08	7,72E+07	3,58E+07	1,22E+07	3,10E+06	5,77E+05	7,93E+04	8,72E-03
			2,5	7,08E+05	3,41E+06	1,19E+07	3,15E+07	6,30E+07	9,44E+07	1,06E+08	8,90E+07	5,52E+07	2,56E+07	8,72E+06	2,22E+06	4,13E+05	5,67E+04	6,24E-03
			2,9	3,30E+05	1,59E+06	5,54E+06	1,47E+07	2,93E+07	4,40E+07	4,95E+07	4,15E+07	2,58E+07	1,19E+07	4,06E+06	1,03E+06	1,92E+05	2,64E+04	2,89E-03
		heteroaggregates in sediment	**1,5**	4,82E+01	3,01E+02	1,34E+03	4,93E+03	1,62E+04	5,46E+04	8,41E+04	1,01E+05	1,15E+05	1,52E+05	5,99E+04	2,37E+04	8,55E+03	4,17E+03	5,61E-03
			2	4,62E+01	2,93E+02	1,31E+03	4,84E+03	1,58E+04	5,22E+04	8,04E+04	9,65E+04	1,09E+05	1,43E+05	5,65E+04	2,23E+04	8,04E+03	3,92E+03	5,26E-03
			2,5	3,77E+01	2,69E+02	1,36E+03	5,42E+03	1,77E+04	5,18E+04	8,50E+04	1,07E+05	1,14E+05	1,27E+05	5,45E+04	2,16E+04	7,39E+03	3,13E+03	3,77E-03
			2,9	2,62E+01	2,59E+02	1,77E+03	8,94E+03	3,35E+04	9,29E+04	1,96E+05	3,06E+05	3,53E+05	3,03E+05	1,92E+05	9,03E+04	3,12E+04	8,04E+03	1,93E-03

alpha river	Month	State of aggregation	Df	Sizeclass													
				2,00E-07	3,12E-07	4,86E-07	7,58E-07	1,18E-06	1,84E-06	2,87E-06	4,47E-06	6,97E-06	1,09E-05	1,69E-05	2,64E-05	4,12E-05	6,42E-05	1,00E-04
	May	homoaggregates in water	1,5	3,76E+03	2,35E+04	1,04E+05	3,84E+05	1,27E+06	4,26E+06	6,56E+06	7,89E+06	8,93E+06	1,19E+07	4,67E+06	1,85E+06	6,67E+05	3,26E+05	4,39E-01
			2	3,61E+03	2,29E+04	1,02E+05	3,78E+05	1,23E+06	4,07E+06	6,27E+06	7,53E+06	8,48E+06	1,12E+07	4,41E+06	1,74E+06	6,28E+05	3,06E+05	4,11E-01
			2,5	2,94E+03	2,09E+04	1,06E+05	4,22E+05	1,38E+06	4,04E+06	6,62E+06	8,31E+06	8,91E+06	9,93E+06	4,25E+06	1,69E+06	5,76E+05	2,44E+05	2,94E-01
			2,9	2,05E+03	2,02E+04	1,38E+05	6,97E+05	2,61E+06	7,25E+06	1,53E+07	2,39E+07	2,75E+07	2,37E+07	1,50E+07	7,05E+06	2,43E+06	6,27E+05	1,51E-01
		homoaggregates in sediment	1,5	3,63E+08	9,45E+08	6,87E+08	1,37E+08	7,40E+06	1,02E+05	3,41E+02	3,04E-01	6,38E-05	3,05E-09	8,18E-14	0,00E+00	0,00E+00	0,00E+00	0,00E+00
			2	2,15E+09	7,00E+09	6,36E+09	1,58E+09	1,07E+08	1,83E+06	7,64E+03	8,51E+00	2,23E-03	1,33E-07	4,45E-12	0,00E+00	0,00E+00	0,00E+00	0,00E+00
			2,5	9,72E+09	3,95E+10	4,47E+10	1,39E+10	1,17E+09	2,50E+07	1,30E+05	1,78E+02	5,72E-02	4,10E-06	1,59E-10	3,13E-16	0,00E+00	0,00E+00	0,00E+00
			2,9	1,99E+10	9,64E+10	1,30E+11	4,79E+10	4,74E+09	1,17E+08	6,77E+05	9,27E+02	2,37E-01	7,68E-06	3,69E-11	0,00E+00	0,00E+00	0,00E+00	0,00E+00
				Sizeclass														
				1,00E-06	1,39E-06	1,93E-06	2,69E-06	3,74E-06	5,19E-06	7,22E-06	1,00E-05	1,40E-05	1,94E-05	2,70E-05	3,75E-05	5,21E-05	7,24E-05	1,00E-04
		heteroaggregates in water	1,5	2,78E+07	1,34E+08	4,67E+08	1,24E+09	2,47E+09	3,71E+09	4,17E+09	3,49E+09	2,17E+09	1,01E+09	3,42E+08	8,71E+07	1,62E+07	2,23E+06	2,45E-01
			2	2,61E+07	1,26E+08	4,38E+08	1,16E+09	2,32E+09	3,48E+09	3,91E+09	3,28E+09	2,03E+09	9,43E+08	3,21E+08	8,17E+07	1,52E+07	2,09E+06	2,30E-01
			2,5	1,86E+07	8,97E+07	3,13E+08	8,28E+08	1,66E+09	2,48E+09	2,79E+09	2,34E+09	1,45E+09	6,73E+08	2,29E+08	5,84E+07	1,09E+07	1,49E+06	1,64E-01
			2,9	8,70E+06	4,19E+07	1,46E+08	3,86E+08	7,73E+08	1,16E+09	1,30E+09	1,09E+09	6,78E+08	3,14E+08	1,07E+08	2,72E+07	5,07E+06	6,97E+05	7,64E-02
		heteroaggregates in sediment	1,5	3,76E+03	2,35E+04	1,04E+05	3,84E+05	1,27E+06	4,26E+06	6,56E+06	7,89E+06	8,93E+06	1,19E+07	4,67E+06	1,85E+06	6,67E+05	3,26E+05	4,39E-01
			2	3,61E+03	2,29E+04	1,02E+05	3,78E+05	1,23E+06	4,07E+06	6,27E+06	7,53E+06	8,48E+06	1,12E+07	4,41E+06	1,74E+06	6,28E+05	3,06E+05	4,11E-01
			2,5	2,94E+03	2,09E+04	1,06E+05	4,22E+05	1,38E+06	4,04E+06	6,62E+06	8,31E+06	8,91E+06	9,93E+06	4,25E+06	1,69E+06	5,76E+05	2,44E+05	2,94E-01
			2,9	2,05E+03	2,02E+04	1,38E+05	6,97E+05	2,61E+06	7,25E+06	1,53E+07	2,39E+07	2,75E+07	2,37E+07	1,50E+07	7,05E+06	2,43E+06	6,27E+05	1,51E-01
0,001				Sizeclass														
				2,00E-07	3,12E-07	4,86E-07	7,58E-07	1,18E-06	1,84E-06	2,87E-06	4,47E-06	6,97E-06	1,09E-05	1,69E-05	2,64E-05	4,12E-05	6,42E-05	1,00E-04
	August	homoaggregates in water	1,5	2,19E+15	4,54E+15	2,65E+15	4,23E+14	1,82E+13	2,02E+11	5,40E+08	3,85E+05	6,50E+01	2,49E-03	5,33E-08	6,29E-14	0,00E+00	0,00E+00	0,00E+00
			2	2,05E+15	4,26E+15	2,48E+15	3,99E+14	1,71E+13	1,89E+11	5,05E+08	3,61E+05	6,08E+01	2,33E-03	4,98E-08	5,88E-14	0,00E+00	0,00E+00	0,00E+00
			2,5	1,47E+15	3,05E+15	1,77E+15	2,84E+14	1,22E+13	1,34E+11	3,57E+08	2,53E+05	4,19E+01	1,54E-03	3,05E-08	3,10E-14	0,00E+00	0,00E+00	0,00E+00
			2,9	6,84E+14	1,42E+15	8,25E+14	1,31E+14	5,57E+12	5,95E+10	1,47E+08	8,70E+04	9,52E+00	1,33E-04	2,76E-10	1,42E-18	0,00E+00	0,00E+00	0,00E+00
		homoaggregates in sediment	1,5	1,06E+08	2,73E+08	1,99E+08	3,97E+07	2,14E+06	2,95E+04	9,86E+01	8,79E-02	1,85E-05	8,85E-10	2,37E-14	0,00E+00	0,00E+00	0,00E+00	0,00E+00
			2	6,25E+08	2,03E+09	1,84E+09	4,61E+08	3,08E+07	5,31E+05	2,21E+03	2,46E+00	6,47E-04	3,86E-08	1,29E-12	0,00E+00	0,00E+00	0,00E+00	0,00E+00
			2,5	2,83E+09	1,15E+10	1,30E+10	4,04E+09	3,38E+08	7,24E+06	3,75E+04	5,16E+01	1,67E-02	1,19E-06	4,59E-11	9,07E-17	0,00E+00	0,00E+00	0,00E+00
			2,9	5,78E+09	2,79E+10	3,76E+10	1,39E+10	1,37E+09	3,41E+07	1,96E+05	2,69E+02	6,85E-02	2,23E-06	1,07E-11	0,00E+00	0,00E+00	0,00E+00	0,00E+00
				Sizeclass														
				1,00E-06	1,39E-06	1,93E-06	2,69E-06	3,74E-06	5,19E-06	7,22E-06	1,00E-05	1,40E-05	1,94E-05	2,70E-05	3,75E-05	5,21E-05	7,24E-05	1,00E-04
		heteroaggregates in water	1,5	2,02E+06	9,71E+06	3,38E+07	8,97E+07	1,79E+08	2,69E+08	3,02E+08	2,53E+08	1,57E+08	7,29E+07	2,48E+07	6,32E+06	1,18E+06	1,62E+05	1,78E-02
			2	1,89E+06	9,11E+06	3,17E+07	8,41E+07	1,68E+08	2,52E+08	2,84E+08	2,38E+08	1,48E+08	6,84E+07	2,33E+07	5,93E+06	1,10E+06	1,52E+05	1,67E-02
			2,5	1,35E+06	6,52E+06	2,27E+07	6,02E+07	1,20E+08	1,80E+08	2,03E+08	1,70E+08	1,06E+08	4,89E+07	1,67E+07	4,24E+06	7,89E+05	1,08E+05	1,19E-02
			2,9	6,31E+05	3,04E+06	1,06E+07	2,80E+07	5,61E+07	8,40E+07	9,45E+07	7,92E+07	4,92E+07	2,28E+07	7,76E+06	1,98E+06	3,68E+05	5,05E+04	5,54E-03
		heteroaggregates in sediment	1,5	1,91E+02	1,19E+03	5,30E+03	1,95E+04	6,44E+04	2,16E+05	3,33E+05	4,01E+05	4,54E+05	6,03E+05	2,37E+05	9,38E+04	3,39E+04	1,65E+04	2,23E-02
			2	1,83E+02	1,16E+03	5,20E+03	1,92E+04	6,27E+04	2,07E+05	3,19E+05	3,83E+05	4,31E+05	5,69E+05	2,24E+05	8,85E+04	3,19E+04	1,55E+04	2,09E-02
			2,5	1,50E+02	1,07E+03	5,39E+03	2,15E+04	7,03E+04	2,06E+05	3,37E+05	4,23E+05	4,54E+05	5,06E+05	2,16E+05	8,59E+04	2,93E+04	1,24E+04	1,50E-02
			2,9	1,04E+02	1,03E+03	7,02E+03	3,54E+04	1,33E+05	3,68E+05	7,77E+05	1,21E+06	1,40E+06	1,20E+06	7,60E+05	3,58E+05	1,24E+05	3,19E+04	7,67E-03

alpha river	Month	State of aggregation	Df	Sizeclass													
				2,00E-07	3,12E-07	4,86E-07	7,58E-07	1,18E-06	1,84E-06	2,87E-06	4,47E-06	6,97E-06	1,09E-05	1,69E-05	2,64E-05	4,12E-05	6,42E-05	1,00E-04
0,001	November	homoaggregates in water	1,5	2,12E+15	4,43E+15	2,57E+15	4,12E+14	1,78E+13	1,95E+11	5,24E+08	3,74E+05	6,31E+01	2,41E-03	5,19E-08	6,11E-14	0,00E+00	0,00E+00	0,00E+00
			2	1,99E+15	4,15E+15	2,41E+15	3,86E+14	1,66E+13	1,83E+11	4,92E+08	3,51E+05	5,91E+01	2,26E-03	4,85E-08	5,70E-14	0,00E+00	0,00E+00	0,00E+00
			2,5	1,43E+15	2,97E+15	1,72E+15	2,75E+14	1,19E+13	1,30E+11	3,49E+08	2,46E+05	4,07E+01	1,49E-03	2,96E-08	3,01E-14	0,00E+00	0,00E+00	0,00E+00
			2,9	6,67E+14	1,38E+15	7,99E+14	1,27E+14	5,40E+12	5,75E+10	1,43E+08	8,45E+04	9,27E+00	1,29E-04	2,68E-10	1,38E-18	0,00E+00	0,00E+00	0,00E+00
		homoaggregates in sediment	1,5	1,33E+08	3,46E+08	2,51E+08	5,02E+07	2,70E+06	3,72E+04	1,24E+02	1,11E-01	2,34E-05	1,11E-09	2,99E-14	0,00E+00	0,00E+00	0,00E+00	0,00E+00
			2	7,89E+08	2,56E+09	2,32E+09	5,79E+08	3,89E+07	6,68E+05	2,80E+03	3,11E+00	8,16E-04	4,86E-08	1,63E-12	0,00E+00	0,00E+00	0,00E+00	0,00E+00
			2,5	3,57E+09	1,45E+10	1,63E+10	5,09E+09	4,26E+08	9,12E+06	4,75E+04	6,52E+01	2,10E-02	1,50E-06	5,79E-11	1,14E-16	0,00E+00	0,00E+00	0,00E+00
			2,9	7,31E+09	3,53E+10	4,73E+10	1,75E+10	1,73E+09	4,28E+07	2,47E+05	3,39E+02	8,65E-02	2,81E-06	1,35E-11	0,00E+00	0,00E+00	0,00E+00	0,00E+00
				Sizeclass														
				1,00E-06	1,39E-06	1,93E-06	2,69E-06	3,74E-06	5,19E-06	7,22E-06	1,00E-05	1,40E-05	1,94E-05	2,70E-05	3,75E-05	5,21E-05	7,24E-05	1,00E-04
		heteroaggregates in water	1,5	3,31E+06	1,59E+07	5,56E+07	1,47E+08	2,95E+08	4,42E+08	4,97E+08	4,16E+08	2,58E+08	1,20E+08	4,08E+07	1,04E+07	1,93E+06	2,65E+05	2,92E-02
			2	3,11E+06	1,50E+07	5,21E+07	1,38E+08	2,76E+08	4,14E+08	4,66E+08	3,90E+08	2,42E+08	1,12E+08	3,82E+07	9,73E+06	1,81E+06	2,49E+05	2,74E-02
			2,5	2,22E+06	1,07E+07	3,73E+07	9,87E+07	1,97E+08	2,96E+08	3,33E+08	2,79E+08	1,73E+08	8,03E+07	2,73E+07	6,96E+06	1,30E+06	1,78E+05	1,96E-02
			2,9	1,04E+06	4,98E+06	1,74E+07	4,60E+07	9,20E+07	1,38E+08	1,55E+08	1,30E+08	8,08E+07	3,74E+07	1,27E+07	3,24E+06	6,04E+05	8,29E+04	9,07E-03
		heteroaggregates in sediment	1,5	4,08E+02	2,55E+03	1,13E+04	4,16E+04	1,37E+05	4,61E+05	7,10E+05	8,54E+05	9,68E+05	1,29E+06	5,06E+05	2,00E+05	7,23E+04	3,53E+04	4,74E-02
			2	3,91E+02	2,48E+03	1,11E+04	4,09E+04	1,34E+05	4,41E+05	6,79E+05	8,16E+05	9,19E+05	1,21E+06	4,77E+05	1,89E+05	6,80E+04	3,31E+04	4,45E-02
			2,5	3,19E+02	2,27E+03	1,15E+04	4,58E+04	1,50E+05	4,38E+05	7,18E+05	9,01E+05	9,66E+05	1,08E+06	4,61E+05	1,83E+05	6,25E+04	2,64E+04	3,18E-02
			2,9	2,22E+02	2,19E+03	1,50E+04	7,55E+04	2,83E+05	7,85E+05	1,66E+06	2,59E+06	2,98E+06	2,56E+06	1,62E+06	7,63E+05	2,63E+05	6,79E+04	1,63E-02

alpha river	Month	State of aggregation	Df	Sizeclass													
				2,00E-07	**3,12E-07**	**4,86E-07**	**7,58E-07**	**1,18E-06**	**1,84E-06**	**2,87E-06**	**4,47E-06**	**6,97E-06**	**1,09E-05**	**1,69E-05**	**2,64E-05**	**4,12E-05**	**6,42E-05**	**1,00E-04**
	January	homoaggregates in water	**1,5**	7,33E+13	1,52E+14	8,86E+13	1,42E+13	6,12E+11	6,77E+09	1,81E+07	1,29E+04	2,18E+00	8,31E-05	1,78E-09	2,11E-15	0,00E+00	0,00E+00	0,00E+00
			2	6,87E+13	1,42E+14	8,31E+13	1,33E+13	5,71E+11	6,31E+09	1,70E+07	1,21E+04	2,04E+00	7,80E-05	1,67E-09	1,97E-15	0,00E+00	0,00E+00	0,00E+00
			2,5	4,92E+13	1,02E+14	5,94E+13	9,51E+12	4,08E+11	4,51E+09	1,20E+07	8,45E+03	1,40E+00	5,15E-05	1,02E-09	1,04E-15	0,00E+00	0,00E+00	0,00E+00
			2,9	2,30E+13	4,73E+13	2,76E+13	4,40E+12	1,86E+11	1,99E+09	4,92E+06	2,91E+03	3,19E-01	4,46E-06	9,24E-12	0,00E+00	0,00E+00	0,00E+00	0,00E+00
		homoaggregates in sediment	**1,5**	3,11E+06	8,07E+06	5,86E+06	1,17E+06	6,32E+04	8,72E+02	2,92E+00	2,59E-03	5,45E-07	2,60E-11	6,96E-16	0,00E+00	0,00E+00	0,00E+00	0,00E+00
			2	1,84E+07	5,96E+07	5,42E+07	1,35E+07	9,04E+05	1,56E+04	6,56E+01	7,24E-02	1,91E-05	1,14E-09	3,79E-14	0,00E+00	0,00E+00	0,00E+00	0,00E+00
			2,5	8,35E+07	3,37E+08	3,82E+08	1,19E+08	9,93E+06	2,14E+05	1,11E+03	1,52E+00	4,90E-04	3,50E-08	1,35E-12	0,00E+00	0,00E+00	0,00E+00	0,00E+00
			2,9	1,71E+08	8,17E+08	1,11E+09	4,11E+08	4,03E+07	1,00E+06	5,76E+03	7,93E+00	2,02E-03	6,56E-08	3,16E-13	0,00E+00	0,00E+00	0,00E+00	0,00E+00
				Sizeclass														
				1,00E-06	**1,39E-06**	**1,93E-06**	**2,69E-06**	**3,74E-06**	**5,19E-06**	**7,22E-06**	**1,00E-05**	**1,40E-05**	**1,94E-05**	**2,70E-05**	**3,75E-05**	**5,21E-05**	**7,24E-05**	**1,00E-04**
		heteroaggregates in water	**1,5**	1,04E+06	5,01E+06	1,75E+07	4,63E+07	9,25E+07	1,39E+08	1,56E+08	1,31E+08	8,12E+07	3,76E+07	1,28E+07	3,26E+06	6,07E+05	8,34E+04	9,18E-03
			2	9,75E+05	4,69E+06	1,64E+07	4,33E+07	8,67E+07	1,30E+08	1,46E+08	1,22E+08	7,60E+07	3,52E+07	1,20E+07	3,05E+06	5,68E+05	7,81E+04	8,60E-03
			2,5	6,98E+05	3,36E+06	1,17E+07	3,10E+07	6,20E+07	9,30E+07	1,05E+08	8,77E+07	5,44E+07	2,52E+07	8,59E+06	2,19E+06	4,07E+05	5,59E+04	6,15E-03
			2,9	3,24E+05	1,56E+06	5,44E+06	1,44E+07	2,88E+07	4,32E+07	4,86E+07	4,07E+07	2,53E+07	1,17E+07	3,99E+06	1,02E+06	1,89E+05	2,60E+04	2,85E-03
		heteroaggregates in sediment	**1,5**	8,67E+01	5,42E+02	2,40E+03	8,86E+03	2,92E+04	9,81E+04	1,51E+05	1,82E+05	2,06E+05	2,74E+05	1,08E+05	4,26E+04	1,54E+04	7,51E+03	1,01E-02
			2	8,31E+01	5,26E+02	2,36E+03	8,70E+03	2,84E+04	9,38E+04	1,44E+05	1,73E+05	1,95E+05	2,58E+05	1,01E+05	4,01E+04	1,44E+04	7,04E+03	9,47E-03
			2,5	6,78E+01	4,83E+02	2,44E+03	9,75E+03	3,19E+04	9,32E+04	1,53E+05	1,92E+05	2,06E+05	2,29E+05	9,80E+04	3,89E+04	1,33E+04	5,62E+03	6,79E-03
			2,9	4,70E+01	4,64E+02	3,17E+03	1,60E+04	6,00E+04	1,67E+05	3,51E+05	5,49E+05	6,33E+05	5,44E+05	3,44E+05	1,62E+05	5,59E+04	1,44E+04	3,47E-03
0,01	March			Sizeclass														
				2,00E-07	**3,12E-07**	**4,86E-07**	**7,58E-07**	**1,18E-06**	**1,84E-06**	**2,87E-06**	**4,47E-06**	**6,97E-06**	**1,09E-05**	**1,69E-05**	**2,64E-05**	**4,12E-05**	**6,42E-05**	**1,00E-04**
		homoaggregates in water	**1,5**	1,36E+15	2,83E+15	1,64E+15	2,63E+14	1,13E+13	1,26E+11	3,36E+08	2,39E+05	4,05E+01	1,54E-03	3,33E-08	3,91E-14	0,00E+00	0,00E+00	0,00E+00
			2	1,27E+15	2,65E+15	1,54E+15	2,46E+14	1,06E+13	1,17E+11	3,15E+08	2,24E+05	3,79E+01	1,44E-06	3,10E-08	3,65E-14	0,00E+00	0,00E+00	0,00E+00
			2,5	9,09E+14	1,90E+15	1,10E+15	1,76E+14	7,58E+12	8,36E+10	2,23E+08	1,57E+05	2,60E+01	9,52E-04	1,90E-08	1,92E-14	0,00E+00	0,00E+00	0,00E+00
			2,9	4,25E+14	8,85E+14	5,12E+14	8,13E+13	3,44E+12	3,70E+10	9,14E+07	5,41E+04	5,90E+00	8,25E-05	1,71E-10	8,80E-19	0,00E+00	0,00E+00	0,00E+00
		homoaggregates in sediment	**1,5**	3,15E+07	8,20E+07	5,94E+07	1,19E+07	6,38E+05	8,84E+03	2,95E+01	2,63E-02	5,55E-06	2,64E-10	7,10E-15	0,00E+00	0,00E+00	0,00E+00	0,00E+00
			2	1,87E+08	6,07E+08	5,49E+08	1,37E+08	9,20E+06	1,59E+05	6,64E+02	7,36E-01	1,94E-04	1,15E-11	3,85E-13	0,00E+00	0,00E+00	0,00E+00	0,00E+00
			2,5	8,43E+08	3,43E+09	3,87E+09	1,20E+09	1,01E+08	2,17E+06	1,12E+04	1,54E+01	4,96E-03	3,54E-07	1,37E-11	2,71E-17	0,00E+00	0,00E+00	0,00E+00
			2,9	1,73E+09	8,35E+09	1,12E+10	4,14E+09	4,08E+08	1,02E+07	5,85E+04	8,05E+01	2,04E-02	6,63E-07	3,20E-12	0,00E+00	0,00E+00	0,00E+00	0,00E+00
				Sizeclass														
				1,00E-06	**1,39E-06**	**1,93E-06**	**2,69E-06**	**3,74E-06**	**5,19E-06**	**7,22E-06**	**1,00E-05**	**1,40E-05**	**1,94E-05**	**2,70E-05**	**3,75E-05**	**5,21E-05**	**7,24E-05**	**1,00E-04**
		heteroaggregates in water	**1,5**	1,06E+07	5,09E+07	1,77E+08	4,70E+08	9,39E+08	1,41E+09	1,58E+09	1,33E+09	8,24E+08	3,82E+08	1,30E+08	3,31E+07	6,16E+06	8,46E+05	9,31E-02
			2	9,90E+06	4,77E+07	1,66E+08	4,40E+08	8,80E+08	1,32E+09	1,48E+09	1,24E+09	7,72E+08	3,58E+08	1,22E+08	3,10E+07	5,77E+06	7,93E+05	8,72E-02
			2,5	7,08E+06	3,41E+07	1,19E+08	3,15E+08	6,30E+08	9,44E+08	1,06E+09	8,90E+08	5,52E+08	2,56E+08	8,71E+07	2,22E+07	4,13E+06	5,67E+05	6,24E-02
			2,9	3,30E+06	1,59E+07	5,54E+07	1,47E+08	2,93E+08	4,40E+08	4,95E+08	4,15E+08	2,58E+08	1,19E+08	4,06E+07	1,03E+07	1,92E+06	2,64E+05	2,89E-02
		heteroaggregates in sediment	**1,5**	4,81E+02	3,01E+03	1,33E+04	4,91E+04	1,62E+05	5,44E+05	8,38E+05	1,01E+06	1,14E+06	1,52E+06	5,97E+05	2,36E+05	8,53E+04	4,16E+04	5,60E-02
			2	4,61E+02	2,92E+03	1,31E+04	4,83E+04	1,58E+05	5,21E+05	8,02E+05	9,63E+05	1,08E+06	1,43E+06	5,63E+05	2,23E+05	8,02E+04	3,91E+04	5,25E-02
			2,5	3,76E+02	2,68E+03	1,35E+04	5,41E+04	1,77E+05	5,17E+05	8,48E+05	1,06E+06	1,14E+06	1,27E+06	5,44E+05	2,16E+05	7,37E+04	3,12E+04	3,76E-02
			2,9	2,62E+02	2,58E+03	1,77E+04	8,91E+04	3,34E+05	9,26E+05	1,96E+06	3,05E+06	3,52E+06	3,03E+06	1,91E+06	9,01E+05	3,11E+05	8,02E+04	1,93E-02

alpha river	Month	State of aggregation	Df	Sizeclass													
				2,00E-07	3,12E-07	4,86E-07	7,58E-07	1,18E-06	1,84E-06	2,87E-06	4,47E-06	6,97E-06	1,09E-05	1,69E-05	2,64E-05	4,12E-05	6,42E-05	1,00E-04
0,01	May	homoaggregates in water	1,5	5,26E+15	1,10E+16	6,40E+15	1,02E+15	4,42E+13	4,86E+11	1,30E+09	9,32E+05	1,57E+02	6,00E-03	1,29E-07	1,52E-13	0,00E+00	0,00E+00	0,00E+00
			2	4,94E+15	1,03E+16	6,00E+15	9,57E+14	4,14E+13	4,55E+11	1,22E+09	8,74E+05	1,47E+02	5,61E-03	1,21E-07	1,42E-13	0,00E+00	0,00E+00	0,00E+00
			2,5	3,53E+15	7,36E+15	4,28E+15	6,84E+14	2,96E+13	3,25E+11	8,65E+08	6,12E+05	1,01E+02	3,72E-03	7,38E-08	7,48E-14	0,00E+00	0,00E+00	0,00E+00
			2,9	1,65E+15	3,44E+15	1,99E+15	3,16E+14	1,35E+13	1,43E+11	3,56E+08	2,10E+05	2,30E+01	3,22E-04	6,66E-10	3,42E-18	0,00E+00	0,00E+00	0,00E+00
		homoaggregates in sediment	1,5	3,63E+08	9,45E+08	6,87E+08	1,37E+08	7,39E+06	1,02E+05	3,40E+02	3,04E-01	6,38E-05	3,05E-09	8,18E-14	0,00E+00	0,00E+00	0,00E+00	0,00E+00
			2	2,15E+09	7,00E+09	6,35E+09	1,58E+09	1,07E+08	1,83E+06	7,64E+03	8,51E+00	2,23E-03	1,33E-07	4,45E-12	0,00E+00	0,00E+00	0,00E+00	0,00E+00
			2,5	9,72E+09	3,95E+10	4,47E+10	1,39E+10	1,17E+09	2,50E+07	1,29E+05	1,78E+02	5,72E-02	4,10E-06	1,58E-10	3,13E-16	0,00E+00	0,00E+00	0,00E+00
			2,9	1,99E+10	9,63E+10	1,30E+11	4,78E+10	4,74E+09	1,17E+08	6,76E+05	9,26E+02	2,37E-01	7,67E-06	3,69E-11	0,00E+00	0,00E+00	0,00E+00	0,00E+00
				Sizeclass														
				1,00E-06	1,39E-06	1,93E-06	2,69E-06	3,74E-06	5,19E-06	7,22E-06	1,00E-05	1,40E-05	1,94E-05	2,70E-05	3,75E-05	5,21E-05	7,24E-05	1,00E-04
		heteroaggregates in water	1,5	2,78E+08	1,34E+09	4,66E+09	1,24E+10	2,47E+10	3,71E+10	4,17E+10	3,49E+10	2,17E+10	1,00E+10	3,42E+09	8,71E+08	1,62E+08	2,23E+07	2,46E+00
			2	2,61E+08	1,26E+09	4,37E+09	1,16E+10	2,32E+10	3,48E+10	3,91E+10	3,28E+10	2,03E+10	9,42E+09	3,21E+09	8,17E+08	1,52E+08	2,09E+07	2,31E+00
			2,5	1,86E+08	8,97E+08	3,12E+09	8,28E+09	1,66E+10	2,48E+10	2,79E+10	2,34E+10	1,45E+10	6,73E+09	2,29E+09	5,83E+08	1,09E+08	1,49E+07	1,65E+00
			2,9	8,69E+07	4,18E+08	1,46E+09	3,86E+09	7,73E+09	1,16E+10	1,30E+10	1,09E+10	6,78E+09	3,14E+09	1,07E+09	2,72E+08	5,07E+07	6,98E+06	7,66E-01
		heteroaggregates in sediment	1,5	3,76E+04	2,35E+05	1,04E+06	3,84E+06	1,27E+07	4,25E+07	6,55E+07	7,88E+07	8,93E+07	1,19E+08	4,67E+07	1,85E+07	6,67E+06	3,25E+06	4,40E+00
			2	3,61E+04	2,29E+05	1,02E+06	3,78E+06	1,23E+07	4,07E+07	6,27E+07	7,53E+07	8,48E+07	1,12E+08	4,40E+07	1,74E+07	6,27E+06	3,06E+06	4,12E+00
			2,5	2,94E+04	2,09E+05	1,06E+06	4,22E+06	1,38E+07	4,04E+07	6,62E+07	8,30E+07	8,91E+07	9,92E+07	4,24E+07	1,69E+07	5,76E+06	2,44E+06	2,95E+00
			2,9	2,05E+04	2,02E+05	1,38E+06	6,97E+06	2,61E+07	7,24E+07	1,53E+08	2,39E+08	2,75E+08	2,37E+08	1,49E+08	7,05E+07	2,43E+07	6,28E+06	1,51E+00
				Sizeclass														
				2,00E-07	3,12E-07	4,86E-07	7,58E-07	1,18E-06	1,84E-06	2,87E-06	4,47E-06	6,97E-06	1,09E-05	1,69E-05	2,64E-05	4,12E-05	6,42E-05	1,00E-04
	August	homoaggregates in water	1,5	2,19E+15	4,54E+15	2,65E+15	4,23E+14	1,82E+13	2,02E+11	5,40E+08	3,85E+05	6,50E+01	2,49E-03	5,33E-08	6,29E-14	0,00E+00	0,00E+00	0,00E+00
			2	2,05E+15	4,26E+15	2,48E+15	3,99E+14	1,71E+13	1,89E+11	5,05E+08	3,61E+05	6,08E+01	2,33E-03	4,98E-08	5,88E-14	0,00E+00	0,00E+00	0,00E+00
			2,5	1,47E+15	3,05E+15	1,77E+15	2,84E+14	1,22E+13	1,34E+11	3,57E+08	2,53E+05	4,19E+01	1,54E-03	3,05E-08	3,10E-14	0,00E+00	0,00E+00	0,00E+00
			2,9	6,84E+14	1,42E+15	8,25E+14	1,31E+14	5,57E+12	5,94E+10	1,47E+08	8,70E+04	9,52E+00	1,33E-04	2,76E-10	1,42E-18	0,00E+00	0,00E+00	0,00E+00
		homoaggregates in sediment	1,5	2,19E+15	4,54E+15	2,65E+15	4,23E+14	1,82E+13	2,02E+11	5,40E+08	3,85E+05	6,50E+01	2,49E-03	5,33E-08	6,29E-14	0,00E+00	0,00E+00	0,00E+00
			2	2,05E+15	4,26E+15	2,48E+15	3,99E+14	1,71E+13	1,89E+11	5,05E+08	3,61E+05	6,08E+01	2,33E-03	4,98E-08	5,88E-14	0,00E+00	0,00E+00	0,00E+00
			2,5	1,47E+15	3,05E+15	1,77E+15	2,84E+14	1,22E+13	1,34E+11	3,57E+08	2,53E+05	4,19E+01	1,54E-03	3,05E-08	3,10E-14	0,00E+00	0,00E+00	0,00E+00
			2,9	6,84E+14	1,42E+15	8,25E+14	1,31E+14	5,57E+12	5,94E+10	1,47E+08	8,70E+04	9,52E+00	1,33E-04	2,76E-10	1,42E-18	0,00E+00	0,00E+00	0,00E+00
				Sizeclass														
				1,00E-06	1,39E-06	1,93E-06	2,69E-06	3,74E-06	5,19E-06	7,22E-06	1,00E-05	1,40E-05	1,94E-05	2,70E-05	3,75E-05	5,21E-05	7,24E-05	1,00E-04
		heteroaggregates in water	1,5	2,02E+07	9,71E+07	3,38E+08	8,97E+08	1,79E+09	2,69E+09	3,02E+09	2,53E+09	1,57E+09	7,29E+08	2,48E+08	6,32E+07	1,18E+07	1,62E+06	1,78E-01
			2	1,89E+07	9,11E+07	3,17E+08	8,41E+08	1,68E+09	2,52E+09	2,84E+09	2,38E+09	1,48E+09	6,84E+08	2,33E+08	5,93E+07	1,10E+07	1,52E+06	1,67E-01
			2,5	1,35E+07	6,52E+07	2,27E+08	6,02E+08	1,20E+09	1,80E+09	2,03E+09	1,70E+09	1,06E+09	4,89E+08	1,67E+08	4,24E+07	7,89E+06	1,08E+06	1,19E-01
			2,9	6,31E+06	3,03E+07	1,06E+08	2,80E+08	5,61E+08	8,40E+08	9,45E+08	7,92E+08	4,92E+08	2,28E+08	7,76E+07	1,98E+07	3,68E+06	5,05E+05	5,54E-02
		heteroaggregates in sediment	1,5	1,91E+03	1,19E+04	5,29E+04	1,95E+05	6,43E+05	2,16E+06	3,33E+06	4,00E+06	4,53E+06	6,02E+06	2,37E+06	9,37E+05	3,38E+05	1,65E+05	2,22E-01
			2	1,83E+03	1,16E+04	5,20E+04	1,92E+05	6,26E+05	2,07E+06	3,18E+06	3,82E+06	4,31E+06	5,68E+06	2,24E+06	8,84E+05	3,19E+05	1,55E+05	2,09E-01
			2,5	1,49E+03	1,07E+04	5,38E+04	2,15E+05	7,02E+05	2,05E+06	3,37E+06	4,23E+06	4,53E+06	5,05E+06	2,16E+06	8,58E+05	2,93E+05	1,24E+05	1,49E-01
			2,9	1,04E+03	1,02E+04	7,01E+04	3,54E+05	1,33E+06	3,68E+06	7,76E+06	1,21E+07	1,40E+07	1,20E+07	7,59E+06	3,58E+06	1,23E+06	3,18E+05	7,66E-02

alpha river	Month	State of aggregation	Df	Sizeclass													
				2,00E-07	3,12E-07	4,86E-07	7,58E-07	1,18E-06	1,84E-06	2,87E-06	4,47E-06	6,97E-06	1,09E-05	1,69E-05	2,64E-05	4,12E-05	6,42E-05	1,00E-04
0,01	November	homoaggregates in water	1,5	2,12E+15	4,43E+15	2,57E+15	4,12E+14	1,78E+13	1,95E+11	5,24E+08	3,74E+05	6,31E+01	2,41E-03	5,19E-08	6,11E-14	0,00E+00	0,00E+00	0,00E+00
			2	1,99E+15	4,15E+15	2,41E+15	3,86E+14	1,66E+13	1,83E+11	4,92E+08	3,51E+05	5,91E+01	2,26E-03	4,85E-08	5,70E-14	0,00E+00	0,00E+00	0,00E+00
			2,5	1,43E+15	2,97E+15	1,72E+15	2,75E+14	1,19E+13	1,30E+11	3,49E+08	2,46E+05	4,07E+01	1,49E-03	2,96E-08	3,01E-14	0,00E+00	0,00E+00	0,00E+00
			2,9	6,67E+14	1,38E+15	7,99E+14	1,27E+14	5,39E+12	5,75E+10	1,43E+08	8,45E+04	9,26E+00	1,29E-04	2,68E-10	1,38E-18	0,00E+00	0,00E+00	0,00E+00
		homoaggregates in sediment	1,5	1,33E+08	3,46E+08	2,50E+08	5,02E+07	2,70E+06	3,71E+04	1,24E+02	1,11E-01	2,33E-05	1,11E-09	2,99E-14	0,00E+00	0,00E+00	0,00E+00	0,00E+00
			2	7,88E+08	2,56E+09	2,32E+09	5,79E+08	3,89E+07	6,68E+05	2,80E+03	3,11E+00	8,15E-04	4,85E-08	1,63E-12	0,00E+00	0,00E+00	0,00E+00	0,00E+00
			2,5	3,57E+09	1,45E+10	1,63E+10	5,08E+09	4,26E+08	9,11E+06	4,74E+04	6,51E+01	2,10E-02	1,50E-06	5,78E-11	1,14E-16	0,00E+00	0,00E+00	0,00E+00
			2,9	7,31E+09	3,53E+10	4,73E+10	1,75E+10	1,72E+09	4,27E+07	2,47E+05	3,39E+02	8,64E-02	2,80E-06	1,35E-11	0,00E+00	0,00E+00	0,00E+00	0,00E+00
				Sizeclass														
				1,00E-06	1,39E-06	1,93E-06	2,69E-06	3,74E-06	5,19E-06	7,22E-06	1,00E-05	1,40E-05	1,94E-05	2,70E-05	3,75E-05	5,21E-05	7,24E-05	1,00E-04
		heteroaggregates in water	1,5	3,31E+07	1,59E+08	5,56E+08	1,47E+09	2,94E+09	4,41E+09	4,97E+09	4,16E+09	2,58E+09	1,20E+09	4,08E+08	1,04E+08	1,93E+07	2,65E+06	2,92E-01
			2	3,11E+07	1,50E+08	5,21E+08	1,38E+09	2,76E+09	4,14E+09	4,65E+09	3,90E+09	2,42E+09	1,12E+09	3,82E+08	9,73E+07	1,81E+07	2,49E+06	2,74E-01
			2,5	2,22E+07	1,07E+08	3,72E+08	9,87E+08	1,97E+09	2,96E+09	3,33E+09	2,79E+09	1,73E+09	8,03E+08	2,73E+08	6,96E+07	1,29E+07	1,78E+06	1,96E-01
			2,9	1,03E+07	4,98E+07	1,74E+08	4,60E+08	9,20E+08	1,38E+09	1,55E+09	1,30E+09	8,07E+08	3,74E+08	1,27E+08	3,24E+07	6,04E+06	8,29E+05	9,07E-02
		heteroaggregates in sediment	1,5	4,07E+03	2,54E+04	1,13E+05	4,16E+05	1,37E+06	4,61E+06	7,10E+06	8,54E+06	9,67E+06	1,29E+07	5,06E+06	2,00E+06	7,22E+05	3,52E+05	4,74E-01
			2	3,90E+03	2,47E+04	1,11E+05	4,09E+05	1,33E+06	4,41E+06	6,79E+06	8,15E+06	9,18E+06	1,21E+07	4,77E+06	1,88E+06	6,79E+05	3,31E+05	4,45E-01
			2,5	3,18E+03	2,27E+04	1,15E+05	4,58E+05	1,50E+06	4,38E+06	7,18E+06	9,00E+06	9,66E+06	1,08E+07	4,60E+06	1,83E+06	6,24E+05	2,64E+05	3,18E-01
			2,9	2,21E+03	2,18E+04	1,49E+05	7,54E+05	2,83E+06	7,84E+06	1,65E+07	2,59E+07	2,98E+07	2,56E+07	1,62E+07	7,63E+06	2,63E+06	6,79E+05	1,63E-01

alpha river	Month	State of aggregation	Df	Sizeclass													
				2,00E-07	3,12E-07	4,86E-07	7,58E-07	1,18E-06	1,84E-06	2,87E-06	4,47E-06	6,97E-06	1,09E-05	1,69E-05	2,64E-05	4,12E-05	6,42E-05	1,00E-04
0,1	January	homoaggregates in water	1,5	7,33E+13	1,52E+14	8,85E+13	1,42E+13	6,11E+11	6,76E+09	1,81E+07	1,29E+04	2,18E+00	8,31E-05	1,78E-09	2,11E-15	0,00E+00	0,00E+00	0,00E+00
			2	6,87E+13	1,42E+14	8,29E+13	1,33E+13	5,69E+11	6,29E+09	1,70E+07	1,21E+04	2,04E+00	7,80E-05	1,67E-09	1,97E-15	0,00E+00	0,00E+00	0,00E+00
			2,5	4,92E+13	1,02E+14	5,93E+13	9,49E+12	4,07E+11	4,49E+09	1,20E+07	8,44E+03	1,40E+00	5,15E-05	1,02E-09	1,04E-15	0,00E+00	0,00E+00	0,00E+00
			2,9	2,30E+13	4,73E+13	2,76E+13	4,39E+12	1,86E+11	1,99E+09	4,91E+06	2,91E+03	3,19E-01	4,46E-06	9,24E-12	0,00E+00	0,00E+00	0,00E+00	0,00E+00
		homoaggregates in sediment	1,5	3,11E+06	8,06E+06	5,85E+06	1,17E+06	6,30E+04	8,70E+02	2,91E+00	2,59E-03	5,45E-07	2,60E-11	6,96E-16	0,00E+00	0,00E+00	0,00E+00	0,00E+00
			2	1,84E+07	5,96E+07	5,41E+07	1,35E+07	9,02E+05	1,56E+04	6,55E+01	7,24E-02	1,91E-05	1,14E-09	3,79E-14	0,00E+00	0,00E+00	0,00E+00	0,00E+00
			2,5	8,35E+07	3,37E+08	3,81E+08	1,19E+08	9,90E+06	2,13E+05	1,11E+03	1,52E+00	4,90E-04	3,50E-08	1,35E-12	0,00E+00	0,00E+00	0,00E+00	0,00E+00
			2,9	1,71E+08	8,16E+08	1,11E+09	4,10E+08	4,02E+07	1,00E+06	5,75E+03	7,92E+00	2,02E-03	6,56E-08	3,16E-13	0,00E+00	0,00E+00	0,00E+00	0,00E+00
				Sizeclass														
				1,00E-06	1,39E-06	1,93E-06	2,69E-06	3,74E-06	5,19E-06	7,22E-06	1,00E-05	1,40E-05	1,94E-05	2,70E-05	3,75E-05	5,21E-05	7,24E-05	1,00E-04
		heteroaggregates in water	1,5	1,04E+07	5,01E+07	1,74E+08	4,62E+08	9,24E+08	1,39E+09	1,56E+09	1,31E+09	8,11E+08	3,76E+08	1,28E+08	3,26E+07	6,06E+06	8,33E+05	9,16E-02
			2	9,74E+06	4,69E+07	1,63E+08	4,33E+08	8,66E+08	1,30E+09	1,46E+09	1,22E+09	7,60E+08	3,52E+08	1,20E+08	3,05E+07	5,68E+06	7,80E+05	8,58E-02
			2,5	6,97E+06	3,36E+07	1,17E+08	3,10E+08	6,20E+08	9,29E+08	1,05E+09	8,76E+08	5,44E+08	2,52E+08	8,58E+07	2,18E+07	4,06E+06	5,59E+05	6,14E-02
			2,9	3,24E+06	1,56E+07	5,43E+07	1,44E+08	2,88E+08	4,32E+08	4,86E+08	4,07E+08	2,53E+08	1,17E+08	3,99E+07	1,02E+07	1,89E+06	2,60E+05	2,85E-02
		heteroaggregates in sediment	1,5	8,66E+02	5,41E+03	2,40E+04	8,85E+04	2,92E+05	9,80E+05	1,51E+06	1,82E+06	2,06E+06	2,73E+06	1,08E+06	4,25E+05	1,54E+05	7,50E+04	1,01E-01
			2	8,30E+02	5,26E+03	2,36E+04	8,69E+04	2,84E+05	9,37E+05	1,44E+06	1,73E+06	1,95E+06	2,57E+06	1,01E+06	4,00E+05	1,44E+05	7,03E+04	9,45E-02
			2,5	6,78E+02	4,83E+03	2,44E+04	9,74E+04	3,18E+05	9,31E+05	1,53E+06	1,92E+06	2,05E+06	2,29E+06	9,79E+05	3,89E+05	1,33E+05	5,62E+04	6,77E-02
			2,9	4,70E+02	4,63E+03	3,17E+04	1,60E+05	6,00E+05	1,66E+06	3,51E+06	5,49E+06	6,32E+06	5,43E+06	3,43E+06	1,62E+06	5,58E+05	1,44E+05	3,47E-02
	March			Sizeclass														
				2,00E-07	3,12E-07	4,86E-07	7,58E-07	1,18E-06	1,84E-06	2,87E-06	4,47E-06	6,97E-06	1,09E-05	1,69E-05	2,64E-05	4,12E-05	6,42E-05	1,00E-04
		homoaggregates in water	1,5	1,36E+15	2,83E+15	1,64E+15	2,62E+14	1,13E+13	1,25E+11	3,35E+08	2,39E+05	4,05E+01	1,54E-03	3,33E-08	3,91E-14	0,00E+00	0,00E+00	0,00E+00
			2	1,27E+15	2,65E+15	1,54E+15	2,46E+14	1,06E+13	1,17E+11	3,15E+08	2,24E+05	3,79E+01	1,44E-06	3,10E-08	3,65E-14	0,00E+00	0,00E+00	0,00E+00
			2,5	9,09E+14	1,90E+15	1,10E+15	1,75E+14	7,57E+12	8,35E+10	2,22E+08	1,57E+05	2,60E+01	9,52E-04	1,90E-08	1,92E-14	0,00E+00	0,00E+00	0,00E+00
			2,9	4,25E+14	8,85E+14	5,12E+14	8,12E+13	3,44E+12	3,70E+10	9,14E+07	5,41E+04	5,90E+00	8,25E-05	1,71E-10	8,80E-19	0,00E+00	0,00E+00	0,00E+00
		homoaggregates in sediment	1,5	3,15E+07	8,19E+07	5,94E+07	1,18E+07	6,37E+05	8,83E+03	2,95E+01	2,62E-02	5,55E-06	2,64E-10	7,10E-15	0,00E+00	0,00E+00	0,00E+00	0,00E+00
			2	1,87E+08	6,07E+08	5,48E+08	1,36E+08	9,18E+06	1,58E+05	6,63E+02	7,35E-01	1,94E-04	1,15E-11	3,85E-13	0,00E+00	0,00E+00	0,00E+00	0,00E+00
			2,5	8,43E+08	3,43E+09	3,87E+09	1,20E+09	1,01E+08	2,16E+06	1,12E+04	1,54E+01	4,96E-03	3,54E-07	1,37E-11	2,71E-17	0,00E+00	0,00E+00	0,00E+00
			2,9	1,73E+09	8,35E+09	1,12E+10	4,14E+09	4,07E+08	1,02E+07	5,85E+04	8,04E+01	2,04E-02	6,63E-07	3,20E-12	0,00E+00	0,00E+00	0,00E+00	0,00E+00
				Sizeclass														
				1,00E-06	1,39E-06	1,93E-06	2,69E-06	3,74E-06	5,19E-06	7,22E-06	1,00E-05	1,40E-05	1,94E-05	2,70E-05	3,75E-05	5,21E-05	7,24E-05	1,00E-04
		heteroaggregates in water	1,5	1,06E+08	5,08E+08	1,77E+09	4,69E+09	9,39E+09	1,41E+10	1,58E+10	1,33E+10	8,24E+09	3,82E+09	1,30E+09	3,31E+08	6,16E+07	8,46E+06	9,30E-01
			2	9,90E+07	4,76E+08	1,66E+09	4,40E+09	8,80E+09	1,32E+10	1,48E+10	1,24E+10	7,72E+09	3,58E+09	1,22E+09	3,10E+08	5,77E+07	7,93E+06	8,71E-01
			2,5	7,08E+07	3,41E+08	1,19E+09	3,15E+09	6,29E+09	9,43E+09	1,06E+10	8,89E+09	5,52E+09	2,56E+09	8,71E+08	2,22E+08	4,13E+07	5,67E+06	6,23E-01
			2,9	3,30E+07	1,59E+08	5,53E+08	1,47E+09	2,93E+09	4,40E+09	4,95E+09	4,14E+09	2,57E+09	1,19E+09	4,06E+08	1,03E+08	1,92E+07	2,64E+06	2,89E-01
		heteroaggregates in sediment	1,5	4,81E+03	3,00E+04	1,33E+05	4,91E+05	1,62E+06	5,44E+06	8,38E+06	1,01E+07	1,14E+07	1,52E+07	5,97E+06	2,36E+06	8,53E+05	4,16E+05	5,60E-01
			2	4,61E+03	2,92E+04	1,31E+05	4,83E+05	1,58E+06	5,20E+06	8,01E+06	9,62E+06	1,08E+07	1,43E+07	5,63E+06	2,22E+06	8,02E+05	3,90E+05	5,24E-01
			2,5	3,76E+03	2,68E+04	1,35E+05	5,40E+05	1,77E+06	5,17E+06	8,47E+06	1,06E+07	1,14E+07	1,27E+07	5,43E+06	2,16E+06	7,37E+05	3,12E+05	3,76E-01
			2,9	2,62E+03	2,58E+04	1,76E+05	8,91E+05	3,34E+06	9,26E+06	1,95E+07	3,05E+07	3,52E+07	3,02E+07	1,91E+07	9,01E+06	3,11E+06	8,01E+05	1,92E-01

alpha river	Month	State of aggregation	Df	Sizeclass													
				2,00E-07	**3,12E-07**	**4,86E-07**	**7,58E-07**	**1,18E-06**	**1,84E-06**	**2,87E-06**	**4,47E-06**	**6,97E-06**	**1,09E-05**	**1,69E-05**	**2,64E-05**	**4,12E-05**	**6,42E-05**	**1,00E-04**
0,1	May	homoaggregates in water	**1,5**	5,26E+15	1,10E+16	6,36E+15	1,01E+15	4,37E+13	4,82E+11	1,30E+09	9,29E+05	1,57E+02	6,00E-03	1,29E-07	1,52E-13	0,00E+00	0,00E+00	0,00E+00
			2	4,93E+15	1,03E+16	5,96E+15	9,48E+14	4,10E+13	4,51E+11	1,22E+09	8,71E+05	1,47E+02	5,61E-03	1,21E-07	1,42E-13	0,00E+00	0,00E+00	0,00E+00
			2,5	3,52E+15	7,34E+15	4,25E+15	6,78E+14	2,92E+13	3,22E+11	8,60E+08	6,10E+05	1,01E+02	3,71E-03	7,38E-08	7,48E-14	0,00E+00	0,00E+00	0,00E+00
			2,9	1,65E+15	3,43E+15	1,98E+15	3,13E+14	1,33E+13	1,42E+11	3,54E+08	2,09E+05	2,30E+01	3,22E-04	6,66E-10	3,42E-18	0,00E+00	0,00E+00	0,00E+00
		homoaggregates in sediment	**1,5**	3,62E+08	9,42E+08	6,82E+08	1,36E+08	7,31E+06	1,01E+05	3,38E+02	3,03E-01	6,37E-05	3,05E-09	8,18E-14	0,00E+00	0,00E+00	0,00E+00	0,00E+00
			2	2,15E+09	6,97E+09	6,31E+09	1,56E+09	1,05E+08	1,81E+06	7,59E+03	8,49E+00	2,23E-03	1,33E-07	4,45E-12	0,00E+00	0,00E+00	0,00E+00	0,00E+00
			2,5	9,71E+09	3,94E+10	4,44E+10	1,38E+10	1,16E+09	2,48E+07	1,29E+05	1,78E+02	5,71E-02	4,10E-06	1,58E-10	3,13E-16	0,00E+00	0,00E+00	0,00E+00
			2,9	1,99E+10	9,60E+10	1,29E+11	4,74E+10	4,69E+09	1,16E+08	6,72E+05	9,24E+02	2,36E-01	7,67E-06	3,69E-11	0,00E+00	0,00E+00	0,00E+00	0,00E+00
				Sizeclass														
				1,00E-06	**1,39E-06**	**1,93E-06**	**2,69E-06**	**3,74E-06**	**5,19E-06**	**7,22E-06**	**1,00E-05**	**1,40E-05**	**1,94E-05**	**2,70E-05**	**3,75E-05**	**5,21E-05**	**7,24E-05**	**1,00E-04**
		heteroaggregates in water	**1,5**	2,77E+09	1,33E+10	4,65E+10	1,23E+11	2,46E+11	3,69E+11	4,15E+11	3,48E+11	2,16E+11	1,00E+11	3,41E+10	8,68E+09	1,62E+09	2,22E+08	2,45E+01
			2	2,60E+09	1,25E+10	4,36E+10	1,15E+11	2,31E+11	3,46E+11	3,89E+11	3,26E+11	2,03E+11	9,39E+10	3,20E+10	8,14E+09	1,51E+09	2,08E+08	2,29E+01
			2,5	1,86E+09	8,93E+09	3,11E+10	8,25E+10	1,65E+11	2,47E+11	2,78E+11	2,33E+11	1,45E+11	6,71E+10	2,28E+10	5,81E+09	1,08E+09	1,49E+08	1,64E+01
			2,9	8,66E+08	4,17E+09	1,45E+10	3,85E+10	7,70E+10	1,15E+11	1,30E+11	1,09E+11	6,76E+10	3,13E+10	1,07E+10	2,71E+09	5,05E+08	6,95E+07	7,61E+00
		heteroaggregates in sediment	**1,5**	3,75E+05	2,34E+06	1,04E+07	3,83E+07	1,26E+08	4,24E+08	6,53E+08	7,85E+08	8,90E+08	1,18E+09	4,65E+08	1,84E+08	6,64E+07	3,24E+07	4,37E+01
			2	3,59E+05	2,28E+06	1,02E+07	3,76E+07	1,23E+08	4,06E+08	6,25E+08	7,50E+08	8,45E+08	1,11E+09	4,39E+08	1,73E+08	6,25E+07	3,04E+07	4,10E+01
			2,5	2,93E+05	2,09E+06	1,05E+07	4,21E+07	1,37E+08	4,02E+08	6,59E+08	8,27E+08	8,87E+08	9,89E+08	4,23E+08	1,68E+08	5,74E+07	2,43E+07	2,93E+01
			2,9	2,04E+05	2,01E+06	1,38E+07	6,94E+07	2,60E+08	7,22E+08	1,52E+09	2,38E+09	2,74E+09	2,36E+09	1,49E+09	7,02E+08	2,42E+08	6,26E+07	1,50E+01
	August			**Sizeclass**														
				2,00E-07	**3,12E-07**	**4,86E-07**	**7,58E-07**	**1,18E-06**	**1,84E-06**	**2,87E-06**	**4,47E-06**	**6,97E-06**	**1,09E-05**	**1,69E-05**	**2,64E-05**	**4,12E-05**	**6,42E-05**	**1,00E-04**
		homoaggregates in water	**1,5**	2,19E+15	4,53E+15	2,65E+15	4,22E+14	1,82E+13	2,01E+11	5,39E+08	3,85E+05	6,49E+01	2,49E-03	5,33E-08	6,29E-14	0,00E+00	0,00E+00	0,00E+00
			2	2,05E+15	4,26E+15	2,48E+15	3,98E+14	1,70E+13	1,89E+11	5,05E+08	3,61E+05	6,08E+01	2,33E-03	4,98E-08	5,88E-14	0,00E+00	0,00E+00	0,00E+00
			2,5	1,47E+15	3,05E+15	1,77E+15	2,83E+14	1,22E+13	1,34E+11	3,57E+08	2,53E+05	4,19E+01	1,54E-03	3,05E-08	3,10E-14	0,00E+00	0,00E+00	0,00E+00
			2,9	6,84E+14	1,42E+15	8,24E+14	1,31E+14	5,56E+12	5,94E+10	1,47E+08	8,69E+04	9,52E+00	1,33E-04	2,76E-10	1,42E-18	0,00E+00	0,00E+00	0,00E+00
		homoaggregates in sediment	**1,5**	1,05E+08	2,73E+08	1,99E+08	3,96E+07	2,13E+06	2,95E+04	9,84E+01	8,77E-02	1,85E-05	8,84E-10	2,36E-14	0,00E+00	0,00E+00	0,00E+00	0,00E+00
			2	6,25E+08	2,02E+09	1,84E+09	4,60E+08	3,07E+07	5,30E+05	2,21E+03	2,46E+00	6,46E-04	3,86E-08	1,29E-12	0,00E+00	0,00E+00	0,00E+00	0,00E+00
			2,5	2,83E+09	1,14E+10	1,29E+10	4,02E+09	3,37E+08	7,22E+06	3,74E+04	5,16E+01	1,66E-02	1,19E-06	4,58E-11	9,06E-17	0,00E+00	0,00E+00	0,00E+00
			2,9	5,77E+09	2,79E+10	3,75E+10	1,39E+10	1,37E+09	3,40E+07	1,95E+05	2,69E+02	6,84E-02	2,23E-06	1,07E-11	0,00E+00	0,00E+00	0,00E+00	0,00E+00
				Sizeclass														
				1,00E-06	**1,39E-06**	**1,93E-06**	**2,69E-06**	**3,74E-06**	**5,19E-06**	**7,22E-06**	**1,00E-05**	**1,40E-05**	**1,94E-05**	**2,70E-05**	**3,75E-05**	**5,21E-05**	**7,24E-05**	**1,00E-04**
		heteroaggregates in water	**1,5**	2,02E+08	9,70E+08	3,38E+09	8,96E+09	1,79E+10	2,69E+10	3,02E+10	2,53E+10	1,57E+10	7,28E+09	2,48E+09	6,31E+08	1,17E+08	1,61E+07	1,78E+00
			2	1,89E+08	9,10E+08	3,17E+09	8,41E+09	1,68E+10	2,52E+10	2,83E+10	2,38E+10	1,48E+10	6,83E+09	2,33E+09	5,92E+08	1,10E+08	1,51E+07	1,67E+00
			2,5	1,35E+08	6,51E+08	2,27E+09	6,01E+09	1,20E+10	1,80E+10	2,03E+10	1,70E+10	1,06E+10	4,89E+09	1,67E+09	4,24E+08	7,89E+07	1,08E+07	1,19E+00
			2,9	6,30E+07	3,03E+08	1,06E+09	2,80E+09	5,60E+09	8,40E+09	9,45E+09	7,92E+09	4,92E+09	2,28E+09	7,75E+08	1,97E+08	3,67E+07	5,05E+06	5,53E-01
		heteroaggregates in sediment	**1,5**	1,91E+04	1,19E+05	5,29E+05	1,95E+06	6,42E+06	2,16E+07	3,32E+07	4,00E+07	4,53E+07	6,02E+07	2,37E+07	9,37E+06	3,38E+06	1,65E+06	2,22E+00
			2	1,83E+04	1,16E+05	5,20E+05	1,92E+06	6,26E+06	2,07E+07	3,18E+07	3,82E+07	4,30E+07	5,68E+07	2,24E+07	8,83E+06	3,18E+06	1,55E+06	2,09E+00
			2,5	1,49E+04	1,06E+05	5,38E+05	2,15E+06	7,02E+06	2,05E+07	3,37E+07	4,22E+07	4,53E+07	5,05E+07	2,16E+07	8,57E+06	2,93E+06	1,24E+06	1,49E+00
			2,9	1,04E+04	1,02E+05	7,00E+05	3,54E+06	1,32E+07	3,68E+07	7,76E+07	1,21E+08	1,40E+08	1,20E+08	7,58E+07	3,58E+07	1,23E+07	3,18E+06	7,65E-01

alpha river	Month	State of aggregation	Df	Sizeclass													
				2,00E-07	3,12E-07	4,86E-07	7,58E-07	1,18E-06	1,84E-06	2,87E-06	4,47E-06	6,97E-06	1,09E-05	1,69E-05	2,64E-05	4,12E-05	6,42E-05	1,00E-04
0,1	November	homoaggregates in water	1,5	2,12E+15	4,42E+15	2,56E+15	4,11E+14	1,77E+13	1,95E+11	5,23E+08	3,74E+05	6,31E+01	2,41E-03	5,19E-08	6,11E-14	0,00E+00	0,00E+00	0,00E+00
			2	1,99E+15	4,14E+15	2,40E+15	3,85E+14	1,66E+13	1,83E+11	4,91E+08	3,50E+05	5,90E+01	2,26E-03	4,85E-08	5,70E-14	0,00E+00	0,00E+00	0,00E+00
			2,5	1,42E+15	2,97E+15	1,72E+15	2,75E+14	1,18E+13	1,30E+11	3,48E+08	2,46E+05	4,07E+01	1,49E-03	2,96E-08	3,01E-14	0,00E+00	0,00E+00	0,00E+00
			2,9	6,67E+14	1,38E+15	7,98E+14	1,27E+14	5,38E+12	5,74E+10	1,43E+08	8,44E+04	9,26E+00	1,29E-04	2,68E-10	1,38E-18	0,00E+00	0,00E+00	0,00E+00
		homoaggregates in sediment	1,5	1,33E+08	3,46E+08	2,50E+08	5,00E+07	2,69E+06	3,70E+04	1,24E+02	1,11E-01	2,33E-05	1,11E-09	2,99E-14	0,00E+00	0,00E+00	0,00E+00	0,00E+00
			2	7,88E+08	2,56E+09	2,31E+09	5,77E+08	3,88E+07	6,66E+05	2,79E+03	3,10E+00	8,15E-04	4,85E-08	1,63E-12	0,00E+00	0,00E+00	0,00E+00	0,00E+00
			2,5	3,57E+09	1,45E+10	1,63E+10	5,07E+09	4,25E+08	9,09E+06	4,74E+04	6,51E+01	2,10E-02	1,50E-06	5,78E-11	1,14E-16	0,00E+00	0,00E+00	0,00E+00
			2,9	7,30E+09	3,52E+10	4,72E+10	1,75E+10	1,72E+09	4,26E+07	2,47E+05	3,39E+02	8,64E-02	2,80E-06	1,35E-11	0,00E+00	0,00E+00	0,00E+00	0,00E+00
				Sizeclass														
				1,00E-06	1,39E-06	1,93E-06	2,69E-06	3,74E-06	5,19E-06	7,22E-06	1,00E-05	1,40E-05	1,94E-05	2,70E-05	3,75E-05	5,21E-05	7,24E-05	1,00E-04
		heteroaggregates in water	1,5	3,31E+08	1,59E+09	5,55E+09	1,47E+10	2,94E+10	4,41E+10	4,96E+10	4,16E+10	2,58E+10	1,20E+10	4,07E+09	1,04E+09	1,93E+08	2,65E+07	2,91E+00
			2	3,10E+08	1,49E+09	5,20E+09	1,38E+10	2,76E+10	4,13E+10	4,65E+10	3,90E+10	2,42E+10	1,12E+10	3,82E+09	9,72E+08	1,81E+08	2,48E+07	2,73E+00
			2,5	2,22E+08	1,07E+09	3,72E+09	9,86E+09	1,97E+10	2,96E+10	3,33E+10	2,79E+10	1,73E+10	8,02E+09	2,73E+09	6,95E+08	1,29E+08	1,78E+07	1,95E+00
			2,9	1,03E+08	4,97E+08	1,73E+09	4,59E+09	9,19E+09	1,38E+10	1,55E+10	1,30E+10	8,07E+09	3,74E+09	1,27E+09	3,24E+08	6,03E+07	8,28E+06	9,05E-01
		heteroaggregates in sediment	1,5	4,07E+04	2,54E+05	1,13E+06	4,16E+06	1,37E+07	4,60E+07	7,09E+07	8,53E+07	9,66E+07	1,28E+08	5,05E+07	2,00E+07	7,21E+06	3,52E+06	4,73E+00
			2	3,90E+04	2,47E+05	1,11E+06	4,08E+06	1,33E+07	4,40E+07	6,78E+07	8,14E+07	9,17E+07	1,21E+08	4,76E+07	1,88E+07	6,78E+06	3,30E+06	4,44E+00
			2,5	3,18E+04	2,27E+05	1,14E+06	4,57E+06	1,49E+07	4,37E+07	7,17E+07	8,99E+07	9,64E+07	1,07E+08	4,60E+07	1,83E+07	6,24E+06	2,64E+06	3,18E+00
			2,9	2,21E+04	2,18E+05	1,49E+06	7,53E+06	2,82E+07	7,83E+07	1,65E+08	2,58E+08	2,98E+08	2,56E+08	1,62E+08	7,62E+07	2,63E+07	6,78E+06	1,63E+00

Appendix XI: Number concentrations of aggregates, obtained at point 4, with alpha (T) = 0,001

alpha river	Month	State of aggregation	Df	Size class													
				2,00E-07	3,12E-07	4,86E-07	7,58E-07	1,18E-06	1,84E-06	2,87E-06	4,47E-06	6,97E-06	1,09E-05	1,69E-05	2,64E-05	4,12E-05	6,42E-05	1,00E-04
0	January	homoaggregates in water	1,5	7,33E+13	1,52E+14	8,86E+13	1,42E+13	6,13E+11	6,78E+09	1,83E+07	1,30E+04	2,21E+00	8,59E-05	1,86E-09	2,52E-15	1,36E-27	0,00E+00	0,00E+00
			2	6,87E+13	1,42E+14	8,31E+13	1,34E+13	5,76E+11	6,36E+09	1,71E+07	1,22E+04	2,07E+00	8,03E-05	1,74E-09	2,37E-15	1,35E-27	0,00E+00	0,00E+00
			2,5	4,92E+13	1,02E+14	5,94E+13	9,51E+12	4,09E+11	4,53E+09	1,21E+07	8,54E+03	1,42E+00	5,38E-05	1,17E-09	2,34E-15	8,91E-27	0,00E+00	0,00E+00
			2,9	2,30E+13	4,73E+13	2,76E+13	4,41E+12	1,87E+11	2,00E+09	4,97E+06	2,95E+03	3,37E-01	6,08E-06	3,89E-11	1,55E-16	7,70E-27	0,00E+00	0,00E+00
		homoaggregates in sediment	1,5	3,12E+06	8,08E+06	5,87E+06	1,18E+06	6,32E+04	8,73E+02	2,94E+00	2,62E-03	5,55E-07	2,69E-11	7,28E-16	1,23E-21	0,00E+00	0,00E+00	0,00E+00
			2	1,85E+07	5,97E+07	5,42E+07	1,36E+07	9,13E+05	1,57E+04	6,60E+01	7,33E-02	1,94E-05	1,17E-09	3,96E-14	8,40E-20	0,00E+00	0,00E+00	0,00E+00
			2,5	8,36E+07	3,38E+08	3,82E+08	1,19E+08	9,97E+06	2,15E+05	1,12E+03	1,53E+00	4,98E-04	3,66E-08	1,54E-12	6,04E-18	0,00E+00	0,00E+00	0,00E+00
			2,9	1,71E+08	8,18E+08	1,11E+09	4,11E+08	4,05E+07	1,01E+06	5,82E+03	8,04E+00	2,13E-03	8,95E-08	1,33E-12	1,24E-17	1,42E-27	0,00E+00	0,00E+00
				Sizeclass														
				1,00E-06	1,39E-06	1,93E-06	2,69E-06	3,74E-06	5,19E-06	7,22E-06	1,00E-05	1,40E-05	1,94E-05	2,70E-05	3,75E-05	5,21E-05	7,24E-05	1,00E-04
		heteroaggregates in water	1,5	0	0	0	0	0	0	0	0	0	0	0	0	0	0	0
			2	0	0	0	0	0	0	0	0	0	0	0	0	0	0	0
			2,5	0	0	0	0	0	0	0	0	0	0	0	0	0	0	0
			2,9	0	0	0	0	0	0	0	0	0	0	0	0	0	0	0
		heteroaggregates in sediment	1,5	0	0	0	0	0	0	0	0	0	0	0	0	0	0	0
			2	0	0	0	0	0	0	0	0	0	0	0	0	0	0	0
			2,5	0	0	0	0	0	0	0	0	0	0	0	0	0	0	0
			2,9	0	0	0	0	0	0	0	0	0	0	0	0	0	0	0
	March			Sizeclass														
				2,00E-07	3,12E-07	4,86E-07	7,58E-07	1,18E-06	1,84E-06	2,87E-06	4,47E-06	6,97E-06	1,09E-05	1,69E-05	2,64E-05	4,12E-05	6,42E-05	1,00E-04
		homoaggregates in water	1,5	1,31E+15	2,80E+15	1,70E+15	2,83E+14	1,27E+13	1,46E+11	4,17E+08	3,27E+05	6,54E+01	3,50E-03	1,13E-07	1,14E-12	1,90E-23	0,00E+00	0,00E+00
			2	1,23E+15	2,62E+15	1,59E+15	2,64E+14	1,18E+13	1,36E+11	3,85E+08	3,01E+05	5,99E+01	3,18E-03	1,04E-07	1,15E-12	2,01E-23	0,00E+00	0,00E+00
			2,5	8,88E+14	1,88E+15	1,13E+15	1,85E+14	8,16E+12	9,29E+10	2,60E+08	2,00E+05	4,23E+01	3,33E-03	6,66E-07	4,46E-08	4,72E-10	6,51E-20	0,00E+00
			2,9	1,51E+12	3,10E+12	1,74E+12	2,64E+11	1,05E+10	1,01E+08	2,11E+05	9,84E+01	7,99E-03	1,05E-07	9,43E-13	8,42E-16	4,14E-27	4,63E-06	9,23E-14
		homoaggregates in sediment	1,5	3,05E+07	8,13E+07	6,17E+07	1,28E+07	7,16E+05	1,03E+04	3,67E+01	3,60E-02	8,98E-06	6,00E-10	2,41E-14	3,04E-19	0,00E+00	0,00E+00	0,00E+00
			2	1,81E+08	6,02E+08	5,69E+08	1,47E+08	1,03E+07	1,84E+05	8,12E+02	9,90E-01	3,07E-04	2,54E-08	1,30E-12	2,23E-17	6,08E-28	0,00E+00	0,00E+00
			2,5	8,26E+08	3,41E+09	3,98E+09	1,27E+09	1,09E+08	2,41E+06	1,31E+04	1,97E+01	8,09E-03	1,24E-06	4,83E-10	6,29E-11	1,30E-12	3,48E-22	0,00E+00
			2,9	6,13E+06	2,93E+07	3,82E+07	1,35E+07	1,24E+06	2,78E+04	1,35E+02	1,47E-01	2,77E-05	8,48E-10	1,77E-14	3,66E-17	4,19E-28	1,09E-06	5,04E-14
				Sizeclass														
				1,00E-06	1,39E-06	1,93E-06	2,69E-06	3,74E-06	5,19E-06	7,22E-06	1,00E-05	1,40E-05	1,94E-05	2,70E-05	3,75E-05	5,21E-05	7,24E-05	1,00E-04
		heteroaggregates in water	1,5	0	0	0	0	0	0	0	0	0	0	0	0	0	0	0
			2	0	0	0	0	0	0	0	0	0	0	0	0	0	0	0
			2,5	0	0	0	0	0	0	0	0	0	0	0	0	0	0	0
			2,9	0	0	0	0	0	0	0	0	0	0	0	0	0	0	0
		heteroaggregates in sediment	1,5	0	0	0	0	0	0	0	0	0	0	0	0	0	0	0
			2	0	0	0	0	0	0	0	0	0	0	0	0	0	0	0
			2,5	0	0	0	0	0	0	0	0	0	0	0	0	0	0	0
			2,9	0	0	0	0	0	0	0	0	0	0	0	0	0	0	0

alpha river	Month	State of aggregation	Df	Size class													
				2,00E-07	3,12E-07	4,86E-07	7,58E-07	1,18E-06	1,84E-06	2,87E-06	4,47E-06	6,97E-06	1,09E-05	1,69E-05	2,64E-05	4,12E-05	6,42E-05	1,00E-04
0	May	homoaggregates in water	1,5	5,16E+15	1,09E+16	6,55E+15	1,07E+15	4,77E+13	5,38E+11	1,51E+09	1,14E+06	2,17E+02	1,04E-02	2,91E-07	1,72E-12	1,86E-23	0,00E+00	0,00E+00
			2	4,83E+15	1,02E+16	6,14E+15	1,00E+15	4,44E+13	5,02E+11	1,40E+09	1,06E+06	2,00E+02	9,56E-03	2,72E-07	1,69E-12	1,93E-23	0,00E+00	0,00E+00
			2,5	3,48E+15	7,33E+15	4,35E+15	7,07E+14	3,11E+13	3,48E+11	9,58E+08	7,19E+05	1,39E+02	8,67E-03	8,05E-07	1,49E-09	1,11E-19	0,00E+00	0,00E+00
			2,9	7,41E+12	1,52E+13	8,58E+12	1,30E+12	5,20E+10	4,99E+08	1,05E+06	4,95E+02	4,09E-02	5,71E-07	6,11E-12	1,38E-14	5,64E-26	3,15E-03	5,40E-11
		homoaggregates in sediment	1,5	3,56E+08	9,38E+08	7,04E+08	1,44E+08	7,98E+06	1,13E+05	3,93E+02	3,72E-01	8,82E-05	5,29E-09	1,84E-13	1,36E-18	0,00E+00	0,00E+00	0,00E+00
			2	2,11E+09	6,95E+09	6,50E+09	1,66E+09	1,14E+08	2,01E+06	8,74E+03	1,03E+01	3,03E-03	2,26E-07	1,00E-11	9,73E-17	0,00E+00	0,00E+00	0,00E+00
			2,5	9,58E+09	3,93E+10	4,54E+10	1,44E+10	1,23E+09	2,67E+07	1,43E+05	2,10E+02	7,90E-02	9,57E-06	1,73E-09	6,21E-12	9,07E-22	0,00E+00	0,00E+00
			2,9	8,94E+07	4,25E+08	5,59E+08	1,97E+08	1,83E+07	4,08E+05	2,00E+03	2,19E+00	4,20E-04	1,36E-08	3,39E-13	1,78E-15	1,69E-26	2,19E-03	8,74E-11
				Sizeclass														
				1,00E-06	1,39E-06	1,93E-06	2,69E-06	3,74E-06	5,19E-06	7,22E-06	1,00E-05	1,40E-05	1,94E-05	2,70E-05	3,75E-05	5,21E-05	7,24E-05	1,00E-04
		heteroaggregates in water	1,5	0	0	0	0	0	0	0	0	0	0	0	0	0	0	0
			2	0	0	0	0	0	0	0	0	0	0	0	0	0	0	0
			2,5	0	0	0	0	0	0	0	0	0	0	0	0	0	0	0
			2,9	0	0	0	0	0	0	0	0	0	0	0	0	0	0	0
		heteroaggregates in sediment	1,5	0	0	0	0	0	0	0	0	0	0	0	0	0	0	0
			2	0	0	0	0	0	0	0	0	0	0	0	0	0	0	0
			2,5	0	0	0	0	0	0	0	0	0	0	0	0	0	0	0
			2,9	0	0	0	0	0	0	0	0	0	0	0	0	0	0	0
	August			Sizeclass														
				2,00E-07	3,12E-07	4,86E-07	7,58E-07	1,18E-06	1,84E-06	2,87E-06	4,47E-06	6,97E-06	1,09E-05	1,69E-05	2,64E-05	4,12E-05	6,42E-05	1,00E-04
		homoaggregates in water	1,5	2,09E+15	4,47E+15	2,77E+15	4,67E+14	2,12E+13	2,49E+11	7,25E+08	5,84E+05	1,24E+02	7,39E-03	2,74E-07	9,25E-18	0,00E+00	0,00E+00	0,00E+00
			2	1,96E+15	4,19E+15	2,59E+15	4,37E+14	1,97E+13	2,30E+11	6,67E+08	5,33E+05	1,13E+02	6,67E-03	2,53E-07	8,70E-18	0,00E+00	0,00E+00	0,00E+00
			2,5	1,42E+15	3,02E+15	1,83E+15	3,03E+14	1,35E+13	1,55E+11	4,40E+08	3,51E+05	8,01E+01	7,97E-03	3,51E-06	4,88E-16	0,00E+00	0,00E+00	0,00E+00
			2,9	1,81E+12	3,71E+12	2,12E+12	3,24E+11	1,29E+10	1,25E+08	2,72E+05	1,46E+02	2,40E-02	7,84E-06	1,58E-03	1,61E-04	8,11E-16	4,50E-02	4,95E-13
		homoaggregates in sediment	1,5	1,01E+08	2,69E+08	2,09E+08	4,39E+07	2,49E+06	3,64E+04	1,33E+02	1,33E-01	3,54E-05	2,63E-09	1,22E-13	5,13E-24	0,00E+00	0,00E+00	0,00E+00
			2	5,99E+08	2,00E+09	1,92E+09	5,05E+08	3,56E+07	6,47E+05	2,92E+03	3,64E+00	1,20E-03	1,11E-07	6,55E-12	3,50E-22	0,00E+00	0,00E+00	0,00E+00
			2,5	2,74E+09	1,14E+10	1,34E+10	4,32E+09	3,74E+08	8,37E+06	4,61E+04	7,16E+01	3,18E-02	6,17E-06	5,28E-09	1,43E-18	0,00E+00	0,00E+00	0,00E+00
			2,9	1,53E+07	7,28E+07	9,66E+07	3,44E+07	3,18E+06	7,17E+04	3,61E+02	4,52E-01	1,73E-04	1,31E-07	6,14E-05	1,45E-05	1,70E-16	2,20E-02	5,61E-13
				Sizeclass														
				1,00E-06	1,39E-06	1,93E-06	2,69E-06	3,74E-06	5,19E-06	7,22E-06	1,00E-05	1,40E-05	1,94E-05	2,70E-05	3,75E-05	5,21E-05	7,24E-05	1,00E-04
		heteroaggregates in water	1,5	0	0	0	0	0	0	0	0	0	0	0	0	0	0	0
			2	0	0	0	0	0	0	0	0	0	0	0	0	0	0	0
			2,5	0	0	0	0	0	0	0	0	0	0	0	0	0	0	0
			2,9	0	0	0	0	0	0	0	0	0	0	0	0	0	0	0
		heteroaggregates in sediment	1,5	0	0	0	0	0	0	0	0	0	0	0	0	0	0	0
			2	0	0	0	0	0	0	0	0	0	0	0	0	0	0	0
			2,5	0	0	0	0	0	0	0	0	0	0	0	0	0	0	0
			2,9	0	0	0	0	0	0	0	0	0	0	0	0	0	0	0

alpha river	Month	State of aggregation	Df	Size class														
				2,00E-07	3,12E-07	4,86E-07	7,58E-07	1,18E-06	1,84E-06	2,87E-06	4,47E-06	6,97E-06	1,09E-05	1,69E-05	2,64E-05	4,12E-05	6,42E-05	1,00E-04
0	November	homoaggregates in water	1,5	2,06E+15	4,39E+15	2,65E+15	4,40E+14	1,97E+13	2,25E+11	6,36E+08	4,92E+05	9,72E+01	5,03E-03	1,55E-07	1,32E-12	1,95E-23	0,00E+00	0,00E+00
			2	1,93E+15	4,11E+15	2,48E+15	4,10E+14	1,83E+13	2,09E+11	5,91E+08	4,54E+05	8,91E+01	4,59E-03	1,44E-07	1,32E-12	2,06E-23	0,00E+00	0,00E+00
			2,5	1,39E+15	2,95E+15	1,76E+15	2,88E+14	1,27E+13	1,43E+11	4,00E+08	3,05E+05	6,26E+01	4,59E-03	7,18E-07	1,52E-08	3,07E-13	3,75E-23	0,00E+00
			2,9	2,56E+12	5,24E+12	2,95E+12	4,50E+11	1,79E+10	1,71E+08	3,61E+05	1,69E+02	1,38E-02	1,85E-07	1,74E-12	1,99E-15	9,47E-27	4,50E-05	8,71E-13
		homoaggregates in sediment	1,5	1,29E+08	3,43E+08	2,59E+08	5,36E+07	2,99E+06	4,27E+04	1,51E+02	1,46E-01	3,60E-05	2,33E-09	8,92E-14	9,53E-19	0,00E+00	0,00E+00	0,00E+00
			2	7,67E+08	2,54E+09	2,39E+09	6,16E+08	4,28E+07	7,61E+05	3,36E+03	4,02E+00	1,23E-03	9,89E-08	4,82E-12	6,92E-17	1,68E-27	0,00E+00	0,00E+00
			2,5	3,50E+09	1,44E+10	1,67E+10	5,32E+09	4,58E+08	1,00E+07	5,44E+04	8,08E+01	3,23E-02	4,60E-06	1,40E-09	5,77E-11	2,27E-15	5,39E-25	0,00E+00
			2,9	2,81E+07	1,34E+08	1,75E+08	6,19E+07	5,72E+06	1,27E+05	6,24E+02	6,77E-01	1,29E-04	4,01E-09	8,76E-14	2,33E-16	2,58E-27	2,85E-05	1,28E-12
				Sizeclass														
				1,00E-06	1,39E-06	1,93E-06	2,69E-06	3,74E-06	5,19E-06	7,22E-06	1,00E-05	1,40E-05	1,94E-05	2,70E-05	3,75E-05	5,21E-05	7,24E-05	1,00E-04
		heteroaggregates in water	1,5	0	0	0	0	0	0	0	0	0	0	0	0	0	0	0
			2	0	0	0	0	0	0	0	0	0	0	0	0	0	0	0
			2,5	0	0	0	0	0	0	0	0	0	0	0	0	0	0	0
			2,9	0	0	0	0	0	0	0	0	0	0	0	0	0	0	0
		heteroaggregates in sediment	1,5	0	0	0	0	0	0	0	0	0	0	0	0	0	0	0
			2	0	0	0	0	0	0	0	0	0	0	0	0	0	0	0
			2,5	0	0	0	0	0	0	0	0	0	0	0	0	0	0	0
			2,9	0	0	0	0	0	0	0	0	0	0	0	0	0	0	0

alpha river	Month	State of aggregation	Df	Size class													
				2,00E-07	**3,12E-07**	**4,86E-07**	**7,58E-07**	**1,18E-06**	**1,84E-06**	**2,87E-06**	**4,47E-06**	**6,97E-06**	**1,09E-05**	**1,69E-05**	**2,64E-05**	**4,12E-05**	**6,42E-05**	**1,00E-04**
0,001	January	homoaggregates in water	**1,5**	7,33E+13	1,52E+14	8,86E+13	1,42E+13	6,13E+11	6,78E+09	1,83E+07	1,30E+04	2,21E+00	8,59E-05	1,86E-09	2,52E-15	1,36E-27	0,00E+00	0,00E+00
			2	6,87E+13	1,42E+14	8,31E+13	1,34E+13	5,76E+11	6,36E+09	1,71E+07	1,22E+04	2,07E+00	8,03E-05	1,74E-09	2,37E-15	1,35E-27	0,00E+00	0,00E+00
			2,5	4,92E+13	1,02E+14	5,94E+13	9,51E+12	4,09E+11	4,53E+09	1,21E+07	8,54E+03	1,42E+00	5,38E-05	1,17E-09	2,34E-15	8,91E-27	0,00E+00	0,00E+00
			2,9	2,30E+13	4,73E+13	2,76E+13	4,41E+12	1,87E+11	2,00E+09	4,97E+06	2,95E+03	3,37E-01	6,08E-06	3,89E-11	1,55E-16	7,70E-27	0,00E+00	0,00E+00
		homoaggregates in sediment	**1,5**	3,12E+06	8,08E+06	5,87E+06	1,18E+06	6,32E+04	8,73E+02	2,94E+00	2,62E-03	5,55E-07	2,69E-11	7,28E-16	1,23E-21	0,00E+00	0,00E+00	0,00E+00
			2	1,85E+07	5,97E+07	5,42E+07	1,36E+07	9,13E+05	1,57E+04	6,60E+01	7,33E-02	1,94E-05	1,17E-09	3,96E-14	8,40E-20	0,00E+00	0,00E+00	0,00E+00
			2,5	8,36E+07	3,38E+08	3,82E+08	1,19E+08	9,97E+06	2,15E+05	1,12E+03	1,53E+00	4,98E-04	3,66E-08	1,54E-12	6,04E-18	0,00E+00	0,00E+00	0,00E+00
			2,9	1,71E+08	8,18E+08	1,11E+09	4,11E+08	4,05E+07	1,01E+06	5,82E+03	8,04E+00	2,13E-03	8,95E-08	1,33E-12	1,24E-17	1,42E-27	0,00E+00	0,00E+00
				Sizeclass														
				1,00E-06	**1,39E-06**	**1,93E-06**	**2,69E-06**	**3,74E-06**	**5,19E-06**	**7,22E-06**	**1,00E-05**	**1,40E-05**	**1,94E-05**	**2,70E-05**	**3,75E-05**	**5,21E-05**	**7,24E-05**	**1,00E-04**
		heteroaggregates in water	**1,5**	1,04E+05	5,01E+05	1,75E+06	4,63E+06	9,26E+06	1,39E+07	1,56E+07	1,31E+07	8,12E+06	3,76E+06	1,28E+06	3,26E+05	6,07E+04	8,34E+03	9,19E-04
			2	9,75E+04	4,70E+05	1,64E+06	4,33E+06	8,67E+06	1,30E+07	1,46E+07	1,22E+07	7,61E+06	3,52E+06	1,20E+06	3,05E+05	5,68E+04	7,81E+03	8,61E-04
			2,5	6,98E+04	3,36E+05	1,17E+06	3,10E+06	6,21E+06	9,30E+06	1,05E+07	8,77E+06	5,44E+06	2,52E+06	8,59E+05	2,19E+05	4,07E+04	5,59E+03	6,15E-04
			2,9	3,24E+04	1,56E+05	5,44E+05	1,44E+06	2,88E+06	4,32E+06	4,86E+06	4,07E+06	2,53E+06	1,17E+06	3,99E+05	1,02E+05	1,89E+04	2,60E+03	2,85E-04
		heteroaggregates in sediment	**1,5**	8,68E+00	5,43E+01	2,41E+02	8,87E+02	2,92E+03	9,82E+03	1,51E+04	1,82E+04	2,06E+04	2,74E+04	1,08E+04	4,26E+03	1,54E+03	7,51E+02	1,01E-03
			2	8,32E+00	5,27E+01	2,36E+02	8,71E+02	2,84E+03	9,39E+03	1,45E+04	1,74E+04	1,96E+04	2,58E+04	1,02E+04	4,01E+03	1,45E+03	7,04E+02	9,49E-04
			2,5	6,79E+00	4,84E+01	2,44E+02	9,76E+02	3,19E+03	9,33E+03	1,53E+04	1,92E+04	2,06E+04	2,29E+04	9,81E+03	3,90E+03	1,33E+03	5,63E+02	6,79E-04
			2,9	4,71E+00	4,64E+01	3,18E+02	1,60E+03	6,01E+03	1,67E+04	3,52E+04	5,50E+04	6,34E+04	5,45E+04	3,44E+04	1,62E+04	5,59E+03	1,44E+03	3,48E-04
	March			**Sizeclass**														
				2,00E-07	**3,12E-07**	**4,86E-07**	**7,58E-07**	**1,18E-06**	**1,84E-06**	**2,87E-06**	**4,47E-06**	**6,97E-06**	**1,09E-05**	**1,69E-05**	**2,64E-05**	**4,12E-05**	**6,42E-05**	**1,00E-04**
		homoaggregates in water	**1,5**	1,31E+15	2,80E+15	1,70E+15	2,83E+14	1,27E+13	1,46E+11	4,17E+08	3,27E+05	6,54E+01	3,50E-03	1,13E-07	1,14E-12	1,90E-23	0,00E+00	0,00E+00
			2	1,23E+15	2,62E+15	1,59E+15	2,64E+14	1,18E+13	1,36E+11	3,85E+08	3,01E+05	5,99E+01	3,18E-03	1,04E-07	1,15E-12	2,01E-23	0,00E+00	0,00E+00
			2,5	8,88E+14	1,88E+15	1,13E+15	1,85E+14	8,16E+12	9,29E+10	2,60E+08	2,00E+05	4,23E+01	3,33E-03	6,66E-07	4,46E-08	4,72E-10	6,51E-20	0,00E+00
			2,9	1,51E+12	3,10E+12	1,74E+12	2,64E+11	1,05E+10	1,01E+08	2,11E+05	9,84E+01	7,99E-03	1,05E-07	9,43E-13	8,42E-16	4,14E-27	4,63E-06	9,23E-14
		homoaggregates in sediment	**1,5**	3,04E+07	8,11E+07	6,15E+07	1,28E+07	7,14E+05	1,03E+04	3,66E+01	3,59E-02	8,96E-06	5,99E-10	2,40E-14	3,03E-19	0,00E+00	0,00E+00	0,00E+00
			2	1,81E+08	6,00E+08	5,67E+08	1,47E+08	1,02E+07	1,84E+05	8,10E+02	9,87E-01	3,06E-04	2,54E-08	1,30E-12	2,22E-17	0,00E+00	0,00E+00	0,00E+00
			2,5	8,24E+08	3,40E+09	3,97E+09	1,26E+09	1,09E+08	2,41E+06	1,31E+04	1,96E+01	8,07E-03	1,24E-06	4,81E-10	6,27E-11	1,29E-12	3,47E-22	0,00E+00
			2,9	6,12E+06	2,92E+07	3,81E+07	1,34E+07	1,24E+06	2,77E+04	1,35E+02	1,46E-01	2,76E-05	8,46E-10	1,76E-14	3,65E-17	0,00E+00	1,09E-06	5,03E-14
				Sizeclass														
				1,00E-06	**1,39E-06**	**1,93E-06**	**2,69E-06**	**3,74E-06**	**5,19E-06**	**7,22E-06**	**1,00E-05**	**1,40E-05**	**1,94E-05**	**2,70E-05**	**3,75E-05**	**5,21E-05**	**7,24E-05**	**1,00E-04**
		heteroaggregates in water	**1,5**	1,06E+06	5,11E+06	1,78E+07	4,71E+07	9,42E+07	1,41E+08	1,59E+08	1,33E+08	8,25E+07	3,82E+07	1,30E+07	3,31E+06	6,16E+05	8,47E+04	9,68E-03
			2	9,95E+05	4,79E+06	1,67E+07	4,42E+07	8,82E+07	1,32E+08	1,49E+08	1,25E+08	7,73E+07	3,58E+07	1,22E+07	3,10E+06	5,78E+05	7,94E+04	9,05E-03
			2,5	7,11E+05	3,42E+06	1,19E+07	3,16E+07	6,31E+07	9,45E+07	1,06E+08	8,90E+07	5,53E+07	2,56E+07	8,72E+06	2,22E+06	4,13E+05	5,68E+04	6,40E-03
			2,9	1,14E+03	5,49E+03	1,91E+04	5,08E+04	1,02E+05	1,52E+05	1,71E+05	1,44E+05	8,92E+04	4,14E+04	1,41E+04	3,59E+03	6,67E+02	9,17E+01	9,72E-06
		heteroaggregates in sediment	**1,5**	4,83E+01	3,02E+02	1,34E+03	4,93E+03	1,62E+04	5,45E+04	8,40E+04	1,01E+05	1,14E+05	1,52E+05	5,98E+04	2,36E+04	8,54E+03	4,17E+03	5,82E-03
			2	4,63E+01	2,94E+02	1,31E+03	4,84E+03	1,58E+04	5,22E+04	8,03E+04	9,64E+04	1,09E+05	1,43E+05	5,64E+04	2,23E+04	8,03E+03	3,91E+03	5,44E-03
			2,5	3,77E+01	2,69E+02	1,36E+03	5,42E+03	1,77E+04	5,18E+04	8,49E+04	1,06E+05	1,14E+05	1,27E+05	5,44E+04	2,16E+04	7,38E+03	3,12E+03	3,86E-03
			2,9	9,05E-02	8,92E-01	6,10E+00	3,08E+01	1,16E+02	3,21E+02	6,77E+02	1,06E+03	1,22E+03	1,05E+03	6,62E+02	3,12E+02	1,08E+02	2,78E+01	6,47E-06

alpha river	Month	State of aggregation	Df	Size class													
				2,00E-07	3,12E-07	4,86E-07	7,58E-07	1,18E-06	1,84E-06	2,87E-06	4,47E-06	6,97E-06	1,09E-05	1,69E-05	2,64E-05	4,12E-05	6,42E-05	1,00E-04
	May	homoaggregates in water	1,5	5,16E+15	1,09E+16	6,55E+15	1,07E+15	4,76E+13	5,38E+11	1,51E+09	1,14E+06	2,17E+02	1,04E-02	2,91E-07	1,72E-12	1,86E-23	0,00E+00	0,00E+00
			2	4,83E+15	1,02E+16	6,14E+15	1,00E+15	4,44E+13	5,02E+11	1,40E+09	1,06E+06	2,00E+02	9,56E-03	2,72E-07	1,69E-12	1,93E-23	0,00E+00	0,00E+00
			2,5	3,48E+15	7,33E+15	4,35E+15	7,07E+14	3,11E+13	3,47E+11	9,58E+08	7,19E+05	1,39E+02	8,67E-03	8,05E-07	1,49E-09	1,11E-19	0,00E+00	0,00E+00
			2,9	7,41E+12	1,52E+13	8,58E+12	1,30E+12	5,19E+10	4,99E+08	1,05E+06	4,95E+02	4,09E-02	5,71E-07	6,11E-12	1,38E-14	5,64E-26	3,15E-03	5,40E-11
		homoaggregates in sediment	1,5	3,56E+08	9,38E+08	7,04E+08	1,44E+08	7,98E+06	1,13E+05	3,93E+02	3,72E-01	8,82E-05	5,29E-09	1,84E-13	1,36E-18	0,00E+00	0,00E+00	0,00E+00
			2	2,11E+09	6,95E+09	6,50E+09	1,65E+09	1,14E+08	2,01E+06	8,74E+03	1,03E+01	3,03E-03	2,26E-07	1,00E-11	9,73E-17	0,00E+00	0,00E+00	0,00E+00
			2,5	9,58E+09	3,93E+10	4,54E+10	1,44E+10	1,23E+09	2,67E+07	1,43E+05	2,10E+02	7,90E-02	9,57E-06	1,73E-09	6,21E-12	9,07E-22	0,00E+00	0,00E+00
			2,9	8,94E+07	4,25E+08	5,59E+08	1,97E+08	1,83E+07	4,08E+05	2,00E+03	2,19E+00	4,20E-04	1,36E-08	3,39E-13	1,78E-15	1,69E-26	2,19E-03	8,74E-11
				Sizeclass														
				1,00E-06	1,39E-06	1,93E-06	2,69E-06	3,74E-06	5,19E-06	7,22E-06	1,00E-05	1,40E-05	1,94E-05	2,70E-05	3,75E-05	5,21E-05	7,24E-05	1,00E-04
		heteroaggregates in water	1,5	2,79E+07	1,34E+08	4,68E+08	1,24E+09	2,48E+09	3,71E+09	4,18E+09	3,50E+09	2,17E+09	1,01E+09	3,43E+08	8,72E+07	1,62E+07	2,23E+06	2,52E-01
			2	2,62E+07	1,26E+08	4,39E+08	1,16E+09	2,32E+09	3,48E+09	3,92E+09	3,28E+09	2,04E+09	9,44E+08	3,21E+08	8,18E+07	1,52E+07	2,09E+06	2,36E-01
			2,5	1,87E+07	8,99E+07	3,13E+08	8,30E+08	1,66E+09	2,49E+09	2,80E+09	2,34E+09	1,45E+09	6,74E+08	2,29E+08	5,84E+07	1,09E+07	1,49E+06	1,67E-01
			2,9	3,80E+04	1,83E+05	6,38E+05	1,69E+06	3,38E+06	5,08E+06	5,71E+06	4,79E+06	2,97E+06	1,38E+06	4,69E+05	1,19E+05	2,22E+04	3,05E+03	3,25E-04
		heteroaggregates in sediment	1,5	3,78E+03	2,36E+04	1,05E+05	3,85E+05	1,27E+06	4,26E+06	6,57E+06	7,90E+06	8,95E+06	1,19E+07	4,68E+06	1,85E+06	6,68E+05	3,26E+05	4,50E-01
			2	3,62E+03	2,29E+04	1,03E+05	3,79E+05	1,24E+06	4,08E+06	6,28E+06	7,54E+06	8,49E+06	1,12E+07	4,41E+06	1,74E+06	6,28E+05	3,06E+05	4,22E-01
			2,5	2,95E+03	2,10E+04	1,06E+05	4,23E+05	1,38E+06	4,04E+06	6,63E+06	8,31E+06	8,92E+06	9,93E+06	4,25E+06	1,69E+06	5,76E+05	2,44E+05	2,99E-01
			2,9	8,95E+00	8,82E+01	6,04E+02	3,05E+03	1,14E+04	3,17E+04	6,70E+04	1,05E+05	1,21E+05	1,04E+05	6,55E+04	3,09E+04	1,07E+04	2,75E+03	6,42E-04
0,001				Sizeclass														
	August			2,00E-07	3,12E-07	4,86E-07	7,58E-07	1,18E-06	1,84E-06	2,87E-06	4,47E-06	6,97E-06	1,09E-05	1,69E-05	2,64E-05	4,12E-05	6,42E-05	1,00E-04
		homoaggregates in water	1,5	2,09E+15	4,47E+15	2,77E+15	4,67E+14	2,12E+13	2,49E+11	7,25E+08	5,84E+05	1,24E+02	7,39E-03	2,74E-07	9,25E-18	0,00E+00	0,00E+00	0,00E+00
			2	1,96E+15	4,19E+15	2,59E+15	4,36E+14	1,97E+13	2,30E+11	6,67E+08	5,33E+05	1,13E+02	6,67E-03	2,53E-07	8,70E-18	0,00E+00	0,00E+00	0,00E+00
			2,5	1,42E+15	3,02E+15	1,83E+15	3,03E+14	1,35E+13	1,55E+11	4,40E+08	3,51E+05	8,01E+01	7,97E-03	3,51E-06	4,88E-16	0,00E+00	0,00E+00	0,00E+00
			2,9	1,81E+12	3,71E+12	2,12E+12	3,24E+11	1,29E+10	1,25E+08	2,72E+05	1,46E+02	2,40E-02	7,84E-06	1,58E-03	1,61E-04	8,11E-16	4,50E-02	4,95E-13
		homoaggregates in sediment	1,5	1,01E+08	2,69E+08	2,09E+08	4,39E+07	2,49E+06	3,64E+04	1,33E+02	1,33E-01	3,54E-05	2,63E-09	1,22E-13	5,13E-24	0,00E+00	0,00E+00	0,00E+00
			2	5,99E+08	2,00E+09	1,92E+09	5,05E+08	3,56E+07	6,47E+05	2,92E+03	3,64E+00	1,20E-03	1,11E-07	6,55E-12	3,50E-22	0,00E+00	0,00E+00	0,00E+00
			2,5	2,74E+09	1,14E+10	1,34E+10	4,32E+09	3,74E+08	8,37E+06	4,61E+04	7,16E+01	3,18E-02	6,17E-06	5,28E-09	1,43E-18	0,00E+00	0,00E+00	0,00E+00
			2,9	1,53E+07	7,28E+07	9,66E+07	3,44E+07	3,18E+06	7,17E+04	3,61E+02	4,52E-01	1,73E-04	1,31E-07	6,14E-05	1,45E-05	1,70E-16	2,20E-02	5,61E-13
				Sizeclass														
				1,00E-06	1,39E-06	1,93E-06	2,69E-06	3,74E-06	5,19E-06	7,22E-06	1,00E-05	1,40E-05	1,94E-05	2,70E-05	3,75E-05	5,21E-05	7,24E-05	1,00E-04
		heteroaggregates in water	1,5	2,03E+06	9,78E+06	3,40E+07	9,00E+07	1,80E+08	2,69E+08	3,03E+08	2,54E+08	1,57E+08	7,29E+07	2,48E+07	6,32E+06	1,18E+06	1,62E+05	1,87E-02
			2	1,90E+06	9,16E+06	3,19E+07	8,44E+07	1,69E+08	2,53E+08	2,84E+08	2,38E+08	1,48E+08	6,84E+07	2,33E+07	5,93E+06	1,10E+06	1,52E+05	1,75E-02
			2,5	1,36E+06	6,55E+06	2,28E+07	6,04E+07	1,21E+08	1,81E+08	2,03E+08	1,70E+08	1,06E+08	4,90E+07	1,67E+07	4,24E+06	7,90E+05	1,08E+05	1,24E-02
			2,9	1,64E+03	7,87E+03	2,74E+04	7,28E+04	1,46E+05	2,18E+05	2,46E+05	2,06E+05	1,28E+05	5,92E+04	2,02E+04	5,14E+03	9,56E+02	1,31E+02	1,41E-05
		heteroaggregates in sediment	1,5	1,92E+02	1,20E+03	5,32E+03	1,96E+04	6,46E+04	2,17E+05	3,34E+05	4,01E+05	4,54E+05	6,04E+05	2,37E+05	9,39E+04	3,39E+04	1,65E+04	2,35E-02
			2	1,84E+02	1,17E+03	5,23E+03	1,93E+04	6,28E+04	2,07E+05	3,19E+05	3,83E+05	4,31E+05	5,69E+05	2,24E+05	8,85E+04	3,19E+04	1,55E+04	2,19E-02
			2,5	1,50E+02	1,07E+03	5,40E+03	2,16E+04	7,04E+04	2,06E+05	3,38E+05	4,23E+05	4,54E+05	5,06E+05	2,16E+05	8,59E+04	2,93E+04	1,24E+04	1,55E-02
			2,9	2,70E-01	2,66E+00	1,82E+01	9,20E+01	3,45E+02	9,56E+02	2,02E+03	3,16E+03	3,64E+03	3,13E+03	1,97E+03	9,31E+02	3,21E+02	8,28E+01	1,95E-05

alpha river	Month	State of aggregation	Df	Size class													
				2,00E-07	3,12E-07	4,86E-07	7,58E-07	1,18E-06	1,84E-06	2,87E-06	4,47E-06	6,97E-06	1,09E-05	1,69E-05	2,64E-05	4,12E-05	6,42E-05	1,00E-04
0,001	November	homoaggregates in water	1,5	2,06E+15	4,39E+15	2,65E+15	4,40E+14	1,97E+13	2,25E+11	6,36E+08	4,92E+05	9,72E+01	5,03E-03	1,55E-07	1,32E-12	1,95E-23	0,00E+00	0,00E+00
			2	1,93E+15	4,11E+15	2,48E+15	4,10E+14	1,83E+13	2,09E+11	5,91E+08	4,54E+05	8,91E+01	4,59E-03	1,44E-07	1,32E-12	2,06E-23	0,00E+00	0,00E+00
			2,5	1,39E+15	2,95E+15	1,76E+15	2,88E+14	1,27E+13	1,43E+11	4,00E+08	3,05E+05	6,26E+01	4,59E-03	7,18E-07	1,52E-08	3,07E-13	3,75E-23	0,00E+00
			2,9	2,56E+12	5,24E+12	2,95E+12	4,50E+11	1,79E+10	1,71E+08	3,61E+05	1,69E+02	1,38E-02	1,85E-07	1,74E-12	1,99E-15	9,47E-27	4,50E-05	8,71E-13
		homoaggregates in sediment	1,5	1,29E+08	3,43E+08	2,59E+08	5,36E+07	2,99E+06	4,27E+04	1,51E+02	1,46E-01	3,60E-05	2,33E-09	8,92E-14	9,53E-19	0,00E+00	0,00E+00	0,00E+00
			2	7,67E+08	2,54E+09	2,39E+09	6,16E+08	4,28E+07	7,61E+05	3,36E+03	4,02E+00	1,23E-03	9,89E-08	4,82E-12	6,92E-17	1,68E-27	0,00E+00	0,00E+00
			2,5	3,50E+09	1,44E+10	1,67E+10	5,32E+09	4,58E+08	1,00E+07	5,44E+04	8,08E+01	3,23E-02	4,60E-06	1,40E-09	5,77E-11	2,27E-15	5,39E-25	0,00E+00
			2,9	2,81E+07	1,34E+08	1,75E+08	6,19E+07	5,72E+06	1,27E+05	6,24E+02	6,77E-01	1,29E-04	4,01E-09	8,76E-14	2,33E-16	2,58E-27	2,85E-05	1,28E-12
				Sizeclass														
				1,00E-06	1,39E-06	1,93E-06	2,69E-06	3,74E-06	5,19E-06	7,22E-06	1,00E-05	1,40E-05	1,94E-05	2,70E-05	3,75E-05	5,21E-05	7,24E-05	1,00E-04
		heteroaggregates in water	1,5	3,33E+06	1,60E+07	5,58E+07	1,48E+08	2,95E+08	4,43E+08	4,98E+08	4,17E+08	2,59E+08	1,20E+08	4,08E+07	1,04E+07	1,93E+06	2,66E+05	3,02E-02
			2	3,12E+06	1,50E+07	5,23E+07	1,38E+08	2,77E+08	4,15E+08	4,66E+08	3,91E+08	2,43E+08	1,12E+08	3,83E+07	9,74E+06	1,81E+06	2,49E+05	2,83E-02
			2,5	2,23E+06	1,07E+07	3,73E+07	9,89E+07	1,98E+08	2,96E+08	3,33E+08	2,79E+08	1,73E+08	8,03E+07	2,73E+07	6,96E+06	1,29E+06	1,78E+05	2,00E-02
			2,9	3,88E+03	1,87E+04	6,51E+04	1,73E+05	3,46E+05	5,19E+05	5,83E+05	4,89E+05	3,04E+05	1,41E+05	4,79E+04	1,22E+04	2,27E+03	3,12E+02	3,32E-05
		heteroaggregates in sediment	1,5	4,09E+02	2,56E+03	1,13E+04	4,18E+04	1,38E+05	4,62E+05	7,11E+05	8,56E+05	9,69E+05	1,29E+06	5,07E+05	2,00E+05	7,23E+04	3,53E+04	4,91E-02
			2	3,92E+02	2,49E+03	1,11E+04	4,10E+04	1,34E+05	4,42E+05	6,80E+05	8,17E+05	9,20E+05	1,21E+06	4,78E+05	1,89E+05	6,80E+04	3,31E+04	4,60E-02
			2,5	3,19E+02	2,28E+03	1,15E+04	4,59E+04	1,50E+05	4,38E+05	7,19E+05	9,01E+05	9,66E+05	1,08E+06	4,61E+05	1,83E+05	6,25E+04	2,64E+04	3,26E-02
			2,9	8,32E-01	8,20E+00	5,61E+01	2,83E+02	1,06E+03	2,95E+03	6,23E+03	9,73E+03	1,12E+04	9,64E+03	6,09E+03	2,87E+03	9,90E+02	2,55E+02	5,96E-05

alpha river	Month	State of aggregation	Df	Size class													
				2,00E-07	3,12E-07	4,86E-07	7,58E-07	1,18E-06	1,84E-06	2,87E-06	4,47E-06	6,97E-06	1,09E-05	1,69E-05	2,64E-05	4,12E-05	6,42E-05	1,00E-04
		homoaggregates in water	1,5	7,33E+13	1,52E+14	8,86E+13	1,42E+13	6,12E+11	6,77E+09	1,83E+07	1,30E+04	2,21E+00	8,59E-05	1,86E-09	2,52E-15	0,00E+00	0,00E+00	0,00E+00
			2	6,87E+13	1,42E+14	8,31E+13	1,34E+13	5,75E+11	6,36E+09	1,71E+07	1,22E+04	2,07E+00	8,03E-05	1,74E-09	2,37E-15	0,00E+00	0,00E+00	0,00E+00
			2,5	4,92E+13	1,02E+14	5,94E+13	9,51E+12	4,09E+11	4,52E+09	1,21E+07	8,54E+03	1,42E+00	5,38E-05	1,17E-09	2,34E-15	0,00E+00	0,00E+00	0,00E+00
			2,9	2,30E+13	4,73E+13	2,76E+13	4,41E+12	1,87E+11	2,00E+09	4,97E+06	2,95E+03	3,37E-01	6,08E-06	3,89E-11	1,55E-16	0,00E+00	0,00E+00	0,00E+00
		homoaggregates in sediment	1,5	3,11E+06	8,07E+06	5,86E+06	1,18E+06	6,32E+04	8,72E+02	2,94E+00	2,62E-03	5,55E-07	2,69E-11	7,27E-16	0,00E+00	0,00E+00	0,00E+00	0,00E+00
			2	1,84E+07	5,96E+07	5,42E+07	1,36E+07	9,12E+05	1,57E+04	6,59E+01	7,33E-02	1,94E-05	1,17E-09	3,96E-14	0,00E+00	0,00E+00	0,00E+00	0,00E+00
			2,5	8,35E+07	3,37E+08	3,82E+08	1,19E+08	9,96E+06	2,14E+05	1,12E+03	1,53E+00	4,98E-04	3,66E-08	1,54E-12	0,00E+00	0,00E+00	0,00E+00	0,00E+00
			2,9	1,71E+08	8,17E+08	1,11E+09	4,11E+08	4,04E+07	1,00E+06	5,81E+03	8,03E+00	2,13E-03	8,94E-08	1,33E-12	0,00E+00	0,00E+00	0,00E+00	0,00E+00
	January			Sizeclass														
				1,00E-06	1,39E-06	1,93E-06	2,69E-06	3,74E-06	5,19E-06	7,22E-06	1,00E-05	1,40E-05	1,94E-05	2,70E-05	3,75E-05	5,21E-05	7,24E-05	1,00E-04
		heteroaggregates in water	1,5	1,04E+06	5,01E+06	1,75E+07	4,63E+07	9,26E+07	1,39E+08	1,56E+08	1,31E+08	8,12E+07	3,76E+07	1,28E+07	3,26E+06	6,07E+05	8,34E+04	9,19E-03
			2	9,75E+05	4,69E+06	1,64E+07	4,33E+07	8,67E+07	1,30E+08	1,46E+08	1,22E+08	7,61E+07	3,52E+07	1,20E+07	3,05E+06	5,68E+05	7,81E+04	8,61E-03
			2,5	6,98E+05	3,36E+06	1,17E+07	3,10E+07	6,20E+07	9,30E+07	1,05E+08	8,77E+07	5,44E+07	2,52E+07	8,59E+06	2,19E+06	4,07E+05	5,59E+04	6,15E-03
			2,9	3,24E+05	1,56E+06	5,44E+06	1,44E+07	2,88E+07	4,32E+07	4,86E+07	4,07E+07	2,53E+07	1,17E+07	3,99E+06	1,02E+06	1,89E+05	2,60E+04	2,85E-03
		heteroaggregates in sediment	1,5	8,68E+01	5,42E+02	2,40E+03	8,86E+03	2,92E+04	9,81E+04	1,51E+05	1,82E+05	2,06E+05	2,74E+05	1,08E+05	4,26E+04	1,54E+04	7,51E+03	1,01E-02
			2	8,31E+01	5,27E+02	2,36E+03	8,70E+03	2,84E+04	9,38E+04	1,44E+05	1,73E+05	1,95E+05	2,58E+05	1,01E+05	4,01E+04	1,45E+04	7,04E+03	9,48E-03
			2,5	6,78E+01	4,83E+02	2,44E+03	9,75E+03	3,19E+04	9,32E+04	1,53E+05	1,92E+05	2,06E+05	2,29E+05	9,80E+04	3,89E+04	1,33E+04	5,62E+03	6,79E-03
			2,9	4,70E+01	4,64E+02	3,17E+03	1,60E+04	6,00E+04	1,67E+05	3,51E+05	5,49E+05	6,33E+05	5,44E+05	3,44E+05	1,62E+05	5,59E+04	1,44E+04	3,47E-03
0,01				Sizeclass														
				2,00E-07	3,12E-07	4,86E-07	7,58E-07	1,18E-06	1,84E-06	2,87E-06	4,47E-06	6,97E-06	1,09E-05	1,69E-05	2,64E-05	4,12E-05	6,42E-05	1,00E-04
		homoaggregates in water	1,5	1,31E+15	2,80E+15	1,70E+15	2,83E+14	1,27E+13	1,46E+11	4,17E+08	3,27E+05	6,54E+01	3,50E-03	1,13E-07	1,14E-12	0,00E+00	0,00E+00	0,00E+00
			2	1,23E+15	2,62E+15	1,59E+15	2,64E+14	1,18E+13	1,36E+11	3,85E+08	3,01E+05	5,99E+01	3,18E-03	1,04E-07	1,15E-12	0,00E+00	0,00E+00	0,00E+00
			2,5	8,88E+14	1,88E+15	1,13E+15	1,85E+14	8,16E+12	9,29E+10	2,60E+08	2,00E+05	4,23E+01	3,33E-03	6,66E-07	4,46E-08	4,72E-10	6,51E-20	0,00E+00
			2,9	1,51E+12	3,10E+12	1,74E+12	2,64E+11	1,05E+10	1,01E+08	2,11E+05	9,84E+01	7,99E-03	1,05E-07	9,43E-13	8,42E-16	0,00E+00	4,63E-06	9,23E-14
		homoaggregates in sediment	1,5	3,04E+07	8,11E+07	6,15E+07	1,28E+07	7,14E+05	1,03E+04	3,66E+01	3,59E-02	8,96E-06	5,99E-10	2,40E-14	0,00E+00	0,00E+00	0,00E+00	0,00E+00
			2	1,81E+08	6,00E+08	5,67E+08	1,47E+08	1,02E+07	1,84E+05	8,10E+02	9,87E-01	3,06E-04	2,54E-08	1,30E-12	2,22E-17	0,00E+00	0,00E+00	0,00E+00
			2,5	8,24E+08	3,40E+09	3,97E+09	1,26E+09	1,09E+08	2,41E+06	1,31E+04	1,96E+01	8,07E-03	1,24E-06	4,81E-10	6,27E-11	1,29E-12	0,00E+00	0,00E+00
			2,9	6,12E+06	2,92E+07	3,81E+07	1,34E+07	1,24E+06	2,77E+04	1,35E+02	1,46E-01	2,76E-05	8,46E-10	1,76E-14	3,65E-17	0,00E+00	1,09E-06	5,03E-14
	March			Sizeclass														
				1,00E-06	1,39E-06	1,93E-06	2,69E-06	3,74E-06	5,19E-06	7,22E-06	1,00E-05	1,40E-05	1,94E-05	2,70E-05	3,75E-05	5,21E-05	7,24E-05	1,00E-04
		heteroaggregates in water	1,5	1,06E+07	5,11E+07	1,78E+08	4,71E+08	9,42E+08	1,41E+09	1,59E+09	1,33E+09	8,25E+08	3,82E+08	1,30E+08	3,31E+07	6,16E+06	8,47E+05	9,68E-02
			2	9,95E+06	4,79E+07	1,67E+08	4,41E+08	8,82E+08	1,32E+09	1,49E+09	1,25E+09	7,73E+08	3,58E+08	1,22E+08	3,10E+07	5,78E+06	7,94E+05	9,05E-02
			2,5	7,11E+06	3,42E+07	1,19E+08	3,15E+08	6,31E+08	9,45E+08	1,06E+09	8,90E+08	5,53E+08	2,56E+08	8,72E+07	2,22E+07	4,13E+06	5,68E+05	6,40E-02
			2,9	1,14E+04	5,49E+04	1,91E+05	5,08E+05	1,02E+06	1,52E+06	1,71E+06	1,44E+06	8,92E+05	4,13E+05	1,41E+05	3,59E+04	6,67E+03	9,17E+02	9,72E-05
		heteroaggregates in sediment	1,5	4,83E+02	3,02E+03	1,34E+04	4,93E+04	1,62E+05	5,45E+05	8,40E+05	1,01E+06	1,14E+06	1,52E+06	5,98E+05	2,36E+05	8,54E+04	4,17E+04	5,82E-02
			2	4,63E+02	2,94E+03	1,31E+04	4,84E+04	1,58E+05	5,22E+05	8,03E+05	9,64E+05	1,09E+06	1,43E+06	5,64E+05	2,23E+05	8,03E+04	3,91E+04	5,44E-02
			2,5	3,77E+02	2,69E+03	1,36E+04	5,42E+04	1,77E+05	5,18E+05	8,49E+05	1,06E+06	1,14E+06	1,27E+06	5,44E+05	2,16E+05	7,38E+04	3,12E+04	3,86E-02
			2,9	9,05E-01	8,92E+00	6,10E+01	3,08E+02	1,16E+03	3,21E+03	6,77E+03	1,06E+04	1,22E+04	1,05E+04	6,62E+03	3,12E+03	1,08E+03	2,78E+02	6,47E-05

alpha river	Month	State of aggregation	Df	Size class													
				2,00E-07	3,12E-07	4,86E-07	7,58E-07	1,18E-06	1,84E-06	2,87E-06	4,47E-06	6,97E-06	1,09E-05	1,69E-05	2,64E-05	4,12E-05	6,42E-05	1,00E-04
	May	homoaggregates in water	1,5	5,16E+15	1,09E+16	6,55E+15	1,07E+15	4,76E+13	5,38E+11	1,51E+09	1,14E+06	2,17E+02	1,04E-02	2,91E-07	1,72E-12	0,00E+00	0,00E+00	0,00E+00
			2	4,83E+15	1,02E+16	6,14E+15	1,00E+15	4,43E+13	5,02E+11	1,40E+09	1,06E+06	2,00E+02	9,56E-03	2,72E-07	1,69E-12	0,00E+00	0,00E+00	0,00E+00
			2,5	3,47E+15	7,33E+15	4,35E+15	7,06E+14	3,11E+13	3,47E+11	9,58E+08	7,19E+05	1,39E+02	8,67E-03	8,05E-07	1,49E-09	1,11E-19	0,00E+00	0,00E+00
			2,9	7,41E+12	1,52E+13	8,58E+12	1,30E+12	5,19E+10	4,98E+08	1,05E+06	4,95E+02	4,09E-02	5,71E-07	6,11E-12	1,38E-14	0,00E+00	3,15E-03	5,40E-11
		homoaggregates in sediment	1,5	3,55E+08	9,38E+08	7,03E+08	1,44E+08	7,97E+06	1,12E+05	3,93E+02	3,72E-01	8,81E-05	5,29E-09	1,84E-13	0,00E+00	0,00E+00	0,00E+00	0,00E+00
			2	2,11E+09	6,95E+09	6,50E+09	1,65E+09	1,14E+08	2,01E+06	8,73E+03	1,03E+01	3,03E-03	2,26E-07	1,00E-11	0,00E+00	0,00E+00	0,00E+00	0,00E+00
			2,5	9,57E+09	3,93E+10	4,54E+10	1,43E+10	1,23E+09	2,67E+07	1,43E+05	2,09E+02	7,90E-02	9,57E-06	1,73E-09	6,21E-12	0,00E+00	0,00E+00	0,00E+00
			2,9	8,93E+07	4,24E+08	5,58E+08	1,97E+08	1,82E+07	4,07E+05	2,00E+03	2,19E+00	4,20E-04	1,36E-08	3,39E-13	1,78E-15	0,00E+00	2,19E-03	8,74E-11
				Sizeclass														
				1,00E-06	1,39E-06	1,93E-06	2,69E-06	3,74E-06	5,19E-06	7,22E-06	1,00E-05	1,40E-05	1,94E-05	2,70E-05	3,75E-05	5,21E-05	7,24E-05	1,00E-04
		heteroaggregates in water	1,5	2,79E+08	1,34E+09	4,68E+09	1,24E+10	2,48E+10	3,71E+10	4,18E+10	3,50E+10	2,17E+10	1,01E+10	3,43E+09	8,72E+08	1,62E+08	2,23E+07	2,53E+00
			2	2,62E+08	1,26E+09	4,39E+09	1,16E+10	2,32E+10	3,48E+10	3,91E+10	3,28E+10	2,04E+10	9,43E+09	3,21E+09	8,18E+08	1,52E+08	2,09E+07	2,36E+00
			2,5	1,87E+08	8,99E+08	3,13E+09	8,29E+09	1,66E+10	2,48E+10	2,79E+10	2,34E+10	1,45E+10	6,73E+09	2,29E+09	5,84E+08	1,09E+08	1,49E+07	1,68E+00
			2,9	3,80E+05	1,83E+06	6,37E+06	1,69E+07	3,38E+07	5,07E+07	5,71E+07	4,78E+07	2,97E+07	1,38E+07	4,69E+06	1,19E+06	2,22E+05	3,06E+04	3,26E-03
		heteroaggregates in sediment	1,5	3,77E+04	2,36E+05	1,05E+06	3,85E+06	1,27E+07	4,26E+07	6,56E+07	7,89E+07	8,94E+07	1,19E+08	4,67E+07	1,85E+07	6,67E+06	3,26E+06	4,51E+00
			2	3,62E+04	2,29E+05	1,03E+06	3,79E+06	1,24E+07	4,08E+07	6,28E+07	7,54E+07	8,49E+07	1,12E+08	4,41E+07	1,74E+07	6,28E+06	3,06E+06	4,23E+00
			2,5	2,94E+04	2,10E+05	1,06E+06	4,23E+06	1,38E+07	4,04E+07	6,63E+07	8,31E+07	8,91E+07	9,93E+07	4,25E+07	1,69E+07	5,76E+06	2,44E+06	3,00E+00
			2,9	8,95E+01	8,82E+02	6,04E+03	3,05E+04	1,14E+05	3,17E+05	6,70E+05	1,05E+06	1,21E+06	1,04E+06	6,55E+05	3,09E+05	1,07E+05	2,75E+04	6,44E-03
0,01				Sizeclass														
	August			2,00E-07	3,12E-07	4,86E-07	7,58E-07	1,18E-06	1,84E-06	2,87E-06	4,47E-06	6,97E-06	1,09E-05	1,69E-05	2,64E-05	4,12E-05	6,42E-05	1,00E-04
		homoaggregates in water	1,5	2,09E+15	4,47E+15	2,77E+15	4,67E+14	2,12E+13	2,49E+11	7,25E+08	5,84E+05	1,24E+02	7,39E-03	2,74E-07	9,25E-18	0,00E+00	0,00E+00	0,00E+00
			2	1,96E+15	4,19E+15	2,59E+15	4,36E+14	1,97E+13	2,30E+11	6,67E+08	5,33E+05	1,13E+02	6,67E-03	2,53E-07	8,70E-18	0,00E+00	0,00E+00	0,00E+00
			2,5	1,42E+15	3,02E+15	1,83E+15	3,03E+14	1,35E+13	1,55E+11	4,40E+08	3,51E+05	8,01E+01	7,97E-03	3,51E-06	4,88E-16	0,00E+00	0,00E+00	0,00E+00
			2,9	1,81E+12	3,71E+12	2,12E+12	3,24E+11	1,29E+10	1,25E+08	2,71E+05	1,46E+02	2,40E-02	7,84E-06	1,58E-03	1,61E-04	8,11E-16	4,50E-02	4,95E-13
		homoaggregates in sediment	1,5	1,01E+08	2,69E+08	2,08E+08	4,39E+07	2,49E+06	3,64E+04	1,32E+02	1,33E-01	3,53E-05	2,63E-09	1,21E-13	0,00E+00	0,00E+00	0,00E+00	0,00E+00
			2	5,98E+08	1,99E+09	1,92E+09	5,04E+08	3,55E+07	6,46E+05	2,92E+03	3,63E+00	1,20E-03	1,10E-07	6,54E-12	0,00E+00	0,00E+00	0,00E+00	0,00E+00
			2,5	2,74E+09	1,13E+10	1,34E+10	4,31E+09	3,74E+08	8,36E+06	4,61E+04	7,15E+01	3,18E-02	6,16E-06	5,27E-09	0,00E+00	0,00E+00	0,00E+00	0,00E+00
			2,9	1,53E+07	7,28E+07	9,65E+07	3,43E+07	3,17E+06	7,16E+04	3,61E+02	4,51E-01	1,72E-04	1,31E-07	6,14E-05	1,45E-05	1,70E-16	2,19E-02	5,61E-13
				Sizeclass														
				1,00E-06	1,39E-06	1,93E-06	2,69E-06	3,74E-06	5,19E-06	7,22E-06	1,00E-05	1,40E-05	1,94E-05	2,70E-05	3,75E-05	5,21E-05	7,24E-05	1,00E-04
		heteroaggregates in water	1,5	2,03E+07	9,77E+07	3,40E+08	9,00E+08	1,80E+09	2,69E+09	3,03E+09	2,54E+09	1,57E+09	7,29E+08	2,48E+08	6,32E+07	1,18E+07	1,62E+06	1,87E-01
			2	1,90E+07	9,16E+07	3,19E+08	8,44E+08	1,69E+09	2,53E+09	2,84E+09	2,38E+09	1,48E+09	6,84E+08	2,33E+08	5,93E+07	1,10E+07	1,52E+06	1,75E-01
			2,5	1,36E+07	6,55E+07	2,28E+08	6,03E+08	1,21E+09	1,81E+09	2,03E+09	1,70E+09	1,06E+09	4,90E+08	1,67E+08	4,24E+07	7,90E+06	1,08E+06	1,24E-01
			2,9	1,64E+04	7,87E+04	2,74E+05	7,27E+05	1,46E+06	2,18E+06	2,46E+06	2,06E+06	1,28E+06	5,92E+05	2,02E+05	5,13E+04	9,56E+03	1,31E+03	1,41E-04
		heteroaggregates in sediment	1,5	1,92E+03	1,20E+04	5,32E+04	1,96E+05	6,45E+05	2,16E+06	3,33E+06	4,01E+06	4,54E+06	6,03E+06	2,37E+06	9,38E+05	3,39E+05	1,65E+05	2,34E-01
			2	1,84E+03	1,17E+04	5,22E+04	1,92E+05	6,28E+05	2,07E+06	3,19E+06	3,83E+06	4,31E+06	5,68E+06	2,24E+06	8,84E+05	3,18E+05	1,55E+05	2,19E-01
			2,5	1,50E+03	1,07E+04	5,40E+04	2,15E+05	7,03E+05	2,06E+06	3,37E+06	4,23E+06	4,54E+06	5,05E+06	2,16E+06	8,58E+05	2,93E+05	1,24E+05	1,55E-01
			2,9	2,70E+00	2,66E+01	1,82E+02	9,19E+02	3,44E+03	9,55E+03	2,02E+04	3,15E+04	3,63E+04	3,12E+04	1,97E+04	9,30E+03	3,21E+03	8,27E+02	1,94E-04

alpha river	Month	State of aggregation	Df	Size class													
				2,00E-07	**3,12E-07**	**4,86E-07**	**7,58E-07**	**1,18E-06**	**1,84E-06**	**2,87E-06**	**4,47E-06**	**6,97E-06**	**1,09E-05**	**1,69E-05**	**2,64E-05**	**4,12E-05**	**6,42E-05**	**1,00E-04**
0,01	November	homoaggregates in water	**1,5**	2,06E+15	4,39E+15	2,65E+15	4,40E+14	1,96E+13	2,24E+11	6,36E+08	4,92E+05	9,72E+01	5,03E-03	1,55E-07	1,32E-12	0,00E+00	0,00E+00	0,00E+00
			2	1,93E+15	4,11E+15	2,48E+15	4,10E+14	1,83E+13	2,09E+11	5,90E+08	4,54E+05	8,91E+01	4,59E-03	1,44E-07	1,32E-12	0,00E+00	0,00E+00	0,00E+00
			2,5	1,39E+15	2,95E+15	1,76E+15	2,88E+14	1,27E+13	1,43E+11	4,00E+08	3,05E+05	6,26E+01	4,59E-03	7,18E-07	1,52E-08	3,07E-13	0,00E+00	0,00E+00
			2,9	2,56E+12	5,24E+12	2,95E+12	4,50E+11	1,79E+10	1,71E+08	3,61E+05	1,68E+02	1,38E-02	1,85E-07	1,74E-12	1,99E-15	0,00E+00	4,50E-05	8,71E-13
		homoaggregates in sediment	**1,5**	1,29E+08	3,43E+08	2,58E+08	5,36E+07	2,99E+06	4,26E+04	1,51E+02	1,46E-01	3,59E-05	2,32E-09	8,92E-14	0,00E+00	0,00E+00	0,00E+00	0,00E+00
			2	7,66E+08	2,54E+09	2,39E+09	6,15E+08	4,27E+07	7,60E+05	3,35E+03	4,02E+00	1,23E-03	9,88E-08	4,82E-12	0,00E+00	0,00E+00	0,00E+00	0,00E+00
			2,5	3,49E+09	1,44E+10	1,67E+10	5,32E+09	4,57E+08	1,00E+07	5,44E+04	8,08E+01	3,23E-02	4,60E-06	1,40E-09	5,76E-11	2,27E-15	0,00E+00	0,00E+00
			2,9	2,81E+07	1,33E+08	1,75E+08	6,19E+07	5,71E+06	1,27E+05	6,23E+02	6,76E-01	1,29E-04	4,01E-09	8,75E-14	2,33E-16	0,00E+00	2,85E-05	1,28E-12
				Sizeclass														
				1,00E-06	**1,39E-06**	**1,93E-06**	**2,69E-06**	**3,74E-06**	**5,19E-06**	**7,22E-06**	**1,00E-05**	**1,40E-05**	**1,94E-05**	**2,70E-05**	**3,75E-05**	**5,21E-05**	**7,24E-05**	**1,00E-04**
		heteroaggregates in water	**1,5**	3,33E+07	1,60E+08	5,58E+08	1,48E+09	2,95E+09	4,43E+09	4,98E+09	4,17E+09	2,59E+09	1,20E+09	4,08E+08	1,04E+08	1,93E+07	2,66E+06	3,02E-01
			2	3,12E+07	1,50E+08	5,23E+08	1,38E+09	2,77E+09	4,15E+09	4,66E+09	3,91E+09	2,43E+09	1,12E+09	3,82E+08	9,74E+07	1,81E+07	2,49E+06	2,83E-01
			2,5	2,23E+07	1,07E+08	3,73E+08	9,89E+08	1,98E+09	2,96E+09	3,33E+09	2,79E+09	1,73E+09	8,03E+08	2,73E+08	6,96E+07	1,29E+07	1,78E+06	2,00E-01
			2,9	3,88E+04	1,87E+05	6,51E+05	1,73E+06	3,46E+06	5,18E+06	5,83E+06	4,89E+06	3,04E+06	1,41E+06	4,79E+05	1,22E+05	2,27E+04	3,12E+03	3,32E-04
		heteroaggregates in sediment	**1,5**	4,09E+03	2,56E+04	1,13E+05	4,17E+05	1,38E+06	4,62E+06	7,11E+06	8,55E+06	9,69E+06	1,29E+07	5,06E+06	2,00E+06	7,23E+05	3,53E+05	4,91E-01
			2	3,92E+03	2,49E+04	1,11E+05	4,10E+05	1,34E+06	4,42E+06	6,80E+06	8,16E+06	9,19E+06	1,21E+07	4,77E+06	1,89E+06	6,80E+05	3,31E+05	4,59E-01
			2,5	3,19E+03	2,28E+04	1,15E+05	4,58E+05	1,50E+06	4,38E+06	7,18E+06	9,00E+06	9,66E+06	1,08E+07	4,60E+06	1,83E+06	6,24E+05	2,64E+05	3,26E-01
			2,9	8,31E+00	8,19E+01	5,61E+02	2,83E+03	1,06E+04	2,95E+04	6,22E+04	9,72E+04	1,12E+05	9,63E+04	6,08E+04	2,87E+04	9,90E+03	2,55E+03	5,96E-04

alpha river	Month	State of aggregation	Df	Size class													
				2,00E-07	3,12E-07	4,86E-07	7,58E-07	1,18E-06	1,84E-06	2,87E-06	4,47E-06	6,97E-06	1,09E-05	1,69E-05	2,64E-05	4,12E-05	6,42E-05	1,00E-04
0,1	January	homoaggregates in water	1,5	7,33E+13	1,52E+14	8,85E+13	1,42E+13	6,11E+11	6,76E+09	1,83E+07	1,30E+04	2,21E+00	8,59E-05	1,86E-09	2,52E-15	0,00E+00	0,00E+00	0,00E+00
			2	6,87E+13	1,42E+14	8,29E+13	1,33E+13	5,74E+11	6,34E+09	1,71E+07	1,22E+04	2,07E+00	8,03E-05	1,74E-09	2,37E-15	0,00E+00	0,00E+00	0,00E+00
			2,5	4,92E+13	1,02E+14	5,93E+13	9,49E+12	4,08E+11	4,51E+09	1,21E+07	8,53E+03	1,42E+00	5,38E-05	1,16E-09	2,34E-15	0,00E+00	0,00E+00	0,00E+00
			2,9	2,30E+13	4,73E+13	2,76E+13	4,40E+12	1,86E+11	1,99E+09	4,96E+06	2,95E+03	3,37E-01	6,08E-06	3,89E-11	1,55E-16	0,00E+00	0,00E+00	0,00E+00
		homoaggregates in sediment	1,5	3,11E+06	8,06E+06	5,85E+06	1,17E+06	6,30E+04	8,70E+02	2,93E+00	2,62E-03	5,55E-07	2,69E-11	7,27E-16	0,00E+00	0,00E+00	0,00E+00	0,00E+00
			2	1,84E+07	5,96E+07	5,41E+07	1,36E+07	9,09E+05	1,57E+04	6,58E+01	7,32E-02	1,94E-05	1,17E-09	3,96E-14	0,00E+00	0,00E+00	0,00E+00	0,00E+00
			2,5	8,35E+07	3,37E+08	3,81E+08	1,19E+08	9,93E+06	2,14E+05	1,12E+03	1,53E+00	4,98E-04	3,66E-08	1,54E-12	0,00E+00	0,00E+00	0,00E+00	0,00E+00
			2,9	1,71E+08	8,16E+08	1,11E+09	4,10E+08	4,03E+07	1,00E+06	5,80E+03	8,02E+00	2,13E-03	8,94E-08	1,33E-12	0,00E+00	0,00E+00	0,00E+00	0,00E+00
				Sizeclass														
				1,00E-06	1,39E-06	1,93E-06	2,69E-06	3,74E-06	5,19E-06	7,22E-06	1,00E-05	1,40E-05	1,94E-05	2,70E-05	3,75E-05	5,21E-05	7,24E-05	1,00E-04
		heteroaggregates in water	1,5	1,04E+07	5,01E+07	1,74E+08	4,62E+08	9,25E+08	1,39E+09	1,56E+09	1,31E+09	8,11E+08	3,76E+08	1,28E+08	3,26E+07	6,06E+06	8,33E+05	9,17E-02
			2	9,74E+06	4,69E+07	1,63E+08	4,33E+08	8,66E+08	1,30E+09	1,46E+09	1,22E+09	7,60E+08	3,52E+08	1,20E+08	3,05E+07	5,68E+06	7,80E+05	8,60E-02
			2,5	6,97E+06	3,36E+07	1,17E+08	3,10E+08	6,20E+08	9,29E+08	1,05E+09	8,76E+08	5,44E+08	2,52E+08	8,58E+07	2,18E+07	4,06E+06	5,59E+05	6,14E-02
			2,9	3,24E+06	1,56E+07	5,43E+07	1,44E+08	2,88E+08	4,32E+08	4,86E+08	4,07E+08	2,53E+08	1,17E+08	3,99E+07	1,02E+07	1,89E+06	2,60E+05	2,85E-02
		heteroaggregates in sediment	1,5	8,67E+02	5,42E+03	2,40E+04	8,85E+04	2,92E+05	9,80E+05	1,51E+06	1,82E+06	2,06E+06	2,73E+06	1,08E+06	4,26E+05	1,54E+05	7,50E+04	1,01E-01
			2	8,30E+02	5,26E+03	2,36E+04	8,69E+04	2,84E+05	9,37E+05	1,44E+06	1,73E+06	1,95E+06	2,57E+06	1,01E+06	4,00E+05	1,44E+05	7,03E+04	9,47E-02
			2,5	6,78E+02	4,83E+03	2,44E+04	9,74E+04	3,18E+05	9,31E+05	1,53E+06	1,92E+06	2,05E+06	2,29E+06	9,79E+05	3,89E+05	1,33E+05	5,62E+04	6,77E-02
			2,9	4,70E+02	4,63E+03	3,17E+04	1,60E+05	6,00E+05	1,66E+06	3,51E+06	5,49E+06	6,32E+06	5,43E+06	3,43E+06	1,62E+06	5,58E+05	1,44E+05	3,47E-02
	March			Sizeclass														
				2,00E-07	3,12E-07	4,86E-07	7,58E-07	1,18E-06	1,84E-06	2,87E-06	4,47E-06	6,97E-06	1,09E-05	1,69E-05	2,64E-05	4,12E-05	6,42E-05	1,00E-04
		homoaggregates in water	1,5	1,31E+15	2,80E+15	1,70E+15	2,83E+14	1,27E+13	1,46E+11	4,16E+08	3,27E+05	6,54E+01	3,50E-03	1,13E-07	1,14E-12	0,00E+00	0,00E+00	0,00E+00
			2	1,23E+15	2,62E+15	1,59E+15	2,64E+14	1,18E+13	1,36E+11	3,85E+08	3,01E+05	5,99E+01	3,18E-03	1,04E-07	1,15E-12	0,00E+00	0,00E+00	0,00E+00
			2,5	8,88E+14	1,88E+15	1,13E+15	1,85E+14	8,15E+12	9,28E+10	2,59E+08	2,00E+05	4,22E+01	3,33E-03	6,66E-07	4,46E-08	4,72E-10	6,51E-20	0,00E+00
			2,9	1,51E+12	3,09E+12	1,73E+12	2,64E+11	1,05E+10	1,01E+08	2,11E+05	9,83E+01	7,99E-03	1,05E-07	9,43E-13	8,42E-16	0,00E+00	4,63E-06	9,23E-14
		homoaggregates in sediment	1,5	3,04E+07	8,11E+07	6,15E+07	1,28E+07	7,13E+05	1,03E+04	3,66E+01	3,59E-02	8,96E-06	5,99E-10	2,40E-14	0,00E+00	0,00E+00	0,00E+00	0,00E+00
			2	1,81E+08	6,00E+08	5,67E+08	1,46E+08	1,02E+07	1,83E+05	8,09E+02	9,87E-01	3,06E-04	2,54E-08	1,30E-12	2,22E-17	0,00E+00	0,00E+00	0,00E+00
			2,5	8,24E+08	3,40E+09	3,96E+09	1,26E+09	1,08E+08	2,40E+06	1,31E+04	1,96E+01	8,07E-03	1,24E-06	4,81E-10	6,27E-11	1,29E-12	0,00E+00	0,00E+00
			2,9	6,12E+06	2,92E+07	3,80E+07	1,34E+07	1,24E+06	2,77E+04	1,35E+02	1,46E-01	2,76E-05	8,46E-10	1,76E-14	3,65E-17	0,00E+00	1,09E-06	5,03E-14
				Sizeclass														
				1,00E-06	1,39E-06	1,93E-06	2,69E-06	3,74E-06	5,19E-06	7,22E-06	1,00E-05	1,40E-05	1,94E-05	2,70E-05	3,75E-05	5,21E-05	7,24E-05	1,00E-04
		heteroaggregates in water	1,5	1,06E+08	5,11E+08	1,78E+09	4,71E+09	9,41E+09	1,41E+10	1,59E+10	1,33E+10	8,25E+09	3,82E+09	1,30E+09	3,31E+08	6,16E+07	8,46E+06	9,67E-01
			2	9,94E+07	4,79E+08	1,67E+09	4,41E+09	8,82E+09	1,32E+10	1,49E+10	1,24E+10	7,73E+09	3,58E+09	1,22E+09	3,10E+08	5,77E+07	7,93E+06	9,04E-01
			2,5	7,10E+07	3,42E+08	1,19E+09	3,15E+09	6,30E+09	9,45E+09	1,06E+10	8,90E+09	5,52E+09	2,56E+09	8,71E+08	2,22E+08	4,13E+07	5,67E+06	6,40E-01
			2,9	1,14E+05	5,49E+05	1,91E+06	5,07E+06	1,02E+07	1,52E+07	1,71E+07	1,44E+07	8,92E+06	4,13E+06	1,41E+06	3,58E+05	6,67E+04	9,16E+03	9,71E-04
		heteroaggregates in sediment	1,5	4,83E+03	3,02E+04	1,34E+05	4,93E+05	1,62E+06	5,45E+06	8,39E+06	1,01E+07	1,14E+07	1,52E+07	5,98E+06	2,36E+06	8,53E+05	4,16E+05	5,82E-01
			2	4,63E+03	2,93E+04	1,31E+05	4,84E+05	1,58E+06	5,21E+06	8,02E+06	9,63E+06	1,08E+07	1,43E+07	5,63E+06	2,23E+06	8,02E+05	3,91E+05	5,44E-01
			2,5	3,77E+03	2,69E+04	1,36E+05	5,42E+05	1,77E+06	5,17E+06	8,48E+06	1,06E+07	1,14E+07	1,27E+07	5,44E+06	2,16E+06	7,37E+05	3,12E+05	3,86E-01
			2,9	9,04E+00	8,91E+01	6,10E+02	3,08E+03	1,16E+04	3,21E+04	6,77E+04	1,06E+05	1,22E+05	1,05E+05	6,62E+04	3,12E+04	1,08E+04	2,78E+03	6,46E-04

alpha river	Month	State of aggregation	Df	Size class													
				2,00E-07	**3,12E-07**	**4,86E-07**	**7,58E-07**	**1,18E-06**	**1,84E-06**	**2,87E-06**	**4,47E-06**	**6,97E-06**	**1,09E-05**	**1,69E-05**	**2,64E-05**	**4,12E-05**	**6,42E-05**	**1,00E-04**
0,1	May	homoaggregates in water	**1,5**	5,15E+15	1,09E+16	6,51E+15	1,06E+15	4,71E+13	5,33E+11	1,50E+09	1,14E+06	2,16E+02	1,04E-02	2,91E-07	1,72E-12	0,00E+00	0,00E+00	0,00E+00
			2	4,83E+15	1,02E+16	6,10E+15	9,93E+14	4,39E+13	4,97E+11	1,39E+09	1,05E+06	1,99E+02	9,56E-03	2,72E-07	1,69E-12	0,00E+00	0,00E+00	0,00E+00
			2,5	3,47E+15	7,30E+15	4,32E+15	7,00E+14	3,08E+13	3,44E+11	9,52E+08	7,17E+05	1,39E+02	8,67E-03	8,05E-07	1,49E-09	1,11E-19	0,00E+00	0,00E+00
			2,9	7,41E+12	1,51E+13	8,53E+12	1,29E+12	5,13E+10	4,94E+08	1,05E+06	4,94E+02	4,09E-02	5,71E-07	6,11E-12	1,38E-14	0,00E+00	3,15E-03	5,40E-11
		homoaggregates in sediment	**1,5**	3,55E+08	9,35E+08	6,99E+08	1,42E+08	7,88E+06	1,11E+05	3,91E+02	3,71E-01	8,80E-05	5,29E-09	1,84E-13	0,00E+00	0,00E+00	0,00E+00	0,00E+00
			2	2,10E+09	6,93E+09	6,46E+09	1,64E+09	1,13E+08	1,99E+06	8,68E+03	1,03E+01	3,03E-03	2,26E-07	1,00E-11	0,00E+00	0,00E+00	0,00E+00	0,00E+00
			2,5	9,56E+09	3,92E+10	4,51E+10	1,42E+10	1,22E+09	2,65E+07	1,42E+05	2,09E+02	7,89E-02	9,56E-06	1,73E-09	6,21E-12	0,00E+00	0,00E+00	0,00E+00
			2,9	8,92E+07	4,23E+08	5,55E+08	1,95E+08	1,81E+07	4,04E+05	1,99E+03	2,18E+00	4,20E-04	1,36E-08	3,39E-13	1,78E-15	0,00E+00	2,19E-03	8,74E-11
				Sizeclass														
				1,00E-06	**1,39E-06**	**1,93E-06**	**2,69E-06**	**3,74E-06**	**5,19E-06**	**7,22E-06**	**1,00E-05**	**1,40E-05**	**1,94E-05**	**2,70E-05**	**3,75E-05**	**5,21E-05**	**7,24E-05**	**1,00E-04**
		heteroaggregates in water	**1,5**	2,78E+09	1,34E+10	4,66E+10	1,23E+11	2,47E+11	3,70E+11	4,16E+11	3,48E+11	2,16E+11	1,00E+11	3,41E+10	8,69E+09	1,62E+09	2,22E+08	2,51E+01
			2	2,61E+09	1,25E+10	4,37E+10	1,16E+11	2,31E+11	3,47E+11	3,90E+11	3,27E+11	2,03E+11	9,40E+10	3,20E+10	8,14E+09	1,52E+09	2,08E+08	2,35E+01
			2,5	1,86E+09	8,95E+09	3,12E+10	8,26E+10	1,65E+11	2,48E+11	2,78E+11	2,33E+11	1,45E+11	6,71E+10	2,28E+10	5,82E+09	1,08E+09	1,49E+08	1,67E+01
			2,9	3,79E+06	1,82E+07	6,35E+07	1,68E+08	3,37E+08	5,05E+08	5,69E+08	4,77E+08	2,96E+08	1,37E+08	4,67E+07	1,19E+07	2,22E+06	3,05E+05	3,24E-02
		heteroaggregates in sediment	**1,5**	3,76E+05	2,35E+06	1,04E+07	3,84E+07	1,26E+08	4,24E+08	6,54E+08	7,86E+08	8,91E+08	1,18E+09	4,66E+08	1,84E+08	6,65E+07	3,25E+07	4,48E+01
			2	3,60E+05	2,28E+06	1,02E+07	3,77E+07	1,23E+08	4,06E+08	6,25E+08	7,51E+08	8,46E+08	1,12E+09	4,39E+08	1,73E+08	6,25E+07	3,05E+07	4,20E+01
			2,5	2,93E+05	2,09E+06	1,06E+07	4,21E+07	1,38E+08	4,03E+08	6,60E+08	8,28E+08	8,88E+08	9,89E+08	4,23E+08	1,68E+08	5,74E+07	2,43E+07	2,98E+01
			2,9	8,91E+02	8,78E+03	6,01E+04	3,04E+05	1,14E+06	3,16E+06	6,67E+06	1,04E+07	1,20E+07	1,03E+07	6,53E+06	3,08E+06	1,06E+06	2,74E+05	6,40E-02
	August			**Sizeclass**														
				2,00E-07	**3,12E-07**	**4,86E-07**	**7,58E-07**	**1,18E-06**	**1,84E-06**	**2,87E-06**	**4,47E-06**	**6,97E-06**	**1,09E-05**	**1,69E-05**	**2,64E-05**	**4,12E-05**	**6,42E-05**	**1,00E-04**
		homoaggregates in water	**1,5**	2,09E+15	4,47E+15	2,77E+15	4,67E+14	2,12E+13	2,48E+11	7,24E+08	5,84E+05	1,24E+02	7,39E-03	2,74E-07	9,25E-18	0,00E+00	0,00E+00	0,00E+00
			2	1,96E+15	4,19E+15	2,59E+15	4,36E+14	1,97E+13	2,30E+11	6,66E+08	5,32E+05	1,13E+02	6,67E-03	2,53E-07	8,70E-18	0,00E+00	0,00E+00	0,00E+00
			2,5	1,42E+15	3,02E+15	1,83E+15	3,03E+14	1,35E+13	1,55E+11	4,39E+08	3,50E+05	8,01E+01	7,97E-03	3,51E-06	4,88E-16	0,00E+00	0,00E+00	0,00E+00
			2,9	1,81E+12	3,71E+12	2,11E+12	3,24E+11	1,29E+10	1,25E+08	2,71E+05	1,46E+02	2,40E-02	7,84E-06	1,58E-03	1,61E-04	8,11E-16	4,50E-02	4,95E-13
		homoaggregates in sediment	**1,5**	1,01E+08	2,69E+08	2,08E+08	4,38E+07	2,48E+06	3,63E+04	1,32E+02	1,33E-01	3,53E-05	2,63E-09	1,21E-13	0,00E+00	0,00E+00	0,00E+00	0,00E+00
			2	5,98E+08	1,99E+09	1,92E+09	5,03E+08	3,54E+07	6,45E+05	2,91E+03	3,63E+00	1,20E-03	1,10E-07	6,54E-12	0,00E+00	0,00E+00	0,00E+00	0,00E+00
			2,5	2,74E+09	1,13E+10	1,34E+10	4,31E+09	3,73E+08	8,35E+06	4,60E+04	7,15E+01	3,18E-02	6,16E-06	5,27E-09	0,00E+00	0,00E+00	0,00E+00	0,00E+00
			2,9	1,53E+07	7,27E+07	9,64E+07	3,43E+07	3,17E+06	7,15E+04	3,61E+02	4,51E-01	1,72E-04	1,31E-07	6,14E-05	1,45E-05	1,70E-16	2,19E-02	5,61E-13
				Sizeclass														
				1,00E-06	**1,39E-06**	**1,93E-06**	**2,69E-06**	**3,74E-06**	**5,19E-06**	**7,22E-06**	**1,00E-05**	**1,40E-05**	**1,94E-05**	**2,70E-05**	**3,75E-05**	**5,21E-05**	**7,24E-05**	**1,00E-04**
		heteroaggregates in water	**1,5**	2,03E+08	9,77E+08	3,40E+09	9,00E+09	1,80E+10	2,69E+10	3,03E+10	2,54E+10	1,57E+10	7,29E+09	2,48E+09	6,32E+08	1,18E+08	1,62E+07	1,87E+00
			2	1,90E+08	9,15E+08	3,19E+09	8,43E+09	1,68E+10	2,52E+10	2,84E+10	2,38E+10	1,48E+10	6,83E+09	2,33E+09	5,92E+08	1,10E+08	1,51E+07	1,75E+00
			2,5	1,36E+08	6,54E+08	2,28E+09	6,03E+09	1,21E+10	1,81E+10	2,03E+10	1,70E+10	1,06E+10	4,89E+09	1,67E+09	4,24E+08	7,89E+07	1,08E+07	1,23E+00
			2,9	1,64E+05	7,86E+05	2,74E+06	7,27E+06	1,45E+07	2,18E+07	2,45E+07	2,06E+07	1,28E+07	5,92E+06	2,02E+06	5,13E+05	9,55E+04	1,31E+04	1,40E-03
		heteroaggregates in sediment	**1,5**	1,92E+04	1,20E+05	5,31E+05	1,96E+06	6,44E+06	2,16E+07	3,33E+07	4,00E+07	4,54E+07	6,03E+07	2,37E+07	9,37E+06	3,38E+06	1,65E+06	2,34E+00
			2	1,84E+04	1,17E+05	5,22E+05	1,92E+06	6,27E+06	2,07E+07	3,19E+07	3,82E+07	4,31E+07	5,68E+07	2,24E+07	8,83E+06	3,18E+06	1,55E+06	2,19E+00
			2,5	1,50E+04	1,07E+05	5,39E+05	2,15E+06	7,03E+06	2,06E+07	3,37E+07	4,23E+07	4,53E+07	5,05E+07	2,16E+07	8,58E+06	2,93E+06	1,24E+06	1,55E+00
			2,9	2,69E+01	2,66E+02	1,82E+03	9,18E+03	3,44E+04	9,55E+04	2,02E+05	3,15E+05	3,63E+05	3,12E+05	1,97E+05	9,29E+04	3,21E+04	8,27E+03	1,94E-03

alpha river	Month	State of aggregation	Df	Size class													
				2,00E-07	3,12E-07	4,86E-07	7,58E-07	1,18E-06	1,84E-06	2,87E-06	4,47E-06	6,97E-06	1,09E-05	1,69E-05	2,64E-05	4,12E-05	6,42E-05	1,00E-04
0,1	November	homoaggregates in water	1,5	2,06E+15	4,38E+15	2,64E+15	4,38E+14	1,96E+13	2,24E+11	6,35E+08	4,92E+05	9,72E+01	5,03E-03	1,55E-07	1,32E-12	0,00E+00	0,00E+00	0,00E+00
			2	1,93E+15	4,11E+15	2,47E+15	4,09E+14	1,82E+13	2,08E+11	5,89E+08	4,54E+05	8,91E+01	4,59E-03	1,44E-07	1,32E-12	0,00E+00	0,00E+00	0,00E+00
			2,5	1,39E+15	2,94E+15	1,75E+15	2,87E+14	1,27E+13	1,43E+11	3,99E+08	3,05E+05	6,26E+01	4,59E-03	7,18E-07	1,52E-08	3,07E-13	0,00E+00	0,00E+00
			2,9	2,56E+12	5,24E+12	2,95E+12	4,49E+11	1,78E+10	1,71E+08	3,60E+05	1,68E+02	1,38E-02	1,85E-07	1,74E-12	1,99E-15	0,00E+00	4,50E-05	8,71E-13
		homoaggregates in sediment	1,5	1,29E+08	3,43E+08	2,58E+08	5,34E+07	2,98E+06	4,25E+04	1,51E+02	1,46E-01	3,59E-05	2,32E-09	8,92E-14	0,00E+00	0,00E+00	0,00E+00	0,00E+00
			2	7,66E+08	2,54E+09	2,38E+09	6,14E+08	4,26E+07	7,58E+05	3,35E+03	4,02E+00	1,23E-03	9,88E-08	4,82E-12	0,00E+00	0,00E+00	0,00E+00	0,00E+00
			2,5	3,49E+09	1,44E+10	1,66E+10	5,30E+09	4,56E+08	9,97E+06	5,43E+04	8,07E+01	3,23E-02	4,60E-06	1,40E-09	5,76E-11	2,27E-15	0,00E+00	0,00E+00
			2,9	2,80E+07	1,33E+08	1,74E+08	6,17E+07	5,69E+06	1,27E+05	6,22E+02	6,76E-01	1,29E-04	4,01E-09	8,75E-14	2,33E-16	0,00E+00	2,85E-05	1,28E-12
				Sizeclass														
				1,00E-06	1,39E-06	1,93E-06	2,69E-06	3,74E-06	5,19E-06	7,22E-06	1,00E-05	1,40E-05	1,94E-05	2,70E-05	3,75E-05	5,21E-05	7,24E-05	1,00E-04
		heteroaggregates in water	1,5	3,32E+08	1,60E+09	5,57E+09	1,48E+10	2,95E+10	4,42E+10	4,97E+10	4,16E+10	2,58E+10	1,20E+10	4,08E+09	1,04E+09	1,93E+08	2,65E+07	3,02E+00
			2	3,11E+08	1,50E+09	5,22E+09	1,38E+10	2,76E+10	4,14E+10	4,66E+10	3,90E+10	2,42E+10	1,12E+10	3,82E+09	9,73E+08	1,81E+08	2,49E+07	2,82E+00
			2,5	2,22E+08	1,07E+09	3,73E+09	9,87E+09	1,97E+10	2,96E+10	3,33E+10	2,79E+10	1,73E+10	8,02E+09	2,73E+09	6,95E+08	1,29E+08	1,78E+07	2,00E+00
			2,9	3,88E+05	1,87E+06	6,51E+06	1,73E+07	3,45E+07	5,18E+07	5,83E+07	4,88E+07	3,03E+07	1,41E+07	4,79E+06	1,22E+06	2,27E+05	3,12E+04	3,31E-03
		heteroaggregates in sediment	1,5	4,09E+04	2,55E+05	1,13E+06	4,17E+06	1,37E+07	4,61E+07	7,10E+07	8,54E+07	9,67E+07	1,29E+08	5,06E+07	2,00E+07	7,22E+06	3,52E+06	4,90E+00
			2	3,92E+04	2,48E+05	1,11E+06	4,10E+06	1,34E+07	4,41E+07	6,79E+07	8,15E+07	9,18E+07	1,21E+08	4,77E+07	1,88E+07	6,79E+06	3,31E+06	4,58E+00
			2,5	3,19E+04	2,27E+05	1,15E+06	4,58E+06	1,50E+07	4,38E+07	7,17E+07	8,99E+07	9,65E+07	1,07E+08	4,60E+07	1,83E+07	6,23E+06	2,64E+06	3,25E+00
			2,9	8,30E+01	8,18E+02	5,60E+03	2,83E+04	1,06E+05	2,94E+05	6,21E+05	9,71E+05	1,12E+06	9,62E+05	6,08E+05	2,87E+05	9,89E+04	2,55E+04	5,94E-03

Appendix XI: Number concentrations of aggregates, obtained at point 5, with alpha (NN) = 0,1

alpha river	Month	Aggregation state	Df	Sizeclass														
				2,00E-07	3,12E-07	4,86E-07	7,58E-07	1,18E-06	1,84E-06	2,87E-06	4,47E-06	6,97E-06	1,09E-05	1,69E-05	2,64E-05	4,12E-05	6,42E-05	1,00E-04
0,001	January	homoaggregates in water	1,5	0,00E+00	0,00E+00	0,00E+00	0,00E+00	0,00E+00	0,00E+00	0,00E+00	0,00E+00	0,00E+00	0,00E+00	0,00E+00	0,00E+00	0,00E+00	0,00E+00	0,00E+00
			2	0,00E+00	0,00E+00	0,00E+00	0,00E+00	0,00E+00	0,00E+00	0,00E+00	0,00E+00	0,00E+00	0,00E+00	0,00E+00	0,00E+00	0,00E+00	0,00E+00	0,00E+00
			2,5	0,00E+00	0,00E+00	0,00E+00	0,00E+00	0,00E+00	0,00E+00	0,00E+00	0,00E+00	0,00E+00	0,00E+00	0,00E+00	0,00E+00	0,00E+00	0,00E+00	0,00E+00
			2,9	0,00E+00	0,00E+00	0,00E+00	0,00E+00	0,00E+00	0,00E+00	0,00E+00	0,00E+00	0,00E+00	0,00E+00	0,00E+00	0,00E+00	0,00E+00	0,00E+00	0,00E+00
		homoaggregates in sediment	1,5	0,00E+00	0,00E+00	0,00E+00	0,00E+00	0,00E+00	0,00E+00	0,00E+00	0,00E+00	0,00E+00	0,00E+00	0,00E+00	0,00E+00	0,00E+00	0,00E+00	0,00E+00
			2	0,00E+00	0,00E+00	0,00E+00	0,00E+00	0,00E+00	0,00E+00	0,00E+00	0,00E+00	0,00E+00	0,00E+00	0,00E+00	0,00E+00	0,00E+00	0,00E+00	0,00E+00
			2,5	0,00E+00	0,00E+00	0,00E+00	0,00E+00	0,00E+00	0,00E+00	0,00E+00	0,00E+00	0,00E+00	0,00E+00	0,00E+00	0,00E+00	0,00E+00	0,00E+00	0,00E+00
			2,9	0,00E+00	0,00E+00	0,00E+00	0,00E+00	0,00E+00	0,00E+00	0,00E+00	0,00E+00	0,00E+00	0,00E+00	0,00E+00	0,00E+00	0,00E+00	0,00E+00	0,00E+00
				Sizeclass														
				1,00E-06	1,39E-06	1,93E-06	2,69E-06	3,74E-06	5,19E-06	7,22E-06	1,00E-05	1,40E-05	1,94E-05	2,70E-05	3,75E-05	5,21E-05	7,24E-05	1,00E-04
		heteroaggregates in water	1,5	0,00E+00	0,00E+00	0,00E+00	0,00E+00	0,00E+00	0,00E+00	0,00E+00	0,00E+00	0,00E+00	0,00E+00	0,00E+00	0,00E+00	0,00E+00	0,00E+00	0,00E+00
			2	0,00E+00	0,00E+00	0,00E+00	0,00E+00	0,00E+00	0,00E+00	0,00E+00	0,00E+00	0,00E+00	0,00E+00	0,00E+00	0,00E+00	0,00E+00	0,00E+00	0,00E+00
			2,5	0,00E+00	0,00E+00	0,00E+00	0,00E+00	0,00E+00	0,00E+00	0,00E+00	0,00E+00	0,00E+00	0,00E+00	0,00E+00	0,00E+00	0,00E+00	0,00E+00	0,00E+00
			2,9	0,00E+00	0,00E+00	0,00E+00	0,00E+00	0,00E+00	0,00E+00	0,00E+00	0,00E+00	0,00E+00	0,00E+00	0,00E+00	0,00E+00	0,00E+00	0,00E+00	0,00E+00
		heteroaggregates in sediment	1,5	0,00E+00	0,00E+00	0,00E+00	0,00E+00	0,00E+00	0,00E+00	0,00E+00	0,00E+00	0,00E+00	0,00E+00	0,00E+00	0,00E+00	0,00E+00	0,00E+00	0,00E+00
			2	0,00E+00	0,00E+00	0,00E+00	0,00E+00	0,00E+00	0,00E+00	0,00E+00	0,00E+00	0,00E+00	0,00E+00	0,00E+00	0,00E+00	0,00E+00	0,00E+00	0,00E+00
			2,5	0,00E+00	0,00E+00	0,00E+00	0,00E+00	0,00E+00	0,00E+00	0,00E+00	0,00E+00	0,00E+00	0,00E+00	0,00E+00	0,00E+00	0,00E+00	0,00E+00	0,00E+00
			2,9	0,00E+00	0,00E+00	0,00E+00	0,00E+00	0,00E+00	0,00E+00	0,00E+00	0,00E+00	0,00E+00	0,00E+00	0,00E+00	0,00E+00	0,00E+00	0,00E+00	0,00E+00
	March			Sizeclass														
				2,00E-07	3,12E-07	4,86E-07	7,58E-07	1,18E-06	1,84E-06	2,87E-06	4,47E-06	6,97E-06	1,09E-05	1,69E-05	2,64E-05	4,12E-05	6,42E-05	1,00E-04
		homoaggregates in water	1,5	4,63E+14	9,60E+14	5,63E+14	9,10E+13	3,97E+12	4,47E+10	1,29E+08	1,13E+05	3,64E+01	1,04E-02	0,00E+00	0,00E+00	0,00E+00	0,00E+00	0,00E+00
			2	4,30E+14	9,10E+14	5,30E+14	8,61E+13	3,64E+12	4,30E+10	1,21E+08	1,03E+05	3,31E+01	8,28E-03	0,00E+00	0,00E+00	0,00E+00	0,00E+00	0,00E+00
			2,5	3,14E+14	6,45E+14	3,81E+14	6,12E+13	2,65E+12	2,98E+10	8,28E+07	6,79E+04	1,82E+01	3,14E-03	0,00E+00	0,00E+00	0,00E+00	0,00E+00	0,00E+00
			2,9	1,46E+14	2,98E+14	1,82E+14	2,81E+13	1,22E+12	1,36E+10	3,64E+07	2,81E+04	6,62E+00	9,60E-04	0,00E+00	0,00E+00	0,00E+00	0,00E+00	0,00E+00
		homoaggregates in sediment	1,5	3,45E+07	8,91E+07	6,52E+07	1,32E+07	7,18E+05	1,01E+04	3,64E+01	3,96E-02	1,60E-05	0,00E+00	0,00E+00	0,00E+00	0,00E+00	0,00E+00	0,00E+00
			2	2,02E+08	6,67E+08	6,05E+08	1,53E+08	1,01E+07	1,86E+05	8,15E+02	1,08E+00	5,43E-04	2,11E-07	0,00E+00	0,00E+00	0,00E+00	0,00E+00	0,00E+00
			2,5	9,36E+08	3,74E+09	4,29E+09	1,34E+09	1,13E+08	2,47E+06	1,34E+04	2,13E+01	1,11E-02	3,75E-06	0,00E+00	0,00E+00	0,00E+00	0,00E+00	0,00E+00
			2,9	1,90E+09	9,01E+09	1,28E+10	4,60E+09	4,65E+08	1,20E+07	7,47E+04	1,34E+02	7,34E-02	2,47E-05	0,00E+00	0,00E+00	0,00E+00	0,00E+00	0,00E+00
				Sizeclass														
				1,00E-06	1,39E-06	1,93E-06	2,69E-06	3,74E-06	5,19E-06	7,22E-06	1,00E-05	1,40E-05	1,94E-05	2,70E-05	3,75E-05	5,21E-05	7,24E-05	1,00E-04
		heteroaggregates in water	1,5	3,70E+04	1,78E+05	6,22E+05	1,65E+06	3,28E+06	4,94E+06	5,54E+06	4,65E+06	2,89E+06	1,33E+06	4,55E+05	1,16E+05	2,15E+04	2,96E+03	3,28E-04
			2	3,49E+04	1,67E+05	5,86E+05	1,55E+06	3,09E+06	4,65E+06	5,22E+06	4,38E+06	2,72E+06	1,25E+06	4,28E+05	1,09E+05	2,02E+04	2,79E+03	3,09E-04
			2,5	2,50E+04	1,20E+05	4,20E+05	1,11E+06	2,22E+06	3,33E+06	3,74E+06	3,14E+06	1,95E+06	8,98E+05	3,07E+05	7,81E+04	1,45E+04	2,00E+03	2,21E-04
			2,9	1,17E+04	5,60E+04	1,96E+05	5,18E+05	1,03E+06	1,55E+06	1,74E+06	1,46E+06	9,08E+05	4,19E+05	1,43E+05	3,64E+04	6,76E+03	9,32E+02	1,04E-04
		heteroaggregates in sediment	1,5	5,41E+00	3,37E+01	1,50E+02	5,52E+02	1,82E+03	6,12E+03	9,41E+03	1,13E+04	1,28E+04	1,70E+04	6,70E+03	2,65E+03	9,54E+02	4,67E+02	6,32E-04
			2	5,21E+00	3,29E+01	1,48E+02	5,45E+02	1,78E+03	5,88E+03	9,04E+03	1,09E+04	1,22E+04	1,61E+04	6,35E+03	2,51E+03	9,01E+02	4,40E+02	5,96E-04
			2,5	4,26E+00	3,02E+01	1,53E+02	6,12E+02	1,99E+03	5,85E+03	9,58E+03	1,20E+04	1,29E+04	1,43E+04	6,14E+03	2,44E+03	8,30E+02	3,52E+02	4,27E-04
			2,9	2,97E+00	2,92E+01	2,00E+02	1,01E+03	3,77E+03	1,05E+04	2,21E+04	3,46E+04	3,98E+04	3,41E+04	2,16E+04	1,02E+04	3,50E+03	9,06E+02	2,21E-04

alpha river	Month	Aggregation state	Df	Sizeclass													
				2,00E-07	3,12E-07	4,86E-07	7,58E-07	1,18E-06	1,84E-06	2,87E-06	4,47E-06	6,97E-06	1,09E-05	1,69E-05	2,64E-05	4,12E-05	6,42E-05	1,00E-04
0,001	May	homoaggregates in water	1,5	1,18E+15	2,52E+15	1,50E+15	2,36E+14	1,02E+13	1,18E+11	3,15E+08	2,52E+05	6,23E+01	7,88E-03	0,00E+00	0,00E+00	0,00E+00	0,00E+00	0,00E+00
			2	1,10E+15	2,36E+15	1,34E+15	2,21E+14	9,46E+12	1,10E+11	3,00E+08	2,36E+05	5,60E+01	6,70E-03	0,00E+00	0,00E+00	0,00E+00	0,00E+00	0,00E+00
			2,5	7,88E+14	1,66E+15	9,46E+14	1,58E+14	6,78E+12	7,57E+10	2,05E+08	1,58E+05	3,55E+01	3,23E-03	0,00E+00	0,00E+00	0,00E+00	0,00E+00	0,00E+00
			2,9	3,78E+14	7,88E+14	4,57E+14	7,25E+13	3,15E+12	3,47E+10	9,46E+07	6,86E+04	1,34E+01	1,02E-03	0,00E+00	0,00E+00	0,00E+00	0,00E+00	0,00E+00
		homoaggregates in sediment	1,5	3,78E+08	1,01E+09	7,46E+08	1,47E+08	7,95E+06	1,15E+05	3,81E+02	3,81E-01	1,17E-04	0,00E+00	0,00E+00	0,00E+00	0,00E+00	0,00E+00	0,00E+00
			2	2,23E+09	7,44E+09	6,58E+09	1,69E+09	1,13E+08	2,05E+06	8,68E+03	1,07E+01	3,94E-03	0,00E+00	0,00E+00	0,00E+00	0,00E+00	0,00E+00	0,00E+00
			2,5	1,01E+10	4,12E+10	4,58E+10	1,48E+10	1,24E+09	2,70E+07	1,42E+05	2,13E+02	9,32E-02	1,65E-05	0,00E+00	0,00E+00	0,00E+00	0,00E+00	0,00E+00
			2,9	2,11E+10	1,02E+11	1,38E+11	5,09E+10	5,14E+09	1,31E+08	8,33E+05	1,40E+03	6,38E-01	1,13E-04	0,00E+00	0,00E+00	0,00E+00	0,00E+00	0,00E+00
				Sizeclass														
				1,00E-06	1,39E-06	1,93E-06	2,69E-06	3,74E-06	5,19E-06	7,22E-06	1,00E-05	1,40E-05	1,94E-05	2,70E-05	3,75E-05	5,21E-05	7,24E-05	1,00E-04
		heteroaggregates in water	1,5	6,06E+05	2,91E+06	1,02E+07	2,69E+07	5,37E+07	8,07E+07	9,06E+07	7,60E+07	4,72E+07	2,17E+07	7,43E+06	1,89E+06	3,51E+05	4,84E+04	5,38E-03
			2	5,59E+05	2,68E+06	9,39E+06	2,49E+07	4,96E+07	7,46E+07	8,37E+07	7,02E+07	4,36E+07	2,01E+07	6,87E+06	1,75E+06	3,24E+05	4,47E+04	4,93E-03
			2,5	3,94E+05	1,89E+06	6,62E+06	1,75E+07	3,50E+07	5,26E+07	5,90E+07	4,96E+07	3,07E+07	1,42E+07	4,85E+06	1,23E+06	2,29E+05	3,15E+04	3,49E-03
			2,9	1,89E+05	9,05E+05	3,17E+06	8,38E+06	1,67E+07	2,52E+07	2,82E+07	2,37E+07	1,47E+07	6,78E+06	2,32E+06	5,89E+05	1,09E+05	1,51E+04	1,65E-03
		heteroaggregates in sediment	1,5	3,80E+02	2,37E+03	1,05E+04	3,88E+04	1,27E+05	4,29E+05	6,60E+05	7,95E+05	9,00E+05	1,19E+06	4,70E+05	1,86E+05	6,69E+04	3,28E+04	4,46E-02
			2	3,59E+02	2,27E+03	1,02E+04	3,75E+04	1,22E+05	4,05E+05	6,22E+05	7,48E+05	8,43E+05	1,11E+06	4,37E+05	1,73E+05	6,20E+04	3,03E+04	4,08E-02
			2,5	2,88E+02	2,05E+03	1,04E+04	4,15E+04	1,35E+05	3,97E+05	6,49E+05	8,15E+05	8,74E+05	9,69E+05	4,16E+05	1,65E+05	5,62E+04	2,39E+04	2,90E-02
			2,9	2,06E+02	2,02E+03	1,39E+04	7,01E+04	2,62E+05	7,29E+05	1,54E+06	2,40E+06	2,77E+06	2,37E+06	1,50E+06	7,07E+05	2,43E+05	6,29E+04	1,52E-02
	August			Sizeclass														
				2,00E-07	3,12E-07	4,86E-07	7,58E-07	1,18E-06	1,84E-06	2,87E-06	4,47E-06	6,97E-06	1,09E-05	1,69E-05	2,64E-05	4,12E-05	6,42E-05	1,00E-04
		homoaggregates in water	1,5	6,57E+14	1,34E+15	7,82E+14	1,28E+14	5,63E+12	6,25E+10	1,78E+08	1,47E+05	4,07E+01	7,51E-03	0,00E+00	0,00E+00	0,00E+00	0,00E+00	0,00E+00
			2	6,25E+14	1,28E+15	7,51E+14	1,19E+14	5,32E+12	5,94E+10	1,66E+08	1,34E+05	3,75E+01	6,25E-03	0,00E+00	0,00E+00	0,00E+00	0,00E+00	0,00E+00
			2,5	4,38E+14	9,07E+14	5,32E+14	8,44E+13	3,75E+12	4,07E+10	1,16E+08	9,07E+04	2,19E+01	2,69E-03	0,00E+00	0,00E+00	0,00E+00	0,00E+00	0,00E+00
			2,9	2,03E+14	4,38E+14	2,47E+14	4,07E+13	1,72E+12	1,91E+10	5,00E+07	3,75E+04	8,13E+00	9,07E-04	0,00E+00	0,00E+00	0,00E+00	0,00E+00	0,00E+00
		homoaggregates in sediment	1,5	8,36E+07	2,14E+08	1,55E+08	3,18E+07	1,74E+06	2,42E+04	8,60E+01	8,85E-02	3,06E-05	0,00E+00	0,00E+00	0,00E+00	0,00E+00	0,00E+00	0,00E+00
			2	5,04E+08	1,61E+09	1,47E+09	3,62E+08	2,53E+07	4,40E+05	1,91E+03	2,42E+00	1,05E-03	0,00E+00	0,00E+00	0,00E+00	0,00E+00	0,00E+00	0,00E+00
			2,5	2,23E+09	8,99E+09	1,03E+10	3,17E+09	2,74E+08	5,78E+06	3,20E+04	4,88E+01	2,29E-02	5,49E-06	0,00E+00	0,00E+00	0,00E+00	0,00E+00	0,00E+00
			2,9	4,53E+09	2,27E+10	2,97E+10	1,14E+10	1,12E+09	2,88E+07	1,76E+05	3,06E+02	1,54E-01	4,00E-05	0,00E+00	0,00E+00	0,00E+00	0,00E+00	0,00E+00
				Sizeclass														
				1,00E-06	1,39E-06	1,93E-06	2,69E-06	3,74E-06	5,19E-06	7,22E-06	1,00E-05	1,40E-05	1,94E-05	2,70E-05	3,75E-05	5,21E-05	7,24E-05	1,00E-04
		heteroaggregates in water	1,5	1,28E+05	6,16E+05	2,16E+06	5,71E+06	1,14E+07	1,71E+07	1,92E+07	1,61E+07	1,00E+07	4,62E+06	1,58E+06	4,01E+05	7,45E+04	1,03E+04	1,14E-03
			2	1,22E+05	5,88E+05	2,06E+06	5,44E+06	1,09E+07	1,63E+07	1,83E+07	1,54E+07	9,55E+06	4,40E+06	1,51E+06	3,83E+05	7,11E+04	9,80E+03	1,08E-03
			2,5	8,65E+04	4,15E+05	1,45E+06	3,85E+06	7,67E+06	1,15E+07	1,29E+07	1,09E+07	6,74E+06	3,11E+06	1,06E+06	2,70E+05	5,02E+04	6,92E+03	7,63E-04
			2,9	4,10E+04	1,97E+05	6,88E+05	1,82E+06	3,63E+06	5,47E+06	6,13E+06	5,15E+06	3,19E+06	1,47E+06	5,03E+05	1,28E+05	2,38E+04	3,28E+03	3,60E-04
		heteroaggregates in sediment	1,5	3,21E+01	2,00E+02	8,91E+02	3,28E+03	1,08E+04	3,63E+04	5,59E+04	6,73E+04	7,62E+04	1,01E+05	3,98E+04	1,57E+04	5,66E+03	2,77E+03	3,75E-03
			2	3,13E+01	1,98E+02	8,90E+02	3,28E+03	1,07E+04	3,54E+04	5,44E+04	6,54E+04	7,36E+04	9,67E+04	3,82E+04	1,51E+04	5,42E+03	2,65E+03	3,56E-03
			2,5	2,52E+01	1,79E+02	9,09E+02	3,63E+03	1,18E+04	3,47E+04	5,68E+04	7,13E+04	7,64E+04	8,48E+04	3,64E+04	1,44E+04	4,92E+03	2,09E+03	2,52E-03
			2,9	1,78E+01	1,75E+02	1,20E+03	6,07E+03	2,27E+04	6,32E+04	1,33E+05	2,08E+05	2,40E+05	2,05E+05	1,30E+05	6,12E+04	2,11E+04	5,45E+03	1,32E-03

alpha river	Month	Aggregation state	Df	Sizeclass													
				2,00E-07	3,12E-07	4,86E-07	7,58E-07	1,18E-06	1,84E-06	2,87E-06	4,47E-06	6,97E-06	1,09E-05	1,69E-05	2,64E-05	4,12E-05	6,42E-05	1,00E-04
0,001	November	homoaggregates in water	1,5	4,14E+15	8,82E+15	5,09E+15	8,14E+14	3,66E+13	4,27E+11	1,36E+09	1,42E+06	8,82E+02	1,90E+00	3,32E+01	0,00E+00	0,00E+00	0,00E+00	0,00E+00
			2	3,87E+15	8,14E+15	4,82E+15	8,14E+14	3,46E+13	4,00E+11	1,22E+09	1,29E+06	7,46E+02	1,29E+00	9,50E+00	0,00E+00	0,00E+00	0,00E+00	0,00E+00
			2,5	2,78E+15	5,83E+15	3,39E+15	5,50E+14	2,44E+13	2,78E+11	8,14E+08	8,14E+05	3,39E+02	2,44E-01	8,14E-02	0,00E+00	0,00E+00	0,00E+00	0,00E+00
			2,9	1,29E+15	2,71E+15	1,56E+15	2,51E+14	1,09E+13	1,22E+11	3,53E+08	2,99E+05	1,02E+02	5,43E-02	0,00E+00	0,00E+00	0,00E+00	0,00E+00	0,00E+00
		homoaggregates in sediment	1,5	3,61E+08	9,61E+08	6,92E+08	1,38E+08	7,77E+06	1,13E+05	4,49E+02	5,88E-01	4,54E-04	1,22E-06	2,67E-05	0,00E+00	0,00E+00	0,00E+00	0,00E+00
			2	2,13E+09	7,01E+09	6,46E+09	1,70E+09	1,13E+08	2,03E+06	9,67E+03	1,59E+01	1,44E-02	3,87E-05	4,44E-04	0,00E+00	0,00E+00	0,00E+00	0,00E+00
			2,5	9,71E+09	3,96E+10	4,49E+10	1,41E+10	1,22E+09	2,71E+07	1,54E+05	3,01E+02	2,44E-01	3,41E-04	2,22E-04	0,00E+00	0,00E+00	0,00E+00	0,00E+00
			2,9	1,97E+10	9,63E+10	1,29E+11	4,81E+10	4,84E+09	1,26E+08	8,49E+05	1,67E+03	1,32E+00	1,64E-03	0,00E+00	0,00E+00	0,00E+00	0,00E+00	0,00E+00
				Sizeclass														
				1,00E-06	1,39E-06	1,93E-06	2,69E-06	3,74E-06	5,19E-06	7,22E-06	1,00E-05	1,40E-05	1,94E-05	2,70E-05	3,75E-05	5,21E-05	7,24E-05	1,00E-04
		heteroaggregates in water	1,5	1,58E+06	7,60E+06	2,66E+07	7,04E+07	1,40E+08	2,11E+08	2,37E+08	1,99E+08	1,23E+08	5,69E+07	1,95E+07	4,95E+06	9,18E+05	1,27E+05	1,40E-02
			2	1,48E+06	7,13E+06	2,49E+07	6,59E+07	1,31E+08	1,98E+08	2,22E+08	1,86E+08	1,15E+08	5,33E+07	1,82E+07	4,63E+06	8,59E+05	1,18E+05	1,34E-02
			2,5	1,05E+06	5,06E+06	1,77E+07	4,69E+07	9,35E+07	1,41E+08	1,58E+08	1,32E+08	8,22E+07	3,79E+07	1,30E+07	3,29E+06	6,11E+05	8,43E+04	9,34E-03
			2,9	4,88E+05	2,34E+06	8,19E+06	2,17E+07	4,33E+07	6,51E+07	7,31E+07	6,13E+07	3,80E+07	1,75E+07	6,00E+06	1,52E+06	2,83E+05	3,90E+04	4,29E-03
		heteroaggregates in sediment	1,5	2,71E+02	1,69E+03	7,53E+03	2,77E+04	9,11E+04	3,07E+05	4,72E+05	5,69E+05	6,44E+05	8,52E+05	3,36E+05	1,33E+05	4,79E+04	2,34E+04	3,16E-02
			2	2,60E+02	1,64E+03	7,39E+03	2,72E+04	8,86E+04	2,93E+05	4,51E+05	5,42E+05	6,10E+05	8,01E+05	3,16E+05	1,25E+05	4,49E+04	2,19E+04	3,03E-02
			2,5	2,11E+02	1,50E+03	7,59E+03	3,03E+04	9,87E+04	2,90E+05	4,74E+05	5,96E+05	6,38E+05	7,08E+05	3,04E+05	1,21E+05	4,11E+04	1,74E+04	2,12E-02
			2,9	1,46E+02	1,43E+03	9,83E+03	4,96E+04	1,85E+05	5,16E+05	1,09E+06	1,70E+06	1,96E+06	1,68E+06	1,06E+06	5,00E+05	1,72E+05	4,45E+04	1,07E-02

alpha river	Month	Aggregation state	Df	Sizeclass														
				2,00E-07	3,12E-07	4,86E-07	7,58E-07	1,18E-06	1,84E-06	2,87E-06	4,47E-06	6,97E-06	1,09E-05	1,69E-05	2,64E-05	4,12E-05	6,42E-05	1,00E-04
0,01	January	homoaggregates in water	1,5	0,00E+00	0,00E+00	0,00E+00	0,00E+00	0,00E+00	0,00E+00	0,00E+00	0,00E+00	0,00E+00	0,00E+00	0,00E+00	0,00E+00	0,00E+00	0,00E+00	0,00E+00
			2	0,00E+00	0,00E+00	0,00E+00	0,00E+00	0,00E+00	0,00E+00	0,00E+00	0,00E+00	0,00E+00	0,00E+00	0,00E+00	0,00E+00	0,00E+00	0,00E+00	0,00E+00
			2,5	0,00E+00	0,00E+00	0,00E+00	0,00E+00	0,00E+00	0,00E+00	0,00E+00	0,00E+00	0,00E+00	0,00E+00	0,00E+00	0,00E+00	0,00E+00	0,00E+00	0,00E+00
			2,9	0,00E+00	0,00E+00	0,00E+00	0,00E+00	0,00E+00	0,00E+00	0,00E+00	0,00E+00	0,00E+00	0,00E+00	0,00E+00	0,00E+00	0,00E+00	0,00E+00	0,00E+00
		homoaggregates in sediment	1,5	0,00E+00	0,00E+00	0,00E+00	0,00E+00	0,00E+00	0,00E+00	0,00E+00	0,00E+00	0,00E+00	0,00E+00	0,00E+00	0,00E+00	0,00E+00	0,00E+00	0,00E+00
			2	0,00E+00	0,00E+00	0,00E+00	0,00E+00	0,00E+00	0,00E+00	0,00E+00	0,00E+00	0,00E+00	0,00E+00	0,00E+00	0,00E+00	0,00E+00	0,00E+00	0,00E+00
			2,5	0,00E+00	0,00E+00	0,00E+00	0,00E+00	0,00E+00	0,00E+00	0,00E+00	0,00E+00	0,00E+00	0,00E+00	0,00E+00	0,00E+00	0,00E+00	0,00E+00	0,00E+00
			2,9	0,00E+00	0,00E+00	0,00E+00	0,00E+00	0,00E+00	0,00E+00	0,00E+00	0,00E+00	0,00E+00	0,00E+00	0,00E+00	0,00E+00	0,00E+00	0,00E+00	0,00E+00
				Sizeclass														
				1,00E-06	1,39E-06	1,93E-06	2,69E-06	3,74E-06	5,19E-06	7,22E-06	1,00E-05	1,40E-05	1,94E-05	2,70E-05	3,75E-05	5,21E-05	7,24E-05	1,00E-04
		heteroaggregates in water	1,5	0,00E+00	0,00E+00	0,00E+00	0,00E+00	0,00E+00	0,00E+00	0,00E+00	0,00E+00	0,00E+00	0,00E+00	0,00E+00	0,00E+00	0,00E+00	0,00E+00	0,00E+00
			2	0,00E+00	0,00E+00	0,00E+00	0,00E+00	0,00E+00	0,00E+00	0,00E+00	0,00E+00	0,00E+00	0,00E+00	0,00E+00	0,00E+00	0,00E+00	0,00E+00	0,00E+00
			2,5	0,00E+00	0,00E+00	0,00E+00	0,00E+00	0,00E+00	0,00E+00	0,00E+00	0,00E+00	0,00E+00	0,00E+00	0,00E+00	0,00E+00	0,00E+00	0,00E+00	0,00E+00
			2,9	0,00E+00	0,00E+00	0,00E+00	0,00E+00	0,00E+00	0,00E+00	0,00E+00	0,00E+00	0,00E+00	0,00E+00	0,00E+00	0,00E+00	0,00E+00	0,00E+00	0,00E+00
		heteroaggregates in sediment	1,5	0,00E+00	0,00E+00	0,00E+00	0,00E+00	0,00E+00	0,00E+00	0,00E+00	0,00E+00	0,00E+00	0,00E+00	0,00E+00	0,00E+00	0,00E+00	0,00E+00	0,00E+00
			2	0,00E+00	0,00E+00	0,00E+00	0,00E+00	0,00E+00	0,00E+00	0,00E+00	0,00E+00	0,00E+00	0,00E+00	0,00E+00	0,00E+00	0,00E+00	0,00E+00	0,00E+00
			2,5	0,00E+00	0,00E+00	0,00E+00	0,00E+00	0,00E+00	0,00E+00	0,00E+00	0,00E+00	0,00E+00	0,00E+00	0,00E+00	0,00E+00	0,00E+00	0,00E+00	0,00E+00
			2,9	0,00E+00	0,00E+00	0,00E+00	0,00E+00	0,00E+00	0,00E+00	0,00E+00	0,00E+00	0,00E+00	0,00E+00	0,00E+00	0,00E+00	0,00E+00	0,00E+00	0,00E+00
	March			Sizeclass														
				2,00E-07	3,12E-07	4,86E-07	7,58E-07	1,18E-06	1,84E-06	2,87E-06	4,47E-06	6,97E-06	1,09E-05	1,69E-05	2,64E-05	4,12E-05	6,42E-05	1,00E-04
		homoaggregates in water	1,5	4,63E+14	9,60E+14	5,63E+14	9,10E+13	3,97E+12	4,47E+10	1,29E+08	1,13E+05	3,64E+01	1,04E-02	0,00E+00	0,00E+00	0,00E+00	0,00E+00	0,00E+00
			2	4,30E+14	9,10E+14	5,30E+14	8,61E+13	3,64E+12	4,30E+10	1,21E+08	1,03E+05	3,31E+01	8,28E-03	0,00E+00	0,00E+00	0,00E+00	0,00E+00	0,00E+00
			2,5	3,14E+14	6,45E+14	3,81E+14	6,12E+13	2,65E+12	2,98E+10	8,28E+07	6,79E+04	1,82E+01	3,14E-03	0,00E+00	0,00E+00	0,00E+00	0,00E+00	0,00E+00
			2,9	1,46E+14	2,98E+14	1,82E+14	2,81E+13	1,22E+12	1,36E+10	3,64E+07	2,81E+04	6,62E+00	9,60E-04	0,00E+00	0,00E+00	0,00E+00	0,00E+00	0,00E+00
		homoaggregates in sediment	1,5	3,45E+07	8,91E+07	6,52E+07	1,32E+07	7,18E+05	1,01E+04	3,64E+01	3,96E-02	1,60E-05	5,72E-09	0,00E+00	0,00E+00	0,00E+00	0,00E+00	0,00E+00
			2	2,02E+08	6,67E+08	6,05E+08	1,53E+08	1,01E+07	1,86E+05	8,15E+02	1,08E+00	5,43E-04	2,11E-07	0,00E+00	0,00E+00	0,00E+00	0,00E+00	0,00E+00
			2,5	9,36E+08	3,74E+09	4,29E+09	1,34E+09	1,13E+08	2,47E+06	1,34E+04	2,13E+01	1,11E-02	3,75E-06	0,00E+00	0,00E+00	0,00E+00	0,00E+00	0,00E+00
			2,9	1,90E+09	9,01E+09	1,28E+10	4,60E+09	4,65E+08	1,20E+07	7,47E+04	1,34E+02	7,34E-02	2,47E-05	0,00E+00	0,00E+00	0,00E+00	0,00E+00	0,00E+00
				Sizeclass														
				1,00E-06	1,39E-06	1,93E-06	2,69E-06	3,74E-06	5,19E-06	7,22E-06	1,00E-05	1,40E-05	1,94E-05	2,70E-05	3,75E-05	5,21E-05	7,24E-05	1,00E-04
		heteroaggregates in water	1,5	3,70E+05	1,78E+06	6,22E+06	1,65E+07	3,28E+07	4,94E+07	5,54E+07	4,65E+07	2,89E+07	1,33E+07	4,55E+06	1,16E+06	2,15E+05	2,96E+04	3,28E-03
			2	3,49E+05	1,67E+06	5,86E+06	1,55E+07	3,09E+07	4,65E+07	5,22E+07	4,38E+07	2,72E+07	1,25E+07	4,28E+06	1,09E+06	2,02E+05	2,79E+04	3,09E-03
			2,5	2,50E+05	1,20E+06	4,20E+06	1,11E+07	2,22E+07	3,33E+07	3,74E+07	3,14E+07	1,95E+07	8,98E+06	3,07E+06	7,81E+05	1,45E+05	2,00E+04	2,21E-03
			2,9	1,17E+05	5,60E+05	1,96E+06	5,18E+06	1,03E+07	1,55E+07	1,74E+07	1,46E+07	9,08E+06	4,19E+06	1,43E+06	3,64E+05	6,76E+04	9,32E+03	1,04E-03
		heteroaggregates in sediment	1,5	5,41E+01	3,37E+02	1,50E+03	5,52E+03	1,82E+04	6,12E+04	9,41E+04	1,13E+05	1,28E+05	1,70E+05	6,70E+04	2,65E+04	9,54E+03	4,67E+03	6,32E-03
			2	5,21E+01	3,29E+02	1,48E+03	5,45E+03	1,78E+04	5,88E+04	9,04E+04	1,09E+05	1,22E+05	1,61E+05	6,35E+04	2,51E+04	9,01E+03	4,40E+03	5,96E-03
			2,5	4,26E+01	3,02E+02	1,53E+03	6,12E+03	1,99E+04	5,85E+04	9,58E+04	1,20E+05	1,29E+05	1,43E+05	6,14E+04	2,44E+04	8,30E+03	3,52E+03	4,27E-03
			2,9	2,97E+01	2,92E+02	2,00E+03	1,01E+04	3,77E+04	1,05E+05	2,21E+05	3,46E+05	3,98E+05	3,41E+05	2,16E+05	1,02E+05	3,50E+04	9,06E+03	2,21E-03

alpha river	Month	Aggregation state	Df	Sizeclass													
				2,00E-07	3,12E-07	4,86E-07	7,58E-07	1,18E-06	1,84E-06	2,87E-06	4,47E-06	6,97E-06	1,09E-05	1,69E-05	2,64E-05	4,12E-05	6,42E-05	1,00E-04
0,01	May	homoaggregates in water	1,5	1,18E+15	2,52E+15	1,50E+15	2,36E+14	1,02E+13	1,18E+11	3,15E+08	2,52E+05	6,23E+01	7,88E-03	0,00E+00	0,00E+00	0,00E+00	0,00E+00	0,00E+00
			2	1,10E+15	2,36E+15	1,34E+15	2,21E+14	9,46E+12	1,10E+11	3,00E+08	2,36E+05	5,60E+01	6,70E-03	0,00E+00	0,00E+00	0,00E+00	0,00E+00	0,00E+00
			2,5	7,88E+14	1,66E+15	9,46E+14	1,58E+14	6,78E+12	7,57E+10	2,05E+08	1,58E+05	3,55E+01	3,23E-03	0,00E+00	0,00E+00	0,00E+00	0,00E+00	0,00E+00
			2,9	3,78E+14	7,88E+14	4,57E+14	7,25E+13	3,15E+12	3,47E+10	9,46E+07	6,86E+04	1,34E+01	1,02E-03	0,00E+00	0,00E+00	0,00E+00	0,00E+00	0,00E+00
		homoaggregates in sediment	1,5	3,78E+08	1,01E+09	7,45E+08	1,47E+08	7,95E+06	1,15E+05	3,81E+02	3,81E-01	1,17E-04	0,00E+00	0,00E+00	0,00E+00	0,00E+00	0,00E+00	0,00E+00
			2	2,23E+09	7,44E+09	6,58E+09	1,69E+09	1,13E+08	2,05E+06	8,68E+03	1,07E+01	3,94E-03	0,00E+00	0,00E+00	0,00E+00	0,00E+00	0,00E+00	0,00E+00
			2,5	1,01E+10	4,12E+10	4,58E+10	1,48E+10	1,24E+09	2,70E+07	1,42E+05	2,13E+02	9,32E-02	1,65E-05	0,00E+00	0,00E+00	0,00E+00	0,00E+00	0,00E+00
			2,9	2,11E+10	1,02E+11	1,38E+11	5,09E+10	5,14E+09	1,31E+08	8,33E+05	1,40E+03	6,38E-01	1,13E-04	0,00E+00	0,00E+00	0,00E+00	0,00E+00	0,00E+00
				Sizeclass														
				1,00E-06	1,39E-06	1,93E-06	2,69E-06	3,74E-06	5,19E-06	7,22E-06	1,00E-05	1,40E-05	1,94E-05	2,70E-05	3,75E-05	5,21E-05	7,24E-05	1,00E-04
		heteroaggregates in water	1,5	6,06E+06	2,91E+07	1,02E+08	2,69E+08	5,37E+08	8,07E+08	9,06E+08	7,60E+08	4,71E+08	2,17E+08	7,43E+07	1,89E+07	3,51E+06	4,84E+05	5,38E-02
			2	5,59E+06	2,68E+07	9,39E+07	2,49E+08	4,96E+08	7,46E+08	8,37E+08	7,02E+08	4,36E+08	2,01E+08	6,87E+07	1,75E+07	3,24E+06	4,47E+05	4,93E-02
			2,5	3,94E+06	1,89E+07	6,62E+07	1,75E+08	3,50E+08	5,26E+08	5,90E+08	4,95E+08	3,07E+08	1,42E+08	4,85E+07	1,23E+07	2,29E+06	3,15E+05	3,49E-02
			2,9	1,89E+06	9,05E+06	3,17E+07	8,38E+07	1,67E+08	2,52E+08	2,82E+08	2,37E+08	1,47E+08	6,78E+07	2,32E+07	5,89E+06	1,09E+06	1,51E+05	1,65E-02
		heteroaggregates in sediment	1,5	3,80E+03	2,37E+04	1,05E+05	3,88E+05	1,27E+06	4,29E+06	6,60E+06	7,95E+06	9,00E+06	1,19E+07	4,70E+06	1,86E+06	6,69E+05	3,28E+05	4,46E-01
			2	3,59E+03	2,27E+04	1,02E+05	3,75E+05	1,22E+06	4,05E+06	6,22E+06	7,48E+06	8,43E+06	1,11E+07	4,37E+06	1,73E+06	6,20E+05	3,03E+05	4,08E-01
			2,5	2,88E+03	2,05E+04	1,04E+05	4,15E+05	1,35E+06	3,97E+06	6,49E+06	8,15E+06	8,74E+06	9,69E+06	4,16E+06	1,65E+06	5,62E+05	2,39E+05	2,90E-01
			2,9	2,06E+03	2,02E+04	1,39E+05	7,01E+05	2,62E+06	7,29E+06	1,54E+07	2,40E+07	2,77E+07	2,37E+07	1,50E+07	7,07E+06	2,43E+06	6,29E+05	1,52E-01
	August			Sizeclass														
				2,00E-07	3,12E-07	4,86E-07	7,58E-07	1,18E-06	1,84E-06	2,87E-06	4,47E-06	6,97E-06	1,09E-05	1,69E-05	2,64E-05	4,12E-05	6,42E-05	1,00E-04
		homoaggregates in water	1,5	6,57E+14	1,34E+15	7,82E+14	1,28E+14	5,63E+12	6,25E+10	1,78E+08	1,47E+05	4,07E+01	7,51E-03	0,00E+00	0,00E+00	0,00E+00	0,00E+00	0,00E+00
			2	6,25E+14	1,28E+15	7,51E+14	1,19E+14	5,32E+12	5,94E+10	1,66E+08	1,34E+05	3,75E+01	6,25E-03	0,00E+00	0,00E+00	0,00E+00	0,00E+00	0,00E+00
			2,5	4,38E+14	9,07E+14	5,32E+14	8,44E+13	3,75E+12	4,07E+10	1,16E+08	9,07E+04	2,19E+01	2,69E-03	0,00E+00	0,00E+00	0,00E+00	0,00E+00	0,00E+00
			2,9	2,03E+14	4,38E+14	2,47E+14	4,07E+13	1,72E+12	1,91E+10	5,00E+07	3,75E+04	8,13E+00	9,07E-04	0,00E+00	0,00E+00	0,00E+00	0,00E+00	0,00E+00
		homoaggregates in sediment	1,5	8,36E+07	2,14E+08	1,55E+08	3,18E+07	1,74E+06	2,42E+04	8,60E+01	8,85E-02	3,06E-05	0,00E+00	0,00E+00	0,00E+00	0,00E+00	0,00E+00	0,00E+00
			2	5,04E+08	1,61E+09	1,47E+09	3,62E+08	2,53E+07	4,40E+05	1,91E+03	2,42E+00	1,05E-03	0,00E+00	0,00E+00	0,00E+00	0,00E+00	0,00E+00	0,00E+00
			2,5	2,23E+09	8,99E+09	1,03E+10	3,17E+09	2,74E+08	5,78E+06	3,20E+04	4,88E+01	2,29E-02	5,49E-06	0,00E+00	0,00E+00	0,00E+00	0,00E+00	0,00E+00
			2,9	4,53E+09	2,27E+10	2,97E+10	1,14E+10	1,12E+09	2,88E+07	1,76E+05	3,06E+02	1,54E-01	4,00E-05	0,00E+00	0,00E+00	0,00E+00	0,00E+00	0,00E+00
				Sizeclass														
				1,00E-06	1,39E-06	1,93E-06	2,69E-06	3,74E-06	5,19E-06	7,22E-06	1,00E-05	1,40E-05	1,94E-05	2,70E-05	3,75E-05	5,21E-05	7,24E-05	1,00E-04
		heteroaggregates in water	1,5	1,28E+06	6,16E+06	2,16E+07	5,71E+07	1,14E+08	1,71E+08	1,92E+08	1,61E+08	1,00E+08	4,62E+07	1,58E+07	4,01E+06	7,45E+05	1,03E+05	1,14E-02
			2	1,22E+06	5,88E+06	2,06E+07	5,44E+07	1,09E+08	1,63E+08	1,83E+08	1,54E+08	9,55E+07	4,40E+07	1,51E+07	3,83E+06	7,11E+05	9,80E+04	1,08E-02
			2,5	8,65E+05	4,15E+06	1,45E+07	3,85E+07	7,67E+07	1,15E+08	1,29E+08	1,09E+08	6,74E+07	3,11E+07	1,06E+07	2,70E+06	5,02E+05	6,92E+04	7,63E-03
			2,9	4,10E+05	1,97E+06	6,88E+06	1,82E+07	3,63E+07	5,47E+07	6,13E+07	5,15E+07	3,19E+07	1,47E+07	5,03E+06	1,28E+06	2,38E+05	3,28E+04	3,60E-03
		heteroaggregates in sediment	1,5	3,21E+02	2,00E+03	8,91E+03	3,28E+04	1,08E+05	3,63E+05	5,59E+05	6,73E+05	7,62E+05	1,01E+06	3,98E+05	1,57E+05	5,66E+04	2,77E+04	3,75E-02
			2	3,13E+02	1,98E+03	8,90E+03	3,28E+04	1,07E+05	3,54E+05	5,44E+05	6,54E+05	7,36E+05	9,67E+05	3,82E+05	1,51E+05	5,42E+04	2,65E+04	3,56E-02
			2,5	2,52E+02	1,79E+03	9,09E+03	3,63E+04	1,18E+05	3,47E+05	5,68E+05	7,13E+05	7,64E+05	8,48E+05	3,64E+05	1,44E+05	4,92E+04	2,09E+04	2,52E-02
			2,9	1,78E+02	1,75E+03	1,20E+04	6,07E+04	2,27E+05	6,32E+05	1,33E+06	2,08E+06	2,40E+06	2,05E+06	1,30E+06	6,12E+05	2,11E+05	5,45E+04	1,32E-02

alpha river	Month	Aggregation state	Df	Sizeclass													
				2,00E-07	**3,12E-07**	**4,86E-07**	**7,58E-07**	**1,18E-06**	**1,84E-06**	**2,87E-06**	**4,47E-06**	**6,97E-06**	**1,09E-05**	**1,69E-05**	**2,64E-05**	**4,12E-05**	**6,42E-05**	**1,00E-04**
0,01	November			Sizeclass														
				2,00E-07	3,12E-07	4,86E-07	7,58E-07	1,18E-06	1,84E-06	2,87E-06	4,47E-06	6,97E-06	1,09E-05	1,69E-05	2,64E-05	4,12E-05	6,42E-05	1,00E-04
		homoaggregates in water	**1,5**	4,14E+15	8,82E+15	5,09E+15	8,14E+14	3,66E+13	4,27E+11	1,36E+09	1,42E+06	8,82E+02	1,90E+00	3,32E+01	0,00E+00	0,00E+00	0,00E+00	0,00E+00
			2	3,87E+15	8,14E+15	4,82E+15	8,14E+14	3,46E+13	4,00E+11	1,22E+09	1,29E+06	7,46E+02	1,29E+00	9,50E+00	0,00E+00	0,00E+00	0,00E+00	0,00E+00
			2,5	2,78E+15	5,83E+15	3,39E+15	5,49E+14	2,44E+13	2,78E+11	8,14E+08	8,14E+05	3,39E+02	2,44E-01	8,14E-02	0,00E+00	0,00E+00	0,00E+00	0,00E+00
			2,9	1,29E+15	2,71E+15	1,56E+15	2,51E+14	1,09E+13	1,22E+11	3,53E+08	2,98E+05	1,02E+02	5,43E-02	0,00E+00	0,00E+00	0,00E+00	0,00E+00	0,00E+00
		homoaggregates in sediment	**1,5**	3,61E+08	9,61E+08	6,92E+08	1,38E+08	7,77E+06	1,13E+05	4,49E+02	5,88E-01	4,54E-04	1,22E-06	2,67E-05	0,00E+00	0,00E+00	0,00E+00	0,00E+00
			2	2,13E+09	7,01E+09	6,46E+09	1,70E+09	1,13E+08	2,03E+06	9,67E+03	1,59E+01	1,44E-02	3,87E-05	4,44E-04	0,00E+00	0,00E+00	0,00E+00	0,00E+00
			2,5	9,71E+09	3,96E+10	4,49E+10	1,41E+10	1,22E+09	2,71E+07	1,54E+05	3,01E+02	2,44E-01	3,41E-04	2,22E-04	0,00E+00	0,00E+00	0,00E+00	0,00E+00
			2,9	1,97E+10	9,63E+10	1,29E+11	4,81E+10	4,84E+09	1,26E+08	8,49E+05	1,67E+03	1,32E+00	1,64E-03	0,00E+00	0,00E+00	0,00E+00	0,00E+00	0,00E+00
				Sizeclass														
				1,00E-06	**1,39E-06**	**1,93E-06**	**2,69E-06**	**3,74E-06**	**5,19E-06**	**7,22E-06**	**1,00E-05**	**1,40E-05**	**1,94E-05**	**2,70E-05**	**3,75E-05**	**5,21E-05**	**7,24E-05**	**1,00E-04**
		heteroaggregates in water	**1,5**	1,58E+07	7,60E+07	2,66E+08	7,04E+08	1,40E+09	2,11E+09	2,37E+09	1,99E+09	1,23E+09	5,69E+08	1,95E+08	4,95E+07	9,18E+06	1,27E+06	1,40E-01
			2	1,48E+07	7,13E+07	2,49E+08	6,59E+08	1,31E+09	1,98E+09	2,22E+09	1,86E+09	1,15E+09	5,33E+08	1,82E+08	4,63E+07	8,59E+06	1,18E+06	1,34E-01
			2,5	1,05E+07	5,06E+07	1,77E+08	4,69E+08	9,35E+08	1,41E+09	1,58E+09	1,32E+09	8,22E+08	3,79E+08	1,30E+08	3,29E+07	6,11E+06	8,43E+05	9,34E-02
			2,9	4,88E+06	2,34E+07	8,19E+07	2,17E+08	4,33E+08	6,51E+08	7,31E+08	6,13E+08	3,80E+08	1,75E+08	6,00E+07	1,52E+07	2,83E+06	3,90E+05	4,29E-02
		heteroaggregates in sediment	**1,5**	2,71E+03	1,69E+04	7,53E+04	2,77E+05	9,11E+05	3,07E+06	4,72E+06	5,69E+06	6,44E+06	8,52E+06	3,36E+06	1,33E+06	4,79E+05	2,34E+05	3,16E-01
			2	2,60E+03	1,64E+04	7,39E+04	2,72E+05	8,86E+05	2,93E+06	4,51E+06	5,42E+06	6,10E+06	8,01E+06	3,16E+06	1,25E+06	4,49E+05	2,19E+05	3,03E-01
			2,5	2,11E+03	1,50E+04	7,59E+04	3,03E+05	9,87E+05	2,90E+06	4,74E+06	5,96E+06	6,38E+06	7,08E+06	3,04E+06	1,21E+06	4,11E+05	1,74E+05	2,12E-01
			2,9	1,46E+03	1,43E+04	9,83E+04	4,96E+05	1,85E+06	5,16E+06	1,09E+07	1,70E+07	1,96E+07	1,67E+07	1,06E+07	5,00E+06	1,72E+06	4,45E+05	1,07E-01

alpha river	Month	Aggregation state	Df	Sizeclass														
				2,00E-07	3,12E-07	4,86E-07	7,58E-07	1,18E-06	1,84E-06	2,87E-06	4,47E-06	6,97E-06	1,09E-05	1,69E-05	2,64E-05	4,12E-05	6,42E-05	1,00E-04
0,1	January	homoaggregates in water	1,5	0,00E+00	0,00E+00	0,00E+00	0,00E+00	0,00E+00	0,00E+00	0,00E+00	0,00E+00	0,00E+00	0,00E+00	0,00E+00	0,00E+00	0,00E+00	0,00E+00	0,00E+00
			2	0,00E+00	0,00E+00	0,00E+00	0,00E+00	0,00E+00	0,00E+00	0,00E+00	0,00E+00	0,00E+00	0,00E+00	0,00E+00	0,00E+00	0,00E+00	0,00E+00	0,00E+00
			2,5	0,00E+00	0,00E+00	0,00E+00	0,00E+00	0,00E+00	0,00E+00	0,00E+00	0,00E+00	0,00E+00	0,00E+00	0,00E+00	0,00E+00	0,00E+00	0,00E+00	0,00E+00
			2,9	0,00E+00	0,00E+00	0,00E+00	0,00E+00	0,00E+00	0,00E+00	0,00E+00	0,00E+00	0,00E+00	0,00E+00	0,00E+00	0,00E+00	0,00E+00	0,00E+00	0,00E+00
		homoaggregates in sediment	1,5	0,00E+00	0,00E+00	0,00E+00	0,00E+00	0,00E+00	0,00E+00	0,00E+00	0,00E+00	0,00E+00	0,00E+00	0,00E+00	0,00E+00	0,00E+00	0,00E+00	0,00E+00
			2	0,00E+00	0,00E+00	0,00E+00	0,00E+00	0,00E+00	0,00E+00	0,00E+00	0,00E+00	0,00E+00	0,00E+00	0,00E+00	0,00E+00	0,00E+00	0,00E+00	0,00E+00
			2,5	0,00E+00	0,00E+00	0,00E+00	0,00E+00	0,00E+00	0,00E+00	0,00E+00	0,00E+00	0,00E+00	0,00E+00	0,00E+00	0,00E+00	0,00E+00	0,00E+00	0,00E+00
			2,9	0,00E+00	0,00E+00	0,00E+00	0,00E+00	0,00E+00	0,00E+00	0,00E+00	0,00E+00	0,00E+00	0,00E+00	0,00E+00	0,00E+00	0,00E+00	0,00E+00	0,00E+00
				Sizeclass														
				1,00E-06	1,39E-06	1,93E-06	2,69E-06	3,74E-06	5,19E-06	7,22E-06	1,00E-05	1,40E-05	1,94E-05	2,70E-05	3,75E-05	5,21E-05	7,24E-05	1,00E-04
		heteroaggregates in water	1,5	0,00E+00	0,00E+00	0,00E+00	0,00E+00	0,00E+00	0,00E+00	0,00E+00	0,00E+00	0,00E+00	0,00E+00	0,00E+00	0,00E+00	0,00E+00	0,00E+00	0,00E+00
			2	0,00E+00	0,00E+00	0,00E+00	0,00E+00	0,00E+00	0,00E+00	0,00E+00	0,00E+00	0,00E+00	0,00E+00	0,00E+00	0,00E+00	0,00E+00	0,00E+00	0,00E+00
			2,5	0,00E+00	0,00E+00	0,00E+00	0,00E+00	0,00E+00	0,00E+00	0,00E+00	0,00E+00	0,00E+00	0,00E+00	0,00E+00	0,00E+00	0,00E+00	0,00E+00	0,00E+00
			2,9	0,00E+00	0,00E+00	0,00E+00	0,00E+00	0,00E+00	0,00E+00	0,00E+00	0,00E+00	0,00E+00	0,00E+00	0,00E+00	0,00E+00	0,00E+00	0,00E+00	0,00E+00
		heteroaggregates in sediment	1,5	0,00E+00	0,00E+00	0,00E+00	0,00E+00	0,00E+00	0,00E+00	0,00E+00	0,00E+00	0,00E+00	0,00E+00	0,00E+00	0,00E+00	0,00E+00	0,00E+00	0,00E+00
			2	0,00E+00	0,00E+00	0,00E+00	0,00E+00	0,00E+00	0,00E+00	0,00E+00	0,00E+00	0,00E+00	0,00E+00	0,00E+00	0,00E+00	0,00E+00	0,00E+00	0,00E+00
			2,5	0,00E+00	0,00E+00	0,00E+00	0,00E+00	0,00E+00	0,00E+00	0,00E+00	0,00E+00	0,00E+00	0,00E+00	0,00E+00	0,00E+00	0,00E+00	0,00E+00	0,00E+00
			2,9	0,00E+00	0,00E+00	0,00E+00	0,00E+00	0,00E+00	0,00E+00	0,00E+00	0,00E+00	0,00E+00	0,00E+00	0,00E+00	0,00E+00	0,00E+00	0,00E+00	0,00E+00
	March			Sizeclass														
				2,00E-07	3,12E-07	4,86E-07	7,58E-07	1,18E-06	1,84E-06	2,87E-06	4,47E-06	6,97E-06	1,09E-05	1,69E-05	2,64E-05	4,12E-05	6,42E-05	1,00E-04
		homoaggregates in water	1,5	4,63E+14	9,60E+14	5,63E+14	9,10E+13	3,97E+12	4,47E+10	1,29E+08	1,13E+05	3,64E+01	1,04E-02	0,00E+00	0,00E+00	0,00E+00	0,00E+00	0,00E+00
			2	4,30E+14	9,10E+14	5,30E+14	8,60E+13	3,64E+12	4,30E+10	1,21E+08	1,03E+05	3,31E+01	8,28E-03	0,00E+00	0,00E+00	0,00E+00	0,00E+00	0,00E+00
			2,5	3,14E+14	6,45E+14	3,81E+14	6,12E+13	2,65E+12	2,98E+10	8,27E+07	6,79E+04	1,82E+01	3,14E-03	0,00E+00	0,00E+00	0,00E+00	0,00E+00	0,00E+00
			2,9	1,46E+14	2,98E+14	1,82E+14	2,81E+13	1,22E+12	1,36E+10	3,64E+07	2,81E+04	6,62E+00	9,60E-04	0,00E+00	0,00E+00	0,00E+00	0,00E+00	0,00E+00
		homoaggregates in sediment	1,5	3,45E+07	8,91E+07	6,52E+07	1,32E+07	7,18E+05	1,01E+04	3,64E+01	3,96E-02	1,60E-05	0,00E+00	0,00E+00	0,00E+00	0,00E+00	0,00E+00	0,00E+00
			2	2,02E+08	6,67E+08	6,05E+08	1,53E+08	1,01E+07	1,86E+05	8,15E+02	1,08E+00	5,43E-04	2,11E-07	0,00E+00	0,00E+00	0,00E+00	0,00E+00	0,00E+00
			2,5	9,36E+08	3,74E+09	4,29E+09	1,34E+09	1,13E+08	2,47E+06	1,34E+04	2,13E+01	1,11E-02	3,75E-06	0,00E+00	0,00E+00	0,00E+00	0,00E+00	0,00E+00
			2,9	1,90E+09	9,01E+09	1,28E+10	4,60E+09	4,65E+08	1,20E+07	7,47E+04	1,34E+02	7,34E-02	2,47E-05	0,00E+00	0,00E+00	0,00E+00	0,00E+00	0,00E+00
				Sizeclass														
				1,00E-06	1,39E-06	1,93E-06	2,69E-06	3,74E-06	5,19E-06	7,22E-06	1,00E-05	1,40E-05	1,94E-05	2,70E-05	3,75E-05	5,21E-05	7,24E-05	1,00E-04
		heteroaggregates in water	1,5	3,70E+06	1,78E+07	6,22E+07	1,65E+08	3,28E+08	4,94E+08	5,54E+08	4,65E+08	2,89E+08	1,33E+08	4,55E+07	1,16E+07	2,15E+06	2,96E+05	3,28E-02
			2	3,49E+06	1,67E+07	5,86E+07	1,55E+08	3,09E+08	4,65E+08	5,22E+08	4,38E+08	2,72E+08	1,25E+08	4,28E+07	1,09E+07	2,02E+06	2,79E+05	3,09E-02
			2,5	2,50E+06	1,20E+07	4,20E+07	1,11E+08	2,22E+08	3,33E+08	3,74E+08	3,14E+08	1,95E+08	8,98E+07	3,07E+07	7,80E+06	1,45E+06	2,00E+05	2,21E-02
			2,9	1,17E+06	5,60E+06	1,96E+07	5,18E+07	1,03E+08	1,55E+08	1,74E+08	1,46E+08	9,08E+07	4,19E+07	1,43E+07	3,64E+06	6,76E+05	9,32E+04	1,04E-02
		heteroaggregates in sediment	1,5	5,41E+02	3,37E+03	1,50E+04	5,52E+04	1,82E+05	6,12E+05	9,41E+05	1,13E+06	1,28E+06	1,70E+06	6,70E+05	2,65E+05	9,53E+04	4,67E+04	6,32E-02
			2	5,21E+02	3,29E+03	1,48E+04	5,45E+04	1,78E+05	5,88E+05	9,04E+05	1,09E+06	1,22E+06	1,61E+06	6,35E+05	2,51E+05	9,01E+04	4,40E+04	5,96E-02
			2,5	4,26E+02	3,02E+03	1,53E+04	6,12E+04	1,99E+05	5,85E+05	9,58E+05	1,20E+06	1,29E+06	1,43E+06	6,14E+05	2,44E+05	8,30E+04	3,52E+04	4,27E-02
			2,9	2,97E+02	2,92E+03	2,00E+04	1,01E+05	3,77E+05	1,05E+06	2,21E+06	3,46E+06	3,98E+06	3,41E+06	2,16E+06	1,02E+06	3,50E+05	9,06E+04	2,21E-02

alpha river	Month	Aggregation state	Df	Sizeclass													
				2,00E-07	3,12E-07	4,86E-07	7,58E-07	1,18E-06	1,84E-06	2,87E-06	4,47E-06	6,97E-06	1,09E-05	1,69E-05	2,64E-05	4,12E-05	6,42E-05	1,00E-04
0,1	May	homoaggregates in water	1,5	1,18E+15	2,52E+15	1,50E+15	2,36E+14	1,02E+13	1,18E+11	3,15E+08	2,52E+05	6,23E+01	7,88E-03	0,00E+00	0,00E+00	0,00E+00	0,00E+00	0,00E+00
			2	1,10E+15	2,36E+15	1,34E+15	2,20E+14	9,45E+12	1,10E+11	2,99E+08	2,36E+05	5,60E+01	6,70E-03	0,00E+00	0,00E+00	0,00E+00	0,00E+00	0,00E+00
			2,5	7,88E+14	1,65E+15	9,45E+14	1,57E+14	6,77E+12	7,56E+10	2,05E+08	1,58E+05	3,55E+01	3,23E-03	0,00E+00	0,00E+00	0,00E+00	0,00E+00	0,00E+00
			2,9	3,78E+14	7,88E+14	4,57E+14	7,24E+13	3,15E+12	3,46E+10	9,45E+07	6,86E+04	1,34E+01	1,02E-03	0,00E+00	0,00E+00	0,00E+00	0,00E+00	0,00E+00
		homoaggregates in sediment	1,5	3,78E+08	1,01E+09	7,45E+08	1,47E+08	7,94E+06	1,14E+05	3,81E+02	3,81E-01	1,17E-04	0,00E+00	0,00E+00	0,00E+00	0,00E+00	0,00E+00	0,00E+00
			2	2,23E+09	7,44E+09	6,57E+09	1,69E+09	1,13E+08	2,05E+06	8,67E+03	1,07E+01	3,94E-03	0,00E+00	0,00E+00	0,00E+00	0,00E+00	0,00E+00	0,00E+00
			2,5	1,01E+10	4,11E+10	4,57E+10	1,48E+10	1,24E+09	2,70E+07	1,42E+05	2,13E+02	9,32E-02	1,65E-05	0,00E+00	0,00E+00	0,00E+00	0,00E+00	0,00E+00
			2,9	2,11E+10	1,02E+11	1,38E+11	5,08E+10	5,13E+09	1,31E+08	8,33E+05	1,40E+03	6,38E-01	1,13E-04	0,00E+00	0,00E+00	0,00E+00	0,00E+00	0,00E+00
				Sizeclass														
				1,00E-06	1,39E-06	1,93E-06	2,69E-06	3,74E-06	5,19E-06	7,22E-06	1,00E-05	1,40E-05	1,94E-05	2,70E-05	3,75E-05	5,21E-05	7,24E-05	1,00E-04
		heteroaggregates in water	1,5	6,06E+07	2,91E+08	1,02E+09	2,69E+09	5,36E+09	8,07E+09	9,05E+09	7,60E+09	4,71E+09	2,17E+09	7,43E+08	1,89E+08	3,51E+07	4,83E+06	5,38E-01
			2	5,59E+07	2,68E+08	9,38E+08	2,48E+09	4,96E+09	7,46E+09	8,37E+09	7,02E+09	4,36E+09	2,01E+09	6,87E+08	1,75E+08	3,24E+07	4,47E+06	4,93E-01
			2,5	3,94E+07	1,89E+08	6,62E+08	1,75E+09	3,50E+09	5,26E+09	5,90E+09	4,95E+09	3,07E+09	1,42E+09	4,84E+08	1,23E+08	2,29E+07	3,15E+06	3,49E-01
			2,9	1,89E+07	9,04E+07	3,16E+08	8,38E+08	1,67E+09	2,51E+09	2,82E+09	2,37E+09	1,47E+09	6,78E+08	2,32E+08	5,89E+07	1,09E+07	1,51E+06	1,65E-01
		heteroaggregates in sediment	1,5	3,80E+04	2,37E+05	1,05E+06	3,88E+06	1,27E+07	4,29E+07	6,60E+07	7,95E+07	9,00E+07	1,19E+08	4,70E+07	1,86E+07	6,69E+06	3,27E+06	4,45E+00
			2	3,58E+04	2,26E+05	1,02E+06	3,75E+06	1,22E+07	4,05E+07	6,22E+07	7,48E+07	8,42E+07	1,11E+08	4,37E+07	1,72E+07	6,20E+06	3,03E+06	4,08E+00
			2,5	2,88E+04	2,05E+05	1,04E+06	4,14E+06	1,35E+07	3,97E+07	6,49E+07	8,15E+07	8,74E+07	9,69E+07	4,16E+07	1,65E+07	5,62E+06	2,39E+06	2,89E+00
			2,9	2,06E+04	2,02E+05	1,39E+06	7,01E+06	2,62E+07	7,29E+07	1,54E+08	2,40E+08	2,77E+08	2,37E+08	1,50E+08	7,06E+07	2,43E+07	6,29E+06	1,51E+00
	August			Sizeclass														
				2,00E-07	3,12E-07	4,86E-07	7,58E-07	1,18E-06	1,84E-06	2,87E-06	4,47E-06	6,97E-06	1,09E-05	1,69E-05	2,64E-05	4,12E-05	6,42E-05	1,00E-04
		homoaggregates in water	1,5	6,57E+14	1,34E+15	7,82E+14	1,28E+14	5,63E+12	6,25E+10	1,78E+08	1,47E+05	4,07E+01	7,51E-03	0,00E+00	0,00E+00	0,00E+00	0,00E+00	0,00E+00
			2	6,25E+14	1,28E+15	7,50E+14	1,19E+14	5,31E+12	5,94E+10	1,66E+08	1,34E+05	3,75E+01	6,25E-03	0,00E+00	0,00E+00	0,00E+00	0,00E+00	0,00E+00
			2,5	4,38E+14	9,07E+14	5,32E+14	8,44E+13	3,75E+12	4,06E+10	1,16E+08	9,07E+04	2,19E+01	2,69E-03	0,00E+00	0,00E+00	0,00E+00	0,00E+00	0,00E+00
			2,9	2,03E+14	4,38E+14	2,47E+14	4,06E+13	1,72E+12	1,91E+10	5,00E+07	3,75E+04	8,13E+00	9,07E-04	0,00E+00	0,00E+00	0,00E+00	0,00E+00	0,00E+00
		homoaggregates in sediment	1,5	8,36E+07	2,14E+08	1,55E+08	3,18E+07	1,74E+06	2,42E+04	8,60E+01	8,85E-02	3,06E-05	0,00E+00	0,00E+00	0,00E+00	0,00E+00	0,00E+00	0,00E+00
			2	5,04E+08	1,61E+09	1,47E+09	3,62E+08	2,53E+07	4,40E+05	1,91E+03	2,42E+00	1,05E-03	0,00E+00	0,00E+00	0,00E+00	0,00E+00	0,00E+00	0,00E+00
			2,5	2,23E+09	8,99E+09	1,03E+10	3,17E+09	2,74E+08	5,78E+06	3,20E+04	4,88E+01	2,29E-02	5,49E-06	0,00E+00	0,00E+00	0,00E+00	0,00E+00	0,00E+00
			2,9	4,53E+09	2,27E+10	2,97E+10	1,14E+10	1,12E+09	2,88E+07	1,76E+05	3,06E+02	1,54E-01	4,00E-05	0,00E+00	0,00E+00	0,00E+00	0,00E+00	0,00E+00
				Sizeclass														
				1,00E-06	1,39E-06	1,93E-06	2,69E-06	3,74E-06	5,19E-06	7,22E-06	1,00E-05	1,40E-05	1,94E-05	2,70E-05	3,75E-05	5,21E-05	7,24E-05	1,00E-04
		heteroaggregates in water	1,5	1,28E+07	6,16E+07	2,16E+08	5,71E+08	1,14E+09	1,71E+09	1,92E+09	1,61E+09	1,00E+09	4,62E+08	1,58E+08	4,01E+07	7,45E+06	1,03E+06	1,13E-01
			2	1,22E+07	5,88E+07	2,06E+08	5,44E+08	1,09E+09	1,63E+09	1,83E+09	1,54E+09	9,55E+08	4,40E+08	1,50E+08	3,83E+07	7,10E+06	9,80E+05	1,08E-01
			2,5	8,65E+06	4,15E+07	1,45E+08	3,85E+08	7,67E+08	1,15E+09	1,29E+09	1,09E+09	6,74E+08	3,11E+08	1,06E+08	2,70E+07	5,02E+06	6,92E+05	7,63E-02
			2,9	4,10E+06	1,97E+07	6,88E+07	1,82E+08	3,63E+08	5,46E+08	6,13E+08	5,15E+08	3,19E+08	1,47E+08	5,03E+07	1,28E+07	2,38E+06	3,28E+05	3,60E-02
		heteroaggregates in sediment	1,5	3,21E+03	2,00E+04	8,90E+04	3,28E+05	1,08E+06	3,63E+06	5,59E+06	6,73E+06	7,62E+06	1,01E+07	3,98E+06	1,57E+06	5,66E+05	2,77E+05	3,75E-01
			2	3,13E+03	1,98E+04	8,89E+04	3,28E+05	1,07E+06	3,54E+06	5,44E+06	6,54E+06	7,36E+06	9,66E+06	3,82E+06	1,51E+06	5,42E+05	2,65E+05	3,56E-01
			2,5	2,52E+03	1,79E+04	9,09E+04	3,63E+05	1,18E+06	3,47E+06	5,68E+06	7,13E+06	7,64E+06	8,48E+06	3,64E+06	1,44E+06	4,92E+05	2,09E+05	2,52E-01
			2,9	1,78E+03	1,75E+04	1,20E+05	6,07E+05	2,27E+06	6,32E+06	1,33E+07	2,08E+07	2,40E+07	2,05E+07	1,30E+07	6,12E+06	2,11E+06	5,45E+05	1,32E-01

alpha river	Month	Aggregation state	Df	Sizeclass													
				2,00E-07	3,12E-07	4,86E-07	7,58E-07	1,18E-06	1,84E-06	2,87E-06	4,47E-06	6,97E-06	1,09E-05	1,69E-05	2,64E-05	4,12E-05	6,42E-05	1,00E-04
0,1	November	homoaggregates in water	1,5	4,14E+15	8,82E+15	5,09E+15	8,13E+14	3,66E+13	4,27E+11	1,36E+09	1,42E+06	8,82E+02	1,90E+00	3,32E+01	0,00E+00	0,00E+00	0,00E+00	0,00E+00
			2	3,87E+15	8,14E+15	4,81E+15	8,13E+14	3,46E+13	4,00E+11	1,22E+09	1,29E+06	7,46E+02	1,29E+00	9,50E+00	0,00E+00	0,00E+00	0,00E+00	0,00E+00
			2,5	2,78E+15	5,83E+15	3,39E+15	5,49E+14	2,44E+13	2,78E+11	8,14E+08	8,14E+05	3,39E+02	2,44E-01	8,14E-02	0,00E+00	0,00E+00	0,00E+00	0,00E+00
			2,9	1,29E+15	2,71E+15	1,56E+15	2,51E+14	1,08E+13	1,22E+11	3,53E+08	2,98E+05	1,02E+02	5,43E-02	0,00E+00	0,00E+00	0,00E+00	0,00E+00	0,00E+00
		homoaggregates in sediment	1,5	3,61E+08	9,61E+08	6,92E+08	1,38E+08	7,76E+06	1,13E+05	4,48E+02	5,88E-01	4,54E-04	1,22E-06	2,67E-05	0,00E+00	0,00E+00	0,00E+00	0,00E+00
			2	2,13E+09	7,00E+09	6,46E+09	1,70E+09	1,13E+08	2,03E+06	9,67E+03	1,59E+01	1,44E-02	3,87E-05	4,44E-04	0,00E+00	0,00E+00	0,00E+00	0,00E+00
			2,5	9,71E+09	3,96E+10	4,48E+10	1,41E+10	1,22E+09	2,71E+07	1,54E+05	3,00E+02	2,44E-01	3,41E-04	2,22E-04	0,00E+00	0,00E+00	0,00E+00	0,00E+00
			2,9	1,97E+10	9,63E+10	1,29E+11	4,81E+10	4,83E+09	1,26E+08	8,49E+05	1,67E+03	1,32E+00	1,64E-03	0,00E+00	0,00E+00	0,00E+00	0,00E+00	0,00E+00
				Sizeclass														
				1,00E-06	1,39E-06	1,93E-06	2,69E-06	3,74E-06	5,19E-06	7,22E-06	1,00E-05	1,40E-05	1,94E-05	2,70E-05	3,75E-05	5,21E-05	7,24E-05	1,00E-04
		heteroaggregates in water	1,5	1,58E+08	7,60E+08	2,66E+09	7,04E+09	1,40E+10	2,11E+10	2,37E+10	1,99E+10	1,23E+10	5,69E+09	1,94E+09	4,95E+08	9,18E+07	1,27E+07	1,40E+00
			2	1,48E+08	7,12E+08	2,49E+09	6,59E+09	1,31E+10	1,98E+10	2,22E+10	1,86E+10	1,15E+10	5,32E+09	1,82E+09	4,63E+08	8,59E+07	1,18E+07	1,34E+00
			2,5	1,05E+08	5,06E+08	1,77E+09	4,69E+09	9,35E+09	1,41E+10	1,58E+10	1,32E+10	8,22E+09	3,79E+09	1,29E+09	3,29E+08	6,11E+07	8,43E+06	9,33E-01
			2,9	4,88E+07	2,34E+08	8,19E+08	2,17E+09	4,33E+09	6,51E+09	7,30E+09	6,13E+09	3,80E+09	1,75E+09	5,99E+08	1,52E+08	2,83E+07	3,90E+06	4,29E-01
		heteroaggregates in sediment	1,5	2,71E+04	1,69E+05	7,53E+05	2,77E+06	9,11E+06	3,07E+07	4,72E+07	5,69E+07	6,44E+07	8,52E+07	3,36E+07	1,33E+07	4,78E+06	2,34E+06	3,16E+00
			2	2,60E+04	1,64E+05	7,39E+05	2,72E+06	8,86E+06	2,93E+07	4,51E+07	5,42E+07	6,10E+07	8,01E+07	3,16E+07	1,25E+07	4,49E+06	2,19E+06	3,02E+00
			2,5	2,11E+04	1,50E+05	7,59E+05	3,03E+06	9,87E+06	2,90E+07	4,74E+07	5,96E+07	6,38E+07	7,08E+07	3,04E+07	1,21E+07	4,11E+06	1,74E+06	2,12E+00
			2,9	1,46E+04	1,43E+05	9,83E+05	4,96E+06	1,85E+07	5,16E+07	1,09E+08	1,70E+08	1,96E+08	1,67E+08	1,06E+08	5,00E+07	1,72E+07	4,45E+06	1,07E+00

Appendix XI: Number concentrations of aggregates, obtained at point 5, with alpha (NN) = 0,5

alpha river	Month	Aggregation state	Df	Sizeclass													
				2,00E-07	3,12E-07	4,86E-07	7,58E-07	1,18E-06	1,84E-06	2,87E-06	4,47E-06	6,97E-06	1,09E-05	1,69E-05	2,64E-05	4,12E-05	6,42E-05	1,00E-04
0,001	January	homoaggregates in water	1,5	0	0	0	0	0	0	0	0	0	0	0	0	0	0	0
			2	0	0	0	0	0	0	0	0	0	0	0	0	0	0	0
			2,5	0	0	0	0	0	0	0	0	0	0	0	0	0	0	0
			2,9	0	0	0	0	0	0	0	0	0	0	0	0	0	0	0
		homoaggregates in sediment	1,5	0	0	0	0	0	0	0	0	0	0	0	0	0	0	0
			2	0	0	0	0	0	0	0	0	0	0	0	0	0	0	0
			2,5	0	0	0	0	0	0	0	0	0	0	0	0	0	0	0
			2,9	0	0	0	0	0	0	0	0	0	0	0	0	0	0	0
				Sizeclass														
				1,00E-06	1,39E-06	1,93E-06	2,69E-06	3,74E-06	5,19E-06	7,22E-06	1,00E-05	1,40E-05	1,94E-05	2,70E-05	3,75E-05	5,21E-05	7,24E-05	1,00E-04
		heteroaggregates in water	1,5	0	0	0	0	0	0	0	0	0	0	0	0	0	0	0
			2	0	0	0	0	0	0	0	0	0	0	0	0	0	0	0
			2,5	0	0	0	0	0	0	0	0	0	0	0	0	0	0	0
			2,9	0	0	0	0	0	0	0	0	0	0	0	0	0	0	0
		heteroaggregates in sediment	1,5	0	0	0	0	0	0	0	0	0	0	0	0	0	0	0
			2	0	0	0	0	0	0	0	0	0	0	0	0	0	0	0
			2,5	0	0	0	0	0	0	0	0	0	0	0	0	0	0	0
			2,9	0	0	0	0	0	0	0	0	0	0	0	0	0	0	0
	March			Sizeclass														
				2,00E-07	3,12E-07	4,86E-07	7,58E-07	1,18E-06	1,84E-06	2,87E-06	4,47E-06	6,97E-06	1,09E-05	1,69E-05	2,64E-05	4,12E-05	6,42E-05	1,00E-04
		homoaggregates in water	1,5	4,52E+14	9,53E+14	5,76E+14	9,60E+13	4,40E+12	5,53E+10	2,05E+08	3,53E+05	8,31E+02	1,94E+02	0,00E+00	0,00E+00	0,00E+00	0,00E+00	0,00E+00
			2	4,24E+14	8,94E+14	5,40E+14	8,95E+13	4,09E+12	5,10E+10	1,85E+08	3,03E+05	6,21E+02	8,57E+01	0,00E+00	0,00E+00	0,00E+00	0,00E+00	0,00E+00
			2,5	3,06E+14	6,42E+14	3,84E+14	6,29E+13	2,83E+12	3,41E+10	1,15E+08	1,54E+05	1,79E+02	3,49E+00	0,00E+00	0,00E+00	0,00E+00	0,00E+00	0,00E+00
			2,9	1,44E+14	3,01E+14	1,77E+14	2,86E+13	1,26E+12	1,45E+10	4,40E+07	4,77E+04	3,76E+01	6,31E-01	0,00E+00	0,00E+00	0,00E+00	0,00E+00	0,00E+00
		homoaggregates in sediment	1,5	3,36E+07	8,85E+07	6,68E+07	1,39E+07	7,96E+05	1,25E+04	5,78E+01	1,24E-01	3,65E-04	1,06E-04	0,00E+00	0,00E+00	0,00E+00	0,00E+00	0,00E+00
			2	1,99E+08	6,55E+08	6,17E+08	1,60E+08	1,14E+07	2,21E+05	1,25E+03	3,19E+00	1,02E-02	2,19E-03	0,00E+00	0,00E+00	0,00E+00	0,00E+00	0,00E+00
			2,5	9,11E+08	3,72E+09	4,33E+09	1,38E+09	1,21E+08	2,83E+06	1,85E+04	4,83E+01	1,09E-01	4,16E-03	0,00E+00	0,00E+00	0,00E+00	0,00E+00	0,00E+00
			2,9	1,88E+09	9,11E+09	1,24E+10	4,68E+09	4,78E+08	1,28E+07	9,03E+04	2,27E+02	4,16E-01	1,62E-02	0,00E+00	0,00E+00	0,00E+00	0,00E+00	0,00E+00
				Sizeclass														
				1,00E-06	1,39E-06	1,93E-06	2,69E-06	3,74E-06	5,19E-06	7,22E-06	1,00E-05	1,40E-05	1,94E-05	2,70E-05	3,75E-05	5,21E-05	7,24E-05	1,00E-04
		heteroaggregates in water	1,5	3,71E+04	1,78E+05	6,24E+05	1,65E+06	3,29E+06	4,95E+06	5,55E+06	4,65E+06	2,89E+06	1,33E+06	4,55E+05	1,16E+05	2,15E+04	2,96E+03	3,37E-04
			2	3,48E+04	1,67E+05	5,84E+05	1,55E+06	3,08E+06	4,63E+06	5,20E+06	4,36E+06	2,71E+06	1,25E+06	4,26E+05	1,08E+05	2,01E+04	2,78E+03	3,16E-04
			2,5	2,49E+04	1,20E+05	4,18E+05	1,11E+06	2,21E+06	3,32E+06	3,72E+06	3,13E+06	1,94E+06	8,94E+05	3,06E+05	7,77E+04	1,44E+04	1,99E+03	2,24E-04
			2,9	1,16E+04	5,58E+04	1,95E+05	5,16E+05	1,03E+06	1,55E+06	1,74E+06	1,46E+06	9,05E+05	4,17E+05	1,43E+05	3,63E+04	6,73E+03	9,28E+02	1,03E-04
		heteroaggregates in sediment	1,5	5,42E+00	3,38E+01	1,50E+02	5,54E+02	1,82E+03	6,13E+03	9,42E+03	1,13E+04	1,28E+04	1,70E+04	6,70E+03	2,65E+03	9,54E+02	4,67E+02	6,51E-04
			2	5,20E+00	3,29E+01	1,48E+02	5,44E+02	1,77E+03	5,86E+03	9,00E+03	1,08E+04	1,22E+04	1,60E+04	6,32E+03	2,49E+03	8,97E+02	4,38E+02	6,09E-04
			2,5	4,24E+00	3,02E+01	1,53E+02	6,10E+02	1,99E+03	5,83E+03	9,54E+03	1,20E+04	1,28E+04	1,42E+04	6,11E+03	2,42E+03	8,26E+02	3,51E+02	4,33E-04
			2,9	2,95E+00	2,90E+01	1,99E+02	1,01E+03	3,75E+03	1,05E+04	2,20E+04	3,44E+04	3,97E+04	3,39E+04	2,15E+04	1,01E+04	3,49E+03	9,02E+02	2,20E-04

alpha river	Month	Aggregation state	Df	Sizeclass													
				2,00E-07	**3,12E-07**	**4,86E-07**	**7,58E-07**	**1,18E-06**	**1,84E-06**	**2,87E-06**	**4,47E-06**	**6,97E-06**	**1,09E-05**	**1,69E-05**	**2,64E-05**	**4,12E-05**	**6,42E-05**	**1,00E-04**
0,001	May	homoaggregates in water	**1,5**	1,19E+15	2,50E+15	1,47E+15	2,40E+14	1,07E+13	1,27E+11	4,07E+08	4,82E+05	3,89E+02	1,97E+00	0,00E+00	0,00E+00	0,00E+00	0,00E+00	0,00E+00
			2	1,12E+15	2,34E+15	1,38E+15	2,25E+14	1,00E+13	1,18E+11	3,74E+08	4,30E+05	3,19E+02	1,22E+00	0,00E+00	0,00E+00	0,00E+00	0,00E+00	0,00E+00
			2,5	8,04E+14	1,68E+15	9,85E+14	1,59E+14	7,02E+12	8,12E+10	2,47E+08	2,52E+05	1,33E+02	1,76E-01	0,00E+00	0,00E+00	0,00E+00	0,00E+00	0,00E+00
			2,9	3,76E+14	7,84E+14	4,58E+14	7,35E+13	3,20E+12	3,62E+10	1,03E+08	9,14E+04	3,61E+01	3,50E-02	0,00E+00	0,00E+00	0,00E+00	0,00E+00	0,00E+00
		homoaggregates in sediment	**1,5**	3,80E+08	9,96E+08	7,34E+08	1,49E+08	8,32E+06	1,23E+05	4,92E+02	7,28E-01	7,33E-04	4,64E-06	0,00E+00	0,00E+00	0,00E+00	0,00E+00	0,00E+00
			2	2,26E+09	7,37E+09	6,77E+09	1,72E+09	1,19E+08	2,20E+06	1,08E+04	1,94E+01	2,25E-02	1,34E-04	0,00E+00	0,00E+00	0,00E+00	0,00E+00	0,00E+00
			2,5	1,03E+10	4,17E+10	4,77E+10	1,50E+10	1,29E+09	2,90E+07	1,71E+05	3,41E+02	3,50E-01	8,99E-04	0,00E+00	0,00E+00	0,00E+00	0,00E+00	0,00E+00
			2,9	2,10E+10	1,02E+11	1,38E+11	5,15E+10	5,22E+09	1,37E+08	9,10E+05	1,87E+03	1,72E+00	3,87E-03	0,00E+00	0,00E+00	0,00E+00	0,00E+00	0,00E+00
				Sizeclass														
				1,00E-06	**1,39E-06**	**1,93E-06**	**2,69E-06**	**3,74E-06**	**5,19E-06**	**7,22E-06**	**1,00E-05**	**1,40E-05**	**1,94E-05**	**2,70E-05**	**3,75E-05**	**5,21E-05**	**7,24E-05**	**1,00E-04**
		heteroaggregates in water	**1,5**	6,02E+05	2,89E+06	1,01E+07	2,67E+07	5,33E+07	8,02E+07	9,00E+07	7,55E+07	4,68E+07	2,16E+07	7,38E+06	1,88E+06	3,49E+05	4,81E+04	5,37E-03
			2	5,64E+05	2,71E+06	9,47E+06	2,51E+07	5,00E+07	7,51E+07	8,43E+07	7,08E+07	4,39E+07	2,03E+07	6,92E+06	1,76E+06	3,27E+05	4,50E+04	5,02E-03
			2,5	4,04E+05	1,94E+06	6,78E+06	1,79E+07	3,58E+07	5,38E+07	6,04E+07	5,07E+07	3,14E+07	1,45E+07	4,96E+06	1,26E+06	2,34E+05	3,23E+04	3,58E-03
			2,9	1,88E+05	9,03E+05	3,16E+06	8,36E+06	1,67E+07	2,51E+07	2,82E+07	2,36E+07	1,47E+07	6,76E+06	2,31E+06	5,88E+05	1,09E+05	1,50E+04	1,66E-03
		heteroaggregates in sediment	**1,5**	3,77E+02	2,35E+03	1,05E+04	3,85E+04	1,27E+05	4,27E+05	6,56E+05	7,90E+05	8,94E+05	1,18E+06	4,67E+05	1,84E+05	6,65E+04	3,25E+04	4,45E-02
			2	3,61E+02	2,28E+03	1,03E+04	3,78E+04	1,23E+05	4,08E+05	6,27E+05	7,54E+05	8,49E+05	1,11E+06	4,40E+05	1,74E+05	6,25E+04	3,05E+04	4,16E-02
			2,5	2,95E+02	2,10E+03	1,06E+04	4,24E+04	1,38E+05	4,06E+05	6,64E+05	8,34E+05	8,94E+05	9,91E+05	4,26E+05	1,69E+05	5,75E+04	2,44E+04	2,97E-02
			2,9	2,05E+02	2,02E+03	1,39E+04	6,99E+04	2,61E+05	7,27E+05	1,53E+06	2,40E+06	2,76E+06	2,36E+06	1,50E+06	7,05E+05	2,43E+05	6,28E+04	1,52E-02
	August			**Sizeclass**														
				2,00E-07	**3,12E-07**	**4,86E-07**	**7,58E-07**	**1,18E-06**	**1,84E-06**	**2,87E-06**	**4,47E-06**	**6,97E-06**	**1,09E-05**	**1,69E-05**	**2,64E-05**	**4,12E-05**	**6,42E-05**	**1,00E-04**
		homoaggregates in water	**1,5**	6,41E+14	1,34E+15	8,07E+14	1,33E+14	6,04E+12	7,35E+10	2,53E+08	3,57E+05	4,66E+02	1,26E+01	0,00E+00	0,00E+00	0,00E+00	0,00E+00	0,00E+00
			2	6,00E+14	1,26E+15	7,54E+14	1,24E+14	5,63E+12	6,82E+10	2,31E+08	3,13E+05	3,66E+02	6,75E+00	0,00E+00	0,00E+00	0,00E+00	0,00E+00	0,00E+00
			2,5	4,32E+14	9,04E+14	5,38E+14	8,76E+13	3,91E+12	4,63E+10	1,47E+08	1,71E+05	1,30E+02	5,82E-01	0,00E+00	0,00E+00	0,00E+00	0,00E+00	0,00E+00
			2,9	2,03E+14	4,22E+14	2,49E+14	4,00E+13	1,75E+12	2,00E+10	5,91E+07	5,79E+04	3,35E+01	1,62E-01	0,00E+00	0,00E+00	0,00E+00	0,00E+00	0,00E+00
		homoaggregates in sediment	**1,5**	8,16E+07	2,14E+08	1,60E+08	3,30E+07	1,87E+06	2,84E+04	1,22E+02	2,15E-01	3,50E-04	1,19E-05	0,00E+00	0,00E+00	0,00E+00	0,00E+00	0,00E+00
			2	4,84E+08	1,58E+09	1,47E+09	3,80E+08	2,68E+07	5,05E+05	2,67E+03	5,63E+00	1,03E-02	2,96E-04	0,00E+00	0,00E+00	0,00E+00	0,00E+00	0,00E+00
			2,5	2,20E+09	8,96E+09	1,04E+10	3,29E+09	2,86E+08	6,58E+06	4,08E+04	9,21E+01	1,37E-01	1,19E-03	0,00E+00	0,00E+00	0,00E+00	0,00E+00	0,00E+00
			2,9	4,53E+09	2,19E+10	2,99E+10	1,12E+10	1,14E+09	3,03E+07	2,08E+05	4,72E+02	6,35E-01	7,14E-03	0,00E+00	0,00E+00	0,00E+00	0,00E+00	0,00E+00
				Sizeclass														
				1,00E-06	**1,39E-06**	**1,93E-06**	**2,69E-06**	**3,74E-06**	**5,19E-06**	**7,22E-06**	**1,00E-05**	**1,40E-05**	**1,94E-05**	**2,70E-05**	**3,75E-05**	**5,21E-05**	**7,24E-05**	**1,00E-04**
		heteroaggregates in water	**1,5**	1,29E+05	6,21E+05	2,17E+06	5,75E+06	1,15E+07	1,72E+07	1,93E+07	1,62E+07	1,01E+07	4,64E+06	1,59E+06	4,03E+05	7,49E+04	1,03E+04	1,17E-03
			2	1,21E+05	5,82E+05	2,03E+06	5,38E+06	1,07E+07	1,61E+07	1,81E+07	1,52E+07	9,42E+06	4,35E+06	1,49E+06	3,78E+05	7,01E+04	9,66E+03	1,09E-03
			2,5	8,67E+04	4,16E+05	1,45E+06	3,85E+06	7,68E+06	1,15E+07	1,30E+07	1,09E+07	6,75E+06	3,11E+06	1,06E+06	2,70E+05	5,02E+04	6,92E+03	7,75E-04
			2,9	4,04E+04	1,94E+05	6,78E+05	1,79E+06	3,58E+06	5,38E+06	6,04E+06	5,07E+06	3,14E+06	1,45E+06	4,95E+05	1,26E+05	2,34E+04	3,23E+03	3,58E-04
		heteroaggregates in sediment	**1,5**	3,24E+01	2,02E+02	8,97E+02	3,30E+03	1,09E+04	3,66E+04	5,62E+04	6,77E+04	7,66E+04	1,01E+05	4,00E+04	1,58E+04	5,69E+03	2,79E+03	3,86E-03
			2	3,10E+01	1,96E+02	8,80E+02	3,24E+03	1,05E+04	3,49E+04	5,37E+04	6,45E+04	7,26E+04	9,54E+04	3,77E+04	1,49E+04	5,35E+03	2,61E+03	3,60E-03
			2,5	2,53E+01	1,80E+02	9,10E+02	3,63E+03	1,18E+04	3,47E+04	5,68E+04	7,13E+04	7,64E+04	8,48E+04	3,64E+04	1,44E+04	4,92E+03	2,09E+03	2,57E-03
			2,9	1,76E+01	1,73E+02	1,19E+03	5,98E+03	2,23E+04	6,22E+04	1,31E+05	2,05E+05	2,36E+05	2,02E+05	1,28E+05	6,03E+04	2,07E+04	5,37E+03	1,31E-03

alpha river	Month	Aggregation state	Df	Sizeclass													
				2,00E-07	3,12E-07	4,86E-07	7,58E-07	1,18E-06	1,84E-06	2,87E-06	4,47E-06	6,97E-06	1,09E-05	1,69E-05	2,64E-05	4,12E-05	6,42E-05	1,00E-04
0,001	November	homoaggregates in water	1,5	0,00E+00	0,00E+00	0,00E+00	0,00E+00	0,00E+00	0,00E+00	0,00E+00	0,00E+00	0,00E+00	0,00E+00	0,00E+00	0,00E+00	0,00E+00	0,00E+00	1,67E+14
			2	0,00E+00	0,00E+00	0,00E+00	0,00E+00	0,00E+00	0,00E+00	0,00E+00	0,00E+00	0,00E+00	0,00E+00	0,00E+00	0,00E+00	0,00E+00	0,00E+00	1,56E+14
			2,5	0,00E+00	0,00E+00	0,00E+00	0,00E+00	0,00E+00	0,00E+00	0,00E+00	0,00E+00	0,00E+00	0,00E+00	0,00E+00	0,00E+00	0,00E+00	0,00E+00	1,02E+14
			2,9	2,38E+12	4,92E+12	2,85E+12	4,50E+11	1,91E+10	2,10E+08	6,38E+05	8,48E+02	1,99E+00	1,03E+01	5,53E+00	4,65E+00	1,61E-03	0,00E+00	6,04E+13
		homoaggregates in sediment	1,5	0,00E+00	0,00E+00	0,00E+00	0,00E+00	0,00E+00	0,00E+00	0,00E+00	0,00E+00	0,00E+00	0,00E+00	0,00E+00	0,00E+00	0,00E+00	0,00E+00	3,26E+08
			2	0,00E+00	0,00E+00	0,00E+00	0,00E+00	0,00E+00	0,00E+00	0,00E+00	0,00E+00	0,00E+00	0,00E+00	0,00E+00	0,00E+00	0,00E+00	0,00E+00	4,31E+10
			2,5	0,00E+00	0,00E+00	0,00E+00	0,00E+00	0,00E+00	0,00E+00	0,00E+00	0,00E+00	0,00E+00	0,00E+00	0,00E+00	0,00E+00	0,00E+00	0,00E+00	4,00E+12
			2,9	3,64E+07	1,75E+08	2,35E+08	8,64E+07	8,50E+06	2,18E+05	1,54E+03	4,75E+00	2,59E-02	3,12E-01	3,88E-01	7,59E-01	6,13E-04	0,00E+00	1,24E+14
				Sizeclass														
				1,00E-06	1,39E-06	1,93E-06	2,69E-06	3,74E-06	5,19E-06	7,22E-06	1,00E-05	1,40E-05	1,94E-05	2,70E-05	3,75E-05	5,21E-05	7,24E-05	1,00E-04
		heteroaggregates in water	1,5	0,00E+00	0,00E+00	0,00E+00	0,00E+00	0,00E+00	0,00E+00	0,00E+00	0,00E+00	0,00E+00	0,00E+00	0,00E+00	0,00E+00	0,00E+00	0,00E+00	0,00E+00
			2	0,00E+00	0,00E+00	0,00E+00	0,00E+00	0,00E+00	0,00E+00	0,00E+00	0,00E+00	0,00E+00	0,00E+00	0,00E+00	0,00E+00	0,00E+00	0,00E+00	0,00E+00
			2,5	0,00E+00	0,00E+00	0,00E+00	0,00E+00	0,00E+00	0,00E+00	0,00E+00	0,00E+00	0,00E+00	0,00E+00	0,00E+00	0,00E+00	0,00E+00	0,00E+00	0,00E+00
			2,9	8,89E+02	4,27E+03	1,49E+04	3,95E+04	7,88E+04	1,19E+05	1,33E+05	1,12E+05	6,93E+04	3,20E+04	1,09E+04	2,78E+03	5,16E+02	7,12E+01	7,77E-06
		heteroaggregates in sediment	1,5	0,00E+00	0,00E+00	0,00E+00	0,00E+00	0,00E+00	0,00E+00	0,00E+00	0,00E+00	0,00E+00	0,00E+00	0,00E+00	0,00E+00	0,00E+00	0,00E+00	0,00E+00
			2	0,00E+00	0,00E+00	0,00E+00	0,00E+00	0,00E+00	0,00E+00	0,00E+00	0,00E+00	0,00E+00	0,00E+00	0,00E+00	0,00E+00	0,00E+00	0,00E+00	0,00E+00
			2,5	0,00E+00	0,00E+00	0,00E+00	0,00E+00	0,00E+00	0,00E+00	0,00E+00	0,00E+00	0,00E+00	0,00E+00	0,00E+00	0,00E+00	0,00E+00	0,00E+00	0,00E+00
			2,9	2,65E-01	2,61E+00	1,79E+01	9,04E+01	3,38E+02	9,40E+02	1,98E+03	3,10E+03	3,57E+03	3,05E+03	1,93E+03	9,11E+02	3,14E+02	8,12E+01	1,95E-05

alpha river	Month	Aggregation state	Df	Sizeclass														
				2,00E-07	3,12E-07	4,86E-07	7,58E-07	1,18E-06	1,84E-06	2,87E-06	4,47E-06	6,97E-06	1,09E-05	1,69E-05	2,64E-05	4,12E-05	6,42E-05	1,00E-04
0,01	January	homoaggregates in water	1,5	0	0	0	0	0	0	0	0	0	0	0	0	0	0	0
			2	0	0	0	0	0	0	0	0	0	0	0	0	0	0	0
			2,5	0	0	0	0	0	0	0	0	0	0	0	0	0	0	0
			2,9	0	0	0	0	0	0	0	0	0	0	0	0	0	0	0
		homoaggregates in sediment	1,5	0	0	0	0	0	0	0	0	0	0	0	0	0	0	0
			2	0	0	0	0	0	0	0	0	0	0	0	0	0	0	0
			2,5	0	0	0	0	0	0	0	0	0	0	0	0	0	0	0
			2,9	0	0	0	0	0	0	0	0	0	0	0	0	0	0	0
				Sizeclass														
				1,00E-06	1,39E-06	1,93E-06	2,69E-06	3,74E-06	5,19E-06	7,22E-06	1,00E-05	1,40E-05	1,94E-05	2,70E-05	3,75E-05	5,21E-05	7,24E-05	1,00E-04
		heteroaggregates in water	1,5	0	0	0	0	0	0	0	0	0	0	0	0	0	0	0
			2	0	0	0	0	0	0	0	0	0	0	0	0	0	0	0
			2,5	0	0	0	0	0	0	0	0	0	0	0	0	0	0	0
			2,9	0	0	0	0	0	0	0	0	0	0	0	0	0	0	0
		heteroaggregates in sediment	1,5	0	0	0	0	0	0	0	0	0	0	0	0	0	0	0
			2	0	0	0	0	0	0	0	0	0	0	0	0	0	0	0
			2,5	0	0	0	0	0	0	0	0	0	0	0	0	0	0	0
			2,9	0	0	0	0	0	0	0	0	0	0	0	0	0	0	0
	March			Sizeclass														
				2,00E-07	3,12E-07	4,86E-07	7,58E-07	1,18E-06	1,84E-06	2,87E-06	4,47E-06	6,97E-06	1,09E-05	1,69E-05	2,64E-05	4,12E-05	6,42E-05	1,00E-04
		homoaggregates in water	1,5	4,52E+14	9,53E+14	5,76E+14	9,60E+13	4,40E+12	5,53E+10	2,05E+08	3,53E+05	8,31E+02	1,94E+02	0,00E+00	0,00E+00	0,00E+00	0,00E+00	0,00E+00
			2	4,24E+14	8,94E+14	5,40E+14	8,95E+13	4,09E+12	5,10E+10	1,85E+08	3,03E+05	6,21E+02	8,57E+01	0,00E+00	0,00E+00	0,00E+00	0,00E+00	0,00E+00
			2,5	3,06E+14	6,42E+14	3,84E+14	6,29E+13	2,83E+12	3,41E+10	1,15E+08	1,54E+05	1,79E+02	3,49E+00	0,00E+00	0,00E+00	0,00E+00	0,00E+00	0,00E+00
			2,9	1,44E+14	3,01E+14	1,77E+14	2,86E+13	1,26E+12	1,45E+10	4,40E+07	4,77E+04	3,76E+01	6,31E-01	0,00E+00	0,00E+00	0,00E+00	0,00E+00	0,00E+00
		homoaggregates in sediment	1,5	3,36E+07	8,85E+07	6,68E+07	1,39E+07	7,96E+05	1,25E+04	5,78E+01	1,24E-01	3,65E-04	1,06E-04	0,00E+00	0,00E+00	0,00E+00	0,00E+00	0,00E+00
			2	1,99E+08	6,55E+08	6,17E+08	1,60E+08	1,14E+07	2,21E+05	1,25E+03	3,19E+00	1,02E-02	2,19E-03	0,00E+00	0,00E+00	0,00E+00	0,00E+00	0,00E+00
			2,5	9,11E+08	3,72E+09	4,33E+09	1,38E+09	1,21E+08	2,83E+06	1,85E+04	4,83E+01	1,09E-01	4,16E-03	0,00E+00	0,00E+00	0,00E+00	0,00E+00	0,00E+00
			2,9	1,88E+09	9,11E+09	1,24E+10	4,68E+09	4,78E+08	1,28E+07	9,03E+04	2,27E+02	4,16E-01	1,62E-02	0,00E+00	0,00E+00	0,00E+00	0,00E+00	0,00E+00
				Sizeclass														
				1,00E-06	1,39E-06	1,93E-06	2,69E-06	3,74E-06	5,19E-06	7,22E-06	1,00E-05	1,40E-05	1,94E-05	2,70E-05	3,75E-05	5,21E-05	7,24E-05	1,00E-04
		heteroaggregates in water	1,5	3,71E+05	1,78E+06	6,24E+06	1,65E+07	3,29E+07	4,95E+07	5,55E+07	4,65E+07	2,89E+07	1,33E+07	4,55E+06	1,16E+06	2,15E+05	2,96E+04	3,37E-03
			2	3,48E+05	1,67E+06	5,84E+06	1,55E+07	3,08E+07	4,63E+07	5,20E+07	4,36E+07	2,71E+07	1,25E+07	4,26E+06	1,08E+06	2,01E+05	2,78E+04	3,16E-03
			2,5	2,49E+05	1,20E+06	4,18E+06	1,11E+07	2,21E+07	3,32E+07	3,72E+07	3,13E+07	1,94E+07	8,94E+06	3,06E+06	7,77E+05	1,44E+05	1,99E+04	2,24E-03
			2,9	1,16E+05	5,58E+05	1,95E+06	5,16E+06	1,03E+07	1,55E+07	1,74E+07	1,46E+07	9,05E+06	4,17E+06	1,43E+06	3,63E+05	6,73E+04	9,28E+03	1,03E-03
		heteroaggregates in sediment	1,5	5,42E+01	3,38E+02	1,50E+03	5,54E+03	1,82E+04	6,13E+04	9,42E+04	1,13E+05	1,28E+05	1,70E+05	6,70E+04	2,65E+04	9,54E+03	4,67E+03	6,51E-03
			2	5,20E+01	3,29E+02	1,48E+03	5,44E+03	1,77E+04	5,86E+04	9,00E+04	1,08E+05	1,22E+05	1,60E+05	6,32E+04	2,49E+04	8,97E+03	4,38E+03	6,09E-03
			2,5	4,24E+01	3,02E+02	1,53E+03	6,10E+03	1,99E+04	5,83E+04	9,54E+04	1,20E+05	1,28E+05	1,42E+05	6,11E+04	2,42E+04	8,26E+03	3,51E+03	4,33E-03
			2,9	2,95E+01	2,90E+02	1,99E+03	1,01E+04	3,75E+04	1,05E+05	2,20E+05	3,44E+05	3,97E+05	3,39E+05	2,15E+05	1,01E+05	3,49E+04	9,02E+03	2,20E-03

alpha river	Month	Aggregation state	Df	Sizeclass													
				2,00E-07	**3,12E-07**	**4,86E-07**	**7,58E-07**	**1,18E-06**	**1,84E-06**	**2,87E-06**	**4,47E-06**	**6,97E-06**	**1,09E-05**	**1,69E-05**	**2,64E-05**	**4,12E-05**	**6,42E-05**	**1,00E-04**
0,01	May	homoaggregates in water	**1,5**	1,19E+15	2,50E+15	1,47E+15	2,40E+14	1,07E+13	1,27E+11	4,07E+08	4,82E+05	3,89E+02	1,97E+00	0,00E+00	0,00E+00	0,00E+00	0,00E+00	0,00E+00
			2	1,12E+15	2,34E+15	1,38E+15	2,25E+14	1,00E+13	1,18E+11	3,74E+08	4,30E+05	3,19E+02	1,22E+00	0,00E+00	0,00E+00	0,00E+00	0,00E+00	0,00E+00
			2,5	8,04E+14	1,68E+15	9,85E+14	1,59E+14	7,02E+12	8,12E+10	2,47E+08	2,52E+05	1,33E+02	1,76E-01	0,00E+00	0,00E+00	0,00E+00	0,00E+00	0,00E+00
			2,9	3,76E+14	7,84E+14	4,58E+14	7,35E+13	3,20E+12	3,62E+10	1,03E+08	9,14E+04	3,61E+01	3,50E-02	0,00E+00	0,00E+00	0,00E+00	0,00E+00	0,00E+00
		homoaggregates in sediment	**1,5**	3,80E+08	9,96E+08	7,34E+08	1,49E+08	8,32E+06	1,23E+05	4,92E+02	7,28E-01	7,33E-04	4,64E-06	0,00E+00	0,00E+00	0,00E+00	0,00E+00	0,00E+00
			2	2,26E+09	7,37E+09	6,77E+09	1,72E+09	1,19E+08	2,20E+06	1,08E+04	1,94E+01	2,25E-02	1,34E-04	0,00E+00	0,00E+00	0,00E+00	0,00E+00	0,00E+00
			2,5	1,03E+10	4,17E+10	4,77E+10	1,50E+10	1,29E+09	2,90E+07	1,71E+05	3,41E+02	3,50E-01	8,99E-04	0,00E+00	0,00E+00	0,00E+00	0,00E+00	0,00E+00
			2,9	2,10E+10	1,02E+11	1,38E+11	5,15E+10	5,22E+09	1,37E+08	9,09E+05	1,87E+03	1,72E+00	3,87E-03	0,00E+00	0,00E+00	0,00E+00	0,00E+00	0,00E+00
				Sizeclass														
				1,00E-06	**1,39E-06**	**1,93E-06**	**2,69E-06**	**3,74E-06**	**5,19E-06**	**7,22E-06**	**1,00E-05**	**1,40E-05**	**1,94E-05**	**2,70E-05**	**3,75E-05**	**5,21E-05**	**7,24E-05**	**1,00E-04**
		heteroaggregates in water	**1,5**	6,02E+06	2,89E+07	1,01E+08	2,67E+08	5,33E+08	8,02E+08	9,00E+08	7,55E+08	4,68E+08	2,16E+08	7,38E+07	1,88E+07	3,48E+06	4,80E+05	5,37E-02
			2	5,64E+06	2,71E+07	9,47E+07	2,51E+08	5,00E+08	7,51E+08	8,43E+08	7,08E+08	4,39E+08	2,02E+08	6,92E+07	1,76E+07	3,27E+06	4,50E+05	5,02E-02
			2,5	4,04E+06	1,94E+07	6,78E+07	1,79E+08	3,58E+08	5,38E+08	6,04E+08	5,07E+08	3,14E+08	1,45E+08	4,96E+07	1,26E+07	2,34E+06	3,23E+05	3,58E-02
			2,9	1,88E+06	9,03E+06	3,16E+07	8,36E+07	1,67E+08	2,51E+08	2,82E+08	2,36E+08	1,47E+08	6,76E+07	2,31E+07	5,88E+06	1,09E+06	1,50E+05	1,66E-02
		heteroaggregates in sediment	**1,5**	3,77E+03	2,35E+04	1,05E+05	3,85E+05	1,27E+06	4,27E+06	6,56E+06	7,90E+06	8,94E+06	1,18E+07	4,67E+06	1,84E+06	6,65E+05	3,25E+05	4,45E-01
			2	3,61E+03	2,28E+04	1,03E+05	3,78E+05	1,23E+06	4,08E+06	6,27E+06	7,54E+06	8,49E+06	1,11E+07	4,40E+06	1,74E+06	6,25E+05	3,05E+05	4,16E-01
			2,5	2,95E+03	2,10E+04	1,06E+05	4,24E+05	1,38E+06	4,06E+06	6,64E+06	8,34E+06	8,94E+06	9,91E+06	4,26E+06	1,69E+06	5,75E+05	2,44E+05	2,97E-01
			2,9	2,05E+03	2,02E+04	1,39E+05	6,99E+05	2,61E+06	7,27E+06	1,53E+07	2,40E+07	2,76E+07	2,36E+07	1,50E+07	7,05E+06	2,43E+06	6,28E+05	1,52E-01
	August			**Sizeclass**														
				2,00E-07	**3,12E-07**	**4,86E-07**	**7,58E-07**	**1,18E-06**	**1,84E-06**	**2,87E-06**	**4,47E-06**	**6,97E-06**	**1,09E-05**	**1,69E-05**	**2,64E-05**	**4,12E-05**	**6,42E-05**	**1,00E-04**
		homoaggregates in water	**1,5**	6,41E+14	1,34E+15	8,07E+14	1,33E+14	6,04E+12	7,35E+10	2,53E+08	3,57E+05	4,66E+02	1,26E+01	0,00E+00	0,00E+00	0,00E+00	0,00E+00	0,00E+00
			2	6,00E+14	1,26E+15	7,54E+14	1,24E+14	5,63E+12	6,82E+10	2,31E+08	3,13E+05	3,66E+02	6,75E+00	0,00E+00	0,00E+00	0,00E+00	0,00E+00	0,00E+00
			2,5	4,32E+14	9,04E+14	5,38E+14	8,76E+13	3,91E+12	4,63E+10	1,47E+08	1,71E+05	1,30E+02	5,82E-01	0,00E+00	0,00E+00	0,00E+00	0,00E+00	0,00E+00
			2,9	2,03E+14	4,22E+14	2,49E+14	4,00E+13	1,75E+12	2,00E+10	5,91E+07	5,79E+04	3,35E+01	1,62E-01	0,00E+00	0,00E+00	0,00E+00	0,00E+00	0,00E+00
		homoaggregates in sediment	**1,5**	8,16E+07	2,14E+08	1,60E+08	3,30E+07	1,87E+06	2,84E+04	1,22E+02	2,15E-01	3,50E-04	1,19E-05	0,00E+00	0,00E+00	0,00E+00	0,00E+00	0,00E+00
			2	4,84E+08	1,58E+09	1,47E+09	3,80E+08	2,68E+07	5,05E+05	2,67E+03	5,63E+00	1,03E-02	2,96E-04	0,00E+00	0,00E+00	0,00E+00	0,00E+00	0,00E+00
			2,5	2,20E+09	8,96E+09	1,04E+10	3,29E+09	2,86E+08	6,58E+06	4,08E+04	9,21E+01	1,37E-01	1,19E-03	0,00E+00	0,00E+00	0,00E+00	0,00E+00	0,00E+00
			2,9	4,53E+09	2,19E+10	2,99E+10	1,12E+10	1,14E+09	3,03E+07	2,08E+05	4,72E+02	6,35E-01	7,14E-03	0,00E+00	0,00E+00	0,00E+00	0,00E+00	0,00E+00
				Sizeclass														
				1,00E-06	**1,39E-06**	**1,93E-06**	**2,69E-06**	**3,74E-06**	**5,19E-06**	**7,22E-06**	**1,00E-05**	**1,40E-05**	**1,94E-05**	**2,70E-05**	**3,75E-05**	**5,21E-05**	**7,24E-05**	**1,00E-04**
		heteroaggregates in water	**1,5**	1,29E+06	6,21E+06	2,17E+07	5,75E+07	1,15E+08	1,72E+08	1,93E+08	1,62E+08	1,01E+08	4,64E+07	1,59E+07	4,03E+06	7,49E+05	1,03E+05	1,17E-02
			2	1,21E+06	5,82E+06	2,03E+07	5,38E+07	1,07E+08	1,61E+08	1,81E+08	1,52E+08	9,42E+07	4,35E+07	1,48E+07	3,78E+06	7,01E+05	9,66E+04	1,09E-02
			2,5	8,67E+05	4,16E+06	1,45E+07	3,85E+07	7,68E+07	1,15E+08	1,30E+08	1,09E+08	6,75E+07	3,11E+07	1,06E+07	2,70E+06	5,02E+05	6,92E+04	7,75E-03
			2,9	4,04E+05	1,94E+06	6,78E+06	1,79E+07	3,58E+07	5,38E+07	6,04E+07	5,07E+07	3,14E+07	1,45E+07	4,95E+06	1,26E+06	2,34E+05	3,23E+04	3,58E-03
		heteroaggregates in sediment	**1,5**	3,24E+02	2,02E+03	8,97E+03	3,30E+04	1,09E+05	3,66E+05	5,62E+05	6,77E+05	7,66E+05	1,01E+06	4,00E+05	1,58E+05	5,69E+04	2,79E+04	3,86E-02
			2	3,10E+02	1,96E+03	8,80E+03	3,24E+04	1,05E+05	3,49E+05	5,37E+05	6,45E+05	7,26E+05	9,54E+05	3,77E+05	1,49E+05	5,35E+04	2,61E+04	3,60E-02
			2,5	2,53E+02	1,80E+03	9,10E+03	3,63E+04	1,18E+05	3,47E+05	5,68E+05	7,13E+05	7,64E+05	8,48E+05	3,64E+05	1,44E+05	4,92E+04	2,09E+04	2,57E-02
			2,9	1,76E+02	1,73E+03	1,19E+04	5,98E+04	2,23E+05	6,22E+05	1,31E+06	2,05E+06	2,36E+06	2,02E+06	1,28E+06	6,03E+05	2,07E+05	5,37E+04	1,31E-02

alpha river	Month	Aggregation state	Df	Sizeclass													
				2,00E-07	3,12E-07	4,86E-07	7,58E-07	1,18E-06	1,84E-06	2,87E-06	4,47E-06	6,97E-06	1,09E-05	1,69E-05	2,64E-05	4,12E-05	6,42E-05	1,00E-04
0,01	November	homoaggregates in water	1,5	0,00E+00	0,00E+00	0,00E+00	0,00E+00	0,00E+00	0,00E+00	0,00E+00	0,00E+00	0,00E+00	0,00E+00	0,00E+00	0,00E+00	0,00E+00	0,00E+00	1,67E+14
			2	0,00E+00	0,00E+00	0,00E+00	0,00E+00	0,00E+00	0,00E+00	0,00E+00	0,00E+00	0,00E+00	0,00E+00	0,00E+00	0,00E+00	0,00E+00	0,00E+00	1,56E+14
			2,5	0,00E+00	0,00E+00	0,00E+00	0,00E+00	0,00E+00	0,00E+00	0,00E+00	0,00E+00	0,00E+00	0,00E+00	0,00E+00	0,00E+00	0,00E+00	0,00E+00	1,02E+14
			2,9	2,38E+12	4,92E+12	2,85E+12	4,50E+11	1,91E+10	2,10E+08	6,38E+05	8,48E+02	1,99E+00	1,03E+01	5,53E+00	4,65E+00	1,61E-03	0,00E+00	6,04E+13
		homoaggregates in sediment	1,5	0,00E+00	0,00E+00	0,00E+00	0,00E+00	0,00E+00	0,00E+00	0,00E+00	0,00E+00	0,00E+00	0,00E+00	0,00E+00	0,00E+00	0,00E+00	0,00E+00	3,26E+08
			2	0,00E+00	0,00E+00	0,00E+00	0,00E+00	0,00E+00	0,00E+00	0,00E+00	0,00E+00	0,00E+00	0,00E+00	0,00E+00	0,00E+00	0,00E+00	0,00E+00	4,31E+10
			2,5	0,00E+00	0,00E+00	0,00E+00	0,00E+00	0,00E+00	0,00E+00	0,00E+00	0,00E+00	0,00E+00	0,00E+00	0,00E+00	0,00E+00	0,00E+00	0,00E+00	4,00E+12
			2,9	3,64E+07	1,75E+08	2,35E+08	8,64E+07	8,49E+06	2,18E+05	1,54E+03	4,75E+00	2,59E-02	3,12E-01	3,88E-01	7,59E-01	6,13E-04	0,00E+00	1,24E+14
				Sizeclass														
				1,00E-06	1,39E-06	1,93E-06	2,69E-06	3,74E-06	5,19E-06	7,22E-06	1,00E-05	1,40E-05	1,94E-05	2,70E-05	3,75E-05	5,21E-05	7,24E-05	1,00E-04
		heteroaggregates in water	1,5	0,00E+00	0,00E+00	0,00E+00	0,00E+00	0,00E+00	0,00E+00	0,00E+00	0,00E+00	0,00E+00	0,00E+00	0,00E+00	0,00E+00	0,00E+00	0,00E+00	0,00E+00
			2	0,00E+00	0,00E+00	0,00E+00	0,00E+00	0,00E+00	0,00E+00	0,00E+00	0,00E+00	0,00E+00	0,00E+00	0,00E+00	0,00E+00	0,00E+00	0,00E+00	0,00E+00
			2,5	0,00E+00	0,00E+00	0,00E+00	0,00E+00	0,00E+00	0,00E+00	0,00E+00	0,00E+00	0,00E+00	0,00E+00	0,00E+00	0,00E+00	0,00E+00	0,00E+00	0,00E+00
			2,9	0,00E+00	0,00E+00	0,00E+00	0,00E+00	0,00E+00	0,00E+00	0,00E+00	0,00E+00	0,00E+00	0,00E+00	0,00E+00	0,00E+00	0,00E+00	0,00E+00	0,00E+00
		heteroaggregates in sediment	1,5	0,00E+00	0,00E+00	0,00E+00	0,00E+00	0,00E+00	0,00E+00	0,00E+00	0,00E+00	0,00E+00	0,00E+00	0,00E+00	0,00E+00	0,00E+00	0,00E+00	0,00E+00
			2	0,00E+00	0,00E+00	0,00E+00	0,00E+00	0,00E+00	0,00E+00	0,00E+00	0,00E+00	0,00E+00	0,00E+00	0,00E+00	0,00E+00	0,00E+00	0,00E+00	0,00E+00
			2,5	0,00E+00	0,00E+00	0,00E+00	0,00E+00	0,00E+00	0,00E+00	0,00E+00	0,00E+00	0,00E+00	0,00E+00	0,00E+00	0,00E+00	0,00E+00	0,00E+00	0,00E+00
			2,9	0,00E+00	0,00E+00	0,00E+00	0,00E+00	0,00E+00	0,00E+00	0,00E+00	0,00E+00	0,00E+00	0,00E+00	0,00E+00	0,00E+00	0,00E+00	0,00E+00	0,00E+00

alpha river	Month	Aggregation state	Df	Sizeclass														
				2,00E-07	3,12E-07	4,86E-07	7,58E-07	1,18E-06	1,84E-06	2,87E-06	4,47E-06	6,97E-06	1,09E-05	1,69E-05	2,64E-05	4,12E-05	6,42E-05	1,00E-04
	January	homoaggregates in water	1,5	0	0	0	0	0	0	0	0	0	0	0	0	0	0	0
			2	0	0	0	0	0	0	0	0	0	0	0	0	0	0	0
			2,5	0	0	0	0	0	0	0	0	0	0	0	0	0	0	0
			2,9	0	0	0	0	0	0	0	0	0	0	0	0	0	0	0
		homoaggregates in sediment	1,5	0	0	0	0	0	0	0	0	0	0	0	0	0	0	0
			2	0	0	0	0	0	0	0	0	0	0	0	0	0	0	0
			2,5	0	0	0	0	0	0	0	0	0	0	0	0	0	0	0
			2,9	0	0	0	0	0	0	0	0	0	0	0	0	0	0	0
				Sizeclass														
				1,00E-06	1,39E-06	1,93E-06	2,69E-06	3,74E-06	5,19E-06	7,22E-06	1,00E-05	1,40E-05	1,94E-05	2,70E-05	3,75E-05	5,21E-05	7,24E-05	1,00E-04
		heteroaggregates in water	1,5	0	0	0	0	0	0	0	0	0	0	0	0	0	0	0
			2	0	0	0	0	0	0	0	0	0	0	0	0	0	0	0
			2,5	0	0	0	0	0	0	0	0	0	0	0	0	0	0	0
			2,9	0	0	0	0	0	0	0	0	0	0	0	0	0	0	0
		heteroaggregates in sediment	1,5	0	0	0	0	0	0	0	0	0	0	0	0	0	0	0
			2	0	0	0	0	0	0	0	0	0	0	0	0	0	0	0
			2,5	0	0	0	0	0	0	0	0	0	0	0	0	0	0	0
			2,9	0	0	0	0	0	0	0	0	0	0	0	0	0	0	0
0,1				0														
				0,00E+00	3,12E-07	4,86E-07	7,58E-07	1,18E-06	1,84E-06	2,87E-06	4,47E-06	6,97E-06	1,09E-05	1,69E-05	2,64E-05	4,12E-05	6,42E-05	1,00E-04
		homoaggregates in water	1,5	4,52E+14	9,53E+14	5,76E+14	9,60E+13	4,40E+12	5,53E+10	2,05E+08	3,53E+05	8,31E+02	1,94E+02	0,00E+00	0,00E+00	0,00E+00	0,00E+00	0,00E+00
			2	4,24E+14	8,94E+14	5,39E+14	8,95E+13	4,09E+12	5,10E+10	1,85E+08	3,03E+05	6,21E+02	8,57E+01	0,00E+00	0,00E+00	0,00E+00	0,00E+00	0,00E+00
			2,5	3,06E+14	6,42E+14	3,84E+14	6,29E+13	2,83E+12	3,41E+10	1,15E+08	1,54E+05	1,79E+02	3,49E+00	0,00E+00	0,00E+00	0,00E+00	0,00E+00	0,00E+00
			2,9	1,44E+14	3,01E+14	1,77E+14	2,86E+13	1,26E+12	1,45E+10	4,40E+07	4,77E+04	3,76E+01	6,31E-01	0,00E+00	0,00E+00	0,00E+00	0,00E+00	0,00E+00
		homoaggregates in sediment	1,5	3,36E+07	8,85E+07	6,68E+07	1,39E+07	7,95E+05	1,25E+04	5,78E+01	1,24E-01	3,65E-04	1,06E-04	0,00E+00	0,00E+00	0,00E+00	0,00E+00	0,00E+00
			2	1,99E+08	6,55E+08	6,17E+08	1,60E+08	1,14E+07	2,21E+05	1,25E+03	3,19E+00	1,02E-02	2,19E-03	0,00E+00	0,00E+00	0,00E+00	0,00E+00	0,00E+00
			2,5	9,11E+08	3,72E+09	4,33E+09	1,38E+09	1,21E+08	2,83E+06	1,85E+04	4,83E+01	1,09E-01	4,16E-03	0,00E+00	0,00E+00	0,00E+00	0,00E+00	0,00E+00
			2,9	1,88E+09	9,11E+09	1,24E+10	4,68E+09	4,78E+08	1,28E+07	9,03E+04	2,27E+02	4,16E-01	1,62E-02	0,00E+00	0,00E+00	0,00E+00	0,00E+00	0,00E+00
	March			Sizeclass														
				1,00E-06	1,39E-06	1,93E-06	2,69E-06	3,74E-06	5,19E-06	7,22E-06	1,00E-05	1,40E-05	1,94E-05	2,70E-05	3,75E-05	5,21E-05	7,24E-05	1,00E-04
		heteroaggregates in water	1,5	3,71E+06	1,78E+07	6,24E+07	1,65E+08	3,29E+08	4,94E+08	5,55E+08	4,65E+08	2,89E+08	1,33E+08	4,55E+07	1,16E+07	2,15E+06	2,96E+05	3,37E-02
			2	3,48E+06	1,67E+07	5,84E+07	1,55E+08	3,08E+08	4,63E+08	5,20E+08	4,36E+08	2,71E+08	1,25E+08	4,26E+07	1,08E+07	2,01E+06	2,77E+05	3,16E-02
			2,5	2,49E+06	1,20E+07	4,18E+07	1,11E+08	2,21E+08	3,32E+08	3,72E+08	3,13E+08	1,94E+08	8,94E+07	3,06E+07	7,77E+06	1,44E+06	1,99E+05	2,24E-02
			2,9	1,16E+06	5,58E+06	1,95E+07	5,16E+07	1,03E+08	1,55E+08	1,74E+08	1,46E+08	9,05E+07	4,17E+07	1,43E+07	3,63E+06	6,73E+05	9,28E+04	1,03E-02
		heteroaggregates in sediment	1,5	5,42E+02	3,38E+03	1,50E+04	5,54E+04	1,82E+05	6,13E+05	9,42E+05	1,13E+06	1,28E+06	1,70E+06	6,70E+05	2,65E+05	9,54E+04	4,67E+04	6,51E-02
			2	5,20E+02	3,29E+03	1,48E+04	5,44E+04	1,77E+05	5,86E+05	9,00E+05	1,08E+06	1,22E+06	1,60E+06	6,32E+05	2,49E+05	8,97E+04	4,38E+04	6,09E-02
			2,5	4,24E+02	3,02E+03	1,53E+04	6,10E+04	1,99E+05	5,83E+05	9,54E+05	1,20E+06	1,28E+06	1,42E+06	6,11E+05	2,42E+05	8,26E+04	3,51E+04	4,33E-02
			2,9	2,95E+02	2,90E+03	1,99E+04	1,01E+05	3,75E+05	1,05E+06	2,20E+06	3,44E+06	3,97E+06	3,39E+06	2,15E+06	1,01E+06	3,49E+05	9,02E+04	2,20E-02

alpha river	Month	Aggregation state	Df	Sizeclass													
				2,00E-07	**3,12E-07**	**4,86E-07**	**7,58E-07**	**1,18E-06**	**1,84E-06**	**2,87E-06**	**4,47E-06**	**6,97E-06**	**1,09E-05**	**1,69E-05**	**2,64E-05**	**4,12E-05**	**6,42E-05**	**1,00E-04**
0,1	May	homoaggregates in water	**1,5**	1,19E+15	2,50E+15	1,47E+15	2,40E+14	1,07E+13	1,27E+11	4,06E+08	4,82E+05	3,89E+02	1,97E+00	0,00E+00	0,00E+00	0,00E+00	0,00E+00	0,00E+00
			2	1,12E+15	2,34E+15	1,38E+15	2,24E+14	1,00E+13	1,18E+11	3,73E+08	4,30E+05	3,19E+02	1,22E+00	0,00E+00	0,00E+00	0,00E+00	0,00E+00	0,00E+00
			2,5	8,04E+14	1,68E+15	9,85E+14	1,59E+14	7,02E+12	8,11E+10	2,47E+08	2,52E+05	1,33E+02	1,76E-01	0,00E+00	0,00E+00	0,00E+00	0,00E+00	0,00E+00
			2,9	3,76E+14	7,84E+14	4,58E+14	7,34E+13	3,20E+12	3,61E+10	1,03E+08	9,14E+04	3,61E+01	3,50E-02	0,00E+00	0,00E+00	0,00E+00	0,00E+00	0,00E+00
		homoaggregates in sediment	**1,5**	3,80E+08	9,96E+08	7,33E+08	1,49E+08	8,31E+06	1,23E+05	4,92E+02	7,28E-01	7,33E-04	4,64E-06	0,00E+00	0,00E+00	0,00E+00	0,00E+00	0,00E+00
			2	2,26E+09	7,37E+09	6,77E+09	1,72E+09	1,19E+08	2,20E+06	1,08E+04	1,94E+01	2,25E-02	1,34E-04	0,00E+00	0,00E+00	0,00E+00	0,00E+00	0,00E+00
			2,5	1,03E+10	4,17E+10	4,76E+10	1,50E+10	1,29E+09	2,89E+07	1,71E+05	3,41E+02	3,50E-01	8,99E-04	0,00E+00	0,00E+00	0,00E+00	0,00E+00	0,00E+00
			2,9	2,10E+10	1,02E+11	1,38E+11	5,15E+10	5,21E+09	1,37E+08	9,09E+05	1,87E+03	1,72E+00	3,87E-03	0,00E+00	0,00E+00	0,00E+00	0,00E+00	0,00E+00
				Sizeclass														
				1,00E-06	**1,39E-06**	**1,93E-06**	**2,69E-06**	**3,74E-06**	**5,19E-06**	**7,22E-06**	**1,00E-05**	**1,40E-05**	**1,94E-05**	**2,70E-05**	**3,75E-05**	**5,21E-05**	**7,24E-05**	**1,00E-04**
		heteroaggregates in water	**1,5**	6,01E+07	2,89E+08	1,01E+09	2,67E+09	5,33E+09	8,02E+09	8,99E+09	7,55E+09	4,68E+09	2,16E+09	7,38E+08	1,88E+08	3,48E+07	4,80E+06	5,37E-01
			2	5,64E+07	2,71E+08	9,46E+08	2,50E+09	4,99E+09	7,51E+09	8,43E+09	7,07E+09	4,39E+09	2,02E+09	6,92E+08	1,76E+08	3,27E+07	4,50E+06	5,02E-01
			2,5	4,04E+07	1,94E+08	6,77E+08	1,79E+09	3,58E+09	5,38E+09	6,04E+09	5,07E+09	3,14E+09	1,45E+09	4,95E+08	1,26E+08	2,34E+07	3,22E+06	3,58E-01
			2,9	1,88E+07	9,03E+07	3,16E+08	8,36E+08	1,67E+09	2,51E+09	2,81E+09	2,36E+09	1,47E+09	6,76E+08	2,31E+08	5,87E+07	1,09E+07	1,50E+06	1,66E-01
		heteroaggregates in sediment	**1,5**	3,77E+04	2,35E+05	1,05E+06	3,85E+06	1,27E+07	4,26E+07	6,55E+07	7,90E+07	8,94E+07	1,18E+08	4,67E+07	1,84E+07	6,64E+06	3,25E+06	4,45E+00
			2	3,61E+04	2,28E+05	1,03E+06	3,78E+06	1,23E+07	4,08E+07	6,27E+07	7,54E+07	8,48E+07	1,11E+08	4,40E+07	1,74E+07	6,25E+06	3,05E+06	4,16E+00
			2,5	2,95E+04	2,10E+05	1,06E+06	4,24E+06	1,38E+07	4,06E+07	6,64E+07	8,34E+07	8,93E+07	9,91E+07	4,25E+07	1,69E+07	5,75E+06	2,44E+06	2,97E+00
			2,9	2,05E+04	2,02E+05	1,39E+06	6,99E+06	2,61E+07	7,27E+07	1,53E+08	2,40E+08	2,76E+08	2,36E+08	1,50E+08	7,05E+07	2,42E+07	6,28E+06	1,52E+00
	August			**Sizeclass**														
				2,00E-07	**3,12E-07**	**4,86E-07**	**7,58E-07**	**1,18E-06**	**1,84E-06**	**2,87E-06**	**4,47E-06**	**6,97E-06**	**1,09E-05**	**1,69E-05**	**2,64E-05**	**4,12E-05**	**6,42E-05**	**1,00E-04**
		homoaggregates in water	**1,5**	6,41E+14	1,34E+15	8,07E+14	1,33E+14	6,03E+12	7,35E+10	2,53E+08	3,56E+05	4,66E+02	1,26E+01	0,00E+00	0,00E+00	0,00E+00	0,00E+00	0,00E+00
			2	6,00E+14	1,26E+15	7,53E+14	1,24E+14	5,63E+12	6,81E+10	2,31E+08	3,13E+05	3,66E+02	6,75E+00	0,00E+00	0,00E+00	0,00E+00	0,00E+00	0,00E+00
			2,5	4,32E+14	9,04E+14	5,38E+14	8,75E+13	3,91E+12	4,63E+10	1,47E+08	1,71E+05	1,30E+02	5,82E-01	0,00E+00	0,00E+00	0,00E+00	0,00E+00	0,00E+00
			2,9	2,03E+14	4,22E+14	2,49E+14	4,00E+13	1,75E+12	2,00E+10	5,91E+07	5,78E+04	3,35E+01	1,62E-01	0,00E+00	0,00E+00	0,00E+00	0,00E+00	0,00E+00
		homoaggregates in sediment	**1,5**	8,16E+07	2,14E+08	1,60E+08	3,30E+07	1,87E+06	2,84E+04	1,22E+02	2,15E-01	3,50E-04	1,19E-05	0,00E+00	0,00E+00	0,00E+00	0,00E+00	0,00E+00
			2	4,84E+08	1,58E+09	1,47E+09	3,80E+08	2,68E+07	5,05E+05	2,67E+03	5,63E+00	1,03E-02	2,96E-04	0,00E+00	0,00E+00	0,00E+00	0,00E+00	0,00E+00
			2,5	2,20E+09	8,96E+09	1,04E+10	3,29E+09	2,86E+08	6,58E+06	4,08E+04	9,21E+01	1,37E-01	1,19E-03	0,00E+00	0,00E+00	0,00E+00	0,00E+00	0,00E+00
			2,9	4,53E+09	2,19E+10	2,99E+10	1,12E+10	1,14E+09	3,03E+07	2,08E+05	4,72E+02	6,35E-01	7,14E-03	0,00E+00	0,00E+00	0,00E+00	0,00E+00	0,00E+00
				Sizeclass														
				1,00E-06	**1,39E-06**	**1,93E-06**	**2,69E-06**	**3,74E-06**	**5,19E-06**	**7,22E-06**	**1,00E-05**	**1,40E-05**	**1,94E-05**	**2,70E-05**	**3,75E-05**	**5,21E-05**	**7,24E-05**	**1,00E-04**
		heteroaggregates in water	**1,5**	1,29E+07	6,21E+07	2,17E+08	5,75E+08	1,15E+09	1,72E+09	1,93E+09	1,62E+09	1,01E+09	4,64E+08	1,59E+08	4,03E+07	7,49E+06	1,03E+06	1,17E-01
			2	1,21E+07	5,82E+07	2,03E+08	5,38E+08	1,07E+09	1,61E+09	1,81E+09	1,52E+09	9,42E+08	4,35E+08	1,48E+08	3,78E+07	7,01E+06	9,66E+05	1,09E-01
			2,5	8,67E+06	4,16E+07	1,45E+08	3,85E+08	7,68E+08	1,15E+09	1,30E+09	1,09E+09	6,74E+08	3,11E+08	1,06E+08	2,70E+07	5,02E+06	6,92E+05	7,75E-02
			2,9	4,04E+06	1,94E+07	6,77E+07	1,79E+08	3,58E+08	5,38E+08	6,04E+08	5,07E+08	3,14E+08	1,45E+08	4,95E+07	1,26E+07	2,34E+06	3,22E+05	3,58E-02
		heteroaggregates in sediment	**1,5**	3,23E+03	2,02E+04	8,97E+04	3,30E+05	1,09E+06	3,66E+06	5,62E+06	6,77E+06	7,66E+06	1,01E+07	4,00E+06	1,58E+06	5,69E+05	2,79E+05	3,86E-01
			2	3,10E+03	1,96E+04	8,80E+04	3,24E+05	1,05E+06	3,49E+06	5,37E+06	6,45E+06	7,26E+06	9,54E+06	3,77E+06	1,49E+06	5,35E+05	2,61E+05	3,60E-01
			2,5	2,53E+03	1,80E+04	9,10E+04	3,63E+05	1,18E+06	3,47E+06	5,68E+06	7,13E+06	7,64E+06	8,48E+06	3,64E+06	1,44E+06	4,92E+05	2,09E+05	2,57E-01
			2,9	1,76E+03	1,73E+04	1,19E+05	5,98E+05	2,23E+06	6,22E+06	1,31E+07	2,05E+07	2,36E+07	2,02E+07	1,28E+07	6,02E+06	2,07E+06	5,37E+05	1,31E-01

alpha river	Month	Aggregation state	Df	Sizeclass													
				2,00E-07	**3,12E-07**	**4,86E-07**	**7,58E-07**	**1,18E-06**	**1,84E-06**	**2,87E-06**	**4,47E-06**	**6,97E-06**	**1,09E-05**	**1,69E-05**	**2,64E-05**	**4,12E-05**	**6,42E-05**	**1,00E-04**
0,1	November			Sizeclass														
				2,00E-07	3,12E-07	4,86E-07	7,58E-07	1,18E-06	1,84E-06	2,87E-06	4,47E-06	6,97E-06	1,09E-05	1,69E-05	2,64E-05	4,12E-05	6,42E-05	1,00E-04
		homoaggregates in water	**1,5**	0,00E+00	0,00E+00	0,00E+00	0,00E+00	0,00E+00	0,00E+00	0,00E+00	0,00E+00	0,00E+00	0,00E+00	0,00E+00	0,00E+00	0,00E+00	0,00E+00	1,67E+14
			2	0,00E+00	0,00E+00	0,00E+00	0,00E+00	0,00E+00	0,00E+00	0,00E+00	0,00E+00	0,00E+00	0,00E+00	0,00E+00	0,00E+00	0,00E+00	0,00E+00	1,56E+14
			2,5	0,00E+00	0,00E+00	0,00E+00	0,00E+00	0,00E+00	0,00E+00	0,00E+00	0,00E+00	0,00E+00	0,00E+00	0,00E+00	0,00E+00	0,00E+00	0,00E+00	1,02E+14
			2,9	2,38E+12	4,92E+12	2,85E+12	4,50E+11	1,90E+10	2,10E+08	6,37E+05	8,48E+02	1,99E+00	1,03E+01	5,53E+00	4,65E+00	1,61E-03	0,00E+00	6,04E+13
		homoaggregates in sediment	**1,5**	0,00E+00	0,00E+00	0,00E+00	0,00E+00	0,00E+00	0,00E+00	0,00E+00	0,00E+00	0,00E+00	0,00E+00	0,00E+00	0,00E+00	0,00E+00	0,00E+00	3,26E+08
			2	0,00E+00	0,00E+00	0,00E+00	0,00E+00	0,00E+00	0,00E+00	0,00E+00	0,00E+00	0,00E+00	0,00E+00	0,00E+00	0,00E+00	0,00E+00	0,00E+00	4,31E+10
			2,5	0,00E+00	0,00E+00	0,00E+00	0,00E+00	0,00E+00	0,00E+00	0,00E+00	0,00E+00	0,00E+00	0,00E+00	0,00E+00	0,00E+00	0,00E+00	0,00E+00	4,00E+12
			2,9	3,64E+07	1,75E+08	2,35E+08	8,63E+07	8,49E+06	2,18E+05	1,53E+03	4,74E+00	2,59E-02	3,12E-01	3,88E-01	7,59E-01	6,13E-04	0,00E+00	1,24E+14
				Sizeclass														
				1,00E-06	**1,39E-06**	**1,93E-06**	**2,69E-06**	**3,74E-06**	**5,19E-06**	**7,22E-06**	**1,00E-05**	**1,40E-05**	**1,94E-05**	**2,70E-05**	**3,75E-05**	**5,21E-05**	**7,24E-05**	**1,00E-04**
		heteroaggregates in water	**1,5**	0,00E+00	0,00E+00	0,00E+00	0,00E+00	0,00E+00	0,00E+00	0,00E+00	0,00E+00	0,00E+00	0,00E+00	0,00E+00	0,00E+00	0,00E+00	0,00E+00	0,00E+00
			2	0,00E+00	0,00E+00	0,00E+00	0,00E+00	0,00E+00	0,00E+00	0,00E+00	0,00E+00	0,00E+00	0,00E+00	0,00E+00	0,00E+00	0,00E+00	0,00E+00	0,00E+00
			2,5	0,00E+00	0,00E+00	0,00E+00	0,00E+00	0,00E+00	0,00E+00	0,00E+00	0,00E+00	0,00E+00	0,00E+00	0,00E+00	0,00E+00	0,00E+00	0,00E+00	0,00E+00
			2,9	8,89E+04	4,27E+05	1,49E+06	3,95E+06	7,88E+06	1,19E+07	1,33E+07	1,12E+07	6,93E+06	3,20E+06	1,09E+06	2,78E+05	5,16E+04	7,11E+03	7,77E-04
		heteroaggregates in sediment	**1,5**	0,00E+00	0,00E+00	0,00E+00	0,00E+00	0,00E+00	0,00E+00	0,00E+00	0,00E+00	0,00E+00	0,00E+00	0,00E+00	0,00E+00	0,00E+00	0,00E+00	0,00E+00
			2	0,00E+00	0,00E+00	0,00E+00	0,00E+00	0,00E+00	0,00E+00	0,00E+00	0,00E+00	0,00E+00	0,00E+00	0,00E+00	0,00E+00	0,00E+00	0,00E+00	0,00E+00
			2,5	0,00E+00	0,00E+00	0,00E+00	0,00E+00	0,00E+00	0,00E+00	0,00E+00	0,00E+00	0,00E+00	0,00E+00	0,00E+00	0,00E+00	0,00E+00	0,00E+00	0,00E+00
			2,9	2,65E+01	2,61E+02	1,79E+03	9,03E+03	3,37E+04	9,40E+04	1,98E+05	3,10E+05	3,57E+05	3,05E+05	1,93E+05	9,11E+04	3,14E+04	8,11E+03	1,95E-03

Appendix XI: Number concentrations of aggregates, obtained at point 5, with alpha (NN) = 1

alpha river	Month	Aggregation state	Df	Sizeclass													
				2,00E-07	3,12E-07	4,86E-07	7,58E-07	1,18E-06	1,84E-06	2,87E-06	4,47E-06	6,97E-06	1,09E-05	1,69E-05	2,64E-05	4,12E-05	6,42E-05	1,00E-04
0,001	January	homoaggregates in water	1,5	0,00E+00	0,00E+00	0,00E+00	0,00E+00	0,00E+00	0,00E+00	0,00E+00	0,00E+00	0,00E+00	0,00E+00	0,00E+00	0,00E+00	0,00E+00	0,00E+00	0,00E+00
			2,0	0,00E+00	0,00E+00	0,00E+00	0,00E+00	0,00E+00	0,00E+00	0,00E+00	0,00E+00	0,00E+00	0,00E+00	0,00E+00	0,00E+00	0,00E+00	0,00E+00	0,00E+00
			2,5	0,00E+00	0,00E+00	0,00E+00	0,00E+00	0,00E+00	0,00E+00	0,00E+00	0,00E+00	0,00E+00	0,00E+00	0,00E+00	0,00E+00	0,00E+00	0,00E+00	0,00E+00
			2,9	0,00E+00	0,00E+00	0,00E+00	0,00E+00	0,00E+00	0,00E+00	0,00E+00	0,00E+00	0,00E+00	0,00E+00	0,00E+00	0,00E+00	0,00E+00	0,00E+00	0,00E+00
		homoaggregates in sediment	1,5	0,00E+00	0,00E+00	0,00E+00	0,00E+00	0,00E+00	0,00E+00	0,00E+00	0,00E+00	0,00E+00	0,00E+00	0,00E+00	0,00E+00	0,00E+00	0,00E+00	0,00E+00
			2,0	0,00E+00	0,00E+00	0,00E+00	0,00E+00	0,00E+00	0,00E+00	0,00E+00	0,00E+00	0,00E+00	0,00E+00	0,00E+00	0,00E+00	0,00E+00	0,00E+00	0,00E+00
			2,5	0,00E+00	0,00E+00	0,00E+00	0,00E+00	0,00E+00	0,00E+00	0,00E+00	0,00E+00	0,00E+00	0,00E+00	0,00E+00	0,00E+00	0,00E+00	0,00E+00	0,00E+00
			2,9	0,00E+00	0,00E+00	0,00E+00	0,00E+00	0,00E+00	0,00E+00	0,00E+00	0,00E+00	0,00E+00	0,00E+00	0,00E+00	0,00E+00	0,00E+00	0,00E+00	0,00E+00
				Sizeclass														
				1,00E-06	1,39E-06	1,93E-06	2,69E-06	3,74E-06	5,19E-06	7,22E-06	1,00E-05	1,40E-05	1,94E-05	2,70E-05	3,75E-05	5,21E-05	7,24E-05	1,00E-04
		heteroaggregates in water	1,5	0,00E+00	0,00E+00	0,00E+00	0,00E+00	0,00E+00	0,00E+00	0,00E+00	0,00E+00	0,00E+00	0,00E+00	0,00E+00	0,00E+00	0,00E+00	0,00E+00	0,00E+00
			2,0	0,00E+00	0,00E+00	0,00E+00	0,00E+00	0,00E+00	0,00E+00	0,00E+00	0,00E+00	0,00E+00	0,00E+00	0,00E+00	0,00E+00	0,00E+00	0,00E+00	0,00E+00
			2,5	0,00E+00	0,00E+00	0,00E+00	0,00E+00	0,00E+00	0,00E+00	0,00E+00	0,00E+00	0,00E+00	0,00E+00	0,00E+00	0,00E+00	0,00E+00	0,00E+00	0,00E+00
			2,9	0,00E+00	0,00E+00	0,00E+00	0,00E+00	0,00E+00	0,00E+00	0,00E+00	0,00E+00	0,00E+00	0,00E+00	0,00E+00	0,00E+00	0,00E+00	0,00E+00	0,00E+00
		heteroaggregates in sediment	1,5	0,00E+00	0,00E+00	0,00E+00	0,00E+00	0,00E+00	0,00E+00	0,00E+00	0,00E+00	0,00E+00	0,00E+00	0,00E+00	0,00E+00	0,00E+00	0,00E+00	0,00E+00
			2,0	0,00E+00	0,00E+00	0,00E+00	0,00E+00	0,00E+00	0,00E+00	0,00E+00	0,00E+00	0,00E+00	0,00E+00	0,00E+00	0,00E+00	0,00E+00	0,00E+00	0,00E+00
			2,5	0,00E+00	0,00E+00	0,00E+00	0,00E+00	0,00E+00	0,00E+00	0,00E+00	0,00E+00	0,00E+00	0,00E+00	0,00E+00	0,00E+00	0,00E+00	0,00E+00	0,00E+00
			2,9	0,00E+00	0,00E+00	0,00E+00	0,00E+00	0,00E+00	0,00E+00	0,00E+00	0,00E+00	0,00E+00	0,00E+00	0,00E+00	0,00E+00	0,00E+00	0,00E+00	0,00E+00
	March			Sizeclass														
				2,00E-07	3,12E-07	4,86E-07	7,58E-07	1,18E-06	1,84E-06	2,87E-06	4,47E-06	6,97E-06	1,09E-05	1,69E-05	2,64E-05	4,12E-05	6,42E-05	1,00E-04
		homoaggregates in water	1,5	9,42E+05	1,89E+06	1,06E+06	1,54E+05	5,71E+03	5,23E+01	1,26E-01	1,34E-04	0,00E+00	2,95E-06	0,00E+00	0,00E+00	0,00E+00	0,00E+00	1,85E+13
			2,0	2,05E+10	4,24E+10	2,50E+10	3,96E+09	1,67E+08	1,89E+06	6,27E+03	1,12E+01	6,52E-02	2,57E+00	6,84E-01	1,46E-01	4,90E-05	0,00E+00	1,74E+13
			2,5	3,00E+14	6,37E+14	3,91E+14	6,59E+13	3,08E+12	4,04E+10	1,67E+08	3,81E+05	2,23E+03	1,80E+04	1,20E-03	0,00E+00	0,00E+00	0,00E+00	0,00E+00
			2,9	1,43E+14	3,00E+14	1,79E+14	2,93E+13	1,31E+12	1,59E+10	5,46E+07	8,67E+04	2,63E+02	1,75E+03	0,00E+00	0,00E+00	0,00E+00	0,00E+00	0,00E+00
		homoaggregates in sediment	1,5	7,00E-02	1,75E-01	1,22E-01	2,23E-02	1,03E-03	1,18E-05	0,00E+00	0,00E+00	0,00E+00	0,00E+00	0,00E+00	0,00E+00	0,00E+00	0,00E+00	3,08E+07
			2,0	9,65E+03	3,11E+04	2,86E+04	7,05E+03	4,64E+02	8,17E+00	4,23E-02	1,18E-04	1,07E-06	6,56E-05	2,72E-05	9,09E-06	0,00E+00	0,00E+00	4,09E+09
			2,5	8,91E+08	3,69E+09	4,40E+09	1,44E+09	1,31E+08	3,35E+06	2,70E+04	1,20E+02	1,37E+00	2,15E+01	2,79E-06	0,00E+00	0,00E+00	0,00E+00	0,00E+00
			2,9	1,86E+09	9,06E+09	1,26E+10	4,79E+09	4,98E+08	1,40E+07	1,12E+05	4,14E+02	2,92E+00	4,52E+01	0,00E+00	0,00E+00	0,00E+00	0,00E+00	0,00E+00
				Sizeclass														
				1,00E-06	1,39E-06	1,93E-06	2,69E-06	3,74E-06	5,19E-06	7,22E-06	1,00E-05	1,40E-05	1,94E-05	2,70E-05	3,75E-05	5,21E-05	7,24E-05	1,00E-04
		heteroaggregates in water	1,5	7,16E-05	3,43E-04	1,20E-03	3,19E-03	6,36E-03	9,58E-03	1,08E-02	9,03E-03	5,60E-03	2,59E-03	8,83E-04	2,25E-04	4,17E-05	5,75E-06	0,00E+00
			2,0	1,64E+00	7,86E+00	2,75E+01	7,28E+01	1,45E+02	2,18E+02	2,45E+02	2,06E+02	1,28E+02	5,88E+01	2,01E+01	5,11E+00	9,49E-01	1,31E-01	1,44E-08
			2,5	2,50E+04	1,20E+05	4,19E+05	1,11E+06	2,21E+06	3,32E+06	3,72E+06	3,12E+06	1,94E+06	8,93E+05	3,05E+05	7,76E+04	1,44E+04	1,99E+03	2,29E-04
			2,9	1,16E+04	5,58E+04	1,95E+05	5,16E+05	1,03E+06	1,55E+06	1,74E+06	1,46E+06	9,04E+05	4,17E+05	1,42E+05	3,62E+04	6,73E+03	9,27E+02	1,04E-04
		heteroaggregates in sediment	1,5	0,00E+00	0,00E+00	0,00E+00	1,07E-06	3,52E-06	1,19E-05	1,83E-05	2,20E-05	2,49E-05	3,30E-05	1,30E-05	5,14E-06	1,85E-06	9,07E-07	0,00E+00
			2,0	2,44E-04	1,54E-03	6,94E-03	2,56E-02	8,33E-02	2,76E-01	4,24E-01	5,10E-01	5,74E-01	7,54E-01	2,98E-01	1,18E-01	4,23E-02	2,07E-02	0,00E+00
			2,5	4,25E+00	3,02E+01	1,53E+02	6,10E+02	1,99E+03	5,83E+03	9,53E+03	1,20E+04	1,28E+04	1,42E+04	6,11E+03	2,42E+03	8,25E+02	3,50E+02	4,43E-04
			2,9	2,95E+00	2,91E+01	1,99E+02	1,01E+03	3,75E+03	1,05E+04	2,20E+04	3,44E+04	3,96E+04	3,39E+04	2,15E+04	1,01E+04	3,48E+03	9,01E+02	2,22E-04

alpha river	Month	Aggregation state	Df	Sizeclass													
				2,00E-07	3,12E-07	4,86E-07	7,58E-07	1,18E-06	1,84E-06	2,87E-06	4,47E-06	6,97E-06	1,09E-05	1,69E-05	2,64E-05	4,12E-05	6,42E-05	1,00E-04
0,001	May	homoaggregates in water	1,5	1,17E+15	2,48E+15	1,50E+15	2,48E+14	1,14E+13	1,44E+11	5,47E+08	1,00E+06	2,91E+03	1,47E+03	1,16E-02	0,00E+00	0,00E+00	0,00E+00	0,00E+00
			2,0	1,10E+15	2,33E+15	1,40E+15	2,32E+14	1,06E+13	1,33E+11	4,94E+08	8,59E+05	2,14E+03	6,05E+02	0,00E+00	0,00E+00	0,00E+00	0,00E+00	0,00E+00
			2,5	7,96E+14	1,67E+15	9,93E+14	1,63E+14	7,34E+12	8,91E+10	3,03E+08	4,26E+05	5,71E+02	1,84E+01	0,00E+00	0,00E+00	0,00E+00	0,00E+00	0,00E+00
			2,9	3,74E+14	7,83E+14	4,60E+14	7,42E+13	3,27E+12	3,78E+10	1,16E+08	1,28E+05	1,07E+02	2,09E+00	0,00E+00	0,00E+00	0,00E+00	0,00E+00	0,00E+00
		homoaggregates in sediment	1,5	3,75E+08	9,90E+08	7,46E+08	1,54E+08	8,87E+06	1,40E+05	6,62E+02	1,51E+00	5,48E-03	3,45E-03	0,00E+00	0,00E+00	0,00E+00	0,00E+00	0,00E+00
			2,0	2,23E+09	7,32E+09	6,85E+09	1,77E+09	1,27E+08	2,48E+06	1,43E+04	3,88E+01	1,50E-01	6,64E-02	0,00E+00	0,00E+00	0,00E+00	0,00E+00	0,00E+00
			2,5	1,02E+10	4,15E+10	4,81E+10	1,54E+10	1,34E+09	3,18E+07	2,11E+05	5,76E+02	1,50E+00	9,40E-02	0,00E+00	0,00E+00	0,00E+00	0,00E+00	0,00E+00
			2,9	2,09E+10	1,02E+11	1,39E+11	5,20E+10	5,33E+09	1,43E+08	1,02E+06	2,61E+03	5,10E+00	2,31E-01	0,00E+00	0,00E+00	0,00E+00	0,00E+00	0,00E+00
				Sizeclass														
				1,00E-06	1,39E-06	1,93E-06	2,69E-06	3,74E-06	5,19E-06	7,22E-06	1,00E-05	1,40E-05	1,94E-05	2,70E-05	3,75E-05	5,21E-05	7,24E-05	1,00E-04
		heteroaggregates in water	1,5	6,03E+05	2,89E+06	1,01E+07	2,68E+07	5,34E+07	8,03E+07	9,00E+07	7,55E+07	4,69E+07	2,16E+07	7,38E+06	1,88E+06	3,49E+05	4,81E+04	5,47E-03
			2,0	5,64E+05	2,71E+06	9,46E+06	2,50E+07	4,99E+07	7,51E+07	8,42E+07	7,07E+07	4,38E+07	2,02E+07	6,91E+06	1,76E+06	3,26E+05	4,50E+04	5,10E-03
			2,5	4,04E+05	1,94E+06	6,78E+06	1,79E+07	3,58E+07	5,38E+07	6,03E+07	5,06E+07	3,14E+07	1,45E+07	4,95E+06	1,26E+06	2,34E+05	3,22E+04	3,62E-03
			2,9	1,88E+05	9,03E+05	3,16E+06	8,36E+06	1,67E+07	2,51E+07	2,81E+07	2,36E+07	1,47E+07	6,76E+06	2,31E+06	5,87E+05	1,09E+05	1,50E+04	1,67E-03
		heteroaggregates in sediment	1,5	3,78E+02	2,36E+03	1,05E+04	3,86E+04	1,27E+05	4,27E+05	6,56E+05	7,90E+05	8,95E+05	1,18E+06	4,67E+05	1,85E+05	6,65E+04	3,26E+04	4,53E-02
			2,0	3,61E+02	2,29E+03	1,03E+04	3,78E+04	1,23E+05	4,08E+05	6,26E+05	7,53E+05	8,48E+05	1,11E+06	4,40E+05	1,73E+05	6,24E+04	3,05E+04	4,23E-02
			2,5	2,95E+02	2,10E+03	1,06E+04	4,24E+04	1,38E+05	4,06E+05	6,63E+05	8,33E+05	8,93E+05	9,91E+05	4,25E+05	1,69E+05	5,75E+04	2,44E+04	3,01E-02
			2,9	2,05E+02	2,02E+03	1,39E+04	6,99E+04	2,61E+05	7,27E+05	1,53E+06	2,40E+06	2,76E+06	2,36E+06	1,50E+06	7,05E+05	2,42E+05	6,27E+04	1,53E-02
	August			Sizeclass														
				2,00E-07	3,12E-07	4,86E-07	7,58E-07	1,18E-06	1,84E-06	2,87E-06	4,47E-06	6,97E-06	1,09E-05	1,69E-05	2,64E-05	4,12E-05	6,42E-05	1,00E-04
		homoaggregates in water	1,5	9,16E+11	1,91E+12	1,14E+12	1,83E+11	7,97E+09	9,23E+07	3,16E+05	5,29E+02	1,87E+00	6,22E+00	3,88E+00	4,22E+00	4,50E-02	0,00E+00	2,60E+13
			2,0	5,88E+14	1,25E+15	7,69E+14	1,31E+14	6,19E+12	8,19E+10	3,44E+08	7,97E+05	4,72E+03	3,35E+04	4,00E+04	2,38E+04	9,91E+02	1,67E-03	0,00E+00
			2,5	4,25E+14	9,01E+14	5,44E+14	9,10E+13	4,19E+12	5,29E+10	1,98E+08	3,50E+05	9,19E+02	3,57E+02	0,00E+00	0,00E+00	0,00E+00	0,00E+00	0,00E+00
			2,9	2,02E+14	4,22E+14	2,50E+14	4,10E+13	1,82E+12	2,15E+10	6,97E+07	9,35E+04	1,58E+02	8,47E+01	0,00E+00	0,00E+00	0,00E+00	0,00E+00	0,00E+00
		homoaggregates in sediment	1,5	1,17E+05	3,03E+05	2,25E+05	4,54E+04	2,47E+03	3,56E+01	1,52E-01	3,18E-04	1,41E-06	5,84E-06	4,54E-06	6,18E-06	0,00E+00	0,00E+00	7,40E+07
			2,0	4,74E+08	1,57E+09	1,51E+09	4,00E+08	2,94E+07	6,07E+05	3,97E+03	1,44E+01	1,33E-01	1,46E+00	2,73E+00	2,53E+00	1,64E-01	0,00E+00	0,00E+00
			2,5	2,17E+09	8,93E+09	1,05E+10	3,42E+09	3,06E+08	7,52E+06	5,47E+04	1,89E+02	9,64E-01	7,27E-01	0,00E+00	0,00E+00	0,00E+00	0,00E+00	0,00E+00
			2,9	4,50E+09	2,19E+10	3,01E+10	1,15E+10	1,18E+09	3,24E+07	2,45E+05	7,63E+02	3,00E+00	3,74E+00	0,00E+00	0,00E+00	0,00E+00	0,00E+00	0,00E+00
				Sizeclass														
				1,00E-06	1,39E-06	1,93E-06	2,69E-06	3,74E-06	5,19E-06	7,22E-06	1,00E-05	1,40E-05	1,94E-05	2,70E-05	3,75E-05	5,21E-05	7,24E-05	1,00E-04
		heteroaggregates in water	1,5	1,83E+02	8,79E+02	3,07E+03	8,13E+03	1,62E+04	2,44E+04	2,74E+04	2,30E+04	1,42E+04	6,57E+03	2,25E+03	5,71E+02	1,06E+02	1,46E+01	1,63E-06
			2,0	1,21E+05	5,84E+05	2,04E+06	5,39E+06	1,07E+07	1,62E+07	1,81E+07	1,52E+07	9,43E+06	4,35E+06	1,49E+06	3,78E+05	7,01E+04	9,67E+03	1,12E-03
			2,5	8,68E+04	4,17E+05	1,46E+06	3,86E+06	7,69E+06	1,16E+07	1,30E+07	1,09E+07	6,75E+06	3,11E+06	1,06E+06	2,70E+05	5,02E+04	6,92E+03	7,90E-04
			2,9	4,05E+04	1,94E+05	6,79E+05	1,80E+06	3,58E+06	5,39E+06	6,05E+06	5,08E+06	3,15E+06	1,45E+06	4,96E+05	1,26E+05	2,34E+04	3,23E+03	3,62E-04
		heteroaggregates in sediment	1,5	4,58E-02	2,85E-01	1,27E+00	4,67E+00	1,54E+01	5,17E+01	7,95E+01	9,58E+01	1,08E+02	1,43E+02	5,66E+01	2,24E+01	8,06E+00	3,95E+00	5,38E-06
			2,0	3,11E+01	1,96E+02	8,82E+02	3,25E+03	1,06E+04	3,50E+04	5,37E+04	6,46E+04	7,27E+04	9,54E+04	3,77E+04	1,49E+04	5,35E+03	2,61E+03	3,70E-03
			2,5	2,53E+01	1,80E+02	9,12E+02	3,64E+03	1,18E+04	3,48E+04	5,68E+04	7,14E+04	7,65E+04	8,48E+04	3,64E+04	1,44E+04	4,92E+03	2,09E+03	2,61E-03
			2,9	1,76E+01	1,73E+02	1,19E+03	5,99E+03	2,24E+04	6,23E+04	1,31E+05	2,05E+05	2,36E+05	2,02E+05	1,28E+05	6,03E+04	2,08E+04	5,37E+03	1,32E-03

alpha river	Month	Aggregation state	Df	Sizeclass													
				2,00E-07	3,12E-07	4,86E-07	7,58E-07	1,18E-06	1,84E-06	2,87E-06	4,47E-06	6,97E-06	1,09E-05	1,69E-05	2,64E-05	4,12E-05	6,42E-05	1,00E-04
0,001	November	homoaggregates in water	1,5	0,00E+00	0,00E+00	0,00E+00	0,00E+00	0,00E+00	0,00E+00	0,00E+00	0,00E+00	0,00E+00	0,00E+00	0,00E+00	0,00E+00	0,00E+00	0,00E+00	1,67E+14
			2,0	0,00E+00	0,00E+00	0,00E+00	0,00E+00	0,00E+00	0,00E+00	0,00E+00	0,00E+00	0,00E+00	0,00E+00	0,00E+00	0,00E+00	0,00E+00	0,00E+00	1,56E+14
			2,5	0,00E+00	0,00E+00	0,00E+00	0,00E+00	0,00E+00	0,00E+00	0,00E+00	0,00E+00	0,00E+00	0,00E+00	0,00E+00	0,00E+00	0,00E+00	0,00E+00	9,70E+13
			2,9	0,00E+00	0,00E+00	0,00E+00	0,00E+00	0,00E+00	0,00E+00	0,00E+00	0,00E+00	0,00E+00	0,00E+00	0,00E+00	0,00E+00	0,00E+00	0,00E+00	7,87E+10
		homoaggregates in sediment	1,5	0,00E+00	0,00E+00	0,00E+00	0,00E+00	0,00E+00	0,00E+00	0,00E+00	0,00E+00	0,00E+00	0,00E+00	0,00E+00	0,00E+00	0,00E+00	0,00E+00	3,26E+08
			2,0	0,00E+00	0,00E+00	0,00E+00	0,00E+00	0,00E+00	0,00E+00	0,00E+00	0,00E+00	0,00E+00	0,00E+00	0,00E+00	0,00E+00	0,00E+00	0,00E+00	4,31E+10
			2,5	0,00E+00	0,00E+00	0,00E+00	0,00E+00	0,00E+00	0,00E+00	0,00E+00	0,00E+00	0,00E+00	0,00E+00	0,00E+00	0,00E+00	0,00E+00	0,00E+00	3,79E+12
			2,9	0,00E+00	0,00E+00	0,00E+00	0,00E+00	0,00E+00	0,00E+00	0,00E+00	0,00E+00	0,00E+00	0,00E+00	0,00E+00	0,00E+00	0,00E+00	0,00E+00	1,61E+11
				Sizeclass														
				1,00E-06	1,39E-06	1,93E-06	2,69E-06	3,74E-06	5,19E-06	7,22E-06	1,00E-05	1,40E-05	1,94E-05	2,70E-05	3,75E-05	5,21E-05	7,24E-05	1,00E-04
		heteroaggregates in water	1,5	0,00E+00	0,00E+00	0,00E+00	0,00E+00	0,00E+00	0,00E+00	0,00E+00	0,00E+00	0,00E+00	0,00E+00	0,00E+00	0,00E+00	0,00E+00	0,00E+00	0,00E+00
			2,0	0,00E+00	0,00E+00	0,00E+00	0,00E+00	0,00E+00	0,00E+00	0,00E+00	0,00E+00	0,00E+00	0,00E+00	0,00E+00	0,00E+00	0,00E+00	0,00E+00	0,00E+00
			2,5	0,00E+00	0,00E+00	0,00E+00	0,00E+00	0,00E+00	0,00E+00	0,00E+00	0,00E+00	0,00E+00	0,00E+00	0,00E+00	0,00E+00	0,00E+00	0,00E+00	0,00E+00
			2,9	0,00E+00	0,00E+00	0,00E+00	0,00E+00	0,00E+00	0,00E+00	0,00E+00	0,00E+00	0,00E+00	0,00E+00	0,00E+00	0,00E+00	0,00E+00	0,00E+00	0,00E+00
		heteroaggregates in sediment	1,5	0,00E+00	0,00E+00	0,00E+00	0,00E+00	0,00E+00	0,00E+00	0,00E+00	0,00E+00	0,00E+00	0,00E+00	0,00E+00	0,00E+00	0,00E+00	0,00E+00	0,00E+00
			2,0	0,00E+00	0,00E+00	0,00E+00	0,00E+00	0,00E+00	0,00E+00	0,00E+00	0,00E+00	0,00E+00	0,00E+00	0,00E+00	0,00E+00	0,00E+00	0,00E+00	0,00E+00
			2,5	0,00E+00	0,00E+00	0,00E+00	0,00E+00	0,00E+00	0,00E+00	0,00E+00	0,00E+00	0,00E+00	0,00E+00	0,00E+00	0,00E+00	0,00E+00	0,00E+00	0,00E+00
			2,9	0,00E+00	0,00E+00	0,00E+00	0,00E+00	0,00E+00	0,00E+00	0,00E+00	0,00E+00	0,00E+00	0,00E+00	0,00E+00	0,00E+00	0,00E+00	0,00E+00	0,00E+00

alpha river	Month	Aggregation state	Df	Sizeclass														
				2,00E-07	3,12E-07	4,86E-07	7,58E-07	1,18E-06	1,84E-06	2,87E-06	4,47E-06	6,97E-06	1,09E-05	1,69E-05	2,64E-05	4,12E-05	6,42E-05	1,00E-04
0,01	January	homoaggregates in water	1,5	0	0	0	0	0	0	0	0	0	0	0	0	0	0	0
			2,0	0	0	0	0	0	0	0	0	0	0	0	0	0	0	0
			2,5	0	0	0	0	0	0	0	0	0	0	0	0	0	0	0
			2,9	0	0	0	0	0	0	0	0	0	0	0	0	0	0	0
		homoaggregates in sediment	1,5	0	0	0	0	0	0	0	0	0	0	0	0	0	0	0
			2,0	0	0	0	0	0	0	0	0	0	0	0	0	0	0	0
			2,5	0	0	0	0	0	0	0	0	0	0	0	0	0	0	0
			2,9	0	0	0	0	0	0	0	0	0	0	0	0	0	0	0
				Sizeclass														
				1,00E-06	1,39E-06	1,93E-06	2,69E-06	3,74E-06	5,19E-06	7,22E-06	1,00E-05	1,40E-05	1,94E-05	2,70E-05	3,75E-05	5,21E-05	7,24E-05	1,00E-04
		heteroaggregates in water	1,5	0	0	0	0	0	0	0	0	0	0	0	0	0	0	0
			2,0	0	0	0	0	0	0	0	0	0	0	0	0	0	0	0
			2,5	0	0	0	0	0	0	0	0	0	0	0	0	0	0	0
			2,9	0	0	0	0	0	0	0	0	0	0	0	0	0	0	0
		heteroaggregates in sediment	1,5	0	0	0	0	0	0	0	0	0	0	0	0	0	0	0
			2,0	0	0	0	0	0	0	0	0	0	0	0	0	0	0	0
			2,5	0	0	0	0	0	0	0	0	0	0	0	0	0	0	0
			2,9	0	0	0	0	0	0	0	0	0	0	0	0	0	0	0
	March			Sizeclass														
				2,00E-07	3,12E-07	4,86E-07	7,58E-07	1,18E-06	1,84E-06	2,87E-06	4,47E-06	6,97E-06	1,09E-05	1,69E-05	2,64E-05	4,12E-05	6,42E-05	1,00E-04
		homoaggregates in water	1,5	9,42E+05	1,89E+06	1,06E+06	1,54E+05	5,71E+03	5,23E+01	1,26E-01	1,34E-04	0,00E+00	2,95E-06	0,00E+00	0,00E+00	0,00E+00	0,00E+00	1,85E+13
			2,0	2,05E+10	4,24E+10	2,50E+10	3,96E+09	1,67E+08	1,89E+06	6,27E+03	1,12E+01	6,52E-02	2,57E+00	6,84E-01	1,46E-01	4,90E-05	0,00E+00	1,74E+13
			2,5	3,00E+14	6,37E+14	3,91E+14	6,59E+13	3,08E+12	4,04E+10	1,67E+08	3,81E+05	2,23E+03	1,80E+04	1,20E-03	0,00E+00	0,00E+00	0,00E+00	0,00E+00
			2,9	1,43E+14	3,00E+14	1,79E+14	2,93E+13	1,31E+12	1,59E+10	5,46E+07	8,67E+04	2,63E+02	1,75E+03	0,00E+00	0,00E+00	0,00E+00	0,00E+00	0,00E+00
		homoaggregates in sediment	1,5	7,00E-02	1,75E-01	1,22E-01	2,23E-02	1,03E-03	1,18E-05	0,00E+00	0,00E+00	0,00E+00	0,00E+00	0,00E+00	0,00E+00	0,00E+00	0,00E+00	3,08E+07
			2,0	9,65E+03	3,11E+04	2,86E+04	7,05E+03	4,64E+02	8,17E+00	4,23E-02	1,18E-04	1,07E-06	6,56E-05	2,72E-05	9,09E-06	0,00E+00	0,00E+00	4,09E+09
			2,5	8,91E+08	3,69E+09	4,40E+09	1,44E+09	1,31E+08	3,35E+06	2,70E+04	1,20E+02	1,37E+00	2,15E+01	2,79E-06	0,00E+00	0,00E+00	0,00E+00	0,00E+00
			2,9	1,86E+09	9,06E+09	1,26E+10	4,79E+09	4,98E+08	1,40E+07	1,12E+05	4,14E+02	2,92E+00	4,52E+01	0,00E+00	0,00E+00	0,00E+00	0,00E+00	0,00E+00
				Sizeclass														
				1,00E-06	1,39E-06	1,93E-06	2,69E-06	3,74E-06	5,19E-06	7,22E-06	1,00E-05	1,40E-05	1,94E-05	2,70E-05	3,75E-05	5,21E-05	7,24E-05	1,00E-04
		heteroaggregates in water	1,5	7,16E-04	3,43E-03	1,20E-02	3,19E-02	6,36E-02	9,58E-02	1,08E-01	9,03E-02	5,60E-02	2,59E-02	8,83E-03	2,25E-03	4,17E-04	5,75E-05	0,00E+00
			2,0	1,64E+01	7,86E+01	2,75E+02	7,28E+02	1,45E+03	2,18E+03	2,45E+03	2,06E+03	1,28E+03	5,88E+02	2,01E+02	5,11E+01	9,49E+00	1,31E+00	1,44E-07
			2,5	2,50E+05	1,20E+06	4,19E+06	1,11E+07	2,21E+07	3,32E+07	3,72E+07	3,12E+07	1,94E+07	8,93E+06	3,05E+06	7,76E+05	1,44E+05	1,99E+04	2,29E-03
			2,9	1,16E+05	5,58E+05	1,95E+06	5,16E+06	1,03E+07	1,55E+07	1,74E+07	1,46E+07	9,04E+06	4,17E+06	1,42E+06	3,62E+05	6,73E+04	9,27E+03	1,04E-03
		heteroaggregates in sediment	1,5	0,00E+00	6,50E-07	2,90E-06	1,07E-05	3,52E-05	1,19E-04	1,83E-04	2,20E-04	2,49E-04	3,30E-04	1,30E-04	5,14E-05	1,85E-05	9,07E-06	0,00E+00
			2,0	2,44E-03	1,54E-02	6,94E-02	2,56E-01	8,33E-01	2,76E+00	4,24E+00	5,10E+00	5,74E+00	7,54E+00	2,98E+00	1,18E+00	4,23E-01	2,07E-01	0,00E+00
			2,5	4,25E+01	3,02E+02	1,53E+03	6,10E+03	1,99E+04	5,83E+04	9,53E+04	1,20E+05	1,28E+05	1,42E+05	6,11E+04	2,42E+04	8,25E+03	3,50E+03	4,43E-03
			2,9	2,95E+01	2,91E+02	1,99E+03	1,01E+04	3,75E+04	1,05E+05	2,20E+05	3,44E+05	3,96E+05	3,39E+05	2,15E+05	1,01E+05	3,48E+04	9,01E+03	2,22E-03

alpha river	Month	Aggregation state	Df	Sizeclass													
				2,00E-07	3,12E-07	4,86E-07	7,58E-07	1,18E-06	1,84E-06	2,87E-06	4,47E-06	6,97E-06	1,09E-05	1,69E-05	2,64E-05	4,12E-05	6,42E-05	1,00E-04
0,01	May	homoaggregates in water	1,5	1,17E+15	2,48E+15	1,50E+15	2,48E+14	1,14E+13	1,44E+11	5,47E+08	1,00E+06	2,91E+03	1,47E+03	1,16E-02	0,00E+00	0,00E+00	0,00E+00	0,00E+00
			2,0	1,10E+15	2,33E+15	1,40E+15	2,32E+14	1,06E+13	1,33E+11	4,94E+08	8,59E+05	2,14E+03	6,05E+02	0,00E+00	0,00E+00	0,00E+00	0,00E+00	0,00E+00
			2,5	7,96E+14	1,67E+15	9,93E+14	1,63E+14	7,34E+12	8,91E+10	3,03E+08	4,26E+05	5,71E+02	1,84E+01	0,00E+00	0,00E+00	0,00E+00	0,00E+00	0,00E+00
			2,9	3,74E+14	7,83E+14	4,60E+14	7,42E+13	3,27E+12	3,78E+10	1,16E+08	1,28E+05	1,07E+02	2,09E+00	0,00E+00	0,00E+00	0,00E+00	0,00E+00	0,00E+00
		homoaggregates in sediment	1,5	3,75E+08	9,90E+08	7,45E+08	1,54E+08	8,87E+06	1,40E+05	6,62E+02	1,51E+00	5,48E-03	3,45E-03	0,00E+00	0,00E+00	0,00E+00	0,00E+00	0,00E+00
			2,0	2,23E+09	7,32E+09	6,85E+09	1,77E+09	1,27E+08	2,48E+06	1,43E+04	3,88E+01	1,50E-01	6,64E-02	0,00E+00	0,00E+00	0,00E+00	0,00E+00	0,00E+00
			2,5	1,02E+10	4,15E+10	4,80E+10	1,54E+10	1,34E+09	3,18E+07	2,11E+05	5,76E+02	1,50E+00	9,40E-02	0,00E+00	0,00E+00	0,00E+00	0,00E+00	0,00E+00
			2,9	2,09E+10	1,02E+11	1,39E+11	5,20E+10	5,33E+09	1,43E+08	1,02E+06	2,61E+03	5,10E+00	2,31E-01	0,00E+00	0,00E+00	0,00E+00	0,00E+00	0,00E+00
				Sizeclass														
				1,00E-06	1,39E-06	1,93E-06	2,69E-06	3,74E-06	5,19E-06	7,22E-06	1,00E-05	1,40E-05	1,94E-05	2,70E-05	3,75E-05	5,21E-05	7,24E-05	1,00E-04
		heteroaggregates in water	1,5	6,03E+06	2,89E+07	1,01E+08	2,68E+08	5,34E+08	8,02E+08	9,00E+08	7,55E+08	4,69E+08	2,16E+08	7,38E+07	1,88E+07	3,49E+06	4,81E+05	5,47E-02
			2,0	5,64E+06	2,71E+07	9,46E+07	2,50E+08	4,99E+08	7,51E+08	8,42E+08	7,07E+08	4,38E+08	2,02E+08	6,91E+07	1,76E+07	3,26E+06	4,50E+05	5,10E-02
			2,5	4,04E+06	1,94E+07	6,78E+07	1,79E+08	3,58E+08	5,38E+08	6,03E+08	5,06E+08	3,14E+08	1,45E+08	4,95E+07	1,26E+07	2,34E+06	3,22E+05	3,62E-02
			2,9	1,88E+06	9,03E+06	3,16E+07	8,36E+07	1,67E+08	2,51E+08	2,81E+08	2,36E+08	1,47E+08	6,76E+07	2,31E+07	5,87E+06	1,09E+06	1,50E+05	1,67E-02
		heteroaggregates in sediment	1,5	3,78E+03	2,36E+04	1,05E+05	3,86E+05	1,27E+06	4,27E+06	6,56E+06	7,90E+06	8,94E+06	1,18E+07	4,67E+06	1,85E+06	6,65E+05	3,25E+05	4,53E-01
			2,0	3,61E+03	2,28E+04	1,03E+05	3,78E+05	1,23E+06	4,08E+06	6,26E+06	7,53E+06	8,48E+06	1,11E+07	4,40E+06	1,73E+06	6,24E+05	3,05E+05	4,23E-01
			2,5	2,95E+03	2,10E+04	1,06E+05	4,24E+05	1,38E+06	4,06E+06	6,63E+06	8,33E+06	8,93E+06	9,91E+06	4,25E+06	1,69E+06	5,75E+05	2,44E+05	3,01E-01
			2,9	2,05E+03	2,02E+04	1,39E+05	6,99E+05	2,61E+06	7,27E+06	1,53E+07	2,40E+07	2,76E+07	2,36E+07	1,50E+07	7,05E+06	2,42E+06	6,27E+05	1,53E-01
	August			Sizeclass														
				2,00E-07	3,12E-07	4,86E-07	7,58E-07	1,18E-06	1,84E-06	2,87E-06	4,47E-06	6,97E-06	1,09E-05	1,69E-05	2,64E-05	4,12E-05	6,42E-05	1,00E-04
		homoaggregates in water	1,5	9,16E+11	1,91E+12	1,14E+12	1,83E+11	7,97E+09	9,23E+07	3,16E+05	5,29E+02	1,87E+00	6,22E+00	3,88E+00	4,22E+00	4,50E-02	0,00E+00	2,60E+13
			2,0	5,88E+14	1,25E+15	7,69E+14	1,31E+14	6,19E+12	8,19E+10	3,44E+08	7,97E+05	4,72E+03	3,35E+04	4,00E+04	2,38E+04	9,91E+02	1,67E-03	0,00E+00
			2,5	4,25E+14	9,01E+14	5,44E+14	9,10E+13	4,19E+12	5,28E+10	1,98E+08	3,50E+05	9,19E+02	3,57E+02	0,00E+00	0,00E+00	0,00E+00	0,00E+00	0,00E+00
			2,9	2,02E+14	4,22E+14	2,50E+14	4,10E+13	1,82E+12	2,15E+10	6,97E+07	9,35E+04	1,58E+02	8,47E+01	0,00E+00	0,00E+00	0,00E+00	0,00E+00	0,00E+00
		homoaggregates in sediment	1,5	1,17E+05	3,03E+05	2,25E+05	4,54E+04	2,47E+03	3,56E+01	1,52E-01	3,18E-04	1,41E-06	5,84E-06	4,54E-06	6,18E-06	0,00E+00	0,00E+00	7,40E+07
			2,0	4,74E+08	1,57E+09	1,51E+09	4,00E+08	2,94E+07	6,07E+05	3,97E+03	1,44E+01	1,33E-01	1,46E+00	2,73E+00	2,53E+00	1,64E-01	0,00E+00	0,00E+00
			2,5	2,17E+09	8,93E+09	1,05E+10	3,42E+09	3,06E+08	7,52E+06	5,47E+04	1,89E+02	9,64E-01	7,27E-01	0,00E+00	0,00E+00	0,00E+00	0,00E+00	0,00E+00
			2,9	4,50E+09	2,19E+10	3,01E+10	1,15E+10	1,18E+09	3,24E+07	2,45E+05	7,63E+02	3,00E+00	3,74E+00	0,00E+00	0,00E+00	0,00E+00	0,00E+00	0,00E+00
				Sizeclass														
				1,00E-06	1,39E-06	1,93E-06	2,69E-06	3,74E-06	5,19E-06	7,22E-06	1,00E-05	1,40E-05	1,94E-05	2,70E-05	3,75E-05	5,21E-05	7,24E-05	1,00E-04
		heteroaggregates in water	1,5	1,83E+03	8,79E+03	3,07E+04	8,13E+04	1,62E+05	2,44E+05	2,74E+05	2,30E+05	1,42E+05	6,57E+04	2,25E+04	5,71E+03	1,06E+03	1,46E+02	1,63E-05
			2,0	1,21E+06	5,84E+06	2,04E+07	5,39E+07	1,07E+08	1,62E+08	1,81E+08	1,52E+08	9,43E+07	4,35E+07	1,49E+07	3,78E+06	7,01E+05	9,67E+04	1,12E-02
			2,5	8,68E+05	4,17E+06	1,46E+07	3,86E+07	7,69E+07	1,16E+08	1,30E+08	1,09E+08	6,75E+07	3,11E+07	1,06E+07	2,70E+06	5,02E+05	6,92E+04	7,90E-03
			2,9	4,05E+05	1,94E+06	6,79E+06	1,80E+07	3,58E+07	5,39E+07	6,05E+07	5,08E+07	3,15E+07	1,45E+07	4,96E+06	1,26E+06	2,34E+05	3,23E+04	3,62E-03
		heteroaggregates in sediment	1,5	4,58E-01	2,85E+00	1,27E+01	4,67E+01	1,54E+02	5,17E+02	7,95E+02	9,58E+02	1,08E+03	1,43E+03	5,66E+02	2,24E+02	8,06E+01	3,95E+01	5,38E-05
			2,0	3,11E+02	1,96E+03	8,82E+03	3,25E+04	1,06E+05	3,50E+05	5,37E+05	6,46E+05	7,27E+05	9,54E+05	3,77E+05	1,49E+05	5,35E+04	2,61E+04	3,70E-02
			2,5	2,53E+02	1,80E+03	9,12E+03	3,64E+04	1,18E+05	3,48E+05	5,68E+05	7,14E+05	7,65E+05	8,48E+05	3,64E+05	1,44E+05	4,92E+04	2,09E+04	2,61E-02
			2,9	1,76E+02	1,73E+03	1,19E+04	5,99E+04	2,24E+05	6,23E+05	1,31E+06	2,05E+06	2,36E+06	2,02E+06	1,28E+06	6,03E+05	2,08E+05	5,37E+04	1,32E-02

alpha river	Month	Aggregation state	Df	Sizeclass														
				2,00E-07	3,12E-07	4,86E-07	7,58E-07	1,18E-06	1,84E-06	2,87E-06	4,47E-06	6,97E-06	1,09E-05	1,69E-05	2,64E-05	4,12E-05	6,42E-05	1,00E-04
0,01	November	homoaggregates in water	1,5	0,00E+00	0,00E+00	0,00E+00	0,00E+00	0,00E+00	0,00E+00	0,00E+00	0,00E+00	0,00E+00	0,00E+00	0,00E+00	0,00E+00	0,00E+00	0,00E+00	1,67E+14
			2,0	0,00E+00	0,00E+00	0,00E+00	0,00E+00	0,00E+00	0,00E+00	0,00E+00	0,00E+00	0,00E+00	0,00E+00	0,00E+00	0,00E+00	0,00E+00	0,00E+00	1,56E+14
			2,5	0,00E+00	0,00E+00	0,00E+00	0,00E+00	0,00E+00	0,00E+00	0,00E+00	0,00E+00	0,00E+00	0,00E+00	0,00E+00	0,00E+00	0,00E+00	0,00E+00	9,70E+13
			2,9	0,00E+00	0,00E+00	0,00E+00	0,00E+00	0,00E+00	0,00E+00	0,00E+00	0,00E+00	0,00E+00	0,00E+00	0,00E+00	0,00E+00	0,00E+00	0,00E+00	7,87E+10
		homoaggregates in sediment	1,5	0,00E+00	0,00E+00	0,00E+00	0,00E+00	0,00E+00	0,00E+00	0,00E+00	0,00E+00	0,00E+00	0,00E+00	0,00E+00	0,00E+00	0,00E+00	0,00E+00	3,26E+08
			2,0	0,00E+00	0,00E+00	0,00E+00	0,00E+00	0,00E+00	0,00E+00	0,00E+00	0,00E+00	0,00E+00	0,00E+00	0,00E+00	0,00E+00	0,00E+00	0,00E+00	4,31E+10
			2,5	0,00E+00	0,00E+00	0,00E+00	0,00E+00	0,00E+00	0,00E+00	0,00E+00	0,00E+00	0,00E+00	0,00E+00	0,00E+00	0,00E+00	0,00E+00	0,00E+00	3,79E+12
			2,9	0,00E+00	0,00E+00	0,00E+00	0,00E+00	0,00E+00	0,00E+00	0,00E+00	0,00E+00	0,00E+00	0,00E+00	0,00E+00	0,00E+00	0,00E+00	0,00E+00	1,61E+11
				Sizeclass														
				1,00E-06	1,39E-06	1,93E-06	2,69E-06	3,74E-06	5,19E-06	7,22E-06	1,00E-05	1,40E-05	1,94E-05	2,70E-05	3,75E-05	5,21E-05	7,24E-05	1,00E-04
		heteroaggregates in water	1,5	0	0	0	0	0	0	0	0	0	0	0	0	0	0	0
			2,0	0	0	0	0	0	0	0	0	0	0	0	0	0	0	0
			2,5	0	0	0	0	0	0	0	0	0	0	0	0	0	0	0
			2,9	0	0	0	0	0	0	0	0	0	0	0	0	0	0	0
		heteroaggregates in sediment	1,5	0	0	0	0	0	0	0	0	0	0	0	0	0	0	0
			2,0	0	0	0	0	0	0	0	0	0	0	0	0	0	0	0
			2,5	0	0	0	0	0	0	0	0	0	0	0	0	0	0	0
			2,9	0	0	0	0	0	0	0	0	0	0	0	0	0	0	0

alpha river	Month	Aggregation state	Df	Sizeclass													
				2,00E-07	3,12E-07	4,86E-07	7,58E-07	1,18E-06	1,84E-06	2,87E-06	4,47E-06	6,97E-06	1,09E-05	1,69E-05	2,64E-05	4,12E-05	6,42E-05	1,00E-04
	January	homoaggregates in water	1,5	0	0	0	0	0	0	0	0	0	0	0	0	0	0	0
			2,0	0	0	0	0	0	0	0	0	0	0	0	0	0	0	0
			2,5	0	0	0	0	0	0	0	0	0	0	0	0	0	0	0
			2,9	0	0	0	0	0	0	0	0	0	0	0	0	0	0	0
		homoaggregates in sediment	1,5	0	0	0	0	0	0	0	0	0	0	0	0	0	0	0
			2,0	0	0	0	0	0	0	0	0	0	0	0	0	0	0	0
			2,5	0	0	0	0	0	0	0	0	0	0	0	0	0	0	0
			2,9	0	0	0	0	0	0	0	0	0	0	0	0	0	0	0
				Sizeclass														
				1,00E-06	1,39E-06	1,93E-06	2,69E-06	3,74E-06	5,19E-06	7,22E-06	1,00E-05	1,40E-05	1,94E-05	2,70E-05	3,75E-05	5,21E-05	7,24E-05	1,00E-04
		heteroaggregates in water	1,5	0	0	0	0	0	0	0	0	0	0	0	0	0	0	0
			2,0	0	0	0	0	0	0	0	0	0	0	0	0	0	0	0
			2,5	0	0	0	0	0	0	0	0	0	0	0	0	0	0	0
			2,9	0	0	0	0	0	0	0	0	0	0	0	0	0	0	0
		heteroaggregates in sediment	1,5	0	0	0	0	0	0	0	0	0	0	0	0	0	0	0
			2,0	0	0	0	0	0	0	0	0	0	0	0	0	0	0	0
			2,5	0	0	0	0	0	0	0	0	0	0	0	0	0	0	0
			2,9	0	0	0	0	0	0	0	0	0	0	0	0	0	0	0
0,1				Sizeclass														
				2,00E-07	3,12E-07	4,86E-07	7,58E-07	1,18E-06	1,84E-06	2,87E-06	4,47E-06	6,97E-06	1,09E-05	1,69E-05	2,64E-05	4,12E-05	6,42E-05	1,00E-04
	March	homoaggregates in water	1,5	9,42E+05	1,89E+06	1,06E+06	1,54E+05	5,71E+03	5,23E+01	1,26E-01	1,34E-04	0,00E+00	2,95E-06	0,00E+00	0,00E+00	0,00E+00	0,00E+00	1,85E+13
			2,0	2,05E+10	4,24E+10	2,50E+10	3,95E+09	1,67E+08	1,89E+06	6,27E+03	1,12E+01	6,52E-02	2,57E+00	6,84E-01	1,46E-01	4,90E-05	0,00E+00	1,74E+13
			2,5	3,00E+14	6,37E+14	3,91E+14	6,59E+13	3,08E+12	4,04E+10	1,67E+08	3,81E+05	2,23E+03	1,80E+04	1,20E-03	0,00E+00	0,00E+00	0,00E+00	0,00E+00
			2,9	1,43E+14	3,00E+14	1,79E+14	2,93E+13	1,31E+12	1,59E+10	5,46E+07	8,67E+04	2,63E+02	1,75E+03	0,00E+00	0,00E+00	0,00E+00	0,00E+00	0,00E+00
		homoaggregates in sediment	1,5	7,00E-02	1,75E-01	1,22E-01	2,23E-02	1,03E-03	1,18E-05	0,00E+00	0,00E+00	0,00E+00	0,00E+00	0,00E+00	0,00E+00	0,00E+00	0,00E+00	3,08E+07
			2,0	9,65E+03	3,11E+04	2,86E+04	7,05E+03	4,64E+02	8,17E+00	4,23E-02	1,18E-04	1,07E-06	6,56E-05	2,72E-05	9,09E-06	0,00E+00	0,00E+00	4,09E+09
			2,5	8,91E+08	3,69E+09	4,40E+09	1,44E+09	1,31E+08	3,35E+06	2,70E+04	1,20E+02	1,37E+00	2,15E+01	2,79E-06	0,00E+00	0,00E+00	0,00E+00	0,00E+00
			2,9	1,86E+09	9,06E+09	1,26E+10	4,79E+09	4,98E+08	1,40E+07	1,12E+05	4,13E+02	2,92E+00	4,52E+01	0,00E+00	0,00E+00	0,00E+00	0,00E+00	0,00E+00
				Sizeclass														
				1,00E-06	1,39E-06	1,93E-06	2,69E-06	3,74E-06	5,19E-06	7,22E-06	1,00E-05	1,40E-05	1,94E-05	2,70E-05	3,75E-05	5,21E-05	7,24E-05	1,00E-04
		heteroaggregates in water	1,5	7,16E-03	3,43E-02	1,20E-01	3,19E-01	6,36E-01	9,58E-01	1,08E+00	9,03E-01	5,60E-01	2,59E-01	8,83E-02	2,25E-02	4,17E-03	5,75E-04	0,00E+00
			2,0	1,64E+02	7,86E+02	2,75E+03	7,28E+03	1,45E+04	2,18E+04	2,45E+04	2,06E+04	1,28E+04	5,88E+03	2,01E+03	5,11E+02	9,49E+01	1,31E+01	1,44E-06
			2,5	2,50E+06	1,20E+07	4,19E+07	1,11E+08	2,21E+08	3,32E+08	3,72E+08	3,12E+08	1,94E+08	8,93E+07	3,05E+07	7,76E+06	1,44E+06	1,99E+05	2,29E-02
			2,9	1,16E+06	5,58E+06	1,95E+07	5,16E+07	1,03E+08	1,55E+08	1,74E+08	1,46E+08	9,04E+07	4,17E+07	1,42E+07	3,62E+06	6,73E+05	9,27E+04	1,04E-02
		heteroaggregates in sediment	1,5	1,05E-06	6,50E-06	2,90E-05	1,07E-04	3,52E-04	1,19E-03	1,83E-03	2,20E-03	2,49E-03	3,30E-03	1,30E-03	5,14E-04	1,85E-04	9,07E-05	0,00E+00
			2,0	2,44E-02	1,54E-01	6,94E-01	2,56E+00	8,33E+00	2,76E+01	4,24E+01	5,10E+01	5,74E+01	7,54E+01	2,98E+01	1,18E+01	4,23E+00	2,07E+00	2,78E-06
			2,5	4,25E+02	3,02E+03	1,53E+04	6,10E+04	1,99E+05	5,83E+05	9,53E+05	1,20E+06	1,28E+06	1,42E+06	6,11E+05	2,42E+05	8,25E+04	3,50E+04	4,43E-02
			2,9	2,95E+02	2,91E+03	1,99E+04	1,01E+05	3,75E+05	1,05E+06	2,20E+06	3,44E+06	3,96E+06	3,39E+06	2,15E+06	1,01E+06	3,48E+05	9,01E+04	2,22E-02

alpha river	Month	Aggregation state	Df	Sizeclass													
				2,00E-07	3,12E-07	4,86E-07	7,58E-07	1,18E-06	1,84E-06	2,87E-06	4,47E-06	6,97E-06	1,09E-05	1,69E-05	2,64E-05	4,12E-05	6,42E-05	1,00E-04
0,1	May	homoaggregates in water	1,5	1,17E+15	2,48E+15	1,50E+15	2,48E+14	1,14E+13	1,44E+11	5,47E+08	1,00E+06	2,91E+03	1,47E+03	1,16E-02	0,00E+00	0,00E+00	0,00E+00	0,00E+00
			2,0	1,10E+15	2,32E+15	1,39E+15	2,32E+14	1,06E+13	1,33E+11	4,94E+08	8,59E+05	2,14E+03	6,05E+02	0,00E+00	0,00E+00	0,00E+00	0,00E+00	0,00E+00
			2,5	7,96E+14	1,67E+15	9,93E+14	1,63E+14	7,33E+12	8,90E+10	3,03E+08	4,26E+05	5,71E+02	1,84E+01	0,00E+00	0,00E+00	0,00E+00	0,00E+00	0,00E+00
			2,9	3,74E+14	7,82E+14	4,59E+14	7,41E+13	3,27E+12	3,78E+10	1,16E+08	1,28E+05	1,07E+02	2,09E+00	0,00E+00	0,00E+00	0,00E+00	0,00E+00	0,00E+00
		homoaggregates in sediment	1,5	3,75E+08	9,90E+08	7,45E+08	1,54E+08	8,86E+06	1,40E+05	6,61E+02	1,51E+00	5,48E-03	3,45E-03	0,00E+00	0,00E+00	0,00E+00	0,00E+00	0,00E+00
			2,0	2,23E+09	7,32E+09	6,84E+09	1,77E+09	1,27E+08	2,47E+06	1,43E+04	3,88E+01	1,50E-01	6,64E-02	0,00E+00	0,00E+00	0,00E+00	0,00E+00	0,00E+00
			2,5	1,02E+10	4,15E+10	4,80E+10	1,53E+10	1,34E+09	3,17E+07	2,10E+05	5,76E+02	1,50E+00	9,40E-02	0,00E+00	0,00E+00	0,00E+00	0,00E+00	0,00E+00
			2,9	2,09E+10	1,02E+11	1,39E+11	5,20E+10	5,33E+09	1,43E+08	1,02E+06	2,61E+03	5,10E+00	2,31E-01	0,00E+00	0,00E+00	0,00E+00	0,00E+00	0,00E+00
				Sizeclass														
				1,00E-06	1,39E-06	1,93E-06	2,69E-06	3,74E-06	5,19E-06	7,22E-06	1,00E-05	1,40E-05	1,94E-05	2,70E-05	3,75E-05	5,21E-05	7,24E-05	1,00E-04
		heteroaggregates in water	1,5	6,03E+07	2,89E+08	1,01E+09	2,68E+09	5,33E+09	8,02E+09	9,00E+09	7,55E+09	4,68E+09	2,16E+09	7,38E+08	1,88E+08	3,48E+07	4,80E+06	5,46E-01
			2,0	5,64E+07	2,71E+08	9,46E+08	2,50E+09	4,99E+09	7,50E+09	8,42E+09	7,07E+09	4,38E+09	2,02E+09	6,91E+08	1,76E+08	3,26E+07	4,49E+06	5,10E-01
			2,5	4,04E+07	1,94E+08	6,77E+08	1,79E+09	3,57E+09	5,38E+09	6,03E+09	5,06E+09	3,14E+09	1,45E+09	4,95E+08	1,26E+08	2,34E+07	3,22E+06	3,62E-01
			2,9	1,88E+07	9,03E+07	3,16E+08	8,36E+08	1,67E+09	2,51E+09	2,81E+09	2,36E+09	1,47E+09	6,76E+08	2,31E+08	5,87E+07	1,09E+07	1,50E+06	1,67E-01
		heteroaggregates in sediment	1,5	3,78E+04	2,35E+05	1,05E+06	3,86E+06	1,27E+07	4,27E+07	6,56E+07	7,90E+07	8,94E+07	1,18E+08	4,67E+07	1,84E+07	6,64E+06	3,25E+06	4,53E+00
			2,0	3,61E+04	2,28E+05	1,03E+06	3,78E+06	1,23E+07	4,08E+07	6,26E+07	7,53E+07	8,47E+07	1,11E+08	4,39E+07	1,73E+07	6,24E+06	3,05E+06	4,22E+00
			2,5	2,95E+04	2,10E+05	1,06E+06	4,24E+06	1,38E+07	4,05E+07	6,63E+07	8,33E+07	8,93E+07	9,90E+07	4,25E+07	1,69E+07	5,74E+06	2,44E+06	3,00E+00
			2,9	2,05E+04	2,02E+05	1,39E+06	6,99E+06	2,61E+07	7,27E+07	1,53E+08	2,39E+08	2,76E+08	2,36E+08	1,50E+08	7,04E+07	2,42E+07	6,27E+06	1,53E+00
	August			Sizeclass														
				2,00E-07	3,12E-07	4,86E-07	7,58E-07	1,18E-06	1,84E-06	2,87E-06	4,47E-06	6,97E-06	1,09E-05	1,69E-05	2,64E-05	4,12E-05	6,42E-05	1,00E-04
		homoaggregates in water	1,5	9,16E+11	1,91E+12	1,13E+12	1,83E+11	7,97E+09	9,22E+07	3,16E+05	5,28E+02	1,87E+00	6,22E+00	3,88E+00	4,22E+00	4,50E-02	0,00E+00	2,60E+13
			2,0	5,88E+14	1,25E+15	7,69E+14	1,31E+14	6,19E+12	8,19E+10	3,44E+08	7,97E+05	4,72E+03	3,35E+04	4,00E+04	2,38E+04	9,91E+02	1,67E-03	0,00E+00
			2,5	4,25E+14	9,01E+14	5,44E+14	9,10E+13	4,19E+12	5,28E+10	1,98E+08	3,50E+05	9,19E+02	3,57E+02	0,00E+00	0,00E+00	0,00E+00	0,00E+00	0,00E+00
			2,9	2,02E+14	4,22E+14	2,50E+14	4,10E+13	1,82E+12	2,14E+10	6,97E+07	9,35E+04	1,58E+02	8,47E+01	0,00E+00	0,00E+00	0,00E+00	0,00E+00	0,00E+00
		homoaggregates in sediment	1,5	1,17E+05	3,03E+05	2,25E+05	4,54E+04	2,47E+03	3,56E+01	1,52E-01	3,18E-04	1,41E-06	5,84E-06	4,54E-06	6,18E-06	0,00E+00	0,00E+00	7,40E+07
			2,0	4,73E+08	1,57E+09	1,51E+09	4,00E+08	2,94E+07	6,07E+05	3,97E+03	1,44E+01	1,33E-01	1,46E+00	2,73E+00	2,53E+00	1,64E-01	0,00E+00	0,00E+00
			2,5	2,17E+09	8,93E+09	1,05E+10	3,42E+09	3,06E+08	7,51E+06	5,47E+04	1,89E+02	9,64E-01	7,27E-01	0,00E+00	0,00E+00	0,00E+00	0,00E+00	0,00E+00
			2,9	4,50E+09	2,19E+10	3,01E+10	1,15E+10	1,18E+09	3,24E+07	2,45E+05	7,63E+02	3,00E+00	3,74E+00	0,00E+00	0,00E+00	0,00E+00	0,00E+00	0,00E+00
				Sizeclass														
				1,00E-06	1,39E-06	1,93E-06	2,69E-06	3,74E-06	5,19E-06	7,22E-06	1,00E-05	1,40E-05	1,94E-05	2,70E-05	3,75E-05	5,21E-05	7,24E-05	1,00E-04
		heteroaggregates in water	1,5	1,83E+04	8,78E+04	3,07E+05	8,13E+05	1,62E+06	2,44E+06	2,74E+06	2,30E+06	1,42E+06	6,57E+05	2,25E+05	5,71E+04	1,06E+04	1,46E+03	1,63E-04
			2,0	1,21E+07	5,84E+07	2,04E+08	5,39E+08	1,07E+09	1,62E+09	1,81E+09	1,52E+09	9,43E+08	4,35E+08	1,49E+08	3,78E+07	7,01E+06	9,67E+05	1,12E-01
			2,5	8,68E+06	4,17E+07	1,46E+08	3,86E+08	7,68E+08	1,16E+09	1,30E+09	1,09E+09	6,75E+08	3,11E+08	1,06E+08	2,70E+07	5,02E+06	6,92E+05	7,90E-02
			2,9	4,04E+06	1,94E+07	6,79E+07	1,80E+08	3,58E+08	5,39E+08	6,05E+08	5,07E+08	3,15E+08	1,45E+08	4,96E+07	1,26E+07	2,34E+06	3,23E+05	3,61E-02
		heteroaggregates in sediment	1,5	4,57E+00	2,85E+01	1,27E+02	4,67E+02	1,54E+03	5,17E+03	7,95E+03	9,58E+03	1,08E+04	1,43E+04	5,66E+03	2,24E+03	8,06E+02	3,95E+02	5,38E-04
			2,0	3,10E+03	1,96E+04	8,82E+04	3,25E+05	1,06E+06	3,50E+06	5,37E+06	6,46E+06	7,27E+06	9,54E+06	3,77E+06	1,49E+06	5,35E+05	2,61E+05	3,70E-01
			2,5	2,53E+03	1,80E+04	9,12E+04	3,64E+05	1,18E+06	3,48E+06	5,68E+06	7,14E+06	7,65E+06	8,48E+06	3,64E+06	1,44E+06	4,92E+05	2,09E+05	2,61E-01
			2,9	1,76E+03	1,73E+04	1,19E+05	5,99E+05	2,24E+06	6,23E+06	1,31E+07	2,05E+07	2,36E+07	2,02E+07	1,28E+07	6,03E+06	2,08E+06	5,37E+05	1,32E-01

alpha river	Month	Aggregation state	Df	Sizeclass														
				2,00E-07	3,12E-07	4,86E-07	7,58E-07	1,18E-06	1,84E-06	2,87E-06	4,47E-06	6,97E-06	1,09E-05	1,69E-05	2,64E-05	4,12E-05	6,42E-05	1,00E-04
0,1	November	homoaggregates in water	1,5	0,00E+00	0,00E+00	0,00E+00	0,00E+00	0,00E+00	0,00E+00	0,00E+00	0,00E+00	0,00E+00	0,00E+00	0,00E+00	0,00E+00	0,00E+00	0,00E+00	1,67E+14
			2,0	0,00E+00	0,00E+00	0,00E+00	0,00E+00	0,00E+00	0,00E+00	0,00E+00	0,00E+00	0,00E+00	0,00E+00	0,00E+00	0,00E+00	0,00E+00	0,00E+00	1,56E+14
			2,5	0,00E+00	0,00E+00	0,00E+00	0,00E+00	0,00E+00	0,00E+00	0,00E+00	0,00E+00	0,00E+00	0,00E+00	0,00E+00	0,00E+00	0,00E+00	0,00E+00	9,70E+13
			2,9	0,00E+00	0,00E+00	0,00E+00	0,00E+00	0,00E+00	0,00E+00	0,00E+00	0,00E+00	0,00E+00	0,00E+00	0,00E+00	0,00E+00	0,00E+00	0,00E+00	7,87E+10
		homoaggregates in sediment	1,5	0,00E+00	0,00E+00	0,00E+00	0,00E+00	0,00E+00	0,00E+00	0,00E+00	0,00E+00	0,00E+00	0,00E+00	0,00E+00	0,00E+00	0,00E+00	0,00E+00	3,26E+08
			2,0	0,00E+00	0,00E+00	0,00E+00	0,00E+00	0,00E+00	0,00E+00	0,00E+00	0,00E+00	0,00E+00	0,00E+00	0,00E+00	0,00E+00	0,00E+00	0,00E+00	4,31E+10
			2,5	0,00E+00	0,00E+00	0,00E+00	0,00E+00	0,00E+00	0,00E+00	0,00E+00	0,00E+00	0,00E+00	0,00E+00	0,00E+00	0,00E+00	0,00E+00	0,00E+00	3,79E+12
			2,9	0,00E+00	0,00E+00	0,00E+00	0,00E+00	0,00E+00	0,00E+00	0,00E+00	0,00E+00	0,00E+00	0,00E+00	0,00E+00	0,00E+00	0,00E+00	0,00E+00	1,61E+11
				Sizeclass														
				1,00E-06	1,39E-06	1,93E-06	2,69E-06	3,74E-06	5,19E-06	7,22E-06	1,00E-05	1,40E-05	1,94E-05	2,70E-05	3,75E-05	5,21E-05	7,24E-05	1,00E-04
		heteroaggregates in water	1,5	0	0	0	0	0	0	0	0	0	0	0	0	0	0	0
			2,0	0	0	0	0	0	0	0	0	0	0	0	0	0	0	0
			2,5	0	0	0	0	0	0	0	0	0	0	0	0	0	0	0
			2,9	0	0	0	0	0	0	0	0	0	0	0	0	0	0	0
		heteroaggregates in sediment	1,5	0	0	0	0	0	0	0	0	0	0	0	0	0	0	0
			2,0	0	0	0	0	0	0	0	0	0	0	0	0	0	0	0
			2,5	0	0	0	0	0	0	0	0	0	0	0	0	0	0	0
			2,9	0	0	0	0	0	0	0	0	0	0	0	0	0	0	0

Appendix XIIA: Ecotoxicity values measured on *G. roeseli* (adapted from LIEC communication, to be published in autumn 2015 in J. Andrei's Ph.D dissertation) and integrated in the BN. Green boxes indicate positive effects, orange boxes indicate negative effects.

NP type	TAC (Trolox eq/gprot/min)			LOOH (nmol/gprot)			Locomotion (% individus mobiles)		
	d7	d14	d21	d7	d14	d21	d7	d14	d21
Control	8,63	23,13	21,68	434,34	431,73	388,08	42,22	36,54	21,11
AB	8,52	45,62	39,55	511,17	522,24	338,04	39,75	18,02	13,89
AC	4,01	28,89	36,15	470,06	454,26	355,18	24,20	17,46	9,18
NP type	TAC (% to control)			LOOH (% to control)			Locomotion (% to control)		
	d7	d14	d21	d7	d14	d21	d7	d14	d21
Control	0	0	0	0	0	0	0	0	0
AB	-1,28	97,24	82,47	17,69	20,96	-12,89	-5,85	-50,68	-34,21
AC	-53,54	24,89	66,78	8,23	5,22	-8,48	-42,69	-52,22	-56,52

NP type	Ventilation (pleopod fluttering/min)			Osmolality (mOsm/L)			Mortality (% mortality)		
	d7	d14	d21	d7	d14	d21	t7	t14	t21
Control	214,22	218,00	181,33	284,69	280,28	-	20,00	69,33	92,67
AB	220,44	206,67	168,11	259,37	251,11	-	17,33	68,00	92,67
AC	206,89	210,43	174,33	265,50	239,85	-	22,00	59,33	94,00
NP type	Ventilation (% to control)			Osmolality (% to control)			Mortality (% survival)		
	t7	t14	t21	t7	t14	t21	t7	t14	t21
Control	0	0	0	0	0	-	0	0	0
AB	2,90	-5,20	-7,29	-8,89	-10,41	-	-13,35	-1,92	0,00
AC	-3,42	-3,47	-3,86	-6,74	-14,42	-	10,00	-14,42	1,44

Appendix XIIB: Ecotoxicity values measured on *D. polymorpha* (adapted from LIEC communication, to be published by October 2015 in M. Garaud Ph.D dissertation) and integrated in the BN. Green boxes indicate positive effects, orange boxes indicate negative effects.

NP type	Dammaged cells (%)			ROS production (AU)			Phagocytosis performance (% of phagocytic cells)		
	d7	d14	d21	d7	d14	d21	d7	d14	d21
Control	12,2	13,7	10,87	44,03	44,7	49,23	75,23	61,7	91,17
AB	14,93	15,4	37,6	46,83	43,4	53,83	72,03	63,57	59,9
AC	14,93	12,93	29	33	37,5	51,93	65,5	70,63	79,77
NP type	Dammaged cells (% to control)			ROS production (% to control)			Phagocytosis performance (% to control)		
	d7	d14	d21	d7	d14	d21	d7	d14	d21
Control	0	0	0	0	0	0	0	0	0
AB	22,38	12,41	245,91	6,36	-2,91	9,34	-4,25	3,03	-34,30
AC	22,38	-5,62	166,79	-25,05	-16,11	5,48	-12,93	14,47	-12,50

NP type	TAC (Trolox eq/gprot/min)			LOOH (nmol/gprot)			Filtration (mL/ind/h)	Mortality (% mortality)
	d7	d14	d21	d7	d14	d21	d21	d28
Control	43,37	35,9	65,27	30,2	28,17	30,4	7,3	11
AB	35,93	47,83	48,93	30,93	31,9	26,43	5,8	5
AC	34,87	44,5	63,83	31,1	30,2	33,13	7,7	5
NP type	TAC (%)			LOOH (% to control)			Filtration (% to control)	Mortality (% to control)
	d7	d14	d21	d7	d14	d21	d21	d28
Control	0	0	0	0	0	0	0	0
AB	-17,15	33,23	-25,03	2,42	13,24	-13,06	-20,55	-54,55
AC	-19,60	23,96	-2,21	2,98	7,21	8,98	5,48	-54,55

COMMUNICATIONS AND PUBLICATIONS RELATED TO THIS THESIS

Communications

V. Adam. Environmental Risk and Impact Assessment of TiO_2 Nanomaterials. Presentation. CEINT internal meeting, Durham, NC, USA, 13/05/2015

V. Adam. Environmental risk and impact assessment of TiO_2 nanomaterials. Presentation. CREIDD, Troyes, France, 20/04/2015

V. Adam, G. Quaranta, S. Lawniczak. LCA-RA combined approach using a Bayesian model: Example of the aquatic ecotoxicity impact/risk of the nano-TiO_2 production. Presentation. SETAC Europe, Basel, Switzerland, 14/05/2014

V. Adam. Evaluation des impacts et des risques des nanomatériaux de TiO_2 sur l'eau douce par la mise en place d'un modèle combiné Evaluation des Risques – Analyse du Cycle de Vie (ER-ACV). Presentation. ADEME Ph.D. students conference, Angers, France, 04/02/2014

V. Adam, G. Quaranta, S. Lawniczak. Impact and Risk Assessment of Nano-TiO_2 on Freshwater by Risk Assessment and Life Cycle Assessment (RA-LCA) Modeling. Poster. Ph.D. students conference, Doctoral School of Earth and Environmental Sciences (ED413), Strasbourg, France, 27/11/2013

V. Adam, G. Quaranta, S. Loyaux-Lawniczak. Combining Life Cycle (LCA) and Risk (RA) Assessments of TiO_2 Nanomaterials: Use of a Bayesian Network. Poster. Goldschmidt Conference, Florence, Italy, 29/08/2013

V. Adam. Evaluation des impacts et des risques toxiques des nanomatériaux manufactures de TiO_2 par la mise au point d'un modèle ER-ACV (Evaluation des Risques – Analyse du Cycle de Vie). Poster. ADEME Ph.D. students conference, Angers, France, 15/02/2013

Publications

Published

V. Adam, S. Loyaux-Lawniczak, G. Quaranta (2015) Characterization of Engineered TiO_2 Nanomaterials in a Life Cycle and Risk Assessments Perspective". Environmental Sciences and Pollution Research. DOI 10.1007/s11356-015-4661-x.

G. Quaranta, V. Adam (2015) Nano TiO_2 Life Cycle Assessment Perspective, Encyclopedia of Nanotechnology [128803] edited by Bharat Bhushan, Springer, 17p.

Under review

V. Adam, G. Quaranta, S. Loyaux-Lawniczak. Life Cycle Assessment and Ecological Risk Assessment of Nanomaterials - Review of single and combined approaches. Submitted to Environmental Science and Pollution Research, July 2015.

V. Adam, S. Loyaux-Lawniczak, J. Labille, C. Galindo, M. del Nero, T.Weber, G. Quaranta. Aggregation behavior of TiO_2 ENMs in natural river water. Accepted in the Journal of Nanoparticle Research, September 2015.

Véronique ADAM

Ecotoxicological impact and risk assessment of engineered TiO2 nanomaterials on water, sediments and soil bu building a combined RA-LCA (Risk Assessment – Life Cycle Assessment) model

Résumé

L'analyse du cycle de vie et l'évaluation du risque ont été combinées afin d'évaluer les impacts et risques potentiels de NMs de TiO_2 dans l'eau, les sols et les sédiments à une échelle site-spécifique. Une approche analytique a permis de caractériser les NMs industriels dans les eaux, sols et sédiments et de déterminer leur comportement dans l'eau. Un modèle bayésien a été réalisé pour évaluer leur devenir dans les eaux et sédiments de la rivière, ainsi que leurs effets et risques associés en mésocosmes. Il a ainsi été montré que le TiO_2 est présent en faible concentration dans l'eau de rivière. En mésocosmes, des risques ont été quantifiés sur deux espèces : *Dreissena polymorpha* et *Gammarus roeseli*. Il est apparu nécessaire de mieux caractériser la dimension fractale des agrégats de NMs pour comprendre leur sédimentation et de quantifier les effets des nano-TiO_2 dans le milieu naturel, en dépassant l'approche par mésocosmes.

Devenir des nano-TiO_2, Effet des nano-TiO_2, Analyse du Cycle de Vie, Evaluation du Risque, Réseau bayésien.

Abstract

In this work, life cycle and risk assessments were combined in order to assess the potential impacts and risks of TiO_2 NMs in water, soils and sediments at a site-specific scale. Two approaches were used: (1) An analytical approach allowed the analyzes of waters, sediments and soils, the characterization of industrial NMs and the determination of their aggregation behavior in water; (2) A Bayesian modeling approach was used to assess their fate in the river water and sediments, as well as their potential effects and risks in mesocosms. It was thus shown the TiO_2 occurs at low concentrations in the river water. Quantifying the TiO_2 mass which deposits on the sediment requires characterizing more precisely their fractal dimension. Finally, nano-TiO_2 were shown to induce risks to two species in mesocosms: it is consequently necessary to assess the potential effects of the nano-TiO_2 produced in the study area in mesocosms, simulating realistic conditions.

Fate of nano-TiO_2, Effect of nano-TiO_2, Life Cycle Assessment, Risk Assessment, Bayesian network.